

# **Novel therapeutic interventions that blunt hyperglycemia-induced cardiac contractile dysfunction**

by

Rudo Fiona Mapanga

*Thesis presented in fulfilment of the requirements for the degree of Doctor of Philosophy (Physiological Sciences) in the Faculty of Science at Stellenbosch University*



Supervisor: Professor M Faadiel Essop

March 2013

## DECLARATION

By submitting this thesis/dissertation, I declare that the entirety of the work contained therein is my own, original work, that I am the sole author thereof (save to the extent explicitly otherwise stated), that reproduction and publication thereof by Stellenbosch University will not infringe any third party rights and that I have not previously in its entirety or in part submitted it for obtaining any qualification.

March 2013

Copyright © 2013 Stellenbosch University

All rights reserved

## Abstract

### Introduction

Diabetes constitutes a major health challenge. Since cardiovascular complications are common in diabetic patients this will further increase the overall burden of disease. Furthermore, stress-induced hyperglycemia in non-diabetic patients with acute myocardial infarction is associated with higher in-hospital mortality. Hyperglycemia-induced oxidative stress results in DNA damage and subsequent activation of poly-ADP-ribose polymerase (PARP) as a restorative mechanism. However, PARP attenuates glyceraldehyde-3-phosphate dehydrogenase (GAPDH) activity, thereby diverting upstream glycolytic metabolites into damaging non-oxidative glucose pathways (NOGP). For example, hyperglycemia-induced stimulation of four NOGP, i.e. the polyol pathway, hexosamine biosynthetic pathway (HBP), advanced glycation end products (AGE), and PKC activation elicit cardiovascular complications. The current thesis examined the regulation of NOGP in the setting of ischemia and reperfusion under hyperglycemic conditions.

Here we hypothesized that administration of two unique therapeutic interventions, i.e. oleanolic acid (OA; clove extract) and benfotiamine (BFT; vitamin B1 derivative), can blunt oxidative stress and NOGP-induced cardiac dysfunction under hyperglycemic conditions following ischemia and reperfusion. Our choice for these agents was based on the principle that OA possesses antioxidant properties; and BFT stimulates transketolase (pentose phosphate pathway [PPP] enzyme) thereby shunting flux away from the NOGP pathways. Additionally, hyperglycemia-induced oxidative stress can also result in dysregulation of the ubiquitin-proteasome system (UPS) that removes misfolded proteins. There are conflicting data whether increased/decreased UPS is detrimental with hyperglycemia and/or in response to ischemia and reperfusion. In light of this, we also hypothesized that BFT and OA act as novel cardio-protective agents by diminishing myocardial UPS activity in response to ischemia and reperfusion under acute hyperglycemic conditions.

### Materials and Methods

For the first part of the study, we employed several experimental systems: 1) H9c2 cardiac myoblasts were exposed to 33 mM glucose for 48 hr vs. controls (5 mM glucose); and subsequently treated with two OA doses (20 and 50  $\mu$ M) for 6 and 24 hr, respectively; 2) Isolated rat hearts were perfused *ex vivo* with Krebs-Henseleit buffer containing 33 mM glucose vs. controls (11 mM glucose) for 60 min, followed by 20 min global ischemia and 60 min reperfusion  $\pm$  OA treatment; 3) Infarct size was

determined using Evans Blue dye and 1% 2,3,5-triphenyl tetrazolium chloride (TTC) staining with 20 min regional ischemia and 2 hr reperfusion 4) *In vivo* coronary ligations were performed on streptozotocin-diabetic rats  $\pm$  0.45 mg/kg OA administration within the first two minutes of reperfusion; and 5) Effects of long-term OA treatment (2 weeks) on heart function were assessed in streptozotocin (STZ)-diabetic rats. Here, STZ was dissolved in citrate buffer (p.H 6.3) and diabetes was induced by administering 60 mg/kg i.p Tissues were collected at the end of the global ischemia experiments and analyzed for oxidative stress, apoptosis, UPS activity and HBP activation.

For the second part of the study we employed several experimental systems: 1) Isolated rat hearts were perfused *ex vivo* with Krebs-Henseleit buffer containing 33 mM glucose vs. controls (11 mM glucose) for 90 min, followed by 30 min global ischemia and 60 min reperfusion  $\pm$  25, 50 and 100  $\mu$ M BFT treatment, respectively, added during the first 20 min of reperfusion; 2) Infarct size determination as in #3 above but with 30 min regional ischemia and 2 hr reperfusion  $\pm$  100  $\mu$ M BFT treatment; and 3) *In vivo* coronary ligations performed on streptozotocin-diabetic rats  $\pm$  0.50 mg/kg BFT treatment within the first two min of reperfusion. In parallel experiments, NOGP inhibitors were added during the first 20 min of reperfusion. The following inhibitors were individually employed: AGE pathway (100  $\mu$ M aminoguanidine); PKC (5  $\mu$ M chelerythrine chloride); HBP (40  $\mu$ M 6-diazo-5-oxo-L-norleucine); and polyol pathway (1  $\mu$ M zopolrestat); Infarct size determination as in #2) with 30 min regional ischemia and 120 min reperfusion  $\pm$  similar treatments.

## Results

Our data show decreased cardiac contractile function in response to ischemia and reperfusion under hyperglycemic conditions. This was linked to increased PARP and attenuated GAPDH activities, together with higher activation of the NOGP. Moreover, we found elevated myocardial oxidative stress, UPS and cell death under these conditions. OA treatment resulted in cardio-protection, i.e. for *ex vivo* and *in vivo* rat hearts exposed to ischemia and reperfusion under hyperglycemic conditions. In parallel, OA decreased oxidative stress, apoptosis, HBP flux and UPS activity following ischemia and reperfusion. Long-term OA treatment also improved heart function in streptozotocin-diabetic rats. Our data also reveal that acute BFT treatment significantly decreased myocardial oxidative stress and apoptosis, and provided cardio-protection in response to ischemia and reperfusion under hyperglycemic conditions. In parallel, BFT blunted hyperglycemia-induced activation of four NOGP in the rat heart.

Acute administration of each of the NOGP inhibitors decreased PARP and enhanced GAPDH activities, while diminishing oxidative stress and myocardial apoptosis. Moreover, each of the NOGP inhibitors (individually) employed blunted activation of the other three pathways here examined. Hearts treated with NOGP inhibitors also displayed improved functional recovery and smaller infarct sizes following ischemia and reperfusion. Interestingly, NOGP inhibitors resulted in the same degree of change (for all above-mentioned parameters evaluated) when compared to each other.

## **Conclusions**

This study shows that acute and chronic hyperglycemia trigger myocardial oxidative stress that eventually results in NOGP activation and contractile dysfunction following ischemia and reperfusion. Moreover, our findings establish - for the first time as far as we are aware - that there is a convergence of downstream NOGP effects in our model, i.e. increased myocardial oxidative stress, further NOGP pathway activation, apoptosis, and impaired contractile function. Thus a vicious metabolic cycle is established whereby hyperglycemia-induced NOGP further fuels its own activation by generating even more oxidative stress, thereby exacerbating damaging effects on the heart under these conditions. We also found that both OA and BFT treatment blunted high glucose-induced detrimental effects and provided robust cardio-protection in response to ischemia and reperfusion under hyperglycemic conditions (acute and chronic). These findings suggest that the UPS may be a unique therapeutic target to treat ischemic heart disease in individuals that present with stress-induced, acute hyperglycemia. Moreover, BFT exhibited its cardio-protective effects by NOGP inhibition after ischemia and reperfusion under acute and chronic high glucose conditions. A similar effect was observed at baseline although the underlying mechanisms driving this process still need to be elucidated. In summary, the findings of this thesis are highly promising since it may eventually result in novel, cost-effective therapeutic interventions to treat acute hyperglycemia (in non-diabetic patients) and diabetic patients with associated cardiovascular complications.

## **Uittreksel**

### **Inleiding**

Diabetes skep 'n groot gesondheidsuitdaging. Omrede kardiovaskulêre komplikasies algemeen onder diabetiese pasiënte is, sal dit oorkoepelend die las van hierdie siekte verder laat toeneem. Verder word stresgeïnduseerde hiperglukemie in nie-diabetiese pasiënte met akute miokardiale infarksie geassosieër met 'n hoër binne-hospitaalmortaliteit. Hiperglukemies-geïnduseerde oksidatiewe stres veroorsaak DNA skade, en gevolglike aktivering van poli-ADF-ribose polimerase (PARP), as 'n herstelmechanisme. Nietemin, PARP verminder gliseraldehid-3-fosfaatdehidrogenase (GAPDH) aktiwiteit om sodoende die opstroom glikolitiese metaboliete te herlei na skadelike nie-oksidatiewe glukose weë (NOGW). Byvoorbeeld, hiperglukemie-geïnduseerde stimulasie van vier NOGW, i.e. die poliolweg, heksosamienbiosintetiese weg, (HBW), gevorderde glukasie eindprodukte (GGE), en PKC aktivering, lei tot kardiovaskulêre komplikasies. Die huidige tesis ondersoek die regulering van NOGW in 'n isgemiese-reperfussie onder hiperglukemiese toestande.

Ons hipotetiseer dat die toediening van twee unieke terapeutiese intervensies, i.e. oleanoliese suur (OS, naaltjie ekstrak), en benfotiamien (BFT, vitamien B1 derivaat) oksidatiewe stress kan versag, en NOGW geïnduseerde kardiaal disfunksie onder hiperglukemiese toestande na isemie en reperfussie. Ons keuse vir hierdie middels is gebaseer op die beginsel dat OS anti-oksidanteienskappe bevat, en dat BFT transketolase (pentosefosfaat weg (PFW) ensiem) stimuleer en sodoende die fluks weg van die NOGW weg veroorsaak. Addisioneel kan hiperglukemie-geïnduseerde oksidatiewe stres ook tot wanregulering van die ubikwities-proteosoomsisteem (UPS) wat wangevoude proteïene verwyder, aanleiding gee. Daar bestaan kontrasterende data oor 'n verhoogde/verlaagde UPS, tesame met hiperglukemie en/of in reaksie tot isemie-reperfussie. In die lig hiervan, hipotetiseer ons dat BFT en OS as 'n nuwe kardiobeskeringsmiddel kan optree deur miokardiale oksidatiewe stres en UPS aktiwiteit in reaksie op isemie-reperfussie tydens akute hiperglukemiese toestande kan verlaag.

### **Materiale en Metodes**

Vir die eerste deel van die studie het ons van verskeie eksperimentele sisteme gebruik gemaak: 1) H9c2 kardiaal mioblaste is aan 33 mM glukose vir 48 uur vs. kontrole (5 mM glukose) blootgestel; en gevolglik met twee OS dosisse (20 en 50  $\mu$ M) vir 6 en 24 hr, onderskeidelik behandel; 2) geïsoleerde rotharte is *ex vivo* met Krebs-Henseleit buffer, wat, 33 mM glukose vs. kontrole (11 mM glukose)

bevat, vir 60 min geperfuseer, daarna is dit deur 20 min globale isemie gevolg en 60 min reperfusie ± OS behandeling; 3) Infarkgrootte is bepaal deur Evans bou kleursel en 1% 2,3,5-tripheniel tetrazoliumchloried (TTC) kleuring met 20 minute regionale isemie, en 2 uur reperfusie 4) *In vivo* koronêre liggasies is op streptozotosien-diabetiese rotte uitgevoer ± 0.45 mg/kg OS toediening binne die eerste twee minute van reperfusie; en 5) effekte van langtermyn OS behandeling (2 weke) op hartfunksie is in hierdie streptozotosien-diabetiese rotte ondersoek. Hier is STZ opgelos in 'n sitraatbuffer (pH 6.3), en diabetes is geïnduseer deur 60mg/kg i.p. toe te dien. Weefsels is aan die einde van die globale isemie eksperimente versamel, en vir oksidatiewe stres, apoptose, UPS aktiwiteit en HBW aktivering, ontleed.

Vir die tweede deel van die studie het ons van verskeie eksperimentele sisteme gebruik gemaak: 1) geïsoleerde rotharte is *ex vivo* met Krebs-Henseleit buffer, wat 33 mM glukose vs. kontrole (11 mM glukose) bevat, vir 90 min geperfuseer. Daarna is dit gevolg met 30 min globale isemie en 60 min reperfusie ± 25, 50 en 100 µM BFT behandeling onderskeidelik, gevolg, bykomend, gedurende die eerste 20 min reperfusie; 2) Infarkgrootte is bepaal soos in #3 hierbo, maar met 30 minute regionale isemie en 2 uur reperfusie ± 100 µM BFT behandeling; en 3) *In vivo* koronêre liggasies is op streptozotosien-diabetiese rotte uitgevoer ± 0.50 mg/kg BFT behandeling binne die eerste twee minute van reperfusie. Met parallele eksperimente is NOGW inhibeerders bygevoeg binne die eerste 20 min van reperfusie. Die volgende inhibeerders is individueel ontplooi: GGE weeg (100 µM aminoguanidien); PKC (5 µM chelleritrienchloried); HBW (40 µM 6-diazo-5-oxo-L-nor-leusien); en poliolweg (1 µM zopolrestaat); 2) Infarkgrootte is bepaal soos in #2) met die uitsondering van 30 min regionale isemie en 120 min reperfusie ± identiese behandelings.

## Resultate

Ons data toon aan dat kardiaal kontraktiele funksie, in reaksie op isemie-reperfusie onder hiperglukemiese toestande, verlaag. Dit is verwant aan verhoogde PARP en verminderde GAPDH aktiwiteit, tesame met 'n hoër aktivering van die NOGW. Verder het ons bevind dat verhoogde miokardiale oksidatiewe stres, UPS en seldood onder die toestande voorkom. OS behandeling lei tot kardiaal beskerming, i.e. vir *ex vivo* en *in vivo* rotharte wat aan isemie-reperfusie onder hiperglukemiese toestande blootgestel is. Parallel hiermee het OS oksidatiewe stres, apoptose, HBW invloed, en UPS aktiwiteit na isemie-reperfusie, verlaag. Langtermyn OS behandeling het ook hartfunksie in streptozotosien-diabetiese rotte verbeter. Ons data vertoon verder dat akute BFT behandeling, miokardiale oksidatiewe stres en apoptose, betekenisvol verlaag het in reaksie op

isgemie-reperfussie onder hiperglukemiese toestande. Parallel hiermee het BFT hiperglukemie-geïnduseerde aktivering van vier NOGWë in die rothart, verminder.

Akute toediening van die elk van die NOGW inhibeerders het PARP verlaag, en GAPDH aktiwiteite verhoog, terwyl oksidatiewe stres, en miokardiale apoptose verminder. Verder het elk van die NOGW inhibeerders wat (individueel) toegedien is, aktivering van die ander drie weë, hier ondersoek, verlaag. Die harte wat met NOGW inhibeerders behandel is het ook 'n verbeterde herstel en kleiner infarkgrootte na isgemie-reperfussie getoon. Interessant is hoe die NOGW inhibeerders tot dieselfde graad verandering (vir al die bogemelde parameters wat geevalueer is) indien dit vergelyk word teen mekaar, gelei het.

### **Gevolgtrekking**

Hierdie studie het bevind dat akute en chroniese hiperglukemie, miokardiale oksidatiewe stres ontlok, en dat dit geleidelik tot NOGW aktivering en kontraktiele wanfunksionering na isgemie-reperfussie lei. Verder het ons bevindinge vir die eerste keer, volgens ons wete, bewys dat daar 'n ineenloping is van afstroom NOGW effekte in ons model, i.e. verhoogde miokardiale oksidatiewe stres, verdere NOGW weg aktivering, apoptose, en ingeperkte kontraktiele funksie. Dus, 'n gebrekkige metaboliese siklus word verkry waarby hiperglukemies-geïnduseerde NOGW verder sy eie aktivering aanvuur deur meer oksidatiewe stres, en sodoende die skadelike effekte op die hart onder hierdie toestande verder versleg. Ons het verder bevind dat beide OS en BFT behandeling, hoë glukose-geïnduseerde skadelike effekte onderdruk, en kragtige kardiaal-beskerming in reaksie op isgemie-reperfussie onder hiperglukemiese toestande (akuut en chronies), teweeg bring. Hierdie bevindinge dui moontlik daarop dat die UPS 'n unieke terapeutiese teiken kan wees vir die behandeling van isgemiese hartsiekte in individue wat presenteer met stres-geïnduseerde, akute hiperglukemie. BFT het ook sy kardiaal beskermende effekte getoon deur NOGW inhibering na isgemie-geïnduseerde reperfussie onder akute en chroniese hoë glukose toestande. 'n Soorgelyke effek is tydens die basislyn waargeneem, alhoewel die onderliggende meganisme wat hierdie proses dryf verder ondersoek moet word. Opsommend is ons bevindinge baie belowend omrede dit daartoe kan aanleiding gee tot 'n nuwe, meer koste-effektiewe terapeutiese intervensie vir die behandeling van akute hiperglukemie (in nie-diabetiese pasiënte) en diabetiese pasiënte met geassosieëerde kardiovaskulêre komplikasies.



## ACKNOWLEDGEMENTS

First and foremost I thank **God Almighty** for granting me such an opportunity to reach this level and make it through. I also want to thank the following people whose input made this work achievable:

To my supervisor and mentor, **Professor M. Faadiel Essop** words in this space are not enough to express my gratitude. You have made attaining this PhD possible in every way, allowing growth of myself as a human being in a holistic approach. I hope I have attained some of your qualities as a leader and an intellectual. With your open door policy I have received constant and committed guidance, constructive criticisms and financial support for all the requirements of this research all the way through. I truly appreciate all that I learnt from him;

I am very grateful to **Dr Meiring** and **Dr Kelly-Laubscher** for the training supervision, advice and training during my *ex vivo* and *in vivo* studies in this study;

**Dr Theo Nell** thank you for all the assistance, guidance, mentorship and positive criticisms throughout the course of this study and translating my abstract;

I wish to acknowledge the assistance rendered to me by staff members of the Department of Physiological Sciences, especially **Noel Markgraff**, **Katrina**, **Grazelda** and **Jonnifer** not forgetting the Animal Unit staff at the University of Cape Town, Health Sciences;

I also wish to acknowledge the contribution I received on some of the work from **Dr U Rajamani**, **Dr M Zungu-Edmondson** and her student (**N Dlamini**), **Prof E Bourdon** and his colleague (**Dr P Rondeau**), **Prof MA Fahim** and his students (**M Shafiullah** and **A Wahab**).

I pay my sincere thanks to my family, particularly to my **mother**, for the constant support and a warm heart to accommodate all my doings (right and wrong) and also my daughter, **Makatendeka** for being an inspiration and always there to cheer me up; to my sisters (**Lucy** and **Angie**) and brother **Ian** for all the support, love and care throughout, hope I have been a good role model; to **Munya Mavhunga** thanks for the love and support;

To my colleagues in CMRG and PhD room (**Danzil** and **Charlene**) thank you for your sense of humor, all I learnt from you and being true friends always, same goes for the rest of **CMRG** group, thank you

for being a family closer to me away from home. Last but not least I would like to thank the **Oppenheimer, Beit Trust** and **Harry Crossley** for granting me the funds to pursue my studies.

## DEDICATION

*This is especially dedicated to my family; I love you guys for being there for me at all times. I am glad to grow up as part of you; in all these years as a student you made everything possible. To Makatendeka, my daughter, from the day you came in this world you have brightened all my days. To my mother, you are the backbone of my life and have been a good role model to all of us. Maka, grow wiser, with a God fearing character and personality, loving others more. All things are possible my dear if you believe. Fly high in all that you do and aim to achieve more.....love you all.*

**TABLE OF CONTENTS**

Declaration	ii
Abstract (English)	iii
Uittreksel (Afrikaans)	vi
Acknowledgements	ix
Dedication	xi
Table of contents	xii
List of Tables	xvii
List of Figures	xviii
List of Conference Proceedings	xxii
List of Publications	xxiii
List of Abbreviations	xxiv
Units of Measurements	xxxv

**CHAPTER 1 Cardiac metabolism and function under homeostatic conditions**

1.1	Background	1
1.2	Cardiac energy metabolism	4
1.2.1	Substrate utilization by the heart	4
1.2.2	Mechanisms regulating cardiomyocyte glucose uptake	5
1.2.3	Role of insulin in substrate utilization	6
1.2.4	Fate of glucose after uptake by cardiomyocytes	9
1.2.4.1	Glycolysis	9
1.2.5	Myocardial fatty acid (FA) uptake	12
1.2.5.1	Fate of FAs in cardiomyocytes	13
1.2.6	The tricarboxylic acid (TCA)/ Krebs/ citric acid cycle	16
1.2.7	The role of the mitochondria in oxidative phosphorylation	18
1.2.7.1	The electron transport chain (ETC)/ respiratory chain	19
1.2.8	The creatine kinase system of the heart	21
1.2.9	Inter-relationship between glucose and fatty acid metabolism (Randle cycle)	22
1.2.10	Summary and conclusion	25
1.2.11	References	26

**CHAPTER 2 The effects of hyperglycemia on cardiac metabolism and function with ischemia and reperfusion**

2.1	Introduction	41
-----	--------------	----

2.2	Diabetes mellitus	41
2.3	How does hyperglycemia occur with diabetes?	42
2.4	The link between hyperglycemia and the onset of CVDs	45
2.4.1	Chronic hyperglycemia and CVD	45
2.4.2	Acute (stress-induced) hyperglycemia and CVD	48
2.4.3	Acute post-prandial and fasting hyperglycemia	49
2.5	Mechanisms for adverse cardiovascular effects of hyperglycemia	53
2.5.1	Hyperglycemia-induced oxidative stress	53
2.5.1.1	Sources and types of ROS in diabetes and/or ischemia and reperfusion	54
2.5.2	Mitochondrial antioxidant defense mechanisms	60
2.6	Glucose flux through the non-oxidative pathways	61
2.6.1	Polyol pathway	62
2.6.1.1	Contribution of the polyol pathway to diabetic oxidative stress and complications	63
2.6.2	Advanced glycosylation end products	64
2.6.2.1	Contribution of AGE pathway to diabetic oxidative stress and complications	67
2.6.3	Protein kinase C	70
2.6.3.1	Contribution of PKC activation to diabetic oxidative stress and complications	71
2.6.4	The hexosamine biosynthetic pathway	72
2.6.4.1	Contribution of the HBP to diabetic oxidative stress and complications	73
2.6.5	Pentose phosphate pathway	76
2.6.5.1	Non-oxidative branch of the PPP	76
2.6.5.2	Oxidative branch of the PPP	78
2.6.6	Non-oxidative glucose pathways and cardiac function	80
2.7.	Diabetic complications	82
2.7.1	Micro-vascular complications	82
2.7.1.1	Diabetic neuropathy	82
2.7.1.2	Diabetic retinopathy	83
2.7.1.3	Diabetic nephropathy	85
2.7.2	Macro-vascular complications	87
2.7.2.1	Arterial diseases	87
2.7.2.2	Atherosclerosis	88
2.7.2.3	Diabetic cardiomyopathy	91
2.8	Diabetes mellitus management	92
2.8.1	Insulin	93
2.8.2	Insulin sensitizers	94

2.8.2.1 Biguanides	94
2.8.2.2 Thiazolidinediones	95
2.8.3 Insulin secretagogues	96
2.8.3.1 Sulphonylureas	96
2.8.3.2 Meglitinides	96
2.8.4 $\alpha$ -Glucosidase inhibitors	97
2.8.5 Peptide analogues	97
2.8.6 Glycemic control and outcome	98
2.9 Metabolic changes during ischemia and reperfusion	101
2.9.1 Effects of ischemia on substrate utilization	102
2.9.2 Ionic imbalances during ischemia and reperfusion	105
2.9.3 Myocardial ischemia/reperfusion injury	107
2.9.4 ROS in reperfusion injury	109
2.9.4.1 Interventions to attenuate myocardial ischemia and reperfusion injury	109
2.10 The cardiomyocyte stress response	110
2.10.1 Necrosis	111
2.10.2 Apoptosis	113
2.10.2.1 Extrinsic /external/death receptor pathway	114
2.10.2.2 Intrinsic/ mitochondrial pathway	115
2.10.3 Autophagy	117
2.11 The UPS	118
2.11.1 The role of the UPS in response to ischemia and reperfusion and under hyperglycemic conditions	121
2.12 Conclusion	122
2.13 References	124

### **CHAPTER 3 Oleanolic acid: a novel cardio-protective agent that blunts hyperglycemia-induced contractile dysfunction**

3.1 Introduction	186
3.2 Materials and Methods	188
3.2.1 Isolation of oleanolic acid from clove extract	188
3.2.2 Cell culture and oleanolic acid treatments	189
3.2.3 Measurement of intracellular ROS levels and apoptosis	190
3.2.4 Animals and ethics statement	192
3.2.5 <i>Ex-vivo</i> global ischemia during (simulated acute hyperglycemia)	192

3.2.6	<i>Ex-vivo</i> regional ischemia and reperfusion during simulated acute hyperglycemia	194
3.2.6.1	Determination of infarct size	195
3.2.7	<i>In vivo</i> regional ischemia and reperfusion in streptozotocin-treated rats during chronic hyperglycemia	195
3.2.8	Effects of long-term OA treatment on heart function in streptozotocin-treated rats (chronic hyperglycemia)	197
3.2.9	Western blot analysis	198
3.2.10	Measurement of superoxide dismutase	198
3.2.11	Myocardial superoxide levels	199
3.2.12	Isolation of proteins for carbonylation and proteasome activity experiments	199
3.2.13	ELISA carbonyl protocol	200
3.2.14	Proteasome activity measurements	201
3.2.15	Statistical analysis	201
3.3	Results	202
3.3.1	Isolation of oleanolic acid from clove extract	202
3.3.2	Structural elucidation of OA	202
3.3.3	Effects of OA treatment on ROS levels and apoptosis in heart cells	206
3.3.4	Evaluation of <i>ex vivo</i> heart function during global ischemia and reperfusion (simulated acute hyperglycemia)	212
3.3.5	<i>In vivo</i> coronary artery ligations in streptozotocin-treated rats (chronic hyperglycemia)	218
3.3.6	Effects of long-term OA treatment on heart function in streptozotocin-treated rats (chronic hyperglycemia)	221
3.3.7	Effects of OA treatment on <i>ex vivo</i> myocardial ROS levels and apoptosis	222
3.3.8	Evaluating the effects of OA treatment on myocardial proteasomal activity in hearts subjected to ischemia and reperfusion under high glucose conditions	228
3.4	Discussion	231
3.5	References	237

#### **CHAPTER 4 Acute benfotiamine treatment counteract hyperglycemia-mediated contractile dysfunction following ischemia and reperfusion** **245**

4.1	Introduction	246
4.2	Materials and methods	251
4.2.2	Animals and ethics statement	251
4.2.3	<i>Ex vivo</i> global ischemia and reperfusion during simulated acute hyperglycemia	251

4.2.4	<i>Ex vivo</i> regional ischemia and reperfusion during simulated acute hyperglycemia	254
4.2.5	Determination of infarct size	255
4.2.6	<i>In vivo</i> regional ischemia and reperfusion in streptozotocin-treated rats (chronic hyperglycemia)	255
4.2.7	Myocardial superoxide levels	257
4.2.8	Measurement of superoxide dismutase (SOD) activity	257
4.2.9	Isolation of proteins for carbonylation and proteasome activity experiments	258
4.2.10	ELISA carbonyl protocol	258
4.2.11	Proteasome activity measurements	259
4.2.12	Evaluation of myocardial apoptosis	260
4.2.13	PARP assay	261
4.2.14	GAPDH assay	261
4.2.15	Determination of non-oxidative pathway activation	262
4.2.15.1	AGE	262
4.2.15.2	PKC assay	263
4.2.15.3	Hexosamine biosynthetic pathway (HBP)	264
4.2.15.4	Polyol pathway	264
4.2.15.5	Non-oxidative pentose phosphate pathway (PPP) assay	265
4.2.16	Statistical analysis	266
4.3	Results	267
4.3.1	Acute high glucose exposure impairs contractile heart function following ischemia and reperfusion	267
4.3.2	Acute BFT treatment enhances non and post-ischemic contractile function	270
4.3.3	Acute BFT administration decreases infarct size and attenuates high glucose induced oxidative stress and apoptosis	275
4.3.4	BFT treatment decreased chymotrypsin proteasomal activity	281
4.3.5	BFT blunts high glucose-induced metabolic dysfunction and activation of non-oxidative glucose utilizing pathways	282
4.3.6	Acute inhibition of damaging non-oxidative glucose pathways blunts high glucose-induced contractile dysfunction following ischemia and reperfusion	287
4.3.7	Hyperglycemia-induced oxidative stress and apoptosis is blunted by acute inhibition of flux through the damaging non-oxidative glucose pathways	291
4.3.8	The interlink between the damaging non-oxidative glucose pathways in attenuating hyperglycemia-induced metabolic dysfunction	292
4.4	Discussion	297



4.4.1	Acute hyperglycemia triggers oxidative stress, the coordinated induction of non-oxidative glucose metabolic pathways and impaired contractile function	297
4.4.2	Acute BFT treatment attenuates the detrimental effects of hyperglycemia with ischemia and reperfusion	300
4.4.3	Individual acute inhibition of NOGP attenuates the detrimental effects of hyperglycemia with ischemia and reperfusion	303
4.5	References	308
<b>CHAPTER 5 Final Conclusions, limitations and recommendations</b>		<b>320</b>
5.1.	Conclusions	320
5.2.	Limitations and future recommendations	321
5.3	References	322
<b>APPENDICES</b>		<b>323</b>

## LIST OF TABLES

### CHAPTER 1

Table 1.1: Examples of studies that show the effect of substrate utilization on cardiac function

### CHAPTER 2

Table 2.1: Epidemiological studies showing the link between glycemic control and CVDs

### CHAPTER 3

Table 3.1:  $^{13}\text{C}$  (100.64 MHz) Bruker Avance III NMR spectral data of plant-derived and reported OA

Table 3.2: Effects of OA on *ex vivo* coronary flow and end-diastolic pressure during the first ten min of stabilization and at the end of reperfusion

Table 3.3: Body weight and blood glucose levels after 1 week of STZ injection.

Table 3.4: Effects of OA on *in vivo* heart rate, ST height, systolic and diastolic blood pressures during early reperfusion

### CHAPTER 4

Table 4.1: Coronary flow and end-diastolic pressure under high vs. baseline glucose conditions hearts

Table 4.2: Body weight and blood glucose levels after 1 week of STZ injection.

Table 4.3: Coronary flow, end-diastolic pressure, heart rate and velocity of contraction for hearts under high glucose (33 mM) vs. control (11 mM)  $\pm$  NOGP inhibitors at the end of reperfusion

## LIST OF FIGURES

### CHAPTER 1

- Figure 1.1: The role of insulin on glucose and fatty acid uptake
- Figure 1.2: Cardiomyocyte glucose uptake and metabolism by glycolysis
- Figure 1.3: Fatty acid uptake and regulation of metabolism by the cardiomyocyte under normal conditions
- Figure 1.4: The tricarboxylic acid cycle/ Krebs cycle/ citric acid cycle
- Figure 1.5: Schematic diagram of the mitochondrial electron transport chain
- Figure 1.6: The Randle cycle showing the interrelationship between myocardial fatty acid and glucose metabolism

### CHAPTER 2

- Figure 2.1: Mechanism of FA-induced insulin resistance as proposed by Randle et al
- Figure 2.2: Proposed alternative mechanism of FA-induced insulin resistance
- Figure 2.3: Mechanisms of formation of hyperglycemia-induced ROS
- Figure 2.4: Role of polyol pathway in hyperglycemia-induced oxidative stress
- Figure 2.5: Simplified biochemistry of advanced glycation end product formation
- Figure 2.6: Activation and downstream targets of the hexosamine biosynthetic pathway in diabetes
- Figure 2.7: The non-oxidative reactions of the pentose phosphate pathway
- Figure 2.8: Effect of hyperglycemia on atherosclerosis
- Figure 2.9: ATP balance in the heart mitochondria
- Figure 2.10: Ionic imbalances during myocardial ischemia and reperfusion
- Figure 2.11: Protein ubiquitination process and 26S proteasome structure

### CHAPTER 3

- Figure 3.1: Schematic diagrams showing the perfusion protocol for assessment of effects of OA
- Figure 3.2: *Syzygium aromaticum* (cloves)-derived OA 1D and 2D  $^1\text{H}$  and  $^{13}\text{C}$ - NMR spectra
- Figure 3.3: Structure and numbering of oleanolic acid according to IUPAC.
- Figure 3.4: OA treatment attenuates oxidative stress in H9c2 cells.
- Figure 3.5: Representative images on the effects of OA treatments on *in vitro* ROS levels.
- Figure 3.6: Decreased apoptotic cell death in H9c2 cells treated with OA (caspase activity)
- Figure 3.7: Diminished apoptosis in OA-treated H9c2 cells (flow cytometry).
- Figure 3.8: OA treatment does not affect pre-ischemic cardiac function
- Figure 3.9: OA treatment blunts high glucose-induced cardiac dysfunction following ischemia and reperfusion.

- Figure 3.10: OA treatment blunts high glucose-induced cardiac dysfunction following ischemia and reperfusion.
- Figure 3.11: OA administration decreases infarct size under high glucose perfusion conditions.
- Figure 3.12: OA treatment decreases infarct size following coronary artery ligation in streptozotocin-diabetic rats
- Figure 3.13: Long-term OA treatment improves cardiac function in STZ-diabetic rats
- Figure 3.14: OA treatment does not affect superoxide dismutase and caspase activities without ischemia.
- Figure 3.15: Anti-oxidant effects of OA in hearts subjected to ischemia and reperfusion under high glucose perfusion conditions.
- Figure 3.16: OA treatment decreases carbonylation levels in hearts subjected to ischemia and reperfusion under high glucose conditions
- Figure 3.17: Anti-apoptotic effects of OA in hearts subjected to ischemia and reperfusion under high glucose conditions
- Figure 3.18: OA treatment attenuates O-GlcNAcylation in hearts subjected to ischemia and reperfusion under high glucose conditions
- Figure 3.19: Increased proteasomal activity in hearts under high glucose conditions without ischemia and reperfusion.
- Figure 3.20: Increased proteasomal activity in hearts subjected to ischemia and reperfusion under high glucose conditions
- Figure 3.21: OA attenuates high glucose-induced proteasomal activity following ischemia and reperfusion

#### **CHAPTER 4**

- Figure 4.1: Hyperglycemia activates non-oxidative pathways of glucose metabolism
- Figure 4.2: Schematic diagrams showing protocols for assessment of effects of BFT
- Figure 4.3: Target sites for inhibition of non-oxidative glucose pathways
- Figure 4.4: High glucose-induced cardiac contractile dysfunction
- Figure 4.5: High glucose-induced cardiac contractile dysfunction
- Figure 4.6: Acute BFT treatment increases cardiac contractile function under baseline glucose and non-ischemic conditions
- Figure 4.7: Acute BFT treatment blunts cardiac dysfunction following ischemia and reperfusion at baseline glucose conditions
- Figure 4.8: Acute BFT treatment blunts high glucose-induced cardiac dysfunction following ischemia and reperfusion

- Figure 4.9: Acute BFT treatment blunts high glucose-induced cardiac dysfunction following ischemia and reperfusion
- Figure 4.10: Acute BFT treatment decreases infarct size following ischemia and reperfusion *ex vivo*
- Figure 4.11: Acute BFT treatment decreases infarct size following ischemia and reperfusion *in vivo*
- Figure 4.12: Acute BFT treatment blunts high glucose-induced oxidative stress
- Figure 4.13: Myocardial apoptosis in response to high glucose conditions
- Figure 4.14: Anti-apoptotic effects of BFT in hearts subjected to ischemia and reperfusion under high glucose conditions
- Figure 4.15: BFT attenuates proteasomal activity under baseline glucose conditions following ischemia and reperfusion
- Figure 4.16: BFT attenuates high glucose-induced proteasomal activity following ischemia and reperfusion
- Figure 4.17: BFT treatment attenuates O-GlcNAcylation in hearts subjected to ischemia and reperfusion
- Figure 4.18: Acute BFT administration attenuates high glucose-induced metabolic dysfunction and activation of non-oxidative pathways
- Figure 4.19: Activation of non-oxidative pathways in high glucose perfusions relative to baseline conditions  $\pm$  BFT treatment
- Figure 4.20: High-glucose induced cardiac dysfunction blunted by acute non-oxidative pathway inhibition following ischemia and reperfusion.
- Figure 4.21: Acute inhibition of non-oxidative glucose pathways decreases infarct size
- Figure 4.22: Effects of pathway inhibitors on oxidative stress and myocardial apoptosis
- Figure 4.23: Cardiac metabolic function at baseline glucose conditions with acute non-oxidative pathway inhibition following ischemia and reperfusion
- Figure 4.24: High-glucose induced cardiac metabolic dysfunction blunted by acute non-oxidative pathway inhibition following ischemia and reperfusion
- Figure 4.25: Activation of non-oxidative pathways in high glucose perfusions with pathway inhibitors relative to high glucose conditions without treatment.

## LIST OF CONFERENCE PROCEEDINGS

### International

- **Mapanga RF** and Essop MF. Benfotiamine: A novel cardio-protective agent that blunts hyperglycemia-induced cardiac dysfunction. *Experimental Biology* (April 21-25, 2012), San Diego, CA.

### National

- **Mapanga RF** & M Faadiel Essop. Oleonic Acid: A Novel Cardio-protective Agent that Blunts Hyperglycemia-induced Contractile Dysfunction. 40<sup>th</sup> PSSA Annual conference, University of Stellenbosch (10-13 September 2012). Abstract accepted for oral presentation.
- **Mapanga RF** & M Faadiel Essop. Novel ways to blunt hyperglycemia-induced cardiac dysfunction. Society for Endocrinology, Metabolism and Diabetes of South Africa (8-12 April 2011). Best oral science presentation.
- **Mapanga RF**, Rajamani U, Dlamini IN, Zungu M and Essop MF. Clove extract: able to blunt hyperglycemia-induced contractile dysfunction? 39<sup>th</sup> PSSA Annual conference, University of Western Cape (29<sup>th</sup> -31<sup>st</sup> August 2011). Abstract accepted as a poster presentation.
- **Mapanga RF** and Essop MF. Exploring novel ways to blunt hyperglycemia-induced contractile dysfunction. 39<sup>th</sup> PSSA Annual conference, University of Western Cape (29<sup>th</sup> -31<sup>st</sup> August 2011). Runner-up oral presentation
- Meiring JJ, **Mapanga RF** and Essop MF. Hyperglycemia-induced flux through the hexosamine biosynthetic pathway impairs cardiac contractile function. 38<sup>th</sup> PSSA Annual Conference, Walter Sisulu University (6<sup>th</sup> -8<sup>th</sup> September 2010). Accepted for poster presentation.

## LIST OF PUBLICATIONS

- **Mapanga R**, Rajamani U, Dlamini N, Zungu-Edmondson M, Kelly-Laubscher R, Shafiullah M, Wahab A, Hasan M, Fahim M, Rondeau P, Bourdon E, Essop M. Oleanolic acid: a novel cardio-protective agent that blunts hyperglycemia-induced contractile dysfunction. *PloS one* 7: e47322, 2012. The candidate was involved in conceiving and designing the study, performing the bulk of the experiments, analyzing data and writing the paper.
- **Mapanga RF**, Kelly-Laubscher R, M Faadiel Essop. Acute benfotiamine treatment counteracts hyperglycemia-mediated contractile dysfunction following ischemia and reperfusion. (Manuscript in preparation for submission to *Antioxidant Redox & Signaling*).

## LIST OF ABBREVIATIONS

### **A**

A	absorbance
AAR	area at risk
ACBP	acyl-CoA binding protein
ACC1/2	acetyl-CoA carboxylase 1/2
ACCORD	Action to Control Cardiovascular Risk in Diabetes
ADA	American Diabetes Association
ADP	adenosine diphosphate
ADVANCE	Action in Diabetes and Vascular Disease: Preterax and Diamicron Modified Release Controlled Evaluation
AGE(s)	Advanced glycation end-product(s)
AIF	apoptosis inducing factor
AKR	aldo-keto reductase
ALEs	advanced lipoxidation end products
AMG	aminoguanidine
AMI	acute myocardial infarction
AMP	adenosine monophosphate
AMPK	adenosine monophosphate protein kinase
ANOVA	one way analysis of variance
AP-1	activator protein-1
Apaf-1	adaptor protein apoptotic protease activating factor-1
AR	aldose reductase
ARE	antioxidant response elements
ATP	adenosine triphosphate

### **B**

Bad	Bcl-2 associated death promoter
Bak	Bcl-2 homologous antagonist /killer
Bax	Bcl-2-associated X protein
BCA	bicinchoninic acid assay
Bcl-2	B cell leukemia/lymphoma-2
Bcl-x <sub>L</sub>	B cell leukemia/lymphoma-x-isoform
BFT	benfotiamine



BH3	Bcl-2 homology domain 3
BH <sub>4</sub>	tetrahydro biopterin
Bid	BH3-only interacting protein domain
Bim	Bcl-2 like protein 11
Bok	Bcl-2 related ovarian killer
BSA	bovine serum albumin

## **C**

CA	California state
Ca <sup>2+</sup>	calcium
CACT	carnitine/acylcarnitine transferase
cAMP	cyclic adenosine monophosphate
CD36	cluster of differentiation 36
CHE	chelerythrine chloride
CHS	Cardiovascular Health Study
CML	carboxy-methyl lysine
CO <sub>3</sub> <sup>•-</sup>	carbonate radical
CPT-I/II	carnitine palmitoyl transferase I/II
CuSOD	copper superoxide dismutase
CVD	cardiovascular

## **D**

DAG	diacylglycerol
DCCT	Diabetes Control and Complications Trial
DCFDA	2',7'-dichlorodihydrofluorescein diacetate
DECODE	Diabetes Epidemiology Collaborative Analysis of Diagnostic Criteria in Europe
DHAP	dihydroxy acetone phosphate
DIS	Diabetes Intervention Study
DISC	death-inducing signaling complex
DMEM	Dulbecco's modified Eagle's medium
DMSO	dimethyl sulphoxide
DNA	deoxy-ribonucleic acid
DNPH	dinitrophenylhydrazine
DON	6-diazo-5-oxo-L-norleucine
dP/dtmax	maximal velocity of contraction

**E**

E1	ubiquitin-activating enzymes
E2	ubiquitin-conjugating enzymes
E3	ubiquitin–protein ligases
EAS	ethyl acetate solubles
ECG	electrocardiogram
EDC	Epidemiology of Diabetes Complications
EDIC	Epidemiology of Diabetes Interventions and Complications
EDP	end-diastolic pressure
EHDF	endothelium-derived hyperpolarizing factor
eNOS	endothelium nitric oxide synthase
EPIC	European Prospective Investigation of Cancer and Nutrition
ER	endoplasmic reticulum
ERK	extracellular regulated kinase
ESRD	end-stage renal disease
ET-1	endothelin-1
ETF	electron transfer flavoprotein
ETRA	endothelin receptor A

**F**

F2,6 BP	fructose 2,6 biphosphate
FA(s)	fatty acid(s)
FABPpm	fatty acid binding protein (plasma membrane)
FAD	flavin adenine dinucleotide
FADD	Fas-associated death domain protein
FADH2	reduced flavin adenine dinucleotide
FAO	fatty acid oxidation
FAT	fatty acyl translocase
FATP1/6	fatty acid transporter 1/6

**G**

G 3-P	glyceraldehyde 3-phosphate
GADPH	glyceraldehyde-3-phosphate dehydrogenase
GBM	glomerular basement membrane
GDH	glycerophosphate dehydrogenase

GDP	guanosine diphosphate
GFAT	glutamine:fructose-6-phosphate amidotransferase
GFR	glomerular filtration rate
GIK	glucose insulin potassium
GLP	glucagon like peptide
GLUT-1	Glucose transporter-1
GLUT-2	Glucose transporter-2
GLUT-3	Glucose transporter-3
GPAT	glycerol-3-phosphate acyltransferase
G6PD	glyceraldehyde phosphate dehydrogenase
GSH	glutathione
GSK	glycogen synthase kinase
GSSG	glutathione disulfide
GTP	guanosine triphosphate

## **H**

HbA <sub>1c</sub>	glycosylated hemoglobin
HBP	Hexosamine biosynthetic pathway
HCl	hydrochloric acid
HDL	high density lipoprotein
HF	heart failure
H-FABPc	cytoplasmic heart-type fatty acid binding protein
HK	hexokinase
HMQC	Heteronuclear multiple quantum coherence
HR	heart rate
HRP	horse radish peroxidase

## **I**

i.p	intraperitoneal
IA	infarct area
IAP	inhibitor of apoptosis
ICAM-1	intracellular cell adhesion molecule-1
IFM	interfibrillar mitochondria
IFN- $\gamma$	interferon gamma
IGT	impaired glucose tolerance

IMS	mitochondrial inter-membrane space
IR	insulin receptor
IRS 1/2	insulin receptor substrate 1/2
<b><u>J</u></b>	
JAK	janus kinase
JNK	c-Jun NH <sub>2</sub> terminal kinase
<b><u>K</u></b>	
K <sup>+</sup>	potassium
KATP	Adenosine-5'- triphosphate sensitive potassium channels
<b><u>L</u></b>	
LCFAs	long chain fatty acids
LDA	lipid peroxidation-derived aldehydes
LDL	low density lipoprotein
LLE-NA	N-Cbz-Leu-Leu-Glu-b-naphthylamide
LLVY-MCA	Suc-Leu-Leu-Val-Tyr-7-amido-4-methylcoumarin
LPL	lipoprotein lipase
LSTR-MCA	N-t-Boc-Leu-Ser-Thr-Arg-7-amido-4-methylcoumarin
LTD	limited
LVDP	left ventricular developed pressure
<b><u>M</u></b>	
M	molar
MA	Massachusetts state
MAP	mean arterial pressure
MAPK	mitogen activated protein kinase
MCD	malonyl-CoA decarboxylase
MCT-1	monocarboxylic acid transporter-1
MD	Maryland state
MG	methyglyoxal
MnSOD	manganese superoxide dismutase
MnTBAP	manganese (III) tetrakis (4-Benzoic acid) porphyrin chloride
MO	Missouri state

mPTP	mitochondrial permeability transition pore
mTOR	mammalian target of rapamycin
NaCl	sodium chloride
<b><u>N</u></b>	
NAD <sup>+</sup>	oxidized nicotinamide dinucleotide
NADH	nicotinamide adenine dinucleotide hydrogen
NADPH	nicotinamide adenine dinucleotide phosphate hydrogen
NEI	National Eye Institute
NF- $\kappa\beta$	Nuclear factor-kappa beta
NHANES II/III	Second/Third National Health and Nutrition Examination Survey
NMR	Nuclear Magnetic Resonance
NO	nitric oxide
NO <sub>2</sub> <sup>•-</sup>	nitrogen dioxide
NOGP	non-oxidative glucose pathways
Nox	NADPH oxidase
NPDR	non-proliferative diabetic retinopathy
Nrf2	nuclear factor erythroid 2 p45-related factor 2
NSW	New South Wales
3-NT	3-nitrotyrosine
NY	New York state

**O**

O <sub>2</sub> <sup>•-</sup>	superoxide radical
OA	oleanolic acid
OGTT	oral glucose tolerance test
OH <sup>•-</sup>	hydroxyl radical
OMM	outer mitochondrial membrane
ONCOO <sup>•-</sup>	nitrosoperoxy carbonate
ORIGIN	Outcome Reduction with an Initial Glargine Intervention
ox-LDL	Oxidized low density lipoprotein

**P**

PA	phosphatidic acid
PAGE	polyacrylamide gel electrophoresis

PAI-1	Plasminogen activator inhibitor-1
PARP	poly(ADP)ribose polymerase
PBS	phosphate-buffered saline
PCO	protein carbonyl content
PDH	pyruvate dehydrogenase
PDK4	pyruvate dehydrogenase kinase 4
PFK 1/2	phosphofructokinase ½
6PGD	6-phosphogluconate dehydrogenase
PI	phosphatidylinositol
PI	propidium iodide
PI 3-K	Phosphatidyl inositol-3-kinase
PKA	protein kinase A
PKB	protein kinase B
PKC	protein kinase C
PKC-θ	protein kinase C-theta
PKC-α	protein kinase C-alpha
PKC-β	protein kinase C-beta
PKC-γ	protein kinase C-gamma
PKC-δ	protein kinase C-delta
PKC-ε	protein kinase C-epsilon
PKC-ξ	protein kinase-xi
PLC	phospholipase C
PMNs	polymorphonuclear leukocytes
PPAR-α	peroxisome proliferator alpha
PPAR-γ	peroxisome proliferator gamma
PRKAG2	gene encoding for 5'-AMP-activated protein kinase subunit gamma-2
ProACTIVE	PROspective pioglitAzone Clinical Trial In macroVascular Events

**R**

R 5-P	ribose 5-phosphate
RAGE	Receptor for advanced glycation end product
RAS	renin angiotensin system
RECORD	Rosiglitazone evaluated for cardiovascular outcomes in oral agent combination therapy for type 2 diabetes
RFC	reduced folate carrier-1

RIAD	Risk factors in Impaired Glucose Tolerance for Atherosclerosis and Diabetes
RIPA	radio-immunoprecipitation assay buffer
RLU	relative luminescence units
RNS	reactive nitrogen species
ROI	reactive oxygen intermediates
ROS	reactive oxygen species
RPP	rate pressure product
<b><u>S</u></b>	
SDH	sorbitol dehydrogenase
SDS	sodium dodecyl sulfate
SEM	standard error of means
SERCA	sarco(endo)plasmic reticulum Ca <sup>2+</sup> -ATPase
SGLT	Sodium glucose transporter
SGLT-1	Sodium glucose transporter-1
SGLT-2	Sodium glucose transporter-2
SH2	Src homology 2
SLC	solute carrier family
Smac/DIABLO	second mitochondria-derived activator of caspase/direct IAP-binding protein with low PI
SQR	succinate: ubiquinone oxidoreductase
SSM	subsarcolemmal mitochondria
STAT	signal transducers and activators of transcription
STZ	Streptozotocin
SU	Sulphonylurea
SUR-1	Sulphonylurea receptor-1
SUR-2	Sulphonylurea receptor-2
<b><u>I</u></b>	
T1DM	type 1 diabetes mellitus
T2DM	type 2 diabetes mellitus
TAG	triacylglycerides
TBARS	thiobarbituric acid reactive substances
TCA	tricarboxylic acid
TDP	thiamine diphosphate

TGF- $\beta$	transforming growth factor beta
TK	transketolase
TKTL 1/2	transketolase like 1/2
TLC	thin layer chromatography
TMB	3,3',5,5' Tetramethylbenzidine
TNF- $\alpha$	Tumour necrosis factor alpha
TPI	triphosphate isomerase
TPP	triphenylphosphonium
TPP	thiamine pyrophosphate
TTC	2,3,5-triphenyl tetrazolium chloride
tBID	truncated BID
TZD	Thiazolidinediones

## U

Ub	ubiquitin
ucNOS	uncoupling nitric oxide synthase
UDP	uridine diphosphate
UDP-GlcNac	uridine diphosphate acetylglucosamine
UK	United Kingdom
UKPDS	United Kingdom Prospective Diabetes Study
UPS	ubiquitin proteasome system
USA	United States of America

## V

VADT	Veterans Affairs diabetes trial
VCAM-1	Vascular cell adhesion molecule-1
VEGF	Vascular endothelial growth factor
VLDL	very low density lipoprotein
VT	Vermont state

## W

WHO	World Health Organisation
WST-1	water-soluble tetrazolium salt



**X**

X 5-P xylulose 5-phosphate  
XIAP X-linked inhibitor of apoptosis protein

**Z**

ZnSOD zinc superoxide dismutase  
ZOPO zopolrestat

## UNITS OF MEASUREMENT

%	percent/percentage
AU	arbitrary units
cm	centimeter
°C	degrees Celsius
g	gram
hr/s	hour/s
kDa	kilodalton
Hz	Hertz
l/L	litre
IU	international units
M	molar
mg	milligram
mg/kg	milligram per kilogram
min	minutes
ml	millilitres
mHz	milliHertz
ml/min	millilitre per minute
mm	millimetre
mM	millimolar
mmol/l	millimoles per liters
mm/Hg	millimetres of mercury
ng/μl	nanograms per microliter
nm	nanometre
nM	nanomolar
pmol	picomole
RLU	relative light units
ppm	parts per million
sec	seconds
V	volt
μg	microgram
μg/ml	microgram per millilitre
μmol/L	micromoles per litre
μl	microlitre
μm	micrometre

$\mu\text{M}$	micromolar
v/v	volume per volume
w/v	weight per volume

## CHAPTER 1

### Cardiac metabolism and function under homeostatic state

#### 1.1 Background

Diabetes mellitus poses a huge health burden that may have devastating effects if there are no approximate measures taken immediately (129). Currently, diabetes affects ~171 million people worldwide, and this number is predicted to increase to 366 million by the year 2030, thus making it an epidemic (2, 189). Moreover, diabetes is associated with long-term cardiovascular complications, particularly atherosclerosis, thus further contributing to the overall burden of disease (2, 68, 85). Diabetes is defined as a complex chronic metabolic disorder arising from absolute or relative insulin deficiency or due to insulin resistance (2, 175). This condition can be classified into four main categories: type 1, type 2, gestational diabetes, and secondary to other underlying disease or cause (123).

Type 1 diabetes occurs due to autoimmune destructive lesions of pancreatic  $\beta$ -cells leading to an absolute lack of insulin secretion. However, for type 2 diabetes mellitus (T2DM) (~ 90-95% of all diabetics) there is a combination of impaired insulin secretion and sensitivity (175, 189). T2DM also constitutes one of the phenotypes for the metabolic syndrome i.e. together with obesity, insulin resistance, dyslipidemia and high blood pressure (21). The increased prevalence of T2DM is alarming and poor lifestyle choices mean that it is now manifesting at a much younger age than before. Alarmingly ~ 20% newly diagnosed T2DM cases are from children and adolescents (145). Gestational diabetes is defined as the first onset of diabetes mellitus in women during pregnancy precipitated by an excess production of glucocorticoids (2). The fourth type of diabetes is presence of hyperglycemia

in the existence of pancreatic or hormonal disease or secondary to drug or chemical exposure and in certain genetic syndromes (123).

Hyperglycemia is a common symptom for all types of diabetes and is the main risk factor predisposing to the development of microvascular (mostly in type 1 diabetic patients), and macrovascular (mostly in type 2 diabetic patients) complications (43, 179). Indeed, diabetic patients have a greater risk for fatal myocardial infarction than non-diabetic individuals with an impaired recovery of the myocardium from ischemic events (38, 90, 166). Moreover, stress-induced, acute hyperglycemia in non-diabetic patients with acute myocardial infarction is associated with increased in-hospital deaths (126, 189). In light of this, the current study focused on the role of acute and chronic hyperglycemia and its link to a well-known macro-vascular complication, i.e. myocardial infarction.

It is proposed that diabetic complications occur as a result of hyperglycemia-induced oxidative stress that increases flux through non-oxidative pathways of glucose metabolism (18, 19). These pathways are the main focus of this thesis, and include the hexosamine biosynthetic pathway (HBP), the polyol pathway, activation of protein kinase C (PKC), and formation of advanced glycation end products (AGEs). This is our focus since previous studies suggest that increased flux through the non-oxidative pathways can lead to altered protein function, thereby exacerbating oxidative stress and leading to pathologic cardio-metabolic sequelae (18, 93). Thus, the goal for the management of diabetes mellitus should be to achieve near normal or improved glycemic control thereby diminishing the risk of long-term pathophysiologic complications (39, 99, 142, 197). There are many standard anti-diabetic drugs used in the management of diabetes mellitus, including various insulin formulations and oral anti-diabetic agents. These can be used as monotherapy, or in combination, in order to achieve improved glycemic regulation (83, 142).

Evidence from epidemiological and clinical trials on glycemic control indicate that management of blood glucose (moderately or intensively) still predisposes diabetic patients to development of both micro- and macrovascular complications. This implies that the burden of diabetes still requires much attention, and necessitates a comprehensive understanding of the underlying molecular mechanisms since it will enable the development of effective, novel therapies that aim to reduced development of the diabetic associated complications. Therefore, this thesis was designed to investigate the role of novel therapeutic interventions to help improve cardiac function following ischemia and reperfusion under hyperglycemic conditions. These include a) S-benzoyl-thiamine monophosphate or benfotiamine (BFT), and b) oleanolic acid ( $3\beta$ -hydroxy-olea-12-en-28-oic acid [OA]). BFT is a lipid soluble vitamin B1 analog that activates the enzyme transketolase (pentose phosphate pathway), thereby shunting glucose away from the four non-oxidative pathways mentioned earlier. Our approach was to identify feasible cardio-protective agents that will allow for easy translation into the clinic, especially within the developing world context. BFT was investigated as previous studies reported beneficial effects in preventing/reducing complications that occur with diabetes mellitus. Moreover, OA is a triterpenoid found in many medicinal plants, food spices, and vegetables and is also implicated in cardio-protection (104). OA possesses various beneficial medicinal effects, we were particularly focusing on its ability to decrease oxidative stress (antioxidant) for example, it has been reported to quench superoxide (1, 158). However, the efficacy of these compounds has not been investigated in the hyperglycemic context associated with myocardial ischemia.

Chronic hyperglycemia that occurs with diabetes is mainly due to derangements in carbohydrate, lipid and protein metabolism (137, 189). Such metabolic perturbations may impair cardiac function with ischemia and reperfusion by triggering a range of biochemical and electrophysiological changes (174). In diabetes there is shift in substrate utilization in the heart with fatty acids prominent. This leads to increased fatty acid oxidation (FAO), transport and metabolism. This shift consequently results in both diastolic and systolic cardiac function (3). The first chapter of this dissertation will review cardiac

energy metabolism of the normal adult mammalian heart and aims to set a platform for better understanding the biochemical and molecular mechanisms involved in cardiac pathophysiology under hyperglycemic conditions (to be reviewed in detail in Chapter 2). Cardiac energy metabolism is complex, and to simplify matters this chapter will focus on its three basic components, i.e. substrate utilization; oxidative phosphorylation, and the creatine kinase system. These are discussed in the sections below.

## **1.2 Cardiac energy metabolism**

### **1.2.1 Substrate utilization by the heart**

The heart is an omnivorous organ that can rapidly switch its substrate selection to accommodate different physiologic and pathophysiologic conditions. Substrate utilization depends on the concentration of extracellular hormones, substrate availability, rate of oxidative phosphorylation, and energy demand (4, 63, 94, 124, 168, 173). Fatty acids (predominantly long-chain) provide the main source of energy for the normal adult mammalian heart, accounting for ~60-80% of its energetic requirements. The remainder is provided by the oxidation of lactate and carbohydrates (primarily glucose) in equal proportions by glycolysis and the tri-carboxylic acid cycle as guanine triphosphate (GTP) (63, 86). However, the first step for effective substrate utilization involves its uptake by cardiomyocytes. Thus, in the following sections the mechanisms regulating transport, uptake and metabolism of glucose and free fatty acids are described in more detail.

### 1.2.2 Mechanisms regulating cardiomyocyte glucose uptake

Under normal physiological conditions, glucose is one of the major carbohydrates utilized by the heart. Sources of glucose supply include both exogenous (dietary intake) and endogenous sources (glycogenolysis or gluconeogenesis). The metabolism of glucose is regulated through multiple steps that include uptake, glycolysis and pyruvate decarboxylation (3). Extracellular glucose uptake by cardiac myocytes is regulated by the transmembrane glucose concentration gradient, and also the amount, subcellular distribution and activity of glucose transporters (108, 121, 195). For the mammalian heart three facilitative glucose transport proteins (GLUTs) have thus far been identified, i.e. GLUT1, GLUT3 (159) and GLUT4. These transporters are members of a family of 50 kDa integral proteins that contain 12 membrane-spanning domains and six extracellular loops (121).

There are no studies on the role of GLUT3 in the heart in the literature. However, most of myocardial glucose uptake is carried out by GLUT1 and GLUT4. GLUT1 is largely found in the plasma membrane and accounts for glucose uptake under basal conditions (17, 120). GLUT4 is the most abundant transporter in the adult heart and is mainly located in intracellular storage vesicles under basal conditions (~90%) compared to the cell membrane (~3-10%) (77). GLUT4 is the classic insulin-stimulated glucose transporter that ensures increased trafficking from intracellular locations to the cell membrane (8, 53, 108, 118, 187). More recently, sodium-dependent glucose co-transporters I and II (SGLTI and II) were identified in the heart (5, 198), but their precise functional roles in the heart requires further elucidation. However, early studies showed the importance of SGLTI in a glycogen storage cardiomyopathy in transgenic mice (TG<sup>400N</sup>) due to mutations in the PRKAG2 gene that encodes the  $\gamma$ -2 subunit of 5' AMP-activated protein kinase (AMPK). These mice have been shown to exhibit inappropriate activation of AMPK with consequent increased glucose uptake, glycogen synthesis and storage as a result of increased SGLTI mRNA levels and protein expression (5).



Since intracellular glucose levels are usually very low (117), high extracellular glucose concentrations drive glucose transport and *vice versa* e.g. occurring during hypoglycemia or ischemia (95). GLUT transporters have distinct structural components and immune-adsorption studies show that they reside in different subcellular pools, and travel to the membrane independently (53, 169). Increased availability of transporters on the cell membrane involves four processes namely; signaling, translocation, docking and fusion (84, 87). The primary mechanism involved in the acute activation of GLUT transporters from the intracellular pool to the cell membrane is known as translocation (150). This primarily involves outward movement of transporters to the cell membrane, and to some extent it may also be a reflection of the decreased degree of recycling of glucose transporters by endocytosis (150). Insulin increases the incorporation of GLUT1 and GLUT4 into the cell membrane although GLUT4 is the main insulin-dependent isoform in the heart (mechanism is explained in more detail below). Although the cell membrane is the primary site for glucose transporter translocation, glucose transporters can also translocate to the T-tubules (162). In addition to insulin several other stimuli also lead to the translocation of myocardial glucose transporters and these include, ischemia (refer to Chapter 2), exercise and catecholamines.

### **1.2.3 Role of insulin in substrate utilization**

Insulin is a potent anabolic hormone that promotes synthesis and storage of carbohydrates, lipids and proteins, thereby inhibiting their degradation and release into circulation (96). This hormone activates two major signaling events, the mitogen activated protein kinase (MAPK) and phosphoinositide-3-kinase (PI 3-K)-dependent pathway (34, 96, 183). The MAPK pathway plays a prominent role in transcriptional and mitogenic processes such as alterations in growth and regulation of gene expression, while the PI 3-K pathway is crucial in metabolic signaling, i.e. glucose and fatty acid transport (Figure 1.1). Indeed, PI 3-K inhibitors (class Ia) or transfections with dominant negative PI 3-K constructs inhibit the effects of insulin on glucose transport, glycogen and lipid synthesis (160).

The proximal part of the insulin signal transduction pathway is common to all its metabolic effects. The insulin receptor is a tetrameric enzyme comprising of two extracellular  $\alpha$ -subunits and two transmembrane  $\beta$ -subunits. The sequence begins by insulin binding to the extracellular part of the alpha subunits on the insulin receptor. This in turn causes a conformational change in the receptor that induces activation of the intrinsic tyrosine kinase activity on the  $\beta$ -subunits of the receptor. The activated kinase domain leads to an auto-phosphorylation where one  $\beta$ -subunit phosphorylates the other on several tyrosine residues of the receptor as well as in the interacting protein; insulin receptor-substrate 1 (IRS1) (10, 36, 73). Once activated IRS1 then bind with Src homology two proteins (SH2-phosphotyrosine binding sites), including PI 3-K, Ras GTPase-activating protein, phospholipase C and others (122, 148). PI 3-K catalyzes the formation of phospho-inositol triphosphate which activates protein kinase B (PKB) (see Figure 1.1). PKB phosphorylates glycogen synthase kinase  $3\beta$  (GSK  $3\beta$ ) thereby inactivating it; hence resulting in increased glycogen stores (50, 167, 169). In addition PKB also facilitates vesicle fusion, resulting in an increase in glucose and fatty acid transporters (Figure 1.1) (113).

After the signal has been produced its termination occurs mainly by endocytosis and degradation. Signaling can also be terminated by de-phosphorylation of the receptor and IRS tyrosine residues by tyrosine phosphatases (PTPases). Most attention thus far has focused on protein tyrosine phosphatase 1B (PTP 1B) also known as tyrosine-protein phosphatase non-receptor type 1 (PTPN1), e.g. transgenic mice lacking PTP 1B showed greater insulin sensitivity with increased tyrosine phosphorylation of both the receptor and IRS1 (50). The activity of the insulin receptor may be attenuated by serine/threonine kinases that may decrease insulin-stimulated tyrosine phosphorylation and promote interaction with 14-3-3 proteins (36, 73). Such inhibitory phosphorylation provides negative feedback to insulin signaling and serve as a cross-talk mechanism with other pathways that may lead to insulin resistance. Several kinases have been implicated in this process, including PI 3-K, Akt/PKB, glycogen synthase kinase (GSK)- $3\beta$  and mammalian target of rapamycin (mTOR) (148).

As discussed before, with insulin stimulation there is elevated myocardial uptake of both LCFAs and glucose due to increased translocation of FAT/CD36 transporters (49, 59, 101, 165) and GLUT1/4 (8, 49, 117, 150, 169, 182, 186), respectively (see Figure 1.1 below). More recent data show that insulin can also increase myocardial glucose uptake by SGLT1 acting via the PI 3-K pathway (103). Furthermore, studies in isolated rat hearts found that insulin causes the release of hexokinase from the outer mitochondrial membrane of the mitochondria, thereby increasing glucose uptake and phosphorylation (174). Insulin-mediated glucose phosphorylation is the rate-limiting step for insulin-stimulated glucose utilization.

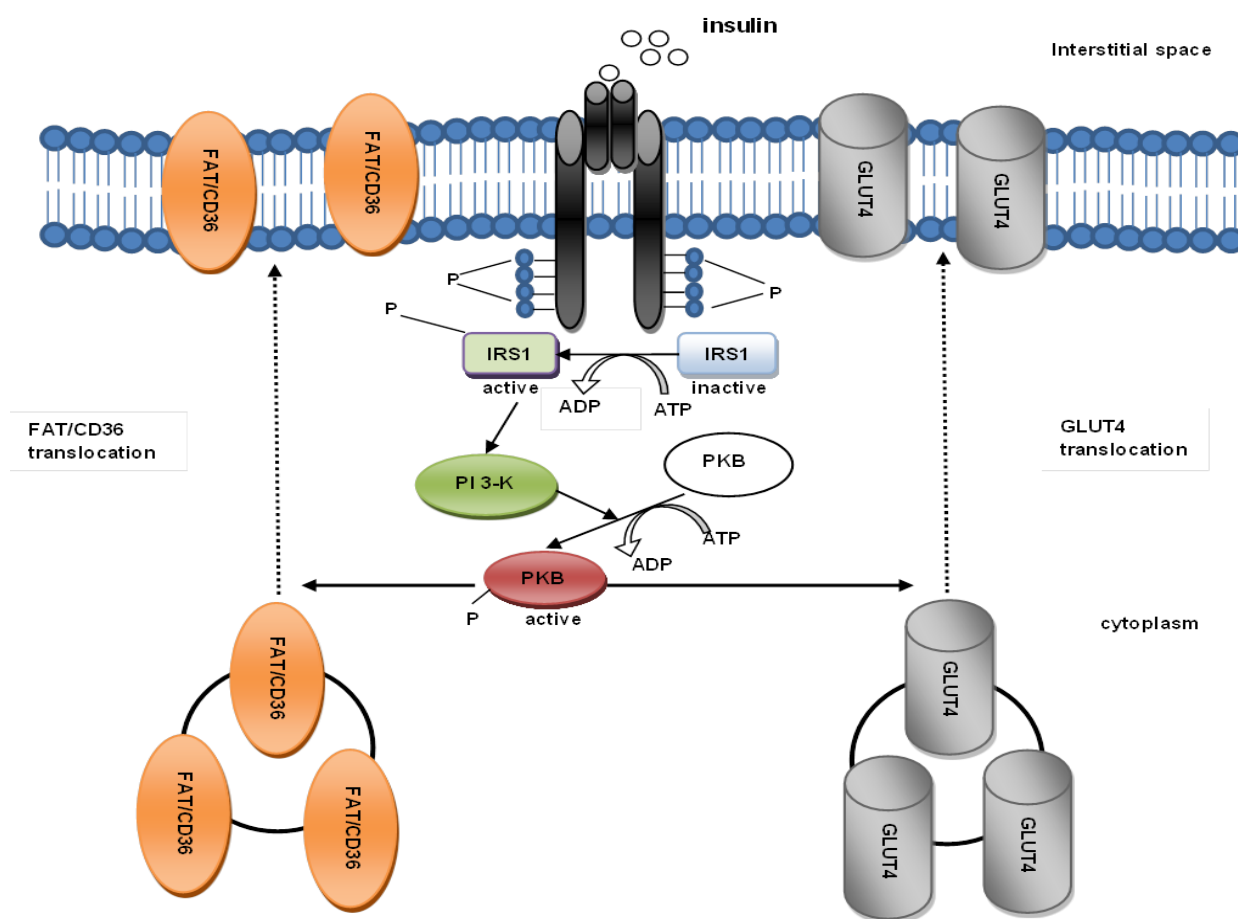
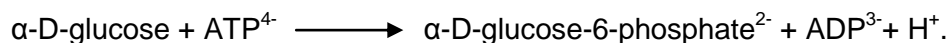


**Figure 1.1. The role of insulin on glucose and fatty acid uptake.** FAT/CD36 (fatty acid translocase), GLUT4 (glucose transporter 4), IRS1 (insulin receptor substrate 1), PI 3-K (phosphoinositide 3-kinase), PKB (protein kinase B/Akt), ADP (adenosine diphosphate), ATP (adenosine triphosphate, P (phosphate residue)).

## 1.2.4 Fate of glucose after uptake by cardiomyocytes

### 1.2.4.1 Glycolysis

Upon entering the cardiac myocytes glucose is rapidly phosphorylated by hexokinase II (in adult hearts) into glucose-6-phosphate in the presence of magnesium ions. Thus, it is trapped in the cell since the membrane is impermeable to phosphate esters (14):



The  $\text{Mg}^{2+}$  is complexed with  $\text{ATP}^{4-}$  and is present as  $\text{MgATP}^{2-}$ . Several steps are involved in controlling the glycolytic rate in the heart, including glucose transport, phosphorylation, and the reaction catalyzed by phosphofructokinase-1 (PFK-1) (140). PFK-1 catalyzes the generation of fructose 1,6-bisphosphate from fructose-6-phosphate (42, 140), and is a multi-modulated enzyme inhibited by low pH, high intracellular citrate or ATP (Figure 1.2). Conversely it is activated by ADP, AMP, phosphate and fructose 2,6-bisphosphate (F2,6-BP) (41, 140) (refer to Figure 1.2). F2,6-BP is formed from fructose-6-phosphate by phosphofructokinase-2 (PFK-2) (75). The production of F2,6-BP itself is highly regulated; here PFK-2 activity can be increased by phosphorylation mediated by hormones such as insulin, glucagon (166), epinephrine and thyroid hormone (75), or kinases e.g. 5' adenosine monophosphate-activated protein kinase (AMPK) and increased levels of citrate (Figure 1.2). Additionally activation of protein kinase C (PKC), protein kinase A (PKA) and PI 3-K can increase PFK-2 activity (3, 40, 111) (Figure 1.2). Stimulation of PFK-2 through these mechanisms increases F2,6-BP generation, activates PFK-1, and subsequently promotes glycolysis. The second rate-limiting enzyme of glycolysis is glyceraldehyde-3-phosphate dehydrogenase (GAPDH) which catalyzes the conversion of glyceraldehyde 3-phosphate to 1,3-diphosphoglycerate, with production of NADH (see Figure 1.2). Since the factors regulating GAPDH activity become prominent during ischemia, this will be discussed within the context of ischemia and reperfusion (114).

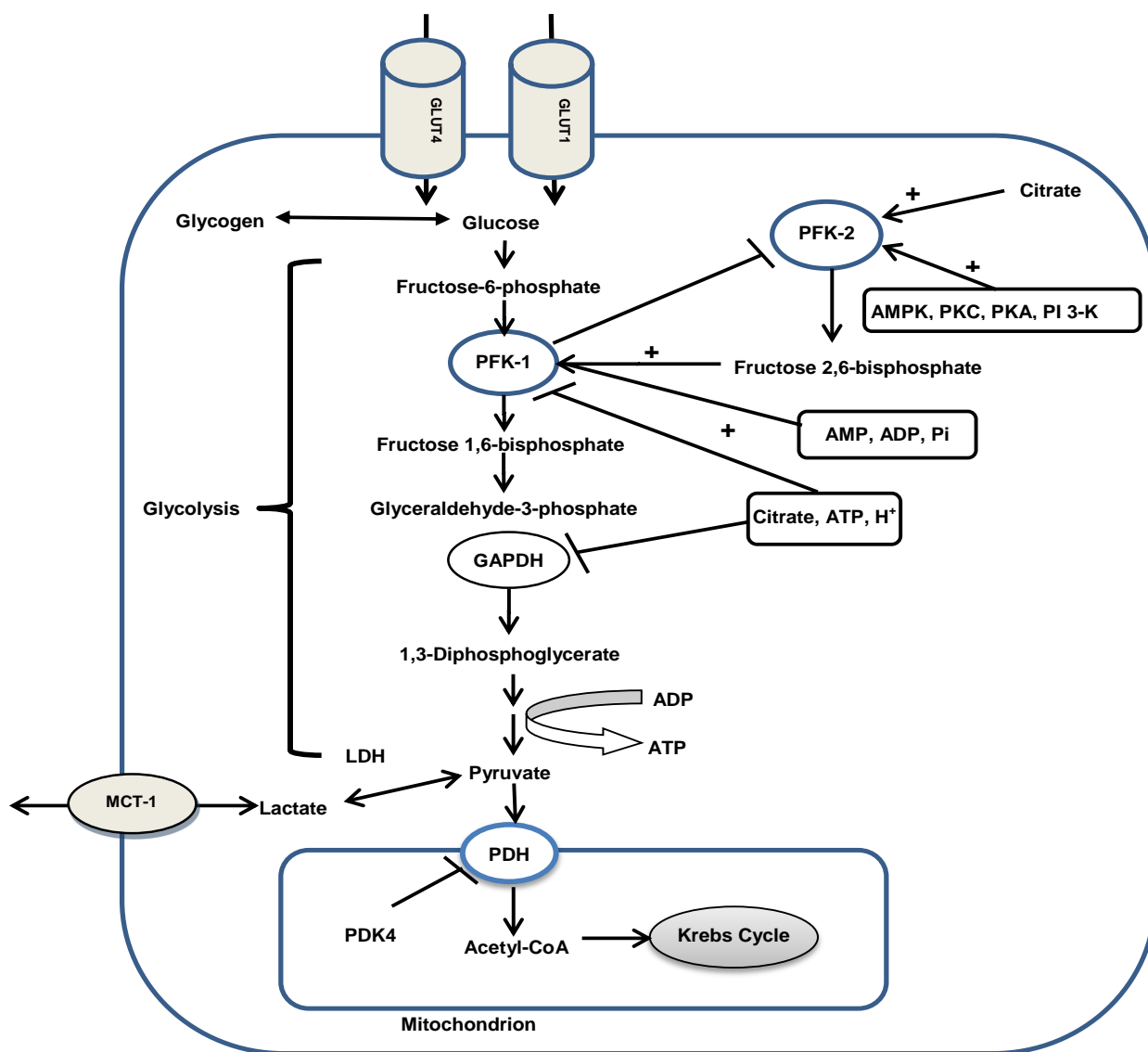


**Figure 1.2: Cardiomyocyte glucose uptake and metabolism by glycolysis.** Key regulatory enzymes; PFK-1 and GAPDH with their respective modulators are shown. PFK-1 or 2 (phosphofructokinase 1/2); GAPDH (glyceraldehyde-3-phosphate dehydrogenase); AMP (adenosine monophosphate); AMPK (AMP-activated kinase); MCT (monocarboxylic translocase); PDH (pyruvate dehydrogenase); ADP (adenosine diphosphate); ATP (adenosine triphosphate); LDH (lactate dehydrogenase); PDK4 (pyruvate dehydrogenase kinase 4).

During conditions when oxygen is not limiting, glycolysis contributes ~10% of total myocardial ATP, i.e. two ATPs generated per glucose molecule (127). Glycolytic ATP is thought to play a critical role in the maintenance of ion pump function due to the proximity of glycolytic enzymes and the ATPases (67, 127). In support, studies in isolated heart tissues found that glycolytically-derived ATP can be employed for calcium re-uptake by the sarcoplasmic reticulum, and also for optimal diastolic relaxation

(67, 80, 102, 156, 184). Additionally key glycolytic enzymes are associated with the cardiac ATP-sensitive  $K^+$  channels that are inhibited by glycolytic ATP (185). Glycolysis is also important for optimal function of the  $Na^+/K^+$  ATPase and prevention of  $Na^+$  accumulation during ischemia (185).

The end products of glycolysis; reduced nicotinamide adenine dinucleotide (NADH) and pyruvate, can thereafter be shuttled into the mitochondrial matrix to eventually generate carbon dioxide and oxidized nicotinamide dinucleotide ( $NAD^+$ ), or in some instances converted to lactate and  $NAD^+$  in the cytosol (non-oxidative glycolysis) (166). The latter is especially important in conditions where oxygen is limiting and pyruvate is converted to lactate by lactate dehydrogenase while oxidizing NADH to  $NAD^+$ . Lactate transport across the cardiac cell membrane is facilitated by the monocarboxylic acid transporter-1 (MCT-1) (see Figure 1.2). Lactate, ketone bodies and amino acids are not major contributors to ATP production under normal aerobic conditions since it is found in relatively low circulating concentrations (167). Normally the heart is a net consumer of lactate, however, if glycolysis is accelerated (e.g. during ischemia), it becomes a net producer of lactate (167).

Inside the mitochondrial matrix, pyruvate may either be decarboxylated to acetyl-CoA or carboxylated to oxaloacetate or malate. The latter reaction is anaplerotic and acts to maintain the tricarboxylic acid cycle (TCA) pool size of intermediates, and TCA function by counteracting the small constant loss of intermediates through efflux of citrate, succinate and fumarate (32, 51, 58, 131, 180). Pyruvate carboxylation accounts for ~2-6% of the citric acid cycle under normal aerobic conditions (32, 180).

The conversion of pyruvate to acetyl-CoA requires the action of pyruvate decarboxylase, dihydrolipoyl transacetylase, dihydrolipoyl dehydrogenase and five coenzymes, i.e. thiamine pyrophosphate, lipoic acid, coenzyme A, flavin adenine dinucleotide (FAD) and nicotinamide adenine dinucleotide (NAD); collectively referred to as the pyruvate dehydrogenase complex (PDH) located within the mitochondrial matrix (173). PDH is phosphorylated on the  $E_1$  subunit and inactivated by PDH kinase 4 (PDK4).

PDK4 in turn is inhibited by pyruvate and decreases in acetyl-CoA/free CoA and NADH/NAD<sup>+</sup> ratios (15, 72). At another regulatory level, high circulating lipid and intracellular accumulation of long-chain fatty acid moieties (e.g. with diabetes and fasting) enhance peroxisome proliferator activated receptor-alpha (PPAR- $\alpha$ ) gene pathways thereby attenuating PDH and pyruvate oxidation (91, 190). The role of PPAR- $\alpha$  on fatty acid uptake will be discussed in detail below. PDH activity is also regulated by a specific PDH phosphatase (131), and can also be enhanced by calcium and magnesium ions that are increased by adrenergic stimulation (88, 91). The product of this reaction (acetyl Co-A) then enters the TCA cycle (Figure 1.2) where it is converted to either malate or oxaloacetate (166). Thus, PDH activity is finely regulated depending on the degree of activities of upstream modulators, i.e. PDK4, and PDH phosphatase and various metabolites as discussed. In summary, this section has reviewed the mechanisms regulating glucose uptake and its fate in cardiomyocytes, with some emphasis on the importance of insulin in this regard. The next section of this chapter will focus on mechanisms regulating myocardial fatty acid uptake and utilization.

### **1.2.5 Myocardial fatty acid (FA) uptake**

As mentioned earlier, the adult heart uses FAs as its main source of ATP production. Fatty acids are present in the circulation in several forms: complexed with albumin, esterified in the lipid core of very low density lipoproteins (VLDLs), and chylomicrons (163, 181). Normal free fatty acid concentrations in the circulation vary between 0.2 and 0.6 mM. However, this may vary depending on the physio/pathophysiologic states e.g. FA levels are relatively low in the fetus, while it can increase to over 2 mM during ischemia or uncontrolled diabetes (101, 166). Albumin-bound FAs easily dissociate from albumin while esterified FAs are hydrolyzed by lipoprotein lipase at the luminal surface before traversing the cell membrane and entering cells. Although some FAs traverse the cell membrane passively by diffusion, the majority (~90%) are transported via carrier proteins (164).

Several carrier proteins play a role in FA transport across the cell membrane, including the 88 kDa scavenger receptor CD36 (rat homologue called fatty acid translocase [FAT]; 43 kDa plasma membrane fatty acid binding protein (FABPpm); and two isoforms of the fatty acid transport proteins (FATP) i.e. FATP1 and FATP6 (31, 34, 61, 110, 165, 170). FATP6 is exclusively expressed in the heart and it is more abundant than FATP1 (59, 151). Since FATP is associated with the cell membrane and co-localizes with FAT/CD36, it is suggested that these two transporters may act in concert (59). However, the main putative long-chain fatty acid (LCFA) carrier protein is CD36/FAT. Moreover, CD36/FAT is found both in storage vesicles inside the cell and on the cell membrane (similar to GLUT4) (62). Insulin can increase expression of both FAT/CD36 and FATPs for LCFAs uptake (49, 59, 101, 165) (refer Figure 1.1 above) (mechanisms involved are as previously described in section 1.2.3). The *in vivo* translocation of FAT/CD36 upon insulin stimulation, however, has not been demonstrated in the heart (161).

#### **1.2.5.1 Fate of FAs in cardiomyocytes**

After uptake LCFAs bind to a 15 kDa cytoplasmic heart-type fatty acid binding protein (H-FABPc) (refer Figure 1.3) and employ it as a vehicle to migrate towards their site of metabolic conversion or action (60, 97, 152). Subsequently, LCFAs are converted to acyl-CoAs by acyl-CoA synthetase (ACS) whereafter acyl-CoAs bind to the cytoplasmic acyl-CoA binding protein (ACBP) (refer Figure 1.3). Acyl-CoAs can either be used for triacylglycerol synthesis, be incorporated into intracellular lipid pools or undergo mitochondrial  $\beta$ -oxidation. Transport of acyl-CoAs into the mitochondrion is mediated by the action of three carnitine-dependent enzymes (48). As shown in Figure 1.3, carnitine palmitoyl transferase I (CPT-I), located at the outer mitochondrial membrane, catalyzes formation of acylcarnitine, and is the key regulatory enzyme in LCFA mitochondrial uptake. Thereafter, carnitine/acylcarnitine transferase (CACT) transports acylcarnitine into mitochondria in a 1:1 ratio for carnitine or other acylcarnitines. Carnitine palmitoyl transferase II (CPT-II) is located at the inner



mitochondrial membrane, and generates acyl-CoA by transferring acyl residues from acylcarnitine to free CoA, and carnitine (reshuttled back to the intermembrane space by the CACT transporter) (92, 106, 157). The acyl-CoA formed is oxidized via  $\beta$ -oxidation to acetyl-CoA, NADH and FADH<sub>2</sub> (see Figure 1.3). The latter two compounds are reoxidized in the mitochondrial electron transport chain, whereas the acetyl-CoA is oxidized to carbon dioxide in the tricarboxylic acid cycle to regenerate free CoA (34, 157).

As with glucose oxidation, fatty acid oxidation is also enhanced in response to increased AMPK activation following higher intracellular AMP: ATP ratios (66). AMPK facilitates FA utilization through phosphorylation and inactivation of acetyl-CoA carboxylase (ACC) (100). ACC catalyzes the conversion of acetyl-CoA to malonyl-CoA that direct either the inhibition of beta oxidation or the activation of lipid biosynthesis. Two main isoforms of ACC are expressed in mammalian tissues with the heart expressing ACC2 (or  $\beta$ ) in a higher ratio than ACC1 (or  $\alpha$ ) confirming a greater need for FA oxidation in the heart (vs. FA synthesis) (6). Malonyl-CoA is a potent inhibitor of CPT-I and AMPK activation decreases its levels thereby removing the inhibition of CPT-I and elevated FA oxidation as shown in Figure 1.3. AMPK may also regulate FAT/CD36 indirectly by inactivation of ACC, thus promoting increased fatty acid transport and subsequent oxidation (109). Furthermore, malonyl-CoA decarboxylase (MCD) can increase FA oxidation since it catalyzes the production of acetyl-CoA from malonyl-CoA thereby attenuating malonyl-CoA levels (161) (see Figure 1.3).

Another key regulatory component of FA oxidation occurs at the transcriptional level by the nuclear receptor peroxisome proliferator-activated receptor- $\alpha$  (PPAR- $\alpha$ ) a nuclear receptor (66, 92, 100). They are activated by natural ligands such as fatty acids or numerous pharmacological ligands (54). PPAR- $\alpha$  forms a heterodimer retinoid-X-receptor, and subsequently binds to PPAR response elements on the promoter regions of target genes (16, 52, 54). These include for example, medium-chain acyl-CoA dehydrogenase, fatty acid binding proteins, fatty acid transporters, 3-ketoacyl-CoA thiolase (119),

CPT-I (16) and malonyl-CoA decarboxylase (22). FAs are endogenous ligands for PPAR- $\alpha$ , hence if levels are increased they promote expression of genes involved in fatty acid oxidation (FAO), uptake and PDK4 expression (74) (refer to Figure 1.3 below). Similar to PPAR- $\alpha$ , PPAR- $\beta$  (or - $\delta$ ) is expressed abundantly in cardiac tissue (7). Activated by elevated intracellular FA (29), PPAR- $\beta$  (or - $\delta$ ) augments expression of a group of genes that promote FA utilization (46, 188). Cardiac-specific knockout of PPAR- $\beta$  also decreases FA oxidative gene expression and FAO (30). Although the targets of PPAR- $\alpha$  and PPAR- $\beta$  are partially overlapping (188), their unique roles and interaction remains unclear in the heart.

The acetyl-CoA generated by FAO subsequently converges with the end products of glycolysis and thereafter enter the Krebs cycle and mitochondrial electron transport chain discussed in sections 1.2.6 and 1.2.7.1, respectively.

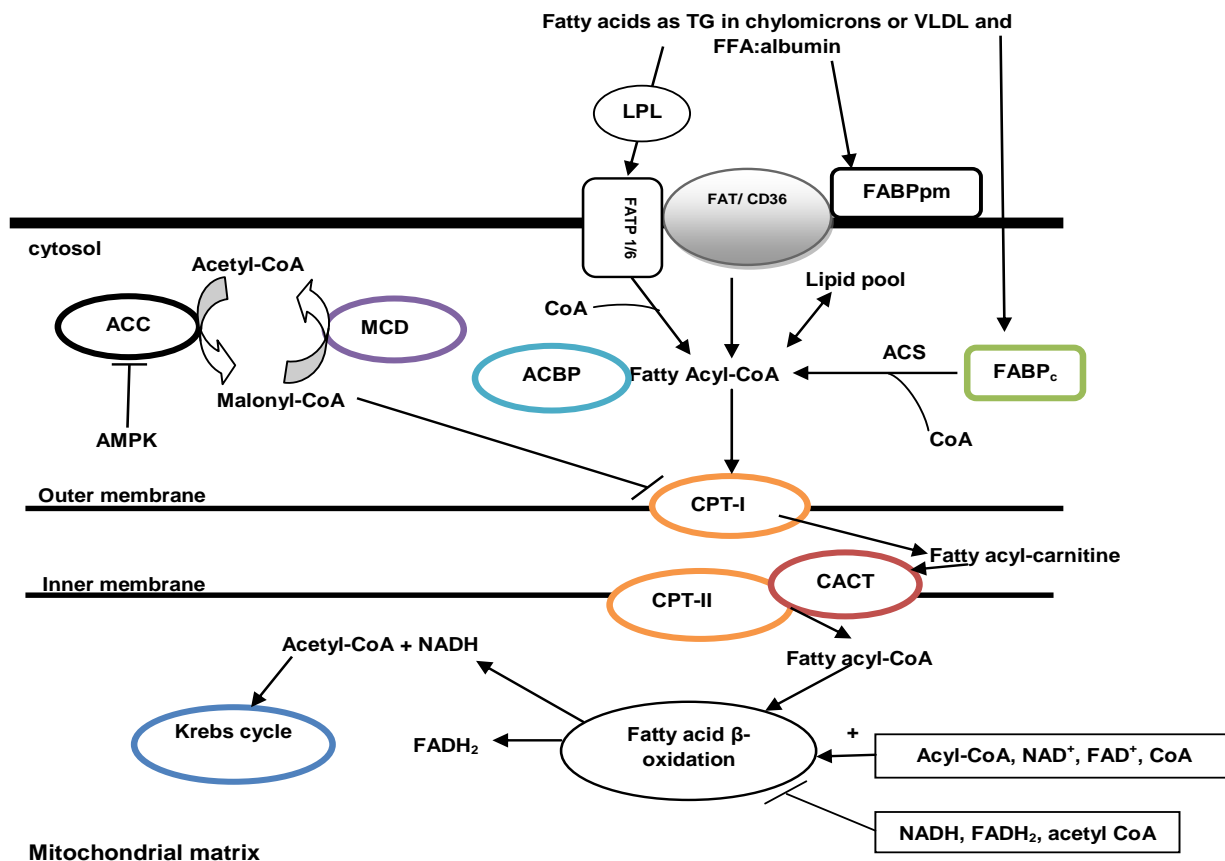


**Figure 1.3: Fatty acid uptake and regulation of metabolism by the cardiomyocyte under normal conditions.** LPL (lipoprotein lipase); FAT/CD36 (fatty acid translocase); FATP (fatty acid transport protein); FABPpm (plasma membrane fatty acid binding protein); FABPc (cytoplasmic heart-type fatty acid binding protein); ACBP (acyl-CoA binding protein); MCD (malonyl-CoA decarboxylase); ACC (acetyl-CoA carboxylase); CPT-I and II (carnitine-palmitoyl transferase I and II); CACT- carnitine/acylcarnitine transferase.

### 1.2.6 The tricarboxylic acid (TCA)/ Krebs/ citric acid cycle

The TCA cycle generates reducing equivalents for mitochondrial oxidative phosphorylation that eventually results in the generation of ATP, carbon dioxide, NADH, FADH<sub>2</sub> and guanosine triphosphate (GTP). In the TCA the most important sites of control are citrate synthase, isocitrate dehydrogenase,  $\alpha$ -ketoglutarate dehydrogenase and malate dehydrogenase. Of these, isocitrate dehydrogenase, pyruvate dehydrogenase and  $\alpha$ -ketoglutarate dehydrogenase activity is increased by calcium ions (Figure 1.3) (128). This is fueled by acetyl-CoA formed primarily from the oxidation of free fatty acids, carbohydrates and proteins (58, 124). Here acetyl-CoA transfers its acetyl group to

oxaloacetate, thereby generating citrate. Citrate provides the precursors (acetyl-CoA, NADH) for fatty acid synthesis, and is a positive allosteric modulator of ACC (112). Citrate exits from mitochondria via the tricarboxylate carrier (173) and regulates glycolysis by negative modulation of 6-phosphofructokinase activity (see above). In a cyclic series of reactions, citrate is subjected to two successive decarboxylations and four oxidative events, generating malate, a four-carbon compound. Only one ATP molecule is directly generated by a singular TCA cycle. Five of the TCA intermediates (malate, 2-oxoglutarate, succinyl-CoA, oxaloacetate and fumarate) are involved in anaplerotic reactions (refer to Figure 1.3) that act to replenish the cycle and are crucial for normal cardiac function (58, 146, 172).

Most studies have focused on  $\alpha$ -ketoglutarate dehydrogenase which catalyzes the conversion of alpha ketoglutarate, CoA and  $\text{NAD}^+$  to succinyl-CoA, NADH and  $\text{CO}_2$ . The production of NADH by  $\alpha$ -ketoglutarate dehydrogenase is crucial for mitochondrial respiration and oxidative phosphorylation (33, 76, 116). This enzyme requires thiamine pyrophosphate as a cofactor (discussed later in Chapter 2), and is highly regulated by modulators that include ATP/ADP and NADH/ $\text{NAD}^+$  ratios, calcium, and substrate availability in mitochondria. It is also a primary site of control for TCA flux (81, 172) e.g. it can be inhibited by its end products succinyl-CoA and NADH (57, 178).

All enzymes of the TCA are located within the mitochondrial matrix, except for succinate dehydrogenase that is embedded within the inner mitochondrial membrane. Thus the reducing equivalents formed (NADH,  $\text{FADH}_2$ ) have easy access to the mitochondrial electron transport chain and thereby ensuring generation of mitochondrial ATP (76, 92).

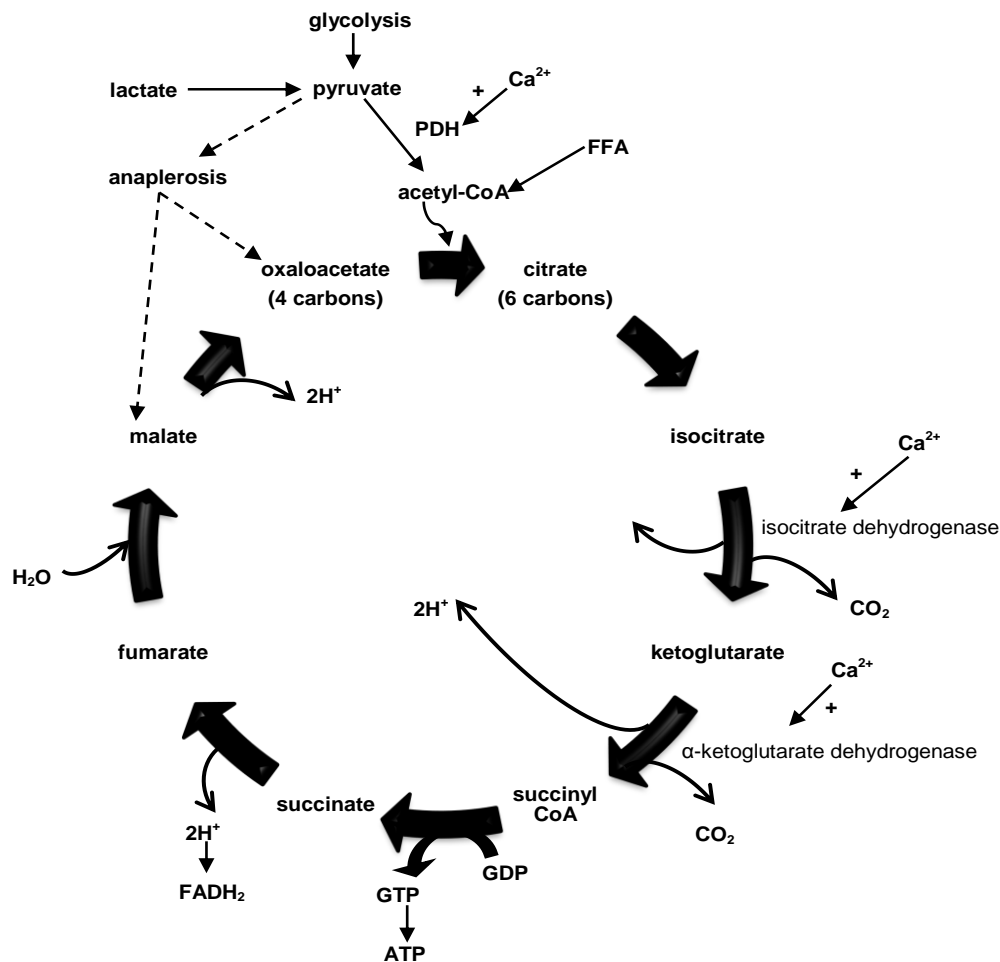


**Figure 1.4: The tricarboxylic acid cycle/ Krebs cycle/citric acid cycle.** The enzymes pyruvate dehydrogenase, isocitrate dehydrogenase and  $\alpha$ -ketoglutarate dehydrogenase can enhance flux into the Krebs cycle in response to increased cytosolic calcium. NADH (nicotinamide adenine dinucleotide hydrogen);  $\text{FADH}_2$  (flavin adenine dinucleotide hydrogen); GTP (guanosine 5-triphosphate); GDP (guanosine 5-diphosphate). The dotted lines indicate anaplerotic reactions.

### 1.2.7 The role of the mitochondria in oxidative phosphorylation

Due to the heart's high energy demands, cardiac cells have a high oxidative capacity with mitochondria making up ~25-35% of total cardiomyocyte volume (44). Two types of mitochondria have been described i.e. interfibrillar mitochondria (IFM) and subsarcolemmal mitochondria (SSM) (130). These types differ in terms of their cristae structure, rates of respiration, and expression of metabolic

proteins (130, 141). Under normal conditions, both SSM and IFM are efficient in meeting demands of the cellular ATP-dependent processes and maintaining ionic homeostasis of cells (71). Mitochondria produce ATP via the TCA and the respiratory chain (in the presence of oxygen), and hence this process is referred to as mitochondrial oxidative phosphorylation. The reducing equivalents generated by the TCA cycle provide electron energy for mitochondrial ATP production. However, glycolytically-derived NADH enters mitochondria via the malate-aspartate cycle, i.e. aspartate is extruded from mitochondria in exchange for malate (89). The process of mitochondrial oxidative phosphorylation occurs via protein complexes within the mitochondria as described in detail below.

#### **1.2.7.1 The electron transport chain (ETC)/ respiratory chain**

The protein components of the respiratory chain are oligomeric complexes that are located within the inner mitochondrial membrane. These complexes are referred to as multi-subunit electron transport complexes I, II, III and IV along with ATP synthase (complex V). Electrons enter the electron transport chain through NADH: ubiquinone oxidoreductase (complex I), the largest respiratory complex (molecular mass > than 900 kDa and contains at least 45 different subunits) (23, 24, 27). Complex I is the main rate-controlling steps of the electron transport chain (35), and catalyzes the electron transfer from NADH to ubiquinone (Q) through a series of redox centers that include a flavin mononucleotide moiety, seven to nine iron-sulfur centers, and up to three detectable ubisemiquinone species (55, 98, 125, 192). Complex I is one of three respiratory complexes where energy is conserved since four protons are translocated across the mitochondrial inner membrane coupled to electron transfer (see Figure 1.5). Therefore, it contributes to the proton-motive force that supports the synthesis of ATP, maintains the  $\text{NAD}^+/\text{NADH}$  ratio in the mitochondrial matrix, and supplies ubiquinol to the complex III (69). Several studies have shown that cardiolipin (a phospholipid) is required for optimal functioning of complex I (47, 56, 132, 135). Cardiolipin also plays an important role in the functioning of other inner

mitochondrial complexes of the electron transport chain and anion carriers, though its precise mechanisms are not yet fully understood (70, 143, 153).

Succinate dehydrogenase (complex II; or succinate: ubiquinone oxidoreductase, SQR) is a functional member of both the Krebs cycle and the aerobic respiratory chain. Complex II couples the oxidation of succinate to fumarate in the mitochondrial matrix with the reduction of ubiquinone in the membrane as shown in Figure 1.5 (26, 191). Ubiquinol produced by the action of membrane-bound dehydrogenases such as complex I, II and electron transfer flavoprotein (ETF)-ubiquinone oxidoreductase (Q-reductase) is oxidized by complex III (ubiquinol-cytochrome c oxidoreductase or cytochrome bc<sub>1</sub> complex). Complex III is located at the “crossroads” of the ETC, independently receiving electrons from complexes I and II (134). Complex III contains two subunits that include a membrane-bound diheme cytochrome b, a membrane-anchored cytochrome c<sub>1</sub>, and [2Fe-2S]-containing Rieske iron-sulfur protein. The electrons from ubiquinol are transferred to cytochrome c, and this reaction develops the proton motive Q cycle (27, 134). The Q cycle receives electrons from complex I and II, and cytochrome b acts as a bridge for electron transfer from the Q cycle to complex IV (136). Complex III is thus another mitochondrial respiratory complex where energy is conserved. In between complex II and complex IV is a mobile electron carrier called cytochrome c (see Figure 1.5) (65). A proton gradient is generated by the terminal cytochrome oxidase (complex IV) (contains 13 subunits) (9, 27, 65, 107, 193, 194) that has four redox metal centers where electrons are transferred, and subsequently reduce oxygen to two water molecules (27, 107, 149, 193, 194).

The final component of the mitochondrial oxidative phosphorylation system is ATP synthase (complex V or F<sub>1</sub>F<sub>0</sub> ATPase). This is a functionally reversible enzyme that can use the proton gradient generated by the electron system to produce ATP. It can also hydrolyze ATP and pump protons against an electrochemical gradient (see Figure 1.5) (27). Thus, mitochondrial F<sub>1</sub>F<sub>0</sub> ATP synthase regenerates ATP utilizing the potential energy produced in the respiratory chain. Myocardial ATP

generated is in close equilibrium with creatine phosphate which acts as a temporary store of high energy phosphate bonds. Creatine kinase plays a key role and this is further discussed below.

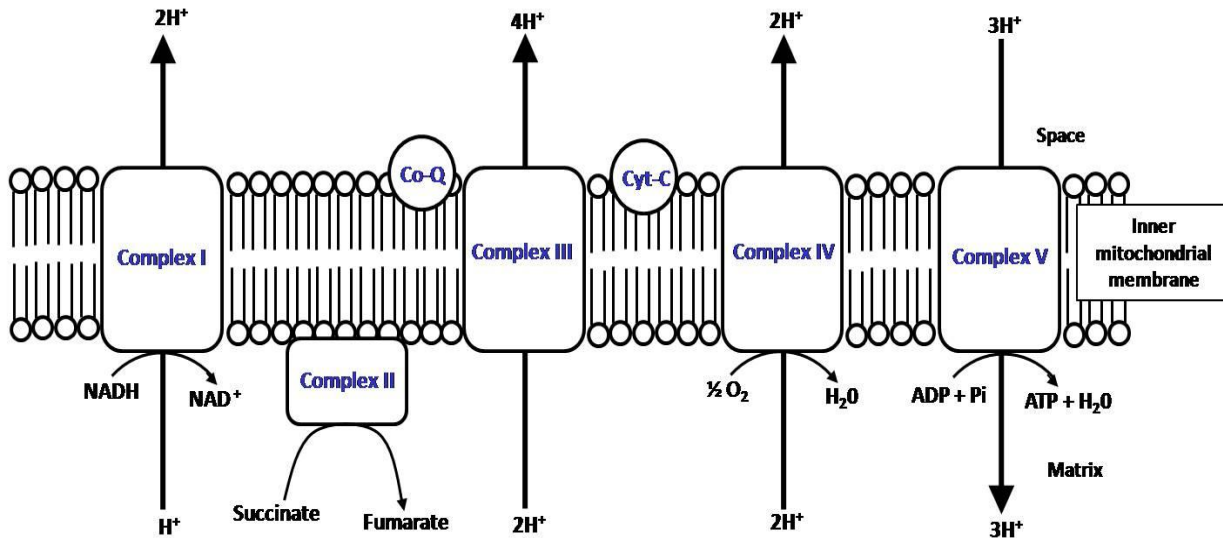


**Figure 1.5: Schematic diagram of the mitochondrial electron transport chain.** Electrons flow from complex I to complex V and subsequently reduce oxygen to water generating ATP via the ATPase. NADH (reduced nicotinamide adenine dinucleotide); ADP (adenosine 5' diphosphate); ATP (adenosine 5' triphosphate).

### 1.2.8 The creatine kinase system of the heart

Creatine kinase enzyme is located within both the mitochondrial intermembrane space and the cytosol (147). It catalyzes the transfer of a high energy phosphate bond from ATP to creatine forming creatine phosphate, acting as a buffer for ATP (82). Bessman *et al.* (1980) proposed the existence and function of the phosphorylcreatine shuttle whereby mitochondrial creatine phosphate/phosphocreatine diffuses to the contractile apparatus to serve as an energy source for myocardial contraction (11). Here creatine kinase binds to the myosin chain and transfers the high energy phosphate moiety from creatine phosphate to ADP thereby regenerating ATP. This is then hydrolyzed by myosin ATPase to



initiate the myocardial contractile processes (45). Free creatine formed by the removal of the high energy phosphate then diffuses back into mitochondria.

The bulk of the creatine is formed by the liver and kidneys, transported to the heart and actively taken up by a creatine phosphate transporter (64). The creatine kinase shuttle system plays a key role to regulate the high demands of the heart that is required to maintain normal contractile function, metabolic processes, and ionic homeostasis (126, 166). At rest, the rate of myocardial ATP hydrolysis is high (~30  $\mu\text{mol/g wet wt/min}$ ), and this result in a complete turnover of the entire myocardial ATP pool every 10 seconds (126, 174). When the heart's energy demands outstrip energy production and supply, phosphocreatine levels decrease to maintain ATP at normal levels, thus fulfilling its role as a buffer system. However, free ADP levels increase in parallel and results in the inhibition of many intracellular enzymes ultimately impairing the heart's contractile mechanisms.

### **1.2.9 Inter-relationship between glucose and fatty acid metabolism (Randle cycle)**

The regulation of glucose and fatty acid metabolism does not occur independently, but rather are inter-linked (138). The preferential use of FAs by cardiomyocytes involves FA-mediated inhibition of carbohydrate utilization at the levels of glucose transport, phosphofructokinase, hexokinase, glycogen phosphorylase, pyruvate dehydrogenase, and stimulation of glycogen synthase (78, 133). The inhibition of glucose transport was first demonstrated by using isolated rat hearts where LCFA or ketone bodies inhibited glucose uptake (133). At another level, inhibition of phosphofructokinase by FAs results via increased tissue levels of cytosolic citrate derived from FAO (see Figure 1.6) (139, 166). This leads to elevated fructose-6-phosphate and glucose-6-phosphate levels that inhibit hexokinase thereby increasing intracellular myocardial glucose concentrations. This decreases the concentration gradient for glucose uptake hence leads to impaired glucose uptake and insulin

resistance in cases of increased dietary FA uptake and/or in diabetes. It is unclear, however, if citrate levels inhibit PFK *in vivo* (167).

Increased glucose-6-phosphate levels also inhibit glycogen utilization through the inhibition of glycogen phosphorylase- $\beta$ . Glycogen phosphorylase- $\beta$  phosphorylates glycogen synthase thereby attenuating glycogen synthesis. Therefore, the net effect of PFK inhibition is decreased utilization of glucose via glycolysis and increased/decreased glycogenesis (28, 176). However, the key effect of fatty acids on glucose oxidation is the inhibition of pyruvate dehydrogenase by increased intra-mitochondrial acetyl-CoA and NADH derived from fatty acids oxidation (see Figure 1.6) (166). Additionally, fatty acyl-CoA blunts insulin-mediated glucose uptake by inhibiting IRS substrates, PKB and hexokinase (154, 155). However, this proposition by Randle (1963) still remains controversial with some studies indicating that the FA-mediated decrease, in glucose oxidation constitutes less than a third of the overall decrease, and that the remainder may be attributed to impaired glucose metabolism in non-oxidative pathways of glucose metabolism (12, 13, 144).

Conversely, inhibition of FAO increases glucose and lactate uptake/oxidation thereby improving cardiac function in some pathological states. This occurs by decreasing citrate levels removing the inhibition on PFK, and also lowering acetyl-CoA and/or NADH levels in the mitochondrial matrix, and thereby relieving the inhibition of PDH (166). This effect was observed in several studies where lipid oxidation was inhibited at various parts. These include inhibition of CPT-I with etomoxir; inhibition of MCD that elevates malonyl-CoA content to decrease CPT-I activity (22); and inhibitors of lipolysis in adipocytes. Conversely, other studies have shown that deficiency of CPT-Ib (an isoform predominantly expressed in the heart) may lead to lipotoxicity and cardiac dysfunction (3). Nevertheless, substrate utilization under different physiological states plays a crucial role on regulating cardiac function. As such Table 1.1 gives examples of studies that show the effect of substrate utilization on cardiac function .

**Table 1:1:** Examples of studies that show the effect of substrate utilization on cardiac function.

Experimental model	Nature of substrate utilization	Effect on function	Reference
<i>Ex vivo</i> neonatal rabbit hearts	Increased FA levels	Increased post-ischemic cardiac contractile function	(79)
<i>Ex vivo</i> Wistar rat hearts	Inhibition of FAO increased glucose oxidation	Improved cardiac functional recovery	(105)
<i>Ex vivo</i> obese Zucker rat hearts	Increased FA availability	Contractile dysfunction	(196)
<i>In vivo</i> <i>ob/ob</i> and <i>db/db</i> mice hearts	Increased FAO and reduced glucose oxidation	Reduced cardiac efficiency and contractile dysfunction	(20)
<i>Ex vivo</i> rat hearts	Hypertriglyceridemia and effect of FAO inhibition	Impaired post-ischemic recovery	(115)
<i>In vivo</i> human hearts	Increased glucose uptake	Improved post-ischemic cardiac function	(25, 37)

FA (fatty acid); FAO (fatty acid oxidation); *ob/ob* (strain of obese mice); *db/db* (strain of diabetic mice)

In summary, increased FAO inhibits glycolysis (Randle cycle) as occurs under both physiological (postprandial increase of plasma FA levels) and pathophysiological conditions (e.g. diabetes, ischemia) (171). It therefore, implies that high FA utilization in diabetes and ischemia and reperfusion impair glucose utilization thereby contributing to hyperglycemia and insulin resistance (28) (refer Chapter 2). As the heart adapts to use of fatty acids for ATP generation there is decreased efficiency since more oxygen will be consumed with less energy produced. This increases the risk of cardiac dysfunction especially during ischemia with reduced oxygen supply for FAO (177).

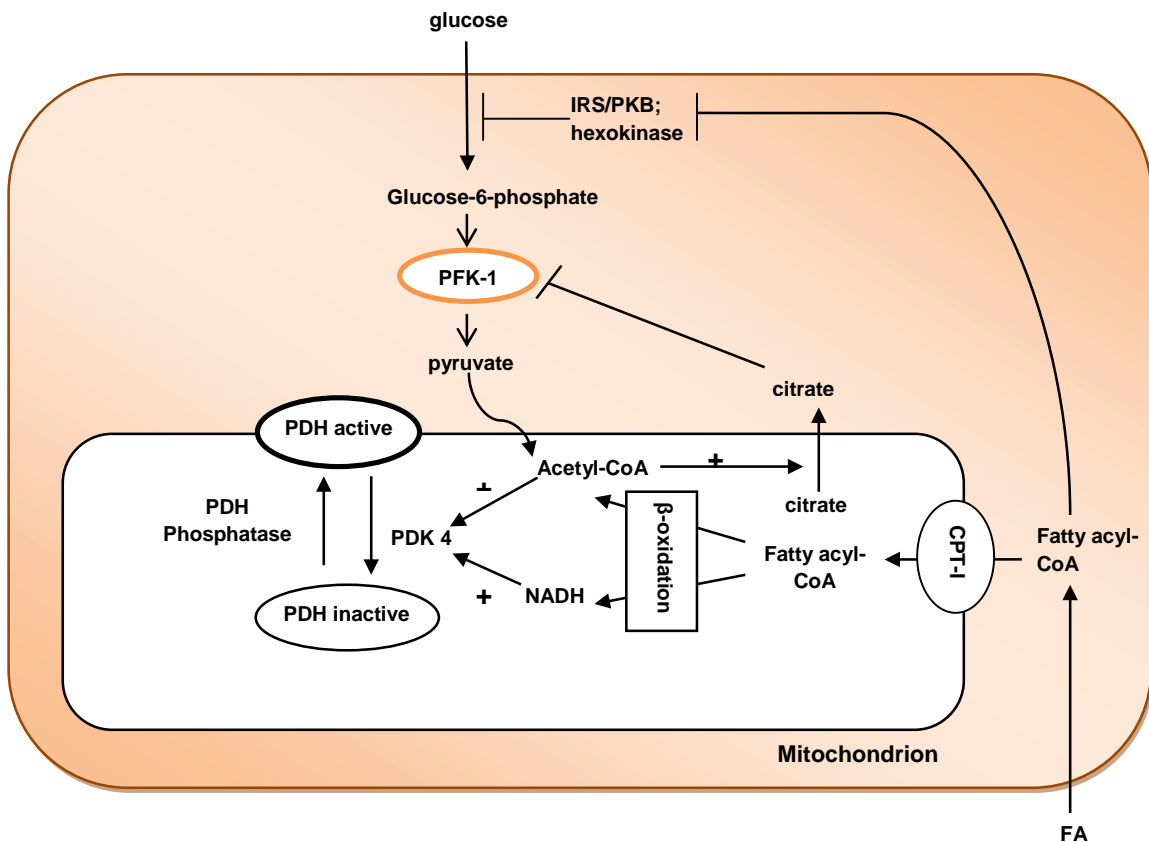


**Figure 1.6: The Randle cycle showing the interrelationship between myocardial fatty acid and glucose metabolism.** IRS/PKB (insulin receptor substrate/protein kinase B); PFK-1 (phosphofruktokinase-1); PDH (pyruvate dehydrogenase); PDK4 (pyruvate dehydrogenase kinase 4); CPT-I (carnitine palmitoyl transferase-I); PPAR- $\alpha$  (peroxisome proliferator-activated receptor- $\alpha$ ); NADH (nicotinamide adenine dinucleotide hydrogen); FA (fatty acids).

### 1.2.10 Summary and conclusion

This chapter briefly reviewed cardiac energy metabolism to set the scene for the focus of this dissertation, i.e. the effects of hyperglycemia on the heart. Such metabolic dysregulation may occur at any or all of the three main components discussed i.e. substrate utilization, mitochondrial energy production, and ATP transfer/utilization. The next chapter of this dissertation will now discuss cardiac energy metabolism, focusing on hyperglycemia within the context of diabetes and myocardial infarction.

## 1.2.11 References

1. **Ali M, Jahangir M, Hussan S, Choudhary M.** Inhibition of  $\alpha$ -glucosidase by oleanolic acid and its synthetic derivatives. *Phytochem* 60: 295–299, 2002.
2. **American Diabetes Association.** Consensus statement: role of cardiovascular risk factors in prevention and treatment of macrovascular disease in diabetes. *Diab Care* 16: 72–78, 1993.
3. **An D, Rodrigues B.** Role of changes in cardiac metabolism in development of diabetic cardiomyopathy. *Am J Physiol. Heart Circ Physiol* 291: H1489–H1506, 2006.
4. **Atkinson LL, Fischer M a, Lopaschuk GD.** Leptin activates cardiac fatty acid oxidation independent of changes in the AMP-activated protein kinase-acetyl-CoA carboxylase-malonyl-CoA axis. *J Biol Chem* 277: 29424–29430, 2002.
5. **Banerjee SK, Wang DW, Alzamora R, Huang XN, Pastor-Soler NM, Hallows KR, McGaffin KR, Ahmad F.** SGLT1, a Novel Cardiac Glucose Transporter, Mediates Increased Glucose Uptake in PRKAG2 Cardiomyopathy. *J Mol Cell Cardiol* 49: 683–692, 2010.
6. **Barber MC, Price NT, Travers MT.** Structure and regulation of acetyl-CoA carboxylase genes of metazoan. *Biochim et Biophys Acta (BBA)* 1733: 1–28, 2005.
7. **Barger PM, Kelly DP.** PPAR signaling in the control of cardiac energy metabolism. *Trends Cardiovasc Med* 10: 238–245, 2000.
8. **Barnard RJ, Youngren JF.** Regulation of glucose transport in skeletal muscle. *FASEB* 6, 1992.
9. **Belevich I, Verkhovsky MI, Wikström M.** Proton-coupled electron transfer drives the proton pump of cytochrome c oxidase. *Nature* 440: 829–32, 2006.
10. **Bertrand L, Horman S, Beauloye C, Vanoverschelde J.** Insulin signalling in the heart. *Cardiovasc Res* 79: 238–48, 2008.
11. **Bessman SP, Yang WC, Geiger PJ, Erickson-Vitanen S.** Intimate coupling of creatine phosphokinase and myofibrillar adenotriphosphatase. *Biochem Biophys Res Commun* 96: 1414–1420, 1980.
12. **Boden G, Chen X, Ruiz J, White J V, Rossetti L.** Mechanisms of fatty acid-induced inhibition of glucose uptake. *J Clin Invest* 93: 2438–46, 1994.
13. **Boden G, Jadali F, White J, Liang Y, Mozzoli M, Chen X, Coleman E, Smith C.** Effects of fat on insulin-stimulated carbohydrate metabolism in normal men. *J Clin Invest* 88: 960–966, 1991.
14. **Bouché C, Serdy S, Kahn CR, Goldfine AB.** The cellular fate of glucose and its relevance in type 2 diabetes. *Endocr Rev* 25: 807–830, 2004.

15. **Bowker-Kinley MM, Davis WI, Wu P, Harris RA, Popov KM.** Evidence for existence of tissue-specific regulation of the mammalian pyruvate dehydrogenase complex. *Biochem J* 329: 191–196, 1998.
16. **Brandt JM, Djouadi F, Kelly DP.** Fatty acids activate transcription of the muscle carnitine palmitoyltransferase I gene in cardiac myocytes via the peroxisome proliferator-activated receptor alpha. *J Biol Chem* 273: 23786–23792, 1998.
17. **Brosius III F, Liu Y, Nguyen N, Sun D, Bartlett J SM.** Persistent myocardial ischemia increases GLUT1 glucose transporter expression in both ischemic and non-ischemic heart regions. *J Mol Cell Cardiol* 29: 1675–1685, 1997.
18. **Brownlee M.** Biochemistry and molecular cell biology of diabetic complications. *Nature* 414: 813–820, 2001.
19. **Brownlee M.** The pathobiology of diabetic complications a unifying mechanism. *Diabetes* 54: 1615–1625, 2005.
20. **Buchanan J, Mazumder PK, Hu P, Chakrabarti G, Roberts MW, Yun UJ, Cooksey RC, Litwin SE, Abel ED.** Reduced cardiac efficiency and altered substrate metabolism precedes the onset of hyperglycemia and contractile dysfunction in two mouse models of insulin resistance and obesity. *Endocrinol* 146: 5341–5349, 2005.
21. **Bugger H, Abel E.** The Metabolic Syndrome and cardiac function. *Adv Pulmon Hypertens* 7: 332–336, 2008.
22. **Campbell FM, Kozak R, Wagner A, Altarejos JY, Dyck JRB, Belke DD, Severson DL, Kelly DP, Lopaschuk GD.** A role for peroxisome proliferator-activated receptor alpha (PPARalpha) in the control of cardiac malonyl-CoA levels: reduced fatty acid oxidation rates and increased glucose oxidation rates in the hearts of mice lacking PPARalpha are associated with high. *J Biol Chem* 277: 4098–4103, 2002.
23. **Carroll J, Fearnley IM, Skehel JM, Runswick MJ, Shannon RJ, Hirst J, Walker JE.** The post-translational modifications of the nuclear encoded subunits of complex I from bovine heart mitochondria. *Mol & Cell Prot: MCP* 4: 693–699, 2005.
24. **Carroll J, Shannon RJ, Fearnley IM, Walker JE, Hirst J.** Definition of the nuclear encoded protein composition of bovine heart mitochondrial complex I. Identification of two new subunits. *J Biol Chem* 277: 50311–50317, 2002.
25. **Carvalho G, Pelletier P, Albacker T, Lachapelle K, Joannisse D, Al E.** Cardioprotective effects of glucose and insulin administration while maintaining normoglycemia (GIN therapy) in patients undergoing coronary artery bypass grafting. *J Clin Endocrinol Metab* 96: 1469–1477, 2011.
26. **Cecchini G, Schröder I, Gunsalus RP, Maklashina E.** Architecture of succinate dehydrogenase and reactive oxygen species generation. *Biochim Biophys Acta* 1553: 140, 2002.

27. **Cecchini G.** Function and structure of complex II of the respiratory chain. *Ann Rev Biochem* 72: 77–109, 2003.
28. **Chalkley SM, Hettiarachchi M, Chisholm DJ, Kraegen EW.** Five-hour fatty acid elevation increases muscle lipids and impairs glycogen synthesis in the rat. *Metab Clin Exp* 47: 1121–1126, 1998.
29. **Chawla A, Lee CH, Barak Y, He W, Rosenfeld J, Liao D, Han J, Kang H, Evans RM.** PPARdelta is a very low-density lipoprotein sensor in macrophages. *Proc Natl Acad Sci USA* 100: 1268–1273, 2003.
30. **Cheng L, Ding G, Qin Q, Huang Y, Lewis W, He N, Evans RM, Schneider MD, Brako FA, Xiao Y, Chen YE, Yang Q.** Cardiomyocyte-restricted peroxisome proliferator-activated receptor-delta deletion perturbs myocardial fatty acid oxidation and leads to cardiomyopathy. *Nat Med* 10: 1245–1250, 2004.
31. **Coburn CT, Hajri T, Ibrahimi A, Abumrad NA.** Role of CD36 in membrane transport and utilization of long-chain fatty acids by different tissues membrane transfer of long-chain. *J Mol Neurosc* 16: 117–121, 2001.
32. **Comte B, Vincent G, Bouchard B, Benderdour M, Des Rosiers C.** Probing the origin of acetyl-CoA and oxaloacetate entering the citric acid cycle from the <sup>13</sup>C labeling of citrate released by the perfused rat hearts. *J Biol Chem* 272: 26117–26124, 1997.
33. **Cooney GJ, Taegtmeyer H, Newsholme EA.** Tricarboxylic acid cycle flux and enzyme activities in the isolated working rat heart. *Biochem J* 200: 701–703, 1981.
34. **Coort SLM, Bonen A, Van der Vusse GJ, Glatz JFC, Luiken JJFP.** Cardiac substrate uptake and metabolism in obesity and type-2 diabetes: role of sarcolemmal substrate transporters. *Mol Cell Biochem* 299: 5–18, 2007.
35. **Cortassa S, O'Rourke B, Winslow RL, Aon M A.** Control and regulation of mitochondrial energetics in an integrated model of cardiomyocyte function. *Biophys J* 96: 2466–2478, 2009.
36. **Craparo A, Freund R, Gustafson TA.** 14-3-3 (e) interacts with the insulin-like growth factor I receptor and insulin receptor substrate I in a phosphoserine-dependent manner. *J Biol Chem* 272: 11663–11669, 1997.
37. **Cross H, Clarke K, Opie L, Radda G.** Is lactate-induced myocardial ischemic injury mediated by decreased pH or increased intracellular lactate? *J Mol Cell Cardiol* 27: 1369–1381, 1995.
38. **DECODE.** Glucose tolerance and cardiovascular mortality: comparison of fasting and 2-hour diagnostic criteria. *Arch Intern Med* 161: 397–405, 2001.
39. **DeFronzo R.** Pharmacologic therapy for type 2 diabetes mellitus. *Annals Intern Med* 131: 281–303, 1999.
40. **Depre C, Ponchaut S, Deprez J, Maisin L, Hue L.** Cyclic AMP suppresses the inhibition of glycolysis by alternative oxidizable substrates in the heart. *J Clin Invest* 101: 390–397, 1998.

41. **Depre C, Rider MH, Veitch K, Hue L.** Role of fructose 2,6-bisphosphate in the control of heart glycolysis. *J Biol Chem* 268: 13274–13279, 1993.
42. **Depre C, Vanoverschelde J-LJ, Taegtmeyer H.** Glucose for the heart. *Circ* 99: 578–588, 1999.
43. **Diabetes Control and Complications Trial Research Group.** The effect of intensive treatment of diabetes on the development and progression of long term complications in insulin-dependent diabetes mellitus. *New Eng J Med* 329: 977–986, 1993.
44. **Dobson GP, Himmelreich U.** Heart design: free ADP scales with absolute mitochondrial and myofibrillar volumes from mouse to human. *Biochim Biophys Acta* 1553: 261–267, 2002.
45. **Dowell RT.** Activity of phosphorylcreatine shuttle enzymes in rat cardiac fast- and slow-twitch skeletal muscles. *Bioch Biophys Res Commun* 104: 740–745, 1982.
46. **Dressel U, Allen TL, Pippal JB, Rohde PR, Lau P, Muscat GE.** The peroxisome proliferator-activated receptor beta/delta agonist, GW501516, regulates the expression of genes involved in lipid catabolism and energy uncoupling in skeletal muscle cells. *Mol Endocrinol* 17: 2477–2493, 2003.
47. **Drose S, Zwicker K, Brandt U.** Full recovery of the NADH. Ubiquinone activity of complex I (NADH: ubiquinone oxidoreductase) from *Yarrowia lipolytica* by the addition of phospholipids. *Biochim Biophys Acta* 1556: 65–72, 2002.
48. **Eaton S.** Control of mitochondrial beta-oxidation flux. *Prog Lipid Res* 41: 197–239, 2002.
49. **Egert S, Nguyen N, Schwaiger M.** Myocardial glucose transporter GLUT1: translocation induced by insulin and ischemia. *J Mol Cell Cardiol* 1344: 1337–1344, 1999.
50. **Elchebly M, Payette P, Michaliszyn E, Cromlish W, Collins S, Loy AL, Normandin D, Cheng A, Himms-Hagen J, Chan C-C, Ramachandran C, Gresser MJ, Tremblay ML, Kenned BP.** Increased insulin sensitivity and obesity resistance in mice lacking the protein tyrosine phosphatase-1B gene. *Science* 283: 1544–1548, 1999.
51. **England PJ, Robinson BH.** The permeability of the rat heart mitochondria to citrate. *Biochem J* 112: 8P, 1969.
52. **Escher P, Wahli W.** Peroxisome proliferator-activated receptors: insight into multiple cellular functions. *Mutation res* 448: 121–138, 2000.
53. **Fischer Y, Thomas J, Sevilla L, Becker C, Holman G, Kozka IJ, Palacı M, Testar X, Kammermeier H, Zorzano A.** Insulin-induced recruitment of glucose transporter 4 (GLUT4) and GLUT1 in isolated rat cardiac myocytes. *J Biol Chem* 272: 7085–7092, 1997.
54. **Forman BM, Chen J, Evans RM.** Hypolipidemic drugs, polyunsaturated fatty acids, and eicosanoids are ligands for peroxisome proliferator-activated receptors alpha and delta. *Proc Natl Acd Sci USA* 94: 4312–4317, 1997.



55. **Friedrich T, Scheide D.** The respiratory complex I of bacteria, archaea and eukarya and its module common with membrane-bound multisubunit hydrogenases 1. *FEBS Lett* 479: 7–11, 2000.
56. **Fry M, Green DE.** Cardiolipin requirement for electron transfer in complex I and III of the mitochondrial respiratory chain. *J Biol Chem* 256: 1874–1880, 1981.
57. **Garland PB.** Some kinetic properties of pig-heart oxoglutarate dehydrogenase that provide a basis for metabolic control of the enzyme activity and also a stoichiometric assay for coenzyme A in tissue extracts. *Biochem J* 92: 10C-12C, 1964.
58. **Gibala MJ, Young ME, Taegtmeyer H.** Anaplerosis of the citric acid cycle: role in energy metabolism of heart and skeletal muscle. *Acat Physiol Scand* 168: 657–665, 2000.
59. **Gimeno RE, Ortegon AM, Patel S, Punreddy S, Ge P, Sun Y, Lodish HF, Stahl A.** Characterization of a heart-specific fatty acid transport protein. *J Biol Chem* 278: 16039–16044, 2003.
60. **Glatz JF, Storch J.** Unravelling the significance of cellular fatty acid-binding proteins. *Curr Opin Lipidol* 12: 267–274, 2001.
61. **Glatz JFC, Luiken JJFP, Bilsen M Van, Vusse GJ Van Der.** Cellular lipid binding proteins as facilitators and regulators of lipid metabolism. *Mol Cell Biochem* 239: 3–7, 2002.
62. **Glatz JFC, Luiken JJFP, Bonen A.** Involvement of membrane-associated proteins in the acute regulation of cellular fatty acid uptake. *J Mol Neurosc* 16: 123–132, 2001.
63. **Grynberg A, Demaison L.** Fatty acid oxidation in the heart. *J Cardiovasc Pharmacol* 28: 11–17, 1996.
64. **Guimbal C, Kilimann MWA.** A Na(+)-dependent creatine transporter in rabbit brain, muscle, heart and kidney: cDNA cloning and functional expression. *J Biol Chem* 268: 8418–8421, 1993.
65. **Gupte SS, Hackenbrock CR.** The role of cytochrome c diffusion in mitochondrial electron transport: multidimensional diffusion modes and collision frequencies of cytochrome c with its redox partners. *J Biol Chem* 263: 5248–5253, 1988.
66. **Hardie DG, Carling D.** The AMP-activated protein kinase-fuel gauge of the mammalian cell? *Eur J Biochem* 246: 259–273, 1997.
67. **Hasin Y, Barry WH.** Myocardial metabolic inhibition and membrane potential, contraction and potassium uptake. *Am J Physiol Heart Circ Physiol* 247: H322–H329, 1984.
68. **Hayashi T, Mori T, Yamashita C, Miyamura M.** Regulation of oxidative stress and cardioprotection in diabetes mellitus. *Curr Cardiol Rev* 4: 251–258, 2008.
69. **Hirst J.** Energy transduction by respiratory complex I – an evaluation of current knowledge. *Biochem Soc Trans* 33: 525–529, 2005.

70. **Hoch FL.** Cardiolipins and biomembrane function. *Biochim Biophys Acta* 1113: 71–133, 1991.
71. **Holmuhamedov EL, Oberlin A, Short K, Terzic A, Jahangir A.** Cardiac subsarcolemmal and interfibrillar mitochondria display distinct responsiveness to protection by diazoxide. *PlosOne* 2012;7:). *PloS One* 7: e44667, 2012.
72. **Holness M, Sugden M.** Regulation of pyruvate dehydrogenase complex activity by reversible phosphorylation. *Biochem Soc Trans* 31: 1143–1151, 2003.
73. **Hotamisligil GS, Peraldi P, Budavari A, Ellis R, White MF, Spiegelman BM.** IRS-1-mediated inhibition of insulin receptor tyrosine kinase activity in TNF- $\alpha$ - and obesity-induced insulin resistance. *Science* 271: 665–668, 1996.
74. **Huang B, Wu P, Popov K, Harris R.** Starvation and diabetes reduce the amount of pyruvate dehydrogenase phosphatase in rat heart and kidney. *Diabetes* 52: 1371–1376, 2003.
75. **Hue L, Rider MH.** Role of fructose 2,6-bisphosphate in the control of glycolysis in mammalian tissues. *Biochem J* 245: 313–324, 1987.
76. **Humphries KM, Szweda LI.** Selective inactivation of alpha-ketoglutarate dehydrogenase and pyruvate dehydrogenase: reaction of lipoic acid with 4-hydroxy-2-nonenal. *Biochem* 37: 15835–15841, 1998.
77. **Ishiki M, Klip A.** Minireview: recent developments in the regulation of glucose transporter-4 traffic: new signals, locations, and partners. *Endocrinol* 146: 5071–5078, 2005.
78. **Itani SI, Zhou Q, Pories WJ, Macdonald KG, Dohm GL.** Involvement of protein kinase c in human skeletal muscle insulin resistance and obesity. *Diabetes* 49: 1353–1358, 2000.
79. **Ito M, Jaswal JS, Lam VH, Oka T, Zhang L, Beker DL, Lopaschuk GD, Rebeyka IM.** High levels of fatty acids increase contractile function of neonatal rabbit hearts during reperfusion following ischemia. *Am J Physiol Heart Circ Physiol* 298: H1426–H1437, 2010.
80. **Jeremy RW, Koretsune Y, Marban E, Becker LC.** Relation between glycolysis and calcium homeostasis in postischemic myocardium. *Circ Res* 70: 1180–1190, 1992.
81. **Johnson RN, Hansford RG.** The control of tricarboxylate-cycle oxidations in blowfly flight muscle. The steady state concentrations of citrate, isocitrate 2-oxoglutarate and malate in flight muscle and isolated mitochondria. *Biochem J* 146: 527–535, 1975.
82. **Joubert F, Mateo P, Gillet B, Beloeil J-C, Mazet J-L, Hoerter JA.** CK flux or direct ATP transfer: versatility of energy transfer pathways evidenced by NMR in the perfused heart. *Mol Cell Biochem* 256/257: 43–58, 2004.
83. **Jung M, Park M, Lee HC, Kang YH, Kang ES, Kim SK.** Antidiabetic agents from medicinal plants. *Curr Med Chem* 13: 1203–1218, 2006.

84. **Kahn BB, Charron MJ, Lodish HF, Cushman SW, Flier JS.** Differential regulation of two glucose transporters in adipose cells from diabetic and insulin-treated diabetic rats. *J Clin Invest* 84: 404–411, 1989.
85. **Kannel WB, McGee DL.** Diabetes and cardiovascular risk factors: the Framingham study. *Circulation* 59: 8–13, 1979.
86. **Kantor P, Dyck JRB, Lopaschuk GD.** Fatty acid oxidation in the reperfused ischemic heart. *Am J Med Sci* 318: 3, 1999.
87. **Karnieli E, Zarnowski MJ, Hissin PJ, Simpson IA, Salans LB, Cushman SW.** Insulin-stimulated translocation of glucose transport systems in the isolated rat adipose cell. *J Biol Chem* 256: 4772–4777, 1981.
88. **Kashiwaya Y, Satos K, Tsuchiya N, Thomas S, Fells DA, Veechn RL, Passonneau J V.** Control of glucose utilization in working perfused rat heart. *J Biol Chem* 269: 25502–25514, 1994.
89. **Kavazis AN, Alvarez S, Talbert E, Lee Y, Powers SK.** Exercise training induces a cardioprotective phenotype and alterations in cardiac subsarcolemmal and intermyofibrillar mitochondrial proteins. *Am J Physiol Heart Circ Physiol* 297: H144–H152, 2009.
90. **Kenchaiah S, Evans J, Levy D, Al E.** Obesity and the risk of heart failure. *N Engl J Med* 347: 305–313, 2002.
91. **Kerbey AL, Randle PJ, Cooper RH, Whitehouse S, Pask HT, Denton RM.** Regulation of Pyruvate Dehydrogenase in Rat Heart: mechanism of regulation of proportions of dephosphorylated and phosphorylated enzyme by oxidation of fatty acids and ketone bodies and of effects of diabetes: role of coenzyme A, Acetyl CoA and reduced an. *Biochem J* 154: 327–348, 1976.
92. **Kerner J, Hoppel C.** Fatty acid import into mitochondria. *Biochim Biophys Acta* 1486: 1–17, 2000.
93. **Khullar M, Al-Shudiefat A, Ludke A, Binopal G, Singal P.** Oxidative stress: a key contributor to diabetic cardiomyopathy. *Can J Physiol. Pharmacol* 88: 233–240, 2010.
94. **King KL, Okere IC, Sharma N, Dyck JRB, Reszko AE, McElfresh T a, Kerner J, Chandler MP, Lopaschuk GD, Stanley WC.** Regulation of cardiac malonyl-CoA content and fatty acid oxidation during increased cardiac power. *Am J Physiol Heart Circ Physiol* 289: H1033–H1037, 2005.
95. **King LM, Opie LH.** Glucose delivery is a major determinant of glucose utilisation in the ischemic myocardium with a residual coronary flow. *Cardiovasc Res* 39: 381–392, 1998.
96. **Koonen DPY, Glatz JFC, Bonen A, Luiken JJFP.** Long-chain fatty acid uptake and FAT/CD36 translocation in heart and skeletal muscle. *Biochim Biophys Acta (BBA)* 1736: 163–80, 2005.

97. **Koonen DPY, Glatz JFC, Bonen A, Luiken JJFP.** Long-chain fatty acid uptake and FAT/CD36 translocation in heart and skeletal muscle. *Biochim Biophys Acta* 1736: 163–80, 2005.
98. **Koopman WJH, Verkaart S, Visch H, Van der Westhuizen FH, Murphy MP, Van den Heuvel LWPJ, Smeitink JAM, Willems PHGM.** Inhibition of complex I of the electron transport chain causes O<sub>2</sub>-mediated mitochondrial outgrowth. *Am J Physiol Cell Physiol* 288: C1440–C1450, 2005.
99. **Krentz AJ, Bailey CJ.** Oral antidiabetic agents: Current role in type 2 diabetes mellitus. *Drugs* 65: 385–411, 2005.
100. **Kudo N, Barr AJ, Barr RL, Desai S, Lopaschuk GD.** High rates of fatty acid oxidation during reperfusion of ischemic hearts are associated with a decrease in malonyl-CoA levels due to an increase in 5'-AMP activated protein kinase inhibition of acetyl-CoA carboxylase. *J Biol Chem* 270: 17513–17520, 1995.
101. **Kurth-Kraczek EJ, Hirshman MF, Goodyear LJ, Winder WW.** 5' AMP-activated protein kinase activation causes GLUT4 translocation in skeletal muscle. *Diabetes* 48: 1–5, 1999.
102. **Kusuoka H, Marban E.** Mechanism of the Diastolic Dysfunction Induced by Glycolytic Inhibition in Ferret Myocardium? *J Clin Invest* 93: 1216–1223, 1994.
103. **Von Lewinski D, Rainer PP, Gasser R, Huber M, Khafaga M, Wilhelm B, Haas T, Mächler H, Rössl U, Pieske B.** Glucose-transporter-mediated positive inotropic effects in human myocardium of diabetic and nondiabetic patients. *Metab Clin Exp* 59: 1020–1028, 2010.
104. **Liu J.** Pharmacology of oleanolic acid and ursolic acid. *J Ethnopharmacol* 49: 57–68, 1995.
105. **Lopaschuk G, Spafford M, Davies N, Wall S.** Glucose and palmitate oxidation in isolated working rat hearts reperfused after a period of transient global ischemia. *Circ Res* 66: 546–553, 1990.
106. **Lopaschuk GD, Witters LA, Itoi T, Barr R, Barr A.** Acetyl-coA carboxylase involvement in the rapid maturation of fatty acid oxidation in the newborn rabbit heart. *J Biol Chem* 269: 25871–25878, 1994.
107. **Ludwig B, Bender E, Arnold S, Hüttemann M, Lee I, Kadenbach N.** Cytochrome c oxidase and the regulation of oxidative phosphorylation. *Chem biochem* 2: 392–403, 2001.
108. **Luiken JJFP, Coort SLM, Koonen DPY, Van der Horst DJ, Bonen A, Zorzano A, Glatz JFC.** Regulation of cardiac long-chain fatty acid and glucose uptake by translocation of substrate transporters. *Eur J Physiol* 448: 1–15, 2004.
109. **Luiken JJFP, Coort SLM, Willems J, Coumans WA, Bonen A, Vusse GJ Van Der, Glatz JFC.** Contraction-induced fatty acid translocase/CD36 translocation in rat cardiac myocytes is mediated through amp-activated protein kinase signaling. *Diabetes* 52: 1627–1634, 2003.

110. **Luiken JJFP, Willems J, Van der Vusse GJ, Glatz JFC.** Electrostimulation enhances FAT/CD36-mediated long chain fatty acid uptake by isolated rat cardiac myocytes. *Am J Physiol Endocrin Metab* 281: E704–E712, 2001.
111. **Marsin A-S, Bertrand L, Rider MH, Deprez J, Beauloye C, Vincent MF, Berghe G Van Den, Carling D, Hue L.** Phosphorylation and activation of heart PFK-2 by AMPK has a role in the stimulation of glycolysis during ischaemia. *Curr Biol* 10: 1247–1255, 2000.
112. **Martin DB, Vagelos PR.** The mechanism of tricarboxylic acid cycle regulation of fatty acid synthesis. *J Biol Chem* 237: 1787–1792, 1962.
113. **McManus EJ, Sakamoto K, Armit LJ, Ronaldson L, Shpiro N, Marquez R, Alessi DR.** Role that phosphorylation of GSK3 plays in insulin and Wnt signaling defined by knockin analysis. *EMBO* 24: 1571–1583, 2005.
114. **Mochizuki S, Neely R.** Control of glyceraldehyde-3-phosphate dehydrogenase in cardiac muscle. *J Mol Cell Cardiol* 11: 221–236, 1979.
115. **Monti LD, Allibardi S, Piatti PM, Valsecchi G, Costa S, Pozza G, Chierchia S, Samaja M.** Triglycerides impair postischemic recovery in isolated hearts: roles of endothelin-1 and trimetazidine. *Am J Physiol Heart Circ Physiol* 281: H1122–H1130, 2001.
116. **Moreno-Sanchez R, Hogue BA, Hansford RG.** Influence of NAD-linked dehydrogenase activity on flux through oxidative phosphorylation. *Biochem J* 268: 421–428, 1990.
117. **Morgan H, Cadenas E, Regen D, Park C.** Regulation of glucose uptake in muscle. II. Rate-limiting steps and effects of insulin and anoxia in heart muscle from diabetic rats. *J Biol Chem* 236: 262–268, 1961.
118. **Morgan HE, Randle PJ, Regen DM.** Regulation of glucose uptake by muscle: the effects of insulin, anoxia, salicylate and 2,4-dinitrophenol on membrane transport and intracellular phosphorylation of glucose in the isolated rat heart. *Biochem J* 73: 573–579, 1959.
119. **Motojima K, Passilly P, Peters JM, Gonzalez FJ, Latruffe N.** Expression of putative fatty acid transporter genes are regulated by peroxisome proliferator-activated receptor alpha and gamma activators in a tissue- and inducer-specific manner. *J Biol Chem* 273: 16710–16714, 1998.
120. **Mueckler M, Hresko RC, Sato M.** Structure, function and biosynthesis of GLUT1. *Biochem Soc Trans* 25: 951–954, 1997.
121. **Mueckler M.** Facilitative glucose transporters. *Eur J Biochem* 219: 713–725, 1994.
122. **Myers MG, Wang LM, Sun XJ, Zhang Y, Yenush L, Schlessinger J, Pierce JH, White MF.** Role of IRS-1-GRB-2 complexes in insulin signaling. *Mol Cell Biol* 14: 3577–3587, 1994.
123. **National Diabetes Data Group.** *National Institutes of Health. National Institute of Diabetes and Digestive and Kidney Diseases.* 1995.

124. **Neely JR, Rovetto MJ, Oram JF.** Myocardial utilization of carbohydrate and lipids. *Prog Cardiovasc Dis* XV: 289–329, 1972.
125. **Ohnishi T.** Iron–sulfur clusters/semiquinones in Complex I. *Biochim Biophys Acta* 1364: 186–206, 1998.
126. **Opie L.** *The Heart: Physiology and Metabolism*. 4th ed. New York: Raven, 1991.
127. **Opie LH, Knuuti J.** The adrenergic-fatty acid load in heart failure. *J Am Coll Cardiol* 54: 1637–1646, 2009.
128. **Opie LH.** *Heart Physiology: from cell to circulation*. 4th ed. Philadelphia, USA: Lippincott Williams & Wilkins, 2004.
129. **Osei K, Schuster DP, Amoah AGB, Owusu SK.** Diabetes in Africa. Pathogenesis of type 1 and type 2 diabetes mellitus in sub-Saharan Africa: implications for transitional populations. *J Cardiovasc Risk* 10: 85–96, 2003.
130. **Palmer J V, Tandler B, Hoppel CL.** Biochemical properties of subsarcolemmal and interfibrillar mitochondria isolated from rat cardiac muscle. *J Biol Chem* 252: 8731–8739, 1977.
131. **Panchal AR, Comte B, Huang H, Kerwin T, Darvish A, Des Rosiers C, Brunengraber H, Stanley WC.** Partitioning of pyruvate between oxidation and anaplerosis in swine hearts. *Am J Physiol Heart Circ* 279: H2390–H2398, 2000.
132. **Paradies G, Petrosillo G, Pistolese M, Ruggiero FM.** Reactive oxygen species generated by the mitochondrial respiratory chain affect the complex III activity via cardiolipin peroxidation in beef-heart submitochondrial particles. *Gene* 282: 135–141, 2001.
133. **Paz K, Hemi R, LeRoith D, Karasik A, Elhanany E, Kanety H, Zick YA.** Molecular basis for insulin resistance. Elevated serine/threonine phosphorylation of IRS-1 and IRS-2 inhibits their binding to the juxtamembrane region of the insulin receptor and impairs their ability to undergo insulin-induced tyrosine phosphorylation. *J Biol Chem* 272: 29911–29918, 1997.
134. **Petrosillo G, Ruggiero FM, Di Venosa N, Paradies G.** Decreased complex III activity in mitochondria isolated from rat heart subjected to ischemia and reperfusion: role of reactive oxygen species and cardiolipin. *Fed Am Soc Exp Biol J* 17: 714–746, 2003.
135. **Ragan CI.** The role of phospholipids in the reduction of ubiquinone analogues by the mitochondrial reduced nicotinamide-adenine dinucleotide-ubiquinone oxidoreductase complex. *Biochem J* 172: 539–547, 1978.
136. **Di Rago JP, Netter P, Slonimski PP.** Intragenic suppressors reveal long distance interactions between inactivating and reactivating amino acid replacements generating three-dimensional constraints in the structure of mitochondrial cytochrome b. *J Biol Chem* 265: 15750–15757, 1990.
137. **Rahimi R, Nikfar S, Larijani B, Abdollahi M.** A review on the role of antioxidants in the management of diabetes and its complications. *Biomed Pharmacother* 59: 365–73, 2005.

138. **Randle PJ, Garland PB, Hales CN, Newsholme EA.** The glucose fatty-acid cycle. Its role in insulin sensitivity and the metabolic disturbances of diabetes mellitus. *Lancet* 1: 785–789, 1963.
139. **Randle PJ, Newsholme EA, Garland PB.** Regulation of Glucose Uptake by Muscle 8: effects of fatty acids, ketone bodies and pyruvate, and of alloxan-diabetes and starvation, on the uptake and metabolic fate of glucose in rat heart and diaphragm muscles. *Biochem J* 93: 652–665, 1964.
140. **Rider MH, Bertrand L, Vertommen D, Michels PA, Rousseau GG, Hue L.** 6-Phosphofructo-2-kinase/fructose-2,6-bisphosphatase: head-to-head with a bifunctional enzyme that controls glycolysis. *Biochem J* 579: 561–579, 2004.
141. **Riva A, Tandler B, Loffredo F, Vazquez E, Hoppel C.** Structural differences in two biochemically defined populations of cardiac mitochondria. *Am J Physiol Heart Circ Physiol* 289: H868–H872, 2005.
142. **Robertson C, Drexler AJ, Vernillo AT.** Update on diabetes diagnosis and management. *J Am Dental Assoc* 134: 16S–23S, 2003.
143. **Robinson NC.** Functional binding of cardiolipin to cytochrome c oxidase. *J Bioenerg Biomembr* 25: 153–163, 1993.
144. **Roden M, Price TB, Perseghin G, Petersen KF, Rothman DL, Cline GW, Shulman GI.** Mechanism of free fatty acid – induced insulin resistance in humans. *J Clin Invest* 97: 2859–2865, 1996.
145. **Rudberg S, Stattin E-L, Dahlquist G.** Familial and perinatal risk factors for micro- and macroalbuminuria in young IDDM patients. *Diabetes* 47: 1121–1126, 1998.
146. **Russell RR, Taegtmeyer H.** Changes in citric acid cycle flux and anaplerosis antedate the functional decline in isolated rat hearts utilizing acetoacetate. *J Clin Invest* 87: 384–390, 1991.
147. **Saks VA, Kongas O, Vendelin M, Kay L.** Role of the creatine/phosphocreatine system in the regulation of mitochondrial respiration. *Acta Physiologica Scand* 168: 635–641, 2000.
148. **Saltiel AR, Kahn CR.** Insulin signaling and the regulation of glucose and lipid metabolism. *Nature* 414: 799–806, 2001.
149. **Saraste M.** Oxidative Phosphorylation at the fin de siècle. *Science* 283: 1488–1493, 1999.
150. **Satoh S, Nishimuras H, Avril E, Kozkan IJ, Vannucci SJ, Sirnpson IA, Quonil MJ, Samuel W, Holmann GD.** Use of bismannose photolabel to elucidate insulin-regulated GLUT4 subcellular trafficking kinetics in rat adipose cells. *J Biol Chem* 268: 17820–17829, 1993.
151. **Schaap F, Hamers L, Van der Vusse GJ, Glatz JFC.** Molecular cloning of fatty acid-transport protein cDNA from rat. *Biochim Biophys Acta* 1354: 29–34, 1997.

152. **Schaap FG, Binas B, Dannenberg H, Van der Vusse GJ, Glatz JF.** Impaired long chain fatty acid utilization by cardiac myocytes isolated from mice lacking the heart-type fatty acid binding protein gene. *Circ Res* 85: 329–337, 1999.
153. **Schlame M, Rua D, Greenberg ML.** The biosynthesis and functional role of cardiolipin. *Prog Lipid Res* 39: 257–288, 2000.
154. **Schmitz-Peiffer C, Craig DL, Biden TJ.** Ceramide generation is sufficient to account for the inhibition of the insulin-stimulated PKB pathway in C2C12 skeletal muscle cells pretreated with palmitate. *J Biol Chem* 274: 24202–24210, 1999.
155. **Schmitz-Peiffer C.** Signalling aspects of insulin resistance in skeletal muscle: mechanisms induced by lipid oversupply. *Cell Signal* 12: 583–594, 2000.
156. **Schonekess BO, Allard MF, Lopaschuk GD.** Propionyl L-carnitine improvement of hyperthyroid heart function is accompanied by an increase in carbohydrates oxidation. *Circ Res* 77: 726–734, 1995.
157. **Schulz H.** Regulation of fatty acid oxidation in heart. *J Nutr* 124: 165–171, 1994.
158. **Senthil S, Sridevi M, Pugalendi K V.** Cardioprotective effect of oleanolic acid on isoproterenol-induced myocardial ischemia in rats. *Toxicol Pathol* 35: 418–423, 2007.
159. **Shepherd PR, Gould GW, Colville CA, McCoid SC, Gibbs EM, Kahn BB.** Distribution of GLUT3 glucose transporter protein in human tissues. *Biochem Biophys Res Commun* 188: 149–154, 1992.
160. **Shepherd PR, Nave BT, Siddle K.** Insulin stimulation of glycogen synthesis and glycogen synthase activity is blocked by wortmannin and rapamycin in 3T3-L1 adipocytes : evidence for the involvement of phosphoinositide 3-kinase and p70 ribosomal protein-S6 kinase. *Biochem J* 28: 25–28, 1995.
161. **Sim AT, Hardie DG.** The low activity of acetyl-CoA carboxylase in basal and glucagon-stimulated hepatocytes is due to phosphorylation by the AMP-activated protein kinase and not cyclic AMP-dependent protein kinase. *FEBS Lett* 233: 294–298, 1988.
162. **Slot JW, Geuze HJ, Gigengack S, James DE, Lienhard GE.** Translocation of the glucose transporter GLUT4 in cardiac myocytes of the rat. *Proc Natl Acad Sci U S A* 88: 7815–7819, 1991.
163. **Spector AA.** Plasma lipid transport. *Clin Physiol Biochem* 2: 123–134, 1984.
164. **Stahl A, Evans JG, Pattel S, Hirsch D, Lodish HF.** Insulin causes fatty acid transport protein translocation and enhanced fatty acid uptake in adipocytes. *Dev Cell* 2: 477–488, 2002.
165. **Stahl A, Gimeno RE, Tartaglia LA, Lodish HF.** Fatty acid transport proteins: a current view of a growing family. *Trends Endocrinol Metab* 12: 266–273, 2001.



166. **Stanley W, Recchia FA, Lopaschuk GD.** Myocardial substrate metabolism in the normal and failing heart. *Physiol Rev* 85: 1093–1129, 2005.
167. **Stanley WC, Lopaschuk GD, Hall JL, McCormack JG.** Regulation of myocardial carbohydrate metabolism under normal and ischaemic conditions: Potential for pharmacological interventions. *Cardiovasc Res* 33: 243–257, 1997.
168. **Stanley WC, Lopaschuk GD, McCormack JG.** Regulation of energy substrate metabolism in the diabetic heart. *Cardiovasc Res* 34: 25–33, 1997.
169. **Steinbusch LKM, Schwenk RW, Ouwens DM, Diamant M, Glatz JFC, Luiken JJFP.** Subcellular trafficking of the substrate transporters GLUT4 and CD36 in cardiomyocytes. *Cell Mol Life Sci : CMLS* 68: 2525–2538, 2011.
170. **Stremmel W, Strohmeyer G, Borchard F, Kochwa S, Berk PD.** Isolation and partial characterization of a fatty acid binding protein in rat liver plasma membranes. *Proc Natl Acad Sci U S A* 82: 4–8, 1985.
171. **Sun KT, Yeatman LA, Buxton DB, Chen K, Johnson JA, Huang SC, Kofoed KF, Weismueller S, Czernin J, Phelps ME, Schelbert HR.** Simultaneous measurement of myocardial oxygen consumption and blood flow using [1-carbon-11]acetate. *J Nucl Med* 39: 272–280, 1998.
172. **Taegtmeyer H, Hems R, Krebs HA.** Utilization of energy-providing substrates in the isolated working rat heart. *Biochem J* 186: 701–711, 1980.
173. **Taegtmeyer H.** Carbohydrate interconversions and production. *Circ* 72: 1–8, 1985.
174. **Taegtmeyer H.** Energy metabolism of the heart: from basic concepts to clinical applications. *Curr Prob Cardiol* 19: 57–116, 1994.
175. **The Committee of the Japan Diabetes Society on the diagnostic criteria of diabetes mellitus.** Report of the Committee on the classification and diagnostic criteria of diabetes mellitus. *Diab Res Clin Prac* 55: 65–85, 2002.
176. **Thompson AL, Lim-Fraser MY, Kraegen EW, Cooney GJ.** Effects of individual fatty acids on glucose uptake and glycogen synthesis in soleus muscle in vitro. *Am J Physiol Endocrinol Metab* 279: E577–E584, 2000.
177. **Tian R, Abel ED.** Responses of GLUT4-deficient hearts to ischemia underscore the importance of glycolysis. *Circ* 103: 2961–2966, 2001.
178. **Tretter L, Adam-Vizi V.** Alpha-ketoglutarate dehydrogenase: a target and generator of oxidative stress. *Philosoph Transact Royal Soc Lond. Series B, Biol Sci* 360: 2335–2345, 2005.
179. **United Kingdom Prospective Diabetes Study (UKPDS) Group.** Intensive blood glucose control with sulphonylureas or insulin compared with conventional treatment and risk of complications in patients with T2DM (UKPDS 33). *Lancet* 352: 837–845, 1998.

180. **Vincent G, Bouchard B, Khairallah M, Des Rosiers C.** Differential modulation of citrate synthesis and release by fatty acids in perfused working rat hearts. *Am J Physiol Heart Circ Physiol* 286: H257–H266, 2004.
181. **Van der Vusse GJ, Van Bilsen M, Glatz JF.** Cardiac fatty acid uptake and transport in health and disease. *Cardiovasc Res* 45: 279–293, 2000. h
182. **Watanabe T, Smith MM, Robinson FW, Kono T.** Insulin action on glucose transport in cardiac muscle. *J Biol Chem* 259: 13117–13122, 1984.
183. **Watson RT, Pessin JE.** Intracellular Organization of Insulin Signaling and GLUT4 Translocation. *Rec Prog Horm Res* 56: 175–193, 2001.
184. **Weiss J, Hiltbrand B.** Functional compartmentation of glycolytic versus oxidative metabolism in isolated rabbit heart. *J Clin Invest* 75: 436–447, 1985.
185. **Weiss JN, Lamp ST.** Cardiac ATP-sensitive K<sup>+</sup> channels: evidence for preferential regulation by glycolysis. *J Gen Physiol* 94: 911–935, 1989.
186. **Wheeler T.** Translocation of glucose transporters in response to anoxia in heart. *J Biol Chem* 263: 19447–19454, 1988.
187. **Wiernsperger N.** Is non-insulin dependent glucose uptake a therapeutic alternative? Part 1: physiology, mechanisms and role of non insulin-dependent glucose uptake in type 2 diabetes *Diab Metab* 31: 415–426, 2005.
188. **Winegar DA, Corton JC, Dohm GL, Kraus WE.** Fatty acid homeostasis and induction of lipid regulatory genes in skeletal muscles of peroxisome proliferator-activated receptor (PPAR) alpha knock-out mice: Evidence for compensatory regulation by PPAR delta. *J Biol Chem* 277: 26089–26097, 2002.
189. **World Health Organization.** *The World Health Report 2006: Working together for health.* 2006.
190. **Wu P, Peters JM, Harris R A.** Adaptive increase in pyruvate dehydrogenase kinase 4 during starvation is mediated by peroxisome proliferator-activated receptor alpha. *Biochem Biophys Res Commun* 287: 391–396, 2001.
191. **Yankovskaya V, Horsefield R, Törnroth S, Luna-Chavez C, Miyoshi H, Léger C, Byrne B, Cecchini G, Iwata S.** Architecture of succinate dehydrogenase and reactive oxygen species generation. *Science (New York, N.Y.)* 299: 700–704, 2003.
192. **Yano T, Magnitsky S, Ohnishi T.** Characterization of the complex I-associated ubisemiquinone species: toward the understanding of their functional roles in the electron/proton transfer reaction. *Biochim Biophys Acta* 1459: 299–304, 2000.
193. **Yoshikawa S, Muramoto K, Shinzawa-Itoh K, Aoyama H, Tsukihara T, Ogura T, Shimokata K, Katayama Y, Shimada H.** Reaction mechanism of bovine heart cytochrome c oxidase. *Biochim Biophys Acta* 1757: 395–400, 2006.

194. **Yoshikawa S.** A cytochrome c oxidase proton pumping mechanism that excludes the O<sub>2</sub> reduction site. *Fed Exp Biol Sci Lett* 555: 8–12, 2003.
195. **Young LH, Coven DL, Russell RR.** Cellular and molecular regulation of cardiac glucose transport. *J Nucl Cardiol* 7: 267–276, 2000.
196. **Young ME, Guthrie PH, Razeghi P, Leighton B, Abbasi S, Patil S, Youker KA, Taegtmeyer H.** Impaired long-chain fatty acid oxidation and contractile dysfunction in the obese Zucker rat heart. *Diabetes* 51: 2587–2595, 2002.
197. **Yurgin N, Secnik K, Lage MJ.** Obesity and the use of insulin: a study of patients with type 2 diabetes in the UK. *J Diab Complic* 22: 235–240, 2008.
198. **Zhou L, Cryan E V, D'Andrea MR, Belkowski S, Conway BR, Demarest KT.** Human cardiomyocytes express high level of Na<sup>+</sup>/glucose cotransporter 1 (SGLT1). *J Cell Biochem* 90: 339–346, 2003.

## CHAPTER 2

# The effects of hyperglycemia on cardiac metabolism and function with ischemia and reperfusion

### 2.1 Introduction

As a follow up from the previous chapter that reviewed cardiac energy metabolism under normal conditions, this chapter's focus is on the detrimental effects of hyperglycemia ± ischemia and reperfusion on the heart. It will highlight evidence that link hyperglycemia to cardiovascular diseases (CVDs), particularly myocardial infarction. Various mechanisms whereby hyperglycemia affects the pathogenesis of cardiovascular disease ± myocardial infarction will be discussed. Moreover, there will be focus on both chronic and acute hyperglycemia as evidence show that both forms have deleterious effects (484). Chronic hyperglycemia is a common symptom of diabetes and/or the metabolic syndrome, whereas acute hyperglycemia can occur in both non-diabetics and diabetics during stress conditions, e.g. following an acute myocardial infarction (AMI), or after eating (post-prandial). Finally, we will discuss ways how the heart adapts during such stressful, pathological conditions- focusing on cell death and protein degradation via the ubiquitin proteasomal system (UPS). Here the aim is also to highlight the need for the establishment of novel therapies to reduce the burden of hyperglycemia and its associated cardiovascular complications.

### 2.2 Diabetes mellitus

Diabetes is defined as a heterogeneous group of metabolic disorders arising from absolute or relative deficiency of insulin or due to insulin resistance characterized by high glucose levels (515, 765) (see section 1.1, Chapter 1 of this thesis). The prevalence and incidence of diabetes is on the rise globally

possibly due to rapidly uncontrolled urbanization, and changing lifestyle and/or greater aging of affected populations (476). The burden of the disease is also exacerbated by the increased association with cardiovascular complications that occur as a result of the chronic hyperglycemia. For example, diabetes causes a 2- to 4-fold increase in the risk of CVDs (50, 93, 655), including stroke (601), atrial fibrillation, flutter, coronary heart disease, and left ventricular hypertrophy (498). Several risk factors are implicated in the pathogenesis of diabetes-related complications and these include: glycemic control, hypertension, dyslipidemia, diet, and smoking (463). **For this thesis the focus is exclusively on hyperglycemia, i.e. both chronic (as in diabetes mellitus) and acutely (as in stress situations).** Before highlighting evidence that demonstrate the link between hyperglycemia *per se* to CVDs, and the mechanisms whereby complications occur, the next section briefly describes how chronic hyperglycemia occurs (as supported by various animal studies).

### **2.3 How does hyperglycemia occur with diabetes?**

Hyperglycemia that manifests during diabetes onset occurs as a result of decreased glucose transport (2, 20, 444), glycolysis and glucose oxidation (Figure 2.1). Defective glucose transport observed in diabetic animal models and patients is attributed to abnormal fatty acid (FA) metabolism, a decrease in total GLUT4 mRNA and protein levels secondary to insulin resistance or lack of insulin (53, 227, 344, 346, 711). Furthermore, impaired recruitment of GLUT4 to the cell membrane upon insulin stimulation that may occur as a result of alterations in the insulin receptor substrates (IRS)/phosphoinositide-3 kinase (PI 3-K)/Protein kinase B (Akt) signaling pathway is also implicated (163, 380, 538, 643) (see Figure 2.1). This may manifest in various ways that include: impaired translocation, persistent docking without fusion (373), partial fusion or altered configuration (rendering them cryptic with inadequate exposure to the extracellular milieu), and reduced activation (133, 345).

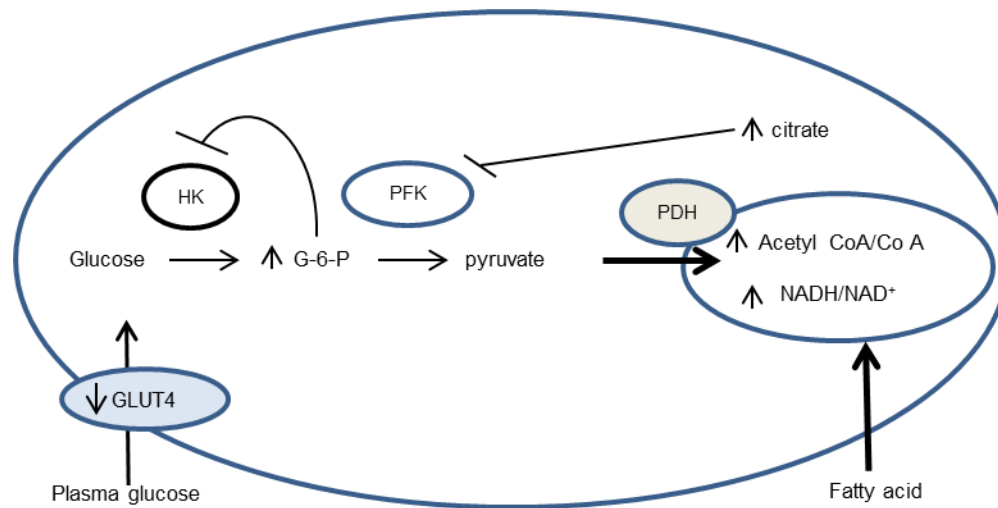


**Figure 2.1: Mechanism of FA-induced insulin resistance as proposed by Randle *et al.* (1963) (581).** An increase in FA concentrations results in an elevation of the intra-mitochondrial acetyl-CoA/CoA and NADH/NAD<sup>+</sup> ratios, with subsequent inactivation of pyruvate dehydrogenase. This causes an increase in citrate concentrations and inhibition of phosphofructokinase. Subsequent elevations in intracellular glucose-6-phosphate concentrations inhibit hexokinase II activity, which results in an increase in intracellular glucose concentration and a decrease in myocardial glucose uptake. GLUT4- glucose transporter 4; HK- hexokinase; G-6-P- glucose-6-phosphate; PFK- phosphofructokinase; PDH- pyruvate dehydrogenase.

The attenuated effects of insulin that occur during the metabolic syndrome and diabetes result in high circulating FA levels that alter glucose metabolism (120, 223, 274, 548, 592, 604, 623, 624, 745). Increased FAs may manifest due to 1) higher lipolysis and release from adipose tissue and liver (174, 256, 551, 582, 588, 599); 2) the augmented and permanent expression of the FAT/CD36 proteins on the cell membrane (139, 449). Enhanced delivery of lipids to the heart increases myocardial FA uptake, metabolism and storage. In support, increased cardiac triacylglycerides (TAGs) content together with greater mRNA levels of glycerol-3-phosphate acyltransferase (GPAT) (805), an enzyme known to direct exogenous FAs into TAGs (327), are found in diabetic patients and animals. Hence the combined elevation of FAT/CD36 and GPAT provides a mechanism for increased FA channeling towards intracellular storage. Indeed, both animal models and human studies of obesity, insulin resistance and diabetes, established that lipids accumulate within the heart (30, 131, 805). Consequently, the diabetes-induced elevation in plasma FA levels together with enhanced fatty acid oxidation (FAO) rates result in an elevation of intra-mitochondrial acetyl-CoA levels (see Figure 2.1),

which likely results in activation of pyruvate dehydrogenase (PDH) kinase 4 and phosphorylation of PDH to its inactive form. In addition, acetyl-CoA inhibits the rate of flux through active dephosphorylated PDH (286) (refer Figure 2.1). It is unclear how much of the decrease in glucose uptake in the diabetic heart is due to impaired pyruvate oxidation and feedback inhibition on the glycolytic pathway. However, the fraction of myocardial PDH in the dephosphorylated active form is significantly reduced in experimentally-induced diabetic rodents (274, 364, 403, 779).

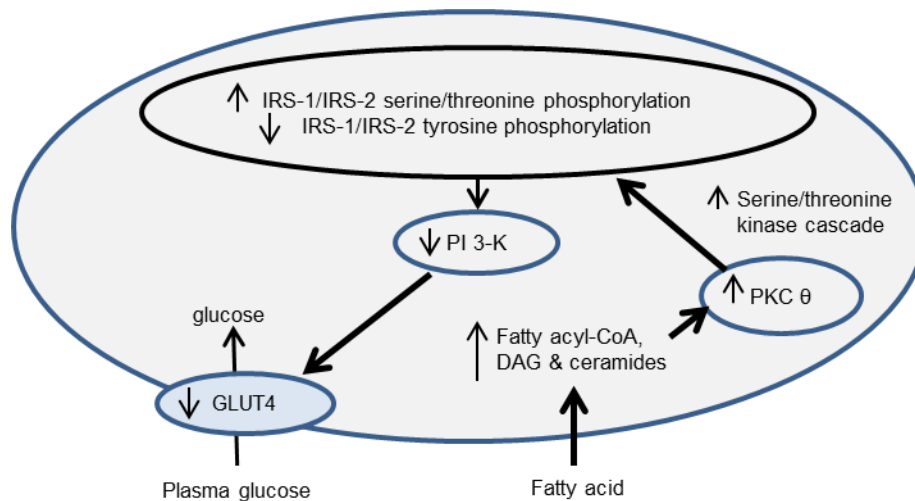


**Figure 2.2 Proposed alternative mechanism for FA-induced insulin resistance.** Enhanced delivery of FAs to muscle or a decrease in intracellular metabolism of FAs lead to increased in intracellular FA metabolites such as DAG, fatty acyl-CoA, and ceramides. HK, hexokinase II; PFK, phosphofructokinase; PDH, pyruvate dehydrogenase; PKC  $\theta$ , protein kinase C  $\theta$ .

Additionally, increased FAs result in elevated lipid metabolite levels such as acyl-CoAs, ceramides and diacylglycerols (DAGs) originating from, or in equilibrium, with the intracellular TAG pool. This in turn is proposed to influence insulin-induced glucose uptake and GLUT4 translocation (Figure 2.2) (7, 333, 672, 717). Acyl-CoAs are precursors for ceramides which are generated via *de novo* synthesis or degradation of sphingomyelin (533). These metabolites activate a serine/threonine kinase cascade (possibly initiated by protein kinase C [PKC]  $\theta$ ) leading to phosphorylation of serine/threonine sites on IRS-1/2, which in turn reduces the ability of the IRS to activate PI 3-K (622) (see Figure 2.2). As a consequence, glucose transport activity, and other events downstream of insulin receptor signaling are diminished (174, 599).

The chronic activation of such pathways can lead to diabetic cardiomyopathy (refer section 2.7.2.3) where both systolic and diastolic dysfunction are present (20). As the heart adapts to high FA utilization for ATP generation there is decreased efficiency since more oxygen will be consumed with less energy produced. This increases the risk of cardiac dysfunction especially during ischemia when reduced oxygen supply is available for FAO. Moreover, under these conditions the heart also increases its dependence on glucose as fuel substrate (707). This section briefly discussed how chronic hyperglycemia can actually occur with diabetes mellitus, and also re-iterated mechanisms already highlighted in Chapter 1. The next part of this review will now focus on the link between hyperglycemia and the onset of CVDs.

## **2.4 The link between hyperglycemia and the onset of CVDs**

Hyperglycemia consists of two forms, i.e. chronic hyperglycemia (diabetes) and acute hyperglycemia that can occur in both diabetic and non-diabetic individuals.

### **2.4.1 Chronic hyperglycemia and CVD**

Chronic hyperglycemia as assessed by glycosylated hemoglobin A<sub>1c</sub> (HbA<sub>1c</sub>) levels is associated with the development of micro- and macro-vascular complications of diabetes (463). There are a number of controlled clinical trials that demonstrate improved glycemic control reducing the risk for CVD, and epidemiologic studies that have established the link of various forms of hyperglycemia to greater risk for CVD (6, 8, 172, 179, 310, 536, 547, 697) (refer Table 2.1). The epidemiological link between diabetes mellitus and the development of CVD was established as early as 1979 (356). Two landmark studies; the Diabetes Control and Complications Trial (DCCT) and the United Kingdom Prospective Diabetes Study (UKPDS) highlighted the direct association between chronic glycemic control and vascular complications in patients with diabetes (167, 722).



A similar observation was also made in the DCCT follow up study, the Epidemiology of Diabetes Interventions and Complications (EDIC) (189); hence these studies have established the link between glycemic control and the risk of developing micro- and macro-vascular complications with T1DM (these complications are further discussed in section 2.7). Acute myocardial infarction is the major contributor to cardiovascular deaths with diabetes and it often progresses into end-stage heart failure (HF) (167, 355, 722). HF is increased with obesity, insulin resistance, and T2DM (57, 363), with incidences 2.4-fold and 5-fold higher in diabetic men and women, respectively (722). This is not only limited to T2DM but also include T1DM. For example, data from the Pittsburgh Epidemiology of Diabetes Complications (EDC) Study indicated that the incidence of major coronary artery disease events was 0.98% per year in young adults (age 28–38 years) with T1DM (20–30 years duration) (542, 595). In part, this increased mortality arising from heart disease ~2 to 4-fold higher in diabetic patients when compared to non-diabetics with the same magnitude of vascular diseases (153, 663).

**Table 3.1** Epidemiological studies showing the link between glycemic control and CVDs.

Trial (year)	Patients (n)	Population characteristics	Age (years)	Diabetes duration (years)	Intervention	Follow up (years)	Endpoint/outcome
DCCT (1993) (167)	1, 441	T1DM	27	6	Intensive insulin vs. standard care	1-15 years	Reduced CV event and outcome Reduced risk of micro-vascular complications
DCCT-EDIC (2005) (697)	1, 340	Follow-up of the DCCT cohort	45	24	Post-interventional follow up	11	Reduced CV events
UKPDS 33 (1998) (722)	3, 867	T2DM	53	Newly diagnosed	Intensive SU or insulin vs. diet	10	Reduced MI and micro-vascular complications
Kumamoto (1995)	110	Japanese with diabetes or 49 vs. 52 without diabetes	49	10	Multiple insulin injection treatment vs. conventional treatment	6	Reduced risk of micro-vascular complications
ProACTIVE (2005) (172)	5, 238	T2DM with macro-vascular disease	62	8	Pioglitazone added vs. placebo	3	Reduced primary CV end point and all cause mortality, non-fatal MI and stroke
STENO-2 (2003) (547)	160	T2DM with microalbuminuria	55	6	Multifactorial intervention vs. standard care	7.8	Reduced CV disease and micro-vascular complications
ACCORD (2008) (6)	10, 251	T2DM	62	10	Intensive vs. standard therapy	3.5	Increased mortality due to severe hypoglycemia
ADVANCE (2008) (8)	11, 140	T2DM (32% with CV events)	66	5	Intensive glucose control with gliclazide + other drugs vs. standard drugs	5	Reduced combined major macro-vascular and micro-vascular events Severe hypoglycemia
VADT (2009) (179)	1, 791	T2DM (40% with CV events)	60	11.5	Intensive glucose control vs. standard care	5.6	No CV benefit
RECORD (2009) (310)	4, 447	T2DM on met or SU	On met 57 on SU 60	On met 6 on SU 8	Add on rosiglitazone vs. combination met + SU	5.5	Increased HF
ORIGIN (2012) (536)	12, 537	T2DM on glargine insulin	45	Newly diagnosed	Glargine insulin vs. standard care and placebo	6	No effect on macro-vascular complications Hypoglycemia and increased weight

DCCT-EDIC (Diabetes Control and Complications Trial/Epidemiology of Diabetes Interventions and Complications); UKPDS (United Kingdom Prospective Diabetes Study); ProACTIVE (PROspective pioglitazone Clinical Trial In macroVascular Events); ACCORD (Action to Control Cardiovascular Risk in Diabetes); ADVANCE (Action in Diabetes and Vascular Disease: Preterax and Diamicon Modified Release Controlled Evaluation); VADT (Veterans Affairs diabetes trial); RECORD (Rosiglitazone evaluated for cardiovascular outcomes in oral agent

Chronic hyperglycemia and HbA<sub>1c</sub> measurements reflect overall glycemc control without revealing much information on individual daily glucose fluctuations (70). However, several studies found that short-term fluctuations in glycemc control also play an important role in the pathogenesis of CVDs in both diabetic and non-diabetic AMI patients - detailed evidence is further elaborated on the section below.

#### **2.4.2 Acute (stress-induced) hyperglycemia and CVD**

The link between acute hyperglycemia and CVD risk was reported in several non-diabetic patients (39, 220, 270, 362, 673) in the absence of chronic hyperglycemia. This link was established in studies where hyperglycemia occurring secondary to stress-induced AMI was associated with increased in-hospital deaths, congestive heart failure or cardiogenic shock (104, 465, 537). High blood glucose levels in patients admitted for AMI are found in both diabetic and non-diabetic individuals (13, 71, 104, 210, 251, 460, 675), and is an independent risk for development of CVD (508). In addition to the elevated plasma glucose in non-diabetics on admission after AMI, glucosuria was also reported since the 1930s (146). Admission hyperglycemia in non-diabetic individuals during the acute phase of AMI probably represents a combination of undiagnosed diabetes, impaired glucose tolerance (IGT) (16, 528) and a severe response to acute stress (104, 414, 537). IGT is defined as a condition where fasting plasma glucose levels are below 7 mmol/L, and 2-hour post-prandial values are between 7.8 mmol/L and 11.0 mmol/L, and precedes the development of T2DM (486).

In the event of undiagnosed diabetes, acute hyperglycemia can add to the damaging effects of chronic hyperglycemia (463). How does this occur? Elevated plasma adrenaline concentrations during the early stages of infarction can stimulate the sympathetic nervous system (104) and increase glycogenolysis, thereby contributing to high plasma glucose levels. Moreover, the relative insulin deficiency (in the event of underlying diabetes), together with lipolysis and excess circulating FAs, limit

uptake of glucose by mechanisms discussed in section 2.3. Likewise, glucose dysregulation of metabolism is also observed in non-diabetic patients during the acute phase of ST-elevation AMI (414) possibly due to an impairment in pancreatic  $\beta$ -cell function and insulin resistance (395). A further point to consider is that since AMI is a stress reaction mediating hyperglycemia, the reverse may also occur i.e. where non-diabetic AMI patients become predisposed to new onset of diabetes (535). In fact, AMI is considered a risk factor for development of diabetes (499), and this is supported by data from a retrospective analysis of the GISSI-PREVENZIONE trial that showed the interrelatedness of AMI and hyperglycemia (311). Despite the robust evidence linking acute hyperglycemia and CVDs, others report on the lack of correlation between the two parameters (103). This discrepancy could be partly due to differences in parameters analyzed to indicate endothelial function, and also the extent duration and pattern of hyperglycemia (590).

#### **2.4.3 Acute post-prandial hyperglycemia and fasting hyperglycemia**

Post-prandial hyperglycemia is a 2-hour post-prandial elevation of blood glucose ( $> 7.8$  mmol/L) in the presence of good glycemic control according to the American Diabetes Association (ADA) criteria, i.e.  $HbA_{1c} < 40\%$  with normal fasting plasma glucose (190). Post-prandial hyperglycemia occurs when the multiple homeostatic mechanisms that minimize glucose fluctuations to restore glucose levels after a meal are blunted. For example, in subjects with IGT insulin-mediated suppression of hepatic glucose production, enhancement of glucose uptake and reduction of FAs are impaired following food intake (39). The development of post-prandial hyperglycemia occurs mainly in the progression towards T2DM, i.e. due to loss of the first phase of insulin secretion (569). The major factor responsible for post-prandial hyperglycemia in individuals with IGT is likely to be impaired early insulin secretion by  $\beta$ -cells. This was observed in studies that reported a negative correlation between impaired post-prandial suppression of glucose and insulin release (486); development of IGT following somatostatin

treatment; and lastly increasing insulin concentrations by different treatments normalizing glucose tolerance (101, 451, 720).

By contrast, fasting hyperglycemia occurs predominantly as a result of increased glucose release by the liver and kidneys through gluconeogenesis (171, 481). Rates of glucose uptake are generally increased in individuals with fasting hyperglycemia, mainly because of the mass action effects of hyperglycemia. Moreover, fasting hyperglycemia may also occur due to antecedent post-prandial hyperglycemia, i.e. the higher the hyperglycemia after an evening meal, the greater the hyperglycemia in the morning and *vice versa*. Hence treatment should therefore aim to control both post-prandial and fasting hyperglycemia.

Post-prandial hyperglycemia is associated with a 2-fold increased risk of death from CVD (230). Some of the effects associated with the effects of acute hyperglycemia on the cardiovascular system include a) myocardial perfusion defects in T2DM patients secondary to micro-vascular function deterioration (628) and, b) alteration of myocardial ventricular repolarization in T1DM patients and increased stiffness/resistance of arteries (247, 248). Another way in which post-prandial hyperglycemia may lead to onset of CVDs may be via suppression of micro-circulation in young healthy adults (218) possibly as a result of micro-vascular dysfunction through leukocyte adhesion, enhanced platelet activation and advanced glycation end products (AGEs) (254, 466). In support of this, Crandall *et al.* (2009) showed that post-prandial hyperglycemia was accompanied by a pro-atherosclerotic and pro-thrombotic vascular profile in older adults with normal or elevated fasting glucose concentrations (141). Moreover, carotid intimal thickness (a marker of atherosclerosis) correlated to 2-hour post-prandial glucose in the Risk factors in Impaired Glucose Tolerance for Atherosclerosis and Diabetes (RIAD) Study (1999) with asymptomatic diabetes (693).

Several epidemiological studies reported the role of post-prandial hyperglycemia in the development of CVD. Examples include the Diabetes Epidemiology Collaborative Analysis of Diagnostic Criteria in Europe (DECODE) study that evaluated the relative risk of death from CVD, coronary heart disease, stroke and all-cause mortality in 22, 514 individuals followed up for 8.8 years. It is from these studies that the converse relationship between given glucose loads, blood glucose level and fasting glucose was established. Using a Cox proportion of hazards it was found that risks for death from CVD was increased in individuals with a 2-hour post-prandial glucose of 7.8-11.0 mmol/L and with T2DM, respectively (153). These results were corroborated in a different ethnic population (Funagata Diabetes Study) which showed that Japanese individuals have a 2-fold increased risk of mortality with post-prandial hyperglycemia, but no risk with impaired fasting blood glucose (709).

The Norfolk cohort of the European Prospective Investigation of Cancer and Nutrition (EPIC Norfolk) Study (1995 - 1999) evaluated 4, 662 individuals (45 - 79 years) and found that the presence or absence of diabetes was not a risk factor, but instead that hyperglycemia *per se* was the key factor (369). Moreover, in the Cardiovascular Health Study (CHS), a prospective study of 4, 515 individuals 65 years or older followed up for eight years, the presence of IGT resulted in an increased risk of 22% for CVD after correcting for other confounding factors such as age, ethnicity and known risk factors for CVD relative to that of normal glucose tolerance (215). These data are similar with those from the Second National Health and Nutrition Examination Survey (NHANES II) Mortality Study (618), a 12-16 year follow-up of a representative sample of the US population who underwent oral glucose tolerance testing between 1979 and 1980. Here relative risk for death was increased by 20% in individuals with IGT and 70% in individuals with previously undiagnosed diabetes.

Furthermore, the Hoorn Study (728), an 8-year follow up of 2, 363 individuals (aged 50 to 70 years) without known diabetes, showed a 62% increased risk for death from CVD in individuals with an elevated 2-hour post-prandial hyperglycemia even after excluding those with pre-existing CVD and

other known risk factors. Similarly, a longitudinal population Polynesian study that followed up on 10,000 individuals after 5 to 12 years, found that those with isolated post-prandial hyperglycemia i.e. 2-hour levels > 11.1 mmol/L displayed an increased CVD mortality of 2.3 to 2.6-fold in men and women, respectively (636). Moreover, the CAPRI cross sectional study (901 patients) on T2DM patients (Italy) reported a link between dietary glycemic index and load with metabolic control in T2DM as it corresponded to the HbA<sub>1c</sub> values and post-prandial glucose levels (193). The Diabetes Intervention Study (DIS), a prospective population-based multicenter study from the University of Dresden with 1,139 patients with newly diagnosed T2DM found that 2-hour post-prandial glucose levels and not fasting glucose measurements or HbA<sub>1c</sub>, predicted mortality (283). A more recent study performed on 1,115 T2DM patients (aged 30-75 years) showed that insulin treatment post-AMI decreased fasting blood glucose with no effect on post-prandial hyperglycemia (587). From all these studies it therefore emerges that post-prandial glycemia in non-diabetic individuals carries a greater risk for cardiovascular complications than increasing fasting glycemia, and hence more emphasis should be placed on its early detection and treatment (31, 231, 271, 406, 549).

Despite evidence from several epidemiological studies, the role of post-prandial glycemia in increasing CVD risk has been questioned by some who emphasized the need for more clinical studies (19). In support of this, Suileman *et al.* (2005) showed that fasting glucose was a better predictor of mortality in non-diabetic patients following AMI than admission blood glucose (679). However, more recent work challenged this notion as data correlated with the NHANES III study, further proving the role of post-prandial glycemia in onset of CVDs (75, 106, 375). Further studies will help clarify this dilemma, but the available evidence strongly implicates post-prandial hyperglycemia as another serious risk factor for CVD. All the available data from clinical trials, epidemiologic studies and some *in vivo* and *in vitro* studies highlight the role of hyperglycemia as an independent risk factor for CVD; the risk is continuous without an apparent threshold and thus there is a great need for better glycemic control to prevent both micro- and macro-vascular diseases with diabetes. The question therefore emerges: how

does hyperglycemia (independently) lead to the development of CVD complications? The next section will discuss the postulated molecular mechanisms whereby hyperglycemia causes damage to the cardiovascular system.

## **2.5 Mechanisms for adverse cardiovascular effects of hyperglycemia**

Hyperglycemia contributes to the development of vascular complications through several mechanisms, however, for this thesis we are focusing on the role of hyperglycemia-induced oxidative stress in the development of cardio-metabolic complications. Evidence in the literature supports the presence of oxidative stress with diabetes, and its role in mediating cardiovascular complications. Furthermore, the effects of hyperglycemia are basically the same irrespective of its nature (acute or chronic), since both activate similar metabolic and hemodynamic pathways from increased mitochondrial production of ROS to the downstream pathways mediating tissue damage (463). For example, both acute (478, 782) and chronic hyperglycemia can elicit endothelial dysfunction (37, 45, 142).

### **2.5.1 Hyperglycemia-induced oxidative stress**

Studies carried out in diabetic individuals, using both *in vitro* and *in vivo* experimental models, show that oxidative stress emerges as the main culprit in the development of cardio-metabolic complications (48, 86, 87, 109, 235, 295, 371, 462, 530, 608, 609, 685, 738) with the heart being at a higher risk due to low levels of antioxidants (127). Oxidative stress occurs when the rate of oxidant production exceeds oxidant scavenging capacities of cells (74, 370, 372). Further support for these concepts come from usage of classic antioxidants e.g. vitamins E/C and  $\alpha$ -lipoic acid that attenuated diabetes-related complications in human (337, 543, 635, 806), *in vitro* and *in vivo* experimental studies. For



example, overexpression of manganese superoxide dismutase (MnSOD) blunted superoxide production in experimental diabetes (127, 526).

### **2.5.1.1 Sources and types of ROS in diabetes and/or ischemia and reperfusion**

The mitochondrial respiratory chain is the principal source of intracellular ROS in diabetes and other stress pathological conditions, e.g. ischemia and reperfusion. The role of cardiac mitochondria under normal circumstances was earlier explained (refer Chapter 1). Briefly, glucose is metabolized through the tricarboxylic acid (TCA) cycle (or FAs through  $\beta$ -oxidation), generating electron donors, four of which reduce oxygen in the final stages of the respiratory chain to water. To be precise, electrons from reduced substrates (NADH and FADH<sub>2</sub>) move from complexes I and II of the electron transport chain through complexes III and IV to oxygen, forming water and causing protons to be pumped across the mitochondrial inner membrane with ATP synthesis (258, 544).

Previous studies show that there is an overlap in the factors that lead to damage or protection of mitochondria. Mitochondria respond to different signals by altering ATP production, calcium homeostasis, ROS production and membrane permeability. Functional integrity of cardiomyocytes requires an abundance of mitochondria capable of producing ATP and involved in calcium homeostasis. However, under stressful conditions mitochondria can contribute to cell death due to increased production of oxidants, activation of apoptotic and necrotic pathways (250). Experimental studies demonstrated that mitochondria are damaged with diabetes (201, 205, 638). Here, a major side effect is that electrons may leak from the respiratory chain and react with oxygen to form free radicals which are highly reactive because of unpaired electrons in their structure.

The primary factor governing mitochondrial ROS generation is the redox state of the respiratory chain (648). If the membrane potential across the inner mitochondrial membrane rises above a certain

threshold value, significant ROS generation occurs (381). Electrons mainly leak from complexes I (43, 44, 126, 229, 301, 396, 405, 409, 534) and complex III (76, 123, 660). Additionally, the stoichiometry of complex III can be altered to generate incompletely reduced forms of oxygen (79, 660). Thus, complex III is considered the major site of ROS production secondary to hyperglycemia and/or ischemia (86, 87, 123). In support, glycation of complex III proteins is attributed to the excess production of superoxide ions in diabetic rats (602).

How is ROS production via the mitochondrial respiratory chain a causal link between high glucose and the main pathways responsible for hyperglycemic damage? The prevailing hypothesis is that the hyperglycemia-induced increase in electron transfer donors (NADH and FADH<sub>2</sub>) increases electron flux through the mitochondrial ETC. There may also be changes in the ETC stoichiometry that can lead to an increase in reverse flow of electrons. Consequently, there is an increase of the ATP/ADP ratio and hyperpolarization of the mitochondrial membrane potential (79, 381, 647, 648). This high electrochemical potential difference generated by the proton gradient leads to partial inhibition of the electron transport in complexes I and III, resulting in an accumulation of electrons to coenzyme Q. In turn, this drives the partial reduction of oxygen to generate superoxide (86, 176, 177). The accelerated reduction of coenzyme Q, and subsequent ROS generation is considered a crucial aspect of mitochondrial dysfunction and diabetes-related metabolic disorders and tissue histopathology.

ROS produced can also damage the respective producing complex itself thereby further decreasing its activity and exacerbating free radical production (544, 799). Superoxide overproduction in the organ systems is an important feature of diabetic complications (176, 177, 526, 773, 774) as it mediates various oxidative chain reactions (86, 112, 116, 117, 176, 177, 526, 773, 774). An example of this is the activation of major, interrelated, pathogenic mechanisms for diabetic complications as modeled in endothelial cells exposed to *in vitro* hyperglycemia (526).

There is also supporting evidence that greater cytosolic generation of ROS may precipitate increased mitochondrial ROS overproduction, which underscores the pathogenic importance of ROS generation from non-mitochondrial sources (225, 804). Other sources for ROS generation include; glucose autoxidation, the membrane NADPH oxidase (Nox), lipoxygenases, cyclo-oxygenases, peroxidases, heme proteins, xanthine oxidase, peroxisomes, or the hepatic P-450 microsomal detoxifying system (see Figure 2.3) (86, 114, 161, 526, 772). Both mitochondrial and non-mitochondrial sources generate three main ROS types, i.e. the superoxide radical ( $O_2^{\bullet-}$ ), hydrogen peroxide ( $H_2O_2$ ), and hydroxyl radical ( $OH^{\bullet}$ ). The hydroxyl radical can be generated by the combination of superoxide radical and hydrogen peroxide in the presence of traces of iron or copper during the Fenton-Haber-Weiss reaction. Increased copper levels may result because of damaged copper binding properties of ceruloplasmin and albumin that occurs with diabetes (25, 181, 572, 783). Thus, hydrogen peroxide (although not a free radical) can generate the hydroxyl and other reactive radicals at multiple intracellular locations, thereby propagating oxidative damage (319, 320). Other ROS that are important for the cardiovascular system include singlet oxygen, nitric oxide (NO) and the perhydroxyl radical, located near membranes where local pH is lower than the rest of the environment as occurs during ischemia and reperfusion.

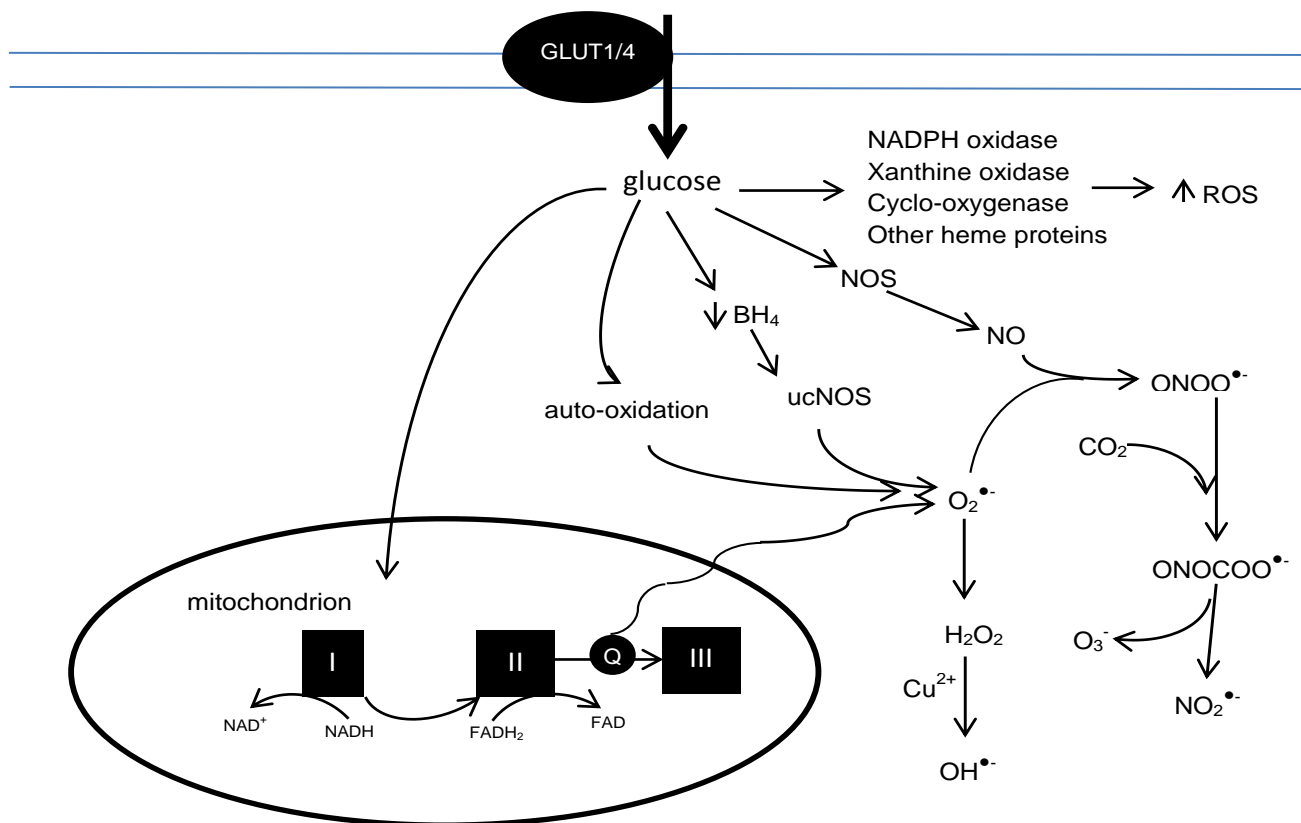


**Figure 2.3 Mechanisms of formation of hyperglycemia-induced ROS.** BH<sub>4</sub>- tetrahydro biopterin; NO- nitric oxide; O<sub>2</sub><sup>•-</sup>- superoxide radical; CO<sub>3</sub><sup>•-</sup>- carbonate radical; ONOO<sup>•-</sup>- peroxynitrite; ucNOS- uncoupled nitric oxide synthase; ONCOO<sup>•-</sup>- nitrosoperoxycarbonate; NO<sub>2</sub><sup>•-</sup>- nitrogen dioxide; Cu<sup>2+</sup>- copper ions; OH<sup>•-</sup>-hydroxyl radical; NAD<sup>+</sup>-oxidized nicotinamide adenine dinucleotide; NADH- reduced nicotinamide adenine dinucleotide; FADH<sub>2</sub>-reduced flavin adenine dinucleotide; FAD- oxidized flavin adenine dinucleotide.

Mitochondrial NO production is much lower than superoxide production. However, it is still an important role player due to its interaction with superoxide and other radicals to produce potent reactive nitrogen species (RNS), e.g. peroxynitrite (86, 114, 117, 161, 275, 526, 772), that causes nitrosative stress in organ systems. A significant increase in serum and tissue 3-nitrotyrosine (3-NT), a by-product of the reaction between peroxynitrite and proteins, is found in diabetic patients (100, 114, 115, 216). Moreover, *in vivo* and *in vitro* studies demonstrated that peroxynitrite is an important causative agent in diabetes-mediated cardiovascular injury (100, 114) (see Figure 2.3), by modifying macromolecules (86, 87). Protonation of peroxynitrite can also yield peroxynitrous acid that can

decompose to yield the hydroxyl radical thus further adding to overall damaging effects (109, 111, 113).

The roles of ROS and RNS in the diabetic complications of multiple organ systems are extensively documented (98, 161, 176, 349, 526, 609, 772), although the exact mechanisms of ROS/RNS-induced pathogenesis are not fully understood yet. However, some of the proposed mechanisms are discussed below. It is now known that peroxynitrite can directly cause oxidative DNA damage and lipid peroxidation (27, 349, 527, 681), and indeed damaged DNA was found in both T1DM and T2DM individuals (135, 246, 390, 419, 439, 616). Furthermore, peroxynitrite can also cause covalent modification of an active thiol site of glyceraldehyde-3-phosphate dehydrogenase (GAPDH) (thus inhibiting its activity), and also able to attenuate creatine kinase activity (684, 736). Here, peroxynitrite-mediated nitration of myofibrillar creatine kinase activity may lead to contractile dysfunction and inhibition of ion pumps including calcium, calcium-activated potassium channels and the membrane  $\text{Na}^+/\text{K}^+$  ATPase (684, 736). As discussed earlier, non-mitochondrial ROS sources include Nox, xanthine oxidase and reduced neuronal nitric oxide synthase (427). For example, Nox activity is high in vascular tissue from diabetic patients and may therefore contribute to superoxide production (268).

Various antioxidants have been used in clinical trials, to ameliorate oxidative stress but with mixed outcomes, i.e. beneficial effects versus none (269, 793). Several antioxidants showed beneficial effects in experimental animals, for example,  $\alpha$ -lipoic acid decreased oxidative stress when administered *in vivo* to diabetic animals (483). Additionally, antioxidant potential is also observed *in vitro* with known antihypertensive agents e.g. nifedipine (a calcium channel blocker) and olmesartan (an angiotensin receptor blocker). For example, olmesartan is a potent scavenger for hydroxyl and tyrosyl radicals and prevents glycooxidation and lipoxidation reactions whereas nifedipine is a potent scavenger of peroxynitrite (487). Interestingly, despite the evidence that superoxide is the major oxidant in hyperglycemia-induced oxidative stress (177, 526, 772), few studies have tested the effects

of decreasing superoxide levels in diabetes (2). Some approaches include the use of catalytic superoxide dismutase (SOD) mimetics, e.g. Mn (III) tetrakis (4-Benzoic acid) porphyrin chloride (MnTBAP), that reduced hepatic superoxide generation, and reversed steato-hepatitis in diabetic *ob/ob* mice (413). Furthermore, mitochondrial targeting of antioxidants by conjugation to cations such as triphenylphosphonium (TPP), leads to preferential mitochondrial uptake. The theory behind this is that these cations initially accumulate within the cytoplasm because of the cell membrane potential (30–60 mV, negative charge inside), then readily permeate the lipid bilayers and become concentrated within mitochondria, because of the large mitochondrial transmembrane potential (150–180 mV, negative charge inside). Eventually, membrane-permeable cations will be predominantly sequestered by mitochondria with much less than 5% remaining outside mitochondria. For example, TPP conjugates of tocopherol (Mito-E) and coenzyme Q (Mito-Q) have successfully been administered to mice (in chow or drinking water) for up to 6 weeks with no evidence of toxicity (649). However, despite these studies, little is known about the impact of pharmacological reduction of mitochondrial superoxide production on cardiac function and substrate metabolism, and this represents new possibilities for future research.

In summary, mitochondrial and non-mitochondrial ROS are key players in the manifestation of cardio-metabolic pathophysiology. Here the initiating event is mitochondrial superoxide production that triggers further ROS generation (other sources) thereby creating a vicious cycle. Subsequently, ROS can induce cellular damage by direct oxidation of proteins, by conversion of lipids to reactive lipid peroxidation products, by increasing protein tyrosine nitration by generation of RNS, and by interaction with DNA. Mitochondrial DNA is particularly susceptible to oxidative damage leading to more ROS production due to altered function (746). It is also important to remember that increased ROS levels not only result from its overproduction, but may also manifest due to decreased efficiency of inhibitory scavenger systems, e.g. SODs (copper/zinc-SOD [Cu/Zn-SOD] and Mn-SOD), catalase, and the

glutathione peroxidase system. These are examples of endogenous mitochondrial antioxidants that prevent tissue damage and dysfunction (361) under normal physiological conditions.

### **2.5.2 Mitochondrial antioxidant defense mechanisms**

Mitochondria together with the other intracellular antioxidant systems have the capability of maintaining oxidative stress homeostasis by a balance between ROS production and its elimination (165). However, these endogenous oxidative stress defense mechanisms are overwhelmed during pathological conditions such as hyperglycemia and/or ischemia-induced oxidative stress. Glutathione reductase and peroxidase play a key role in the recycling of glutathione between its reduced (GSH) and oxidized (GSSG) forms. Glutathione peroxidase removes hydrogen peroxide through the oxidation of GSH to GSSG, while glutathione reductase acts as an antioxidant by converting GSSG to GSH. SOD provides further defensive core by conversion of superoxide to hydrogen peroxide that is then converted to water by catalase (another core antioxidant). SOD is present in three isoforms, i.e. SOD1; a dimer found in the cytoplasm, whereas SOD2 and SOD3 are tetramers found in the mitochondrion and extracellular matrix, respectively (477). Accumulating evidence supports the concept that decreased Cu/Zn-SOD activity leads to apoptotic cell death. Moreover, SOD glycation and reactive oxygen intermediates (ROI) produced from glycated proteins are also involved in many diseases, including diabetic complications (524, 687).

For the present study, we have a particular interest in hyperglycemia and/or ischemia and reperfusion-mediated superoxide generation (by the ETC). Here, superoxide generation leads to peroxynitrite production that subsequently results in the inhibition of the glycolytic enzyme GAPDH, thereby causing increased flux of glycolytic metabolites through the non-oxidative glucose pathways such as polyol pathway, formation of AGEs, the hexosamine biosynthetic pathway (HBP) and activation of protein kinase C (PKC). This will further exacerbate oxidative stress under hyperglycemic conditions and

hence contribute to micro- and macro-vascular complications of diabetes. **One of the aims of this thesis is to elucidate the relative contributions of non-oxidative glucose pathways to cardiac function during ischemia and reperfusion under hyperglycemic conditions.**

## **2.6 Glucose flux through the non-oxidative pathways**

Multiple biochemical pathways are proposed to link the adverse effects of hyperglycemia with vascular complications. As discussed earlier, intracellular hyperglycemia causes overproduction of ROS by the mitochondrial ETC, thereby creating oxidative stress that leads to high glucose-induced superoxide generation. The resultant peroxynitrite causes DNA strand breaks thereby activating poly(ADP)-ribose polymerase (PARP). Poly(ADP-ribosyl)ation represents an immediate cellular response to DNA damage induced by oxidants (97, 136, 168). Indeed, DNA damage is observed in both T1DM and T2DM patients, and can be prevented by vitamin E supplementation (616).

Poly(ADP-ribosyl)ation is usually a very rare event, but it can increase over 100-fold upon DNA damage. Under these conditions, about 90% of poly(ADP-ribose) is synthesized by poly(ADP-ribose) polymerase 1 (PARP-1) (507). PARP-1 is constitutively expressed but enzymatically activated by DNA strand breaks (56, 97). Thus, it functions as a DNA damage sensor and signaling molecule binding to both single- and double-stranded DNA breaks. PARP-1 catalyzes the formation of ADP-ribose from  $\text{NAD}^+$  by cleavage of the glycosidic bond between nicotinamide and ribose (56, 97). Glutamate, aspartate, and carboxyterminal lysine residues of target (“acceptor”) proteins are then covalently modified by the addition of an ADP-ribose subunit, via formation of an ester bond between the protein and the ADP-ribose residue. Here GAPDH is poly(ADP)-ribosylated in a covalent posttranslational modification linked with genome protection (56, 97). It is plausible to suggest that the inhibitory effect of ADP-ribosylation on GAPDH probably represents a feedback loop in order to reduce levels of glycolysis, and transiently block the subsequent flux of metabolites to mitochondria allowing a



decrease in the levels of reducing equivalents and the subsequent mitochondrial ROS production and oxidative cellular and molecular damage (517). However, this causes upstream accumulation of glycolytic metabolites resulting in increased activation of the polyol (531, 532), AGE (754), PKC (388, 389), HBP and enhanced ROS production and actions (86) as discussed below.

### 2.6.1 Polyol pathway

Under normoglycemic conditions in mammalian cells, intracellular glucose is mainly phosphorylated into glucose-6-phosphate by hexokinase thereby entering the glycolytic pathway. Only trace amounts (~3%) of glucose enter the polyol pathway. With hyperglycemia, however, flux through the polyol pathway accounts for more than 30% of glucose metabolism (180, 245, 637, 713, 771). Here the rate limiting step is the reduction of glucose to sorbitol catalyzed by aldose reductase (AR), a member of the aldo-keto reductase (AKR) family of proteins (589). AR is a monomeric oxidoreductase located in the cytosol and is able to catalyze the nicotinamide adenosine dinucleotide phosphate (NADPH)-dependent reduction of several carbonyl compounds, including glucose despite its low affinity for this compound (86, 208, 233). This reaction occurs at the expense of NADPH. Sorbitol is in turn converted to fructose by sorbitol dehydrogenase (SDH) with  $\text{NAD}^+$  as a co-factor (86, 180, 445, 589, 637, 771) (see Figure 2.4). This pathway was first identified in the seminal vesicle by Hers (1956) who demonstrated the conversion of blood glucose into fructose as an energy source for sperm cells (303). AR has since been isolated and identified from several human and animal tissues such as various eye regions (289, 305, 652), ovary (334), kidney (143) and the brain (144).

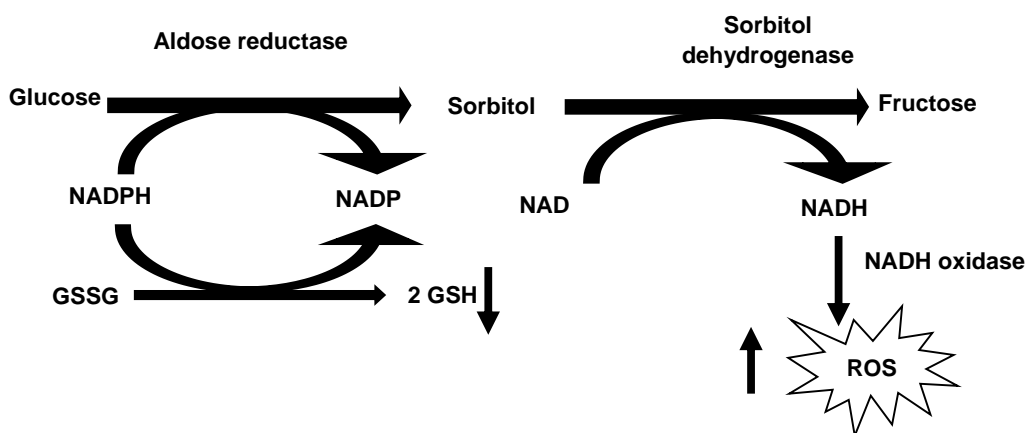


**Figure 2.4 Role of the polyol pathway in hyperglycemia-induced oxidative stress.** NADPH-reduced nicotinamide adenine dinucleotide phosphate; NADP- oxidized nicotinamide adenine dinucleotide phosphate; NAD- oxidized nicotinamide adenine dinucleotide; NADH- reduced nicotinamide adenine dinucleotide, GSSG-oxidized glutathione; GSH- reduced glutathione; ROS- reactive oxygen species.

### 2.6.1.1 Contribution of the polyol pathway to diabetic oxidative stress and complications

With diabetes, the polyol pathway induces oxidative stress through various ways. Firstly it depletes NADPH and consequently decreases reduced glutathione (GSH) levels (86, 445, 637, 694) (refer Figure 2.4). Intracellular depletion of NADPH also leads to lowered NO synthesis since NADPH is a cofactor for NO-synthase which synthesizes NO from L-arginine (694) thus increasing development of vascular complications under hyperglycemic conditions. The conversion of sorbitol into fructose increases NADH levels, a substrate for Nox (see Figure 2.4) and hence elevated superoxide production (180, 497). Furthermore, fructose (end-product), can be further metabolized into fructose-3-phosphate and 3-deoxyglucosone, which are more potent non-enzymatic glycation agents than glucose (278). This implies that flux through the polyol pathway would increase formation of AGEs and ultimately ROS. Studies also show that AR reduces a number of lipid peroxidation-derived aldehydes (LDAs), and their GSH conjugates thereby contributing to cellular toxicity, tissue and DNA damage leading to apoptosis, and necrosis and uncontrolled growth (659). Additional damage also comes from sorbitol (impermeable to biological membranes) that evokes osmotic vascular damage in cataracts of

the eyes as it accumulates inside cells (305, 652). The involvement of sorbitol in osmotic vascular damage, however, is often difficult to rationalize (86, 637).

Based on these putative mechanisms, inhibitors of AR have been used experimentally and in clinical trials for several decades (140), e.g. synthetic drugs such as hydantoins (sorbitol) and carboxylic acids (e.g. tolrestat, penalrestat, epalrestat and zopolrestat) (279, 329, 330, 694, 807). However, some synthetic drugs induced hypersensitivity in clinical trials (78) without much beneficial effect. Other therapeutic options such as supplementation with vitamin C have reduced sorbitol levels in erythrocytes of young T1DM patients (147). AR inhibitors also include flavonoids isolated from various plants such as luteolin, apigenin, linarin and acacetin (416, 417, 474). Moreover, reno-protective effects were observed with berberine, one of the main constituents of *Coptis chinensis* (Franch) [Ranunculaceae] and *Phellodendron amurense* (Ruprecht) [Rutaceae], and this was associated with a concomitant inhibition of oxidative stress (436). Other isolated bioactive compounds from plants that inhibit AR activity include quercetin, silymarin, and puerarin (78). Of note, decreased AR activity prevents production of sorbitol and its downstream stimulation of AGE formation, and PKC pathways which are described in the next sections. Together these data show that the polyol pathway and AR are important targets for therapeutic interventions to treat T1DM and T2DM.

### **2.6.2 Advanced glycosylation end products (AGEs)**

The non-enzymatic glycation reactions were first described around the turn of the century by Louis Camille Maillard who predicted that it would have an important impact on biomedical science - he coined the term “Maillard reaction” (455). Protein glycation occurs through a series of reactions that can be divided into a) stressors, i.e. sources of carbonyl agents that can drive the reaction, b) propagators, i.e. the reactive dicarbonyl agents that arise from the precursor stressors, and c) end products that mark the formation of the AGEs resulting from the Maillard reaction (495). This

distinction is quite helpful in defining the various steps where interference should be targeted, especially since this thesis also focuses on preventing oxidative stress through the non-oxidative pathways.

The protein glycation process starts with a nucleophilic addition reaction between a free  $\epsilon$ -amino group or N-terminal group of proteins, and the carbonyl group of a reducing sugar (normally glucose) to form a reversible Schiff base (10, 11) (see Figure 2.5). The latter can rearrange into a stable, irreversible ketoamine or Amadori product (721, 750). Major sources of the carbonyl group in the glycation reaction include glucose and glyceraldehyde (614). The Schiff base is highly prone to oxidation and free radical generation leading to formation of oxoaldehydes, glyoxal and methyglyoxal, in the so called Namiki pathway of the Maillard reaction (513) (refer Figure 2.5) which occurs early in the glycation process. Further, methyglyoxal can arise by spontaneous  $\beta$ -elimination of phosphate from triose phosphates, which are increased during hyperglycemia from inhibition of glycolysis.

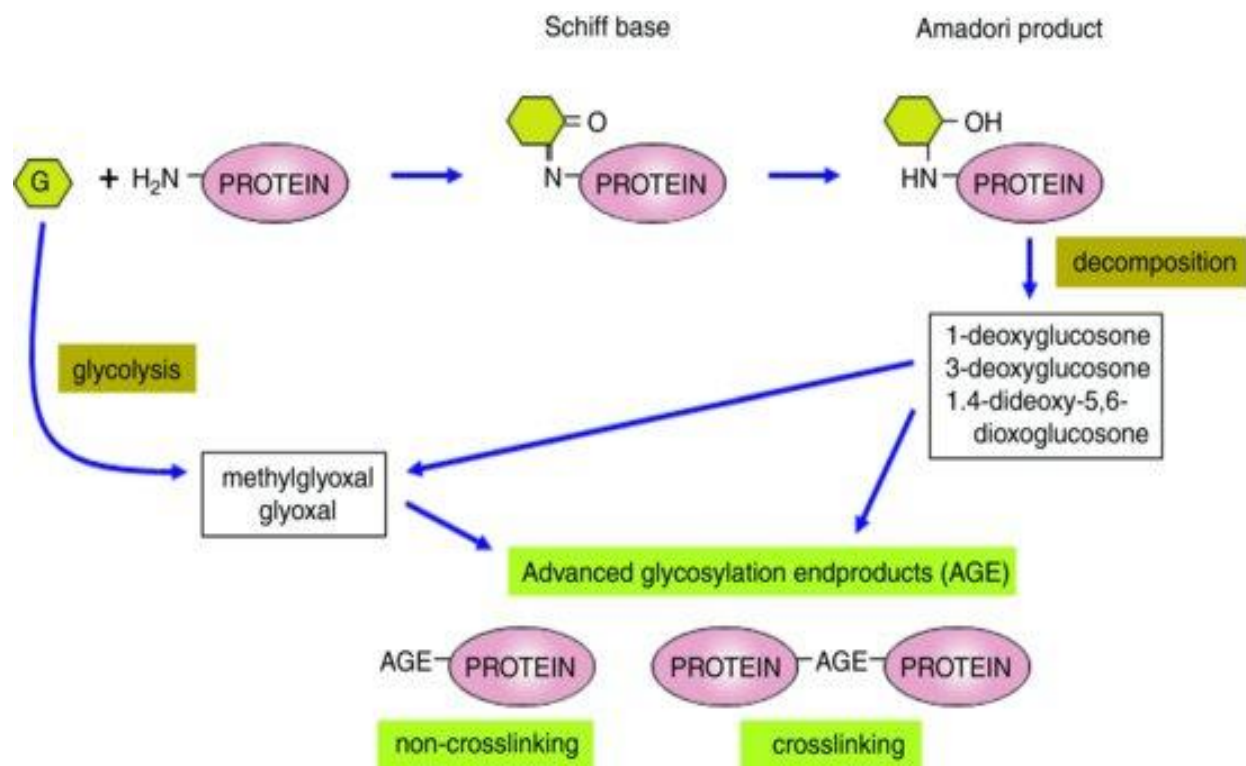


**Figure 2.5 Simplified biochemistry of advanced glycation end product formation.** Prolonged hyperglycemia and oxidative stress during diabetes result in the production and accumulation of advanced glycation end products (AGEs). G-glucose.

Another oxidative pathway suggested that metal-catalyzed auto-oxidation of reducing sugars could be involved in AGE formation (318, 319, 762, 763). For example, fructose-lysine can bind redox-active copper to produce N-carboxy-methyl (lysine) (CML) and generating hydrogen peroxide in the process thus contributing to oxidative stress from AGE formation (617). This is an example of the Fenton reaction where copper ions attached to glycated proteins become reactive or increase reactivity of the glycated protein (25). AGEs can be generated from the Amadori product either by auto-oxidation into reactive dicarbonyl products such as glucosones (for instance methylglyoxal and 1,4-deoxyglucosone) (90) (see Figure 2.5), or be fragmented by glycooxidation to produce CML or pentosidine from lipids (also called advanced lipoxidation end products [ALEs]). It therefore follows that CML is formed by both glycooxidation and lipoxidation (617). The glycation spontaneous reaction, however, depends on the degree and duration of hyperglycemia; turnover of proteins; and availability and reactivity of the

amino groups on proteins. Moreover, it is known that this process is accelerated with diabetes (86, 614, 637, 696, 786).

Since methylglyoxal, the major source of intracellular AGEs (357) is very cytotoxic, eukaryotic cells have developed a system to metabolize it once formed in physiological situations. Together with its two carbon analog (glyoxal), methylglyoxal is physiologically metabolized by the cytosolic glutathione-dependent glyoxalase 1 and 2 to D-lactate (706). Lower expression of glyoxalase was reported with diabetes (583) and glyoxalase 1 deficiency increases intracellular AGEs (3, 488). Furthermore, methylglyoxal can increase oxidative stress by causing glycation and inactivation of glutathione reductase and peroxidase (488). Methylglyoxal can also directly deplete GSH in various cell types so that the cell becomes more sensitive to oxidative stress. Moreover, reduced GSH availability will affect the glyoxalase system and impair methylglyoxal degradation thus establishing a vicious cycle that leads to a further increase of methylglyoxal levels (706).

#### **2.6.2.1 Contribution of AGE pathway to diabetic oxidative stress and complications**

AGEs damaging effects are achieved either directly where glycated proteins cause oxidative stress (502), or indirectly through their interaction with receptors - especially receptors for AGEs (RAGE) (520, 778). Examples of the direct effects of AGEs include altered enzyme activity, decreased ligand binding and modification of protein half-life (737). Additionally, glycation-derived free radicals cause protein fragmentation and oxidation of nucleic acids and lipids (47, 48). Furthermore, AGEs form crosslinks thereby altering the structure and function of proteins, such as serum albumin, lens crystallin, intracellular proteins and collagen in the extra cellular matrix (86, 156, 614, 637, 786). These crosslinkages also reduce matrix protein flexibility hence abnormal interaction with their respective receptors on cells (86, 291).

RAGEs are present on various cells, including endothelial cells, mesangial cells and macrophages (86, 156, 637, 786). The elucidation of RAGE modulatory roles and signal transduction pathways are areas of intensive investigation. Thus, recent evidence suggests that RAGE binding initiates signaling activation of PKC (480, 627), tyrosine phosphorylation of Janus kinase (JAK)/signal transducers and activators of transcription [STAT]), (316), recruitment of PI 3-K to the ras-dependent mitogen-activated protein kinase (MAPK) (430) or PKC (159, 388, 410, 645), and induction of oxidative stress cascades which culminate in nuclear factor (NF)- $\kappa$ B and activator protein-1 (AP-1) transcription (62, 86, 786, 808). One of the crucial pathways impaired in this process is cellular NO signaling (808) which eventually causes the development of atherosclerosis and CVD under hyperglycemic conditions. Such signaling pathways also lead to a tissue-specific pro-inflammatory environment. RAGE activation and stimulate the renin angiotensin system (RAS) leading to increased angiotensin II formation (182, 211, 489). In support, blockade of RAS pathway activation decrease levels of AGEs and prevent associated detrimental effects, e.g. retinopathy (182, 211, 489). AGE pathway is closely associated with the development of cardio-metabolic complications and its accumulation can predict the severity of micro- and macro-vascular in diabetic patients (632).

As such, various strategies have been developed to prevent the detrimental effects of AGEs. These include: trapping of reactive dicarbonyl species; use of antioxidants such as transition chelating metal ions and free radical scavengers; breaking of AGE cross-links; blocking RAGE and its downstream signaling pathways; glycemic control; and AR inhibition and shunting of trioses towards the pentose phosphate pathway by transketolase (TK) activation (553). The inhibitors have multiple sites of action and only a few agents will be discussed. Firstly, glycemic control is a key intervention since AGEs formation is greatly accelerated under high glucose conditions (494) and reduced glucose levels prevent the glucose-dependent first step in the Maillard reaction. To our knowledge there is not much information on the effect of anti-hyperglycemic drugs on non-oxidative glucose pathways. One is

metformin (52, 343). Other drugs such as thiazolidinediones (470) and aspirin formulations are also successfully employed in AGE attenuation (723, 776).

The importance of inhibiting non-oxidative pathways emerged from the DCCT study where CVD complications occurred in association with increased levels of AGEs despite the presence of good glycemic control (189). Thus, this observation is consistent with the hypothesis that other factors e.g. oxidative stress also contribute to the production and accumulation of AGEs (32, 48), and that metabolic memory predisposes diabetic and non-diabetic patients to CVDs even after glycemic control (280).

The inhibition of AGE formation opens several exciting possibilities for the prevention of organ damage with diabetes. Here various approaches were employed including the prevention of AGE-formation, and reducing interaction of AGE with RAGE, i.e. ligand interactions/ signaling pathways effects or break established AGE crosslinks. Interestingly, vitamins and derivatives also exhibit the potent ability to decrease AGEs in diabetic animals (357) and patients (559). Synthetic anti-AGE agents are another focus area and were employed both in experimental animals and clinical trials to combat AGE formation. This included pimagedine (also known as aminoguanidine) that prevents formation of irreversible AGEs by trapping of reactive dicarbonyl intermediates (84, 704, 705). This approach yielded positive outcomes, i.e. slowing progression of overt nephropathy and retinopathy. However, it did not demonstrate statistically significant effects on lowering serum creatinine and urine albumin with T1DM, possibly because of its increased renal clearance (72). Another agent ALT-711/alagebrium breaks pre-accumulated AGEs and showed beneficial effects in preventing diabetic cardiomyopathy (28). In summary, AGEs play a central role in the pathogenesis of diabetic complications. Part of these effects are mediated by generation of increased oxidative stress. One such mechanism involves increased Nox activity via PKC- $\beta$ II (766); hence activation of this pathway in the development of diabetic complications is discussed below.



### 2.6.3 Protein kinase C

PKC, a family of at least twelve enzyme isoforms of the AGC (cAMP-dependent protein kinase/PKG/PKC) family, is a serine/ threonine-related protein kinase that plays a key role in many cellular functions and affects multiple signal transduction pathways (521). It acts by catalyzing the transfer of a phosphate group from ATP to various substrate proteins, and PKC itself undergoes a series of complex phosphorylation steps before activation, during which time it translocates from the cytosol to the cell membrane. Approximately 12 isoforms have been identified to date which differ in structure and substrate requirements (668). Nine of the PKC isoforms (including PKC- $\alpha$ ,  $\beta$ I,  $\beta$ II,  $\gamma$ ,  $\delta$ ,  $\epsilon$  and  $\xi$ ) are activated by the second messenger DAG, a critical signaling molecule that regulates many vascular functions such as permeability, growth factor signaling, vasodilator release and endothelial activation (12, 86, 366, 637).

DAG levels are increased with hyperglycemia, and is formed by multiple pathways, including agonist-induced hydrolysis of phosphatidylinositol (PI) by phospholipase C (PLC) (12, 86, 196, 366, 637), or *de novo* synthesis from the glycolytic intermediates dihydroxyacetone phosphate (DHAP) and glycerol 3-phosphate (767). By contrast, several studies show that the PLC pathway does not contribute to the diabetes-induced increase in DAG levels. For example, exposure of rat aortic smooth muscle cells to elevated glucose concentrations increased DAG levels without changing levels of inositol 1,4,5-triphosphate, a derivative of PI hydrolysis (767). The *de novo* synthesis or direct metabolism of glucose to DAG involves the conversion of the glycolytic intermediate DHAP to lysophosphatic acid and then phosphatidic acid (PA). DAG kinase can convert PA to DAG and *vice versa*. The involvement of this pathway in glucose-induced DAG formation has been confirmed in labeling studies where  $^{14}\text{C}$ -labeled glucose levels revealed the incorporation of glucose into the glycerol backbone of DAG in aortic endothelial cells and smooth muscle cells (328, 767).

### 2.6.3.1 Contribution of PKC activation to diabetic oxidative stress and complications

There is a growing body of evidence for the central role of PKC in signal transduction pathways in hyperglycemia-induced complications (328, 767, 768). Increased flux through the other non-oxidative glucose pathways, partly involves activation of the PKC signaling pathway in eliciting their detrimental effects. Increased PKC levels during diabetes onset are found in a) vascular tissues, including the retina (639) aorta, heart (328) and renal glomeruli (332); and b) non-vascular tissues such as liver and skeletal muscles (300). Moreover, ROS itself e.g. hydrogen peroxide can also activate PKC further exacerbating oxidative stress (12, 86, 196, 366, 637, 732). For example, endogenously formed pro-oxidants from PKC activation promote formation of oxidized low density lipoprotein (ox-LDL) (653) that cause endothelial cell activation and injury (critical in the pathogenesis of atherosclerosis). Here, lysophosphatidylcholine a major constituent of the ox-LDL, further increases activation of PKC and consequently ROS formation (775).

PKC activation mainly results in ROS production through enhancing Nox activity (766). Indeed, lysophosphatidylcholine-induced PKC activation is a critical upstream activator of Nox via phosphorylation of p47phox in various cells (33, 424). Nox activity can be further elevated by increased endothelin-1 (ET-1) levels and associated with enhanced angiotensin II stimulation in endothelial cells that leads to p47phox phosphorylation (33, 424). These data confirm that increased Nox activation by PKC can enhance superoxide production as earlier discussed in section 2.5.1. Also, Quagliaro *et al.* (2003) demonstrated that an intermittent high glucose challenge in endothelial cells resulted in Nox activation that was sensitive to PKC inhibitors (573).

Enhanced PKC activity is associated with changes in blood flow, basement membrane thickening, extra cellular matrix expansion, vascular permeability, angiogenesis, cell growth and enzymatic activity alterations (196). During diabetes, activation of PKC may impair retinal and renal blood flow possibly

by increasing ET-1 levels (86). PKC activation also directly increases the permeability of macromolecules across endothelial or epithelial barriers by phosphorylating cytoskeletal proteins, or indirectly by regulating expression of various growth factors such as vascular endothelial growth factor (VEGF) (12, 86, 196, 366, 637, 732). The effects of PKC activation on NO are unclear, though there is evidence that it can reduce the production of NO (12, 86, 196, 366, 637, 732). All these factors can lead to accelerated atherosclerosis thus predisposing to the development of micro- and macro-vascular complications.

Most of the manifestations due to PKC activation in diabetes mellitus are reversed with the use of PKC inhibitors (12, 86, 196, 366, 637, 732), e.g. ruboxistaurin (PKC- $\beta$  inhibitor) reverses hemodynamic changes that manifest with retinopathy, nephropathy and neuropathy (12, 86, 196, 366, 637, 732).

#### **2.6.4. The hexosamine biosynthetic pathway**

The HBP is a relatively minor branch of glycolysis. It involves conversion of glucose to fructose-6-phosphate, then fructose-6-phosphate to glucosamine-6-phosphate by the first rate-limiting enzyme glutamine: fructose-6-phosphate amidotransferase (GFAT) (see Figure 2.6). The major end-product is uridine diphosphate-*N*-acetylglucosamine (UDP-GlcNAc) (formed from glucosamine-6-phosphate) which along with other HBP generated amino-sugars provide essential building blocks for glycosyl side-chains of proteins and lipids (94) (see Figure 2.6). UDP-GlcNAc is further processed by the second rate-limiting enzyme, *O*-linked GlcNAc transferase (OGT), that transfers GlcNAc to the side-chain hydroxyls of serine and threonine residues to generate  $\beta$ -D *O*-linked glycosylated proteins (see Figure 2.6). Modification of serine and threonine residues of nuclear and cytoplasmic proteins was first identified in 1984 (710), and it occurs at essentially the same serine and threonine side-chains that are targeted by the phosphorylation process, thus *O*-GlcNAc and phosphorylation have potential reciprocity (392, 469). The reversal removal of *O*-GlcNAc residues is carried out by the enzyme *O*-

GlcNAc hydrolase/O-GlcNAcase. The addition of O-GlcNAc to proteins modulates behavior via different mechanisms that include: regulating protein phosphorylation and thus protein function; altering protein degradation; adjusting the localization of proteins; modulating protein-protein interactions and mediating transcription (794).

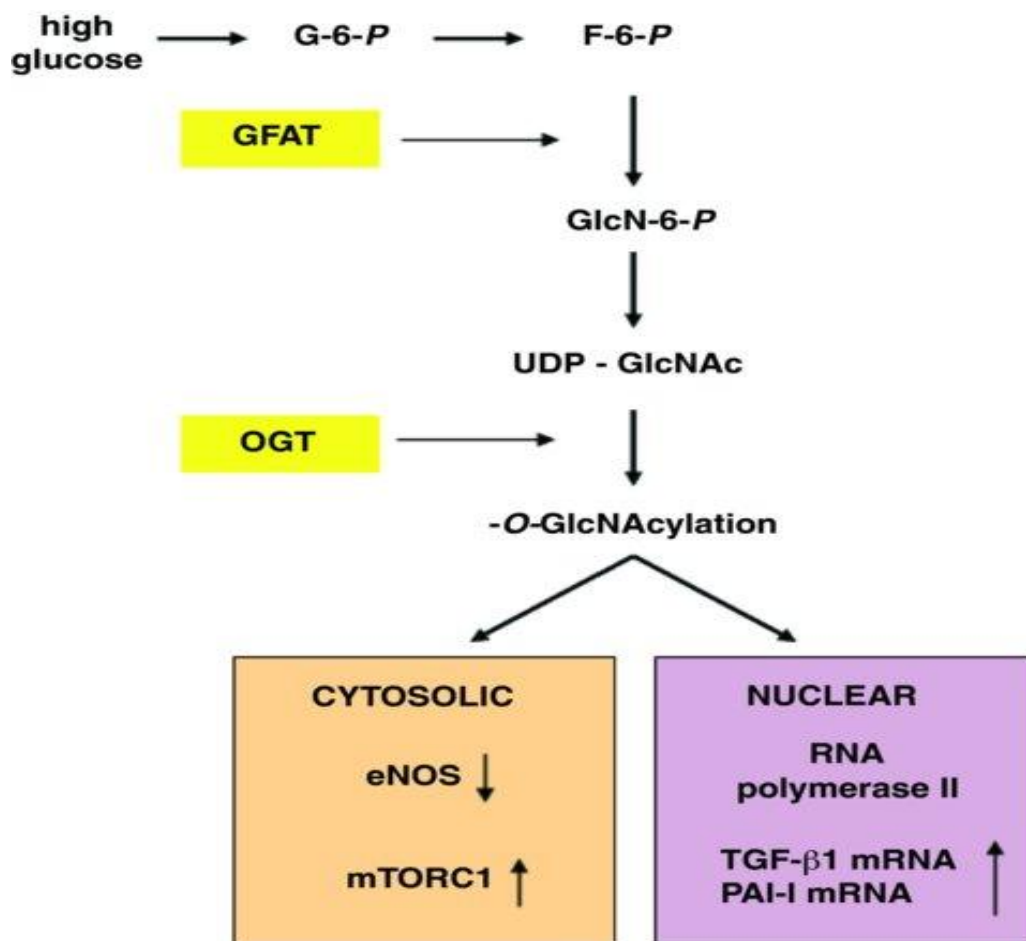


**Figure 2.6 Activation and downstream targets of the hexosamine biosynthetic pathway in diabetes.** Key enzymes in the pathway are highlighted in yellow. G-6-P, fructose-6-phosphate; F-6-P, fructose-6-phosphate; GFAT, glutamine:fructose 6-phosphate amidotransferase; GlcN-6-P, glucosamine 6-phosphate; UDP-GlcNAc, UDP-N-acetylglucosamine; OGT, O-GlcNAc transferase; eNOS, endothelial NO synthase; mTOR, mammalian target of rapamycin; TGF- $\beta$ 1, transforming growth factor- $\beta$ 1; PAI-I, plasminogen activator inhibitor-I.

#### 2.6.4.1 Contribution of the HBP to diabetic oxidative stress and complications

The HBP usually functions as a nutrient sensor under physiological conditions (285). However, during hyperglycemia excess glucose is shunted into the HBP, and this is linked with the development of

insulin resistance (468, 785). This implies that under hyperglycemic conditions increased amounts of fructose-6-phosphate are diverted from glycolysis that provide substrates for reactions that require UDP-*N*-acetylglucosamine, such as proteoglycan synthesis and the formation of O-linked glycoproteins (86). Shunting of excess intracellular glucose into the HBP may account for several manifestations of diabetic renal and vascular complications (94). At present there are very few studies done to show a causal link between HBP activation and high glucose-induced complications in diabetic patients. Recently, a study from our laboratory showed increased HBP activation and O-GlcNAc levels in leukocytes of pre- and full blown diabetic individuals (656). Moreover, an association of GFAT mRNA levels and enzyme activity with post-prandial hyperglycemia and oxidative stress was found in T2DM patients (658). Here, HBP activation correlated with thiobarbituric acid reactive substances (TBARS) and protein carbonyl content (PCO), both markers of oxidative stress. The end-product of this pathway, UDP-GlcNAc, is a substrate for the glycosylation of important intracellular modulators (86) including transcription factors, thereby affecting the expression of several genes, e.g. plasminogen activator inhibitor-1 (PAI-1) (see Figure 2.6). This in turn can lead to the development of diabetes-induced micro-vascular complications (221, 241, 242).

Increased protein O-linked GlcNAcylation can result in diminished expression of sarcoplasmic reticulum Ca<sup>2+</sup>-ATPase (SERCA) in the diabetic heart thereby impairing myocardial contractility (134, 315). Additionally, upregulation of the HBP with hyperglycemia may accelerate atherosclerosis (175, 198, 657) by decreasing eNOS levels (see Figure 2.6) in the vascular endothelium and thereby promoting endoplasmic reticulum stress, lipid accumulation and increased inflammatory gene expression (77, 612, 755) which predispose to AMI.

There is growing evidence (*in vitro* and *in vivo*) that highlight a pivotal role for the HBP in the onset of diabetic nephropathy (473) and (155). This may occur as a result of HBP-mediated induction of TGF- $\beta$  and PAI-1 in vascular smooth muscle, mesangial (379, 753) and aortic endothelial cells (94).

Following TGF- $\beta$  production, it is converted to its active form (TGF- $\beta$ 1) that causes the subsequent production of matrix components (heparan sulphate, proteoglycan, fibronectin). These (matrix components) in turn, alter protein structure and function thus leading to micro-vascular complications. This can result in kidney cellular hypertrophy as previously demonstrated (473). Moreover, PAI-1 induction is mediated by the transcription factor, Sp1 that can be regulated by the HBP. Here PKC  $\beta$ I and  $\delta$  (241) activation was required, therefore suggesting a link between the HBP and PKC under hyperglycemic conditions.

When focusing on ischemia and reperfusion, there are contradictory reports whether an increase in protein O-GlcNAcylation is beneficial or detrimental. Chatham and colleagues report on the beneficial effects of increasing flux through the HBP (121, 122), whilst Essop and colleagues found that increased HBP flux under high glucose conditions followed by ischemia and reperfusion elicits detrimental effects on cardiac contractile function together with increased oxidative stress and apoptosis (462, 576). Consistent with these findings, others found that increased HBP can exert both an anti-inflammatory and pro-oxidative effect in endothelial cells under hyperglycemic conditions (578). It is likely that such differences stem from variations in experimental models, the nature of the stress condition (acute vs. chronic), and other unknown factors. This intriguing question is currently being pursued in our laboratory. Thus, it is clear that hyperglycemia-induced intra- and extracellular changes lead to alterations of signal transduction pathways, affecting gene expression and protein function to cause cellular dysfunction and damage. Moreover, data imply that the ultimate result is increased ROS formation and consequently diabetic complications (769). The next section will now discuss another non-oxidative glucose pathway – pentose phosphate pathway - that is altered with hyperglycemia.

## 2.6.5 Pentose phosphate pathway

The pentose phosphate pathway (PPP)/ phosphogluconate/ hexose monophosphate shunt is a multifunctional pathway and one of the two main biochemical pathways involved in glucose metabolism. It consists of two main branches, i.e. the oxidative and the non-oxidative branch, respectively. In addition to glucose oxidation, the PPP mainly generates reducing equivalents in the form of NADPH and pentoses (5-carbon sugars) such as ribose-5-phosphate and erythrose-4-phosphate used in the synthesis of nucleic acids and aromatic amino acids, respectively (747). In mammals this pathway occurs exclusively in the cytoplasm and is most active in the liver, mammary gland and adrenal cortex (440, 597). For the current thesis we have a great interest in the role of the non-oxidative PPP branch with diabetes (hyperglycemia), and in the setting of ischemia and reperfusion.

### 2.6.5.1 Non-oxidative branch of the PPP

Transketolase (TK) catalyzes several reactions in the non-oxidative PPP, and serves as a bridge between the oxidative PPP and the oxidative decarboxyl metabolism of glucose. This therefore allows the cell to adapt to a variety of metabolic needs under different environmental conditions (312). TK recognizes D-xylulose 5-phosphate, D-fructose 6-phosphate and D-sedoheptulose 7-phosphate as donors while D-ribose 5-phosphate, D-erythrose 4-phosphate, D-glyceraldehyde 3-phosphate and glycoaldehyde as receptor substrates (191). The main function of the non-oxidative PPP branch is to convert hexoses into pentoses, particularly glyceraldehyde 3-phosphate into ribose-5-phosphate that is required for nucleic acid synthesis.

TK relies on thiamine pyrophosphate (a thiamine pyrophosphate [TPP] ester) as cofactor for its function. Here the main source is from Vitamin B1 (thiamine) a water-soluble compound that has been

used for decades in the treatment of several disorders such as neurological, diabetic, and cardiovascular complications (23, 55, 560). More recently, studies found that thiamine can prevent diabetes and its associated complications (292, 560, 671, 703). The main sources of thiamine include various foods e.g. pork, poultry, fish, eggs (440). However, due to its water solubility, it has limited durable storage capacity in the body and there is rapid urine excretion, hence decreased bioavailability in comparison with its fat soluble analogs (36, 38, 66, 219, 253). A variety of lipid-soluble thiamine derivatives were discovered (as early as 1954); subsequently named “allithiamines” because they belong to the *Allium* family of vegetables e.g. crushed garlic and onions (219).

As earlier discussed (Chapter 1), a major focus of this thesis is on is the lipid soluble analog of thiamine, i.e. benfotiamine, that exhibits strong antioxidant properties (232, 625). Benfotiamine contains an open thiazole ring, which allows it to pass through the cell membrane (36). The classification of benfotiamine as a lipophilic agent is disputed by findings that showed its increased solubility in aqueous solutions e.g. water at pH < 7; and not in organic solvents e.g. benzene (740, 743). Thus, it is likely that benfotiamine is an amphipathic agent. Thiamine and its analogs are initially metabolized to thiamine monophosphate, then TPP/ thiamine diphosphate (TDP) that is required by TK. TK is a homodimer with two active sites that are localized at the interface between the monomers. Thus far one TK gene and two TK-like genes (TKTL1) and TKTL2) were identified within the human genome (431). TKTL1 may play a role in carcinogenesis and have implications in the nutrition and future treatment of cancer patients. Researchers have found TK variants and reduced activities of TK enzymes in patients with neurodegenerative diseases (e.g. beriberi), diabetes and cancer (440, 597). The role of TK as illustrated in Figure 2.7 is a two-way process; i.e. firstly converting xylulose-5-phosphate and ribose-5-phosphate to glyceraldehyde-phosphate and sedoheptulose 7-phosphate, respectively. These are then converted to erythrose 4-phosphate and fructose 6-phosphate by transaldolase. In the second TK pathway, xylulose 5-phosphate and erythrose 4-phosphate are



converted to glyceraldehyde 3-phosphate and sedoheptulose 7-phosphate. All the reactions are reversible and depend on substrate availability.

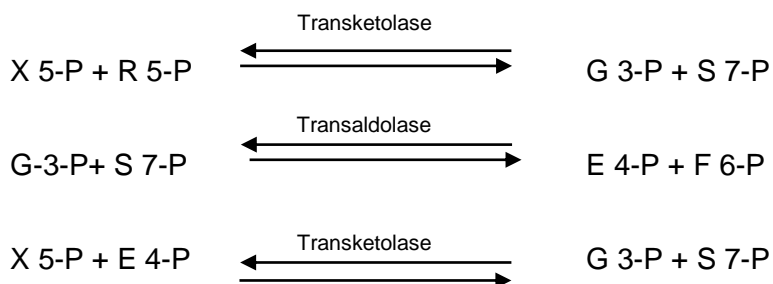


**Figure 2.7 The non-oxidative reactions of the pentose phosphate pathway.** X-5-P (xylulose-5-phosphate); R 5-P (ribose 5-phosphate); G 3-P (glyceraldehyde 3-phosphate); E 4-P (erythrose 4-phosphate); S 7-P (sedoheptulose 7-phosphate).

TPP is also a cofactor of other enzymatic reactions that cleave alpha-keto acids in the TCA cycle, i.e. pyruvate dehydrogenase and  $\alpha$ -ketoglutarate (55, 253, 440, 560). This therefore implies that thiamine and its analogs can promote glucose oxidation. Thiamine is transported across the cell membrane by members of the solute carrier (SLC) family, mainly SLC19A2 and also SLC19A3 found ubiquitously in mammalian tissues (224, 509). Studies reported that benfotiamine is delivered into cells via the reduced folate carrier-1 (RFC-1), and then de-benzoylated to thiamine monophosphate by cellular and plasma esterases (66, 703). Various studies reported reduced levels of thiamin, activity of transketolase (32, 294, 339, 613, 724) and beneficial effects of benfotiamine treatment with diabetes (32, 54, 55, 292, 358, 360).

### 2.6.5.2 Oxidative branch of the PPP

For the oxidative PPP branch, glucose 6-phosphate is oxidized into 6-phosphogluconolactone (6PG) by the rate-limiting enzyme, glucose 6-phosphate dehydrogenase (G6PD). This reaction results in the production of the first NADPH molecule in the pathway. The unstable lactone ring of 6PG is opened up by a lactonase into 6-phosphogluconic acid which undergoes an oxidative decarboxylation by the 6

phosphogluconate dehydrogenase (6PGD) to yield a second NADPH molecule and carbon dioxide. The end product of this pathway, ribulose 5-phosphate, can then be converted into ribose 5-phosphate in the non-oxidative pathway to yield nucleotides via the TK reaction. From these reactions it can be deduced that the main role of the oxidative PPP branch is to produce NADPH which functions in detoxification processes, i.e. reduced glutathione regeneration and lipid biosynthesis (440, 597) as well as provision of ribulose 5-phosphate for nucleotide synthesis.

There are conflicting reports on whether G6PD activity is increased, decreased or not changed with insulin resistance/ diabetes. Some found that G6PD activity increases (263, 633) while others reported decreased activity (105, 107, 359, 678, 747, 800). Such conflicting data further extends to NADPH produced by this pathway, i.e. whether it contributes to or blunts oxidative stress. In fact, almost all the studies show that increased G6PD activity enhances Nox-induced ROS production via PKC activation. Similar findings were observed in various heart failure studies where G6PD activity is increased to provide more NADPH possibly as a compensation mechanism to counter oxidative stress (264, 265). However, the association of G6PD to increased Nox activity has been disputed by Balteau *et al.* (2011) who suggested that this effect is independent of glucose metabolism but relies on glucose uptake via sodium glucose transporter 1 (SGLT1) (40). The differences observed may be attributed to variations of experimental (*in vivo* and *in vitro*) and animal models used (humans, rats and mice), different tissues where G6PD was measured (liver, cardiac, pancreas and neurons). Moreover, G6PD activity varies with ischemia and reperfusion i.e. its activity can be increased (336) or decreased (358) resulting in either detrimental or protective effects. These outcomes imply that G6PD may act as a pro- or antioxidant depending on different ischemia and reperfusion methods and experimental systems (801). In summary, this section highlighted the pathophysiology of hyperglycemia-induced ROS production by increased flux through the non-oxidative glucose pathways. Furthermore, the effect of hyperglycemia on the PPP was considered. The next section will now discuss various complications that occur secondary to the increased activation of pathways discussed above.

## 2.6.6 Non-oxidative glucose pathways and cardiac function

The previous sections have extensively elaborated on the effects of the non-oxidative glucose pathways in general. However, since the focus of this thesis is to link these pathways to alterations in cardiac function, it is essential to clarify how these pathways have shown regulation of cardiac function under various conditions. These will be discussed in the same order as they are above. Firstly, the polyol pathway activation increases three-fold during ischemia and reperfusion (347) and possibly mediates ischemia-reperfusion injury by opening of the mitochondrial permeability transition pore (mPTP) (21, 321, 322) independent of hyperglycemia. The increased activation of the polyol subsequently causes cardiac contractile dysfunction by enhancing tyrosine nitration of the SERCA and oxidation of ryanodine proteins thus impairing its functional role in cardiac contractility (347, 691). Furthermore inhibition of the polyol pathway has shown improved cardiac energy metabolism under both normoglycemic and hyperglycemic conditions (579, 580), attenuation of oxidative stress and a restoration in electrolyte homeostasis (531, 691, 712, 759).

Several studies have shown that AGEs and RAGE do play a role on cardiac function through various mechanisms. AGEs increase following ischemia and reperfusion (88) and enhance myocardial injury through glycation inhibition of thioredoxin activity (748) resulting in contractile dysfunction. Furthermore, AGE-RAGE axis increases ischemia and reperfusion injury via the JNK and STAT pathways causing phosphorylation of GSK-3 $\beta$  (15, 88, 89, 634). In support inhibition of AGE formation (529) or interaction with RAGE (446) has shown an improvement in cardiac function *in vivo* studies.

PKC is increasingly recognized as a key regulatory cardiac enzyme in both normal and pathophysiological conditions. In these circumstances it plays a pivotal role in functional adaptations, with reports on increased activity during ischemia and reperfusion and hyperglycemia (674). This may either be cardio-protective or damaging depending on which isoform is activated and timing of

activation in the protocol (i.e. pre-ischemia, during ischemia, post-ischemia and reperfusion). Various studies highlight the role of PKC $\epsilon$  and  $\zeta$  in cardio-protection at both baseline glucose concentrations (770, 798) and hyperglycemic conditions (457) with/without ischemia and reperfusion. Hyperglycemia activates PKC- $\alpha$ ,  $\beta$  and  $\delta$  causing contractile dysfunction (132, 262, 328, 435).

The role of the HBP on cardiac function has been highlighted earlier as contradictory i.e. whether increased activation is beneficial (121, 122) or harmful (462, 576) to cardiac function. The discrepancy in these experimental findings likely stem from variations in experimental models, the nature of the stress condition (acute vs. chronic), and other unknown factors. Increased O-GlcNAcylation under hyperglycemic conditions has been previously reported to elicit similar detrimental effects on cardiac contractile function (134, 315, 462). It is likely that detrimental effects are mainly due to altered protein function, for e.g. increased protein O-linked GlcNAcylation diminished expression of cardiac SERCA and lead to impaired myocardial contractility (134, 315). Moreover, HBP-mediated induction of FAO may also blunt cardiac function under these conditions (407).

With regards to the PPP various studies have shown pivotal roles of both the oxidative and non-oxidative branches in cardiac function regulating in different conditions. Increased flux via the non-oxidative pathway under hyperglycemic conditions and with ischemia and reperfusion has shown cardio-protective effects in animal studies (336, 358, 801). In contrast, however there are contradicting findings on the outcome of increased activation of G6PD, the rate limiting enzyme of the oxidative PPP branch. The varying effects have been elaborated in section 2.6.5.2 above and clearly indicate that the PPP plays in the regulation of cardiac function.

## **2.7 Diabetic complications**

As discussed, chronic hyperglycemia is one of the main perpetrators predisposing to the development of micro- and macro-vascular complications with diabetes (167, 722). The latter is more common with T2DM, whereas, micro-vascular complications occur mainly in T1DM. Chronic hyperglycemia that occurs with diabetes is mainly due to derangements in carbohydrate, lipid and protein metabolism (575). For the current study, the focus is on one of the macro-vascular complications, i.e. myocardial infarction, since diabetic patients have a greater risk for fatal AMI with an impaired recovery than non-diabetic patients (153, 363, 663). The following section reviews both micro- and macro-vascular complications with diabetes.

### **2.7.1 Micro-vascular complications**

The pathogenesis of micro-vascular complications is similar in T1DM and T2DM (86, 637). Micro-vascular complications most common in T1DM include retinopathy, neuropathy, and nephropathy (47, 230, 744).

#### **2.7.1.1 Diabetic neuropathy**

Diabetic neuropathy is defined as signs and symptoms of peripheral nerve dysfunction in a diabetic patient where other causes of peripheral nerve dysfunction are excluded (41). It is one of the commonest complications of diabetes present in about half of patients (to varying degrees) and typically manifests as polyneuropathy or mononeuropathy (637, 695). The disease can develop in all types of diabetes mellitus, but more typically with T1DM compared to T2DM (433). Diabetic neuropathy leads to increased incidences of ulceration and limb amputations due to the irreversible progressive development of the disease (41, 83). Moreover, it accounts for silent myocardial infarction

and shortens the lifespan of diabetic patients. The prevalence of diabetic neuropathy increases with the duration of the diabetic state (41, 433).

The cause(s) of diabetic neuropathy may include any of the following: oxidative stress, ischemia, and inflammation, leading to dysfunction and loss of axons (433). Here oxidative stress can result due to increased PKC activity (as discussed before). Blood supply to neurons may be impaired by vascular damage and endoneural hypoxia due to oxidative stress (637, 732). Hypoxia further leads to capillary damage aggravating disturbances in axonal metabolism and nerve conduction (41). Distal symmetrical sensorimotor polyneuropathy characterized by thickening of axons of small myelinated and non-myelinated C-fibers is the most common type of diabetic neuropathy (41, 433, 637, 695), and is manifested by paresthesia, dysesthesia, pain, impaired reflexes and decreased vibratory sensation (41, 433, 637, 695).

Inhibition of the pathways involved in the etiology of diabetic complications, glycemic control, antidepressants and analgesics may be used to manage diabetic neuropathy (732, 764). Furthermore, studies indicate that plant derivatives such as  $\alpha$ -lipoic acid, primrose oil and capsaicin offer potential in the management of diabetic neuropathy (272). Also, in this study extensive work on thiamine and its derivative (benfotiamine) show that both agents can attenuate neuropathy (23, 292, 671, 703).

### **2.7.1.2 Diabetic retinopathy**

Diabetic retinopathy, due to damaged blood vessels of the retina, is the most common cause of blindness in diabetic patients (366, 387). Nearly all T1DM individuals and more than half of T2DM develop retinopathy ~ 15-20 years after diagnosis of diabetes (758). Large increases in glucose levels within the retina (if toxic) might damage retinal cells, particularly Müller cells. Because the  $K_m$  of the GLUT1 transporter is 5 mM, it does not saturate with substrate except under pathological conditions

(401). Retinal complications in chronic diabetes may be due to micro-vascular dysfunction, neuroglial abnormalities, and a toxic metabolic environment (366). Diabetic retinopathy is a duration-dependent disease that develops in stages and that may not be detected during the first few years of diabetes (387). It is classified as non-proliferative diabetic retinopathy (NPDR) and proliferative diabetic retinopathy (366, 387, 758). Additionally, NPDR is further divided into progressive stages: mild, moderate and severe (366, 387) and characterized by capillary basement membrane thickening, pericyte loss, micro-aneurysms, increased permeability, exudates deposits, and retinal micro-infarcts. The earliest sign of retinal damage during NPDR results from abnormal permeability and non-perfusion of capillaries, leading to the formation of micro-aneurysms. Visual acuity is impaired by macular edema, following the leakage of fluid and solutes into the surrounding retinal tissue (758). The later stages, sometimes called pre-proliferative retinopathy, show greater retinal damage as evidenced by increased retinal vascular blockage and infarcts (366, 387, 758).

Proliferative retinopathy develops if the pre-proliferative retinopathy is not treated and is characterized by abnormal proliferation of retinal blood vessels. These vessels are, however, fragile and hemorrhage quite easily. The resulting accumulation of blood in the vitreous humor from hemorrhaging vessels impairs vision; this impairment can be permanent due to complications such as retinal detachment (758). Biochemical abnormalities associated with hyperglycemia and identified in diabetic retinas include increased activation of PKC (389), AGEs formation (85, 541, 669), polyol pathway (29), and HBP (297). These lead to increased production of ROS and activation of growth factors that promote apoptosis (512). There is growing evidence that ROS and RNS are present in excess in diabetic retinas (178, 236, 237, 384), and in vascular endothelial cells (176, 570). Both ROS and RNS are toxic to tissues because of high reactivity and ability to non-enzymatically form covalent bonds. The various mitochondrial and non-mitochondrial ways through which they (ROS and RNS) are produced (409, 574, 718) were discussed earlier in section 2.5.1.

The pathways previously described particularly the polyol pathway (see section 2.6.1 - 2.6.4), lead to the structural and functional changes that occur with diabetes mellitus (366). Diabetic retinopathy, like most other complications of diabetes mellitus, does not usually occur in isolation in the diabetic state. Therefore, drugs, medicinal plants and their derivatives that are used to inhibit the pathways involved in the development of diabetic complications may also prevent the onset of diabetic retinopathy. For example, AGE pathway inhibition resulted in beneficial effects i.e. preventing progression of retinopathy and inhibiting hyperglycemia-induced thickening of the retinal basement membrane (9, 226, 280).

### **2.7.1.3 Diabetic nephropathy**

Diabetic nephropathy a leading cause of end-stage renal disorder (ESRD), accounts for significant morbidity and mortality with diabetes (68, 493, 615, 620). The pathophysiology of diabetic nephropathy involves interactions between metabolic and hemodynamic factors. Some metabolic factors include increased formation of AGEs, polyols and PKC activation (137, 138, 584). The involvement of these pathways in the development of diabetic nephropathy has been earlier described. Hemodynamic factors include systemic hypertension and the tone of both afferent and efferent arterioles (138). Diabetic nephropathy progresses from micro-albuminuria to overt proteinuria and then renal failure. During the initial stages of diabetes, there is enlargement of the kidneys and increased glomerular filtration rate (GFR), whereafter GFR progressively decreases (584, 700). The two main hypotheses that describe the initial events of diabetic nephropathy are the 'vascular hypothesis' and the 'tubular hypothesis' (795). The vascular hypothesis states that the initial hyperfiltration is due to a) an excessive production of vasodilator products like nitric oxide and prostaglandins, and b) increased osmolar load (734). Additionally, there is higher glomerular hydrostatic pressure associated with micro-albuminuria (402, 471). These features result in basement membrane thickening, mesangial proliferation, and glomerulosclerosis as a compensatory mechanism



to prevent electrolyte loss. By contrast, the tubular hypothesis proposes that hyperglycemia induces increased production of growth factors and cytokines which cause hyperplasia and hypertrophy of the nephron, particularly the proximal tubule (795). As a result increased reabsorption of sodium occurs in the proximal tubule, consequently reducing the sodium load to the macula densa (795). Experimental animal work indicates that the vascular hypothesis is more applicable considering that the hyperfiltration is observed within 24 hours of diabetes induction (795).

Nephron hypertrophy with diabetic nephropathy occurs because of excessive deposition of extra cellular matrix proteins involved in the architecture of glomerular basement membrane. These include multifunctional glycoproteins, laminin, fibronectin and type IV collagen. At the same time, there is decreased production and under-sulphation of heparan sulphate proteoglycan. This enhances the permeability to macromolecules since the glycoproteins and heparan sulphate proteoglycan normally interact to form a barrier to charged molecules (402). ET-1, which increases five-fold in diabetic animal models is implicated in glomerular hypertrophy mediated by TGF- $\beta$ 1. Indeed, experimental evidence indicates that inhibition of ET-1, TGF- $\beta$ 1 and the endothelin-1 receptor A with plant extracts improves renal function and ameliorates glomerular injury (290, 367, 511, 654). ET-1 production is augmented by vasoconstrictor, profibrotic and inflammatory substances, all of which are increased under hyperglycemic conditions. PKC activation also favors ET-1 production, as this is the signaling pathway leading to its (ET-1) upregulation (654). The effects of ET-1 are mainly directed at mesangial cells, and their proliferation is due to direct or indirect stimulation of mitogenesis (654).

Irrespective of all the other structural and functional changes, the mesangial alterations appear to be the main cause of declining renal function in experimental diabetic animal models (240, 402, 471). Hyper-filtration can be attributed to increased production of the vascular permeability factor in response to stretching of the mesangium (260). The decline in GFR is due to the expanded extracellular mesangial matrix which compresses the glomerular capillaries thereby reducing the

filtration surface area (240, 402, 471). The mesangial cells can also increase glucose uptake through increased expression of GLUT1 (239, 620). Higher glucose uptake exacerbates intracellular hyperglycemia and increases activity of previously described pathways. Various treatment modalities are employed to manage diabetic nephropathy, and these may target oxidative stress (e.g. lisinopril and benfotiamine) (32, 200), and inhibition of the RAS pathway (200).

## **2.7.2 Macro-vascular complications**

Diabetes mellitus is associated with coronary, cerebral and peripheral arterial disease (650). Coronary and cerebral arterial diseases can result in AMI and stroke, respectively. These disorders, with peripheral arterial disease are defined as macro-vascular diseases (86, 733).

### **2.7.2.1 Arterial diseases**

Arterial disease is strongly associated with T2DM rather than T1DM. This is the case since with T2DM the metabolic syndrome usually manifests, i.e. characterized by hypertension, dyslipidemia (increased triglycerides, decreased high density lipoproteins (HDL), and increased low density lipoproteins (LDL) resulting in inflammation and impaired fibrinolysis. All these factors precipitate changes in the vasculature and create an environment conducive for accelerated atherosclerosis (50, 596, 733). A greater risk to develop cardiovascular diseases, as well as increased morbidity and mortality, is thus observed in diabetic patients due to the toxic metabolic milieu found within the circulatory system (50, 596, 733, 734). The chief cause of cardiovascular diseases with diabetes is atherosclerosis which is described below.

### 2.7.2.2 Atherosclerosis

Diabetes is associated with impaired function of the endothelium which contributes to atherosclerosis (142). Endothelial dysfunction arises due to a disruption of the homeostatic factors, usually maintained through integrity of the endothelium barrier and the balance between vasodilators and vasoconstrictors (611, 733). Vasodilators include NO, prostacyclin and endothelium-derived hyperpolarizing factor (EDHF), while the vasoconstrictors ET-1 and angiotensin II are well-known ones (80, 142, 611, 733). However NO, is regarded as the key marker of vascular health (142).

With diabetes mellitus the endothelium barrier is disrupted by the oxidative stress and increased activity of the metalloproteinases resulting in the entrapment of excess atherogenic lipoproteins like VLDL, ox-LDL and lipoprotein (a) (194, 197, 733). This infiltration triggers an inflammatory response thereby attracting monocytes and T-cells (287, 288, 611), and also increased expression of adhesion molecules on the endothelium e.g. VCAM-1 and ICAM-1, P-selectin and E-selectin (194, 197, 514, 733). This in turn triggers adhesion of the attracted monocytes and T-cells to the endothelium (see Figure 2.6). After binding to the arterial wall the monocytes and T-cells can migrate into the sub-endothelial space and differentiate into macrophages and foam cells (287, 288, 611). This migration is attributed to chemo-attractants like ox-LDL, IL-1 and TNF- $\alpha$  produced as a result of activation of the transcription factors NF- $\kappa$ B and AP-1 (50, 194, 197).

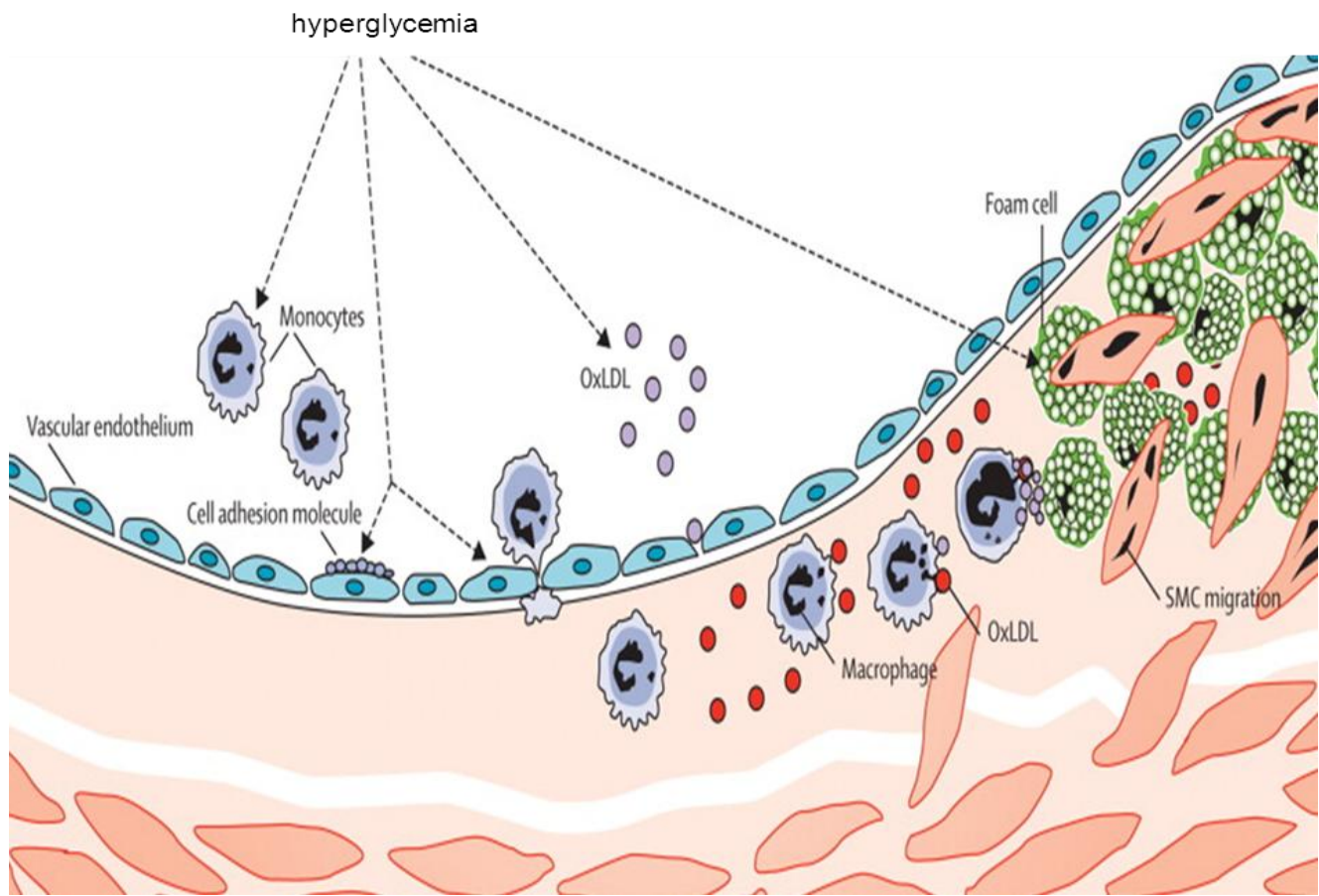


**Figure 2.8 Effect of hyperglycemia on atherosclerosis.** Hyperglycemia can promote several aspects of the atherosclerotic process, including monocyte recruitment and adhesion to the endothelium, penetration into the arterial intima, formation of oxidized LDL (ox-LDL), foam cell formation, vascular smooth muscle cell (SMC) migration and proliferation, leading to fatty streak formation. Modified from (603).

This inflammatory response together with reduced NO formation thus precipitate atherosclerosis with diabetes. Here, reduced NO formation may occur due to the deformed endothelium now exposing eNOS to uncoupling by peroxynitrite and nitrotyrosine. Thus, eNOS produces superoxide free radicals instead of NO (50, 540). NO production may also be inhibited by excessive liberation of FAs from adipose tissue due to PKC-induced inhibition of an eNOS agonist pathway involving PI 3-K (50). Thus, as NO bioavailability progressively decreases, concomitant increases in peroxynitrite further impair production of subsidiary vasodilators like the antiplatelet prostanoid, prostacyclin (50, 142, 733). It is therefore clear that the disordered endothelium exhibits an imbalance between vasodilators and vasoconstrictors, with the latter dominating e.g. increased vasoconstrictors ET-1 and angiotensin II. In

support, angiotensin II-induced increased voltage-gated calcium flux has been observed in vascular smooth muscle from diabetic rats possibly due to increased activity of the canonical transient receptor channels 1/4/5 (TPRC1/4/5) (195, 252). This was observed in association with increased vasoconstriction and accelerated atherosclerosis (195, 252).

Vasoconstriction is further exacerbated by the effects of acetylcholine on smooth muscle muscarinic receptors, thereby fueling the onset of atherosclerosis (50, 733, 734). The processes discussed above, together with hypertension and the impaired fibrinolytic capacity with the prothrombotic milieu, strongly contribute to the onset of atherosclerosis in the setting metabolic syndrome and diabetes mellitus (50, 197). Within the context of this thesis, it is a major cardiovascular risk factor for AMI in non-diabetic and diabetic individuals.

Prevention of atherosclerosis with diabetes mellitus is associated with a reduction in the development of micro- and macro-vascular complications. Some anti-atherosclerotic drugs e.g. statins are not limited to lowering atherogenic lipoprotein levels, but also possess beneficial anti-inflammatory effects (80). Likewise, oral anti-diabetic drugs can elicit similar outcomes (14, 391, 594). Moreover, plant derivatives also offer antioxidant effects, e.g. dietary polyphenols and flavonoids (quercetin) can reduce atherogenic lipoproteins and ameliorate the oxidative stress with diabetes mellitus (453, 670). Other targets implicated in this process include the AGE-RAGE axis. For example, blocking or genetically deleting the RAGE in diabetic experimental animals reverses atherosclerosis (324), while AGE inhibitors (e.g. aminoguanidine, OPB-9195, and pyridoxamine) lead to reno-protective effects in diabetic animals (291, 411). Unfortunately, clinical trials with OPB-9195 resulted in side effects i.e. trapping of pyridoxal leading to vitamin B6 deficiency (351, 644). Furthermore, inhibition of AGEs effects can also be achieved by breaking of the AGE cross links by employing drugs such as alagebrium, and also by attenuating AGE signal transduction e.g. by using incadronate disodium and cerivastatin (291).

Despite all the efforts to control glucose and lipid levels during diabetes the occurrence of HF amongst diabetic patients is increasing. This is secondary to the diabetic cardiomyopathy (discussed below) that occur independent of any other existing pathological condition besides diabetes.

### **2.7.2.3 Diabetic cardiomyopathy**

Diabetic cardiomyopathy is the presence of myocardial dysfunction in the absence of coronary artery disease and hypertension with diabetes, hyperglycemia considered the main trigger (261). This condition was first described by Rubler *et al.* (1972) who reported autopsy data from four patients with diabetic renal micro-angiopathy and dilated left ventricles in the absence of other common causes (606). It is characterized by systolic and diastolic function, with impaired systolic function manifesting as prolonged relaxation and reduced compliance (22). Several mechanisms are proposed for diabetic cardiomyopathy including oxidative stress, impaired glucose metabolism (444, 600), biochemical and physiological changes in hormonal signaling, a number of structural changes in the heart (444), and abnormalities of proteins that control ion movement (particularly calcium) (308, 408, 593).

With diabetes there is a shift in energy production to FAO, with glucose oxidation attenuated due to depleted GLUT1 and 4 levels (600). The end result is the onset of lipotoxicity (excess ceramides triggering apoptosis) and also accumulation FAO toxic intermediates that can impair myocyte calcium handling signaling (hence contractile dysfunction) (1, 183, 429, 458, 459, 600, 688). Excess lipids with diabetic cardiomyopathy enhance atherogenic mechanisms such as ox-LDL, endothelial dysfunction and vascular smooth muscle proliferation and migration (164). Furthermore, inhibited glucose oxidation results in accumulation of glycolytic intermediates that trigger the previously described non-oxidative glucose pathways (183, 429) signaling. Moreover, pathological changes in the diabetic heart are also linked to increased accumulation of ROS or RNS (99, 216).

With hyperglycemia various mechanisms increase myocyte death by both apoptosis and necrosis (216). Some of the mechanisms involved include increased ROS production by AGEs (452), phosphorylation of p53 (203), impaired sympathetic nervous system (65) resistance to IGF-I (124, 216, 261), and increased RAS activation (261). Additionally, these pathologies can result in structural changes of the heart during development and progression of the diabetic cardiomyopathy. Normally the myocardial fibrous tissue is interstitial, perivascular or both, however in pathology there is hypertrophy, interstitial fibrosis, capillary endothelial changes and capillary basal lamina thickening (204). These changes occur as a result of increased deposition of collagen I and II (in the epicardium, and perivascular tissue), and collagen IV (in the endocardium) (640). The collagen ultimately interacts with glucose to form AGEs contributing to the arterial stiffness, endothelial dysfunction and atherosclerotic plaque formation (26, 212). Furthermore, increased TGF- $\beta$ 1 occurs due to overstimulation of fibroblasts and this ultimately results in fibrous tissue deposition and extracellular matrix synthesis which eventually causes myocardial dysfunction (490).

Clearly it can be seen that hyperglycemia-induced toxicity plays an important role in the development of CVDs with diabetes. Since toxic effects are mainly as a result of hyperglycemia-induced oxidative stress that occurs during diabetes, attenuation of these effects may possibly be achieved by normalizing blood glucose levels. Hence, the next section discusses various drugs used during diabetes management, focusing on glycemic control in the diabetic heart.

## **2.8 Diabetes mellitus management**

The importance of blood glucose control in preventing complications of diabetes mellitus is now well recognized and the treatment regimen incorporates a controlled-energy diet, regular aerobic exercises and weight loss (167, 309, 331, 391, 546, 598). However, since most patients fail to achieve adequate blood glucose control with lifestyle interventions alone this also requires pharmaco-therapeutic

approaches (214, 331). There are many standard anti-diabetic drugs used in the management of diabetes mellitus. These include various formulations of insulin and oral anti-diabetic agents which can either be employed as monotherapies or in combination to achieve improved glycemic regulation (342, 598). Here oral anti-diabetic agents such as metformin is more effective when used in combination than when singly administered, e.g. with insulin, sulphonylureas and thiazolidinediones. Indeed, single therapy is less effective in maintaining normoglycemia particularly as diabetes progresses (374, 391). Recently, a 'polypill' treatment was suggested as a potential overall remedy for diabetes and its complications (391, 412), that includes an anti-hyperglycemic, anti-inflammatory, anti-hypertensive, and anti-angiogenic agents. According to Krentz and Bailey (2005), anti-diabetic drugs can be classified as insulin secretagogues, insulin sensitizers and those that delay carbohydrate absorption (391). The following sections discuss the anti-diabetic mechanisms of synthetic drugs.

### **2.8.1 Insulin**

Insulin, discovered in 1921, is the major hypoglycemic agent currently used in the management of T1DM and late stage T2DM (187). Patients who do not achieve effective glycemic control with oral agents, or for whom other oral agents are contraindicated, are also treated with insulin (391, 412). Robertson *et al.* (2003) (598) classify insulin as human insulin and insulin analogs, while another classification is based on the duration of action, i.e. rapid-acting, short-acting, intermediate-acting and long-acting (60, 742).

The short acting type is designed to mimic bolus insulin secretion, while intermediate or long acting insulin analogs are designed to mimic basal glycemic control (209, 742). Insulin is either administered subcutaneously using multiple daily injections, or an external pump for continuous delivery (306). Other delivery routes include oral, inhaled, nasal, rectal, ocular, intra-vaginal and transdermal (306, 689). Severe hypoglycemia is a major disadvantage of insulin usage with over-dosage observed with



several clinical trials such as the ACCORD, ADVANCE, UKPDS and DCCT (4, 8, 167, 722). Additionally Muis et al. (2005) reported increased occurrence of atherosclerosis with insulin usage as it promotes smooth muscle proliferation (501). However, here the combination of insulin with oral anti-diabetic drugs can reduce some of these disadvantages (154, 412, 472, 598, 689).

## **2.8.2 Insulin sensitizers**

### **2.8.2.1 Biguanides**

Phenformin (phenethylbiguanide) and metformin (1,1 dimethylbiguanide hydrochloride) are examples of biguanides. Metformin is derived from *Galega officinalis* (Linnaeus) [Fabaceae] (French lilac), a plant rich in biguanides (259, 391, 492). Metformin can be used alone or in combination with other drugs like sulphonylureas in diabetes management (34). Although the precise mechanisms whereby biguanides trigger hypoglycemia are less clear, the end result is that it can increase insulin sensitivity within the context of T2DM (34). This may occur by it enhancing insulin effects. Metformin's blood glucose lowering effects not only involve suppression of gluconeogenesis and glycogenolysis, but also enhancement of insulin-stimulated glucose uptake by skeletal muscle tissues (14, 391, 594).

Studies indicate that metformin activates AMPK, a heterotrimeric enzyme composed of a catalytic subunit ( $\alpha$ ) and two regulatory subunits ( $\beta$  and  $\gamma$ ) (391, 719). There are two isoforms of the catalytic subunit: AMPK  $\alpha$ 1, which is widely distributed, and AMPK  $\alpha$ 2, which is expressed in skeletal muscle, heart, and liver (217, 506). Previous studies found that AMPK is activated following depletion of cellular ATP, resulting in phosphorylation of AMPK by AMPK kinase at threonine-172 to prevent breakdown of carbohydrates (217, 506). The increase in AMPK activity results in the stimulation of glucose uptake, and the inhibition of hepatic glucose production, cholesterol and triglyceride synthesis, and lipogenesis. By contrast, the enzyme protein phosphatase 2C dephosphorylates AMPK and

results in its inactivation (391, 485, 506). Metformin also lowers blood glucose concentrations by decreasing intestinal absorption of glucose (374). Moreover, novel anti-hyperglycemic mechanisms of metformin may involve enhancement of  $\beta$ -endorphin secretion from adrenal glands and stimulating opioid  $\mu$ -receptors located in peripheral tissues. Here opioid  $\mu$ -receptors stimulation can increase expression and activity of GLUT4 transporters (128).

The efficacy of glycemic control accomplished with metformin is similar to that achieved with sulphonylureas, although their modes of action differ, i.e. metformin mainly acts by decreasing overproduction of glucose in the fasting state (335, 676). For example, its usage also has several beneficial pleiotropic effects (391). Furthermore, it can result in weight reduction, improves lipid profiles, and enhances endothelial function. The use of metformin, however, is contraindicated in conditions such as hypoxia, reduced perfusion of the heart in respiratory insufficiency and impaired renal function (391).

### **2.8.2.2 Thiazolidinediones**

Thiazolidinediones (TZDs) such as troglitazone, pioglitazone and rosiglitazone are selective and potent agonists of peroxisome proliferator-activated receptor (PPAR)- $\gamma$  (129). PPAR- $\gamma$  and its isoforms PPAR- $\alpha$  and PPAR- $\delta$ , are members of the nuclear hormone receptor family of a ligand-activated transcription factors (50, 129, 399). PPAR- $\gamma$  receptors are found on insulin-sensitive tissues and act as lipid sensors to regulate carbohydrate and lipid metabolism. Upon activation, PPAR- $\gamma$  results in an improvement in insulin sensitivity and increases glucose uptake by skeletal muscles, while also reducing hepatic glucose output (50, 129, 399). Other TZDs effects include its ability to protect pancreatic  $\beta$ -cell function (14, 129, 399), modulating most risk factors for CVDs (391, 399) and altering lipid profiles, lowering blood pressure and prevent inflammation and atherosclerosis in vascular tissues (399).

## 2.8.3 Insulin secretagogues

### 2.8.3.1 Sulphonylureas (SUs)

The drugs in the SU group include glibenclamide, chlorpropamide, tolbutamide and gliclazide. Sulphonylureas (SUs) augment glucose-induced late insulin release from pancreatic  $\beta$ -cells (166, 391) by blocking the opening of potassium channels ( $K_{ATP}$ ) by binding to the pancreatic  $\beta$ -cell SU receptor (SUR)1 and depolarize the membrane leading to calcium influx through opened voltage-gated calcium channels (391, 594). Increased intracellular calcium levels mobilize calcium-dependent insulin vesicles to fuse with the membrane and release insulin (14, 391). SUR1 is the regulatory subunit on  $\beta$ -cell  $K_{ATP}$  channels whereas variants of SUR2 are on  $K_{ATP}$  channels of cardiac (SUR2A), and vascular smooth muscles (SUR2B) (166). Tolbutamide and gliclazide block the SUR1 subunit, whereas glibenclamide and glimepiride have affinity for both SUR1 and SUR2 isoforms (166). The binding of SUs to  $K_{ATP}$  channels of coronary vessels causes dilatation to enable the heart to adapt to ischemic conditions (14). However, SUs can cause hypoglycemia, since insulin release is initiated even when glucose concentrations are below the normal threshold required for insulin release (391).

### 2.8.3.2 Meglitinides

Meglitinides include repaglinide and nateglinide and can enhance the initial surge of insulin release in response to meals by binding to specific SUR1 sites on pancreatic  $\beta$ -cell membranes that inhibit potassium channels (230, 391). Activity of meglitinides depends on the concentration of the blood glucose and the dose of the drug used (230). Here medication is taken prior to meals to prevent post-prandial hyperglycemia and because they (meglitinides) relatively have a short half-life (391). Repaglinide has a rapid and short-lived insulinotropic action (539), and is effective in T2DM as reflected by the lower HbA<sub>1c</sub> levels (148, 243, 454). It is also associated with less weight gain and

hypoglycemia and may be used as monotherapy or in combination with metformin, TZDs and long-acting insulin. Nateglinide, is a phenylalanine-derivative that has a lower affinity than repaglinide as it dissociates more rapidly from its receptor (314). Hence, it is less effective in lowering blood glucose levels and HbA<sub>1c</sub> levels (243, 313, 350) but causes less hypoglycemia than repaglinide (539).

#### **2.8.4 $\alpha$ -Glucosidase inhibitors**

$\alpha$ -Glucosidase inhibitor drugs such as acarbose, miglitol and voglibose inhibit intestinal glucose absorption (14, 391, 492).  $\alpha$ -Glucosidase a membrane-bound enzyme on the epithelium of the small intestine hydrolyzes disaccharides and oligosaccharides (14, 391, 492). Inhibition of  $\alpha$ -glucosidase prevents a post-prandial increase in blood glucose concentration due to delayed carbohydrate absorption (14). Acarbose can also increase the secretion of glucagon-like peptide (GLP)-1, an insulinotropic hormone. GLP-1 is a hormone released from intestinal L cells into the circulation after meals (173, 708), whereafter it enhances glucose-dependent insulin secretion through activation of cAMP-dependent protein kinase in pancreatic  $\beta$ -cells (450, 701). GLP-1 is effective in reducing post prandial hyperglycemia (708), enhancing insulin sensitivity and also in preserving  $\beta$ -cell function (516, 701) although the relative contribution to reduction in post-prandial hyperglycemia is unknown (230). However, many patients do not tolerate the  $\alpha$ -glucosidase inhibitors due to flatulence, abdominal pain and diarrhea (284, 631), hence need for development of alternative agents.

#### **2.8.5 Peptide analogues**

This class of anti-diabetic drugs consists of injectable incretin mimetics; glucagon-like analogs/agonists; dipeptidyl peptidase-4 (DPP-4) inhibitors and amylin analogues. Incretins are insulin secretagogues that include glucagon inhibitory peptide (GIP) (702) and the previously mentioned GLP-1. GIP secretion is stimulated by the hyperosmolarity of glucose in the duodenum. GLP-1

promotes insulin secretion and suppression of glucagon levels after meal ingestion. It has beneficial glucose lowering effects in T2DM as it reduces gastric emptying and decreases calorie intake. However, both GIP and GLP-1 have a relatively short half-life and are rapidly inactivated by the enzyme dipeptidyl peptidase-4 (DPP-4), hence development of their agonists (701).

At present only GLP-1 agonists and not GIP agonists have been approved. These include exendin-4/exenatide (GLP-1 homolog) (701), liraglutide and taspoglutide. Exendin-4, a 39 amino acid peptide originally from Gila monster saliva that promotes release and prolongs half-life of GLP-1. It has a relatively longer half-life than GLP-1 and may be used to treat T2DM and diabetes as it delays gastric emptying and reduces calorie intake (184). Exendin-4 is not an analogue of GLP-1 rather an agonist that has increased to resistance to degradation by DPP-4, hence prolonged half-life (222).

Amylin is a pancreatic hormone co-secreted with insulin (from pancreatic  $\beta$ -cells) that reduces post-prandial hyperglycemia by delaying gastric emptying. Its half-life, is however too short for it to be sustained as a routine clinical agent (496). Pramlintide is the only human amylin analogue available clinically and although its administration can reduce post-prandial glucose excursions in diabetics, pramlintide use may be limited by the relatively low efficacy (698, 699) and its adverse effect of nausea. The next section reviews the outcome of agents used for glycemic control in clinical trials and epidemiological studies carried out in diabetic patients, with particular emphasis on cardiovascular diseases. The overall aim of the following section is to highlight the importance of evaluating novel agents that aim to preserve cardiac function under conditions of acute and chronic hyperglycemia.

### **2.8.6 Glycemic control and outcome**

Despite the availability of drugs for diabetes and various treatment modalities to improve cardiac function in coronary artery disease, there is still an increased occurrence of complications secondary

to both pathophysiological conditions, i.e. diabetes and myocardial infarction. It is therefore imperative to investigate alternative treatment modalities that may remedy the *status quo*. Prevention rather than treatment of heart disease can significantly improve patients' quality of life and reduce health care costs. This is even more important considering that the detrimental effects of hyperglycemia not only manifest within the context of diabetes, but also in non-diabetics following AMI and in cases of stress-related hyperglycemia (118). The emphasis of this thesis is therefore on evaluating novel cost-effective therapies to alleviate the damaging effects of acute and chronic hyperglycemia during AMI.

The UKPDS employed various regimens were used in approximately 5, 000 newly-diagnosed diabetic patients that were followed up for ten years, and reported that intensive treatment reduced the risk for AMI by 16% compared with conventional treatment. Moreover, hyperglycemia emerged as an independent risk factor for CVD but with no apparent threshold, i.e. the lower the HbA<sub>1c</sub> the reduction in the risk. Also for every 1% reduction in HbA<sub>1c</sub> (for levels <6% and >10%) there were corresponding reductions in risk for AMI, stroke, HF and amputation or death from peripheral vascular disease (722). The DIGAMI Study was a prospective study of 620 diabetic patients with AMI who were randomly treated with either an intensive insulin regimen (to achieve near normoglycemia), or conventional treatment, and followed up for 3.4 years. Here, mortality was reduced by 27% in the intensively treated group despite high admission blood glucose and HbA<sub>1c</sub> (460). However, experiences from the DIGAMI 2 and CODE studies (82, 428) highlighted that achievement of the targeted fasting glucose level of 5-7 mmol/L with blood glucose lowering treatments is difficult to accomplish (461). The DIGAMI 2 study did, however, establish the role of blood glucose level as a predictor of long-term mortality despite absence of the beneficial effects from acute and long term insulin versus conventional treatment. Hence there is a need for other management routines and improved pharmacological agents for this large group of patients. In this regard there is need for the evaluation of novel therapies to improve outcome (e.g. benfotiamine and oleanolic acid for this study).

In summary, the highlighted clinical trials and epidemiological studies support the notion that intensive glycemic control correlates to a decrease in the incidence of cardiovascular complications. However, it is imperative to note that despite all these measures the incidence of diabetic complications is still on the rise, of especially diabetic cardiomyopathy and HF secondary to AMI. Moreover, the link between intensive glucose control and benefits on CVD prevention has been questioned by several investigators. Here intensive glycemic control can result in increased mortality, likely due to the detrimental effects of hypoglycemia (6, 382, 682) e.g. renal failure (63) and possibly increased CVDs (186).

On the contrary, CVD complications are still prominent despite glycemic control, particularly macro-vascular complications (trials only showed a decrease in micro-vascular complications) (505). The concept of the metabolic memory may help explain the latter phenomenon, i.e. it is linked to the persistent manifestation of complications despite treatment (51, 234, 244, 325, 383, 385, 386, 781). Here pioneering work by Engerman and Kern (1987) found that the increased incidence of retinopathy in dogs was dependent on duration of exposure *before* glycemic control was implemented (188). In essence the concept is that the longer cells are exposed to high glucose, the more it diminishes subsequent metabolic responses when returning to normal glucose levels at a later stage. This effect is attributed to mitochondrial and non-mitochondrial ROS (mainly superoxide and peroxynitrite) and also increased activation of the non-oxidative glucose pathways such as the AGE and PKC pathways (505). With this gap in the current management of diabetes and associated CVDs, it is important to consider the development of drugs that address the fundamental pathophysiologic abnormalities that link diabetes/hyperglycemia and CVD while ensuring that the risk for CVD is not inadvertently increased (162).

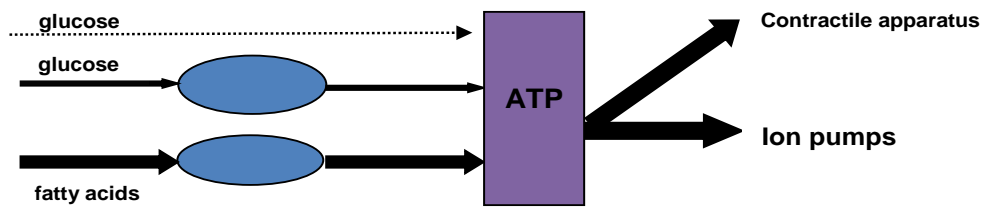
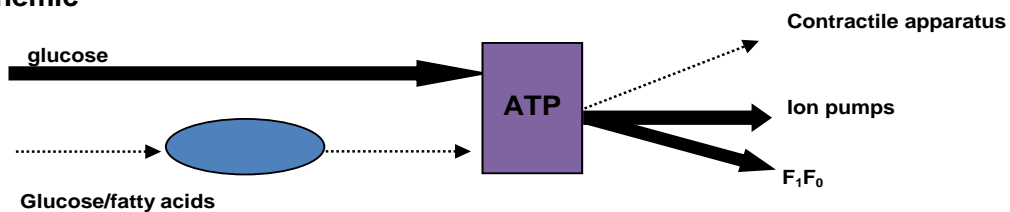
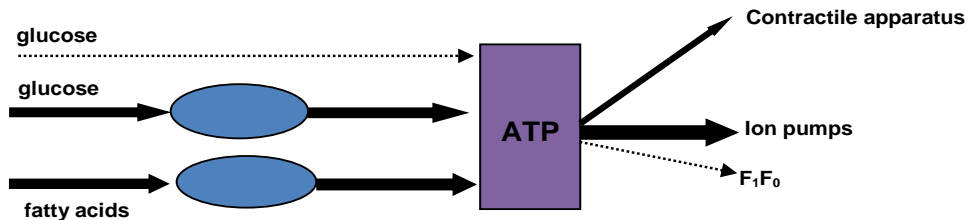
It is also important to understand the molecular mechanisms of events that occur during AMI under hyperglycemic conditions and how this can result in myocardial damage. This pathological aspect is

reviewed in the next section since it may be a putative target for various therapeutic agents to maximize cardio-protection in response to acute and chronic hyperglycemia.

## **2.9 Metabolic changes during ischemia and reperfusion**

As discussed previously, the heart is a highly aerobic tissue that obtains most of its energy from the oxidative phosphorylation of metabolic fuel substrates. Mild or severe impairment of coronary blood supply in large arteries to the myocardium causes myocardial ischemia usually as a result of thrombosis or atherosclerotic plaques. This deprives the myocardium of oxygen, fuel substrates and leads to accumulation of metabolites (545) consequently causing cell death within the infarcted area (491, 651). Myocardial ischemia results in many alterations in cellular function, the reduction in oxygen supply, and its impact on myocardial energetics (150). Studies over the years showed that myocardial cells can compensate for reduced ATP production by lowered metabolic flux and hence able to survive rather relatively long periods, i.e. 60 minutes or more of akinetic oxygen deprivation (provided coronary flow is adequate to remove metabolic products). The ATP balance of cardiac mitochondria under normal conditions and during ischemia and reperfusion is shown in Figure 2.9 below.



**a) Normoxic****b) Ischemic****c) Reperfusion**

**Figure 2.9 ATP balance in the heart mitochondria.** The height of the purple box indicates intracellular ATP concentrations under a) normoxia b) ischemia and c) reperfusion. The sources and sinks of ATP are indicated as black arrows with the relative fluxes corresponding to the thickness of the arrows. The light blue ovals indicate respiratory chain function.

**2.9.1 Effects of ischemia on substrate utilization**

Myocardial substrate utilization is highly dependent on the severity of the ischemia (i.e. mild to moderate and severe ischemia) (665). The changes that are discussed in this section apply to ischemia with/without underlying hyperglycemia i.e. during chronic hyperglycemia as in diabetes or in non-diabetic individuals. As discussed earlier in this chapter, in non-diabetics with AMI, there is an elevation of stress hormone levels, and impaired insulin signaling (104, 118, 395) hence AMI is characterized by hyperglycemia and the metabolic dysfunction that occurs during ischemia is similar in

non-diabetic and diabetic individuals. The main difference is that AMI during chronic hyperglycemia may result in heightened ischemic metabolic changes due to the presence of altered metabolic dysfunction (356). This implies that an excess of FAs (and intermediates e.g. fatty acyl-CoAs, DAG and ceramides) and attenuated glucose oxidation seen with diabetes or metabolic syndrome (422, 429, 441, 442, 610, 665) is further exacerbated during AMI since it manifests in the same way (422, 429, 442, 610, 664). Here increased FA supply occur as a result of ischemia-induced myocardial lipolysis (degradation of endogenous TAGs) as reflected by release of glycerol from ischemic zones thus further increasing the amount of circulating FAs (64, 92, 340, 731). With increased FA levels in diabetes, PPAR- $\alpha$  activation is enhanced further promoting FA uptake, metabolism and FAO (397, 398) and consequently impairing cardiac function with ischemia and reperfusion. For example, overexpressing PPAR- $\alpha$  mice showed decreased functional recovery following global ischemia in comparison to the wild type mice (614). Furthermore, reduced cardiac efficiency occurred due increased CPT-I activity (58, 434) and fatty acyl-CoA-induced inhibition of adenine nucleotide translocase on the inner mitochondrial membrane (exchanges ATP for ADP) thereby uncoupling contractile function in the post-ischemic heart (64).

During ischemia glucose oxidation is also decreased due to lowered GAPDH activity as a result of increased accumulation of NADH, lactate and hydrogen ions (491). Interestingly however, recent studies have reported a more detrimental outcome in non-diabetics compared to diabetics following AMI (104, 118, 119, 460) indicating that there is a need for therapeutic interventions to minimize damage due to acute hyperglycemia. The variations for these observations are not clearly elucidated, however, various studies have reported on the variation of exposure duration to hyperglycemic conditions i.e. more chronic hyperglycemia reducing sensitivity of diabetic myocardium to AMI (456) possibly attenuating ischemia and reperfusion injury (585, 586).

During ischemia there is an elevation of glucose uptake by the myocardial cell membrane (680) that occurs from increased GLUT1/4 translocation and activity (81, 125, 185, 607, 756, 788, 789) due to increased AMPK activation (485). The increase in glucose transport with decreased oxygen availability may be of physiological importance, i.e. allowing the heart to obtain more energy from glycolysis under conditions where FAO is predominant (665). This occurs despite decreased glucose delivery and lower interstitial glucose concentrations because glucose transport is determined by the number of glucose transporters present in the cell membrane and the trans-membrane glucose concentration gradient (448, 500, 789). One of the main mechanisms through which this occurs is through AMPK activation (789). The increased ratio of AMP to ATP activates AMPK kinase (AMPKK) leading to production of AMPK. AMPKK is also activated by a decrease in the creatine phosphate to creatine ratio that occurs during ischemia (404, 561). Additionally AMPK promotes glycolysis by increasing activity of PFK-1 and PFK-2 (317). It is, however, important to note that glycolysis varies with the degree of ischemia. For example, during severe ischemia, glycolysis is inhibited by low delivery rates of glucose, glycogen depletion and intracellular acidosis, which all inhibit PFK-1. Moreover, PFK-1 is inactivated by translocating from cytosol to the cell membrane during severe ischemia (296).

The effects of ischemia on PDH, however, have not been clearly elucidated with studies reporting contradictory effects (286, 377, 662, 726) possibly due to differences in ischemia-protocols and experimental models used i.e. *in vivo* and *ex vivo*. The TCA cycle is attenuated and there is less energy production from oxidative phosphorylation (150) thereby decreasing ATP levels and impairing myocardial function in this pathophysiological state (see Figure 2.9) (18). Changes are also found in the process of oxidative phosphorylation and the creatine kinase shuttle. In this instance mitochondrial number may be increased but are structurally abnormal (323); the activity of ETC complexes are reduced (467); and the number of uncoupling proteins are increased (504). Moreover, the low enzyme activity in the creatine kinase shuttle result in a decline in ATP delivery (up to 71% ) to the myofibrils (58, 434).

In summary, FAO increases during reperfusion in association with impaired pyruvate oxidation and accelerated non-oxidative glycolysis (626). Increased FAO inhibits glucose oxidation, resulting in an imbalance between glycolysis and glucose oxidation (610). Prolonged ischemia can also suppresses DNA and protein synthesis (108), although there may be induction of some specific ones e.g. heat shock protein 70 (HSP 70), PKC- $\epsilon$  and inducible nitric oxide synthase (iNOS) (149, 554, 555). In the next section the ionic imbalances that occur during ischemia and reperfusion are discussed.

### **2.9.2 Ionic imbalances during ischemia and reperfusion**

The ionic content of the cytosol changes markedly during ischemia as a result of decreased ATP levels. The Na<sup>+</sup>/K<sup>+</sup>-ATPase and the SERCA become ineffective, thereby causing increases in the cytoplasmic sodium and calcium ions (see Figure 2.10) (556–558). Prolonged inhibition of mitochondrial oxidative phosphorylation during ischemia dampens the proton gradient leading to decreased activity of the mitochondrial calcium uniport and reversed operation of the ATPase possibly contributing to the ATP loss observed during ischemia (130, 150, 151) (see Figures 2.9 and 2.10). The continued production of hydrogen ions during reperfusion has the potential to exacerbate injury to the myocardium (434, 443).

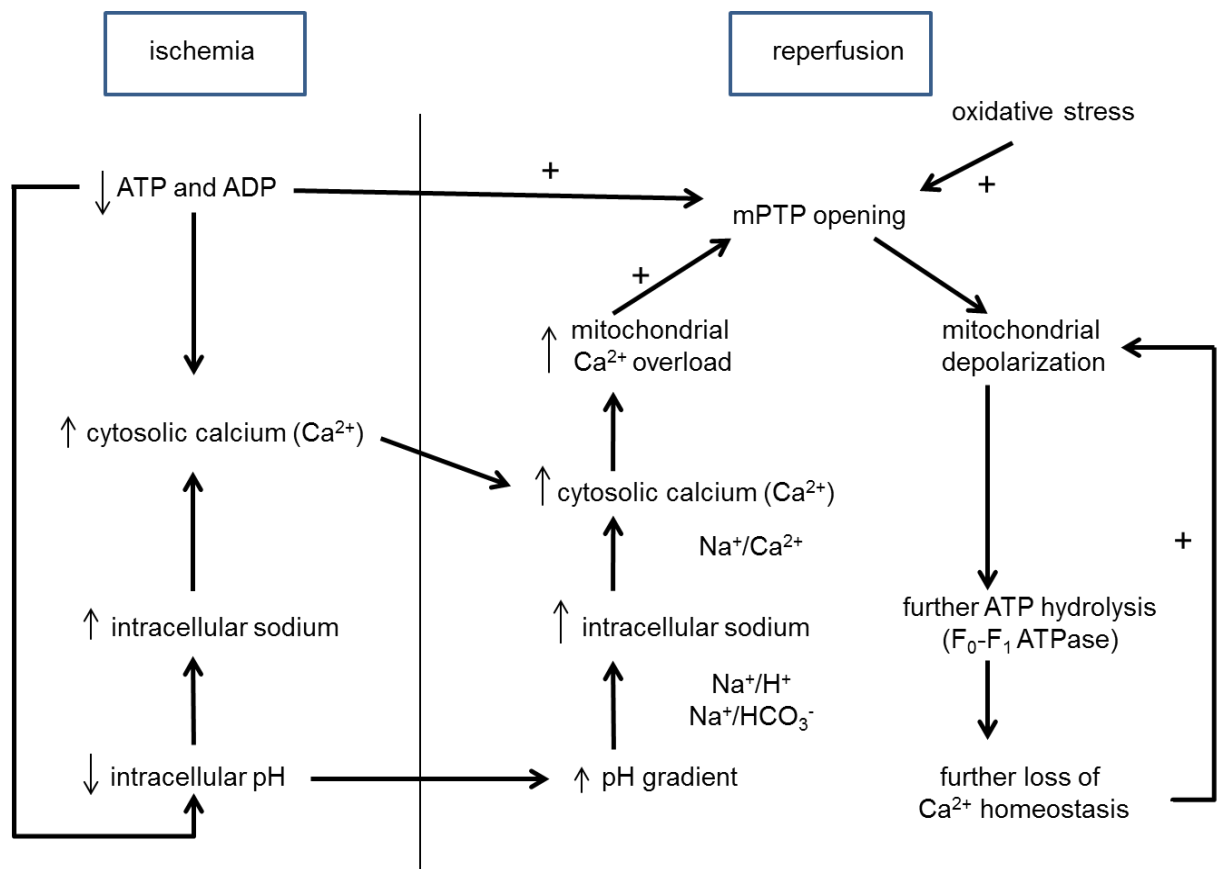


**Figure 2.10 Ionic imbalances during myocardial ischemia and reperfusion.** ATP dissipation during ischemia leads to an increase in resting cytosolic free calcium ( $\text{Ca}^{2+}$ ). Reperfusion leads to excessive mitochondrial  $\text{Ca}^{2+}$  uptake. Mitochondrial  $\text{Ca}^{2+}$  overload together with oxidative stress and the prevailing low ATP provoke mPTP opening. These events initiate a vicious cycle, i. e. inner-membrane depolarization, ATP hydrolysis by the mitochondrial ATP synthase, further increases in cytosolic  $\text{Ca}^{2+}$ , finally leading to cell death.  $\text{Ca}^{2+}$  (calcium ions); ATP (adenosine triphosphate); ADP (adenosine diphosphate);  $\text{Na}^+/\text{H}^+$  (sodium hydrogen exchanger);  $\text{Na}^+/\text{HCO}_3^-$  (sodium hydrogen carbonate exchanger);  $\text{Na}^+/\text{Ca}^{2+}$  (sodium calcium exchanger);  $\text{F}_0\text{-F}_1$  ATPase (ATP synthase); mPTP (mitochondrial permeability transition pore).

The hydrogen ions in the severely ischemic myocardium result from the hydrolysis of glycolytically-derived ATP and is the major contributor of acidosis in the myocardium (158, 619). Ion pumps on the cell membrane respond to remove excess hydrogen in exchange for sodium. In response to elevated levels of intracellular sodium, the  $\text{Na}^+/\text{Ca}^{2+}$ -exchanger (operating in reverse mode) is less capable of removing intracellular calcium culminating in increased cytoplasmic calcium levels (503). The mitochondrial calcium uniporter then transports calcium into mitochondria, that induces calcium - dependent dehydrogenase activation, declines in NADH and electron flux through the ETC, increased ROS, and decreased ATP levels (see Figure 2.10). Calcium uptake into mitochondria dissipates the

mitochondrial membrane potential but its increase in the mitochondrial matrix reaches a plateau under hypoxic conditions (due to limitation of proton gradient). Upon reperfusion, however, restoration of oxygen and ATP-generating capabilities rapidly restores ATP levels and mitochondrial membrane potential, together with marked ROS production (which damage cellular membranes and further induce oxidative stress). These changes regenerate the required ion gradient for more calcium entry into mitochondria, which causes long-lasting opening of mPTP (145, 757).

The mPTP is a non-specific multimeric protein channel located on the inner mitochondrial membrane, initially proposed to consist of a voltage-dependent anion channel, the adenine nucleotide translocase and a cyclophilin D. However, its structure has not yet been completely defined. Under normal physiological conditions (mPTP in closed conformation) the inner mitochondrial membrane is impermeable to almost all metabolites and ions. As the mPTP opens during reperfusion (257, 432), the mitochondrial membrane potential is abolished allowing transition of molecules smaller than ~1 500 daltons. These molecules generate an osmotic force causing mitochondrial swelling and leading to rupture of the outer membrane and release of proapoptotic factors such as cytochrome c (see section 2.10.2 on apoptosis) (273). Experimental and clinical investigations show that although reperfusion does indeed salvage the ischemic myocardium, it can paradoxically also induce some detrimental effects, i.e. a phenomenon referred to as "ischemia/ lethal reperfusion injury" (213, 293, 545, 780, 803). Here, myocardial reperfusion also results in cardiac myocyte death (of cells that were viable immediately before reperfusion) (557, 558). The exact and detailed mechanisms of ischemia/reperfusion injury are described in the section below.

### **2.9.3 Myocardial ischemia/reperfusion injury**

Myocardial reperfusion injury was first described by Jennings *et al.* (1960) after observing histological features of the reperfused canine myocardium (338). In essence myocardial reperfusion injury is a

complex pathophysiological event, resulting in serious acute and chronic myocardial damage. It is characterized by a cascade of acutely initiated local inflammatory responses, metabolic disorder, and cell death that leads to myocardial ultra-structural changes/remodeling and subsequent myocardial systolic/diastolic dysfunction. The major mediators of lethal reperfusion injury are oxygen radicals, calcium loading and neutrophils (213, 545, 780, 802). The injury to the heart during reperfusion causes four main types of cardiac dysfunction, namely: myocardial stunning, no-reflow phenomenon, reperfusion arrhythmias and lethal reperfusion injury (780).

During the earliest phase of reperfusion (minutes) there is development of cardiomyocyte contracture which seems to be the main cause for cardiomyocyte necrotic injury (557). Contracture is a sustained shortening and stiffening of myocardium that occurs as a rigor-type mechanism within the ischemic myocardium. It mainly results from increased intracellular calcium ions and reduced ATP levels that occur during ischemia and reperfusion (see Figure 2.10). Studies on skinned cardiac cells found that a force-generating cross bridge is initiated when cytosolic ATP is reduced to low levels (17, 523). Although ATP levels are quickly exhausted with ischemia, onset of contracture does not cause major structural damage, but instead render the cardiomyocytes more fragile and susceptible to mechanical damage (621). When energy depletion is rapidly relieved then the ischemic rigor contracture is usually reversible (556–558). However, if ischemia is prolonged there may be irreversible structural damage to cardiomyocytes leading to increased end diastolic pressure and ventricular compliance (556–558). Reperfusion-induced contractures are caused by: 1) calcium overload during ischemia followed by rapid re-energization and 2) rigor contracture. With calcium-induced contracture, high cytosolic calcium availability leads to uncontrolled activation of the contractile machinery with damaging effects. Of interest in the context of this thesis is that increased flux through the non-oxidative glucose pathways may elevate the degree of ischemia and reperfusion injury (326, 353, 462, 691, 692). It is now appreciated that lethal myocardial injury caused by ischemia/reperfusion accounts for ~ 50% of the final size of a myocardial infarct (784). In essence altered cardiac energy metabolism leads to

activation of a cascade of events that result in oxidative stress and the next section therefore, focuses on the role of ROS in myocardial ischemia- reperfusion.

#### **2.9.4 ROS in reperfusion injury**

Most of the changes that occur to the redox balance during ischemia and reperfusion are similar to what was earlier discussed (refer section on hyperglycemia-induced oxidative stress) particularly regarding the role of mitochondria. Here superoxide anion is the principal ROS produced by several sources e.g. polymorphonuclear leukocytes (PMNs), Nox (255), incomplete oxidative phosphorylation in mitochondria by complex I (409) and III (298, 552), xanthine oxidase (59) and eNOS (562). Nox is a distinct ROS source since its role is to solely produce superoxide, whereas other enzymes produce ROS as by-products of specific catalytic pathways (341). Endothelial dysfunction occurs due to attenuation of NO bioavailability through formation of peroxynitrite after combining with superoxide (199, 558, 741). Such endothelial dysfunction promotes the upregulation of endothelial adhesion molecules (e.g. ICAM-1) thus facilitating adherence of PMNs and infiltration. The ROS and proteolytic enzymes produced by activated leukocytes cause damage to myocytes and vascular cells through lipid peroxidation thereby altering their permeability to ions such as calcium (447, 605). Thus the transmigrated PMNs are mainly responsible for compromising cardiac contractile function during reperfusion (418, 714). The early phase of reperfusion represents an important target for strategies protecting ischemic myocardium (558) as described below.

##### **2.9.4.1 Interventions to ameliorate myocardial ischemia and reperfusion injury**

Early and successful reperfusion with the use of thrombolytic therapy or primary percutaneous coronary intervention is the most effective treatment strategy to salvage the ischemic myocardium from inevitable death, thereby reducing infarct size and improving clinical outcome. Additionally, there



are various approaches used to protect the ischemic tissue and surrounding muscle at risk of the detrimental effects of ischemia. Firstly, promotion of glycolysis by use of glucose/insulin/potassium (GIK) stimulates glucose uptake thereby increasing glycolysis and suppressing blood FA supply. Findings of GIK trials did, however, result in contradictory findings and this may be due to differences in glucose concentrations in patients receiving treatment and the timing of GIK administration (110, 460). Another approach is to better link glycolysis to glucose oxidation, possibly by increasing activity of PDH to enhance glucose entry into the TCA cycle using pharmacologic agents (e.g. dichloroacetate). The rationale in this instance is to blunt the effects of the Randle cycle, i.e. high FAO blunting glucose oxidation during ischemia and reperfusion (discussed earlier; refer section 2.3). Finally a third approach is to directly limit FAO during ischemia and reperfusion to attenuate fat-mediated effects on glucose oxidation e.g. employing drugs such as trimetazidine (443).

Targeting oxidative stress during ischemia and reperfusion is an attractive therapeutic option but the simplistic approach of administering antioxidants to reduce ROS-induced injury has not always yielded beneficial results (735). The protective potential of an antioxidant depends on the scavenging of specific ROS species and its access to strategic intracellular sites (49, 790). Alternatively, “programming” the heart to either generate less ROS or to increase strategic ROS removal by endogenous mechanisms may yield success in attenuating reperfusion injury. Under these pathophysiological conditions (hyperglycemia and ischemia) the heart undergoes various stress responses discussed below.

## **2.10 The cardiomyocyte stress response**

Adult heart cells endure a wide range of stress during their life span and in the process acquire numerous adaptations. The heart is an organ with limited capacity for regeneration and repair; hence it is susceptible to numerous stresses and must respond to these insults in order to adapt to ever-

changing workload demands. We have discussed the damaging effects of hyperglycemia and ischemia and reperfusion on the heart as examples of stress confronting cardiomyocytes. The heart's adaptations occur in the context of continuous mechanical contraction and relaxation and include changes in signaling events (receptor and adaptor proteins), transcriptional events and the replacement of contractile proteins in response to wear and tear (646).

Moreover, cardiomyocytes respond to stress by the accumulation of protective proteins that may counteract damage, thereby temporarily increasing tolerance to such damage. Alternatively, it may trigger programmed cell death (apoptosis) to remove terminally damaged cells (24) which can be eliminated by the UPS and lysosomal-autophagal system. Cell death (progressive or acute) is a hallmark characteristic of various cardiac diseases that include HF, diabetic cardiomyopathy, AMI, and ischemia and reperfusion. All three types of cell death, i.e. autophagy, apoptosis, and necrosis are present during the progression of heart diseases (757). However, since this dissertation mainly focuses on apoptosis, it will be discussed in detail, whereas the other modes of cell death are only briefly discussed.

### **2.10.1 Necrosis**

Necrosis is marked by distinct morphological changes; including cell and organelle swelling, cell membrane damage, and ATP loss. Disruption of cell integrity and release of cellular contents trigger a secondary inflammatory response, with potential pathological consequences (757). Necrosis is mainly caused by physical or chemical trauma to the cell and has long been considered as passive and accidental cell death (725). Recently, however, emerging evidence suggests that part of the necrotic process is regulated by serial signaling events in a controlled and orchestrated manner (757). Several terms have been introduced to describe this form of necrosis, e.g. programmed necrosis, caspase-independent cell death, and necroptosis (157, 299).

A number of proposed mechanisms may explain the initiation and execution of necrosis, including death receptors, ROS, calcium, and mPTP opening (394, 725). Necrosis can occur in at least four ways: (1) direct damage to the cell membrane induced by certain toxic chemicals e.g. products of activated leukocytes and osmotic fluctuations, such as the calcium paradox or disruption of the membrane cytoskeleton; (2) damage to the respiratory apparatus of mitochondria, with inhibition of oxidative phosphorylation leading to decreased ATP production and an increase in hydrogen ions (decrease in pH, intracellular acidosis); (3) proteolysis of membrane-associated cytoskeletal proteins, including dystrophin, dystrophin-associated protein complex and (4) unregulated membrane phospholipid degradation due to activation of phospholipases and membrane lipid peroxidation due to the generation of ROS (757).

Thus necrosis occurs under normo-/hyperglycemic conditions (216) and also  $\pm$  ischemia and reperfusion (757). Based on these observations, three stages of membrane injury emerge during the progression from reversible to irreversible necrotic injury: (1) discrete alterations in ionic transport systems (reversible); (2) increase in permeability of the phospholipid bilayer (potentially reversible); and (3) physical disruption of the cell membrane (irreversible). These stages of necrotic membrane injury are accompanied by progressive morphologic changes including organelle and cell, membrane blebbing/rupture and cell rupture (73). Leakage of intracellular constituents from cells undergoing necrosis provokes inflammation (299, 420, 757).

However, with myocardial infarction there remains controversy regarding the predominant mode of cell death i.e. amongst necrosis, apoptosis, and autophagy (35, 249, 348, 475, 525). The discrepancy may be due to variations in timing, incidence, and prevalence of the different cell death markers. Moreover, the various cell death markers have different sensitivities and windows of detection during ischemia and reperfusion. Some suggested, however, that apoptosis becomes maximal within the first

four hours of permanent coronary occlusion, whereas necrosis peaks at 24 hours (348). To gain a better understanding of the differences between these two processes, apoptosis is discussed below.

### **2.10.2 Apoptosis**

Apoptosis is an active evolutionarily conserved form of cell self-destruction (programmed cell death Type I) that is precisely regulated by a genetic program resulting in cell death (365, 393, 438). Apoptotic cells are characterized by specific morphological changes, including chromatin condensation and fragmentation and cell membrane blebbing (73, 393). During the late stages of apoptosis the cell becomes fragmented into vesicles called apoptotic bodies, which contain cytosolic, nuclear and organelle material (393). Apoptotic bodies are subsequently recognized by macrophages and cleared from the tissue to avoid inflammatory responses. Furthermore, cells undergoing apoptosis lose the normal phospholipid asymmetry of the cell membrane and accumulate large amounts of phosphatidylserine in the outer cell membrane leaflet. However, the semi-permeable property of the membrane is maintained, preventing leakage of intracellular constituents (unlike necrosis). The exposed phosphatidylserine moieties can be recognized by receptors on adjacent cells leading to rapid phagocytosis of apoptotic fragments, thereby avoiding a stimulus for exudative inflammation. All these features are found in atherosclerotic tissue which can be an underlying cause of AMI (67, 228, 281, 378). Oxidative stress (mitochondrial and non-mitochondrial sources) is the main cause of apoptosis in cardiac tissues under hyperglycemic conditions. The latter mainly include increased activation of non-oxidative glucose pathways which mainly converge on the activation of PKC and TNF- $\alpha$  (169, 170, 192, 207, 425, 683) as earlier discussed.

Apoptosis induction involves activation of specific enzymes, the caspases (cytosolic aspartate residue-specific cysteine proteases) that are a family of proteases thought to be the most important effector molecules of this process (69, 727). A catalytic cascade, much resembling the complement or clotting

cascade, is suggested for caspase activation and it can be initiated by several factors. Data indicate that the route for caspase activation differs depending on the pro-apoptotic stimuli and that not all caspases are active in all mechanisms (69, 727). In addition to caspases, the B cell leukemia/lymphoma-2 (Bcl-2) family member proteins also take part in the process. These are divided into three subfamilies according to their function and degree of homology shared within four Bcl-2 homology domains (BH1-4). In general, the anti-apoptotic Bcl-2 family members contain BH domains 1–4 (e.g. Bcl-2 and B cell leukemia/lymphoma-x-isoform [Bcl-x<sub>L</sub>]) (757) and need to be neutralized or down-regulated by other Bcl-2 family members for apoptosis to progress. The pro-apoptotic members can be subdivided into two groups, i.e. the first group is often referred to as the multidomain pro-apoptotic members that contain BH domains 1–3 and includes Bcl-2-associated X protein (Bax) and Bcl-2 homologous antagonist /killer (Bak) and Bcl-2 related ovarian killer (Bok). The second group is made up of the Bcl-2 homology domain 3 (BH3)-only proteins (BH3-only interacting protein [Bid], Bcl-2 like protein 11 [Bim], Bcl-2 associated death promoter [Bad]) (591). Apoptosis in cardiomyocytes is mediated by the activation of the extrinsic or intrinsic pathways (see below).

### **2.10.2.1 Extrinsic /external/death receptor pathway**

The external pathway is activated by binding of death ligands to cell surface receptors (endonucleases). The best known receptors are those for TNF- $\alpha$  and Fas (also called APO-1) ligand receptor (550). The activated death receptor subsequently conveys signals to the Fas-associated death domain protein (FADD). Both Fas and TNF- $\alpha$  receptors are expressed in cardiac myocytes and implicated in cardiovascular pathology. Since TNF- $\alpha$  signaling is more complex as it can promote survival or death; events following binding of Fas ligand are described. The resultant macromolecular complex constitutes a death-inducing signaling complex (DISC) that activates initiator caspases, including the conversion of procaspase-8 or -10 to active caspase-8 or -10 which in turn activates downstream procaspases (42, 69). Furthermore, the active caspase-8 can also activate the intrinsic

pathway by the proteolysis of BID to truncated BID (t-BID) leading to translocation of its carboxyl portion to the mitochondrion triggering apoptotic events (423).

### **2.10.2.2 The intrinsic/mitochondrial pathway**

The intrinsic pathway is activated in response to a wide variety of extra- and intracellular stimuli, including loss of survival or trophic factors, toxins, radiation, hypoxia, oxidative stress, ischemia and reperfusion, and DNA damage. These stimuli converge at the mitochondrion to trigger a conformational change, characterized by mPTP opening and release of apoptogenic proteins (629). In addition, it causes the ER to release calcium and activate procaspase-12 to caspase-12 (522, 630). Death signals to mitochondria and ER are transduced by two classes of proapoptotic proteins, i.e. Bax and BH3-only proteins (160, 206, 365). Here Bax is proposed to undergo a conformational change and then translocates to mitochondria and the ER. However, the precise mechanisms mediating its activation are not completely understood (160, 206, 365). In contrast to the general involvement of Bax, BH3-only proteins transduce death signals in a stimulus-specific manner (591, 787). Moreover, death signals regulate abundance, activity and localization of these proteins through various transcriptional mechanisms, post-translational modifications (e.g. phosphorylation and cleavage). Deficiency of certain survival factors results in dephosphorylation of Bad, releasing it from 14-3-3 protein and translocation to the mitochondrion (796)

The key event leading to the release of apoptogens and execution of cell death is permeabilization of the outer mitochondrial membrane (OMM) and the subsequent release of apoptogenic factors from the mitochondrial inter-membrane space (IMS) (i.e. cytochrome c, second mitochondria-derived activator of caspase/direct inhibitor of apoptosis [IAP]-binding protein with low PI [Smac/DIABLO], Endonuclease G, and apoptosis inducing factor (AIF) (629). OMM permeabilization is tightly regulated by the Bcl-2 family of proteins, Bax and Bak (751). The specific mechanism by which these respective

Bcl-2 proteins induce OMM permeabilization remains controversial; however, it is known that they both undergo a complex pattern of BH3-induced homo- and hetero-oligomerization at the mitochondria (522, 630). Apoptogen release is opposed by antiapoptotic Bcl-2 proteins, i.e. Bcl-2 and Bcl-x<sub>L</sub> (368, 376).

Once released from mitochondria, cytochrome c binds the adaptor protein apoptotic protease activating factor-1 (Apaf-1) in an ATP-dependent oligomerization causing recruitment of procaspase-9 and ultimately formation of the 'apoptosome' (5, 426). This facilitates the clustering and activation of caspase-9 which, in turn, cleaves and activates caspase-3 and caspase-7 leading to many of the morphological changes associated with apoptosis (757). Activated caspase-3 mediates cleavage of a number of protein substrates and activation of calcium-dependent endonucleases, leading to the characteristic double-stranded inter-nucleosomal DNA fragmentation (180–200 base pairs) (757).

Some or all of these discussed mechanisms are involved in high-glucose and/or ischemia and reperfusion-induced apoptosis (depending on the cell type or tissues studied). Of note, cardiac myocytes are naturally resistant to apoptosis due to their low-level expression of Apaf-1, caspases, and high expression of X-linked inhibitor of apoptosis protein (XIAP). However, apoptosis could be the major form of cell death during myocardial infarction, preceding necrosis (24, 206) and could also be the major determinant of infarct size (348). With hyperglycemia oxidative stress is proposed as the main cause of apoptosis, especially linked with mitochondrial dysfunction (61, 96, 307, 727, 749). Hyperglycemia may also cause apoptosis through the activation of non-oxidative glucose pathways. Our laboratory demonstrated that increased HBP activation causes apoptosis by increased BAD O-GlcNAcylation thereby reducing its phosphorylation (510, 576, 577). Similarly, p53 activity increased following its O-GlcNAcylation under hyperglycemic conditions thereby causing angiotensin-induced apoptosis (203).

High glucose can also initiate oxidative stress-induced apoptosis via Bax-mediated mitochondrial permeability and cytochrome c release (mesangial cells) that could be prevented by insulin-like growth factor-I (IGF-I), which results in phosphorylation of Bad (354). Furthermore, p38 mitogen-activated protein kinases (MAPK) can also play a role in high glucose-induced apoptosis (510). Here high glucose caused sustained phosphorylation of p38 MAPK, caspase-3 activation and Bax-mediated apoptosis in endothelial cells.

### 2.9.3 Autophagy

One of the key cellular pathways that mediate stress-induced adaptation and damage control is autophagy (also called macro-autophagy). Autophagy is a highly conserved process of delivery of intracellular components, including mitochondria and long-lived macromolecules, via a double membrane structure (autophagosome) to lysosomes for degradation (525). Autophagy plays a crucial role in the turnover of organelles in cardiac cells at baseline conditions (250, 266, 267, 421, 525). Furthermore, it is increased under stressful conditions (e.g. with starvation/nutrient deprivation, hypoxia, ROS, and damaged organelles) in a mTOR-dependent process.

The functional role of autophagy with ischemia and reperfusion is complex and it is unclear whether increased or decreased autophagy results in cardio-protective or detrimental effects on the heart. Most studies show increased autophagy with ischemia and reperfusion *in vitro* and *in vivo* studies (152, 276, 475, 777). Activation of autophagy with ischemia and reperfusion showed cardio-protection in association with activation of Bcl-2/adenovirus E1B 19 kDa protein-interacting protein 3 (BNIP3) (277) or AMPK (95, 686). This outcome, however, depends on the duration of ischemia, i.e. if prolonged the autophagic response becomes dysfunctional, as evidenced by the existence of impaired autolysosomes (421, 482). Interestingly, metformin can also activate mTOR thereby blunting cardiac remodeling and improving cardiac function after an AMI (95). Autophagy is further up-regulated during



reperfusion, even though the delivery of oxygen and nutrients is restored, and AMPK rapidly inactivated (276, 475). The continued activation of autophagy is qualitatively different during reperfusion versus ischemia with the involvement of oxidative stress, mitochondrial damage, ER stress, and calcium overload having more important roles in maintaining autophagy at a higher level. By contrast, a decline in autophagy with ischemia and reperfusion as evidenced by reduced levels of lysosomal-associated membrane protein 2 (LAMP2) (a protein critical for autophagosome–lysosome fusion) thus impairing autophagosome processing, culminates in increased ROS generation, mitochondrial permeabilization, and cardiomyocyte death (352). Although autophagy is strongly involved in lysosomal protein degradation, our interest here is the non-lysosomal UPS and its role in protein degradation in the heart under hyperglycemic conditions with ischemia and reperfusion.

## **2.10 The UPS**

Cellular homeostasis and function require properly folded proteins. Proteins can be misfolded or damaged by factors such as thermal, osmotic and oxidative stress leading to exposure of hydrophobic amino acid residues normally located inside the protein. This leads to aggregation or impairment of protein and cellular function and potentially cell death (567, 715). Eukaryotic cells have developed the UPS in order to maintain protein quality by removal of damaged, oxidized and/or misfolded proteins (238, 304, 642). This is particularly important for non-dividing cells such as neurons and cardiomyocytes, where cells are not diluted during cell proliferation. Indeed, proteasomal dysfunction and cell death are found in many neurodegenerative diseases and the initiation/progression of cardiac diseases (568, 715, 716, 791, 792, 809). Also, recent studies indicate that alterations in the UPS contribute to pathogenesis and progression of a variety of cardiac diseases (479, 568, 715, 716, 791, 792, 809).

The UPS plays a central role in the non-lysosomal degradation of most intracellular proteins (80 -90%) as well as regulation of cellular processes such as the cell cycle, transcriptional control, immune response, cell signaling, apoptosis antigen presentation, cellular mass regulation and sarcomere quality control (519, 760). The UPS regulates these processes by rapid ATP-dependent proteolysis of poly-ubiquitinated (through lysine 48) targeted intracellular proteins by the 26S proteasome (479, 518, 519, 715, 792).

The cardiac proteasome (26S), a large multi-catalytic multi-subunit protease complex, constitutes the central proteolytic machinery of the UPS. It is composed of a barrel-shaped 20S proteolytic core and one or two 19S regulatory caps. The 19S complex recognizes, unfolds and removes the ubiquitin from the so-marked proteins and facilitates entry into the 20S for degradation. It binds ubiquitinated proteins via the ubiquitin-interacting motifs of the S5a subunit (Rpn10) (238, 667). The 20S catalytic core complex is composed of four axially stacked rings. Each outer ring consists of seven different non-proteolytic  $\alpha$  subunits that allow conformational flexibility and substrate translocation into the central cavity of the 20S complex; the two inner rings are formed by seven different but related  $\beta$ -subunits giving the complex the general stoichiometry of  $\alpha_{1-7}\beta_{1-7}\beta_{1-7}\alpha_{1-7}$  (46, 518, 519, 739). The two internal rings ( $\beta$ -rings) contain the catalytic units whereas the outer  $\alpha$  -rings form a gated channel through which polypeptides enter the central chamber to be exposed to multiple proteolytic sites. Of the 14 subunits, three are catalytically active i.e. harbor proteolytic sites formed by N-terminal threonine residues that face the central cavity of the 20S complex. These are defined (based on oligopeptidyl specificity) as follows:  $\beta$ 1/post glutamyl peptide hydrolyzing/caspase like/LLE (cleaves after acidic residues),  $\beta$ 2/trypsin like/LSTR (cleaves after basic residues), and  $\beta$ 5/chymotrypsin like/LLVY (cleaves after hydrophobic residues) (46, 304, 716, 739, 760, 761). The chymotrypsin subunit is of utmost importance for overall proteasome function since it is the main one involved in removal of oxidized proteins (238, 304, 642).

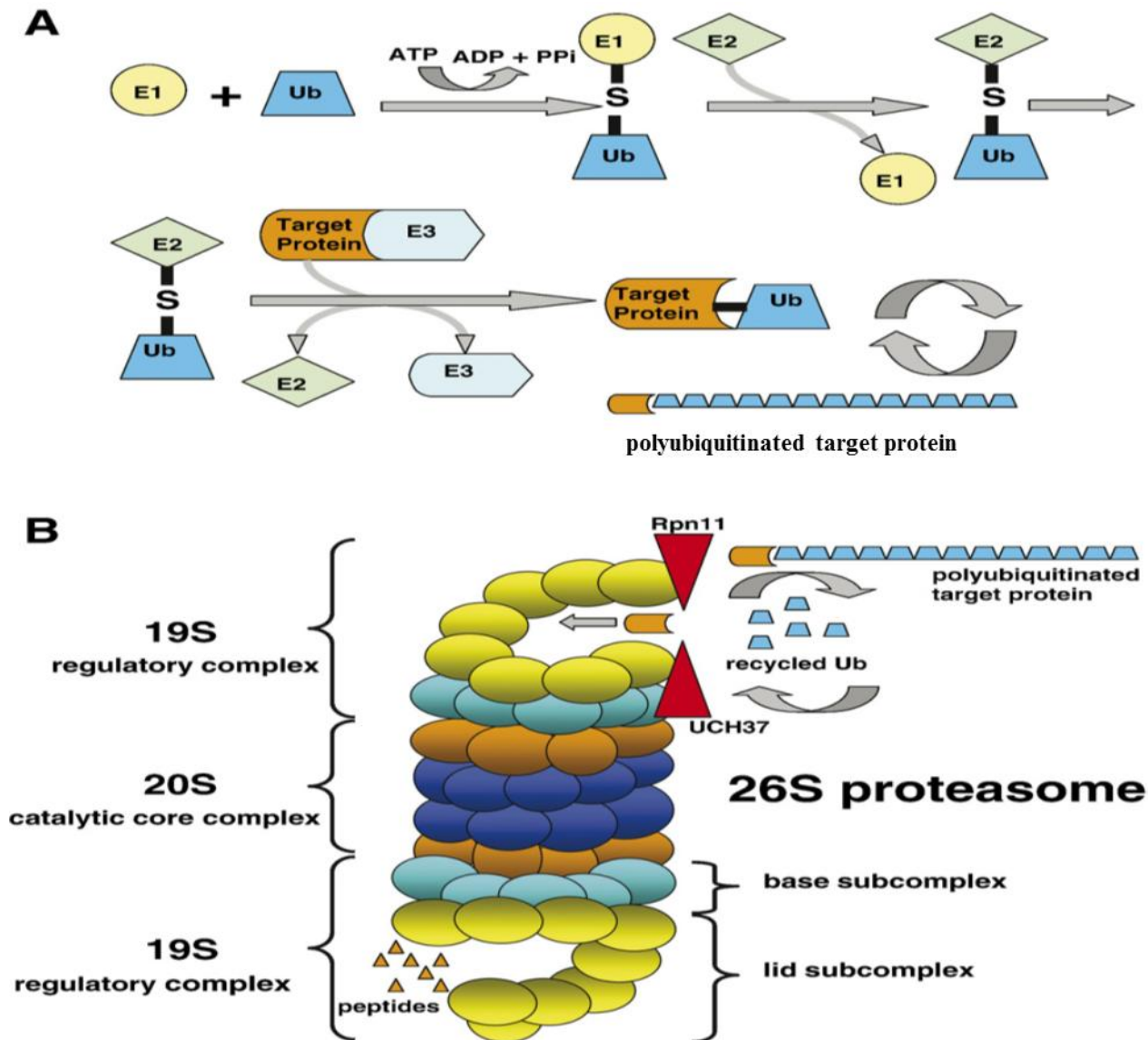


**Figure 2.11 A. Protein ubiquitination process:** with enzymes E1 (ubiquitin-activating); E2 (ubiquitin-conjugating); E3 (ubiquitin protein ligases) and Ub (ubiquitin) **B. structure of the 26S proteasome** composed of two 19S regulatory complexes on both ends and a 20S catalytic core in the middle.

Protein ubiquitination, takes place in a multistep reaction and requires three classes of enzymes: ubiquitin-activating enzymes (E1), ubiquitin-conjugating enzymes (E2), and ubiquitin-protein ligases (E3). E1 activates ubiquitin by forming a high-energy thiol ester bond between an E1 active site-located cysteine residue and the C-terminal glycine residue of ubiquitin in a reaction that requires the hydrolysis of ATP. This activated ubiquitin moiety is then transferred to E2 via the formation of an

additional thiol ester bond, and finally transferred to E3 which catalyzes the covalent attachment of ubiquitin to the target protein by the formation of isopeptide bonds. Multiple cycles of ubiquitination finally result in the synthesis and attachment of poly-ubiquitin chains that serve as a recognition signal for the degradation of the target protein by the 26S proteasome (238, 304). The 20S subunits can be observed in a variety of forms as the constitutive catalytic subunits may be substituted by inducible  $\beta$  subunits forming immunoproteasomes with additional proteolytic activities. Interferon gamma (IFN- $\gamma$ ) or TNF- $\alpha$  can result in the up-regulation of the immunoproteasomes ( $\beta$ 1i,  $\beta$ 2i and  $\beta$ 5i) and in turn alter the specificity and selectivity of the proteasome for substrates under various conditions (715, 716).

### **2.10.1 The role of the UPS in response to ischemia and reperfusion and under hyperglycemic conditions**

There is controversy regarding the role of the UPS in CVDs. For example, some studies report increased proteasomal activity in atherosclerosis due to greater oxidative stress (302, 415, 690, 729, 730). Moreover, with ischemia and reperfusion various studies found decreased UPS activity (particularly 26S proteasome) possibly as a result of ATP depletion, direct inhibition by protein aggregates and oxidative damage to the proteasome and/or regulatory subunits (91, 563, 564). By contrast, inhibition of UPS is linked to cardio-protective effects (by attenuating NF- $\kappa$ B inflammatory and apoptotic effects) with ischemia and reperfusion (91, 102, 462, 571, 666). Decreased UPS may also protect by ensuring increased levels of heat shock proteins in the heart (661).

What about the effects of the UPS during hyperglycemia? Depending on the distinct proteasome inhibitors and experimental systems employed, the role of the UPS with hyperglycemia is controversial and it is not clear whether decreased/increased activity is beneficial or not. Some found that UPS inhibition elicits beneficial effects while others observed that it caused detrimental effects on the heart (400, 464, 566–568, 715, 716, 752). 26S ATP-dependent activity decreased in response to chronic

hyperglycemia, whereas 11S activity increased together with higher oxidative stress and impaired cardiac function. This shows that increased 11S activity may be a compensatory mechanism to reduce effects of oxidative stress in response to chronic hyperglycemia. The decreased 26S activity may occur secondarily to hyperglycemia-induced alterations e.g. O-GlcNAc modification (282, 641, 677, 797) and 4-hydroxynonenal (202). Furthermore, others found that elevated levels of ubiquitinated proteins indicated a dysfunctional UPS (565, 566). However, the notion of reference to levels of ubiquitinated proteins as an indicator of UPS activity was questioned by Liu *et al.* (2000) who suggested that the rate-limiting step of enhanced protein degradation in diabetic rat heart/skeletal muscle may be located at ubiquitin conjugation and/or its binding to the proteasome, and not at the level of ubiquitin availability or the proteasome itself (437).

Conversely, hyperglycemia can initially increase UPS activity. However, this appears to occur in a temporal fashion since with chronic exposure it is inhibited to subsequently cause oxidative stress. The differences observed for UPS activity may be attributed to variations in experimental models used (*in vivo* versus *in vitro*), experimental protocols (i.e. time grading for acute and chronic periods), proteasomal components assessed and the degree of oxidative stress. Thus, further studies are required to determine the regulation of the myocardial UPS in response to ischemia and reperfusion under hyperglycemic conditions.

## **2.11 Conclusion**

This chapter has elaborated on the causal link between high glucose (acute or chronic) in the development and prognosis of cardiovascular diseases (specifically AMI). There are several shortfalls in the current medications for glycemic control (e.g. onset of hypoglycemia) and also the issue of prevailing occurrences of cardiovascular complications despite glycemic control. This demonstrates the strong need for the development of novel therapies that are more accessible (particularly in

developing nations) that may help to combat the increased burden of high glucose-induced cardiovascular complications. The main aims of this thesis were to:

1. Determine the antioxidant and anti-apoptotic effects of OA in an *in vitro* model (H9c2 myoblasts) of hyperglycemia
2. Assess functional recovery of *ex-vivo* perfused rat hearts in response to ischemia-reperfusion under baseline & hyperglycemic conditions
3. Evaluate whether OA and BFT improve functional recovery of *ex-vivo* perfused hearts and *in vivo* STZ-diabetic rat hearts after ischemia and reperfusion (baseline & hyperglycemic conditions)
4. To evaluate the anti-oxidant and anti-apoptotic effects of OA and BFT in *ex vivo* perfused hearts under baseline & hyperglycemic conditions
5. Determine mechanisms of OA cardio-protection by evaluating its impact on the HBP pathway flux
6. Evaluate the relative contributions of non-oxidative glucose pathways (HBP, polyol, AGE and PKC) to oxidative stress under baseline & hyperglycemic conditions in *ex vivo* hearts
7. To determine the mechanisms of BFT-induced cardio-protection by evaluating its effect of on flux of pathways mentioned in 6. above under baseline & hyperglycemic conditions in *ex vivo* hearts
8. Determine activity of UPS after ischemia and reperfusion under both baseline and hyperglycemic conditions in *ex vivo* hearts
9. Evaluate the effects of ischemia and reperfusion on protein carbonylation under both baseline and hyperglycemic conditions in *ex vivo* hearts
10. Investigate the effects of both OA and BFT on UPS activity after ischemia and reperfusion under baseline and hyperglycemic conditions in *ex vivo* hearts

The next chapter will therefore, discuss evaluation of OA as a potential therapy for cardiac function under hyperglycemic conditions following ischemia and reperfusion.

## 2.12 References

1. **Abe T, Ohga Y, Tabayashi N, Kobayashi S, Misawa H, Tsuji T, Kohzuki H, Suga H, Taniguchi S, Takaki M.** Left ventricular diastolic dysfunction in type 2 diabetes mellitus model rats. *Am J Physiol Heart Circ Physiol* 282: H138–H148, 2002.
2. **Abel ED.** Myocardial insulin resistance and cardiac complications of diabetes. *Curr Drug Targets Immune Endocr Metabol Disord* 5: 219–226, 2005.
3. **Abordo E, Minhas H, Thornalley P.** Accumulation of alpha-oxoaldehydes during oxidative stress: a role in cytotoxicity. *Biochem Pharmacol* 58: 641–648, 1999.
4. **ACCORD Study Group, Gerstein H, Miller M, Genuth S, Ismail-Beigi F, Buse J, Goff DJ, Probstfield J, Cushman W, Ginsberg H, Bigger J, Grimm RJ, Byington R, Rosenberg Y, Friedewald W.** Long-term effects of intensive glucose lowering on cardiovascular outcomes. *N Engl J Med* 364: 818–828, 2011.
5. **Acehan D, Jiang X, Morgan D, Heuser J, Wang X, Akey C.** Three-dimensional structure of the apoptosome: implications for assembly, procaspase-9 binding, and activation. *Mol Cell* 9: 423–432, 2002.
6. **Action to Control Cardiovascular Risk in Diabetes Study Group, Gerstein H, Miller M, Byington R, Goff DJ, Bigger J, Buse J, Cushman W, Genuth S, Ismail-Beigi F, Grimm RJ, Probstfield J, Simons-Morton D, Friedewald W.** Effects of intensive glucose lowering in type 2 diabetes. *N Engl J Med* 358: 2545–2559, 2008.
7. **Adams JM, Pratipanawatr T, Berria R, Wang E, DeFronzo R, Sullards M, Mandarino L.** Ceramide content is increased in skeletal muscle from obese insulin-resistant humans. *Diabetes* 53: 25–31, 2004.
8. **ADVANCE Collaborative Group, Patel A, MacMahon S, Chalmers J, Neal B, Billot L, Woodward M, Marre M, Cooper M, Glasziou P, Grobbee D, Hamet P, Harrap S, Heller S, Liu L, Mancia G, Mogensen C, Pan C, Poulter N, Rodgers A, Williams B, Bompoint S, De Galan B, Joshi R, Travert F.** Intensive blood glucose control and vascular outcomes in patients with type 2 diabetes. *N Engl J Med* 358: 2560–2572, 2008.
9. **Agardh E, Hultberg B, Agardh C.** Effects of inhibition of glycation and oxidative stress on the development of cataract and retinal vessel abnormalities in diabetic rats. *Curr Eye Res* 21: 543–549, 2000.
10. **Ahmed MU, Dunn JA, Walla MD, Thorpe SR, Baynes JW.** Oxidative degradation of glucose adducts to protein. *J Biol Chem* 263: 8816–8821, 1988.
11. **Ahmed N.** Advanced glycation endproducts--role in pathology of diabetic complications. *Diab Res Clin Prac* 67: 3–21, 2005.

12. **Aiello L.** The potential role of PKC beta in diabetic retinopathy and macular edema. *Survey of ophthalmology* 47: S263–S269, 2002.
13. **Ainla T, Baburin A, Teesalu R, Rahu M.** The association between hyperglycaemia on admission and 180-day mortality in acute myocardial infarction patients with and without diabetes. *Diabet Med* 22: 1321–1325, 2005.
14. **Ajjan R, Grant P.** Cardiovascular disease prevention in patients with type 2 diabetes: The role of oral anti-diabetic agents. *Diab Vasc Dis Res* 3: 147–158, 2006.
15. **Aleshin A, Ananthkrishnan R, Li Q, Rosario R, Lu Y.** RAGE modulates myocardial injury consequent to LAD infarction via impact on JNK and STAT signaling in a murine model. *Am J Physiol Heart Circ Physiol* 294: H1823–1832 294: H1823–H1832, 2008.
16. **Allison S, Tomlin P, Chamberlain M.** Some effects of anesthesia and surgery on carbohydrate and fat metabolism. *Br J Anaesthesia* 41: 588–592, 1969.
17. **Altschuld R, Wenger W, Lamka K, Kindig O, Capen C, Mizuhira V, Vander Heide R, Brierley G.** Structural and functional properties of adult rat heart myocytes lysed with digitonin. *J Biol Chem* 260: 14325–14334, 1985.
18. **Ambrosios G, Zweierjt JL, Duilio C, Kuppusamyj P, Santoro G, Elia PP, Tritto I, Condorelli M, Chiariello M, Flahertyj JT.** Evidence that mitochondrial respiration is a source of potentially toxic oxygen free radicals in intact rabbit hearts subjected to ischemia and reflow. *J Biol Chem* 268: 18532–18541, 1993.
19. **American Diabetes Association.** Postprandial blood glucose. American Diabetes Association. *Diab Care* 24: 775–778, 2001.
20. **An D, Rodrigues B.** Role of changes in cardiac metabolism in development of diabetic cardiomyopathy. *Am J Physiol Heart Circ Physiol* 291: H1489–H1506, 2006.
21. **Ananthkrishnan R, Kaneko M, Hwang YC, Quadri N, Gomez T, Li Q, Caspersen C, Ramasamy R.** Aldose reductase mediates myocardial ischemia-reperfusion injury in part by opening mitochondrial permeability transition pore. *Am J Physiol Heart Circ Physiol* 296: H333–H341, 2009.
22. **Aneja A, Tang W, Bansilal S, Garcia M, Farkouh M.** Diabetic cardiomyopathy: insights into pathogenesis, diagnostic challenges, and therapeutic options. *Am J Med* 121: 748–757, 2008.
23. **Ang C, Alviar M, Dans A, Bautista-Velez G, Villaruz-Sulit M, Tan J, Co H, Bautista M, Roxas A.** Vitamin B for treating peripheral neuropathy. *Cochrane Database Syst Rev* 3: CD004573, 2008.
24. **Anversa P, Cheng W, Liu Y, Leri A, Redaelli G, Kajstura J.** Apoptosis and myocardial infarction. *Basic Res Cardiol* 93: 8–12, 1998.
25. **Argirova M, Ortwerth B.** Activation of protein-bound copper ions during early glycation: study on two proteins. *Arch Biochem Biophys* 420: 176–184, 2003.



26. **Aronson D.** Cross-linking of glycated collagen in the pathogenesis of arterial and myocardial stiffening of aging and diabetes. *J Hypertens* 21: 3–12, 2003.
27. **Arteel G, Briviba K, Sies H.** Protection against peroxynitrite. *FEBS Lett* 445: 226–230, 1999.
28. **Asif M, Egan J, Vasan S, Jyothirmayi, GN, Masurekar M, Lopez S, Williams C, Torres R, Wagle D, Ulrich P, Cerami A, Brines M, Regan T.** An advanced glycation endproduct cross-link breaker can reverse age-related increases in myocardial stiffness. *Proc Natl Acad Sci U S A* 97: 2809–2813, 2000.
29. **Asnaghi V, Gerhardinger C, Hoehn T, Adeboje A, Lorenzi M.** A role for the polyol pathway in the early neuroretinal apoptosis and glial changes induced by diabetes in the rat. *Diabetes* 52: 506–511, 2003.
30. **Atkinson L, Kozak R, Kelly S, Onay Besikci A, Russell J, GD L.** Potential mechanisms and consequences of cardiac triacylglycerol accumulation in insulin-resistant rats. *Am J Physiol Endocrinol Metab* 284: E923–E930, 2003.
31. **Avignon A, Radauceanu A, Monnier L.** Nonfasting plasma glucose is a better marker of diabetic control than fasting plasma glucose in type 2 diabetes. *Diab Care* 20: 1822–1826, 1997.
32. **Babaei-jadidi R, Karachalias N, Ahmed N, Battah S, Thornalley PJ.** Prevention of incipient diabetic nephropathy by high-dose thiamine and benfotiamine. *Diabetes* 52: 2110–2120, 2003.
33. **Babior B.** NADPH oxidase: an update. *Blood* 93: 1464–1476, 1999.
34. **Bailey C, Turner R.** Metformin. *N Engl J Med* 334: 574–579, 1996.
35. **Baines C, Kaiser R, Purcell N, Blair N, Osinska H, Hambleton M, Brunskill E, Sayen M, Gottlieb R, Dorn G, Robbins J, Molkentin J.** Loss of cyclophilin D reveals a critical role for mitochondrial permeability transition in cell death. *Nature* 434: 658–662, 2005.
36. **Baker H, Frank O.** Absorption, utilization and clinical effectiveness of allithiamines compared to water-soluble thiamines. *J Nutr Sci Vitaminol (Tokyo)* 22: 63–68, 1976.
37. **Bakker W, Eringa EC, Sipkema P, Van Hinsbergh VWM.** Endothelial dysfunction and diabetes: roles of hyperglycemia, impaired insulin signaling and obesity. *Cell Tissue Res* 335: 165–189, 2009.
38. **Balakumar P, Rohilla A, Krishan P, Solairaj P, Thangathirupathi A.** The multifaceted therapeutic potential of benfotiamine. *Pharmacol Res* 61: 482–488, 2010.
39. **Balkau B, Bertrais S, Ducimetiere P, Eschwege E.** Is there a glycemic threshold for mortality risk? *Diab Care* 22: 696–699, 1999.

40. **Balteau M, Tajeddine N, De Meester C, Ginion A, Des Rosiers C, Brady NR, Sommereyns C, Horman S, Vanoverschelde J-L, Gailly P, Hue L, Bertrand L, Beauloye C.** NADPH oxidase activation by hyperglycaemia in cardiomyocytes is independent of glucose metabolism but requires SGLT1. *Cardiovasc Res* 92: 237–246, 2011.
41. **Bansal V, Kalita J, Misra U.** Diabetic neuropathy. *Postgrad Med J* 82: 95–100, 2006.
42. **Bao Q, Shi Y.** Apoptosome: a platform for the activation of initiator caspases. *Cell Death Differ* 14: 56–65, 2007.
43. **Barja G, Herrero A.** Localization at complex I and mechanism of the higher free radical production of brain nonsynaptic mitochondria in the short-lived rat than in the longevous pigeon. *J Bioenerg Biomembr* 30: 235–243, 1998.
44. **Barja G.** Mitochondrial oxygen radical generation and leak : sites of production in states 4 and 3 , organ specificity , and relation to aging and longevity. *J Bioenerg* 31: 347–366, 1999.
45. **Basha B, Samuel SM, Triggle CR, Ding H.** Endothelial dysfunction in diabetes mellitus: possible involvement of endoplasmic reticulum stress? *Exp Diab Res* 2012: 481840, 2012.
46. **Baumeister W, Walz J, Zühl F, Seemüller E.** The proteasome: paradigm of a self-compartmentalizing protease. *Cell* 92: 367–380, 1998.
47. **Baynes J.** Role of oxidative stress in development of complications in diabetes. *Diabetes* 40: 405–412, 1991.
48. **Baynes JW, Thorpe SR.** The role of oxidative stress in diabetic complications. *Curr Opin Endocrinol* 3: 277–284, 1996.
49. **Becker L.** New concepts in reactive oxygen species and cardiovascular reperfusion physiology. *Cardiovasc Res* 61: 461–470, 2004.
50. **Beckman JA, Creager MA, Libby P.** Diabetes and atherosclerosis: epidemiology, pathophysiology, and management. *JAMA* 287: 2570–2581, 2002.
51. **Beisswenger P, Howell S, Nelson R, Mauer M, Szwegold B.** Alpha-oxoaldehyde metabolism and diabetic complications. *Biochem Soc Trans* 31: 1358–1363, 2003.
52. **Beisswenger P, Ruggiero-Lopez D.** Metformin inhibition of glycation processes. *Diab Metab* 29: 6S95–6S103, 2003.
53. **Belke DD, Larsen TS, Gibbs EM, Severson DL.** Altered metabolism causes cardiac dysfunction in perfused hearts from diabetic (db/db) mice. *Am J Physiol Endocrinol Metab* 279: E1104–E1113, 2000.
54. **Beltramo E, Berrone E, Tarallo S, Porta M.** Effects of thiamine and benfotiamine on intracellular glucose metabolism and relevance in the prevention of diabetic complications. *Acta Diabetol* 45: 131–141, 2008.

55. **Beltramo E, Nizheradze K, Berrone E, Tarallo S, Porta M.** Thiamine and benfotiamine prevent apoptosis induced by high glucose-conditioned extracellular matrix in human retinal pericytes. *Diab Metab Res Rev* 25: 647–656, 2009.
56. **Beneke S, Bürkle A.** Poly(ADP-ribosyl)ation in mammalian ageing. *Nucleic Acids Res* 35: 7456–7465, 2007.
57. **Benjamin E, Larson M, Kannel W, Vasan R.** Obesity and the risk of heart failure. *N Eng J Med* 347: 305–313, 2002.
58. **Benzi R, Lerch R.** Dissociation between contractile function and oxidative metabolism in postischemic myocardium. Attenuation by ruthenium red administered during reperfusion. *Circ Res* 71: 567–576, 1992.
59. **Berry C, Hare J.** Xanthine oxidoreductase and cardiovascular disease: molecular mechanisms and pathophysiological implications. *J Physiol* 16: 589–606, 2004.
60. **Bethel M, Feinglos M.** Insulin analogues: new therapies for type 2 diabetes mellitus. *Curr Diab Rep* 2: 403–408, 2002.
61. **Bhat N, Zhang P.** Hydrogen peroxide activation of multiple mitogen-activated protein kinases in an oligodendrocyte cell line: role of extracellular signal-regulated kinase in hydrogen peroxide-induced cell death. *J Neurochem* 72: 112–119, 1999.
62. **Bierhaus A, Schiekofler S, Schwaninger M, Andrassy M, Humpert PM, Chen J, Hong M, Luther T, Henle T, Kloting I, Morcos M, Hofmann M, Tritschler H, Weigle B, Kasper M, Smith M, Perry G, Schmidt A-M, Stern DM, Haring H-U, Schleicher E, Nawroth PP.** Diabetes-associated sustained activation of the transcription factor nuclear factor- $\kappa$ B. *Diabetes* 50: 2792–2808, 2001.
63. **Biesenbach G, Raml A, Schmekal B, Eichbauer-Sturm G.** Decreased insulin requirement in relation to GFR in nephropathic Type 1 and insulin-treated Type 2 diabetic patients. *Diabet Med* 20: 642–645, 2003.
64. **Van Bilsen M, Van der Vusse GJ, Willemsen PH, Coumans WA, Roemen TH, Reneman RS.** Lipid alterations in isolated, working rat hearts during ischemia and reperfusion: its relation to myocardial damage. *Circ Res* 64: 304–314, 1989.
65. **Bisognano J, Weinberger H, Bohlmeier T, Pende A, Reynolds M, Sastravaha A, Roden R, Asano K, Blaxall B, Wu S, Communal C, Singh K, Colucci W, Bristow M, Port D.** Myocardial-directed overexpression of the human beta(1)-adrenergic receptor in transgenic mice. *J Mol Cell Cardiol* 32: 817–830, 2000.
66. **Bitsch R, Wolf M, Möller J, Heuzeroth L, Grünekle D.** Bioavailability assessment of the lipophilic benfotiamine as compared to a water-soluble thiamin derivative. *Ann Nutr Metab* 35: 292–296, 1991.

67. **Björkerud S, Björkerud B.** Apoptosis is abundant in human atherosclerotic lesions, especially in inflammatory cells (macrophages and T cells), and may contribute to the accumulation of gruel and plaque instability. *Am J Pathol* 149: 367–380, 1996.
68. **Bloomgarden ZT.** Diabetic nephropathy. *Diabetes care* 31: 823–827, 2008.
69. **Boatright K, Renatus M, Scott F, Sperandio S, Shin H, Pedersen I, Ricci J, Edris W, Sutherlin D, Green D, Salvesen G.** A unified model for apical caspase activation. *Mol Cell* 11: 529–541, 2003.
70. **Bode D.** Defining the importance of daily glycemic control and implications for type 2 diabetes management. *Postgrad Med* 121: 82–93, 2009.
71. **Bolk J, Van der Ploeg T, Cornel JH, Arnold AE, Sepers J, Umans VA.** Impaired glucose metabolism predicts mortality after a myocardial infarction. *Int J Cardiol* 79: 207–214, 2001.
72. **Bolton W, Cattran D, Williams M, Adler S, Appel G, Cartwright K, Foiles P, Freedman B, Raskin P, Ratner R, Spinowitz B, Whittier F, Wuerth J.** Randomized trial of an inhibitor of formation of advanced glycation end products in diabetic nephropathy. ; ACTION I Investigator Group. *Am J Nephrol* 24: 32–40, 2004.
73. **Bonfoco E, Krainc D, Ankarcona M, Nicotera P, Lipton S.** Apoptosis and necrosis: two distinct events induced, respectively, by mild and intense insults with N-methyl-D-aspartate or nitric oxide/superoxide in cortical cell cultures. *Proc Natl Acad Sci U S A* 92: 7162–7166, 1995.
74. **Bonnefont-Rousselot D, Bastard J, Jaudon M, Delattre J.** Consequences of diabetic status on the oxidant/antioxidant balance. *Diab Metab (Paris)* 26: 163–176, 2000.
75. **Bonora E, Calcaterra F, Lombardi S, Bonfante N, Formentini G, Bonadonna R, Muggeo M.** Plasma glucose levels throughout the day and HbA(1c) interrelationships in type 2 diabetes: implications for treatment and monitoring of metabolic control. *Diab Care* 24: 2023–2029, 2001.
76. **Boveris A, Cadenas E, Stoppani A.** Role of ubiquinone in the mitochondrial generation of hydrogen peroxide. *Biochem J* 156: 435–444, 1976.
77. **Bowes A, Khan M, Shi Y, Robertson L, Werstuck G.** Valproate attenuates accelerated atherosclerosis in hyperglycemic apoE-deficient mice: evidence in support of a role for endoplasmic reticulum stress and glycogen synthase kinase-3 in lesion development and hepatic steatosis. *Am J Pathol* 174: 330–342, 2009.
78. **Bozdağ-Dündar O, Verspohl E, Daş-Evcimen N, Kaup R, Bauer K, Sarikaya M, Evranos B, Ertan R.** Synthesis and biological activity of some new flavonyl-2,4-thiazolidinediones. *Bioorg Med Chem* 16: 6747–6751, 2008.
79. **Brand M, Affourtit C, Esteves T, Green K, Lambert A, Miwa S, Pakay J, Parker N.** Mitochondrial superoxide: production, biological effects, and activation of uncoupling proteins. *Free Radic Biol Med* 37: 755–767, 2004.

80. **Brandes R, Behra A, Lebherz C, Böger R, Bode-Böger S, Mügge A.** Lovastatin maintains nitric oxide--but not EDHF-mediated endothelium-dependent relaxation in the hypercholesterolemic rabbit carotid artery. *Atheroscl* 142: 97–104, 1999.
81. **Brosius III F, Liu Y, Nguyen N, Sun D, Bartlett J SM.** Persistent myocardial ischemia increases GLUT1 glucose transporter expression in both ischemic and non-ischemic heart regions. *J Mol Cell Cardiol* 29: 1675–1685, 1997.
82. **Brown J, Nichols G.** Slow response to loss of glycemic control in type 2 diabetes mellitus. *Am J Manag Care* 9: 213–217, 2003.
83. **Brown M, Bird S, Watling S, Kaleta H, Hayes L, Eckert S, Foyt H.** Natural progression of diabetic peripheral neuropathy in the Zenarestat study population. *Diab Care* 27: 1153–1159, 2004.
84. **Brownlee M, Vlassara H, Kooney A, Ulrich P, Cerami A.** Aminoguanidine prevents diabetes-induced arterial wall protein cross-linking. *Science* 232: 1629–1632, 1986.
85. **Brownlee M.** Advanced protein glycosylation in diabetes and aging. *Annu Rev Med* 46: 223–234, 1995.
86. **Brownlee M.** Biochemistry and molecular cell biology of diabetic complications. *Nature* 414: 813–820, 2001.
87. **Brownlee M.** The pathobiology of diabetic complications a unifying mechanism. *Diabetes* 54: 1615–1625, 2005.
88. **Bucciarelli LG, Ananthkrishnan R, Hwang YC, Kaneko M, Song F, Sell DR, Strauch C, Monnier VM, Yan SF, Schmidt AM, Ramasamy R.** RAGE and modulation of ischemic injury in the diabetic myocardium. *Diabetes* 57: 1941–1951, 2008.
89. **Bucciarelli LG, Kaneko M, Ananthkrishnan R, Harja E, Lee LK, Hwang YC, Lerner S, Bakr S, Li Q, Lu Y, Song F, Qu W, Gomez T, Zou YS, Yan SF, Schmidt AM.** Receptor for advanced-glycation end products: key modulator of myocardial ischemic injury. *Circ* 113: 1226–1234, 2006.
90. **Buettner G.** The pecking order of free radicals and antioxidants: lipid peroxidation, alpha-tocopherol, and ascorbate. *Arch Biochem Biophys* 300: 535–543, 1993.
91. **Bulteau AL, Lundberg KC, Humphries KM, Sadek HA, Szweda PA, Friguet B, Szweda LI.** Oxidative modification and inactivation of the proteasome during coronary occlusion/reperfusion. *J Biol Chem* 276: 30057–30063, 2001.
92. **Burton K, Buja L, Sen A, Willerson J, Chien K.** Accumulation of arachidonate in triacylglycerols and unesterified fatty acids during ischemia and reflow in the isolated rat heart. Correlation with the loss of contractile function and the development of calcium overload. *Am J Pathol* 124: 238–245, 1986.

93. **Buse JB, Ginsberg HN, Bakris GL, Clark NG, Costa F, Eckel R, Fonseca V, Gerstein HC, Grundy S, Nesto RW, Pignone MP, Plutzky J, Porte D, Redberg R, Stitzel KF, Stone NJ, American Heart Association, American Diabetes Association.** Primary prevention of cardiovascular diseases in people with diabetes mellitus: a scientific statement from the American Heart Association and the American Diabetes Association. *Circ* 115: 114–126, 2007.
94. **Buse MG.** Hexosamines, insulin resistance, and the complications of diabetes: current status. *Am J Physiol Endocrinol Metab* 290: E1–E8, 2006.
95. **Buss S, Muenz S, Riffel J, Malekar P, Hagenmueller M, Weiss C, Bea F, Bekeredjian R, Schinke-Braun M, Izumo S, Katus H, Hardt S.** Beneficial effects of mammalian target of rapamycin inhibition on left ventricular remodeling after myocardial infarction. *J Am Coll Cardiol* 54: 2435–2446, 2009.
96. **Buttke T, Sandstrom P.** Oxidative stress as a mediator of apoptosis. *Immunol Today* 15: 7–10, 1994.
97. **Bürkle A.** Poly(ADP-ribose). The most elaborate metabolite of NAD<sup>+</sup>. *FEBS J* 272: 4576–4589, 2005.
98. **Cai L, Kang Y.** Oxidative stress and diabetic cardiomyopathy: a brief review. *Cardiovasc Toxicol* 1: 181–193, 2001.
99. **Cai L, Li W, Wang G, Guo L, Jiang Y, Kang YJ.** hyperglycemia-induced apoptosis in mouse myocardium: mitochondrial cytochrome c-mediated caspase-3 activation pathway. *Diabetes* 51: 1938–1948, 2002.
100. **Cai L, Wang J, Li Y, Sun X, Wang L.** Inhibition of superoxide generation and associated nitrosative damage is involved in metallothionein prevention of diabetic cardiomyopathy. *Diabetes* 54: 1829–1837, 2005.
101. **Calles-Escandon J, Robbins D.** Loss of early phase of insulin release in humans impairs glucose tolerance and blunts thermic effect of glucose. *Diabetes* 36: 1167–1172, 1987.
102. **Campbell B, Adams J, Shin Y, Lefer A.** Cardioprotective effects of a novel proteasome inhibitor following ischemia and reperfusion in the isolated perfused rat heart. *J Mol Cell Cardiol* 31: 467–476, 1999.
103. **Capaldo B, Galderisi M, Turco AA, D’Errico A, Turco S, Rivellese AA, De Simone G, De Divitiis O, Riccardi G.** Acute hyperglycemia does not affect the reactivity of coronary microcirculation in humans. *J Clin Endocrinol Metab* 90: 3871–3876, 2005.
104. **Capes SE, Hunt D, Malmberg K, Gerstein HC.** Stress hyperglycaemia and increased risk of death after myocardial infarction in patients with and without diabetes: a systematic overview. *Lancet* 355: 773–778, 2000.
105. **Cappai G, Songini M, Doria A, Cavallerano J, Lorenzi M.** Increased prevalence of proliferative retinopathy in patients with type 1 diabetes who are deficient in glucose-6-phosphate dehydrogenase. *Diabetol* 54: 1539–1542, 2011.

106. **Caputo S, Pitocco D, Ruotolo V, Ghirlanda G.** What is the real contribution of fasting plasma glucose and postprandial glucose in predicting HbA(1c) and overall blood glucose control? *Diab Care* 24: 2011, 2001.
107. **Carette C, Dubois-Laforgue D, Gautier J, Timsit J.** Diabetes mellitus and glucose-6-phosphate dehydrogenase deficiency: from one crisis to another. *Diabetes Metab* 37: 79–82, 2011.
108. **Casey T, Pakay J, Guppy M, Arthur P.** Hypoxia causes downregulation of protein and RNA synthesis in non-contracting mammalian cardiomyocytes. *Circ Res* 90: 777–783, 2002.
109. **Catherwood MA, Powell LA, Anderson P, McMaster D, Sharpe PC, Trimble ER.** Glucose-induced oxidative stress in mesangial cells. *Kidney Int* 61: 599–608, 2002.
110. **Cave A, Ingwall J, Friedrich J, Liao R, Saupe K, Apstein C, Eberli F.** ATP synthesis during low-flow ischemia: influence of increased glycolytic substrate. *Circ* 101: 2090–2096, 2000.
111. **Cellek S, Qu W, Schmidt A, Moncada S.** Synergistic action of advanced glycation end products and endogenous nitric oxide leads to neuronal apoptosis in vitro: a new insight into selective nitrenergic neuropathy in diabetes. *Diabetol* 47: 331–339, 2004.
112. **Ceriello A, Ihnat M.** Oxidative stress is, convincingly, the mediator of the dangerous effects of glucose variability. *Diab Med* 27: 968, 2010.
113. **Ceriello A, Morocutti A, Mercuri F, Quagliaro L, Moro M, Damante G, Viberti G.** Defective intracellular antioxidant enzyme production in type 1 diabetic patients with nephropathy. *Diabetes* 49: 2170–2177, 2000.
114. **Ceriello A, Quagliaro L, Amico MD, Filippo C Di, Marfella R, Nappo F, Berrino L, Rossi F, Giugliano D.** Acute hyperglycemia induces nitrotyrosine formation and apoptosis in perfused heart from rat. *Diabetes* 51: 1076–1082, 2002.
115. **Ceriello A, Quagliaro L, Catone B, Pascon R, Piazzola M, Bais B, Marra G, Tonutti L, Taboga C, Motz E.** Role of hyperglycemia in nitrotyrosine postprandial generation. *Diabetes Care* 25: 1439–1443, 2002.
116. **Ceriello A.** Oxidative stress and glycemic regulation. *Metab Clin Exp* 49: 27–29, 2000.
117. **Ceriello A.** New insights on oxidative stress and diabetic complications may lead to a “causal” antioxidant therapy. *Diab Care* 26: 1589–1596, 2003.
118. **Ceriello A.** Acute hyperglycaemia: a “new” risk factor during myocardial infarction. *Eur Heart J* 26: 328–231, 2005.
119. **Chakrabarti A, Singh P, Gopalakrishnan L, Kumar V, Elizabeth Doherty M, Abueg C, Wang W, Gibson C.** Admission hyperglycemia and acute myocardial infarction: outcomes and potential therapies for diabetics and nondiabetics. *Cardiol Res Pract* 2012: 704314, 2012.

120. **Chatham JC, Forder JR.** A C-NMR study of glucose oxidation in the intact functioning rat heart following diabetes-induced cardiomyopathy. *J Mol Cell Cardiol* 25: 1203–1213, 1993.
121. **Chatham JC, Marchase RB.** The role of protein O-linked beta-N-acetylglucosamine in mediating cardiac stress responses. *Biochim Biophys Acta* 1800: 57–66, 2010.
122. **Chatham JC, Nöt LG, Fülöp N, Marchase RB.** Hexosamine biosynthesis and protein O-glycosylation: the first line of defense against stress, ischemia, and trauma. *Shock (Augusta, Ga.)* 29: 431–440, 2008.
123. **Chen Q, Vazquez EJ, Moghaddas S, Hoppel CL, Lesnefsky EJ.** Production of reactive oxygen species by mitochondria: central role of complex III. *J Biol Chem* 278: 36027–36031, 2003.
124. **Chen S, Evans T, Mukherjee K, Karmazyn M, Chakrabarti S.** Diabetes-induced myocardial structural changes: role of endothelin-1 and its receptors. *J Mol Cell Cardiol* 32: 1621–1629, 2000.
125. **Chen T, Goodwin G, Guthrie P, Taegtmeyer H.** Effects of insulin on glucose uptake by rat hearts during and after coronary flow reduction. *Am J Physiol* 273: H2170–H2177, 1997.
126. **Chen Y, Chen C, Zhang L, Green-Church K, Zweier J.** Superoxide generation from mitochondrial NADH dehydrogenase induces self-inactivation with specific protein radical formation. *J Biol Chem* 280: 37339–37348, 2005.
127. **Chen Z, Siu B, Ho YS, Vincent R, Chua CC, Hamdy RC, Chua BH.** Overexpression of MnSOD protects against myocardial ischemia/reperfusion injury in transgenic mice. *J Mol Cell Cardiol* 30: 2281–2289, 1998.
128. **Cheng J, Huang C, Liu I, Tzeng T, Chang C.** Novel mechanism for plasma glucose-lowering action of metformin in streptozotocin-induced diabetic rats. *Diabetes* 55: 819–825, 2006.
129. **Chiarelli F, Marzio D Di.** Peroxisome proliferator-activated receptor- $\gamma$  agonists and diabetes: Current evidence and future perspectives. *Vasc Health Risk Manag* 4: 297–304, 2008.
130. **Chien KR, Sen a, Reynolds R, Chang a, Kim Y, Gunn MD, Buja LM, Willerson JT.** Release of arachidonate from membrane phospholipids in cultured neonatal rat myocardial cells during adenosine triphosphate depletion. Correlation with the progression of cell injury. *J Clin Invest* 75: 1770–1780, 1985.
131. **Christoffersen C, Bollano E, Lindegaard M, Bartels E, Goetze J, Andersen C, Nielsen L.** Cardiac lipid accumulation associated with diastolic dysfunction in obese mice. *Endocrinol* 144: 3483–3490, 2003.
132. **Churchill EN, Ferreira JC, Brum PC, Szweda LI, Mochly-Rosen D.** Ischaemic preconditioning improves proteasomal activity and increases the degradation of delta PKC during reperfusion. *Cardiovasc Res* 85: 385–394, 2010.



133. **Clandinin MT, Cheema S, Field CJ, Garg ML, Venkatraman J, Clandinin TR.** Dietary fat: exogenous determination of membrane structure and cell function. *Fed Am Soc Exp Biol J* 5: 2761–2769, 1991.
134. **Clark RJ, McDonough PM, Swanson E, Trost SU, Suzuki M, Fukuda M, Dillman WH.** Diabetes and the accompanying hyperglycemia impairs cardiomyocyte calcium cycling through increased nuclear O-GlcNAcylation. *J Biol Chem* 278: 44230–44237, 2003.
135. **Collins A, Raslová K, Somorovská M, Petrovská H, Ondrusová A, Vohnout B, Fábry R, Dusinská M.** DNA damage in diabetes: correlation with a clinical marker. *Free Radic Biol Med* 25: 373–377, 1998.
136. **Colussi C, Albertini M, Coppola S, Rovidati S, Galli F, Ghibelli L.** H<sub>2</sub>O<sub>2</sub>-induced block of glycolysis as an active ADP-ribosylation reaction protecting cells from apoptosis. *Fed Am Soc Exp Biol J* 14: 2266–2276, 2000.
137. **Cooper M, Gilbert R, Epstein M.** Pathophysiology of diabetic nephropathy. *Metab* 47: 3–6, 1998.
138. **Cooper M.** Pathogenesis, prevention, and treatment of diabetic nephropathy. *Lancet* 352: 213–219, 1998.
139. **Coort S, Luiken J, Van der Vusse G, Bonen A, Glatz J.** Increased FAT (fatty acid translocase)/CD36-mediated long-chain fatty acid uptake in cardiac myocytes from obese Zucker rats. *Biochem Soc Trans* 32: 83–85, 2004.
140. **Crabbe M, Goode D.** Aldose reductase: a window to the treatment of diabetic complications? *Prog Retin Eye Res* 17: 313–383, 1998.
141. **Crandall J, Shamon H, Cohen H, Reid M, Gajavelli S, Trandafirescu G, Tabatabaie V, Barzilai N.** Post-challenge hyperglycemia in older adults is associated with increased cardiovascular risk profile. *J Clin Endocrinol Metab* 94: 1595–1601, 2009.
142. **Creager M, Lüscher T, Cosentino F, Beckman J.** Diabetes and vascular disease: pathophysiology, clinical consequences, and medical therapy: Part I. *Circ* 108: 1527–1532, 2003.
143. **Cromlish J, Flynn T.** Purification and characterization of an enzymically active cleavage product of pig kidney aldehyde reductase. *Biochem J* 209: 597–607, 1983.
144. **Cromlish J, Yoshimoto C, Flynn T.** Purification and characterization of four NADPH-dependent aldehyde reductases from pig brain. *Neurochem* 44: 1477–1484, 1985.
145. **Crompton M.** The mitochondrial permeability transition pore and its role in cell death. *Biochem J* 249: 233–249, 1999.
146. **Cruikshank N.** Coronary thrombosis and myocardial infarction, with glycosuria. *Br Med J* 1: 618–619, 1931.

147. **Cunningham J, Mearkle P, Brown R.** Vitamin C: an aldose reductase inhibitor that normalizes erythrocyte sorbitol in insulin-dependent diabetes mellitus. *J Am Coll Nutr* 13: 344–350, 1994.
148. **Damsbo P, Clauson P, Marbury T, Windfeld K.** A double-blind randomized comparison of meal-related glycemic control by repaglinide and glyburide in well-controlled type 2 diabetic patients. *Diab Care* 22: 789–794, 1999.
149. **Damy T, Ratajczak P, Robidel E, JK B, Oliviero P, Boczkowski J, Ebrahimian T, Marotte F, Samuel J, Heymes C.** Up-regulation of cardiac nitric oxide synthase 1-derived nitric oxide after myocardial infarction in senescent rats. *Fed Am Soc Exp Biol J* 17: 1934–1936, 2003.
150. **Das A, Harris D.** Regulation of the mitochondrial ATP synthase in intact rat cardiomyocytes. *Biochem J* 266: 355–361, 1990.
151. **Das A.** Regulation of the mitochondrial ATP-synthase in health and disease. *Mol Gen Metab* 79: 71–82, 2003.
152. **Decker R, Wildenthal K.** Lysosomal alterations in hypoxic and reoxygenated hearts. I. Ultrastructural and cytochemical changes. *Am J Pathol* 98: 425–444, 1980.
153. **DECODE.** Glucose tolerance and cardiovascular mortality: comparison of fasting and 2-hour diagnostic criteria. *Arch Intern Med* 161: 397–405, 2001.
154. **DeFronzo R.** Pharmacologic therapy for type 2 diabetes mellitus. *Ann Intern Med* 131: 281–303, 1999.
155. **Degrell P, Cseh J, Mohás M, Molnár G, Pajor L, Chatham J, Fülöp N, Wittmann I.** Evidence of O-linked N-acetylglucosamine in diabetic nephropathy. *Life Sci* 84: 389–393, 2009.
156. **DeGroot J.** The AGE of the matrix: chemistry, consequence and cure. *Curr Opinion Pharmacol* 4: 301–305, 2004.
157. **Degterev A, Huang Z, Boyce M, Li Y, Jagtap P, Mizushima N, Cuny G, Mitchison T, Moskowitz M, Yuan J.** Chemical inhibitor of nonapoptotic cell death with therapeutic potential for ischemic brain injury. *Nat Chem Biol* 1: 112–119, 2005.
158. **Dennis S, Gevers W, Opie L.** Protons in ischemia: where do they come from; where do they go to? *J Mol Cell Cardiol* 23: 1077–1086, 1991.
159. **Deora AA, Win T, Vanhaesebroeck B, Lander HM.** A redox-triggered ras-effector interaction. Recruitment of phosphatidylinositol 3'-kinase to Ras by redox stress. *J Biol Chem* 273: 29923–29928, 1998.
160. **Desagher S, Martinou JC.** Mitochondria as the central control point of apoptosis. *Trends Cell Biol* 10: 369–377, 2000.
161. **Desco M, Asensi M, Márquez R, Martínez-Valls J, Vento M, Pallardó F, Sastre J, Viña J.** Xanthine oxidase is involved in free radical production in type 1 diabetes: protection by allopurinol. *Diabetes* 51: 1118–1124, 2002.

162. **DeSouza C, Fonseca V.** Therapeutic targets to reduce cardiovascular disease in type 2 diabetes. *Nat Rev Drug Discov* 8: 361–367, 2009.
163. **Desrois M, Sidell RJ, Gauguier D, King LM, Radda GK, Clarke K.** Initial steps of insulin signaling and glucose transport are defective in the type 2 diabetic rat heart. *Cardiovasc Res* 61: 288–296, 2004.
164. **Devaraj S, Rosenson R, Jialal I.** Metabolic syndrome: an appraisal of the pro-inflammatory and procoagulant status. *Endocrinol Metab Clin North Am* 33: 431–453, 2004.
165. **Dhar A, Desai K, Kazachmov M, Yu P, Wu L.** Methylglyoxal production in vascular smooth muscle cells from different metabolic precursors. *Metab* 57: 1211–1220, 2008.
166. **Dhindsa P, Davis K, Donnelly R.** Comparison of the micro- and macro-vascular effects of glimepiride and gliclazide in metformin-treated patients with Type 2 diabetes: a double-blind, crossover study. *Br J Clin Pharmacol* 55: 616–619, 2003.
167. **Diabetes Control and Complications Trial Research Group.** The effect of intensive treatment of diabetes on the development and progression of long term complications in insulin-dependent diabetes mellitus. *N Engl J Med* 329: 977–986, 1993.
168. **Diefenbach J, Bürkle A.** Introduction to poly(ADP-ribose) metabolism. *Cell Mol Life Sci* 62: 721–730, 2005.
169. **Dimmeler S, Haendeler J, Galle J, Zeiher A.** Oxidized low-density lipoprotein induces apoptosis of human endothelial cells by activation of CPP32-like proteases. A mechanistic clue to the “response to injury” hypothesis. *Circ* 95: 1760–1763, 1997.
170. **Dimmeler S, Haendeler J, Nehls M, Zeiher A.** Suppression of apoptosis by nitric oxide via inhibition of interleukin-1 $\beta$ -converting enzyme (ICE)-like and cysteine protease protein (CPP)-32-like proteases. *J Exp Med* 185: 601–607, 1997.
171. **Dinneen S, Gerich J, Rizza R.** Carbohydrate metabolism in non-insulin-dependent diabetes mellitus. *N Engl J Med* 327: 707–713, 1992.
172. **Dormandy J, Charbonnel B, Eckland D, Erdmann E, Massi-Benedetti M, Moules I, Skene A, Tan M, Lefèbvre P, Murray G, Standl E, Wilcox R, Wilhelmsen L, Betteridge J, Birkeland K, Golay A, Heine R, Korányi L, Laakso M, Mokán M, Norkus A, Pirags V, Podar T, Scheen A, Scherbaum W, Schernthaner G, Schmitz O, Skrha J, Smith U, Taton J, PROactive Investigators.** Secondary prevention of macrovascular events in patients with type 2 diabetes in the PROactive Study (PROspective pioglitAzone Clinical Trial In macroVascular Events): a randomised controlled trial. *Lancet* 366: 1279–1289, 2005.
173. **Doyle M, Egan J.** Glucagon-like peptide-1. *Recent Prog Horm Res* 56: 377–399, 2001.
174. **Dresner A, Laurent D, Marcucci M, Griffin ME, Dufour S, Cline GW, Slezak L a, Andersen DK, Hundal RS, Rothman DL, Petersen KF, Shulman GI.** Effects of free fatty acids on glucose transport and IRS-1-associated phosphatidylinositol 3-kinase activity. *J Clin Invest* 103: 253–259, 1999.

175. **Du X, Edelstein D, Dimmeler S, Ju Q, Sui C, Brownlee M.** Hyperglycemia inhibits endothelial nitric oxide synthase activity by posttranslational modification at the Akt site. *J Clin Invest* 108: 1341–1348, 2001.
176. **Du X, Edelstein D, Rossetti L, Fantus IG, Goldberg H, Ziyadeh F, Wu J, Brownlee M.** Hyperglycemia-induced mitochondrial superoxide overproduction activates the hexosamine pathway and induces plasminogen activator inhibitor-1 expression by increasing Sp1 glycosylation. *Proc Natl Am Sci* 97: 12222–12226, 2000.
177. **Du X, Matsumura T, Edelstein D, Rossetti L, Zsengellér Z, Szabó C, Brownlee M.** Inhibition of GAPDH activity by poly (ADP-ribose) polymerase activates three major pathways of hyperglycemic damage in endothelial cells. *J Clin Invest* 112: 1049–1057, 2003.
178. **Du Y, Miller C, Kern T.** Hyperglycemia increases mitochondrial superoxide in retina and retinal cells. *Free Radic Biol Med* 35: 1491–1499, 2003.
179. **Duckworth W, Abraira C, Moritz T, Reda D, Emanuele N, Reaven P, Zieve F, Marks J, Davis S, Hayward R, Warren S, Goldman S, McCarren M, Vitek M, Henderson W, Huang G, Investigators V.** Glucose control and vascular complications in veterans with type 2 diabetes. *N Engl J Med* 360: 129–139, 2009.
180. **Dunlop M.** Aldose reductase and the role of the polyol pathway in diabetic nephropathy. *Kidney Int Suppl* 77: S3–S12, 2000.
181. **Eaton J, Qian M.** Interactions of copper with glycosylated proteins: possible involvement in the etiology of diabetic neuropathy. *Mol Cell Biochem* 234-235: 135–142, 2002.
182. **Ebrahimian T, Tamarat R, Clergue M, Duriez M, Levy B, Silvestre J.** Dual effect of angiotensin-converting enzyme inhibition on angiogenesis in type 1 diabetic mice. *Arterioscler Thromb Vasc Biol* 25: 65–70, 2005.
183. **Eckel J, Reinauer H.** Insulin action on glucose transport in isolated cardiac myocytes: signalling pathways and diabetes-induced alterations. *Biochem Soc Trans* 18: 1125–1127, 1990.
184. **Edwards, CM, Stanley, SA, Davis, R, Brynes, AE, Frost, GS, Seal, LJ, Ghatei, MA, Bloom S.** Exendin-4 reduces fasting and postprandial glucose and decreases energy intake in healthy volunteers. *Am J Physiol Endocrinol Metab* 281: E155–E161, 2001.
185. **Egert S, Nguyen N, Schwaiger M.** Myocardial glucose transporter GLUT1: translocation induced by insulin and ischemia. *J Mol Cell Cardiol* 1344: 1337–1344, 1999.
186. **Ekundayo O, Muchimba M, Aban I, Ritchie C, Campbell R, Ahmed A.** Multimorbidity due to diabetes mellitus and chronic kidney disease and outcomes in chronic heart failure. *Am J Cardiol* 103: 88–92, 2009.
187. **Emilien G, Maloteaux J, Ponchon M.** Pharmacological management of diabetes: recent progress and future perspective in daily drug treatment. *Pharmacol Ther* 81: 37–51, 1999.

188. **Engerman R, Kern T.** Progression of incipient diabetic retinopathy during good glycaemic control. *Diabetes* 36: 808–812, 1987.
189. **Epidemiology of Diabetes Interventions and Complications (EDIC) study.** Sustained effect of intensive treatment of type 1 diabetes mellitus on development and progression of diabetic nephropathy: the Epidemiology of Diabetes Interventions and Complications (EDIC) study. *J Am Med Assoc* 290: 2159–2167, 2003.
190. **Erlinger T, Brancati F.** Postchallenge hyperglycemia in a national sample of U.S. adults with type 2 diabetes. *Diab Care* 24: 1734–1738, 2001.
191. **Esakova O, Meshalkina L, Golbik R, Hübner G, Kochetov G.** Donor substrate regulation of transketolase. *Eur J Biochem* 271: 4189–4194, 2004.
192. **Escargueil-Blanc I, Meilhac O, Pieraggi M, Arnal J, Salvayre R, Nègre-Salvayre A.** Oxidized LDLs induce massive apoptosis of cultured human endothelial cells through a calcium-dependent pathway. Prevention by aurintricarboxylic acid. *Arterioscler Thromb Vasc Biol* 17: 331–339, 1997.
193. **Esposito K, Majorino M, Di Palo C, Giugliano D.** Campaign post-prandial hyperglycemia study group. Dietary glycaemic index and glycaemic load are associated with metabolic control in type 2 diabetes: The CAPRI experience. *Metab Syndr Relat Disord* 8: 255–261, 2010.
194. **Esposito K, Nappo F, Marfella R, Giugliano G, Giugliano F, Ciotola M, Quagliaro L, Ceriello A, Giugliano D.** Inflammatory cytokine concentrations are acutely increased by hyperglycemia in humans: role of oxidative stress. *Circ* 106: 2067–2072, 2002.
195. **Evans J, Lee J, Ragolia L.** Ang-II-induced Ca(2+) influx is mediated by the 1/4/5 subgroup of the transient receptor potential proteins in cultured aortic smooth muscle cells from diabetic Goto-Kakizaki rats. *Mol Cell Endocrinol* 302: 49–57, 2009.
196. **Das Evcimen N, King G.** The role of protein kinase C activation and the vascular complications of diabetes. *Pharmacol Res* 55: 498–510, 2007.
197. **Fan J, Watanabe T.** Inflammatory reactions in the pathogenesis of atherosclerosis. *J Atheroscler Thromb* 10: 63–71, 2003.
198. **Federici M, Menghini R, Mauriello A, Hribal M, Ferrelli F, Lauro D, Sbraccia P, Spagnoli L, Sesti G, Lauro R.** Insulin-dependent activation of endothelial nitric oxide synthase is impaired by O-linked glycosylation modification of signaling proteins in human coronary endothelial cells. *Circ* 106: 466–472, 2002.
199. **Ferdinandy P, Danial H, Ambrus I, Rothery R, Schulz R.** Peroxynitrite is a major contributor to cytokine-induced myocardial contractile failure. *Circ Res* 87: 241–247, 2000.
200. **Fernandez Juarez G, Luño J, Barrio V, De Vinuesa S, Praga M, Goicoechea M, Cachofeiro V, Nieto J, Fernández Vega F, Tato A, Gutierrez E, Group ;PRONEDI Study.** Effect of dual blockade of the renin-angiotensin system on the progression of type 2 diabetic nephropathy: a randomized trial. *Am J Kidney Dis*. Epub ahead of print, 2012.

201. **Ferreira F, Palmeira C, Seiça R, Moreno A, Santos M.** Diabetes and mitochondrial bioenergetics: alterations with age. *J Biochem Mol Toxicol* 17: 214–222, 2003.
202. **Ferrington D, Kapphahn R.** Catalytic site-specific inhibition of the 20S proteasome by 4-hydroxynonenal. *FEBS Lett* 578: 217–223, 2004.
203. **Fiordaliso F, Leri A, Cesselli D, Limana F, Safai B, Nadal-ginard B, Anversa P, Kajstura J.** Hyperglycemia Activates p53 and p53-Regulated Genes Leading to Myocyte Cell Death. *Diabetes* 50: 2363–2375, 2001.
204. **Fischer V, Barner H, Larose L.** Pathomorphologic aspects of muscular tissue in diabetes mellitus. *Hum Pathol* 15: 1127–1136, 1984.
205. **Fitzl G, Welt K, Wassilew G, Clemens N, Penka K, Mücke N.** The influence of hypoxia on the myocardium of experimentally diabetic rats with and without protection by Ginkgo biloba extract. III: Ultrastructural investigations on mitochondria. *Exp Toxicol Pathol* 52: 557–568, 2001.
206. **Fliss H, Gattinger D.** Apoptosis in ischemic and reperfused rat myocardium. *Circ Res* 79: 949–956, 1996.
207. **Flynn P, Byrne C, Baglin T, Weissberg P, Bennett M.** Thrombin generation by apoptotic vascular smooth muscle cells. *Blood* 89: 4378–4384, 1997.
208. **Folli F, Corradi D, Fanti P, Davalli A, Paez A, Giaccari A, Perego C, Muscogiuri G.** The role of oxidative stress in the pathogenesis of type 2 diabetes mellitus micro- and macrovascular complications: avenues for a mechanistic-based therapeutic approach. *Curr Diabetes Rev* 7: 313–324, 2011.
209. **Fonseca V.** Management of diabetes in the hospital. *Rev Cardiovasc Med* 7: S10–S17, 2006.
210. **Foo K, Cooper J, Deaner A, Knight C, Suliman A, Ranjadayalan K, Timmis AD.** A single serum glucose measurement predicts adverse outcomes across the whole range of acute coronary syndromes. *Heart* 89: 512–516, 2003.
211. **Forbes J, Cooper M, Thallas V, Burns W, Thomas M, Brammar G, Lee F, Grant S, Burrell L, Jerums G, Osicka T.** Reduction of the accumulation of advanced glycation end products by ACE inhibition in experimental diabetic nephropathy. *Diabetes* 51: 3274–3282, 2002.
212. **Forbes JM, Yee LTL, Thallas V, Lassila M, Candido R, Jandeleit-Dahm K a, Thomas MC, Burns WC, Deemer EK, Thorpe SR, Thorpe SM, Cooper ME, Allen TJ.** Advanced glycation end product interventions reduce diabetes-accelerated atherosclerosis. *Diabetes* 53: 1813–23, 2004.
213. **Forman M, Puett D, Virmani R.** Endothelial and myocardial injury during ischemia and reperfusion: pathogenesis and therapeutic implications. *J Am Coll Cardiol* 13: 450–459, 1989.
214. **Fowler MJ.** Diabetes treatment, part 2: oral agents for glycemic management. *Clin Diab* 25: 131–134, 2007.

215. **Fried L, Borhani N, Enright P, Furberg C, Gardin J, Kronmal R, Kuller L, Manolio T, Mittelmark M, Newman A, O'Leary D, Psaty B, Rautaharju P, Tracy R, Weiler P, for the Cardiovascular Health Study Research Group (CHS).** The Cardiovascular Health Study: design and rationale. *Ann Epidemiol* 1: 263–276, 1991.
216. **Frustaci A, Kajstura J, Chimenti C, Jakoniuk I, Leri A, Maseri A, Nadal-ginard B, Anversa P.** Myocardial cell death in human diabetes. *Circ. Res* 87: 1123–1132, 2000.
217. **Fryer LGD, Parbu-Patel A, Carling D.** The Anti-diabetic drugs rosiglitazone and metformin stimulate AMP-activated protein kinase through distinct signaling pathways. *J Biol Chem* 277: 25226–25232, 2002.
218. **Fujimoto K, Hozumi T, Watanabe H, Tokai K, Shimada K, Yoshiyama M, Homma S, Yoshikawa J.** Acute hyperglycemia induced by oral glucose loading suppresses coronary microcirculation on transthoracic Doppler echocardiography in healthy young adults. *Echocardiogr* 23: 829–834, 2006.
219. **Fujiwara M, Sasakawa S, Itokawa Y, Ikeda K.** Affinity of thiamine propyl disulfide-S35 to organs. *Vitaminol (Kyoto)* 10: 79–87, 1964.
220. **Fuller J, Shipley M, Rose G, Jarrett R, Keen H.** Mortality from coronary heart disease and stroke in relation to degree of glycaemia: the Whitehall study. *Br Med J (Clin Res Ed)* 287: 867–870, 1983.
221. **Gabriely I, Yang X, Cases J, Ma X, Rossetti L, Barzilai N.** Hyperglycemia induces PAI-1 gene expression in adipose tissue by activation of the hexosamine biosynthetic pathway. *Atheroscl* 160: 115–122, 2002.
222. **Gallwitz B.** Exenatide in type 2 diabetes: treatment effects in clinical studies and animal study data. *J Clin Pract* 60: 1654–1661, 2006.
223. **Gamble J, Lopaschuk GD.** Glycolysis and glucose oxidation during reperfusion of ischemic hearts from diabetic rats. *Biochim Biophys Acta* 1225: 191–199, 1994.
224. **Ganapathy V, Smith S, Prasad P.** SLC19: the folate/thiamine transporter family. *Pflugers Arch* 447: 641–646, 2004.
225. **Garciarena CD, Caldiz CI, Correa M V, Schinella GR, Mosca SM, Chiappe de Cingolani GE, Cingolani HE, Ennis IL.** Na<sup>+</sup>/H<sup>+</sup> exchanger-1 inhibitors decrease myocardial superoxide production via direct mitochondrial action. *J Appl Physiol (Bethesda : 1985)* 105: 1706–13, 2008.
226. **Gardiner T, Anderson H, Stitt A.** Inhibition of advanced glycation end-products protects against retinal capillary basement membrane expansion during long-term diabetes. *J Pathol* 201: 328–333, 2003.
227. **Garvey WT, Maianu L, Huecksteadt TP, Birnbaum MJ, Molina JM, Ciaraldi TP.** Pretranslational suppression of a glucose transporter protein causes insulin resistance in

- adipocytes from patients with non-insulin-dependent diabetes mellitus and obesity. *J Clin Invest* 87: 1072–1081, 1991.
228. **Geng Y, Henderson L, Levesque E, Muszynski M, Libby P.** Fas is expressed in human atherosclerotic intima and promotes apoptosis of cytokine-primed human vascular smooth muscle cells. *Arterioscler Thromb Vasc Biol* 17: 2200–2208, 1997.
229. **Genova M, Ventura B, Giuliano G, Bovina C, Formiggini G, Parenti Castelli G, Lenaz G.** The site of production of superoxide radical in mitochondrial complex I is not a bound ubisemiquinone but presumably iron-sulfur cluster N2. *FEBS Lett* 505: 364–368, 2001.
230. **Gerich J.** Clinical significance, pathogenesis, and management of postprandial hyperglycemia. *Arch Intern Med* 163: 1306–1316, 2003.
231. **Gerstein H.** Is glucose a continuous risk factor for cardiovascular mortality? *Diabetes Care* 22: 659–660, 1999.
232. **Geyer J, Netzel M, Bitsch I, Frank T, Bitsch R, Krämer K, Hoppe P.** Bioavailability of water- and lipid-soluble thiamin compounds in broiler chickens. *Int J Vitam Nutr Res* 70: 311–316, 2000.
233. **Giacco F, Brownlee M.** Oxidative stress and diabetic complications. *Circ Res* 107: 1058–1070, 2010.
234. **Giardino I, Edelstein D, Brownlee M.** Nonenzymatic glycosylation in vitro and in bovine endothelial cells alters basic fibroblast growth factor activity. A model for intracellular glycosylation in diabetes. *J Clin Invest* 94: 110–117, 1994.
235. **Giardino I, Edelstein D, Brownlee M.** Bcl-2 expression antioxidants prevent hyperglycemia-induced formation of intracellular advanced glycation end products in bovine endothelial cells. *J Clin Invest* 97: 1422–1428, 1996.
236. **Giardino I, Fard A, Hatchell D, Brownlee M.** Aminoguanidine inhibits reactive oxygen species formation, lipid peroxidation, and oxidant-induced apoptosis. *Diabetes* 47: 1114–1120, 1998.
237. **Giugliano D, Ceriello A, Paolisso G.** Oxidative stress and diabetic vascular complications. *Diabetes Care* 19: 257–267, 1996.
238. **Glickman MH, Ciechanover A.** The ubiquitin-proteasome proteolytic pathway: destruction for the sake of construction. *Physiol Rev* 82: 373–428, 2002.
239. **Gnudi L, Thomas SM, Viberti G.** Mechanical forces in diabetic kidney disease: a trigger for impaired glucose metabolism. *J Am Soc Nephrol* 18: 2226–2232, 2007.
240. **Gnudi L, Viberti G, Raij L, Rodriguez V, Burt D, Cortes P, Hartley B, Thomas S, Maestrini S, Gruden G.** GLUT-1 overexpression: Link between hemodynamic and metabolic factors in glomerular injury? *Hypertension* 42: 19–24, 2003.



241. **Goldberg H, Whiteside C, Fantus I.** The hexosamine pathway regulates the plasminogen activator inhibitor-1 gene promoter and Sp1 transcriptional activation through protein kinase C-beta I and -delta. *J Biol Chem* 277: 33833–33841, 2002.
242. **Goldberg H, Whiteside C, Hart G, Fantus I.** Posttranslational, reversible O-glycosylation is stimulated by high glucose and mediates plasminogen activator inhibitor-1 gene expression and Sp1 transcriptional activity in glomerular mesangial cells. *Endocrinol* 147: 222–231, 2006.
243. **Goldberg R, Einhorn D, Lucas C, Rendell M, Damsbo P, Huang W, Strange P, Brodows R.** A randomized placebo-controlled trial of repaglinide in the treatment of type 2 diabetes. *Diab Care* 21: 1897–1903, 1998.
244. **Goldin A, Beckman J, Schmidt A, Creager M.** Advanced glycation end products: sparking the development of diabetic vascular injury. *Circ* 114: 597–605, 2006.
245. **González R, Barnett P, Cheng H, Chylack LJ.** Altered phosphate metabolism in the intact rabbit lens under high glucose conditions and its prevention by an aldose reductase inhibitor. *Exp Eye Res* 39: 553–562, 1984.
246. **Goodarzi M, Navidi A, Rezaei M, Babahmadi-Rezaei H.** Oxidative damage to DNA and lipids: correlation with protein glycation in patients with type 1 diabetes. *J Clin Lab Anal* 24: 72–76, 2010.
247. **Gordin D, Forsblom C, Rönneck M, Groop P.** Acute hyperglycaemia disturbs cardiac repolarization in Type 1 diabetes. *Diabet Med* 25: 101–105, 2008.
248. **Gordin D, Rönneck M, Forsblom C, Heikkilä O, Saraheimo M, Groop PH.** Acute hyperglycaemia rapidly increases arterial stiffness in young patients with type 1 diabetes. *Diabetologia* 50: 1808–1814, 2007.
249. **Gottlieb R, Burleson K, Kloner R, Babior B, Engler R.** Reperfusion injury induces apoptosis in rabbit cardiomyocytes. *J Clin Invest* 94: 1621–1628, 1994.
250. **Gottlieb RA.** Cell death pathways in acute i/r injury. *J Cardiovasc Pharmacol Ther* 16: 233–238, 2011.
251. **Goyal A, Mahaffey KW, Garg J, Nicolau JC, Hochman JS, Weaver WD, Theroux P, Oliveira GB, Todaro TG, Mojcik CF, Armstrong PW, Granger CB.** Prognostic significance of the change in glucose level in the first 24 h after acute myocardial infarction: results from the CARDINAL study. *Eur Heart J* 27: 1289–1297, 2006.
252. **Graham S, Yuan JP, Ma R.** Canonical transient receptor potential channels in diabetes. *Exp Biol Med Maywood, N.J.* 237: 111–118, 2012.
253. **Greb A, Bitsch R.** Comparative bioavailability of various thiamine derivatives after oral administration. *Int J Clin Pharmacol Ther* 36: 216–221, 1998.
254. **Gresele P, Guglielmini G, De Angelis M, Ciferri S, Ciofetta M, Falcinelli E, Lalli C, Ciabattini G, Davi G, Bolli GB.** Acute, short-term hyperglycemia enhances shear stress-

- induced platelet activation in patients with type II diabetes mellitus. *J Am Coll Cardiol* 41: 1013–1020, 2003.
255. **Griendling K, Sorescu D, Ushio-Fukai M.** NAD(P)H oxidase: role in cardiovascular biology and disease. *Circ Res* 86: 494–501, 2000.
256. **Griffin M, Marcucci M, Cline G.** Free fatty acid-induced insulin resistance is associated with activation of protein kinase C theta and alterations in the insulin signaling cascade. *Diabetes* 48, 1999.
257. **Griffiths EJ, Halestrapt AP.** Mitochondrial non-specific pores remain closed during cardiac ischaemia , but open upon reperfusion. 98: 93–98, 1995.
258. **Grivennikova VG, Vinogradov AD.** Generation of superoxide by the mitochondrial Complex I. *Biochim Biophys Acta (BBA)* 1757: 553–561, 2006.
259. **Grover J, Yadav S, Vats V.** Medicinal plants of India with anti-diabetic potential. *J Ethnopharmacol* 81: 81–100, 2002.
260. **Gruden G, Thomas S, Burt D, Lane S, Chusney G, Sacks S, Viberti G.** Mechanical stretch induces vascular permeability factor in human mesangial cells: mechanisms of signal transduction. *Proc Natl Acad Sci U S A* 94: 12112–12116, 1997.
261. **Guleria R, Choudhary R, Tanaka T, Baker KM, Pan J.** Retinoic acid receptor-mediated signaling protects cardiomyocytes from hyperglycemia induced apoptosis : role of the renin-angiotensin system. *J Cell Physiol* 226: 1292–1307, 2011.
262. **Guo M, Wu M, Korompai F, Yuan S.** Upregulation of PKC genes and isozymes in cardiovascular tissues during early stages of experimental diabetes. *Physiol Genomics* 12: 139–146, 2003.
263. **Gupte RS, Floyd BC, Kozicky M, George S, Ungvari ZI, Neito V, Wolin MS, Gupte SA.** Synergistic activation of glucose-6-phosphate dehydrogenase and NAD(P)H oxidase by Src kinase elevates superoxide in type 2 diabetic, Zucker fa/fa, rat liver. *Free Radic Biol Med* 47: 219–228, 2009.
264. **Gupte RS, Vijay V, Marks B, Levine RJ, Sabbah HN, Wolin MS, Recchia FA, Gupte SA.** Upregulation of glucose-6-phosphate dehydrogenase and NAD(P)H oxidase activity increases oxidative stress in failing human heart. *J Cardiac Fail* 13: 497–506, 2007.
265. **Gupte S, Levine RJ, Gupte RS, Young ME, Lionetti V, Labinskyy V, Floyd BC, Ojaimi C, Bellomo M, Wolin MS, Recchia F a.** Glucose-6-phosphate dehydrogenase-derived NADPH fuels superoxide production in the failing heart. *J Mol Cell Cardiol* 41: 340–349, 2006.
266. **Gustafsson AB, Gottlieb RA.** Autophagy in ischemic heart disease. *Circ Res* 104: 150–158, 2009.
267. **Gustafsson ÅB, Gottlieb RA.** Recycle or die : The role of autophagy in cardioprotection. *Heart* 44: 654 –661, 2008.

268. **Guzik T, Mussa S, Gastaldi D, Sadowski J, Ratnatunga C, Pillai R, Channon K.** Mechanisms of increased vascular superoxide production in human diabetes mellitus: role of NAD(P)H oxidase and endothelial nitric oxide synthase. *Circ* 105: 1656–1662, 2002.
269. **Haber C, Lam T, Yu Z, Gupta N, Goh T, Bogdanovic E, Giacca A, Fantus I.** N-acetylcysteine and taurine prevent hyperglycemia-induced insulin resistance in vivo: possible role of oxidative stress. *Am J Physiol Endocrinol Metab* 285: E744–E753, 2003.
270. **Hadjadj S, Coisne D, Mauco G, Ragot S, Duengler F, Sosner P, Torremocha F, Herpin D, Marechaud R.** Prognostic value of admission plasma glucose and HbA<sub>1c</sub> in acute myocardial infarction. *Diabet Med* 21: 305–310, 2004.
271. **Haffner S.** The importance of hyperglycemia in the nonfasting state to the development of cardiovascular disease. *Endocr Rev* 19: 583–592, 1998.
272. **Halat K, Dennehy C.** Botanicals and dietary supplements in diabetic peripheral neuropathy. *J Am Board Fam Pract* 16: 47–57, 2003.
273. **Halestrap A, Clarke S, Javadov S.** Mitochondrial permeability transition pore opening during myocardial reperfusion--a target for cardioprotection. *Cardiovasc Res* 61: 372–385, 2004.
274. **Hall JL, Lopaschuk GD, Barr A, Bringas J, Pizzurro RD, Stanley WC.** Increased cardiac fatty acid uptake with dobutamine infusion in swine is accompanied by a decrease in malonyl CoA levels. *Cardiovasc Res* 32: 879–885, 1996.
275. **Halliwell B.** Biochemistry of oxidative stress. *Biochem Soc Trans* 35: 1147–1150, 2007.
276. **Hamacher-Brady A, Brady N, Gottlieb R.** Enhancing macroautophagy protects against ischemia/ reperfusion injury in cardiac myocytes. *J Biol Chem* 281: 29776–29787, 2006.
277. **Hamacher-Brady A, Brady N, Logue S, Sayen M, Jinno M, Kirshenbaum L, Gottlieb R, Gustafsson A.** Response to myocardial ischemia/reperfusion injury involves Bnip3 and autophagy. *Cell Death Differ* 14: 146–157, 2007.
278. **Hamada Y, Araki N, Koh N, Nakamura J, Horiuchi S, Hotta N.** Rapid formation of advanced glycation end products by intermediate metabolites of glycolytic pathway and polyol pathway. *Biochem Biophys Res Commun* 228: 539–543, 1996.
279. **Hamada Y, Odagaki Y, Sakakibara F, Naruse K, Koh N, Hotta N.** Effects of an aldose reductase inhibitor on erythrocyte fructose 3-phosphate and sorbitol 3-phosphate levels in diabetic patients. *Life Sci* 57: 23–29, 1995.
280. **Hammes H, Martin S, Federlin K, Geisen K, Brownlee M.** Aminoguanidine treatment inhibits the development of experimental diabetic retinopathy. *Proc Natl Acad Sci USA* 88: 11555–11558, 1991.
281. **Han D, Haudenschild C, Hong M, Tinkle B, Leon M, Liao G.** Evidence for apoptosis in human atherogenesis and in a rat vascular injury model. *Am J Pathol* 147: 267–277, 1995.

282. **Han I, Kudlow J.** Reduced O glycosylation of Sp1 is associated with increased proteasome susceptibility. *Mol Cell Biol* 17: 2550–2558, 1997.
283. **Hanefeld M, Fischer S, Julius U, Schulze J, Schwanebeck U, Schmechel H, Ziegelsch H, Lindner J.** Risk factors for myocardial infarction and death in newly detected NIDDM: the Diabetes Intervention Study, 11-year follow-up. *Diabetologia* 39: 1577–1583, 1996.
284. **Hanefeld M.** The role of acarbose in the treatment of non-insulin-dependent diabetes mellitus. *J Diab Comp* 12: 228–237, 1998.
285. **Hanover J, Forsythe M, Hennessey P, Brodigan T, Love D, Ashwell G, Krause M.** A *Caenorhabditis elegans* model of insulin resistance: altered macronutrient storage and dauer formation in an OGT-1 knockout. *Proc Natl Acad Sci U S A* 102: 11266–11271, 2005.
286. **Hansford R, Cohen L.** Relative importance of pyruvate dehydrogenase interconversion and feed-back inhibition in the effect of fatty acids on pyruvate oxidation by rat heart mitochondria. *Arch Biochem Biophys* 191: 65–81, 1978.
287. **Hansson G.** Immune and inflammatory mechanisms in the development of atherosclerosis. *Br Heart J* 69: S38–S41, 1993.
288. **Hansson G.** Inflammation, atherosclerosis, and coronary artery disease. *N Engl J Med* 352: 1685–1695, 2005.
289. **Hara A, Harada T, Nakagawa M, Matsuura K, Nakayama T, Sawada H.** Isolation from pig lens of two proteins with dihydrodiol dehydrogenase and aldehyde reductase activities. *Biochem J* 264: 403–407, 1989.
290. **Hargrove G, Dufresne J, Whiteside C, Muruve D, Wong N.** Diabetes mellitus increases endothelin-1 gene transcription in rat kidney. *Kidney Int* 58: 1534–1545, 2000.
291. **Hartog JW, Voors AA, Bakker SJL, Smit AJ, Van Veldhuisen DJ.** Advanced glycation end-products (AGEs) and heart failure: pathophysiology and clinical implications. *Eur J Heart Fail* 9: 1146–1155, 2007.
292. **Haupt E, Ledermann H, Köpcke W.** Benfotiamine in the treatment of diabetic polyneuropathy--a three-week randomized, controlled pilot study (BEDIP study). *Int J Clin Pharmacol Ther* 43: 71–77, 2005.
293. **Hausenloy D.** Magnitude and relevance of reperfusion injury. *Heart Metab* 54: 5–8, 2012.
294. **Havivi E, Bar On H, Reshef A, Stein P, Raz I.** Vitamins and trace metals status in non insulin dependent diabetes mellitus. *Int J Vitam Nutr Res* 61: 328–333, 1991.
295. **Hayoz D, Ziegler T, Brunner H, Ruiz J.** Diabetes mellitus and vascular lesions. *Metab* 47: 16–19, 1998.

296. **Hazen S, Wolf M, Ford D, Gross R.** The rapid and reversible association of phosphofructokinase with myocardial membranes during myocardial ischemia. *FEBS Lett* 339: 213–216, 1994.
297. **Heath H, Paterson R, Hart J.** Changes in the hydroxyproline, hexosamine and sialic acid of the diabetic human and beta, beta'-iminodipropionitrile-treated rat retinal vascular systems. *Diabetologia* 3: 515–518, 1967.
298. **Heather L, Carr C, Stuckey D, Pope S, Morten K, Carter E, Edwards L, Clarke K.** Critical role of complex III in the early metabolic changes following myocardial infarction. *Cardiovasc Res* 85: 127–136, 2010.
299. **Henriquez M, Armisén R, Stutzin A, Quest A.** Cell death by necrosis, a regulated way to go. *Curr Mol Med* 8: 187–206, 2008.
300. **Van Herpen N, Schrauwen-Hinderling V.** Lipid accumulation in non-adipose tissue and lipotoxicity. *Physiol Behav* 94: 231–241, 2008.
301. **Herrero A, Barja G.** Sites and mechanisms responsible for the low rate of free radical production of heart mitochondria in the long-lived pigeon. 98: 95–111, 1997.
302. **Herrmann J, Edwards W, Holmes DJ, Shogren K, Lerman L, Ciechanover A, Lerman A.** Increased ubiquitin immunoreactivity in unstable atherosclerotic plaques associated with acute coronary syndromes. *J Am Coll Cardiol* 40: 1919–1927, 2002.
303. **Hers H.** The mechanism of the transformation of glucose in fructose in the seminal vesicle. *Biochim Biophys Acta* 22: 202–203, 1956.
304. **Hershko A, Ciechanover A.** The ubiquitin system. *Ann Rev Biochem* 67: 425–479, 1998.
305. **Van Heyningen R.** Sugar alcohols in the pathogenesis of galactose and diabetic cataracts. *Birth Defects Orig Artic Ser* 12: 295–303, 1976.
306. **Hirsch I, Bode B, Garg S, Lane W, Sussman A, Hu P, Santiago O, Kolaczynski J.** Continuous subcutaneous insulin infusion (CSII) of insulin aspart versus multiple daily injection of insulin aspart/insulin glargine in type 1 diabetic patients previously treated with CSII. *Diab Care* 28: 533–538, 2005.
307. **Ho F, Liu S, Liau C, Huang P, Lin-Shiau S.** High glucose-induced apoptosis in human endothelial cells is mediated by sequential activations of c-Jun NH(2)-terminal kinase and caspase-3. *Circ* 101: 2618–2624, 2000.
308. **Hofmann P, Menon V, Gannaway K.** Effects of diabetes on isometric tension as a function of [Ca<sup>2+</sup>] and pH in rat skinned cardiac myocytes. *Am J Physiol* 269: H1656–H1663, 1995.
309. **Holman R, Paul S, Bethel M, Matthews D, Neil H.** 10-year follow-up of intensive glucose control in type 2 diabetes. *N Engl J Med* 359: 1577–1589, 2008.

310. **Home P, Pocock S, Beck-Nielsen H, Curtis P, Gomis R, Hanefeld M, Jones N, Komajda M, McMurray J, RECORD Study Team.** Rosiglitazone evaluated for cardiovascular outcomes in oral agent combination therapy for type 2 diabetes (RECORD): a multicentre, randomised, open-label trial. *Lancet* 373: 2125–2135, 2009.
311. **Hopper L, Ness A, Higgins JP, Moore T, Ebrahim S.** GISSI-Prevenzione trial. *Lancet* 354: 1557, 1999.
312. **Horecker BL.** The pentose phosphate pathway. *J Biol Chem* 277: 47965–47971, 2002.
313. **Horton E, Clinkingbeard C, Gatlin M, Foley J, Mallows S, Shen S.** Nateglinide alone and in combination with metformin improves glycemic control by reducing mealtime glucose levels in type 2 diabetes. *Diab Care* 23: 1660–1665, 2000.
314. **Hu S, Wang S, Fanelli B, Bell P, Dunning B, Geisse S, Schmitz R, Boettcher B.** Pancreatic beta-cell K(ATP) channel activity and membrane-binding studies with nateglinide: A comparison with sulfonylureas and repaglinide. *J Pharmacol Exp Ther* 293: 444–452, 2000.
315. **Hu Y, Belke D, Suarez J, Swanson E, Clark R, Hoshijima M, Dillman WH.** Adenovirus-mediated overexpression of O-GlcNAcase improves contractile function in the diabetic heart. *Circ Res* 96: 1006–1013, 2005.
316. **Huang JS, Guh JY, Hung WC, Yang ML, Lai YH, Chen HC, Chuang LY.** Role of the Janus kinase (JAK)/signal transducers and activators of transcription (STAT) cascade in advanced glycation end-product-induced cellular mitogenesis in NRK-49F cells. *Biochem J* 342: 231–238, 1999.
317. **Hue L, Beauloye C, Marsin A-S, Bertrand L, Horman S, Rider MH.** Insulin and ischemia stimulate glycolysis by acting on the same targets through different and opposing signaling pathways. *J Mol Cell Cardiol* 34: 1091–1097, 2002.
318. **Hunt J, Bottoms M, Mitchinson M.** Oxidative alterations in the experimental glycation model of diabetes mellitus are due to protein-glucose adduct oxidation. Some fundamental differences in proposed mechanisms of glucose oxidation and oxidant production. *Biochem J* 291: 529–535, 1993.
319. **Hunt J, Dean R, Wolff S.** Hydroxyl radical production and autoxidative glycosylation. Glucose autoxidation as the cause of protein damage in the experimental glycation model of diabetes mellitus and ageing. *Biochem J* 256: 205–212, 1988.
320. **Hunt J, Smith C, Wolff S.** Autoxidative glycosylation and possible involvement of peroxides and free radicals in LDL modification by glucose. *Diabetes* 39: 1420–1424, 1990.
321. **Hwang YC, Kaneko M, Bakr S, Liao H, Lu Y, Lewis ER, Yan S, Li S, Itakura M, Rui L, Skopicki H, Homma S, Schmidt AM, Oates PJ, Szabolcs M, Ramasamy R.** Central role for aldose reductase pathway in myocardial ischemic injury. *Fed Am Soc Exp Biol J* 18: 1192–1199, 2004.

322. **Hwang YC, Sato S, Tsai JY, Bakr S, Yan SD, Oates PJ, Ramasamy R.** Aldose reductase activation is a key component of myocardial response to ischemia. *Fed Am Soc Exp Biol J* 16: 243–245, 2002.
323. **Ide T, Tsutsui H, Hayashidani S, Kang D, Suematsu N, Nakamura K, Utsumi H, Hamasaki N, Takeshita A.** Mitochondrial DNA damage and dysfunction associated with oxidative stress in failing hearts after myocardial infarction. *Circ Res* 88: 529–535, 2001.
324. **Ihara Y, Egashira K, Nakano K, Ohtani K, Kubo M, Koga J, Iwai M, Horiuchi M, Gang Z, Yamagishi S, Sunagawa K.** Upregulation of the ligand-RAGE pathway via the angiotensin II type I receptor is essential in the pathogenesis of diabetic atherosclerosis. *J Mol Cell Cardiol* 43: 455–464, 2007.
325. **Ihnat M, Thorpe J, Kamat C, Szabó C, Green D, Warnke L, Lacza Z, Cselenyák A, Ross K, Shakir S, Piconi L, Kaltreider R, Ceriello A.** Reactive oxygen species mediate a cellular “memory” of high glucose stress signalling. *Diabetologia* 50: 1523–1531, 2007.
326. **Ikeda A, Matsushita S, Sakakibara Y.** Inhibition of protein kinase C  $\beta$  ameliorates impaired angiogenesis in type I diabetic mice complicating myocardial infarction. *Circ J* 76: 943 – 949, 2012.
327. **Ingal R, Wang S, Gonzalez-Baro M, Coleman R.** Mitochondrial glycerol phosphate acyltransferase directs the incorporation of exogenous fatty acids into triacylglycerol. *J Biol Chem* 276: 42205–42212, 2001.
328. **Inoguchi T, Battan R, Handler E, Sportsman JR, Heath W, King GL.** Preferential elevation of protein kinase C isoform beta II and diacylglycerol levels in the aorta and heart of diabetic rats: differential reversibility to glycemic control by islet cell transplantation. *Proc Natl Acad Sci USA* 89: 11059–11063, 1992.
329. **Inskeep P, Ronfeld R, Peterson M, Gerber N.** Pharmacokinetics of the aldose reductase inhibitor, zopolrestat, in humans. *J Clin Pharmacol* 34: 760–766, 1994.
330. **Inskeep PB, Reed AE, Ronfeld RA.** Pharmacokinetics of zopolrestat, a carboxylic acid aldose reductase inhibitor, in normal and diabetic rats. *Pharmaceut Res* 8: 1511–1515, 1991.
331. **Inzucchi SE.** Oral antihyperglycemic therapy for type 2 diabetes: scientific review. *J Am Med Assoc* 287: 360–372, 2002.
332. **Ishii H, Jirousek M, Koya D, Takagi C, Xia P, Clermont A, Bursell S, Kern T, Ballas L, Heath W, Stramm L, Feener E, King G.** Amelioration of vascular dysfunctions in diabetic rats by an oral PKC beta inhibitor. *Science* 272: 728–731, 1996.
333. **Itani SI, Ruderman NB, Schmieder F, Boden G.** Lipid-induced insulin resistance in human muscle is associated with changes in diacylglycerol, protein kinase C, and I $\kappa$ B- $\alpha$ . *Diabetes* 51: 2005–2011, 2002.
334. **Iwata N, Inazu N, Satoh T.** The purification and properties of aldose reductase from rat ovary. *Arch Biochem Biophys* 282: 70–77, 1990.

335. **Jackson R, Hawa M, Jaspan J, Sim B, Disilvio L, Featherbe D, Kurtz A.** Mechanism of metformin action in non-insulin-dependent diabetes. *Diabetes* 36: 632–640, 1987.
336. **Jain M, Cui L, Brenner DA, Wang B, Handy DE, Leopold JA, Loscalzo J, Apstein CS, Liao R.** Increased myocardial dysfunction after ischemia-reperfusion in mice lacking glucose-6-phosphate dehydrogenase. *Circ* 109: 898–903, 2004.
337. **Jain S, McVie R, Jaramillo J, Palmer M, Smith T.** Effect of modest vitamin E supplementation on blood glycated hemoglobin and triglyceride levels and red cell indices in type I diabetic patients. *J Am Coll Nutr* 15: 458–461, 1996.
338. **Jennings R, Sommers H, Symth G, Flack H, Linn H.** Myocardial necrosis induced by temporary occlusion of a coronary artery in the dog. *Arch Pathol* 70: 68–78, 1960.
339. **Jermendy G.** Evaluating thiamine deficiency in patients with diabetes. *Diab Vasc Dis Res* 3: 120–121, 2006.
340. **Jesmok G, Wartier D, Gross G, Hardman H.** Transmural triglycerides in acute myocardial ischaemia. *Cardiovasc Res* 12: 659–665, 1978.
341. **Jiang F, Zhang Y, Dusting GJ.** NADPH oxidase-mediated redox signaling : roles in cellular stress response , stress tolerance. *Pharmacol Rev* 63: 218–242, 2011.
342. **Jung M, Park M, Lee HC, Kang YH, Kang ES, Kim SK.** Antidiabetic agents from medicinal plants. *Curr Med Chem* 13: 1203–1218, 2006.
343. **Jyothirmayi G, Soni B, Masurekar M, Lyons M, Regan T.** Effects of metformin on collagen glycation and diastolic dysfunction in diabetic myocardium. *J Cardiovasc Pharmacol Ther* 3: 319–326, 1998.
344. **Kahn BB, Charron MJ, Lodish HF, Cushman SW, Flier JS.** Differential regulation of two glucose transporters in adipose cells from diabetic and insulin-treated diabetic rats. *J Clin Invest* 84: 404–411, 1989.
345. **Kahn BB.** Facilitative glucose transporters: regulatory mechanisms and dysregulation in diabetes. *J Clin Invest* 89: 1367–1374, 1992.
346. **Kainulainen H, Breiner M, Schiirmann A, Marttinen A, Virjo A, Joost G.** In vivo glucose uptake and glucose transporter proteins GLUT1 and GLUT4 in heart and various types of skeletal muscle from streptozotocin-diabetic rats. *Biochim Biophys Acta (BBA)* 1225: 275–282, 1994.
347. **Kaiserova K, Srivastava S, Hoetker JD, Awe SO, Tang X, Cai J, Bhatnagar A.** Redox activation of aldose reductase in the ischemic heart. *J Biol Chem* 281: 15110–15120, 2006.
348. **Kajstura J, Cheng W, Reiss K, Clark W, Sonnenblick E, Krajewski S, Reed J, Olivetti G, Anversa P.** Apoptotic and necrotic myocyte cell deaths are independent contributing variables of infarct size in rats. *Lab Invest* 74: 86–107, 1996.



349. **Kajstura J, Fiordaliso F, Andreoli AM, Li B, Chimenti S, Medow MS, Limana F, Nadalginard B, Leri A, Anversa P.** IGF-1 overexpression inhibits the development of diabetic cardiomyopathy and angiotensin ii-mediated oxidative stress. *Diabetes* 50: 1414–1424, 2001.
350. **Kalbag J, Walter Y, Nedelman J, McLeod J.** Mealtime glucose regulation with nateglinide in healthy volunteers: comparison with repaglinide and placebo. *Diab Care* 24: 73–77, 2001.
351. **Kalousová M, Zima T, Tesar V, Stípek S, Sulková S.** Advanced glycation end products in clinical nephrology. *Kidney Blood Press Res* 27: 18–28, 2004.
352. **Kanamori H, Takemura G, Goto K, Maruyama R, Ono K, Nagao K, Tsujimoto A, Ogino A, Takeyama T, Kawaguchi T, Watanabe T, Kawasaki M, Fujiwara T, Fujiwara H, Seishima M, Minatoguchi S.** Autophagy limits acute myocardial infarction induced by permanent coronary artery occlusion. *Am J Physiol Heart Circ Physiol* 300: H2261–H2271, 2011.
353. **Kaneko M, Bucciarelli L, Hwang YC, Lee L, Yan SF, Schmidt AM, Ramasamy R.** Aldose reductase and AGE-RAGE pathways: key players in myocardial ischemic injury. *Annals New York Acad Sci* 1043: 702–709, 2005.
354. **Kang B, Urbonas A, Baddoo A, Baskin S, Malhotra A, Meggs L.** IGF-1 inhibits the mitochondrial apoptosis program in mesangial cells exposed to high glucose. *Am J Physiol Renal Physiol* 285: F1013–F1024, 2003.
355. **Kannel WB, Hjortland M, Castelli WP.** Role of diabetes in congestive heart failure: the Framingham study. *Am J Cardiol* 34: 29, 1974.
356. **Kannel WB, McGee DL.** Diabetes and cardiovascular risk factors: the Framingham study. *Circulation* 59: 8–13, 1979.
357. **Karachalias N, Babaei-Jadidi R, Ahmed N, Thornalley P.** Accumulation of fructosyl-lysine and advanced glycation end products in the kidney, retina and peripheral nerve of streptozotocin-induced diabetic rats. *Biochem Soc Trans* 31: 1423–1425, 2003.
358. **Katare R, Caporali A, Emanuelli C, Madeddu P.** Benfotiamine improves functional recovery of the infarcted heart via activation of pro-survival G6PD/Akt signaling pathway and modulation of neurohormonal response. *J Mol Cell Cardiol* 49: 625–638, 2010.
359. **Katare R, Oikawa A, Cesselli D, Beltrami A, Avolio E, Muthukrishnan D, Munasinghe P, Angelini G, Emanuelli C, Madeddu P.** Boosting the pentose phosphate pathway restores cardiac progenitor cell availability in diabetes. *Cardiovasc Res* [Epub ahead of print, 2012].
360. **Katare RG, Caporali A, Oikawa A, Meloni M, Emanuelli C, Madeddu P.** Vitamin B1 analog benfotiamine prevents diabetes-induced diastolic dysfunction and heart failure through Akt/Pim-1-mediated survival pathway. *Circ Heart Fail* 3: 294–305, 2010.
361. **Kaul N, Siveski-Iliskovic N, Hill M, Slezak J, Singal P.** Free radicals and the heart. *J Pharmacol Toxicol Methods* 30: 55–67, 1993.

362. **Kawano H, Motoyama T.** Hyperglycemia rapidly suppresses flow-mediated endothelium-dependent vasodilation of brachial artery. *J Afr Coll Cardiol* 34: 146–154, 1999.
363. **Kenchaiah S, Evans J, Levy D, Al E.** Obesity and the risk of heart failure. *N Engl J Med* 347: 305–313, 2002.
364. **Kerbey A, Radcliffe P, Randle P.** Diabetes and the control of pyruvate dehydrogenase in rat heart mitochondria by concentration ratios of adenosine triphosphate/adenosine diphosphate, of reduced/oxidized nicotinamide-adenine dinucleotide and acetylcoenzyme A/coenzyme A. *Biochem J* 164: 509–519, 1977.
365. **Kerr J, Wyllie A, Currie A.** Apoptosis: a basic biological phenomenon with wide-ranging implications in tissue kinetics. *Br J Cancer* 26: 239–257, 1972.
366. **Khan Z, Chakrabarti S.** Cellular signaling and potential new treatment targets in diabetic retinopathy. *Exp Diabetes Res* 2007: 31867, 2007.
367. **Khan Z, Farhangkhoe H, Mahon J, Bere L, Gonder J, Chan B, Uniyal S, Chakrabarti S.** Endothelins: regulators of extracellular matrix protein production in diabetes. *Exp Biol Med (Maywood)* 231: 1022–1029, 2006.
368. **Kharbanda S, Pandey P, Schofield L, Israels S, Roncinske R, Yoshida K, Bharti A, Yuan Z, Saxena S, Weichselbaum R, Nalin C, Kufe D.** Role for Bcl-xL as an inhibitor of cytosolic cytochrome C accumulation in DNA damage-induced apoptosis. *Proc Natl Acad Sci U S A* 94: 6939–6942, 1997.
369. **Khaw K, Wareham N, Luben R, Bingham S, Oakes S, Welch A, Day N.** Glycated haemoglobin, diabetes, and mortality in men in Norfolk cohort of european prospective investigation of cancer and nutrition (EPIC-Norfolk). *Br Med J* 322: 15–18, 2001.
370. **Khullar M, Al-Shudiefat A, Ludke A, Binopal G, Singal P.** Oxidative stress: a key contributor to diabetic cardiomyopathy. *Can J Physiol. Pharmacol* 88: 233–240, 2010.
371. **King G, Brownlee M.** The cellular and molecular mechanisms of diabetic complications. *Endocrinol Metab Clin North Am* 25: 255–270, 1996.
372. **King G, Loeken MR.** Hyperglycemia-induced oxidative stress in diabetic complications. *Histochem Cell Biol* 122: 333–338, 2004.
373. **King PA, Horton ED, Hirshman MF, Horton ES.** Insulin resistance in obese Zucker rat (fa/fa) skeletal muscle is associated with a failure of glucose transporter translocation. *J Clin Invest* 90: 1568–1575, 1992.
374. **Kirpichnikov D, McFarlane S, Sowers J.** Metformin: an update. *Ann Intern Med* 137: 25–33, 2002.
375. **Kitada S, Otsuka Y, Kokubu N, Kasahara Y, Kataoka Y, Noguchi T, Goto Y, Kimura G, Nonogi H.** Post-load hyperglycemia as an important predictor of long-term adverse cardiac events after acute myocardial infarction: a scientific study. *Cardiovasc Diabetol* 9: 75, 2010.

376. **Kluck R, Bossy-Wetzel E, Green D, Newmeyer D.** The release of cytochrome c from mitochondria: a primary site for Bcl-2 regulation of apoptosis. *Science* 275: 1132–1136, 1997.
377. **Kobayashi, K, Neely J.** Effects of ischemia and reperfusion on pyruvate dehydrogenase activity in isolated rat hearts. *J Mol Cell Cardiol* 15: 359–367, 1983.
378. **Kockx M, Cambier B, Bortier H, De Meyer G, Declercq, SC, van Cauwelaert P, Bultinck J.** Foam cell replication and smooth muscle cell apoptosis in human saphenous vein grafts. *Histopathol* 25: 365–371, 1994.
379. **Kolm-Litty V, Sauer U.** High glucose-induced transforming growth factor beta1 production is mediated by the hexosamine pathway in porcine glomerular mesangial cells. *J Clin Invest* 101: 160–169, 1998.
380. **Kolter T, Uphues I, Eckel J.** Molecular analysis of insulin resistance in isolated ventricular cardiomyocytes of obese Zucker rats. *AmJ Physiol* 273: E59–E67, 1997.
381. **Korshunov S, Skulachev V, Starkov A.** High protonic potential actuates a mechanism of production of reactive oxygen species in mitochondria. *FEBS Lett* 416: 15–18, 1997.
382. **Kosiborod M, Inzucchi S, Krumholz H, Xiao L, Jones P, Fiske S, Masoudi F, Marso S, Spertus J.** Glucometrics in patients hospitalized with acute myocardial infarction: defining the optimal outcomes-based measure of risk. *Circ* 117: 1018–1027, 2008.
383. **Kowluru R, Chakrabarti S, Chen S.** Re-institution of good metabolic control in diabetic rats and activation of caspase-3 and nuclear transcriptional factor (NF-kappaB) in the retina. *Acta Diabetol* 41: 194–199, 2004.
384. **Kowluru R, Engerman R, Kern T.** Abnormalities of retinal metabolism in diabetes or experimental galactosemia VIII. Prevention by aminoguanidine. *Curr Eye Res* 21: 814–819, 2000.
385. **Kowluru R, Kanwar M, Kennedy A.** Metabolic memory phenomenon and accumulation of peroxynitrite in retinal capillaries. *Exp Diabetes Res* 2007: 21976, 2007.
386. **Kowluru R.** Effect of reinstatement of good glycemic control on retinal oxidative stress and nitrate stress in diabetic rats. *Diabetes* 52: 818–823, 2003.
387. **Kowluru RA, Chan P.** Oxidative stress and diabetic retinopathy. *Exp Diab Res* 2007: 43603, 2007.
388. **Koya D, Jirousek MR, Lin YW, Ishii H, Kuboki K, King GL.** Characterization of protein kinase C beta isoform activation on the gene expression of transforming growth factor-beta, extracellular matrix components, and prostanoids in the glomeruli of diabetic rats. *J Clin Invest* 100: 115–126, 1997.
389. **Koya D, King G.** Protein kinase C activation and the development of diabetic complications. *Diabetes* 47: 859–866, 1998.

390. **Krapfenbauer K, Birnbacher R, Vierhapper H, Herkner K, Kämpel D, Lubec G.** Glycooxidation, and protein and DNA oxidation in patients with diabetes mellitus. *Clin Sci (Lond)* 95: 331–337, 1998.
391. **Krentz AJ, Bailey CJ.** Oral antidiabetic agents: Current role in type 2 diabetes mellitus. *Drugs* 65: 385–411, 2005.
392. **Kreppel L, Hart G.** Regulation of a cytosolic and nuclear O-GlcNAc transferase. Role of the tetratricopeptide repeats. *J Biol Chem* 274: 32015–32022, 1999.
393. **Kroemer G, El-Deiry, WS, Golstein P, Peter M, Vaux D, Vandenabeele, P, Zhivotovsky, B, Blagosklonny M, Malorni W, Knight R, Piacentini M, Nagata S, Melino G, Nomenclature Committee on Cell Death.** Classification of cell death: recommendations of the Nomenclature Committee on Cell Death. *Cell Death Differ* 12: 1463–1467, 2005.
394. **Kroemer, G, Galluzzi, L, Brenner C.** Mitochondrial membrane permeabilization in cell death. *Physiol Rev* 87: 99–163, 2007.
395. **Kruyt N, Van Westerloo D, DeVries J.** Stress-induced hyperglycemia in healthy bungee jumpers without diabetes due to decreased pancreatic  $\beta$ -cell function and increased insulin resistance. *Diabetes Technol Ther* 14: 311–314, 2012.
396. **Kudin AP, Bimpong-Buta NY-B, Vielhaber S, Elger CE, Kunz WS.** Characterization of superoxide-producing sites in isolated brain mitochondria. *J Biol Chem* 279: 4127–4135, 2004.
397. **Kudo N, Barr AJ, Barr RL, Desai S, Lopaschuk GD.** High rates of fatty acid oxidation during reperfusion of ischemic hearts are associated with a decrease in malonyl-CoA levels due to an increase in 5'-AMP activated protein kinase inhibition of acetyl-CoA carboxylase. *J Biol Chem* 270: 17513–17520, 1995.
398. **Kudo N, Gillespie J, Kung L, Witters L, Schulz R, Clanachan A, Lopaschuk G.** Characterization of 5'AMP-activated protein kinase activity in the heart and its role in inhibiting acetyl-CoA carboxylase during reperfusion following ischemia. *Biochim Biophys Acta* 1301: 67–75, 1996.
399. **Kudzma D.** Effects of thiazolidinediones for early treatment of type 2 diabetes mellitus. *Am J Manag Care* 8: S472–S482, 2002.
400. **Kuhn D, Zeger E, Orlowski R.** Proteasome inhibitors and modulators of heat shock protein function. *Update Cancer Therap* 1: 91–116, 2006.
401. **Kumagai A, Vinore S, Pardridge W.** Pathological upregulation of inner blood-retinal barrier Glut1 glucose transporter expression in diabetes mellitus. *Brain Res* 706: 313–317, 1996.
402. **Kumar GS, Shetty AK, Salimath P V.** Modulatory effect of bitter melon (*Momordica charantia* LINN.) on alterations in kidney heparan sulfate in streptozotocin-induced diabetic rats. *J Ethnopharmacol* 115: 276–283, 2008.

403. **Kuo T, Giacomelli F, Wiener J, Lapanowski-Netzel K.** Pyruvate dehydrogenase activity in cardiac mitochondria from genetically diabetic mice. *Diabetes* 34: 1075–1108, 1985.
404. **Kurth-Kraczek EJ, Hirshman MF, Goodyear LJ, Winder WW.** 5' AMP-Activated Protein Kinase Activation Causes GLUT4 Translocation in Skeletal Muscle. *Diabetes* 48: 1–5, 1999.
405. **Kushnareva Y, Murphy A, Andreyev A.** Complex I-mediated reactive oxygen species generation: modulation by cytochrome c and NAD(P)<sup>+</sup> oxidation-reduction state. *Biochem J* 368: 545–553, 2002.
406. **Laakso M.** Hyperglycemia and cardiovascular disease in type 2 diabetes. *Diabetes* 48: 937–942, 1999.
407. **Laczy B, Fülöp N, Onay-Besikci A, Des Rosiers C, Chatham JC.** Acute regulation of cardiac metabolism by the hexosamine biosynthesis pathway and protein O-GlcNAcylation. *PlosOne* 6: e18417, 2011.
408. **Lagadic-Gossmann D, Buckler K, Le Prigent K, Feuvray D.** Altered Ca<sup>2+</sup> handling in ventricular myocytes isolated from diabetic rats. *Am J Physiol* 270: H1529–H1537, 1996.
409. **Lambert A, Brand M.** Inhibitors of the quinone-binding site allow rapid superoxide production from mitochondrial NADH:ubiquinone oxidoreductase (complex I). *J Biol Chem* 279: 39414–39420, 2004.
410. **Lander HM, Tauras JM, Ogiste JS, Hori O, Moss RA, Schmidt AM.** Activation of the receptor for advanced glycation end products triggers a p21ras-dependent mitogen-activated protein kinase pathway regulated by oxidant stress. *J Biol Chem* 272: 17810–17814, 1997.
411. **Lassila M, Seah K, Allen T, Thallas V, Thomas M, Candido R, Burns W, Forbes J, Calkin A, Cooper M, Jandeleit-Dahm K.** Accelerated nephropathy in diabetic apolipoprotein e-knockout mouse: role of advanced glycation end products. *J Am Soc Nephrol* 15: 2125–2138, 2004.
412. **Laube BL.** Advances in treating diabetes with aerosolized insulin. *Diabetes Technol Ther* 4: 515–518, 2002.
413. **Laurent A, Nicco C, Tran Van Nhieu J, Borderie D, Chéreau C, Conti F, Jaffray P, Soubrane O, Calmus Y, Weill B, Batteux F.** Pivotal role of superoxide anion and beneficial effect of antioxidant molecules in murine steatohepatitis. *Hepatology* 39: 1277–1285, 2004.
414. **Lazzeri C, Tarquini R, Giunta F, Gensini GF.** Glucose dysmetabolism and prognosis in critical illness. *Intern Emerg Med* 4: 147–156, 2009.
415. **Lee M, Hyun D, Jenner P, Halliwell B.** Effect of proteasome inhibition on cellular oxidative damage, antioxidant defences and nitric oxide production. *J Neurochem* 78: 32–41, 2001.
416. **Lee S, Shim S, Kim J, Shin K, Kang S.** Aldose reductase inhibitors from the fruiting bodies of *Ganoderma applanatum*. *Biol Pharm Bull* 28: 1103–1105, 2005.

417. **Lee Y, Lee S, Lee H, Kim B, Ohuchi K, Shin K.** Inhibitory effects of isorhamnetin-3-O-beta-D-glucoside from *Salicornia herbacea* on rat lens aldose reductase and sorbitol accumulation in streptozotocin-induced diabetic rat tissues. *Biol Pharm Bull* 28: 916–918, 2005.
418. **Lefer A, Lefer D.** The role of nitric oxide and cell adhesion molecules on the microcirculation in ischaemia-reperfusion. *Cardiovasc Res* 32: 743–751, 1996.
419. **Leinonen J, Lehtimäki, T Toyokuni S, Okada, K Tanaka T, Hiai H, Ochi H, Laippala P, Rantalaiho, V Wirta O, Pasternack A, Alho H.** New biomarker evidence of oxidative DNA damage in patients with non-insulin-dependent diabetes mellitus. *FEBS Lett* 417: 150–152, 1997.
420. **Leist BM, Single B, Castoldi AF, Kühnle S.** A switch in the decision between apoptosis and necrosis. *J Exp Med* 185: 1481–1486, 1997.
421. **Levine B, Klionsky D.** Development by self-digestion: molecular mechanisms and biological functions of autophagy. *Dev Cell* 6: 463–477, 2004.
422. **Lewandowski E, White L.** Pyruvate dehydrogenase influences postischemic heart function. *Circulation* 91: 2071–2079, 1995.
423. **Li H, Zhu H, Xu C, Yuan J.** Cleavage of BID by caspase 8 mediates the mitochondrial damage in the Fas pathway of apoptosis. *Cell* 94: 491–501, 1998.
424. **Li J, Shah A.** Mechanism of endothelial cell NADPH oxidase activation by angiotensin II. Role of the p47phox subunit. *J Biol Chem* 278: 12094–12100, 2003.
425. **Li P, Dietz R, Von Harsdorf R.** Differential effect of hydrogen peroxide and superoxide anion on apoptosis and proliferation of vascular smooth muscle cells. *Circ* 96: 3602–3609, 1997.
426. **Li P, Nijhawan D, Budihardjo I, Srinivasula S, Ahmad M, Alnemri E, Wang X.** Cytochrome c and dATP-dependent formation of Apaf-1/caspase-9 complex initiates an apoptotic protease cascade. *Cell* 91: 479–489, 1997.
427. **Li S, Yang X, Ceylan-Isik A, Du M, Sreejayan N, Ren J.** Cardiac contractile dysfunction in Lep/Lep obesity is accompanied by NADPH oxidase activation, oxidative modification of sarco(endo)plasmic reticulum Ca<sup>2+</sup>-ATPase and myosin heavy chain isozyme switch. *Diabetologia* 49: 1434–1446, 2006.
428. **Liebl A, Mata, M, Eschwège E, ODE-2 Advisory Board.** Evaluation of risk factors for development of complications in Type II diabetes in Europe. *Diabetologia* 45: S23–S28, 2002.
429. **Liedtke A, DeMaison L, Eggleston A, Cohen LM, Nellis SH.** Changes in substrate metabolism and effects of excess fatty acids in reperfused myocardium. *Circ Res* 62: 535–542, 1988.
430. **Lin L.** RAGE on the toll road? *Cell Mol Immunol* 3: 351–358, 2006.

431. **Lindqvist Y, Schneider G, Ermler U, Sundström M.** Three-dimensional structure of transketolase, a thiamine diphosphate dependent enzyme, at 2.5 Å resolution. *EMBO Journal* 11: 2373–2379, 1992.
432. **Di Lisa F, Menabò R, Canton M, Barile M, Bernardi P.** Opening of the mitochondrial permeability transition pore causes depletion of mitochondrial and cytosolic NAD<sup>+</sup> and is a causative event in the death of myocytes in postischemic reperfusion of the heart. *J Biol Chem* 276: 2571–2575, 2001.
433. **Little AA, Edwards JL, Feldman EL.** Diabetic neuropathies. *Pract Neurol* 7: 82–92, 2007.
434. **Liu B, El Alaoui-Talibi Z, Clanachan A, Schulz R, Lopaschuk G.** Uncoupling of contractile function from mitochondrial TCA cycle activity and MVO<sub>2</sub> during reperfusion of ischemic hearts. *Am J Physiol* 270: H72–H80, 1996.
435. **Liu Q, Chen X, Macdonnell SM, Kranias EG, John N, Leitges M, Houser SR, Molkenkin JD.** PKC $\alpha$ , but not PKC $\beta$  or PKC $\gamma$ , regulates contractility and heart failure susceptibility: Implications for ruboxistaurin as a novel therapeutic approach. *Circ Res* 105: 194–200, 2009.
436. **Liu W, Hei Z, Nie H, Tang F, Huang H, Li X, Deng Y, Chen S, Guo F, Huang W, Chen F, Liu P.** Berberine ameliorates renal injury in streptozotocin-induced diabetic rats by suppression of both oxidative stress and aldose reductase. *Chin Med J (Engl)* 121: 706–712, 2008.
437. **Liu Z, Miers WR, Wei L, Barrett EJ.** The ubiquitin-proteasome proteolytic pathway in heart vs skeletal muscle: effects of acute diabetes. *Biochem Biophys Res Commun* 276: 1255–1260, 2000.
438. **Lockshin R, Williams C.** Programmed cell death. Cytolytic enzymes in relation to the breakdown of the intersegmental muscles of silkworms. *J Insect Physiol* 11: 831–844, 1965.
439. **Lodovici M, Giovannelli L, Pitozzi V, Bigagli E, Bardini G, Rotella C.** Oxidative DNA damage and plasma antioxidant capacity in type 2 diabetic patients with good and poor glycaemic control. *Mutant Res* 638: 98–102, 2008.
440. **Lonsdale D.** A review of the biochemistry, metabolism and clinical benefits of thiamin(e) and its derivatives. *Evid Complement Alternat Med* 3: 49–59, 2006.
441. **Lopaschuk G, Saddik M.** The relative contribution of glucose and fatty acids to ATP production in hearts reperfused following ischemia. *Mol Cell Biochem* 116: 111–116, 1992.
442. **Lopaschuk G, Spafford M, Davies N, Wall S.** Glucose and palmitate oxidation in isolated working rat hearts reperfused after a period of transient global ischemia. *Circ Res* 66: 546–553, 1990.
443. **Lopaschuk G, Wambolt R, Barr R.** An imbalance between glycolysis and glucose oxidation is a possible explanation for the detrimental effects of high levels of fatty acids during aerobic reperfusion of ischemic hearts. *J Pharmacol Exp Ther* 264: 134–144, 1993.

444. **Lopaschuk GD.** Metabolic abnormalities in the diabetic heart. *Heart failure reviews* 7: 149–159, 2002.
445. **Lorenzi M.** The polyol pathway as a mechanism for diabetic retinopathy: attractive, elusive, and resilient. *Exp Diab Res* 2007: 61038, 2007.
446. **Lu L, Zhang Q, Xu Y, Zhu Z, Geng L, Wang L, Jin C, Chen Q, Schmidt A, Shen W.** Intracoronary administration of soluble receptor for advanced glycation end-products attenuates cardiac remodeling with decreased myocardial transforming growth factor-beta1 expression and fibrosis in minipigs with ischemia-reperfusion injury. *Chin Med J (Engl)* 123: 594–958, 2010.
447. **Lucchesi B, Mullane K.** Leukocytes and ischemia-induced myocardial injury. *Annu Rev Pharmacol Toxicol* 26: 201–224, 1986.
448. **Luiken JJFP, Coort SLM, Koonen DPY, Van der Horst DJ, Bonen A, Zorzano A, Glatz JFC.** Regulation of cardiac long-chain fatty acid and glucose uptake by translocation of substrate transporters. *Pflügers Archiv : Eur J Physiol* 448: 1–15, 2004.
449. **Luiken JJFP, Willems J, Van der Vusse GJ, Glatz JFC.** Electrostimulation enhances FAT/CD36-mediated long chain fatty acid uptake by isolated rat cardiac myocytes. *Am J Physiol Endocrin Metab* 281: E704–E712, 2001.
450. **Luna B, Hughes A, Feinglos M.** The use of insulin secretagogues in the treatment of type 2 diabetes. *Prim Care* 26: 895–915, 1999.
451. **Luzi L, DeFronzo R.** Effect of loss of first-phase insulin secretion on hepatic glucose production and tissue glucose disposal in humans. *Am J Physiol* 257: E241–E246, 1989.
452. **Ma H, Li S, Xu P, Babcock S, Dolence E, Brownlee M, Li J, Ren J.** Advanced glycation endproduct (AGE) accumulation and AGE receptor (RAGE) upregulation contribute to the onset of diabetic cardiomyopathy. *J Cell Mol Med* 13: 1751–1764, 2009.
453. **Machha A, Achike FI, Mustafa AM, Mustafa MR.** Quercetin, a flavonoid antioxidant, modulates endothelium-derived nitric oxide bioavailability in diabetic rat aortas. *Nitric oxide : Biol Chem* 16: 442–447, 2007.
454. **Madsbad S, Kilhovd B, Lager I, Mustajoki P, Dejgaard A, Scandinavian Repaglinide Group.** Comparison between repaglinide and glipizide in Type 2 diabetes mellitus: a 1-year multicentre study. *Diabet Med* 18: 395–401, 2001.
455. **Maillard L.** Action of amino acids on sugars. Formation of melanoidins in a methodical way. *Compt Rend* 154: 66, 1912.
456. **Malfitano C, Alba Loureiro T, Rodrigues B, Sirvente R, Salemi V, Rabechi N, Lacchini S, Rui Curi2 and MCCI.** Hyperglycaemia protects the heart after myocardial infarction: aspects of programmed cell survival and cell death. *Eur J Heart Fail* 12: 659–667, 2010.
457. **Malhotra A, Kang B, Hashmi S, Meggs L.** PKCepsilon inhibits the hyperglycemia-induced apoptosis signal in adult rat ventricular myocytes. *Mol Cell Biochem.* 268: 169–173, 2005.



458. **Malhotra A, Penpargkul S, Fein FS, Sonnenblick EH, Scheuer J.** The effect of streptozotocin-induced diabetes in rats on cardiac contractile proteins. *Circ Res* 49: 1243–1250, 1981.
459. **Malhotra A, Sanghi V.** Regulation of contractile proteins in diabetic heart. *Cardiovasc Res* 34: 34–40, 1997.
460. **Malmberg K, Norhammar A, Wedel H, Rydén L.** Glycometabolic state at admission: important risk marker of mortality in conventionally treated patients with diabetes mellitus and acute myocardial infarction: long-term results from the diabetes and insulin-glucose infusion in acute myocardial infarction. *Circ* 99: 2626–2632, 1999.
461. **Malmberg K, Rydén L, Wedel H, Birkeland K, Bootsma A, Dickstein K, Efendic S, Fisher M, Hamsten A, Herlitz J, Hildebrandt P, K M, M L, Torp-Pedersen, C, Waldenström A, DIGAMI 2 Investigators.** Intense metabolic control by means of insulin in patients with diabetes mellitus and acute myocardial infarction (DIGAMI 2): effects on mortality and morbidity. *Eur Heart J* 26: 650–661, 2005.
462. **Mapanga R, Rajamani U, Dlamini N, Zungu-Edmondson M, Kelly-Laubscher R, Shafiullah M, Wahab A, Hasan M, Fahim M, Rondeau P, Bourdon E, Essop M.** Oleanolic acid: a novel cardioprotective agent that blunts hyperglycemia-induced contractile dysfunction. *PloS one* 7: e47322, 2012.
463. **Marcovecchio ML, Lucantoni M, Chiarelli F.** Role of chronic and acute hyperglycemia in the development of diabetes complications. *Diab Technol Therap* 13: 389–394, 2011.
464. **Marfella R, Di C, Portoghese M, Siniscalchi M, Martis S, Ferraraccio F, Guastafierro S, Nicoletti G, Barbieri M, Coppola A, Rossi F.** The ubiquitin – proteasome system contributes to the inflammatory injury in ischemic diabetic myocardium : the role of glycemic control. *Cardiovasc Pathol* 18: 332–345, 2009.
465. **Marfella R, Di Filippo C, Portoghese M, Ferraraccio F, Rizzo MR, Siniscalchi M, Musacchio E, D'Amico M, Rossi F, Paolisso G.** Tight glycemic control reduces heart inflammation and remodeling during acute myocardial infarction in hyperglycemic patients. *J Am Coll Cardiol* 53: 1425–1436, 2009.
466. **Marfella R, Siniscalchi M, Esposito K, Sellitto A, De Fanis U, Romano C, Portoghese M, Siciliano S, Nappo F, Sasso F, Mininni N, Cacciapuoti F, Lucivero G, Giunta R, Verza M, Giugliano D.** Effects of stress hyperglycemia on acute myocardial infarction: role of inflammatory immune process in functional cardiac outcome. *Diab Care* 26: 3129–3135, 2003.
467. **Marin-Garcia J, Goldenthal M, Moe G.** Mitochondrial pathology in cardiac failure. *Cardiovasc Res* 49: 17–26, 2001.
468. **Marshall S, Bacote V, Traxinger R.** Discovery of a metabolic pathway mediating glucose-induced desensitization of the glucose transport system. Role of hexosamine biosynthesis in the induction of insulin resistance. *J Biol Chem* 266: 4706–4712, 1991.
469. **Martinez-Fleites C, He Y, Davies G.** Structural analyses of enzymes involved in the O-GlcNAc modification. *Biochim Biophys Acta* 1800: 122–133, 2010.

470. **Marx N, Walcher D, Ivanova N, Rautzenberg K, Jung A, Friedl R, Hombach V, De Caterina R, Basta G, Wautier M, Wautiers J.** Thiazolidinediones reduce endothelial expression of receptors for advanced glycation end products. *Diabetes* 53: 2662–2668, 2004.
471. **Mason RM.** Extracellular matrix metabolism in diabetic nephropathy. *J Am Soc Nephrol* 14: 1358–1373, 2003.
472. **Massi-Benedetti M, Orsini-Federici M.** Treatment of type 2 diabetes with combined therapy: what are the pros and cons? *Diab Care* 31: S131–S135, 2008.
473. **Masson E, Wiernsperger N, Lagarde M, El Bawab S.** Glucosamine induces cell-cycle arrest and hypertrophy of mesangial cells: implication of gangliosides. *Biochem J* 388: 537–544, 2005.
474. **Matsuda H, Cai H, Kubo M, Tosa H, Iinuma M.** Study on anti-cataract drugs from natural sources. II. Effects of buddlejae flos on in vitro aldose reductase activity. *Biol Pharm Bull* 18: 463–466, 1995.
475. **Matsui Y, Takagi H, Qu X, Abdellatif M, Sakoda H, Asano T, Levine B, Sadoshima J.** Distinct roles of autophagy in the heart during ischemia and reperfusion: roles of AMP-activated protein kinase and Beclin 1 in mediating autophagy. *Circ Res* 100: 914–922, 2007.
476. **Mbanya JC, Motala AA, Sobngwi E, Assah FK, Enoru ST.** Diabetes in sub-Saharan Africa. *Lancet* 375: 2254–2266, 2010.
477. **McCord J, Edeas M.** SOD, oxidative stress and human pathologies: a brief history and a future vision. *Biomed Pharmacother* 59: 139–142, 2005.
478. **McNulty P, Tulli M, Robertson B, Lendel V, Harach L, Scott S, Boehmer J.** Effect of simulated postprandial hyperglycemia on coronary blood flow in cardiac transplant recipients. *Am J Physiol Heart Circ Physiol* 293: H103–H108, 2007.
479. **Mearini G, Schlossarek S, Willis MS, Carrier L.** The ubiquitin-proteasome system in cardiac dysfunction. *Biochim Biophys Acta* 1782: 749–63, 2008.
480. **Menè P, Pascale C, Teti A, Bernardini R, Cinotti GA, Pugliese F.** Effects of advanced glycation end products on cytosolic Ca<sup>2+</sup> signaling of cultured human mesangial cells. *J Am Soc Nephrol* 10: 1478–1486, 1999.
481. **Meyer C, Stumvoll M, Nadkarni V, Dostou J, Mitrakou A, Gerich J.** Abnormal renal and hepatic glucose metabolism in type 2 diabetes mellitus. *J Clin Invest* 102: 619–624, 1998.
482. **De Meyer G, Martinet W.** Autophagy in the cardiovascular system. *Biochim Biophys Acta* 1793: 1485–1495, 2009.
483. **Midaoui A, Elimadi A, Wu L, Haddad P, De Champlain J.** Lipoic acid prevents hypertension, hyperglycemia, and the increase in heart mitochondrial superoxide production. *Am J Hypertens* 16: 173–179, 2003.

484. **Milicevic Z, Raz I, Beattie SD, Campaigne BN, Sarwat S, Gromniak E, Kowalska I, Galic E, Tan M, Hanefeld M.** Natural history of cardiovascular disease in patients with diabetes: role of hyperglycemia. *Diab Care Suppl 2*: S155–S160., 2008.
485. **Misra P, Chakrabarti R.** The role of AMP kinase in diabetes. *Indian J Med Res* 125: 389–398, 2007.
486. **Mitrakou A, Kelley D, Mokan M, Veneman T, Pangburn T, Reilly J, Gerich J.** Role of reduced suppression of glucose production and diminished early insulin release in impaired glucose tolerance. *N Engl J Med* 326: 22–29, 1992.
487. **Miyata T, Kurokawa K.** A detective story for biomedical footprints towards new therapeutic interventions in diabetic nephropathy. *Intern Med* 42: 1165–1171, 2003.
488. **Miyata T, Van Ypersele De Strihou C, Imasawa T, Yoshino A, Ueda Y, Ogura H, Kominami K, Onogi H, Inagi R, Nangaku M, Kurokawa K.** Glyoxalase I deficiency is associated with an unusual level of advanced glycation end products in a hemodialysis patient. *Kidney Intern* 60: 2351–2359, 2001.
489. **Miyata T, Van Ypersele de Strihou C, Ueda Y, Ichimori K, Inagi R, Onogi H, Ishikawa N, Nangaku M, Kurokawa K.** Angiotensin II receptor antagonists and angiotensin-converting enzyme inhibitors lower in vitro the formation of advanced glycation end products: biochemical mechanisms. *J Am Soc Nephrol* 13: 2478–2487, 2002.
490. **Mizushige K, Yao L, Noma T, Kiyomoto H, Yu Y, Hosomi N, Ohmori K, Matsuo H.** Alteration in left ventricular diastolic filling and accumulation of myocardial collagen at insulin-resistant prediabetic stage of a type II diabetic rat model. *Circ* 101: 899–907, 2000.
491. **Mochizuki S, Neely R.** Control of glyceraldehyde-3-phosphate dehydrogenase in cardiac muscle. *J Mol Cell Cardiol* 11: 221–236, 1979.
492. **Modak M, Dixit P, Londhe J, Ghaskadbi S, Paul A Devasagayam T.** Indian herbs and herbal drugs used for the treatment of diabetes. *J Clin Biochem Nutr* 40: 163–173, 2007.
493. **Mogensen CE.** ACE inhibitors and antihypertensive treatment in diabetes: focus on microalbuminuria and macrovascular disease. *J Renin-Angio-Aldo Syst* 1: 234–239, 2000.
494. **Monnier V, Bautista O, Kenny D, Sell D, Fogarty J, Dahms W, Cleary P, Lachin J, Genuth S.** Skin collagen glycation, glycooxidation, and crosslinking are lower in subjects with long-term intensive versus conventional therapy of type 1 diabetes: relevance of glycated collagen products versus HbA1c as markers of diabetic complications. DCCT Skin Co. *Diabetes* 48: 870–880, 1999.
495. **Monnier V.** Intervention against the Maillard reaction in vivo. *Arch Biochem Biophys* 419: 1–15, 2003.
496. **Mooradian A, Thurman J.** Drug therapy of postprandial hyperglycaemia. *Drugs* 57: 19–29, 1999.

497. **Morré D, Lenaz G, Morré D.** Surface oxidase and oxidative stress propagation in aging. *J Exp Biol* 203: 1513–1521, 2000.
498. **Movahed MR, Hashemzadeh M, Jamal MM.** Diabetes mellitus is a strong, independent risk for atrial fibrillation and flutter in addition to other cardiovascular disease. *Int J Cardiol* 105: 315–318, 2005.
499. **Mozaffarian D, Marfisi R, Levantesi G, Silletta MG, Tavazzi L, Tognoni G, Valagussa F, Marchioli R.** Incidence of new-onset diabetes and impaired fasting glucose in patients with recent myocardial infarction and the effect of clinical and lifestyle risk factors. *Lancet* 370: 667–675, 2007.
500. **Mueckler M.** Facilitative glucose transporters. *Eur J Biochem* 219: 713–725, 1994.
501. **Muis M, Bots M, Bilo H, Hoogma R, Hoekstra J, Grobbee D, Stolck R.** High cumulative insulin exposure: a risk factor of atherosclerosis in type 1 diabetes? *Atheroscl* 181: 185–192, 2005.
502. **Mullarkey C, Edelstein D, Brownlee M.** Free radical generation by early glycation products: a mechanism for accelerated atherogenesis in diabetes. *Biochem Biophys Res Commun* 173: 932–939, 1990.
503. **Murphy E, Perlman M, London R, Steenbergen C.** Amiloride delays the ischemia-induced rise in cytosolic free calcium. *Circ Res* 68: 1250–1258, 1991.
504. **Murray AJ, Cole MA, Lygate CA, Carr CA, Stuckey DJ, Little SE, Neubauer S, Clarke K.** Increased mitochondrial uncoupling proteins, respiratory uncoupling and decreased efficiency in the chronically infarcted rat heart. *J Mol Cell Cardiol* 44: 694–700, 2008.
505. **Murray P, Chune G, Vasudevan A.** Legacy effects from DCCT and UKPDS: what they mean and implications for future diabetes trials. *Curr Atheroscler Rep* 12: 432–439, 2010.
506. **Musi N, Hirshman M, Nygren J, Svanfeldt M, Bavenholm, P, Rooyackers O, Zhou G, Williamson J, Ljunqvist O, Efendic S, Moller D, Thorell A, Goodyear L.** Metformin increases AMP-activated protein kinase activity in skeletal muscle of subjects with type 2 diabetes. *Diabetes* 51: 2074–2081, 2002.
507. **Módis K, Gero D, Erdélyi K, Szoleczky P, DeWitt D, Szabo C.** Cellular bioenergetics is regulated by PARP1 under resting conditions and during oxidative stress. *Biochem Pharmacol* 83: 633–643, 2012.
508. **Müdespacher D, Radovanovic D, Camenzind E, Essig M, Bertel O, Erne P, Eberli FR, Gutzwiller F.** Admission glycaemia and outcome in patients with acute coronary syndrome: Amis Plus Investigators. *Diab Vasc Dis Res* 4: 346–352, 2007.
509. **Nabokina S, Said H.** Characterization of the 5'-regulatory region of the human thiamin transporter SLC19A3: in vitro and in vivo studies. *Am J Physiol Gastrointest Liver Physiol* 287: G822–G829, 2004.

510. **Nakagami H, Morishita R, Yamamoto K, Yoshimura S, Taniyama Y, Aoki M, Matsubara H, Kim S, Kaneda Y, Ogihara T.** Phosphorylation of p38 mitogen-activated protein kinase downstream of bax-caspase-3 pathway leads to cell death induced by high D-glucose in human endothelial cells. *Diabetes* 50: 1472–1481, 2001.
511. **Nakagawa T, Goto H, Hikiami H, Yokozawa T, Shibahara N, Shimada Y.** Protective effects of keishibukuryogan on the kidney of spontaneously diabetic WBN/Kob rats. *J Ethnopharmacol* 110: 311–317, 2007.
512. **Nakamura M, Barber AJ, Antonetti DA, LaNoue KF, Robinson KA, Buse MG, Gardner TW.** Excessive hexosamines block the neuroprotective effect of insulin and induce apoptosis in retinal neurons. *J. Biol. Chem* 276: 43748–43755, 2001.
513. **Namiki M, Hayashi T.** A new mechanism of the maillard reaction involving sugar fragmentation and free radical formation in the maillard reaction in foods and nutrition. In: *ACS Symposium Series, 215, American Chemical Society*, edited by Waller G, Feather M. Washington DC: 1983.
514. **Natarajan R, Nadler J.** Lipid inflammatory mediators in diabetic vascular disease. *Arterioscler Thromb Vasc Biol* 24: 1542–1548, 2004.
515. **National Diabetes Data Group.** *National Institutes of Health. National Institute of Diabetes and Digest Kidney Dis.* 1995.
516. **Nauck M.** Therapeutic potential of glucagon-like peptide 1 in type 2 diabetes. *Diabet Med* 13: S39–S43, 1996.
517. **Naudi A, Jove M, Ayala V, Cassanye A, Serrano J, Gonzalo H, Boada J, Prat J, Portero-Otin M, Pamplona R.** Cellular dysfunction in diabetes as maladaptive response to mitochondrial oxidative stress. *Exp Diab Res* 2012: 696215, 2012.
518. **Naujokat C, Berges C, Höh A, Wieczorek H, Fuchs D, Ovens J, Miltz M, Sadeghi M, Opelz G, Daniel V.** Proteasomal chymotrypsin-like peptidase activity is required for essential functions of human monocyte-derived dendritic cells. *Immunol* 120: 120–32, 2007.
519. **Naujokat C, Fuchs D, Berges C.** Adaptive modification and flexibility of the proteasome system in response to proteasome inhibition. *Biochim Biophys Acta (BBA)* 1773: 1389 – 1397, 2007.
520. **Neeper M, Schmidt A, Brett J, Yan S, Wang F, Pan Y, Elliston K, Stern D, Shaw A.** Cloning and expression of a cell surface receptor for advanced glycosylation end products of proteins. *J Biol Chem* 267: 14998–15004, 1992.
521. **Newton A.** Regulation of the ABC kinases by phosphorylation: protein kinase C as a paradigm. *Biochem J* 370: 361–371, 2003.
522. **Nguyen M, Breckenridge D, Ducret A, Shore G.** Caspase-resistant BAP31 inhibits fas-mediated apoptotic membrane fragmentation and release of cytochrome c from mitochondria. *Mol Cell Biol* 20: 6731–6740, 2000.

523. **Nichols C, Lederer W.** The role of ATP in energy deprivation contractures in unloaded rat ventricular myocytes. *Can J Physiol Pharmacol* 68: 183–194, 1990.
524. **Niedowicz D, Daleke D.** The role of oxidative stress in diabetic complications. *Cell Biochem Biophys* 43: 289–330, 2005.
525. **Nishida K, Kyoj S, Yamaguchi O, Sadoshima J, Otsu K.** The role of autophagy in the heart. *Cell Death Different* (2009). doi: 10.1038/cdd.2008.163.
526. **Nishikawa T, Edelstein D, Du XL, Yamagishi S, Matsumura T, Kaneda Y, Yorek MA, Beebek D, Oates PJ, Hammes H, Giardino I, Brownlee M, Ave MP, York N.** Normalizing mitochondrial superoxide production blocks three pathways of hyperglycaemic damage. *Nature* 404: 787–790, 2000.
527. **Noiri E, Nakao A, Uchida K, Tsukahara H, Ohno M, Fujita T, Brodsky S, Goligorsky M.** Oxidative and nitrosative stress in acute renal ischemia. *Am J Physiol Renal Physiol* 281: F948–F957, 2001.
528. **Norhammar A, Tenerz A, Nilsson G, Hamsten A, Efendic S, Ryden L, Malmberg K.** Glucose metabolism in patients with acute myocardial infarction and no previous diagnosis of diabetes mellitus: a prospective study. *Lancet* 359: 2140–2144, 2002.
529. **Norton GR, Candy G, Woodiwiss AJ.** Aminoguanidine prevents the decreased myocardial compliance produced by streptozotocin-induced diabetes mellitus in rats. *Circ* 93: 1905–1912, 1996.
530. **Nourooz-Zadeh J, Rahimi A, Tajaddini-Sarmadi J, Tritschler H, Rosen P, Halliwell B, Betteridge D.** Relationships between plasma measures of oxidative stress and metabolic control in NIDDM. *Diabetologia* 40: 647–653, 1997.
531. **Obrosova IG, Minchenko AG, Vasupuram R, White L, Abatan OI, Kumagai AK, Frank RN, Stevens MJ.** Aldose reductase inhibitor fidarestat prevents retinal oxidative stress and vascular endothelial growth factor overexpression in streptozotocin-diabetic rats. *Diabetes* 52: 864–871, 2003.
532. **Obrosova IG.** Increased sorbitol pathway activity generates oxidative stress in tissue sites for diabetic complications. *Antioxid Redox Signal* 7: 1543–1552, 2005.
533. **Ohanian J, Ohanian V.** Sphingolipids in mammalian cell signalling. *Cell Mol Life Sci* 58: 2053–2068, 2001.
534. **Ohnishi T, Johnson JJ, Yano T, Lobrutto R, Widger W.** Thermodynamic and EPR studies of slowly relaxing ubisemiquinone species in the isolated bovine heart complex I. *FEBS Lett* 579: 500–506, 2005.
535. **Opie L.** Acute myocardial infarction and diabetes. *Lancet* 370: 634–635, 2007.

536. **ORIGIN Trial Investigators, Gerstein H, Bosch J, Dagenais G, Díaz R, Jung H, Maggioni A, Pogue J, Probstfield J, Ramachandran A, Riddle M, Rydén L, Yusuf S.** Basal insulin and cardiovascular and other outcomes in dysglycemia. *N Engl J Med* 367: 319–328, 2012.
537. **Oswald GA, Smith CC, Betteridge DJ, Yudkin JS.** Determinants and importance of stress hyperglycaemia in non-diabetic patients with myocardial infarction. *Br Med J (Clin Res)* 293: 917–22, 1986.
538. **Ouwens DM, Boer C, Fodor M, De Galan P, Heine RJ, Maassen JA, Diamant M.** High-fat diet induced cardiac dysfunction is associated with altered myocardial insulin signalling in rats. *Diabetologia* 48: 1229–1237, 2005.
539. **Owens D.** Repaglinide--prandial glucose regulator: a new class of oral antidiabetic drugs. *Diabet Med* 15: S28–S36, 1998.
540. **Pacher P, Obrosova I, Mabley J, Szabó C.** Role of nitrosative stress and peroxynitrite in the pathogenesis of diabetic complications. Emerging new therapeutical strategies. *Curr Med Chem* 12: 267–275, 2005.
541. **Paget C, Lecomte M, Ruggiero D, Wiernsperger N, Lagarde M.** Modification of enzymatic antioxidants in retinal microvascular cells by glucose or advanced glycation end products. *Free Radic Biol Med* 25: 121–129, 1998.
542. **Pambianco G, Costacou T, Ellis D, Becker D, Klein R, Orchard T.** The 30-year natural history of type 1 diabetes complications: the Pittsburgh Epidemiology of Diabetes Complications Study experience. *Diabetes* 55: 1463–1469, 2006.
543. **Paolisso G, D'Amore A, Galzerano D, Balbi V, Giugliano D, Varricchio M, D'Onofrio F.** Daily vitamin E supplements improve metabolic control but not insulin secretion in elderly type II diabetic patients. *Diab Care* 16: 1433–1437, 1993.
544. **Paradies G, Petrosillo G, Pistolese M, Venosa N Di, Federici A, Ruggiero FM, Reperfused I, Heart R.** Decrease in mitochondrial complex I activity in ischemic/reperfused rat heart: involvement of reactive oxygen species and cardiolipin. *Circ Res* 94: 53–59, 2004.
545. **Park J, Lucchesi B.** Mechanisms of myocardial reperfusion injury. *Ann Thorac Surg* 68: 1905–1912, 1999.
546. **Paterson A, Rutledge B, Cleary P, Lachin J, Crow R, Diabetes Control and Complications Trial/Epidemiology of Diabetes Interventions and Complications Research Group.** The effect of intensive diabetes treatment on resting heart rate in type 1 diabetes: the Diabetes Control and Complications Trial/Epidemiology of Diabetes Interventions and Complications study. *Diab Care* 30: 2107–2112, 2007.
547. **Pedersen O, Gaede P.** Intensified multifactorial intervention and cardiovascular outcome in type 2 diabetes: the Steno-2 study. *Metab* 52: 19–23, 2003.

548. **Pendergrass M, Koval J, Vogt C, Yki-Jarvinen H, Iozzo P, Pipek R, Ardehali H, Printz R, Granner D, DeFronzo RA, Mandarino LJ.** Insulin-induced hexokinase II expression is reduced in obesity and NIDDM. *Diabetes* 47: 387–394, 1998.
549. **Perry R, Baron A.** Impaired glucose tolerance. Why is it not a disease? *Diab Care* 22: 883–885, 1999.
550. **Peter M, Krammer P.** The CD95(APO-1/Fas) DISC and beyond. *Cell Death Differ* 10: 26–35, 2003.
551. **Petersen KF, Hendler R, Price T, Perseghin G, Rothman DL, Held N, Amatruda JM, Shulman GI.** <sup>13</sup>C/<sup>31</sup>P NMR studies on the mechanism of insulin resistance in obesity. *Diabetes* 47: 381–386, 1998.
552. **Petrosillo G, Ruggiero FM, Di Venosa N, Paradies G.** Decreased complex III activity in mitochondria isolated from rat heart subjected to ischemia and reperfusion: role of reactive oxygen species and cardiolipin. *Fed Am Soc Exp Biol J* 17: 714–746, 2003.
553. **Peyroux J, Sternberg M.** Advanced glycation endproducts ( AGEs ): pharmacological inhibition in diabetes Les produits de Maillard ( ou AGEs ) : leur inhibition pharmacologique au cours du diabète. *Pathologie Biologie* 54: 405–419, 2006.
554. **Ping P, Song C, Zhang J, Guo Y, Cao X, Li R, Wu W, Vondriska T, Pass J, Tang X, Pierce W, Bolli R.** Formation of protein kinase C(epsilon)-Lck signaling modules confers cardioprotection. *J Clin Invest* 109: 499–507, 2002.
555. **Ping P, Zhang J, Cao X, Li RCX, Kong D, Qiu Y, Manchikalapudi S, Auchampach JA, G R, Bolli R, Physiol AJ, Circ H, Zhang JUN.** PKC-dependent activation of p44 / p42 MAPKs during myocardial ischemia-reperfusion in conscious rabbits. *Am J Physiol Heart Circ Physiol* 276: 1468–1481, 1999.
556. **Piper H, Abdallah Y, Schäfer C.** The first minutes of reperfusion: a window of opportunity for cardioprotection. *Cardiovasc Res* 61: 365–371, 2004.
557. **Piper H, García-Dorado D, Ovize M.** A fresh look at reperfusion injury. *Cardiovasc Res* 38: 291–300, 1998.
558. **Piper HM, Meuter K, Schäfer C.** Cellular mechanisms of ischemia-reperfusion injury. *Annals Thoracic Surg* 75: S644–S648, 2003.
559. **Polizzi F, Andican G, Çetin E, Civelek S, Yumuk V, Burçak G.** Increased DNA-glycation in type 2 diabetic patients: the effect of thiamine and pyridoxine therapy. *Exp Clin Endocrinol Diabetes* 120: 329–334, 2012.
560. **Pomero F, Molinar Min A, La Selva M, Allione A, Molinatti G, Porta M.** Benfotiamine is similar to thiamine in correcting endothelial cell defects induced by high glucose. *Acta Diabetol* 38: 135–138, 2001.



561. **Ponticos M, Lu QL, Morgan JE, Hardie DG, Partridge T a, Carling D.** Dual regulation of the AMP-activated protein kinase provides a novel mechanism for the control of creatine kinase in skeletal muscle. *EMBO J* 17: 1688–1699, 1998.
562. **Pou S, Pou W, Bredt D, Snyder S, Rosen G.** Generation of superoxide by purified brain nitric oxide synthase. *J Biol Chem* 267: 24173–24176, 1992.
563. **Powell S, Davies K, Divald A.** Optimal determination of heart tissue 26S-proteasome activity requires maximal stimulating ATP concentrations. *J Mol Cell Cardiol* 42: 265–269, 2007.
564. **Powell S, Wang P, Katzeff H, Shringarpure R, Teoh C, Khaliulin I, Das D, Davies K, Schwalb H.** Oxidized and ubiquitinated proteins may predict recovery of postischemic cardiac function: essential role of the proteasome. *Antioxid Redox Signal* 7: 538–546, 2005.
565. **Powell SR, Divald A.** The ubiquitin-proteasome system in myocardial ischaemia and preconditioning. *Cardiovasc Res* 85: 303–311, 2010.
566. **Powell SR, Samuel SM, Wang P, Divald A, Thirunavukkarasu M, Koneru S, Wang X, Maulik N.** Upregulation of myocardial 11S-activated proteasome in experimental hyperglycemia. *J Mol Cell Cardiol* 44: 618–621, 2008.
567. **Powell SR.** Inhibition of the 26S proteasome results in cardiac myocyte apoptosis. *Oxygen* S115: 66081–66081, 1999.
568. **Powell SR.** The ubiquitin-proteasome system in cardiac physiology and pathology. *Am J Physiol Heart Circ Physiol* 291: H1–H19, 2006.
569. **Del Prato S, Tiengo A.** The importance of first phase-secretion: implications for the therapy of type 2 diabetes mellitus. *Diab Metab Res Rev* 17: 164–174, 2001.
570. **Pricci F, Leto G, Amadio L, Iacobini C, Cordone S, Catalano S, Zicari A, Sorcini M, Di Mario U, Pugliese G.** Oxidative stress in diabetes-induced endothelial dysfunction involvement of nitric oxide and protein kinase C. *Free Radic Biol Med* 35: 683–694, 2003.
571. **Pye J, Ardeshirpour F, McCain A, Bellinger D A, Merricks E, Adams J, Elliott PJ, Pien C, Fischer TH, Baldwin AS, Nichols TC.** Proteasome inhibition ablates activation of NF-kappa B in myocardial reperfusion and reduces reperfusion injury. *Am J Physiol Heart Circ Physiol* 284: H919–H926, 2003.
572. **Qian M, Eaton J.** Glycochelates and the etiology of diabetic peripheral neuropathy. *Free Radic Biol Med* 28: 652–656, 2000.
573. **Quagliari L, Piconi L, Assaloni R, Martinelli L, Motz E, Ceriello A.** Intermittent high glucose enhances apoptosis related to oxidative stress in human umbilical vein endothelial cells: the role of protein kinase C and NAD(P)H-oxidase activation. *Diabetes* 52: 2795–2804, 2003.
574. **Raha S, Robinson B.** Mitochondria, oxygen free radicals, disease and ageing. *Trends Biochem Sci* 25: 502–508, 2000.

575. **Rahimi R, Nikfar S, Larijani B, Abdollahi M.** A review on the role of antioxidants in the management of diabetes and its complications. *Biomed Pharmacother* 59: 365–373, 2005.
576. **Rajamani U, Essop MF.** Hyperglycemia-mediated activation of the hexosamine biosynthetic pathway results in myocardial apoptosis. *Am J Physiol Cell Physiol* 299: C139–C147, 2010.
577. **Rajamani U, Joseph D, Roux S, Essop MF.** The hexosamine biosynthetic pathway can mediate myocardial apoptosis in a rat model of diet-induced insulin resistance. *Acta physiologica (Oxford, England)* 202: 151–157, 2011.
578. **Rajapakse A, Ming X, Carvas J, Yang Z.** O-linked beta-N-acetylglucosamine during hyperglycemia exerts both anti-inflammatory and pro-oxidative properties in the endothelial system. *Oxid Med Cell Longev.* 2: 172–175, 2009.
579. **Ramasamy R, Oates PJ, Schaefer S.** Aldose reductase inhibition improves the altered glucose metabolism of isolated diabetic rat hearts. *Diabetes* 46: 292–300, 1997.
580. **Ramasamy R, Trueblood NA, Schaefer S.** Metabolic effects of aldose reductase inhibition during low-flow ischemia and reperfusion. *Am J Physiol Heart Circ Physiol* 275: H195–H203, 1998.
581. **Randle PJ, Garland PB, Hales CN, Newsholme EA.** The glucose fatty-acid cycle. Its role in insulin sensitivity and the metabolic disturbances of diabetes mellitus. *Lancet* 1: 785–789, 1963.
582. **Randle PJ, Newsholme EA, Garland PB.** Regulation of glucose uptake by muscle 8: effects of fatty acids, ketone bodies and pyruvate, and of alloxan-diabetes and starvation, on the uptake and metabolic fate of glucose in rat heart and diaphragm muscles. *Biochem J* 93: 652–665, 1964.
583. **Ranganathan S, Ciaccio P, Walsh E, Tew K.** Genomic sequence of human glyoxalase-I: analysis of promoter activity and its regulation. *Gene* 240: 149–155, 1999.
584. **Rao N, Nammi S.** Antidiabetic and renoprotective effects of the chloroform extract of *Terminalia chebula* Retz. seeds in streptozotocin-induced diabetic rats. *BMC Complement Altern Med* 6: 17, 2006.
585. **Ravingerova T, Neckar J, Kolar F, Stetka R, Volkovova K, Ziegelhoffer A, Styk J.** Ventricular arrhythmias following coronary artery occlusion in rats: is the diabetic heart less or more sensitive to ischaemia? *Basic Res Cardiol* 96: 160–168, 2001.
586. **Ravingerova T, Stetka R, Volkovova K, Pancza D, Dzurba A, Ziegelhoffer A, Styk J.** Acute diabetes modulates response to ischemia in isolated rat heart. *Mol Cell Biochem* 210: 143–151, 2000.
587. **Raz I, Wilson P, Strojek K, Kowalska I, Bozikov V, Gitt A, Jermendy G, Campaigne B, Kerr L, Milicevic Z, Jacober S.** Effects of prandial versus fasting glycemia on cardiovascular outcomes in type 2 diabetes: the HEART2D trial. *Diab Care* 32: 381–386, 2009.

588. **Reaven G, Hollenbeck C, Jeng C, Wu M, Chen Y.** Measurement of plasma glucose, free fatty acid, lactate, and insulin for 24 h in patients with NIDDM. *Diabetes* 37: 1020–1024, 1988.
589. **Reddy ABM, Ramana K V.** Aldose Reductase Inhibition : Emerging Drug Target for the Treatment of Cardiovascular Complications. *Recent Pat Cardiovasc Drug Discov* 5: 25–32, 2010.
590. **Reed A, Charkoudian N, Vella A, Shah P, Rizza R, Joyner MJ.** Forearm vascular control during acute hyperglycemia in healthy humans. *Am J Physiol Endocrinol Metab* 286: E472–E480, 2004.
591. **Reed JC.** Bcl-2 family proteins. *Oncogene* 17: 3225–3236, 1998.
592. **Regen D, Davis W, Morgan H, Park C.** The regulation of hexokinase and phosphofructokinase activity in heart muscle: effects of alloxan diabetes, growth hormone, cortisol and anoxia. *J Biol Chem* 239: 43–49, 1964.
593. **Ren J, Ceylan-Isik A.** Diabetic cardiomyopathy: do women differ from men? *Endocrine* 25: 73–83, 2004.
594. **Rendell M.** Advances in diabetes for the millennium: drug therapy of type 2 diabetes. *MedGenMed* 6: 9, 2004.
595. **Retnakaran R, Zinman B.** Type 1 diabetes, hyperglycaemia, and the heart. *Lancet* 371: 1790–1799, 2008.
596. **Reusch JEB.** Diabetes, microvascular complications, and cardiovascular complications: what is it about glucose? *J Clin Invest* 112: 986–988, 2003.
597. **Riganti C, Gazzano E, Polimeni M, Aldieri E, Ghigo D.** The pentose phosphate pathway: an antioxidant defense and a crossroad in tumor cell fate. *Free Radic Biol Med* 53: 421–436, 2012.
598. **Robertson C, Drexler AJ, Vernillo AT.** Update on diabetes diagnosis and management. *J Am Dental Assoc* 134: 16S–23S, 2003.
599. **Roden M, Price TB, Perseghin G, Petersen KF, Rothman DL, Cline GW, Shulman GI.** Mechanism of free fatty acid – induced insulin resistance in humans. *J Clin Invest* 97: 2859–2865, 1996.
600. **Rodrigues B, Cam MC, McNeill JH.** Metabolic disturbances in diabetic cardiomyopathy. *Mol Cell Biochem* 180: 53–57, 1998.
601. **Rosamond W, Flegal K, Friday G, Furie K, Go A, Greenlund K, Haase N, Ho M, Howard V, Kissela B, Kittner S, Lloyd-Jones D, McDermott M, Meigs J, Moy C, Nichol G, O'Donnell CJ, Roger V, Rumsfeld J, Sorlie P, Steinberger J, Thom T, Wasserthiel-Smoller S, Hong Y, American Heart Association Statistics Committee, Stroke Statistics Subcommittee.** Heart disease and stroke statistics--2007 update: a report from the American Heart Association statistics committee and stroke statistics subcommittee. *Circ* 115: e69–e171, 2007.

602. **Rosca MG, Mustata TG, Kinter MT, Ozdemir AM, Kern TS, Szweda LI, Brownlee M, Monnier VM, Weiss MF.** Glycation of mitochondrial proteins from diabetic rat kidney is associated with excess superoxide formation. *Am J Physiol Renal Physiol* 289: F420–F430, 2005.
603. **Ross R.** Atherosclerosis--an inflammatory disease. *N Engl J Med* 340: 115–126, 1999.
604. **Rothman D, Shulman R, Shulman G.** 31P nuclear magnetic resonance measurements of muscle glucose-6-phosphate. Evidence for reduced insulin-dependent muscle glucose transport or phosphorylation. *J Clin Invest* 89: 1069–1075, 1992.
605. **Rubanyi G, Vanhoutte P.** Oxygen-derived free radicals, endothelium, and responsiveness of vascular smooth muscle. *Am J Physiol* 250: H815–H821, 1986.
606. **Rubler S, Dlugash J, Yuceoglu Y, Kumra I T, Branwood A, Grishman A.** New type of cardiomyopathy associated with diabetic glomerulosclerosis. *Am J Cardiol* 30: 595–602, 1972.
607. **Russell RR, Yin R, Caplan MJ, Hu X, Ren J, Shulman GI, Sinusas AJ, Young LH.** Additive Effects of hyperinsulinemia and ischemia on myocardial GLUT1 and GLUT4 translocation in vivo. *Circ* 98: 2180–2186, 1998.
608. **Rösen P, Du X, Tschöpe D.** Role of oxygen derived radicals for vascular dysfunction in the diabetic heart: prevention with alpha tocopherol? *Mol Cell Biochem* 188: 103–111, 1998.
609. **Rösen P, Nawroth P, King G, Möller W, Tritschler H, Packer L.** The role of oxidative stress in the onset and progression of diabetes and its complications: a summary of a Congress Series sponsored by UNESCO-MCBN, the American Diabetes Association, and the German Diabetes Society. *Diab Metab Res Rev* 17: 189–212, 2001.
610. **Saddik M, Lopaschuk G.** Myocardial triglyceride turnover and contribution to energy substrate utilization in isolated working rat hearts. *J Biol Chem* 266: 8162–8170, 1991.
611. **Sadeghi M.** The pathobiology of the vessel wall: implications for imaging. *J Nucl Cardiol* 13: 402–414, 2006.
612. **Sage A, Walter L, Shi Y, Khan M, Kaneto H, Capretta A, Werstuck G.** Hexosamine biosynthesis pathway flux promotes endoplasmic reticulum stress, lipid accumulation, and inflammatory gene expression in hepatic cells. *Am J Physiol Endocrinol Metab* 298: E499–E511, 2010.
613. **Saito N, Kimura M, Kuchiba A, Itokawa Y.** Blood thiamine levels in outpatients with diabetes mellitus. *J Nutr Sci Vitaminol (Tokyo)* 33: 421–430, 1987.
614. **Sakurai S.** The AGE-RAGE system and diabetic nephropathy. *J Am Soc Nephrol* 14: 259S–263, 2003.
615. **Sarafidis P.** Thiazolidinediones and diabetic nephropathy: need for a closer examination? *J Cardiometab Syndr* 2: 297–301, 2007.

616. **Sardaş S, Yilmaz M, Oztok U, Cakir N, Karakaya A.** Assessment of DNA strand breakage by comet assay in diabetic patients and the role of antioxidant supplementation. *Mutat Res* 490: 123–129, 2001.
617. **Saxena A, Saxena P, Wu X, Obrenovich M, Weiss M, Monnier V.** Protein aging by carboxymethylation of lysines generates sites for divalent metal and redox active copper binding: relevance to diseases of glycoxidative stress. *Biochem Biophys Res Commun* 260: 332–338, 1999.
618. **Saydah S, Loria C, Eberhardt M, Brancati F.** Subclinical states of glucose intolerance and risk of death in the U.S. *Diab Care* 24: 447–453, 2001.
619. **Schaefer S, Ramasamy R.** Short-term inhibition of the Na-H exchanger limits acidosis and reduces ischemic injury in the rat heart. *Cardiovasc Res* 34: 329–36, 1997.
620. **Schena FP.** Pathogenetic mechanisms of diabetic nephropathy. *J Am Soc Nephrol* 16: S30–S33, 2005.
621. **Schlüter K, Jakob G, Ruiz-Meana M, García-Dorado D, Piper H.** Protection of reoxygenated cardiomyocytes against osmotic fragility by NO donors. *Am J Physiol* 271: H428–H434, 1996.
622. **Schmitz-Peiffer C, Browne C, Oakes ND, Watkinson A, Chisholm DJ, Kraegen EW, Biden TJ.** Alterations in the expression and cellular localization of protein kinase C isozymes epsilon and theta are associated with insulin resistance in skeletal muscle of the high-fat-fed rat. *Diabetes* 46: 169–178, 1997.
623. **Schmitz-Peiffer C, Craig DL, Biden TJ.** Ceramide generation is sufficient to account for the inhibition of the insulin-stimulated PKB pathway in C2C12 skeletal muscle cells pretreated with palmitate. *J Biol Chem* 274: 24202–24210, 1999.
624. **Schmitz-Peiffer C.** Signalling aspects of insulin resistance in skeletal muscle: mechanisms induced by lipid oversupply. *Cell Signal* 12: 583–594, 2000.
625. **Schreeb K, Freudenthaler S, Vormfelde S, Gundert-Remy U, Gleiter C.** Comparative bioavailability of two vitamin B1 preparations: benfotiamine and thiamine mononitrate. *Eur J Clin Pharmacol* 52: 319–320, 1997.
626. **Schwaiger M, Neese R, Araujo L, Wyns W, Wisneski J, Sochor H, Swank S, Kulber D, Selin C, Phelps M, Al E.** Sustained nonoxidative glucose utilization and depletion of glycogen in reperfused canine myocardium. *J Am Coll Cardiol* 13: 745–754, 1989.
627. **Scivittaro V, Ganz MB, Weiss MF.** AGEs induce oxidative stress and activate protein kinase C-beta(II) in neonatal mesangial cells. *Am J Physiol Renal Physiol* 278: F676–F683, 2000.
628. **Scognamiglio R, Negut C, De Kreutzenberg S, Tiengo A, Avogaro A.** Postprandial myocardial perfusion in healthy subjects and in type 2 diabetic patients. *Circ* 112: 179–184, 2005.

629. **Scorrano L, Ashiya M, Buttle K, Weiler S, Oakes S, Mannella C, Korsmeyer S.** A distinct pathway remodels mitochondrial cristae and mobilizes cytochrome c during apoptosis. *Dev Cell* 2: 55–67, 2002.
630. **Scorrano L, Oakes S, Opferman J, Cheng E, Sorcinelli M, Pozzan T, Korsmeyer S.** BAX and BAK regulation of endoplasmic reticulum Ca<sup>2+</sup>: a control point for apoptosis. *Science* 300: 135–139, 2003.
631. **Scott L, Spencer C.** Miglitol: a review of its therapeutic potential in type 2 diabetes mellitus. *Drugs* 59: 521–549, 2000.
632. **Sell D, Lapolla A, Odetti P, Fogarty J, Monnier V.** Pentosidine formation in skin correlates with severity of complications in individuals with long-standing IDDM. *Diabetes* 41: 1286–1292, 1992.
633. **Serpillon S, Floyd BC, Gupte RS, George S, Kozicky M, Neito V, Recchia F, Stanley W, Wolin MS, Gupte SA.** Superoxide production by NAD (P)H oxidase and mitochondria is increased in genetically obese and hyperglycemic rat heart and aorta before the development of cardiac dysfunction. The role of glucose-6-phosphate dehydrogenase-derived NADPH. *Am J Physiol Heart Circ Physiol* 297: H153–H162, 2009.
634. **Shang L, Ananthakrishnan R, Li Q, Quadri N, Abdillahi M, Zhu Z, Qu W, Rosario R, Touré F, Yan S, Schmidt A, Ramasamy R.** RAGE modulates hypoxia/reoxygenation injury in adult murine cardiomyocytes via JNK and GSK-3 $\beta$  signaling pathways. *PLoS One* 5: e10092, 2010.
635. **Sharma A, Kharb S, Chugh S, Kakkar R, Singh G.** Evaluation of oxidative stress before and after control of glycemia and after vitamin E supplementation in diabetic patients. *Metab* 49: 160–162, 2000.
636. **Shaw J, Hodge A, De Courten M, Chitson P ZP.** Isolated post-challenge hyperglycaemia confirmed as a risk factor for mortality. *Diabetologia* 42: 1050–1054, 1999.
637. **Sheetz M, King G.** Molecular understanding of hyperglycemia's adverse effects for diabetic complications. *JAMA* 288: 2579–2588, 2002.
638. **Shen X, Zheng S, Thongboonkerd V, Xu M, Pierce WM, Klein JB, Epstein PN.** Cardiac mitochondrial damage and biogenesis in a chronic model of type 1 diabetes. *Am J Physiol Endocrinol Metab* 287: E896–E905, 2004.
639. **Shiba T, Inoguchi T, Sportsman J, Heath W, Bursell S, King G.** Correlation of diacylglycerol level and protein kinase C activity in rat retina to retinal circulation. *Am J Physiol* 265: E783–E793, 1993.
640. **Shimizu M, Umeda K, Sugihara N, Yoshio H, Ino H, Takeda R, Okada Y, Nakanishi I.** Collagen remodelling in myocardia of patients with diabetes. *J Clin Pathol* 46: 32–36, 1993.

641. **Shrikhande G V, Scali ST, Da Silva CG, Damrauer SM, Csizmadia E, Putheti P, Matthey M, Arjoon R, Patel R, Siracuse JJ, Maccariello ER, Andersen ND, Monahan T, Peterson C, Essayagh S, Studer P, Guedes RP, Kocher O, Usheva A, Veves A, Kaczmarek E, Ferran C.** O-glycosylation regulates ubiquitination and degradation of the anti-inflammatory protein A20 to accelerate atherosclerosis in diabetic ApoE-null mice. *PLoS one* 5: e14240, 2010.
642. **Shringarpure R, Grune T, Mehlhase J, Davies KJA.** Ubiquitin conjugation is not required for the degradation of oxidized proteins by proteasome. *Biochem* 278: 311–318, 2003.
643. **Sidell RJ, Cole MA, Draper NJ, Desrois M, Buckingham RE, Clarke K.** Thiazolidinedione treatment normalizes insulin resistance and ischemic injury in the Zucker Fatty rat heart. *Diabetes* 51: 1110–1117, 2002.
644. **Silacci P.** Advanced glycation end-products as a potential target for treatment of cardiovascular disease. *J Hypertens* 20: 1483–1485, 2002.
645. **Simm A, Munch G, Seif F, Schenk O, Heidland A, Richter H, Vamvakas S, Schinzel R.** Advanced glycation endproducts stimulate the MAP-kinase pathway in tubulus cell line LLC-PK1. *FEBS Lett.* .
646. **Simmons S, Fan C, Ramabhadran R.** Cellular stress response pathway system as a sentinel ensemble in toxicological screening. *Toxicol Sci* 111: 202–225, 2009.
647. **Skulachev V.** Role of uncoupled and non-coupled oxidations in maintenance of safely low levels of oxygen and its one-electron reductants. *Q Rev Biophys* 29: 169–202, 1996.
648. **Skulachev V.** Anion carriers in fatty acid-mediated physiological uncoupling. *J Bioenerg Biomembr* 31: 431–445, 1999.
649. **Smith R, Porteous C, Gane A, Murphy M.** Delivery of bioactive molecules to mitochondria in vivo. *Proc Natl Acad Sci USA* 100: 5407–5412, 2003.
650. **Sobel B, Schneider D.** Cardiovascular complications in diabetes mellitus. *Curr Opin Pharmacol* 5: 143–148, 2005.
651. **Solaini G, Harris DA.** Biochemical dysfunction in heart mitochondria exposed to ischaemia and reperfusion. *Biochem J* 394: 377–394, 2005.
652. **Son H, Kim H, H Kwon Y.** Taurine prevents oxidative damage of high glucose-induced cataractogenesis in isolated rat lenses. *J Nutr Sci Vitaminol (Tokyo)* 53: 324–330, 2007.
653. **Sorescu D, Weiss D, Lassègue B, Clempus R, Szöcs K, Sorescu G, Valppu L, Quinn M, Lambeth J, Vega J, Taylor W, Griendling K.** Superoxide production and expression of Nox family proteins in human atherosclerosis. *Circ* 105: 1429–1435, 2002.
654. **Sorokin A, Kohan DE.** Physiology and pathology of endothelin-1 in renal mesangium. *Am J Physiol Renal Physiol* 285: F579–F589, 2003.

655. **Sowers JR, Epstein M, Frohlich ED.** Diabetes, hypertension, and cardiovascular disease: an update. *Hyperten* 37: 1053–1059, 2001.
656. **Springhorn C, Matsha T, Erasmus R, Essop M.** Exploring leukocyte o-glcNacylation as a novel diagnostic tool for the earlier detection of type 2 diabetes mellitus. *J Clin Endocrinol Metab* Epub ahead, 2012.
657. **Srinivasan S, Hatley M, Bolick D, Palmer L, Edelstein D, Brownlee M, Hedrick C.** Hyperglycaemia-induced superoxide production decreases eNOS expression via AP-1 activation in aortic endothelial cells. *Diabetologia* 47: 1727–1734, 2004.
658. **Srinivasan V, Sandhya N, Sampathkumar R, Farooq S, Mohan V, Balasubramanyam M.** Glutamine fructose-6-phosphate amidotransferase (GFAT) gene expression and activity in patients with type 2 diabetes: inter-relationships with hyperglycaemia and oxidative stress. *Clin Biochem* 40: 952–957, 2007.
659. **Srivastava SK, Ramana K V, Bhatnagar A.** Role of aldose reductase and oxidative damage in diabetes and the consequent potential for therapeutic options. *Endocrin Rev* 26: 380–392, 2005.
660. **St-Pierre J, Buckingham J, Roebuck S, Brand M.** Topology of superoxide production from different sites in the mitochondrial electron transport chain. *J Biol Chem* 277: 44784–44790, 2002.
661. **Stangl K, Günther C, Frank T, Lorenz M, Meiners S, Röpke T, Stelter L, Moobed M, Baumann G, Kloetzel P, Stangl V.** Inhibition of the ubiquitin-proteasome pathway induces differential heat-shock protein response in cardiomyocytes and renders early cardiac protection. *Biochem Biophys Res Commun* 291: 542–549, 2002.
662. **Stanley W, Hernandez L, Spires D, Bringas J, Wallace S, McCormack J.** Pyruvate dehydrogenase activity and malonyl CoA levels in normal and ischemic swine myocardium: effects of dichloroacetate. *J Mol Cell Cardiol* 28: 905–914, 1996.
663. **Stanley W, Recchia FA, Lopaschuk GD.** Myocardial substrate metabolism in the normal and failing heart. *Physiol Rev* 85: 1093–1129, 2005.
664. **Stanley W.** Cardiac energetics during ischaemia and the rationale for metabolic interventions. *Coron Artery Dis* 12: S3–S7, 2001.
665. **Stanley WC, Lopaschuk GD, Hall JL, McCormack JG.** Regulation of myocardial carbohydrate metabolism under normal and ischaemic conditions: Potential for pharmacological interventions. *Cardiovasc Res* 33: 243–257, 1997.
666. **Stansfield WE, Moss NC, Willis MS, Tang R, Selzman CH.** Proteasome inhibition attenuates infarct size and preserves cardiac function in a murine model of myocardial ischemia-reperfusion injury. *Annals Thoracic Surg* 84: 120–125, 2007.
667. **Stefani M, Dobson C.** Protein aggregation and aggregate toxicity: new insights into protein folding, misfolding diseases and biological evolution. *J Mol Med (Berl)* 81: 678–699, 2003.



668. **Steinberg S.** Structural basis of protein kinase C isoform function. *Physiol Rev* 88: 1341–1378, 2008.
669. **Stitt AW, Curtis TM.** Advanced glycation and retinal pathology during diabetes. *Pharmacol Rep* 57 Suppl: 156–168, 2005.
670. **Stoclet J, Chataigneau T, Ndiaye M, Oak M, El Bedoui J, Chataigneau M, Schini-Kerth V.** Vascular protection by dietary polyphenols. *Eur J Pharmacol* 500: 299–313, 2004.
671. **Stracke H, Lindemann A, Federlin K.** A benfotiamine-vitamin B combination in treatment of diabetic polyneuropathy. *Exp Clin Endocrinol Diabetes* 104: 311–316, 1996.
672. **Straczkowski M, Kowalska I, Nikolajuk A, Dzienis-Straczkowska S, Kinalska I, Baranowski M, Zendzian-Piotrowska M, Brzezinska Z, Gorski J.** Relationship between insulin sensitivity and sphingomyelin signaling pathway in human skeletal muscle. *Diabetes* 53: 1215–1221, 2004.
673. **Stranders I.** Admission blood glucose level as risk indicator of death after myocardial infarction in patients with and without diabetes mellitus. *Arch Intern Med* 164: 982–988, 2004.
674. **Strasser RH, Braun-Dullaeus R, Walendzik H, Marquetant R.** Alpha 1-receptor-independent activation of protein kinase C in acute myocardial ischemia. Mechanisms for sensitization of the adenylyl cyclase system. *Circ Res* 70: 1304–1312, 1992.
675. **Straumann E, Kurz DJ, Muntwyler J, Stettler I, Furrer M, Naegeli B, Frielingsdorf J, Schuiki E, Mury R, Bertel O, Spinass GA.** Admission glucose concentrations independently predict early and late mortality in patients with acute myocardial infarction treated by primary or rescue percutaneous coronary intervention. *Am Heart J* 150: 1000–1006, 2005.
676. **Stumvoll M, Nurjhan N, Perriello G, Dailey G, Gerich J.** Metabolic effects of metformin in non-insulin-dependent diabetes mellitus. *N Engl J Med* 333, 1995.
677. **Su H, Wang X.** The ubiquitin-proteasome system in cardiac proteinopathy: a quality control perspective. *Cardiovasc Res* 85: 253–62, 2010.
678. **Sudnikovich E, Maksimchik Y, Zabrodskaya S, Kubyshin V, Lapshina E, Bryszewska M, Reiter R, Zavodnik I.** Melatonin attenuates metabolic disorders due to streptozotocin-induced diabetes in rats. *Eur J Pharmacol* 569: 180–187, 2007.
679. **Suleiman M, Hammerman H, Boulos M, Kapeliovich M, Suleiman A, Agmon Y, Markiewicz W, Aronson D.** Fasting glucose is an important independent risk factor for 30-day mortality in patients with acute myocardial infarction: a prospective study. *Circ* 111: 754–760, 2005.
680. **Sun D, Nguyen N, DeGrado TR, Schwaiger M, Brosius FC.** Ischemia induces translocation of the insulin-responsive glucose transporter GLUT4 to the plasma membrane of cardiac myocytes. *Circ* 89: 793–798, 1994.

681. **Supinski G, Stofan D, Callahan L, Nethery D, Nosek T, DiMarco A.** Peroxynitrite induces contractile dysfunction and lipid peroxidation in the diaphragm. *J Appl Physiol* 87: 783–791, 1999.
682. **Svensson A, McGuire D, Abrahamsson P, Dellborg M.** Association between hyper- and hypoglycaemia and 2 year all-cause mortality risk in diabetic patients with acute coronary events. *Eur Heart J* 26: 1255–1261, 2005.
683. **Szabolcs M, Michler R, Yang X, Aji W, Roy D, Athan E, Sciacca R, Minanov O, Cannon P.** Apoptosis of cardiac myocytes during cardiac allograft rejection: relation to induction of nitric oxide synthase. *Circ* 94: 1665–1673, 1996.
684. **Szabó C.** Multiple pathways of peroxynitrite cytotoxicity. *Toxicol Lett* 140-141: 105–112, 2003.
685. **Szaleczky E, Prechl J, Feher J, Somogyi A.** Alterations in enzymatic antioxidant defense in diabetes mellitus- a rationale approach. *Postgrad Med J* 75: 13–17, 1999.
686. **Takagi H, Matsui Y, Hirotani S, Sakoda H, Asano T, Sadoshima J.** AMPK mediates autophagy during myocardial ischemia in vivo. *Autophagy* 3: 405–407, 2007.
687. **Takamiya R, Takahashi M, Myint T, Park Y, Miyazawa N, Endo T, Fujiwara, N Sakiyama H, Misonou, Y Miyamoto Y, Fujii J, Taniguchi N.** Glycation proceeds faster in mutated Cu, Zn-superoxide dismutases related to familial amyotrophic lateral sclerosis. *Fed Am Soc Exp Biol J* 17: 938–940, 2003.
688. **Takeda N, Nakamura I, Hatanaka T, Ohkubo T, Nagano M.** Myocardial mechanical and myosin isoenzyme alterations in streptozotocin-diabetic rats. *Jpn Heart J* 29: 455–463, 1988.
689. **Takei I, Kasatani T.** Future therapy of diabetes mellitus. *Biomed Pharmacother* 58: 578–581, 2004.
690. **Tan C, Li Y, Tan X, Pan H, Huang W.** Inhibition of the ubiquitin-proteasome system: a new avenue for atherosclerosis. *Clin Chem Lab Med* 44: 1218–1225, 2006.
691. **Tang WH, Cheng WT, Kravtsov GM, Tong XY, Hou XY, Chung SK, Chung SSM.** Cardiac contractile dysfunction during acute hyperglycemia due to impairment of SERCA by polyol pathway-mediated oxidative stress. *Am J Physiol Cell Physiol* 299: C643–C653, 2010.
692. **Tang WH, Martin KA, Hwa J.** Aldose reductase, oxidative stress, and diabetic mellitus. *Front Pharmacol* 3: 1–8, 2012.
693. **Temelkova-Kurktschiev T, Koehler C, Henkel E, Leonhardt W, Fuecker K, Hanefeld M.** Postchallenge plasma glucose and glycemic spikes are more strongly associated with atherosclerosis than fasting glucose or HbA1c level. *Diab Care* 23: 1830–1834, 2000.
694. **Tesfamariam B.** Free radicals in diabetic endothelial cell dysfunction. *Free Radic Biol Med* 16: 383–391, 1994.
695. **Tesfaye S.** Diabetic neuropathy: achieving best practice. *Br J Diab Vasc Dis* 3: 112–117, 2003.

696. **Thallas-Bonke V, Thorpe SR, Coughlan MT, Fukami K, Yap FYT, Sourris KC, Penfold SA, Bach LA, Cooper ME, Forbes JM.** Inhibition of NADPH oxidase prevents advanced glycation end product-mediated damage in diabetic nephropathy through a protein kinase C-alpha-dependent pathway. *Diabetes* 57: 460–9, 2008.
697. **The Diabetes Control and Complications Trial/Epidemiology of Diabetes Interventions, and Complications (DCCT/EDIC) Study Research Group.** Intensive diabetes treatment and cardiovascular disease in patients with type 1 diabetes. *N Engl J Med* 353: 2643–2653, 2005.
698. **Thompson R, Gottlieb A, Organ K, Koda J, Kisicki J, Kolterman O.** Pramlintide: a human amylin analogue reduced postprandial plasma glucose, insulin, and C-peptide concentrations in patients with type 2 diabetes. *Diabet Med* 14: 547–555, 1997.
699. **Thompson R, Peterson J, Gottlieb A, Mullane J.** Effects of pramlintide, an analog of human amylin, on plasma glucose profiles in patients with IDDM: results of a multicenter trial. *Diabetes* 46: 632–636, 1997.
700. **Thomson SC, Vallon V, Blantz RC.** Kidney function in early diabetes: the tubular hypothesis of glomerular filtration. *Am J Physiol Renal Physiol* 286: F8–F15, 2004.
701. **Thorens B, Waeber G.** Glucagon-like peptide-I and the control of insulin secretion in the normal state and in NIDDM. *Diabetes* 42: 1219–1225, 1993.
702. **Thorens B.** Glucagon-like peptide-1 and control of insulin secretion. *Diab Metab* 21: 311–318, 1995.
703. **Thornalley P, Babaei-Jadidi R.** Prevention of microvascular complications of diabetes by high dose S-benzoylthiamine monophosphate (benfotiamine): mechanism of thiamine delivery into cells. *Diabetologia* 48: Suppl 1, 2005.
704. **Thornalley P, Yurek-George A, Argirov O.** Kinetics and mechanism of the reaction of aminoguanidine with the alpha-oxoaldehydes glyoxal, methylglyoxal, and 3-deoxyglucosone under physiological conditions. *Biochem Pharmacol* 60: 55–65, 2000.
705. **Thornalley P.** Use of aminoguanidine (pimagedine) to prevent the formation of advanced glycation endproducts. *Arch Biochem Biophys* 419: 31–40, 2003.
706. **Thornalley PJ.** Glutathione-dependent detoxification of alpha-oxoaldehydes by the glyoxalase system: involvement in disease mechanisms and antiproliferative activity of glyoxalase I inhibitors. *Chem Biol Interact* 111: 137–151, 1998.
707. **Tian R, Abel ED.** Responses of GLUT4-deficient hearts to ischemia underscore the importance of glycolysis. *Circ* 103: 2961–2966, 2001.
708. **Todd J, Edwards C, Ghatei M, Mather H, Bloom S.** Subcutaneous glucagon-like peptide-1 improves postprandial glycaemic control over a 3-week period in patients with early type 2 diabetes. *Clin Sci (Lond)* 95: 325–329, 1998.

709. **Tominaga M, Eguchi H, Manaka H, Igarashi K, Kato T, Sekikawa A.** Impaired glucose tolerance is a risk factor for cardiovascular disease, but not impaired fasting glucose. The Funagata Diabetes Study. *Diab Care* 22: 920–924, 1999.
710. **Torres C, Hart G.** Topography and polypeptide distribution of terminal N-acetylglucosamine residues on the surfaces of intact lymphocytes. Evidence for O-linked GlcNAc. *J Biol Chem* 259: 3308–3317, 1984.
711. **Tothman DL, Magnusson I, Cline G, Gerard D, Kahn CR, Shulam RG, Shulman GI.** Decreased muscle glucose transport/phosphorylation is an early defect in the pathogenesis of non-insulin dependent diabetes mellitus. *Proc Natl Acad Sci USA* 92: 983–987, 1995.
712. **Tracey WR, Magee WP, Ellery CA, MacAndrew JT, Smith AH, Knight DR, Oates PJ.** Aldose reductase inhibition alone or combined with an adenosine A3 agonist reduces ischemic myocardial injury. *Am J Physiol Heart Circ Physiol* 279: 1447–1452, 2000.
713. **Travis S, Morrison A, Clements RJ, Winegrad A, Oski F.** Metabolic alterations in the human erythrocyte produced by increases in glucose concentration. The role of the polyol pathway. *J Clin Invest* 50: 2104–2112, 1971.
714. **Tsao P, Lefer A.** Time course and mechanism of endothelial dysfunction in isolated ischemic- and hypoxic-perfused rat hearts. *Am J Physiol* 259: H1660–H1666, 1990.
715. **Tsukamoto O, Minamino T, Kitakaze M.** Functional alterations of cardiac proteasomes under physiological and pathological conditions. *Cardiovasc Res* 85: 339–346, 2010.
716. **Tsukamoto S, Yokosawa H.** Targeting the proteasome pathway. *Exp Opin Therap Targets* 13: 605–622, 2009.
717. **Turinsky J, O'Sullivan D, Bayly B.** 1,2-Diacylglycerol and ceramide levels in insulin-resistant tissues of the rat in vivo. *J Biol Chem* 265: 16880–16885, 1990.
718. **Turrens J, Alexandre A, Lehninger A.** Ubisemiquinone is the electron donor for superoxide formation by complex III of heart mitochondria. *Arch Biochem Biophys* 237: 408–414, 1985.
719. **Ubl J, Chen S, Stucki J.** Anti-diabetic biguanides inhibit hormone-induced intracellular Ca<sup>2+</sup> concentration oscillations in rat hepatocytes. *Biochem J* 567: 561–567, 1994.
720. **Uchino H, Niwa M, Shimizu T, Nishiyama K, Kawamori R.** Impairment of early insulin response after glucose load, rather than insulin resistance, is responsible for postprandial hyperglycemia seen in obese type 2 diabetes: assessment using nateglinide, a new insulin secretagogue. *Endocr J* 47: 639–641, 2000.
721. **Ulrich P, Cerami A.** Protein glycation, diabetes, and aging. *Recent Prog Horm Res* 56: 1–21, 2001.
722. **United Kingdom Prospective Diabetes Study (UKPDS) Group.** Intensive blood glucose control with sulphonylureas or insulin compared with conventional treatment and risk of complications in patients with T2DM (UKPDS 33). *Lancet* 352: 837–845, 1998.

723. **Urios P, Grigorova-Borsos A, Sternberg M.** Aspirin inhibits the formation of pentosidine, a cross-linking advanced glycation end product, in collagen. *Diabetes Res Clin Pract* 77: 337–340, 2007.
724. **Valerio G, Franzese A, Poggi V, Patrini C, Laforenza U, Tenore A.** Lipophilic thiamine treatment in long-standing insulin-dependent diabetes mellitus. *Acta Diabetol* 36: 73–76, 1999.
725. **Vanlangenakker N, Vanden Berghe T, Krysko D, Festjens N, Vandenabeele P.** Molecular mechanisms and pathophysiology of necrotic cell death. *Curr Mol Med* 8: 207–220, 2008.
726. **Vary T, Randle P.** The effect of ischaemia on the activity of pyruvate dehydrogenase complex in rat heart. *J Mol Cell Cardiol* 16: 723–733, 1984.
727. **Vaux D, Strasser A.** The molecular biology of apoptosis. *Proc Natl Acad Sci U S A* 93: 2239–2244, 1996.
728. **De Vegt F, Dekker J, Ruhé H, Stehouwer C, Nijpels G, Bouter L, Heine R.** Hyperglycaemia is associated with all-cause and cardiovascular mortality in the Hoorn population: the Hoorn Study. *Diabetologia* 42: 926–931, 1999.
729. **Versari D, Herrmann J, Gössl M, Mannheim D, Sattler K, Meyer F, Lerman L, Lerman A.** Dysregulation of the ubiquitin-proteasome system in human carotid atherosclerosis. *Arterioscler Thromb Vasc Biol* 26: 2132–2139, 2006.
730. **Vieira O, Escargueil-Blanc I, Jürgens G, Borner C, Almeida L, Salvayre R, Nègre-Salvayre A.** Oxidized LDLs alter the activity of the ubiquitin-proteasome pathway: potential role in oxidized LDL-induced apoptosis. *Fed Am Soc Exp Biol J* 14: 532–542, 2000.
731. **Vik-Mo H, Riemersma R, Mjøs O, Oliver M.** Effect of myocardial ischaemia and antilipolytic agents on lipolysis and fatty acid metabolism in the in situ dog heart. *Scand J Clin Lab Invest* 39: 559–568, 1979.
732. **Vincent A, Russell J, Low P, Feldman E.** Oxidative stress in the pathogenesis of diabetic neuropathy. *Endocr Rev* 25: 612–628, 2004.
733. **Vinik A, Flemmer M.** Diabetes and macrovascular disease. *J Diabetes Complic* 16: 235–245, 2002.
734. **Vinik A, Vinik E.** Prevention of the complications of diabetes. *Am J Manag Care* 9: S63–S80, 2003.
735. **Violi F, Cangemi R, Sabatino G, Pignatelli P.** Vitamin E for the treatment of cardiovascular disease: is there a future? *Ann N Y Acad Sci* 1031: 292–304, 2004.
736. **Virág L, Szabó E, Gergely P, Szabó C.** Peroxynitrite-induced cytotoxicity: mechanism and opportunities for intervention. *Toxicol Lett* 140-141: 113–124, 2003.
737. **Vlassara H, Palace M.** Diabetes and advanced glycation endproducts. *J Intern Med* 251: 87–101, 2002.

738. **Vlassara H, Striker L, Teichberg S, Fuh H, Li Y, Steffes M.** Advanced glycation end products induce glomerular sclerosis and albuminuria in normal rats. *Proc Natl Acad Sci USA* 91: 11704–11708, 1994.
739. **Voges D, Zwickl P, Baumeister W.** The 26S proteasome: a molecular machine designed for controlled proteolysis. *Annu Rev Biochem* 68: 1015–1068, 1999.
740. **Volvert M, Seyen S, Piette M, Evrard B, Gangolf M, Plumier J, Bettendorff L.** Benfotiamine, a synthetic S-acyl thiamine derivative, has different mechanisms of action and a different pharmacological profile than lipid-soluble thiamine disulfide derivatives. *BMC pharmacology* 8: 10, 2008.
741. **Vásquez-Vivar J, Martísek P, Whitsett J, Joseph J, Kalyanaraman B.** The ratio between tetrahydrobiopterin and oxidized tetrahydrobiopterin analogues controls superoxide release from endothelial nitric oxide synthase: an EPR spin trapping study. *Biochem J* 15: 733–739, 2002.
742. **Vázquez-Carrera M, Silvestre J.** Insulin analogues in the management of diabetes. *Methods Find Exp Clin Pharmacol* 26: 445–461, 2004.
743. **Wada T, Takagi H, Minakami H, Hamanaka W, Okamoto K, Ito A, Sahashi Y.** A new thiamine derivative, S-benzoylthiamine O-monophosphate. *Science* 134: 195–196, 1961.
744. **Waisundara V, Hsu A, Huang D, Tan B.** Scutellaria baicalensis enhances the anti-diabetic activity of metformin in streptozotocin-induced diabetic Wistar rats. *Am J Chin Med* 36: 517–540, 2008.
745. **Wall S, Lopaschuk G.** Glucose oxidation rates in fatty acid-perfused isolated working hearts from diabetic rats. *Biochim Biophys Acta (BBA)* 1006: 97–103, 1989.
746. **Wallace D.** Mitochondrial genetics: a paradigm for aging and degenerative diseases? *Science* 256: 628–632, 1992.
747. **Wamelink MMC, Struys EA, Jakobs C.** The biochemistry, metabolism and inherited defects of the pentose phosphate pathway: a review. *J Inher Metab Dis* 31: 703–717, 2008.
748. **Wang X, Lau W, Yuan Y, Wang Y, Yi W, Christopher T, Lopez B, Liu H, Ma X.** Methylglyoxal increases cardiomyocyte ischemia-reperfusion injury via glycation inhibition of thioredoxin activity. *Am J Physiol Endocrinol Metab* 299: E207–E214, 2010.
749. **Wang X, Martindale J, Liu Y, Holbrook N.** The cellular response to oxidative stress: influences of mitogen-activated protein kinase signalling pathways on cell survival. *Biochem J* 333: 291–300, 1998.
750. **Watkins N, Thorpe S, Baynes J.** Glycation of amino groups in protein. Studies on the specificity of modification of RNase by glucose. *J Biol Chem* 260: 10629–10636, 1985.

751. **Wei M, Zong W, Cheng E, Lindsten T, Panoutsakopoulou V, Ross A, Roth K, MacGregor G, Thompson C, Korsmeyer S.** Proapoptotic BAX and BAK: a requisite gateway to mitochondrial dysfunction and death. *Science* 292: 727–730, 2001.
752. **Wei Q, Xia Y.** Proteasome inhibition down-regulates endothelial nitric-oxide synthase phosphorylation and function. *J Biol Chem* 281: 21652–21659, 2006.
753. **Weigert C, Brodbeck K, Sawadogo M, Häring H, Schleicher E.** Upstream stimulatory factor (USF) proteins induce human TGF-beta1 gene activation via the glucose-response element-1013/-1002 in mesangial cells: up-regulation of USF activity by the hexosamine biosynthetic pathway. *J Biol Chem* 279: 15908–15915, 2004.
754. **Wendt T, Harja E, Bucciarelli L, Qu W, Lu Y, Rong L, Jenkins D, Stein G, Schmidt A, Yan S.** RAGE modulates vascular inflammation and atherosclerosis in a murine model of type 2 diabetes. *Atheroscl* 185: 70–77, 2006.
755. **Werstuck G, Khan M, Femia G, Kim A, Tedesco V, Trigatti B, Shi Y.** Glucosamine-induced endoplasmic reticulum dysfunction is associated with accelerated atherosclerosis in a hyperglycemic mouse model. *Diabetes* 55: 93–101, 2006.
756. **Wheeler T.** Translocation of glucose transporters in response to anoxia in heart. *J Biol Chem* 263: 19447–19454, 1988.
757. **Whelan R, Kaplinskiy V, Kitsis R.** Cell death in the pathogenesis of heart disease: mechanisms and significance. *Annu Rev Physiol* 72: 19–44, 2010.
758. **Williams R, Airey M, Baxter H, Forrester J, Kennedy-Martin T, Girach A.** Epidemiology of diabetic retinopathy and macular oedema: a systematic review. *Eye (Lond)* 18: 963–983, 2004.
759. **Williamson JR, Chang K, Frangos M, Hasan KS, Ido Y, Kawamura T, Nyengaard JR, Van den Enden M, Kilo C, Tilton RG.** Hyperglycemic pseudohypoxia and diabetic complications. *Diabetes* 42: 801–813, 1993.
760. **Willis MS, Patterson C.** Into the heart: the emerging role of the ubiquitin-proteasome system. *J Mol Cell Cardiol* 41: 567–579, 2006.
761. **Willis MS, Townley-Tilson WHD, Kang EY, Homeister JW, Patterson C.** Sent to destroy: the ubiquitin proteasome system regulates cell signaling and protein quality control in cardiovascular development and disease. *Circ Res* 106: 463–478, 2010.
762. **Wolff S, Jiang Z, Hunt J.** Protein glycation and oxidative stress in diabetes mellitus and ageing. *Free Radic Biol Med* 10: 339–352, 1991.
763. **Wolff SP, Dean RT.** Glucose autoxidation and protein modification. The potential role of “autoxidative glycosylation” in diabetes. *Biochem. J* 245: 243–250, 1987.
764. **Wong M, Chung JWY, Wong TKS.** Effects of treatments for symptoms of painful diabetic neuropathy: systematic review. *BMJ (Clinical research ed.)* 335: 87, 2007.

765. **World Health Organization.** *The World Health Report 2006: Working together for health.* 2006.
766. **Xia L, Wang H, Goldberg HJ, Munk S, Fantus IG, Whiteside CI.** Mesangial cell NADPH oxidase upregulation in high glucose is protein kinase C dependent and required for collagen IV expression. *Am J Physiol Ren Physiol* 290: F345–F356, 2006.
767. **Xia P, Inoguchi T, Kern TS, Engerman RL, Oates PJ, King GL.** Characterization of the mechanism for the chronic activation of diacylglycerol-protein kinase C pathway in diabetes and hypergalactosemia. *Diabetes* 43: 1122–1129, 1994.
768. **Xia P, Kramer RM, King GL.** Identification of the mechanism for the inhibition of Na<sup>+</sup>,K<sup>(+)</sup>-adenosine triphosphatase by hyperglycemia involving activation of protein kinase C and cytosolic phospholipase A2. *J Clin Invest* 96: 733–740, 1995.
769. **Xu G, Takashi E, Kudo M, Ishiwata T, Naito Z.** Contradictory effects of short- and long-term hyperglycemias on ischemic injury of myocardium via intracellular signalling pathway. *Exp Mol Path* 76: 57–65, 2004.
770. **Xu P, Wang J, Kodavatiganti R, Zeng Y, Kass IS.** Activation of protein kinase C contributes to the isoflurane-induced improvement of functional and metabolic recovery in isolated ischemic rat hearts. *Anesth Analg* 99: 993–1000, 2004.
771. **Yabe-Nishimura C.** Aldose reductase in glucose toxicity: a potential target for the prevention of diabetic complications. *Pharmacol Rev* 50: 21–33, 1998.
772. **Yamagishi S, Edelstein D, Du X, Brownlee M.** Hyperglycemia potentiates collagen-induced platelet activation through mitochondrial superoxide overproduction. *Diabetes* 50: 1491–1494, 2001.
773. **Yamagishi S.** Advanced glycation end products and receptor-oxidative stress system in diabetic vascular complications. *Therapeutic apheresis and dialysis : official peer-reviewed journal of the International Society for Apheresis, the Japanese Society for Apheresis, the Japanese Society for Dialysis Therapy* 13: 534–539, 2009.
774. **Yamagishi S.** Role of advanced glycation end products (AGEs) and receptor for AGEs (RAGE) in vascular damage in diabetes. *Exp Ger* 46: 217–224, 2011.
775. **Yamakawa T, Tanaka S, Yamakawa Y, Kamei J, Numaguchi K, Motley E, Inagami T, Eguchi S.** Lysophosphatidylcholine activates extracellular signal-regulated kinases 1/2 through reactive oxygen species in rat vascular smooth muscle cells. *Arterioscler Thromb Vasc Biol* 22: 752–758, 2002.
776. **Yan H, Guo Y, Zhang J, Ding Z, Ha W, Harding J.** Effect of carnosine, aminoguanidine, and aspirin drops on the prevention of cataracts in diabetic rats. *Mol Vis* 14: 2282–2291, 2008.
777. **Yan L, Vatner D, Kim S, Ge H, Masurekar M, Massover W, Yang G, Matsui Y, Sadoshima J, Vatner S.** Autophagy in chronically ischemic myocardium. *Proc Natl Acad Sci U S A* 102: 13807–13812, 2005.



778. **Yan S, Schmidt A, Anderson G, Zhang J, Brett J, Zou Y, Pinsky D, Stern D.** Enhanced cellular oxidant stress by the interaction of advanced glycation end products with their receptors/binding proteins. *J Biol Chem* 269: 9889–9897, 1994.
779. **Yeaman S.** The 2-oxo acid dehydrogenase complexes: recent advances. *Biochem J* 257: 625–632, 1989.
780. **Yellon DM, Hausenloy DJ.** Mechanisms of disease: myocardial reperfusion injury. *N Engl J Med* 357: 1121–1135, 2007.
781. **Yerneni K, Bai W, Khan B, Medford R, Natarajan R.** Hyperglycemia-induced activation of nuclear transcription factor kappaB in vascular smooth muscle cells. *Diabetes* 48: 855–864, 1999.
782. **Yildiz A, Arat-Ozkan A, Kocas C, Abaci O, Coskun U, Bostan C, Olcay A, Akturk F, Okcun B, Ersanli M, Gurmen T.** Admission hyperglycemia and TIMI frame count in primary percutaneous coronary intervention. *Angiology* 63: 325–329, 2012.
783. **Yim M, Yim H, Lee C, Kang S, Chock P.** Protein glycation: creation of catalytic sites for free radical generation. *Ann N Y Acad Sci* 928: 48–53, 2001.
784. **Yin X, Zheng Y, Zhai X, Zhao X, Cai L.** Diabetic inhibition of preconditioning- and postconditioning-mediated myocardial protection against ischemia/reperfusion injury. *Exp Diab Res* 2012: 198048, 2012.
785. **Yki-Järvinen H, Daniels M, Virkamäki A, Mäkimattila S, DeFronzo R, McClain D.** Increased glutamine:fructose-6-phosphate amidotransferase activity in skeletal muscle of patients with NIDDM. *Diabetes* 45: 302–307, 1996.
786. **Yonekura H, Yamamoto Y, Sakurai S, Watanabe T, Yamamoto H.** Current perspective roles of the receptor for advanced glycation endproducts in diabetes-induced vascular injury. *J Pharmacol Sci* 311: 305–311, 2005.
787. **Youle R, Strasser A.** The BCL-2 protein family: opposing activities that mediate cell death. *Nat Rev Mol Cell Biol* 9: 47–59, 2008.
788. **Young L, Renfu Y, Russell R, Hu X, Caplan M, Ren J, Shulman G, Sinusas A.** Low-flow ischemia leads to translocation of canine heart GLUT-4 and GLUT-1 glucose transporters to the sarcolemma in vivo. *Circ* 95: 415–422, 1997.
789. **Young LH, Coven DL, Russell RR.** Cellular and molecular regulation of cardiac glucose transport. *J Nucl Cardiol* 7: 267–276, 2000.
790. **Yu T, Chen Q, Chen Z, Xiong Z, Ye M.** Protective effects of total flavones of rhododendra against global cerebral ischemia reperfusion injury. *Am J Chin Med* 37: 877–887, 2009.
791. **Yu X, Kem DC.** Proteasome inhibition during myocardial infarction. *Cardiovasc Res* 85: 312–320, 2010.

792. **Yu X, Patterson E, Kem DC.** Targeting proteasomes for cardioprotection. *Curr Opin Pharmacol* 9: 167–172, 2009.
793. **Yue K, Chung W, Leung A, Cheng C.** Redox changes precede the occurrence of oxidative stress in eyes and aorta, but not in kidneys of diabetic rats. *Life Sci* 73: 2557–2570, 2003.
794. **Zachara NE, Hart GW.** Cell signaling, the essential role of O-GlcNAc! *Biochim Biophys Acta* 1761: 599–617, 2006.
795. **Zerbini G, Bonfanti R, Meschi F, Bognetti E, Paesano PL, Gianolli L, Querques M, Maestroni A, Calori G, Del Maschio A, Fazio F, Luzi L, Chiumello G.** Persistent renal hypertrophy and faster decline of glomerular filtration rate precede the development of microalbuminuria in type 1 diabetes. *Diabetes* 55: 2620–2625, 2006.
796. **Zha J, Harada H, Yang E, Jockel J, Korsmeyer S.** Serine phosphorylation of death agonist BAD in response to survival factor results in binding to 14-3-3 not BCL-X(L). *Cell* 87: 619–628, 1996.
797. **Zhang F, Paterson AJ, Huang P, Wang K, Kudlow JE.** Metabolic control of proteasome function. *Physiol (Bethesda, Md.)* 22: 373–379, 2007.
798. **Zhang S, Li H, Yang S.** Tribulosin protects rat hearts from ischemia/ reperfusion injury. *Acta Pharmacol Sin* 31: 671–678, 2010.
799. **Zhang Y, Marcillat O, Giulivi C, Ernster L, Davies JA.** The oxidative inactivation of mitochondrial electron transport chain components and ATPase. *J Biol Chem* 265: 16330–16336, 1990.
800. **Zhang Z, Liew C, Handy D, Zhang Y, Leopold J, Hu J, Guo L, Kulkarni R, Loscalzo J, Stanton R.** High glucose inhibits glucose-6-phosphate dehydrogenase, leading to increased oxidative stress and beta-cell apoptosis. *Fed Am Soc Exp Biol J* 24: 1497–1505, 2010.
801. **Zhao G, Zhao Y, Wang X, Xu Y.** Knockdown of glucose-6-phosphate dehydrogenase (G6PD) following cerebral ischemic reperfusion: The pros and cons. *Neurochem Intern* 61: 146–155, 2012.
802. **Zhao L, Wang Y, Min X, Yang H, Zhang P, Zeng Q.** Ischemia-reperfusion injury up-regulates Pim-3 gene expression in myocardial tissue. *J Huazhong Univ Sci Technol Med Sci* 30: 704–708, 2010.
803. **Zhao Z, Corvera JS, Halkos ME, Kerendi F, Wang N, Guyton RA, Vinten-johansen J.** Inhibition of myocardial injury by ischemic post-conditioning during reperfusion: comparison with ischemic preconditioning. *Am J Physiol Cell Physiol* : 1–35, 2003.
804. **Zhou L, Aon M, Almas T, Cortassa S, Winslow R, O'Rourke B.** A reaction-diffusion model of ROS-induced ROS release in a mitochondrial network. *PLoS Comput Biol* 6: e1000657, 2010.

805. **Zhou Y, Grayburn P, Karim A, Shimabukuro M, Higa M, Baetens D, Orci L, Unger RH.** Lipotoxic heart disease in obese rats : Implications for human obesity. *Proc Natl Acad Sci* 97: 1784–1789, 2000.
806. **Ziegler D, Hanefeld M, Ruhnau K, Meissner H, Lobisch M, Schütte K, Gries F.** Treatment of symptomatic diabetic peripheral neuropathy with the anti-oxidant alpha-lipoic acid. A 3-week multicentre randomized controlled trial (ALADIN Study). *Diabetologia* 38: 1425–1433, 1995.
807. **Ziegler D, Mayer P, Rathmann W, Gries F.** One-year treatment with the aldose reductase inhibitor, ponalrestat, in diabetic neuropathy. *Diabetes Res Clin Pract* 14: 63–73, 1991.
808. **Zieman S, Kass D.** Advanced glycation endproduct crosslinking in the cardiovascular system: potential therapeutic target for cardiovascular disease. *Drugs* 64: 459–470, 2004.
809. **Zolk O, Schenke C, Sarikas A.** The ubiquitin-proteasome system: focus on the heart. *Cardiovasc Res* 70: 410–421, 2006.

## Chapter 3

### **Oleanolic acid: a novel cardio-protective agent that blunts hyperglycemia-induced contractile dysfunction**

Diabetes constitutes a major health challenge. Since cardiovascular complications are common in diabetic patients this will further increase the overall burden of disease. Furthermore, stress-induced hyperglycemia in non-diabetic patients with acute myocardial infarction is associated with higher in-hospital mortality. Previous studies implicate oxidative stress, excessive flux through the hexosamine biosynthetic pathway (HBP) and a dysfunctional ubiquitin-proteasome system (UPS) as potential mediators of this process. Since oleanolic acid (OA; a clove extract) possesses antioxidant properties, we hypothesized that it attenuates acute and chronic hyperglycemia-mediated pathophysiologic molecular events (oxidative stress, apoptosis, HBP, UPS), and thereby improves contractile function in response to ischemia and reperfusion. We employed several experimental systems: 1) H9c2 cardiac myoblasts were exposed to 33 mM glucose for 48 hr vs. controls (5 mM glucose); and subsequently treated with two OA concentrations (20 and 50  $\mu$ M) for 6 and 24 hr, respectively; 2) Isolated rat hearts were perfused *ex vivo* with Krebs-Henseleit buffer containing 33 mM glucose vs. controls (11 mM glucose) for 60 min, followed by 20 min global ischemia and 60 min reperfusion  $\pm$  OA treatment; 3) *In vivo* coronary ligations were performed on streptozotocin treated rats  $\pm$  OA administration during reperfusion; and 4) Effects of long-term OA treatment (2 weeks) on heart function was assessed in streptozotocin-treated rats. Our data demonstrate that OA treatment blunted high glucose-induced oxidative stress and apoptosis in heart cells. OA treatment also resulted in cardio-protection, i.e. for *ex vivo* and *in vivo* rat hearts exposed to ischemia and reperfusion under hyperglycemic conditions. In parallel, we found decreased oxidative stress, apoptosis, HBP flux and proteasomal activity following ischemia and reperfusion. Long-term OA treatment also improved heart function in streptozotocin-diabetic rats. These findings are promising since it may eventually result in novel therapeutic interventions to treat acute hyperglycemia (in non-diabetic patients), and diabetic patients with associated cardiovascular complications.

### 3.1 Introduction

The dramatic surge in diabetes during the past few decades constitutes a major threat to human health in developed and developing nations (6, 84). Since cardiovascular complications and mortalities are common in diabetic patients (5, 58), this will further increase the overall burden of disease. These alarming projections therefore necessitate a comprehensive understanding of the underlying molecular mechanisms orchestrating the onset of cardiovascular diseases (CVD) in diabetic individuals.

Diabetes is characterized by perturbed metabolic pathways usually resulting in hyperlipidemia, hyperinsulinemia and hyperglycemia. Cardiovascular complications frequently present in diabetic patients and chronic hyperglycemia is proposed to be an important risk factor for myocardial infarction (12, 77). Moreover, stress-induced, acute hyperglycemia in non-diabetic patients with acute myocardial infarction is associated with increased in-hospital deaths (56, 62). Acute and chronic hyperglycemia triggers biochemical and electrophysiological changes that may result in impaired cardiac contractile function (15). Furthermore, hyperglycemia generates reactive oxygen species (ROS) and cell death in the myocardium, thereby contributing to the onset of CVD (11, 31, 57, 65). For example, we previously found that hyperglycemia-induced ROS increased flux through the hexosamine biosynthetic pathway (HBP) leading to greater O-GlcNAcylation of target proteins and myocardial apoptosis (65, 66). Hyperglycemia-induced oxidative stress can also result in the formation of misfolded or damaged proteins that may be eliminated by the ubiquitin-proteasome system (UPS). Previous studies revealed dysfunctional UPS with hyperglycemia, linked to greater inflammation and attenuated cardiac function at baseline and in response to ischemia and reperfusion (57, 63). However, it remains unclear whether increased or decreased UPS is detrimental with hyperglycemia and/or in response to ischemia and reperfusion. Pye *et al.* (2003) (64) found that myocardial reperfusion injury is reduced by proteasomal inhibitors, while others determined that UPS over-activity

may enhance the risk of complication during myocardial ischemia in diabetic patients (57). Conversely, others established that proteasomal impairment may contribute to the detrimental effects of myocardial ischemia (10). Additional studies are therefore required to determine the mechanisms underlying dysfunctional UPS in the heart under these conditions.

Despite the prevalence of commercially-available drugs used to treat diabetes, the use of alternative, plant-derived medicines is gaining momentum (33). For example, earlier studies evaluated the anti-diabetic therapeutic potential of *Syzygium aromaticum* [(Linnaeus) Merrill & Perry], belonging to the family Myrtaceae (commonly referred to as cloves). Here research workers established that its active constituent is the triterpenoid, oleanolic acid (OA) that exists in a very wide range of foods, medicinal herbs and plants (38). This triterpene is hydrophobic hence has reduced aqueous solubility (18). In relation to its pharmacokinetics the mean steady-state maximum plasma concentrations ( $C_{max}$ ) and time  $C_{max}$  was reached ( $T_{max}$ ) was reported to be 12.1 ng/ml and 5.2 hr, respectively after oral administration of an OA capsule in humans, indicating delayed *in vivo* absorption. Additionally absolute oral bioavailability of OA was only 0.7 % for oral concentrations of 25 and 50 mg/kg possibly due to poor solubility and extensive metabolic clearance (42). OA has been reported to be relatively non-toxic with reports of a mean lethal dose (LC50) of 0.10 mg/ml (75).

OA medicinal use was reported since the 1960s when its anti-inflammatory properties were reported (32). It is commonly used in traditional medicine for its hepatoprotective effects (49, 51, 52, 79). In addition to the mentioned effects, many of its therapeutic effects have been confirmed by contemporary research and these also include anti-hyperglycemic properties (52, 55, 71); antioxidant (74, 75); anti-tumor (39, 50) and anti-fungal (52). This wide range of effects is mainly attributed to its aglycone structure capable of forming crosslinkages with several molecules leading to molecular structures with different health effects. Furthermore, OA exhibited cardio-protective properties in response to ischemia and reperfusion by up-regulation of myocardial anti-oxidant defenses (24, 75). Commercially OA is now available as capsules or tablets in lipid based formulations to improve its

poor bioavailability and in China for example, it is used clinically used in the treatment of hepatitis B (52).

In light of this, we hypothesized that OA possesses anti-oxidant and anti-apoptotic properties and is thus able to blunt acute and chronic hyperglycemia-mediated pathophysiologic sequelae within the rat heart. Additionally, we proposed that OA attenuates the myocardial UPS and HBP, and thereby improves cardiac contractile function in response to ischemia and reperfusion under hyperglycemic conditions.

## **3.2 Materials and Methods**

### **3.2.1 Isolation of oleanolic acid from clove extract**

We employed *Syzygium aromaticum* [(Linnaeus) Merrill & Perry] (Myrtaceae) cloves (Africa International Food and Cosmetics Technologies, Durban, South Africa) to isolate and purify OA for this study. This approach was adopted since it generates sufficient amounts of OA in a cost-effective manner compared to purchasing purified OA on a regular basis. Cloves (1 kg) were extracted at room temperature for 24 hr sequentially in 3 L of each, dichloromethane and ethyl acetate. This step was repeated 3 times to yield residues of dichloromethane-solubles and ethyl acetate-solubles (EAS), respectively. Previous studies demonstrated that OA is mostly concentrated in the latter fraction (55). Subsequently, filtration was performed with 30 cm filter paper (Whatman International Ltd, Maidstone, England) where after filtrates were concentrated *in vacuo* using a rotary evaporator (Boeco, Hamburg, Germany) at 60°C. This procedure resulted in the isolation of a crude ethyl-acetate extract.

To identify chemical constituents, crude ethyl-acetate extracts were thereafter analyzed by thin layer chromatography (TLC) on pre-coated aluminium plates using Silica Gel 60 F254 (Merck, Darmstadt,

Germany). Here, we spotted a diluted portion of the isolated, crude extract and compared this with commercially obtained OA (Sigma-Aldrich, St Louis, MO). After developing the TLC plate with ethyl acetate/hexane (7:3), it was exposed to ultraviolet light (254-366 nm), sprayed with anisaldehyde/sulphuric acid/alcohol solution and the TLC plate subsequently dried with hot air. The appearance of a blue/violet-blue colouration indicated the presence of triterpenoids (37, 75).

Since the EAS fraction of *S. aromaticum* contained triterpenoids, it was subjected to further purification processes. We fractionated 2 g of EAS on silica gel (70-230 mesh, 3.5 x 45 cm) by open column chromatography with a ratio of 7:3 ethyl acetate and hexane, respectively. An aliquot of each collected fraction was then subjected to TLC as before, and compared to commercially obtained OA. This allowed us to pool the remainder of collected fractions according to TLC profiles (i.e. similar to OA), which was thereafter concentrated *in vacuo* using a rotary evaporator (Boeco, Hamburg, Germany) at 55°C. Concentrates were reconstituted using minimal amounts of chloroform and crystallized OA allowed to air dry. We re-crystallized OA with ethanol and its structure was confirmed by spectroscopic analysis using 1D and 2D <sup>1</sup>H and <sup>13</sup>C nuclear magnetic resonance techniques to a purity of ~98%. For a small part of this study we also employed commercially available OA (Sigma-Aldrich, St. Louis, MO) due to logistic reasons.

### 3.2.2 Cell culture and oleanolic acid treatments

H9c2 rat cardiomyoblasts (ECACC No. 88092904) were maintained at 37°C (5% CO<sub>2</sub> and 95% humidity) in low glucose (5.5 mM) Dulbecco's modified Eagle's medium (DMEM) (Sigma-Aldrich, St. Louis, MO) supplemented with 10% fetal bovine serum (Invitrogen, Carlsbad, CA) as described before by us (65). On the first day, H9c2 cells were split, sub-cultured and allowed to plate for 24 hr. Cells were thereafter cultured in DMEM containing: 5.5 mM glucose (control group), or 33 mM glucose (high glucose). With the high glucose exposure we attempted to simulate chronic hyperglycemia in our cell-



based studies. H9c2 cells were cultured for an additional 48 hr under these conditions followed by treatment with various concentrations of OA i.e. 0, 20, 50  $\mu$ M OA for 6 and 24 hr, respectively. The concentrations were selected based on literature (29, 60). Since these studies were *in vivo* the concentration was initially titrated lower.

### 3.2.3 Measurement of intracellular ROS levels and apoptosis

Intracellular ROS levels were determined by immunofluorescence microscopy as previously described (65). Briefly, cells were grown in special chamber slides and treated with OA as described above. Subsequently, live cells were incubated with 2',7'-dichlorodihydrofluorescein diacetate (DCFDA) stain (1:200; Invitrogen, Carlsbad, CA) for 10 min at 37°C (in the dark). The cells were then further stained with Hoechst dye in PBS at a ratio of 1:200 for 3- 5 min. Stains were then washed off, and cells were visualized using an Olympus Cell<sup>R</sup> fluorescence 1 x 81 inverted microscope (Olympus Biosystems, Planegg, Germany) with an F-view II camera for image acquisition and Cell<sup>R</sup> software for processing images. The temperature of the microscope was maintained at 37°C for live cell imaging using a Solent Scientific microscope incubator chamber (Solent Scientific, Segensworth, UK). Three independent experiments were conducted and at least 3 images per experiment analyzed.

We also measured ROS levels by flow cytometry. After treatment, cells were trypsinized and centrifuged (2 min at 20, 000 g), and the cell pellet treated with 2',7'-dichlorodihydrofluorescein diacetate stain (1:200), resuspended, and incubated at 37°C for 20 min in the dark. Cells not treated with 2',7'-dichlorodihydrofluorescein diacetate acted as negative controls, and stained cells treated with 100  $\mu$ L hydrogen peroxide (30% w/v hydrogen peroxide) incubated for 10 min served as positive controls. ROS levels were measured using a flow cytometer (Becton-Dickinson, Franklin Lakes, NJ) and quantified by determining the mean of fluorescence for each treatment. Three independent experiments were conducted for each condition investigated, with typically 5, 000 – 10, 000 cells analyzed per experiment.

In a separate set of experiments, we evaluated apoptosis by employing a caspase glow assay (Promega, Madison, WI) (see Appendix 4 for the detailed protocol). Briefly, H9c2 myoblasts were trypsinized, counted in a hemocytometer and  $\sim 1 \times 10^4$  cells seeded per well of a 96-well plate (Greiner, Kremsmünster, Austria). Cells were seeded with 300  $\mu\text{L}$  DMEM. DMEM was removed from cells and 100  $\mu\text{L}$  of the reconstituted assay reagent added into each well and gently mixed. Cells were subsequently incubated for  $\sim 2$  hr at room temperature and the degree of luminescence measured in white walled 96-well luminometer plates (Amersham, Buckinghamshire, UK).

We further confirmed our apoptosis data by employing an Annexin V-FITC kit (Macs, Miltenyi Biotec, Germany) according to the manufacturer's instructions. The principle of the assay is that Annexin V can specifically bind to phosphatidyl serine residues exposed outside the membrane of early apoptotic cells. This allows the fluorescein (Annexin V) conjugated stained apoptotic cells to be counted and quantified. Propidium Iodide (PI) is a dye for nucleic acid but can only penetrate into the later stages of apoptotic cells after cells have been permeabilized. Therefore, using both Annexin V and PI, apoptosis at different stages can be distinguished. Samples were gated based on analysis of the physical parameters - forward scatter. Electronic compensation required for Annexin was done in three stages: (1) by analyzing a sample without staining to determine the level of auto fluorescence, (2) by analyzing Annexin-V labeled cells and (3) PI-labeled population. All experiments were performed with these settings. For this experiment the concentration of OA used corresponded to the concentration used in perfusion experiments.

In brief, 100  $\mu\text{M}$  OA was administered for 6 and 24 hr, respectively, as before (refer 'Cell culture and OA treatments' section). After the completion of our experimental protocol, cells were washed with sterile PBS (calcium free), trypsinized and centrifuged at 300 g for three min. The pellet was washed with 1 ml of 1x binding buffer per  $10^6$  cells and re-centrifuged at 300 g for three min. The resulting pellet was resuspended in 100  $\mu\text{l}$  of 1x binding buffer per  $10^6$  cells and thereafter incubated with 10  $\mu\text{l}$

of Annexin V-FITC for 15 min in the dark at room temperature. Cells were subsequently washed with 1 ml of 1x binding buffer and centrifuged at 300 g for 3 min. The pellet was resuspended in 500  $\mu$ l of 1x binding buffer and 5  $\mu$ l of PI solution immediately added, prior to analysis by flow cytometry. Viable cells (Annexin V<sup>-</sup>PI<sup>-</sup>); non-viable, including late apoptotic or necrotic cells (Annexin V<sup>+</sup>PI<sup>+</sup>) or Annexin V<sup>-</sup>PI<sup>+</sup>) and apoptotic cells (Annexin V<sup>+</sup>PI<sup>-</sup>) were detected by the binding of Annexin V to externalized phosphatidylserine in conjunction with PI. Results are presented as the percentage of apoptosis normalized to control (ratio of early apoptotic, Annexin<sup>+</sup>/PI<sup>-</sup> cells to the total population).

### **3.2.4 Animals and ethics statement**

All animals were treated in accordance with the Guide for the Care and use of Laboratory Animals of the National Academy of Sciences (NIH publication No. 85-23, revised 1996). Studies were performed with the approval of the Animal Ethics Committees of Stellenbosch University, and the University of Cape Town (South Africa) (refer Appendices 1 and 2), and the United Arab Emirates University (United Arab Emirates).

### **3.2.5 Ex-vivo global ischemia during (simulated acute hyperglycemia)**

These studies were carried out at Stellenbosch University (South Africa). Male Wistar rats weighing 180-220 gr were used throughout the study. Rats were anesthetized (pentobarbitone, 100 mg/kg i.p) and hearts rapidly excised and perfused in a modified Langendorff model with Krebs-Henseleit buffer (refer Appendix 3 for preparation) equilibrated with 95% O<sub>2</sub>-5% CO<sub>2</sub> (37°C, pH 7.4) at a constant pressure (100 cm). The Krebs-Henseleit buffer contained (in mM) 11 Glucose, 118 NaCl, 4.7 KCl, 1.2 MgSO<sub>4</sub>.7H<sub>2</sub>O, 2.5 CaCl<sub>2</sub>.2H<sub>2</sub>O, 1.2 KH<sub>2</sub>PO<sub>4</sub>, 25 NaHCO<sub>3</sub>. Hearts were randomly distributed into four experimental groups: 1) control (11 mM glucose), untreated; 2) control (11 mM glucose), OA treated; 3) high glucose (33 mM glucose), untreated and 4) high glucose (33 mM glucose), OA treated – n=9

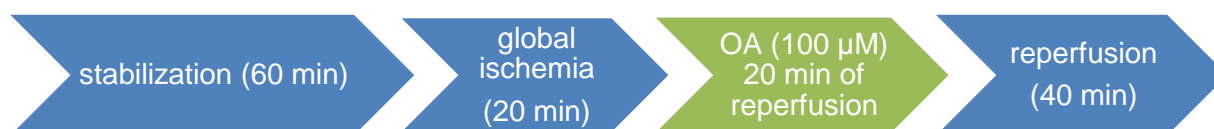
for each group. The buffer mimics the key ionic content of rat plasma or blood (36, 73) and it does not result in any hemodynamic dysfunction in the *ex vivo* heart perfusion system (20). With the high glucose perfusions we are attempting to simulate acute hyperglycemia within the clinical setting. Moreover, since *ex vivo* Langendorff perfusions are typically performed with 11 mM glucose at baseline, we are of the opinion that the 33 mM concentration is representative of a three-fold elevation of glucose levels (above normal) within the clinical setting.

The protocol was divided into two parts, i.e. perfusions a) without ischemia and b) with ischemia and reperfusion. For the non-ischemic protocol, we stabilized for 60 min whereafter 100  $\mu$ M OA was added to the perfusate for an additional 20 min period (Figure 3.1A). The concentration of OA used was chosen based on literature (55). Subsequently, we returned the buffer used in the stabilization period and perfused for a further 20 min (total perfusion time: 100 min). For the ischemic protocol, 100  $\mu$ M OA was added during the first 20 min of reperfusion (for OA experimental groups only; refer details below; see Figure 3.1B). OA was dissolved in a small volume of DMSO and less than 0.0005% (v/v) DMSO was present during perfusion experiments.

**A**



**B**



**C**

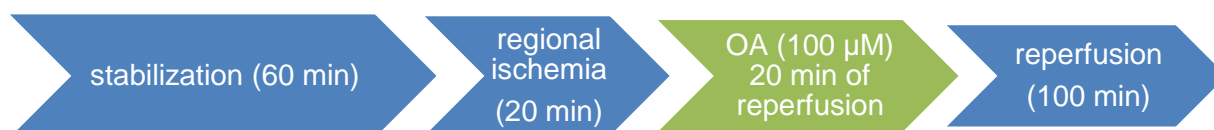


**Figure 3.1** Schematic diagrams showing the perfusion protocols for assessment of effects OA on heart contractile function without ischemia (A), with ischemia (B) and on infarct size (C).

During perfusion, a latex balloon attached to a pressure transducer (Stratham MLT 0380/D, AD Instruments Inc., Bella Vista, NSW, Australia) compatible with the PowerLab System ML410/W (AD Instruments Inc., Bella Vista, NSW, Australia), was inserted into the left ventricle and inflated to produce a diastolic pressure of 4-12 mm Hg. The protocol had a 60 min stabilization period, 20 min of global ischemia, followed by reperfusion for 60 min. Additional experiments were carried out in order to rule out the effects of osmotic pressure on heart function. Here hearts were perfused with 22 mM mannitol plus 11 mM glucose (total molarity = 33 mM) and subjected to ischemia and reperfusion as before. Contractile parameters assessed included heart rate (HR), left ventricular developed pressure (LVDP), and rate-pressure product (RPP;  $RPP = HR \times LVDP$ ). Left ventricular tissues were collected at four time points, i.e. a) within the first two minutes after ischemia, b) 20 and c) 40 min after ischemia, respectively, and d) also after 60 min of reperfusion. Collected tissues were freeze-clamped in liquid nitrogen and stored at  $-80^{\circ}\text{C}$  for further analysis.

### **3.2.6 *Ex-vivo* regional ischemia and reperfusion during simulated acute hyperglycemia**

These studies were carried out at Stellenbosch University (South Africa). To further strengthen our Langendorff perfusion data we also evaluated the effects of OA by infarct size determination. This was performed as described before but with slight modifications (47), i.e. we employed regional ischemia with a reperfusion time of 2 hr (see Figure 3.1C). Here a 3/0 silk suture was placed on the proximal portion of the left anterior descending coronary artery and passing the ends through a plastic tube. For induction of regional ischemia, the ends were tightened by pressing the plastic tube against the surface of the heart (above the artery) for 20 min. The snare was released during the reperfusion period. The efficacy of ischemia was confirmed by regional cyanosis and a substantial decrease in coronary flow.

### 3.2.6.1 Determination of infarct size

After completion of each regional ischemia and reperfusion experiment the snare was re-tightened and 2.5% Evans Blue dye (in Krebs buffer) was perfused through the hearts for infarct development. Hearts were subsequently removed from the Langendorff apparatus, blotted dry, suspended within 50 ml plastic tubes (using suture) and frozen at -20°C for 3 days. Thereafter, frozen hearts were sliced into 2 mm transverse sections and incubated with 1% 2,3,5-triphenyl tetrazolium chloride (TTC) in phosphate-buffered saline for 20 min at 37°C to identify non-infarcted (stained) from infarcted (non-stained) tissues. The area that was not stained with Evans Blue was defined as the area at risk (AAR). The area which demonstrated neither blue nor red was defined as the infarct site. Slices were then fixed in 10% formalin for 24 hr at room temperature before being placed between glass plates for scanning (both sides). The infarct area (IA) size and the area at risk (AAR) were calculated using Image J software (v1.46p, National Institutes of Health, USA) (see Appendices 11 and 12). Values of tissue slices were added together in order to obtain the total IA and AAR for each heart analyzed. We expressed the infarct size as the ratio of IA versus the AAR (%IA/AAR).

### 3.2.7 *In vivo* regional ischemia and reperfusion in streptozotocin-treated rats during chronic hyperglycemia

We next tested the effects of OA on diabetic rats (chronic hyperglycemia) subjected to an ischemic insult. These experiments were completed at the University of Cape Town (South Africa). Hyperglycemia was induced in Wistar rats as previously described (55, 60). In brief, male Wistar rats weighing 250-300 gr were injected (intraperitoneally) with a single dose of streptozotocin (STZ) (60 mg/kg dissolved in freshly prepared 0.1 M citrate buffer, pH 6.2; see Appendix 13). Control rats were injected with the vehicle (citrate buffer). Blood glucose concentrations of  $\geq 20$  mmol/l after 1 week were considered as a stable diabetic state before experimental procedures. We also determined body

weights and non-fasting blood glucose levels before STZ induction and after the one week of diabetes induction.

For the *in vivo* coronary artery ligation experiments, rats were divided into control (citrate-treated) and diabetic (STZ-treated) groups. Each group was subjected to coronary artery ligations  $\pm$  OA treatment (0.45 mg/kg i.v) (as described in detail below). The OA was dissolved in <0.001% DMSO and deionized water; freshly done for each treatment period.

Ligation experiments were performed one week after STZ intraperitoneal injection and confirmation of a stable diabetic state. Rats were anesthetized with sodium pentobarbital (60 mg/kg i.p), intubated, and thereafter ventilated with room air (2.5 ml/stroke) at a rate of 75 strokes per min via a rodent ventilator (Model 681, Harvard Apparatus, USA). Body temperature was monitored by a rectal temperature probe, and a constant temperature was maintained throughout the surgical procedure by placing rats on a custom-made heating block. The depth of anesthesia was checked by assessing the pedal withdrawal reflex and by monitoring heart rate. Maintenance doses of anesthetic (6 mg/kg i.p) were administered as required. Lead II electrocardiogram (ECG) was recorded via an Animal Bio Amplifier (ML136, AD Instruments, Australia). Carotid arterial blood pressure was recorded via a custom-made cannula attached to a pressure transducer (MLT0670, ADInstruments, Australia). Since formation of clots around intra-arterial cannulae poses a potential risk for arterial thrombosis, heparin (1000 IU/kg i.p) was injected concurrently with anesthetic (26, 80).

A left thoracotomy was performed through the 4<sup>th</sup> intercostal space and the left lung collapsed using a damp swab. The left anterior descending coronary artery was thereafter ligated as previously described (22). A 6/0 silk suture was placed around the left anterior descending coronary artery and its ends passed through a plastic tube. For induction of regional ischemia the ends of the suture were used as a snare to occlude the artery by applying it gently onto the ventricular surface for 30 min. The

efficacy of ischemia was confirmed by regional cyanosis and ECG changes. We employed S-T elevation (ECG) to confirm coronary artery ligation. The snare was released during reperfusion.

Rat hearts were subjected to 30 min ischemia followed by 2 hr of reperfusion. The penile vein was cannulated for OA administration, while the vehicle solution was administered to control animals. For the OA rats, a bolus concentration of 0.45 mg/kg i.v (55) was injected immediately on reperfusion (within 1 min of releasing the snare) and thereafter reperused for 2 hr as before. After the reperfusion period, the heart was flushed with saline and the coronary artery was re-occluded with the suture that had been left in place. The heart was then stained with 2.5% Evans blue to reveal the AAR. TTC staining and infarct sizes were determined as described for the *ex vivo* model.

### **3.2.8 Effects of long-term OA treatment on heart function in streptozotocin-treated rats (chronic hyperglycemia)**

We also ascertained the effects of chronic OA treatment within the diabetic context and its effects on cardiac function. These studies were completed at the United Arab Emirates University (Al-Ain, United Arab Emirates) and the candidate not involved with actual experiments; but did analyze all data generated. Here diabetes was induced in male Sprague-Dawley rats by a single intraperitoneal injection of STZ (60 mg/kg body weight) dissolved in citrate buffer. For OA-treated rats daily oral gavage was performed with a dose of 60 mg/kg for the entire 2-week period. The OA was made up freshly on each day and dissolved in DMSO and water. At the end of the two week period, body weights and fasting blood glucose levels for all experiments were determined.

Following STZ treatment, rats were killed by decapitation and hearts rapidly removed, mounted in Langendorff mode and perfused at a constant flow of 8 ml (g heart)<sup>-1</sup> min<sup>-1</sup> at physiological temperature (36–37°C) with Tyrode solution containing: 140 mM NaCl; 5 mM KCl; 1 mM MgCl<sub>2</sub>; 10



mM glucose; 5 mM HEPES; and 1.8 mM CaCl<sub>2</sub>; adjusted to pH 7.4 with NaOH and continuously bubbled with oxygen. When the heart rate stabilized, force was recorded from the left ventricle in spontaneously beating hearts with a purpose-built extracellular suction electrode as previously described (38). Here a clip is fixed at the apex of the hanging heart and a thread tied to the clip. The thread was guided through pulleys and tied to the force transducer that was connected to the Power Lab system. Signals from the electrode were collected at 400 Hz, amplified (ML136 Bioamp, ADInstruments, Castle Hill, New South Wales, Australia), and conveyed via a Powerlab (PL410, ADInstruments, Castle Hill, New South Wales, Australia) to a personal computer. Heart functional data are expressed as force generated (grams).

### **3.2.9 Western blot analysis**

Protein isolation was performed as previously described (65). Briefly, collected heart tissues were homogenized with modified RIPA buffer (see Appendix 5), the supernatant was centrifuged twice at 4, 300 g for 10 min at 4°C then stored at -80°C until further use. Protein expression was determined by Western blotting as described before by us (65, 66) for the following antibodies: BAD, phosphorylated-BAD (Ser 136), caspase 3 (Cell Signaling, MA, USA), and O-GlcNAc (HBP marker; CTD110.6, Santa Cruz Biotechnology Inc.). We employed β-actin (Cell Signaling, MA, USA) as a loading control.

### **3.2.10 Measurement of superoxide dismutase (SOD) activity**

We assessed the total SOD activity (cytosolic and mitochondrial components) as detailed in the instructions of a commercially obtained kit (Biovision K335-100, Mountain View, CA 94043 USA). The assay depends on utilizing a highly water-soluble tetrazolium salt, WST-1 (2-(4-iodophenyl)-3-(4-nitrophenyl)-5-(2,4-disulfo-phenyl)-2H-tetrazolium, monosodium salt), which produces a water-soluble formazan dye upon reduction with a superoxide anion. The rate of WST-1 reduction by superoxide anion is linearly related to the xanthine oxidase activity and is inhibited by SOD. Formazan levels can

be measured by absorption with a spectrophotometer at 450 nm. Briefly, collected heart tissues were homogenized with modified ice cold RIPA buffer, the supernatant was centrifuged twice at 4, 300 g for 10 min at 4°C. The samples were incubated with the enzyme and WST working solutions at 37°C for 20 min in a 96 well-microtiter-plate (Corning, New York, USA) in an orbital shaker incubator. Absorbance was read at 450 nm with a microplate reader (EL 800 KC Junior Universal Microplate reader, Bio-Tek Instruments Inc, Vermont, USA). The assay was optimized by a negative control and a positive control provided with the kit. SOD activity was calculated according to the following formula:

$$\% \text{ inhibition} = (A_{\text{control}} - A_{\text{sample}}) / A_{\text{control}} \times 100.$$

### **3.2.11 Myocardial superoxide levels**

The heart tissue was pulverized and homogenized in 100 volumes of perchloric acid (10% v/v) and centrifuged for 20 min at 13, 000 g (44). Protein-free supernatant (0.1 ml) was subsequently incubated with 0.25 mM lucigenin (Sigma-Aldrich, St. Louis, MO) at room temperature for 5 min in the dark and chemiluminescence measured in a white-walled luminometer 96 well-microtiter plate (Corning, New York, USA). Superoxide levels were expressed as chemiluminescence (RLU) per mg tissue.

### **3.2.12 Isolation of proteins for carbonylation and proteasome activity experiments**

Heart tissues were cut into small slices and homogenized in 1 ml of Tris-HCl buffer (pH 7.4) using an IKA Ultra Turrax T25 homogenizer (IKA Labor Technik, Staufen, Germany) and incubated on ice for 10 min before centrifugation at 9, 000 g for 15 min to remove cell debris. The supernatant was used for protein quantification using the BCA assay.

### 3.2.13 ELISA carbonyl protocol

Protein carbonyls are formed by a variety of oxidative mechanisms and are sensitive indices of oxidative injury. Protein carbonylation was determined by the carbonyl ELISA assay developed in the GEICO laboratory (Université de La Réunion, Saint Denis de La Réunion, France) based on recognition of protein-bound DNPH in carbonylated proteins with an anti-DNP antibody (67). Here 5  $\mu$ l of protein from tissue lysates (0.2-0.6  $\mu$ g) was denatured by adding 10  $\mu$ l 12% SDS solution. Subsequently, proteins were derivatized to DNP hydrazone with 10  $\mu$ l of DNPH solution (10 mM in 6 M guanidine hydrochloride, 0.5 M potassium phosphate buffer, pH 2.5). DNPH is a chemical compound that specifically reacts and binds to carbonylated proteins. Samples were incubated at room temperature for 30 min and the reaction was neutralized and diluted in coating buffer (10 mM sodium carbonate buffer, pH 9.6) to yield a final protein concentration of 0.2 - 0.6 ng/ $\mu$ l.

Diluted samples were added to wells of a Nunc Immuno Plate Maxisorp (Dutscher, Brumath, France) and incubated at 37°C for 3 hr, and thereafter washed 5x with PBS/Tween (0.1%) between each of the following steps: blocking the wells with 1% BSA in PBS/Tween (0.1%) overnight at 4°C; incubation with anti-DNP antibody (Sigma-Aldrich, St Louis, MO) (1:2000 dilution in PBS/Tween [0.1%]/BSA [1%]) at 37°C for 3 hr; incubation with horse radish peroxidase-conjugated polyclonal anti-rabbit immunoglobulin (GE Healthcare, Mannheim, Germany) (1:4000 dilution in PBS/Tween [0.1%]/BSA [1%]) for 1 hr at 37°C; addition of 100  $\mu$ l of TMB substrate solution and incubation for 10 min before stopping the coloration with 100  $\mu$ l of 2 M sulphuric acid. Absorbances were read at 490 nm against the blank (DNP reagent in coating buffer without protein) with a Fluostar microplate reader (BMG Labtech, Ortenberg, Germany). Results are expressed as percentage of absorbance compared to control cells (treatment of samples with 11 mM glucose) after normalization with protein concentrations.

### 3.2.14 Proteasome activity measurements

Chymotrypsin-like, trypsin-like, and caspase-like activities of the proteasome were assayed using fluorogenic peptides (Sigma-Aldrich, St Louis, MO): Suc-Leu-Leu-Val-Tyr-7-amido-4-methylcoumarin (LLVY-MCA at 25  $\mu$ M), N-t-Boc-Leu-Ser-Thr-Arg-7-amido-4-methylcoumarin (LSTR-MCA at 40  $\mu$ M) and N-Cbz-Leu-Leu-Glu-b-naphthylamide (LLE-NA at 150  $\mu$ M), respectively (28). Assays were performed with ~50  $\mu$ g of protein lysate (in 25 mM Tris-HCl, pH 7.5) and the appropriate substrate that were incubated together for 0-30 min at 37°C. Aminomethylcoumarin and  $\beta$ -naphthylamine fluorescence were measured at excitation/emission wavelengths of 350/440 and 333/410 nm, respectively, using a Fluostar fluorometric microplate reader (BMG Labtech, Ortenberg, Germany). Peptidase activities were measured in the absence/presence of 20  $\mu$ M of the proteasome inhibitor, MG132 (N-Cbz-Leu-Leu-leucinal), and the difference between the two values was attributed to proteasome activity. Data were normalized to protein concentrations.

### 3.2.15 Statistical analysis

Data are presented as mean  $\pm$  standard error of mean (SEM). Differences between treatment groups and time points were analyzed using one way analysis of variance (ANOVA). Mann-Whitney unpaired t-test was used when comparisons were made between two groups. Significant changes between groups were further assessed by means of the Tukey – Kramer *post hoc*. All statistical analysis were performed using GraphPad Prism version 5.01 (Graphpad Software, Inc, CA, USA). Values were considered significant when  $p < 0.05$ .

### 3.3 Results

#### 3.3.1 Isolation of oleanolic acid from clove extract

Evaluation of one-dimensional  $^1\text{H}$ - and  $^{13}\text{C}$ -NMR spectra of the isolated OA compound confirmed the presence of the 48 hydrogen and the 30 carbon atoms present in the molecule. For the determination of complex components within the molecule, two-dimensional  $^1\text{H}$ - and  $^{13}\text{C}$ -NMR spectra was conducted and confirmed the chemical structure of OA.

#### 3.3.2 Structural elucidation of OA

The *S. aromaticum* crude leaf extract was sequentially extracted with ethyl acetate to give ethyl acetate-solubles (EAS). The percentage yield of OA from EAS varied from 0.79% to 1.72%. Spectroscopic analyses of the white powder obtained after recrystallization with ethanol carried out using  $^1\text{H}$ - and  $^{13}\text{C}$ -NMR (1D and 2D) are shown in Figure 3.2. Figure 3.2A is the 1D  $^1\text{H}$  NMR spectra showing all the hydrogens in the molecule. Figure 3.2B shows the 1D  $^{13}\text{C}$  NMR spectra of all carbons in the molecule with two carbon signals at 143.6 and 122.7 ppm corresponding to the carbon-carbon double bond at carbon 12 and 13. Figure 3.2C and 3.2D are the two dimensional  $^1\text{H}$  and  $^{13}\text{C}$  NMR spectra of OA. In Figure 3.2C the bottom line shows all the carbons attached to hydrogen atoms; the middle line shows carbons that are attached to one hydrogen atom (CH groups), and in the uppermost line, signals pointing downwards are  $\text{CH}_2$  upwards are CH and  $\text{CH}_3$ . Table 3.1 compares the relative resonance frequencies of all the carbon atoms in the *S. aromaticum*-derived OA with literature data (54) while Figure 3.3 shows the OA structure as elucidated by  $^1\text{H}$ - and  $^{13}\text{C}$ -NMR.

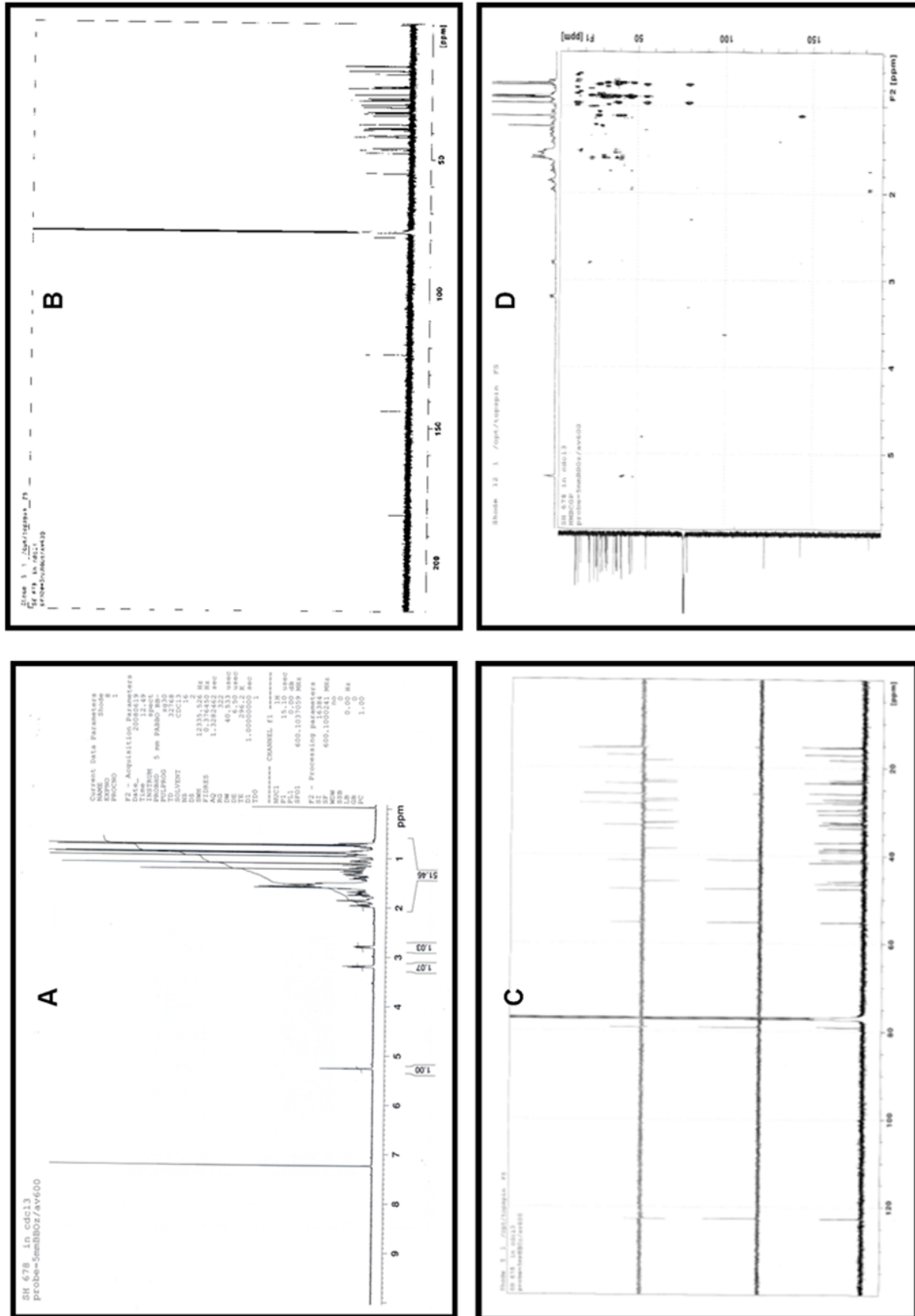
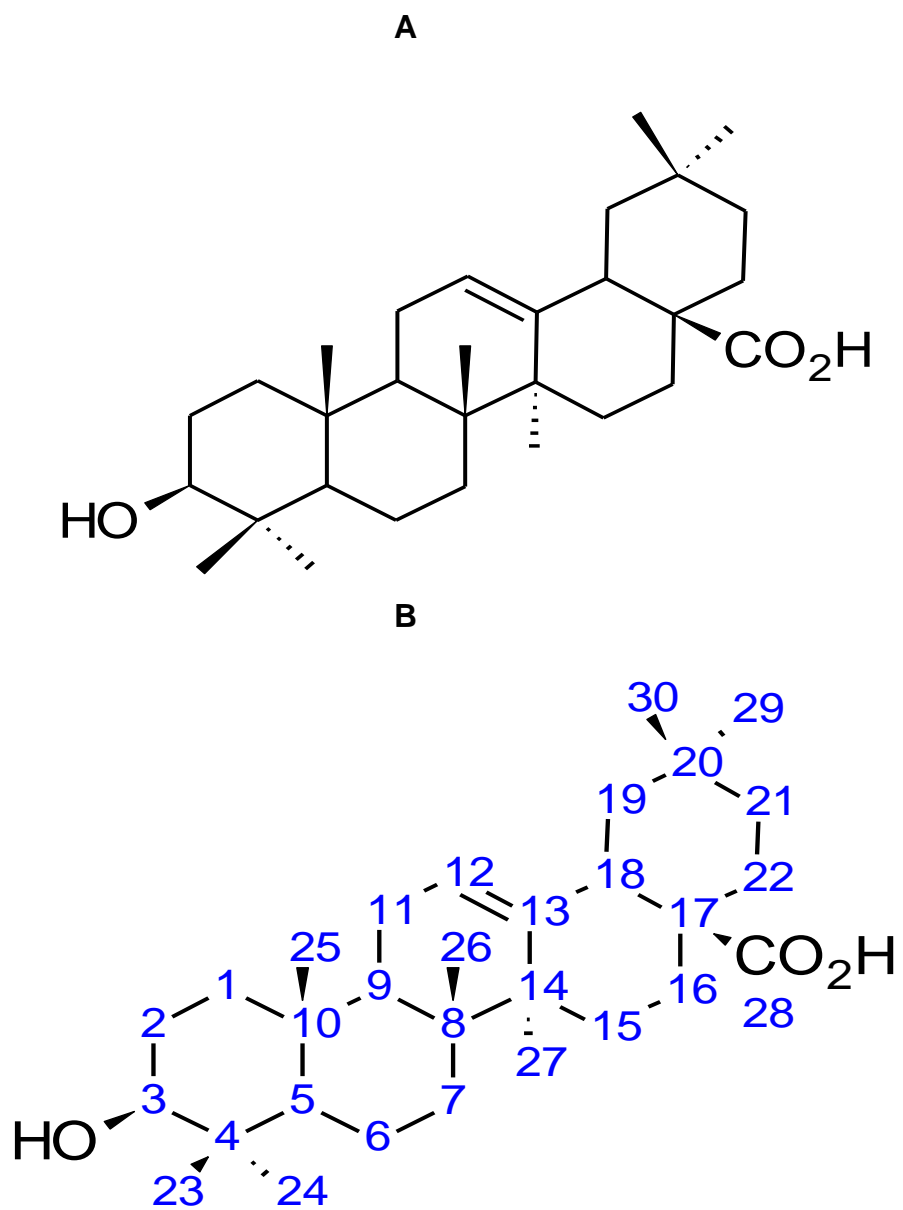


Figure 3.2: *Syzygium aromaticum* (cloves) derived OA one dimensional <sup>1</sup>H and <sup>13</sup>C-NMR spectra (A-B) and two dimensional <sup>1</sup>H and <sup>13</sup>C-NMR spectra by Distortion Enhancement Proton Testing (DEPT) (C) and Heteronuclear multiple quantum coherence (HMQC) (D).

**Table 3.1:**  $^{13}\text{C}$  (100.64 MHz) Bruker Avance III NMR spectral data of plant-derived and reported OA

(54)

<b>Carbon Position</b>	<b>Plant-derived</b>	<b>Reported OA</b>
	<b>OA</b> $^{\circ}\text{C}$	<b>(54)</b> $^{\circ}\text{C}$
<b>1</b>	38.4	38.5
<b>2</b>	27.2	27.4
<b>3</b>	79.0	78.7
<b>4</b>	38.8	38.7
<b>5</b>	55.2	55.2
<b>6</b>	18.3	18.3
<b>7</b>	32.6	32.6
<b>8</b>	39.3	39.3
<b>9</b>	47.6	47.5
<b>10</b>	37.1	37.1
<b>11</b>	23.0	22.9
<b>12</b>	122.7	122.5
<b>13</b>	143.6	143.5
<b>14</b>	41.6	41.6
<b>15</b>	27.7	27.7
<b>16</b>	23.4	23.4
<b>17</b>	46.5	46.5
<b>18</b>	41.0	40.9
<b>19</b>	45.9	45.9
<b>20</b>	30.7	30.6
<b>21</b>	33.8	33.8
<b>22</b>	32.4	32.4
<b>23</b>	28.1	28.1
<b>24</b>	15.5	15.5
<b>25</b>	15.3	15.3
<b>26</b>	17.1	17.1
<b>27</b>	25.9	25.9
<b>28</b>	182.2	183.5
<b>29</b>	33.07	33.1
<b>30</b>	23.6	23.6

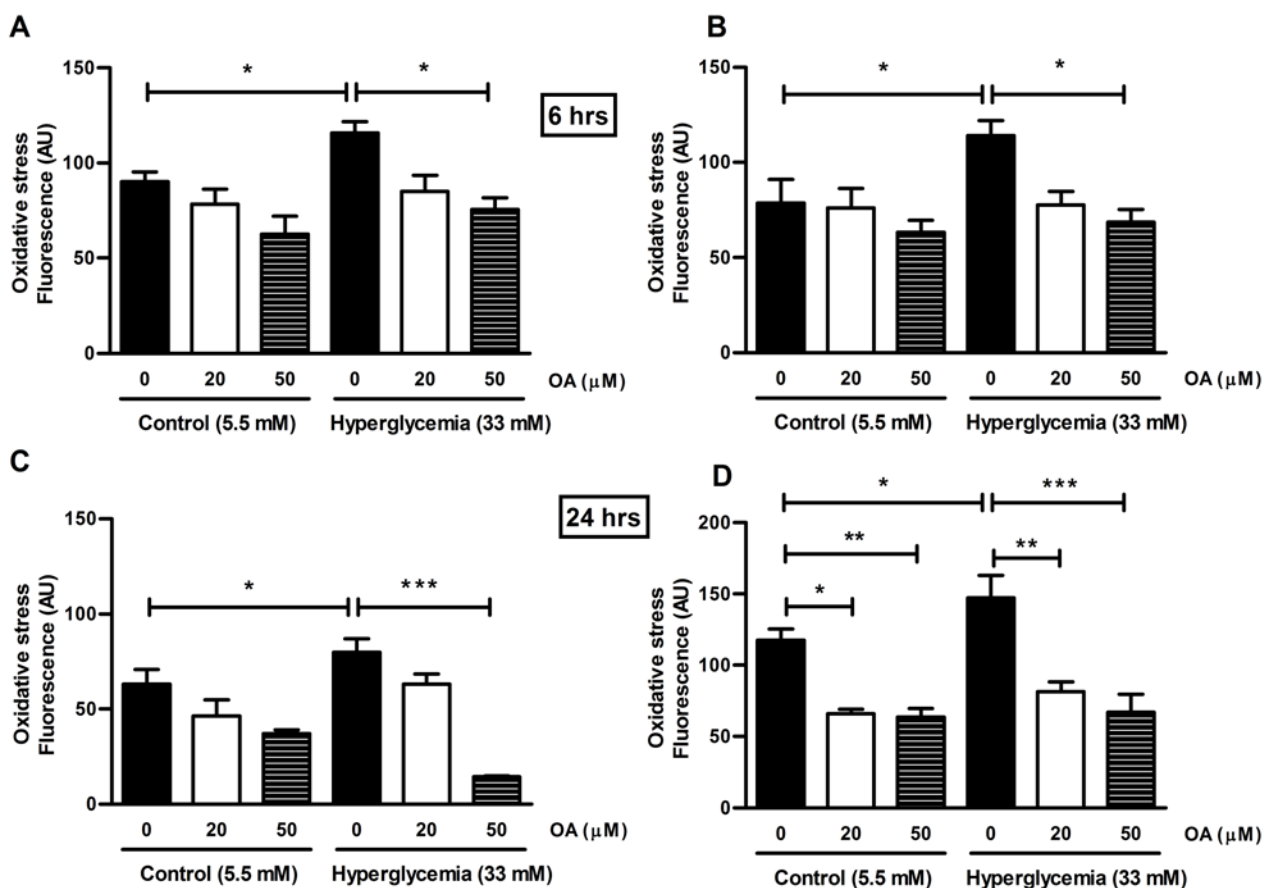


**Figure 3.3:** Structure (A) and numbering (B) of oleanolic acid (International Union of Pure and Applied Chemistry, IUPAC).



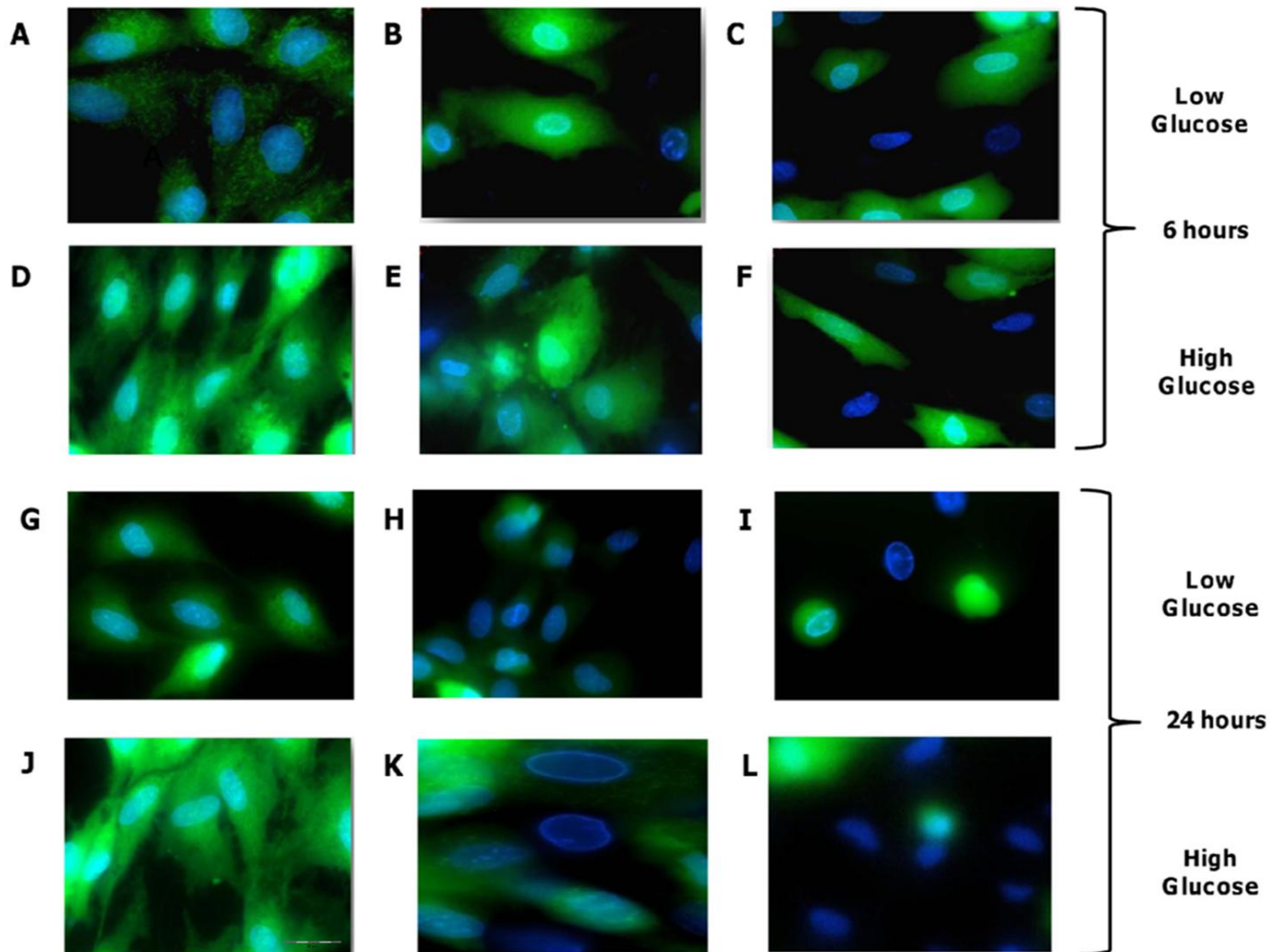
### 3.3.3 Effects of OA treatment on ROS levels and apoptosis in heart cells

We employed both fluorescence microscopy and flow cytometric analysis to evaluate whether OA acts as an anti-oxidant under *in vitro* simulated chronic hyperglycemic conditions. Our data show significantly increased ROS levels in heart cells that were cultured under high glucose conditions (Figure 3.4). However, OA treatment (acute and chronic) significantly decreased myocardial ROS levels under control and high glucose conditions. Here, even the lower OA concentration (20  $\mu$ M) blunted the increase in ROS levels under high glucose culturing conditions ( $p < 0.05$  vs. untreated high glucose cells) (Figure 3.4).



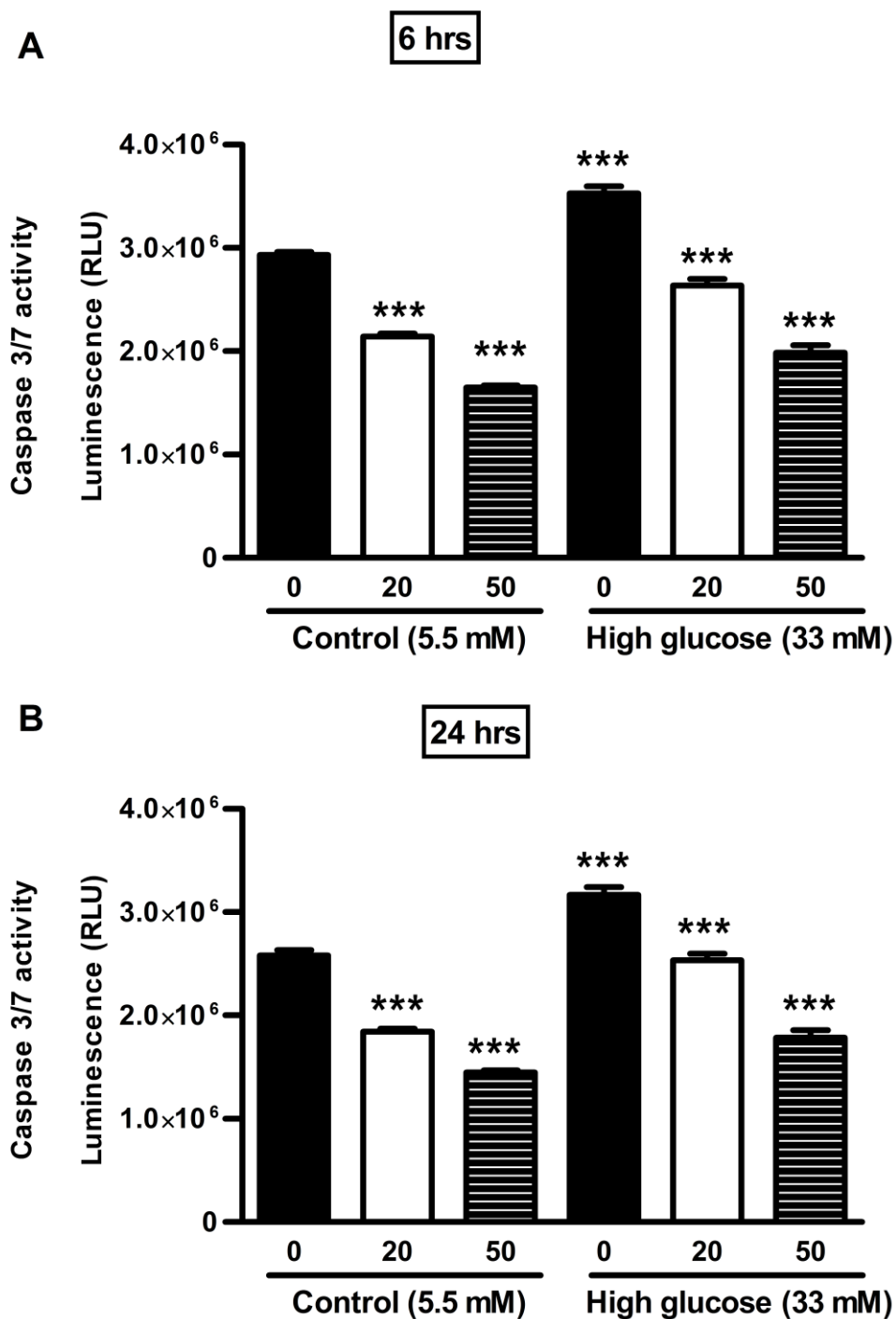
**Figure 3.4 OA treatment attenuates oxidative stress in H9c2 cells under both acute and chronic normoglycemic and hyperglycemic conditions.** Quantification of oxidative stress (DCFDA staining) in H9c2 cells in response to simulated chronic hyperglycemia (33 mM glucose) vs. control (5.5 mM glucose)  $\pm$  treatment with 20  $\mu$ M or 50  $\mu$ M OA for 6 and 24 hr, respectively. (A) and (C) Fluorescence microscopy; (B) and (D) Flow cytometry. Values are expressed as mean  $\pm$  SEM (n=9). \* $p < 0.05$ , \*\* $p < 0.01$ , \*\*\* $p < 0.001$  vs. respective controls.

The effect of OA on ROS levels is also shown by the representative images in Figure 3.5.



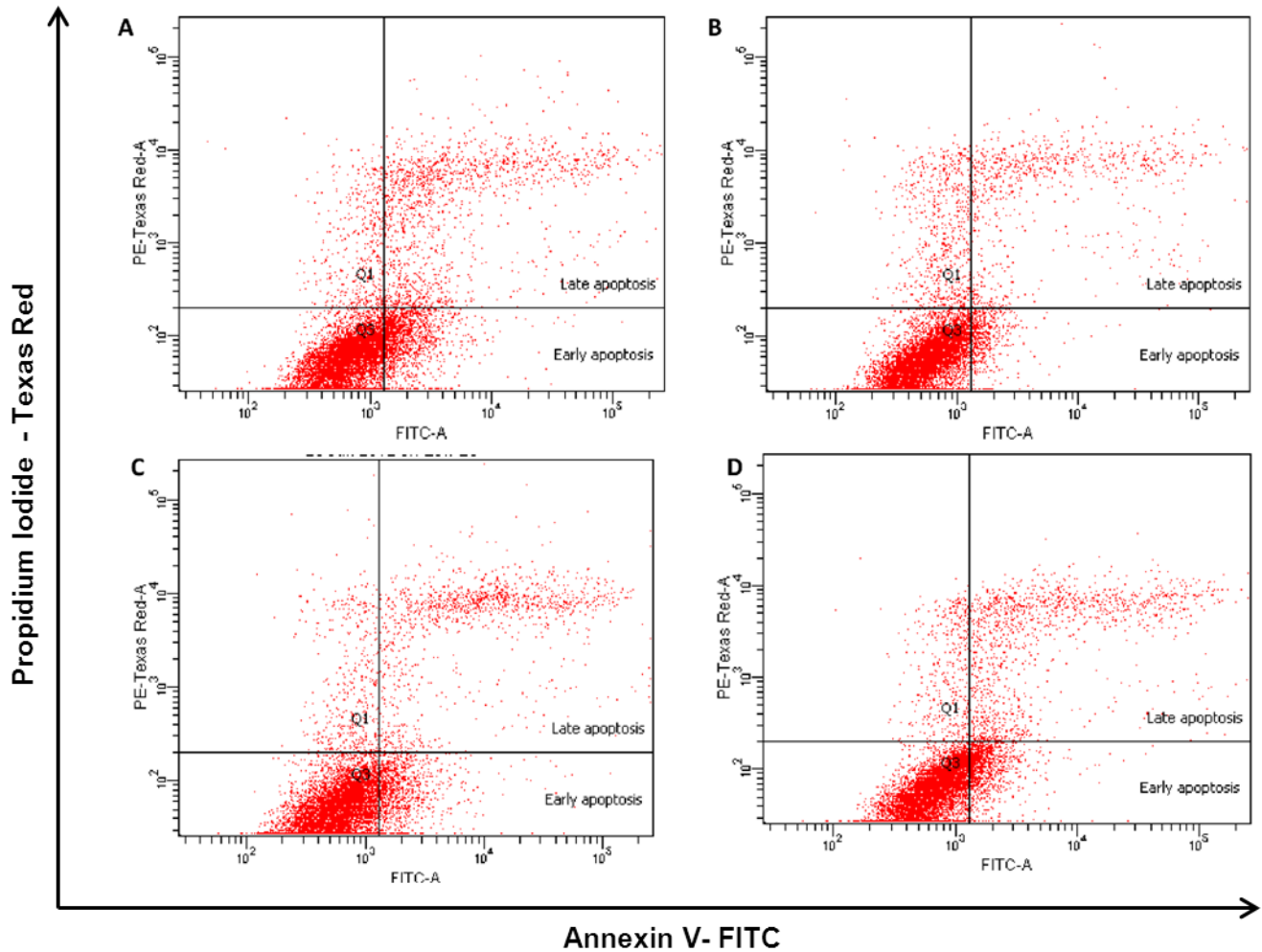
**Figure 3.5 Representative images on the effects of OA treatments on *in vitro* ROS levels.** (A), (B), (C) correspond to control,  $\pm$  20  $\mu$ M or 50  $\mu$ M after 6 hours of treatment, respectively; (D), (E) and (F) show 33 mM (simulated acute hyperglycemia) 20  $\mu$ M or 50  $\mu$ M after 6 hours of treatment respectively. (G), (H) and (I) show the same control groups after 24 hours whereas (J), (K) and (L) show the same corresponding high glucose groups after 24 hours. Scale bar represents 20  $\mu$ m (J), with the original magnification of 60x used for the image acquisition.

To examine whether OA exhibits anti-apoptotic effects, H9c2 cells were treated with 20  $\mu\text{M}$  and 50  $\mu\text{M}$  OA, respectively, for 24 hr and apoptosis determined by aminoluciferin luminescence with the caspase glow assay. Our data revealed increased caspase-3 activity in response to high glucose culturing conditions ( $p < 0.05$  vs. 5.5 mM glucose group) (Figure 3.6). The low glucose-treated cells also exhibited a concentration-dependent reduction in caspase-3 enzymatic activity, i.e. by  $28.4 \pm 2.2\%$  and by  $43.7 \pm 1.5\%$ , respectively, for the 20  $\mu\text{M}$  and 50  $\mu\text{M}$  OA concentrations ( $p < 0.001$  vs. 5.5 mM glucose group). Likewise, high glucose-treated cells displayed a decrease, i.e. by  $19.9 \pm 0.8\%$  and by  $43.4 \pm 3.4\%$ , respectively, for the 20  $\mu\text{M}$  and 50  $\mu\text{M}$  OA concentrations ( $p < 0.001$  vs. 33 mM glucose control) (Figure 3.6B). Our results at the 6 hr time point revealed similar findings (Figure 3.6A).



**Figure 3.6 Decreased apoptotic cell death in H9c2 cells treated with OA as indicated by decreased caspase 3/7 activity measured by aminoluciferin luminescence under both normal and hyperglycemic conditions.** Evaluation of caspase 3/7 activity using the caspase glow assay kit in H9c2 cells in response to simulated acute and chronic hyperglycemia vs. control ± treatment with 20 μM and 50 μM OA, respectively, for 6 and 24 hr. Values are expressed as mean ± SEM (n=9). \*\*\*p<0.001 vs. respective controls.

In support, flow cytometric analysis (Annexin V/FITC PI) showed decreased apoptosis in H9c2 cells exposed to high glucose and treated with 100  $\mu$ M OA for 6 hr ( $p < 0.01$ ) (Figure 3.7). After 24 hr the decrease was observed under both low ( $p < 0.001$  vs. control) and high glucose ( $p < 0.001$  vs. control;  $p < 0.001$  vs. high glucose without OA treatment) culturing conditions (Figure 3.7).



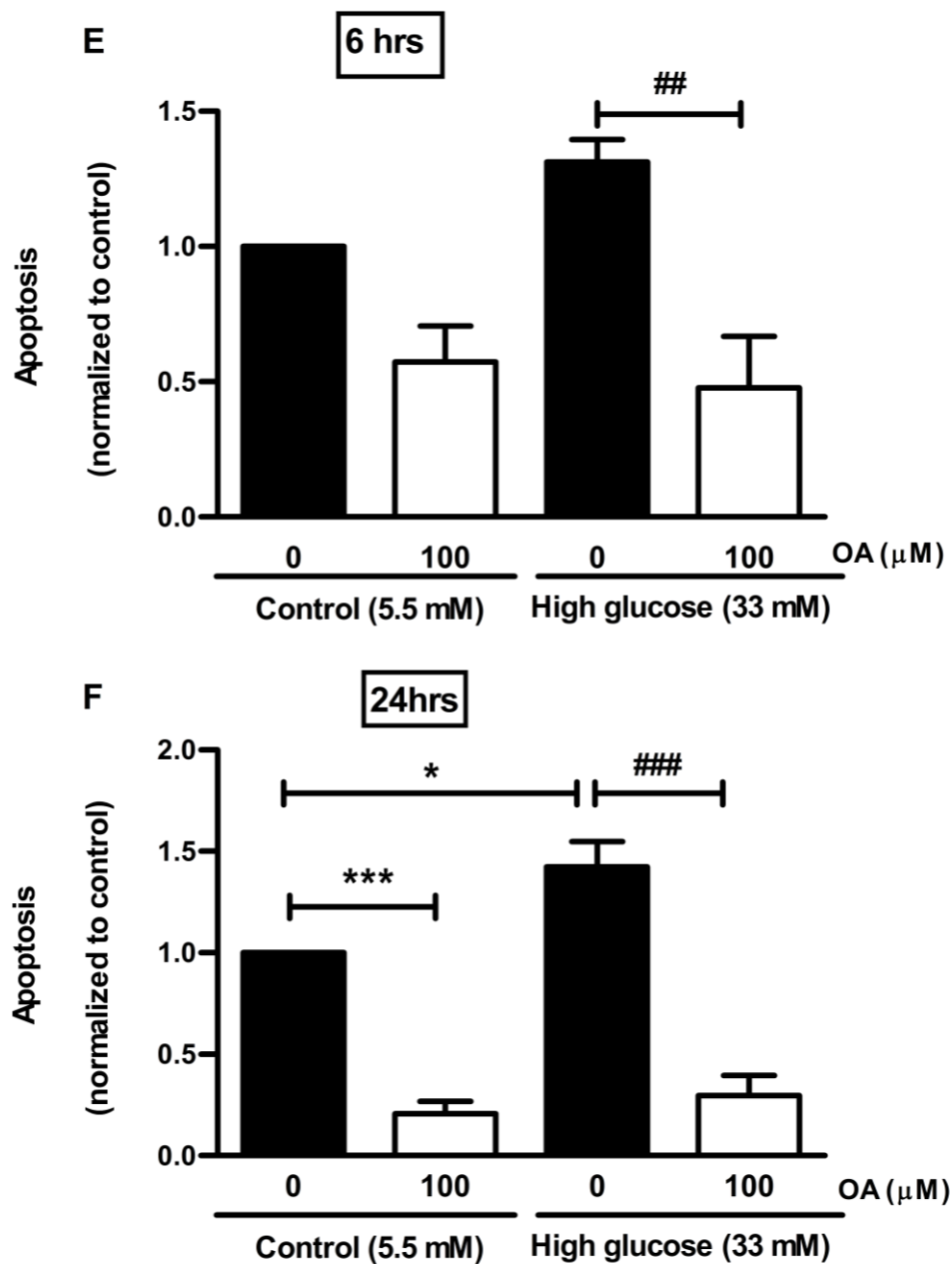


**Figure 3.7 Diminished apoptosis in OA-treated H9c2 cells (flow cytometry) in acute hyperglycemic conditions and both chronic normoglycemic and hyperglycemic conditions.** Flow cytometric analysis using the Annexin V/FITC apoptosis assay kit to evaluate the effects of 100  $\mu$ M OA treatment under control and high glucose culturing conditions (24 hr). (A), (B), (C) and (D) Representative FACS analyses of four individual experiments corresponding to control and high glucose  $\pm$  OA treatment, respectively. (E) and (F) Quantification of OA treatment after 6 and 24 hr, respectively. Values are normalized to the control and expressed as mean  $\pm$  SEM (n=4). \*\*\*p<0.001 vs. controls and, ##, ### p<0.01, p<0.001 vs. high glucose exposure without OA treatment.

### 3.3.4 Evaluation of *ex vivo* heart function during global ischemia and reperfusion (simulated acute hyperglycemia)

The functional data for both low and high glucose perfusions (without ischemia) showed no significant differences with OA treatment on LVDP and RPP (Figure 3.8).

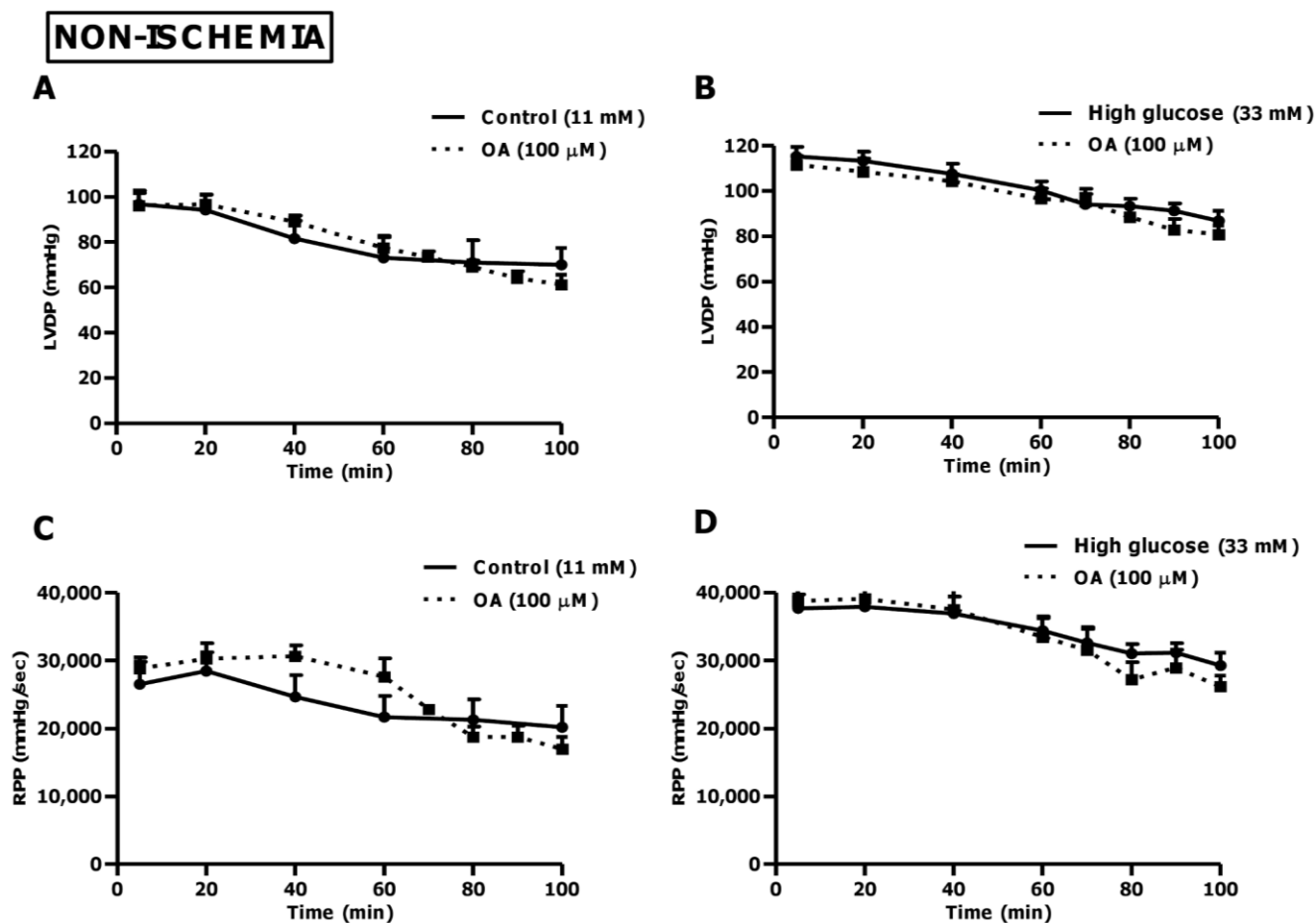


**Figure 3.8 OA treatment does not affect pre-ischemic cardiac function as there was no change in LVDP and RPP between control and OA treated groups.** Isolated rat hearts were perfused under simulated hyperglycemic conditions (33 mM glucose) vs. controls (11 mM glucose)  $\pm$  100  $\mu$ M OA treatment. We initially perfused for 60 min, whereafter OA was added for a further 20 min. Subsequently, the buffer initially used was returned and hearts perfused for an additional 20 min. (A) Left ventricular developed pressure at baseline (11 mM) and (B) high glucose conditions (33 mM). Rate pressure product (RPP) at baseline (C) and (D) high glucose levels. Values are expressed as mean  $\pm$  SEM (n=9).

However, perfusion data with global ischemia and reperfusion show that LVDP recovery for hearts perfused with high glucose was markedly lower compared to the control group ( $p < 0.01$  vs. 11 mM control), ranging between  $12.7 \pm 3.2\%$  and  $23.1 \pm 0.9\%$  of the baseline pre-ischemic values during reperfusion (Figure 3.9). By contrast, the control group's functional recovery during reperfusion ranged from ~28 to 50% of the baseline pre-ischemic value. Our perfusion data revealed that OA treatment markedly improved functional recovery of high glucose perfused hearts during reperfusion ( $p < 0.001$  vs. untreated high glucose), i.e. to  $62 \pm 8\%$  of the baseline pre-ischemic value (Figure 3.9B). In agreement, OA treatment enhanced RPP and  $dP/dt_{max}$  for the high glucose perfused group while it resulted in no significant effects on baseline treated hearts (Figures 3.9 and 3.10).



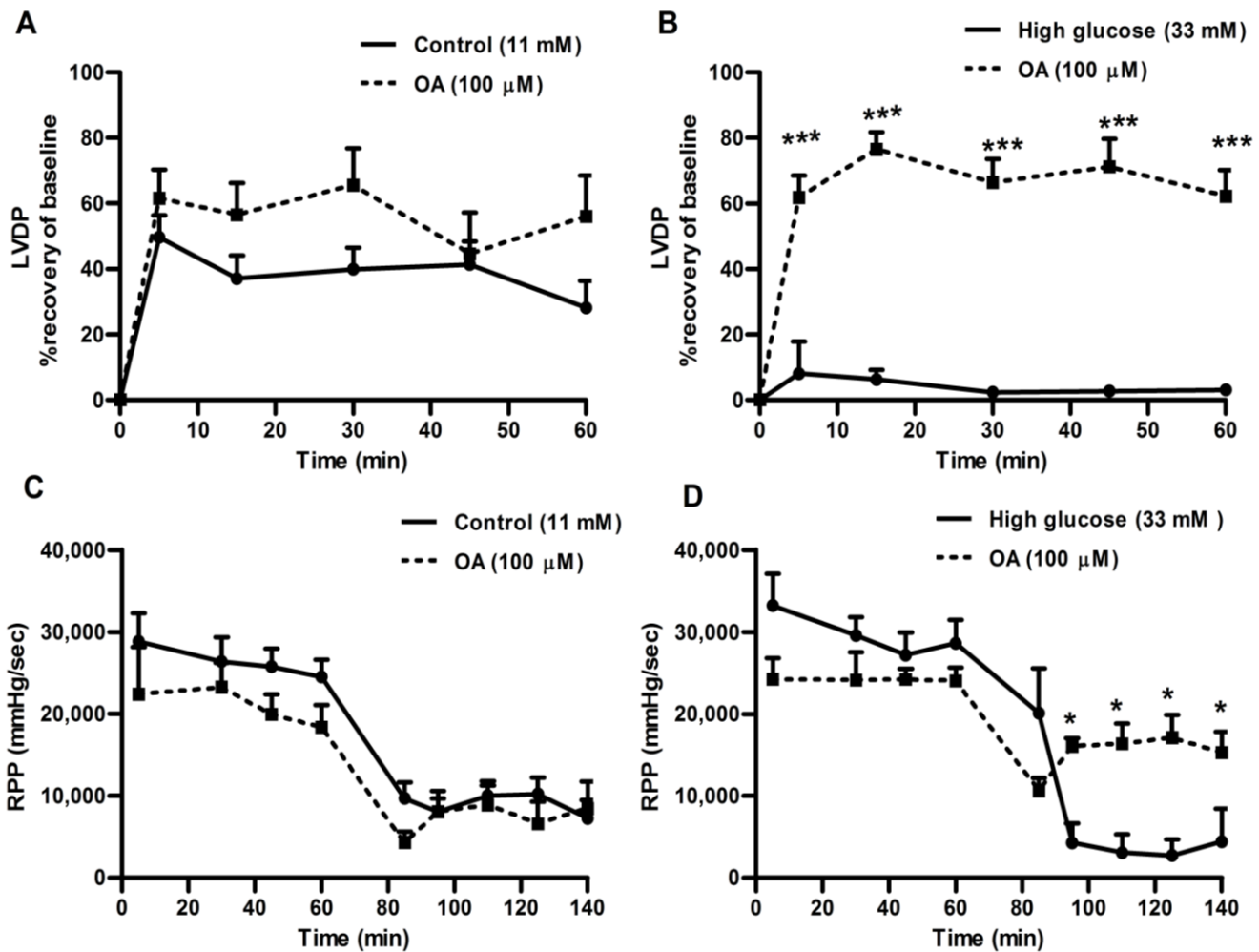


**Figure 3.9 OA treatment during reperfusion blunts high glucose-induced cardiac dysfunction following ischemia and reperfusion as shown by significant post-ischemic recovery of LVDP and RPP under hyperglycemic perfusion conditions.** Isolated rat hearts were perfused under simulated hyperglycemic conditions (33 mM glucose) vs. controls (11 mM glucose) and subjected to 20 min of global ischemia, followed by 60 min of reperfusion. For OA treatments groups, 100  $\mu$ M OA was added during the first 20 min of reperfusion. (A) Left ventricular developed pressure (% recovery) at baseline glucose levels (11 mM), and (B) with high glucose (33 mM). Rate pressure product (RPP) at baseline glucose levels (C), and (D) under high glucose conditions. Values are expressed as mean  $\pm$  SEM (n=9). \*p<0.05, \*\*\*p<0.001 vs. respective controls.

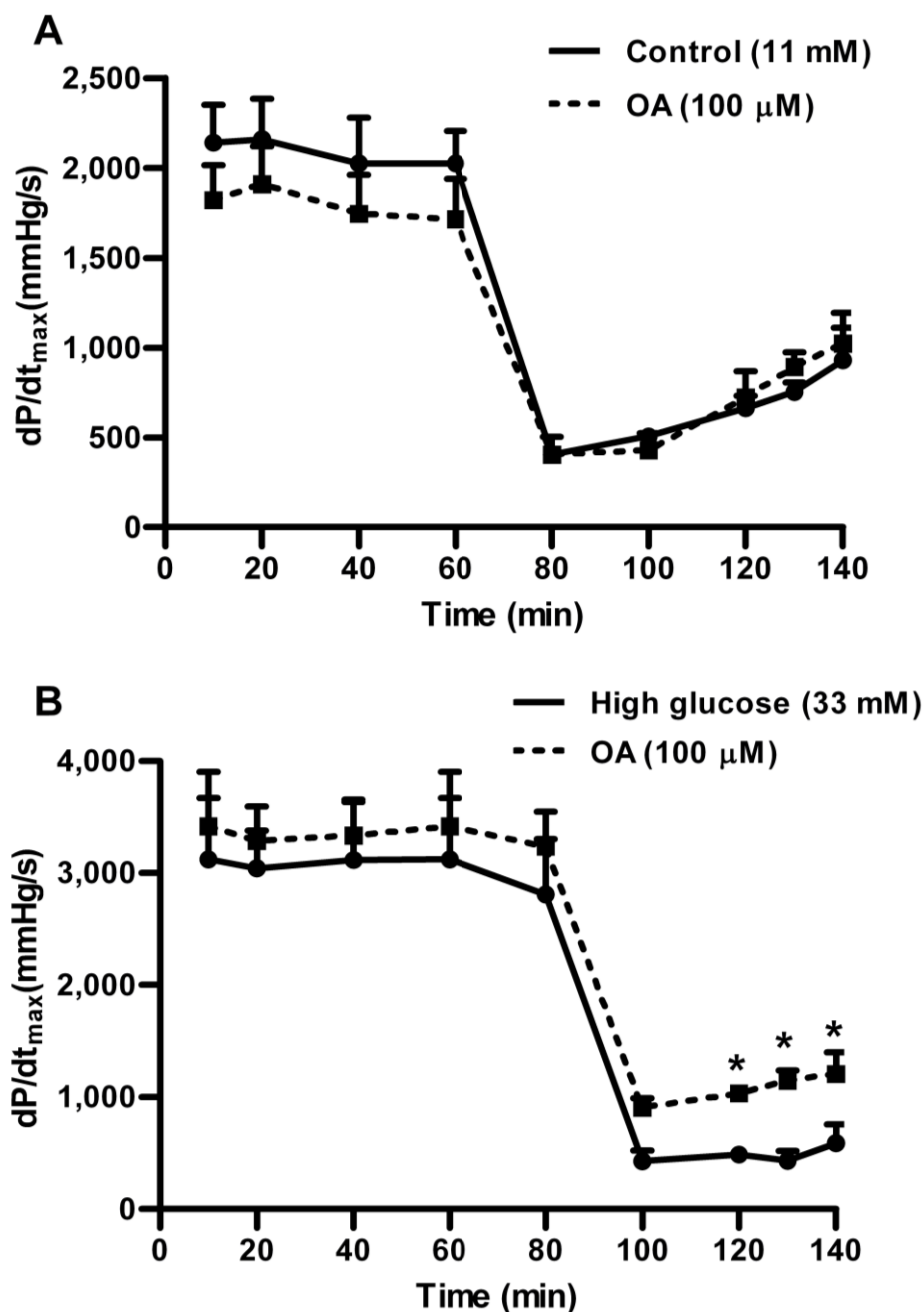


**Figure 3.10 OA treatment blunts high glucose-induced cardiac dysfunction (improved velocity of contraction) following ischemia and reperfusion.** Isolated rat hearts were perfused under simulated hyperglycemic conditions (33 mM glucose) vs. controls (11 mM glucose) and subjected to 20 min of global ischemia, followed by 60 min of reperfusion. For OA treatments groups, 100  $\mu$ M OA was added during the first 20 min of reperfusion. (A) Velocity of contraction (dP/dt<sub>max</sub>) at baseline glucose levels (11 mM), and (B) with high glucose (33 mM). Values are expressed as mean  $\pm$  SEM (n=9). \*p<0.05 vs. respective controls.

Furthermore, OA treatment increased coronary flow vs. untreated group ( $p < 0.01$ ) under high glucose perfusion conditions. This was associated with a decrease in end diastolic pressure in hearts exposed to high glucose conditions, though both coronary flow and end diastolic pressure were not affected by OA treatment (Table 3.2).

**Table 3.2.** Effects of OA on *ex vivo* coronary flow and end-diastolic pressure during the first ten min of stabilization and at the end of reperfusion.

	Coronary Flow (ml/min)		EDP (mmHg)	
	Pre Ischemia	Post Ischemia	Pre Ischemia	Post Ischemia
<b>Control (11 mM)</b>	9 ± 1	7 ± 2	12 ± 0	30 ± 6
<b>+ 100 µM OA</b>	10 ± 1	9 ± 2	8 ± 3	29 ± 7
<b>High Glucose (33 mM)</b>	11 ± 3	4 ± 1	9 ± 3	79 ± 7*
<b>+ 100 µM OA</b>	10 ± 1	13 ± 1**	14 ± 4	22 ± 8**

Values are expressed as mean ± SEM. \* $p < 0.05$ ; \*\* $p < 0.01$  vs. respective control. (n=6 in each group)

Moreover, the regional ischemia and reperfusion experiments (Figure 3.11A) show that OA treatment of high glucose perfused hearts decreased the infarct size from  $59.6 \pm 3.1\%$  vs.  $38.7 \pm 1.6\%$  ( $p < 0.01$  vs. high glucose untreated) with no changes on the area at risk amongst the groups (Figure 3.11B). We also performed additional experiments with 11 mM and 33 mM mannitol, and found no significant effects on functional recovery of hearts following global ischemia and reperfusion, thus ruling out any osmotic effects (data shown in Chapter 4).

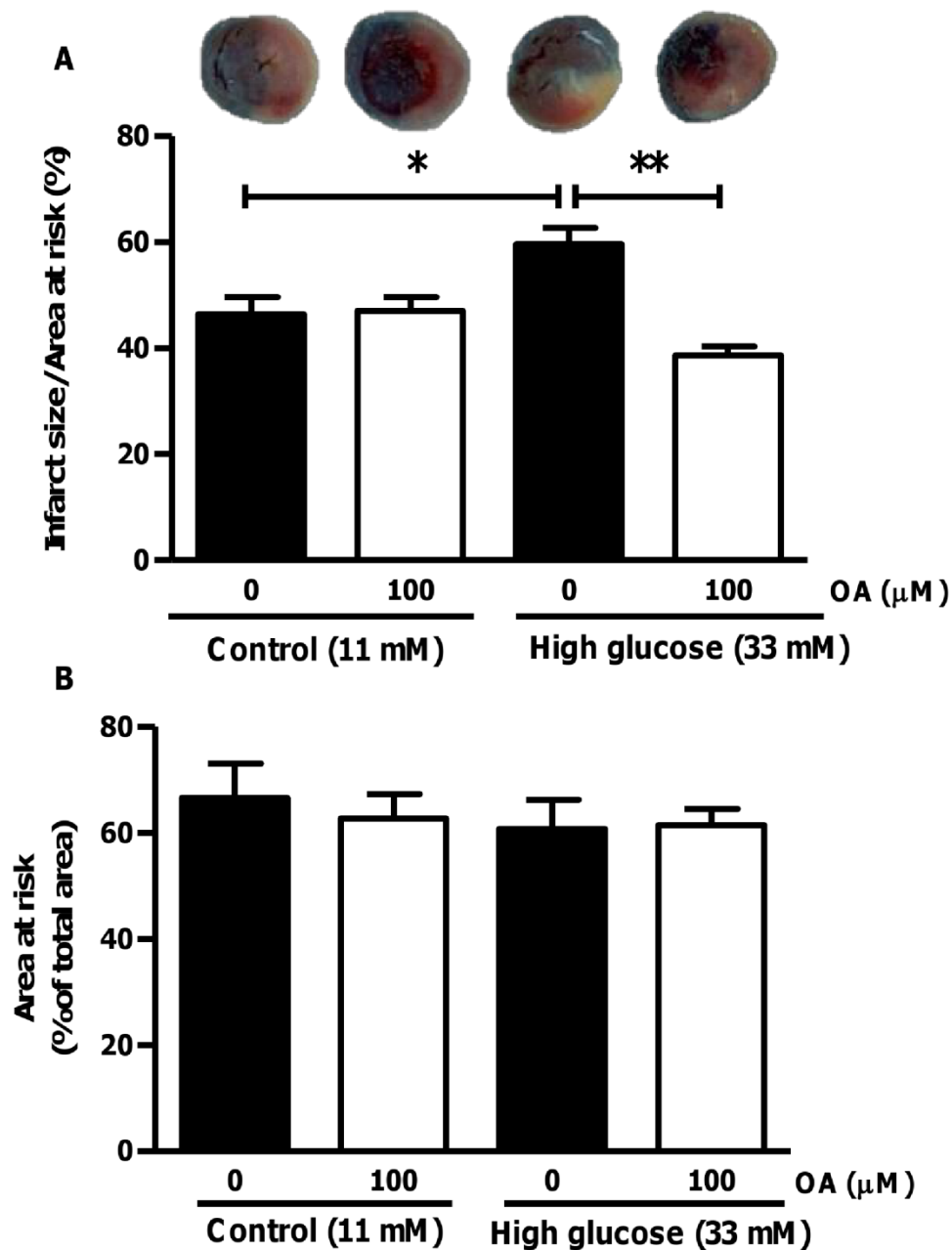


**Figure 3.11 OA administration showed cardio-protective effects as it decreases infarct size under high glucose perfusion conditions following regional ischemia and reperfusion.** Isolated rat hearts were perfused under high glucose conditions vs. controls and subjected to regional ischemia. For OA treated groups, 100  $\mu\text{M}$  OA was added during the first 20 min of the two hr reperfusion period. (A) infarct size/area at risk (%) and (B) area at risk under baseline (simulated normoglycemia) vs. high glucose perfusion conditions (simulated acute hyperglycemia). Evans blue dye and TTC staining enabled visualization of viable tissue (blue), infarcted area (white) and the area at risk (red). Values are expressed as mean  $\pm$  SEM (n=6). \* $p < 0.05$ , \*\*\* $p < 0.001$  vs. respective controls.

### 3.3.5 *In vivo* coronary artery ligations in streptozotocin-treated rats (chronic hyperglycemia)

We next evaluated the cardio-protective effects of OA treatment within the *in vivo* context, i.e. by employing coronary artery ligations in STZ-treated hyperglycemic rats. Our data revealed markedly elevated blood glucose levels in STZ-diabetic rats compared to matched controls ( $p < 0.001$ ) (Table 3.3). This was associated with decreased weight gain in the STZ-diabetic rats.

**Table 3.3** Body weight and blood glucose levels after 1 week of STZ injection.

	% Body weight change	Non-fasting blood glucose (mmol/L)
<b>Non-diabetic</b>	8.1 ± 0.8	6.6 ± 0.5
<b>STZ-diabetic</b>	-4.3 ± 1.2	27.1 ± 1.6***

Data are expressed as mean ± SEM,  $n \geq 4$  in each group. \*\*\* $p < 0.001$  vs. non-diabetic control group.

In agreement with our *ex vivo* perfusion data, we found that infarct size was significantly increased for the STZ-treated rats versus controls ( $47.5 \pm 2.9\%$  vs.  $27.9 \pm 5.2\%$ ) following 30 min coronary artery ligation (Figure 3.12A), and similarly there were no changes in the area at risk amongst the groups (Figure 3.12B).

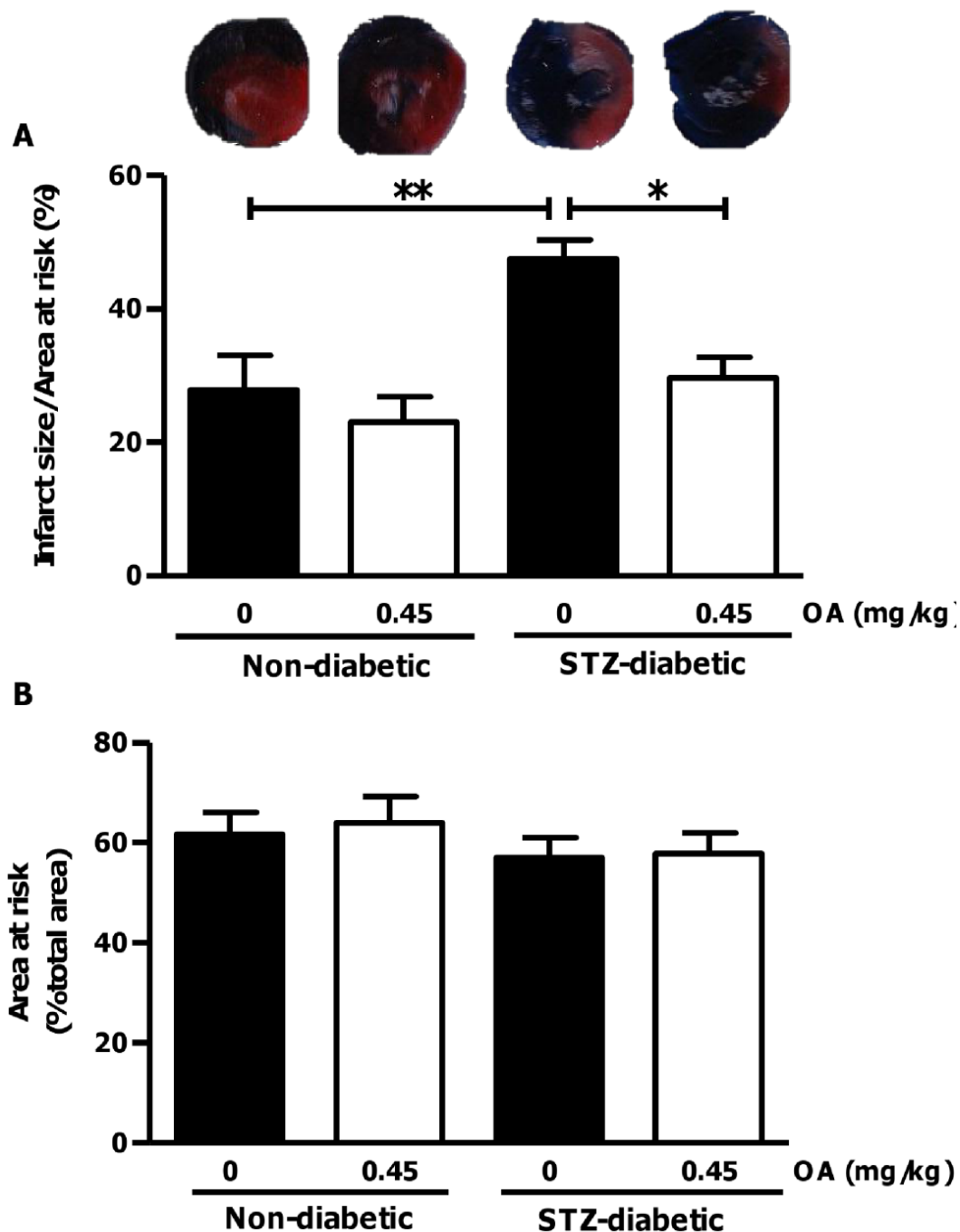


**Figure 3.12** OA treatment decreases infarct size following coronary artery ligation in streptozotocin-diabetic rats. Wistar rats were injected with STZ and followed for a 1-week period. Subsequently, 0.45 mg/kg OA was injected via the penile vein within the first two min of reperfusion. (A) infarct size/area at risk (%) and (B) area at risk under baseline vs. high glucose conditions. Evans blue dye and TTC staining enabled visualization of viable tissue (blue), infarcted area (white) and the area at risk (red). Values are expressed as mean  $\pm$  SEM (n=6). \*p<0.05, \*\*p<0.01 vs. respective controls.

OA administration also decreased systolic and diastolic blood pressures in STZ-diabetic rats vs. untreated STZ-diabetic controls during the early reperfusion period i.e. within the first twenty minutes of reperfusion after the one week of STZ-induction (Table 3.4). There were no significant differences on heart rate and systolic/diastolic blood pressures before the regional ischemia amongst all the groups (Table 3.4).

**Table 3.4** Effects of OA on *in vivo* heart rate, ST height, systolic and diastolic blood pressures during early reperfusion.

	Heart rate (beats/minute)		Systolic BP (mmHg)		Diastolic BP (mmHg)	
	PI	Reperfusion	PI	Reperfusion	PI	Reperfusion
ND	404.7 ± 6.01	411.7 ± 8.5	130.9 ± 8.3	125.3 ± 9.2	81.5 ± 14.1	107.6 ± 7.4
ND + OA	411.6 ± 12.4	399.7 ± 15.1	113.6 ± 13.9	88.6 ± 9.5*	87.5 ± 2.5	62.9 ± 9.1*
STZ	394.3 ± 35.0	429.6 ± 20.4	127.4 ± 8.9	118.4 ± 8.9	63.3 ± 4.7	100.8 ± 3.6
STZ + OA	386.3 ± 14.7	391.0 ± 17.8	117.4 ± 5.8	99.0 ± 5.0*	53.7 ± 4.5	65.0 ± 8.0*

ND (non-diabetic); STZ (STZ-diabetic); BP (blood pressure), PI (pre-ischemia). Data are expressed as mean ±SEM, n ≥ 4 in each group) \*p<0.05 vs. respective control.

### 3.3.6 Effects of long-term OA treatment on heart function in streptozotocin-treated rats (chronic hyperglycemia)

To assess the effects of long-term OA treatment on heart function, rats were injected with STZ and followed for 2 weeks  $\pm$  OA treatment (daily). STZ treatment markedly increased fasting blood glucose ( $16.3 \pm 0.8$  mmol/L) versus matched controls ( $5.4 \pm 0.3$  mmol/L) ( $p < 0.01$ ). Our data show that the force generated by STZ-diabetic rat hearts was significantly lower compared to non-diabetic controls ( $p < 0.01$ ) (Figure 3.13). However, chronic OA treatment for two weeks significantly improved cardiac function in STZ-diabetic rats.

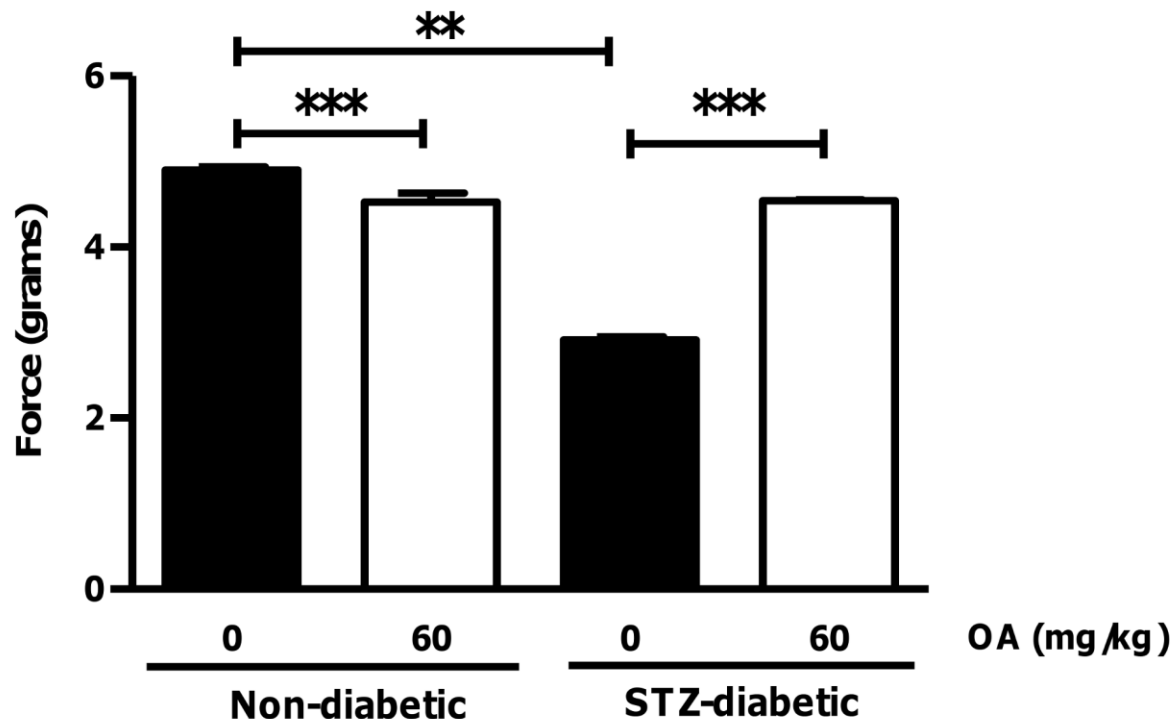


**Figure 3.13 Long-term oral OA treatment improves cardiac function in *ex vivo* STZ-diabetic rats.** Sprague-Dawley rats were injected with STZ and followed for a 2-week period  $\pm$  daily OA treatment. Subsequently, isolated hearts from STZ-diabetic and matched controls were perfused and action potentials recorded via a force transducer. Values are expressed as mean  $\pm$  SEM ( $n=6$ ) \*\* $p < 0.05$  vs. non-diabetic control, and \*\*\* $p < 0.01$  vs. respective controls.



### 3.3.7 Effects of OA treatment on *ex vivo* myocardial ROS levels and apoptosis

To confirm our *in vitro* data, we next evaluated whether OA exhibits anti-oxidant and anti-apoptotic properties within an *ex vivo* context. Under pre-ischemic conditions OA treatment did not significantly affect myocardial SOD activity or apoptosis (Figure 3.14). However, OA administration blunted high glucose-induced myocardial superoxide levels and concomitantly up-regulated SOD activity (Figure 3.15A and 3.15B) following ischemia and reperfusion. To gain further insight into temporal effects, we also performed analyses immediately after ischemia and for several time points thereafter. These data show that OA exerts its main anti-oxidant effects within the first 20 min following ischemia, whereafter it is sustained (Figure 3.15C).

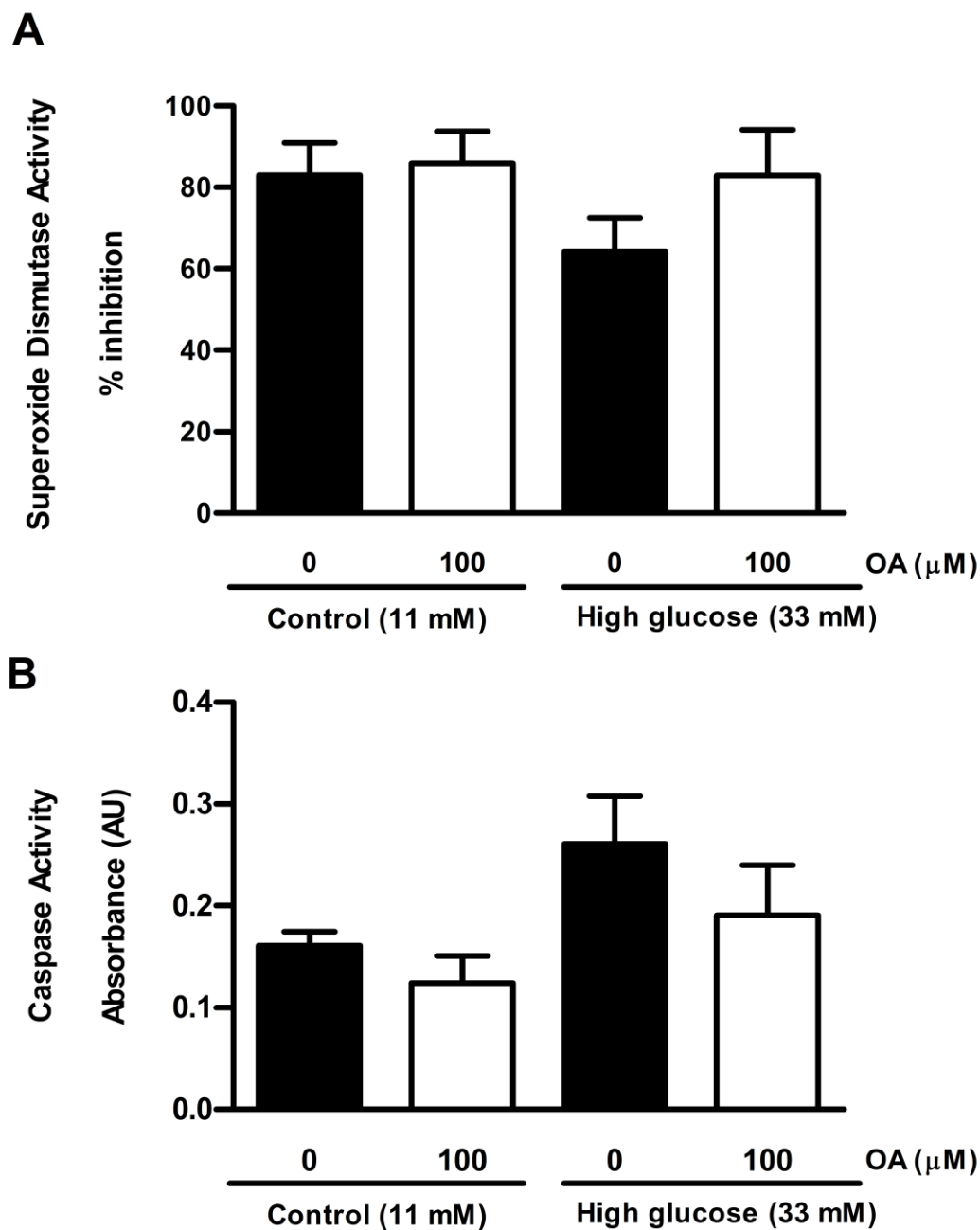


**Figure 3.14 OA treatment does not affect superoxide dismutase and caspase activities without ischemia.** Isolated rat hearts were perfused under simulated hyperglycemic conditions (33 mM glucose) vs. controls (11 mM glucose)  $\pm$  100  $\mu$ M OA treatment. We initially perfused for 60 min, whereafter OA was added for a further 20 min. Subsequently, the buffer initially used was returned and hearts perfused for an additional 20 min. (A) Superoxide dismutase activity (% inhibition) in response to high glucose vs. control  $\pm$  OA treatment; (B) Caspase activity. Values are expressed as mean  $\pm$  SEM (n=6).

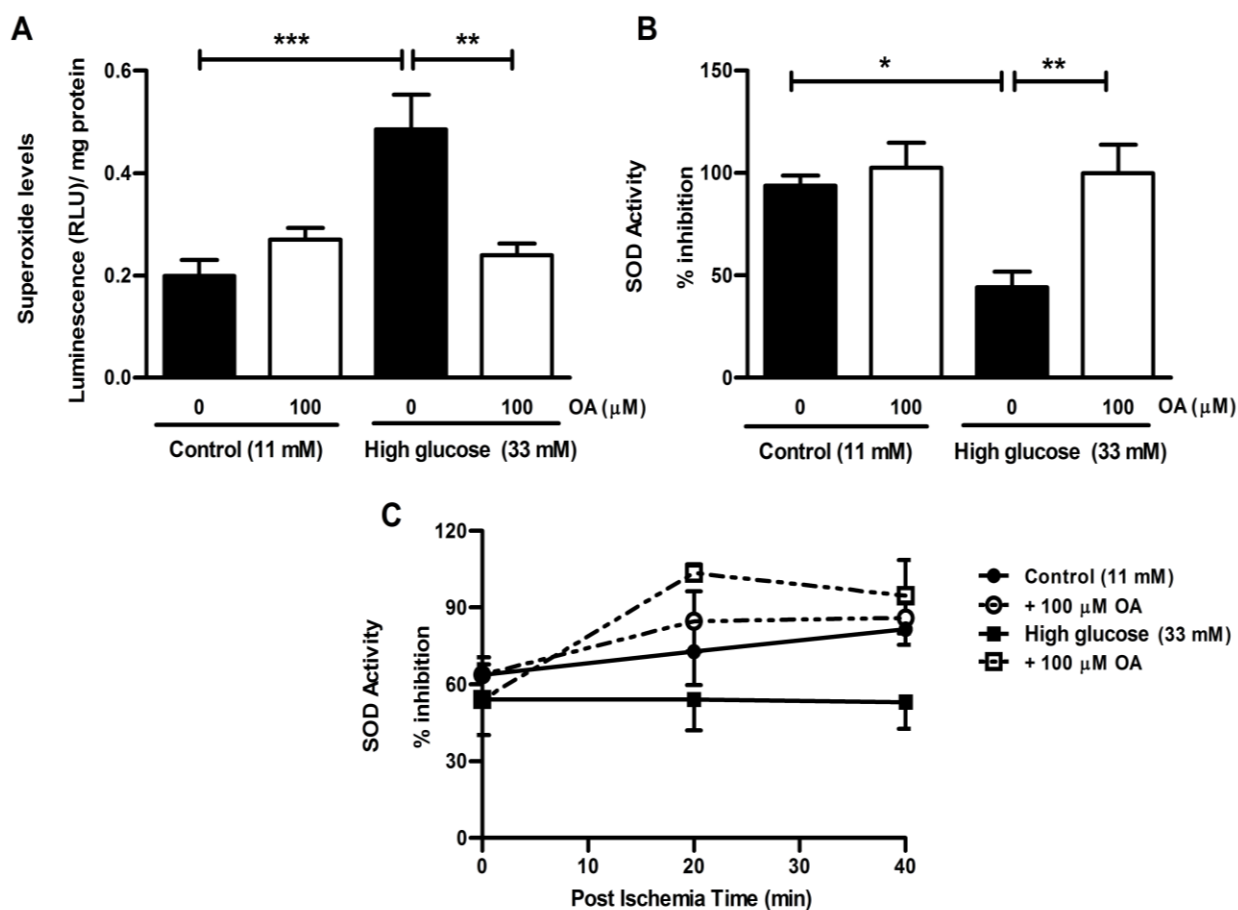


**Figure 3.15 Anti-oxidant effects of OA in hearts subjected to ischemia and reperfusion under high glucose perfusion conditions.** Isolated rat hearts were perfused under high glucose conditions vs. controls and subjected to ischemia and reperfusion. For OA treatments groups, 100  $\mu$ M OA was added during the first 20 min of reperfusion. (A) Superoxide levels under high glucose conditions vs. control  $\pm$  OA treatment; (B) Superoxide dismutase activity (% inhibition) in response to high glucose vs. control  $\pm$  OA treatment; (C) Time course for SOD activity following ischemic insult. Values are expressed as mean  $\pm$  SEM (n=9). \*p<0.05, \*\*p<0.01, \*\*\*p<0.001 vs. respective controls.

We largely confirmed these data by evaluating the degree of protein carbonylation as an additional marker of oxidative stress (Figure 3.16). However, the OA-induced decrease in protein carbonylation under high glucose conditions did not reach statistical significance ( $p=0.076$  vs. untreated high glucose) (Figure 3.16C).

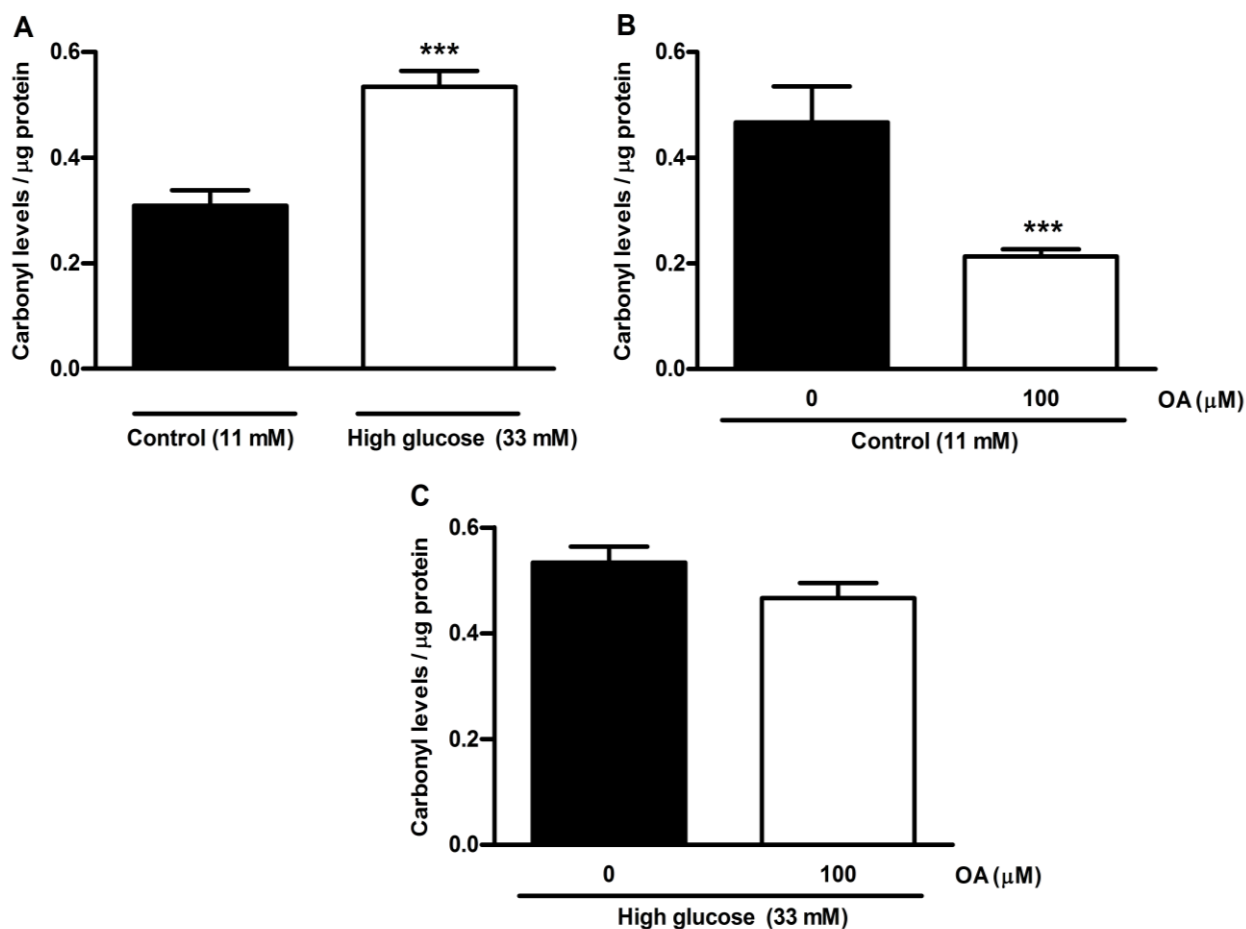


**Figure 3.16 OA treatment decreases carbonylation levels in hearts subjected to ischemia and reperfusion under high glucose conditions.** Isolated rat hearts were perfused under high glucose conditions vs. controls and subjected to ischemia and reperfusion. For OA treatment groups, 100 µM OA was added during the first 20 min of reperfusion. (A) Degree of carbonylation under high glucose conditions vs. control; (B) OA treatment at baseline (11 mM glucose) and (C) under high glucose conditions (33 mM). Values are expressed as mean  $\pm$  SEM ( $n=9$ ). \*\*\* $p<0.001$  vs. respective controls.

We next assessed anti-apoptotic effects of OA in *ex vivo* perfused heart tissues. Myocardial caspase activity levels were increased under high glucose perfusion conditions ( $p < 0.001$  vs. untreated control). This effect was attenuated by OA treatment ( $p < 0.01$  vs. untreated high glucose) (Figure 3.17A). In agreement, OA treatment significantly decreased cardiac caspase-3, and increased p-BAD/BAD peptide levels under high glucose perfusion conditions (Figure 3.17B and 3.17C). We also investigated the temporal nature of myocardial apoptosis following ischemia. Our data show that anti-apoptotic effects emerge at the 40 min time point, suggesting that these effects occur as a result of the earlier upstream reduction of oxidative stress (Figure 3.17D).

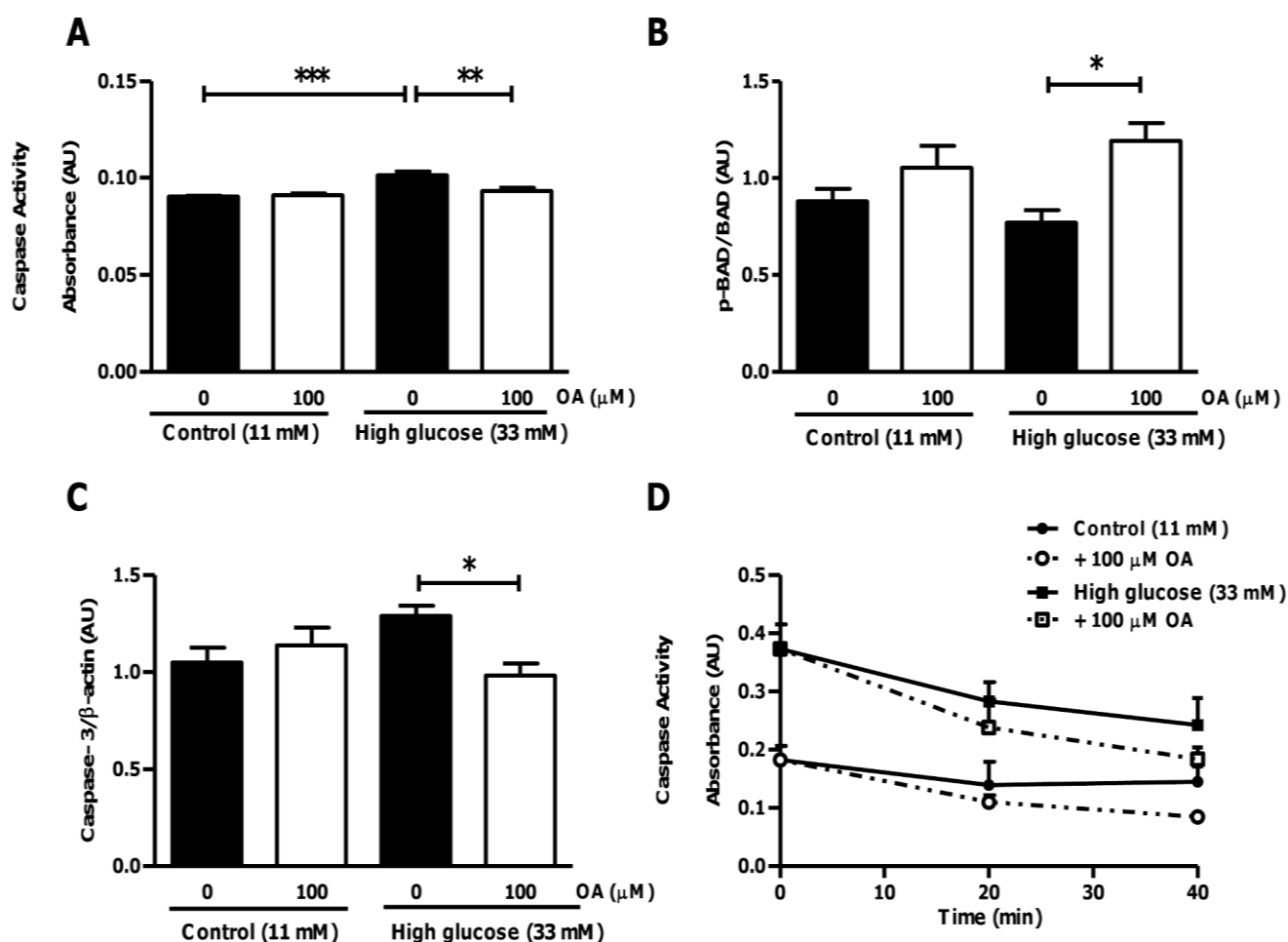


**Figure 3.17 Anti-apoptotic effects of OA in hearts subjected to ischemia and reperfusion under high glucose conditions.** Isolated rat hearts were perfused under high glucose conditions vs. controls and subjected to ischemia and reperfusion. For OA treatments groups, 100  $\mu\text{M}$  OA was added during the first 20 min of reperfusion. (A) Caspase activity; (B) Caspase-3 peptide levels; (C) p-BAD/BAD peptide levels; (D) Time course of myocardial apoptosis following the ischemic insult. Values are expressed as mean  $\pm$  SEM ( $n=9$ ). \* $p < 0.05$ , \*\* $p < 0.01$ , \*\*\* $p < 0.001$  vs. respective controls.

To evaluate whether OA mediates its anti-apoptotic effects via HBP modulation, we next determined the overall degree of O-GlcNAcylation in our experimental system. Our data show increased O-GlcNAcylation in response to high glucose exposure ( $p < 0.05$  vs. untreated high glucose) that was significantly decreased by OA treatment (Figure 3.18).

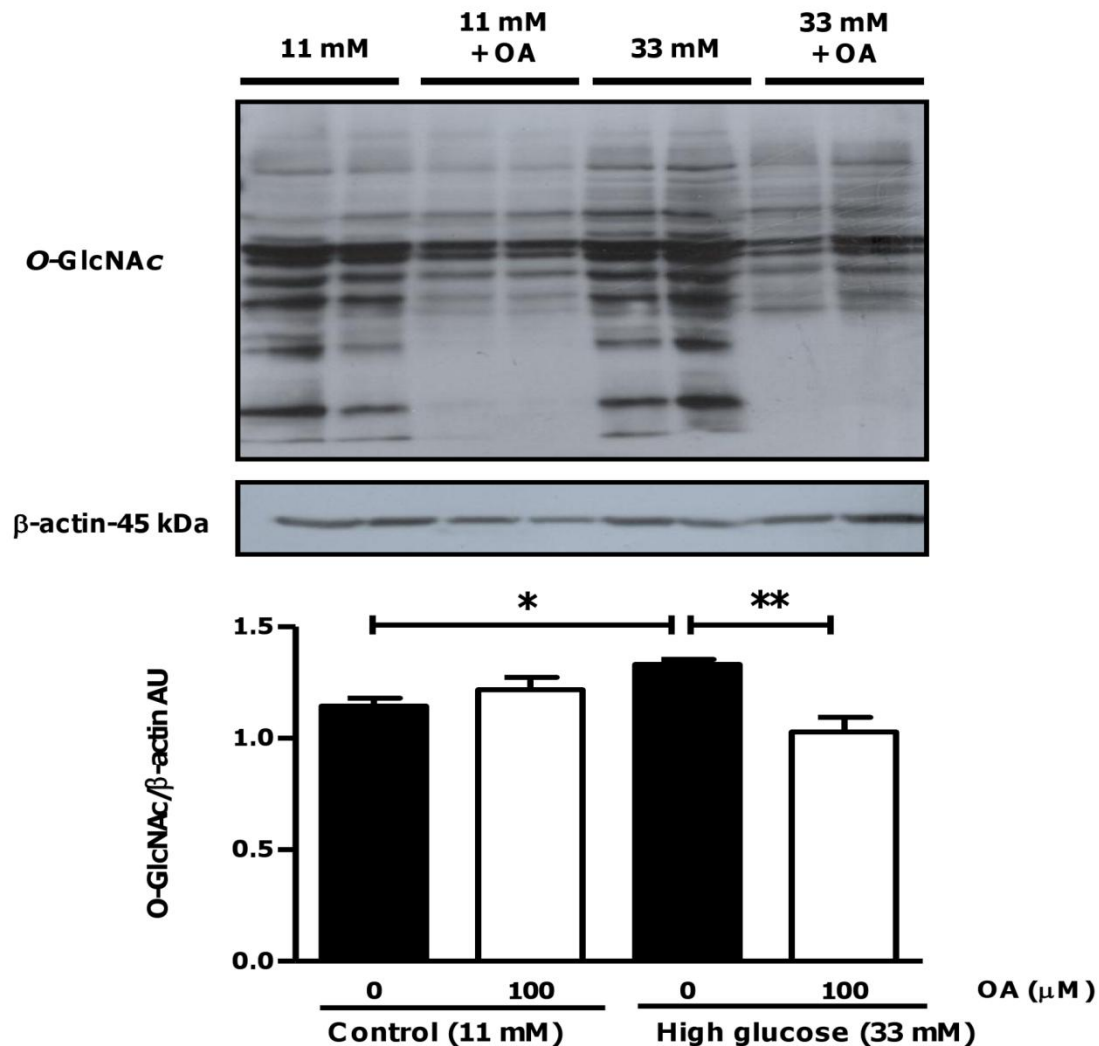


**Figure 3.18 OA treatment attenuates O-GlcNAcylation in hearts subjected to ischemia and reperfusion under high glucose conditions.** Isolated rat hearts were perfused under high glucose conditions vs. controls and subjected to ischemia and reperfusion  $\pm$  OA treatment during reperfusion. Western blot analysis for overall O-GlcNAcylation is shown with  $\beta$ -actin as loading control. Densitometric analysis for O-GlcNAcylation is displayed below gel image (normalized to corresponding  $\beta$ -actin values). Values are expressed as mean  $\pm$  SEM (n=6). \* $p < 0.05$ , \*\* $p < 0.01$  vs. respective controls.

### 3.3.8 Evaluating the effects of OA treatment on myocardial proteasomal activity in hearts subjected to ischemia and reperfusion under high glucose conditions

We initially evaluated pre- and post-ischemic proteasomal activities under high glucose perfusion conditions. Here we found that trypsin-like activity was significantly decreased under baseline glucose concentrations (Figure 3.19A). However, there were no changes on the chymotrypsin- and trypsin-like activities (Figures 3.19B and 3.19C). In contrast hyperglycemia induced a marked increase in all proteasomal activities following ischemia and reperfusion (Figure 3.20).

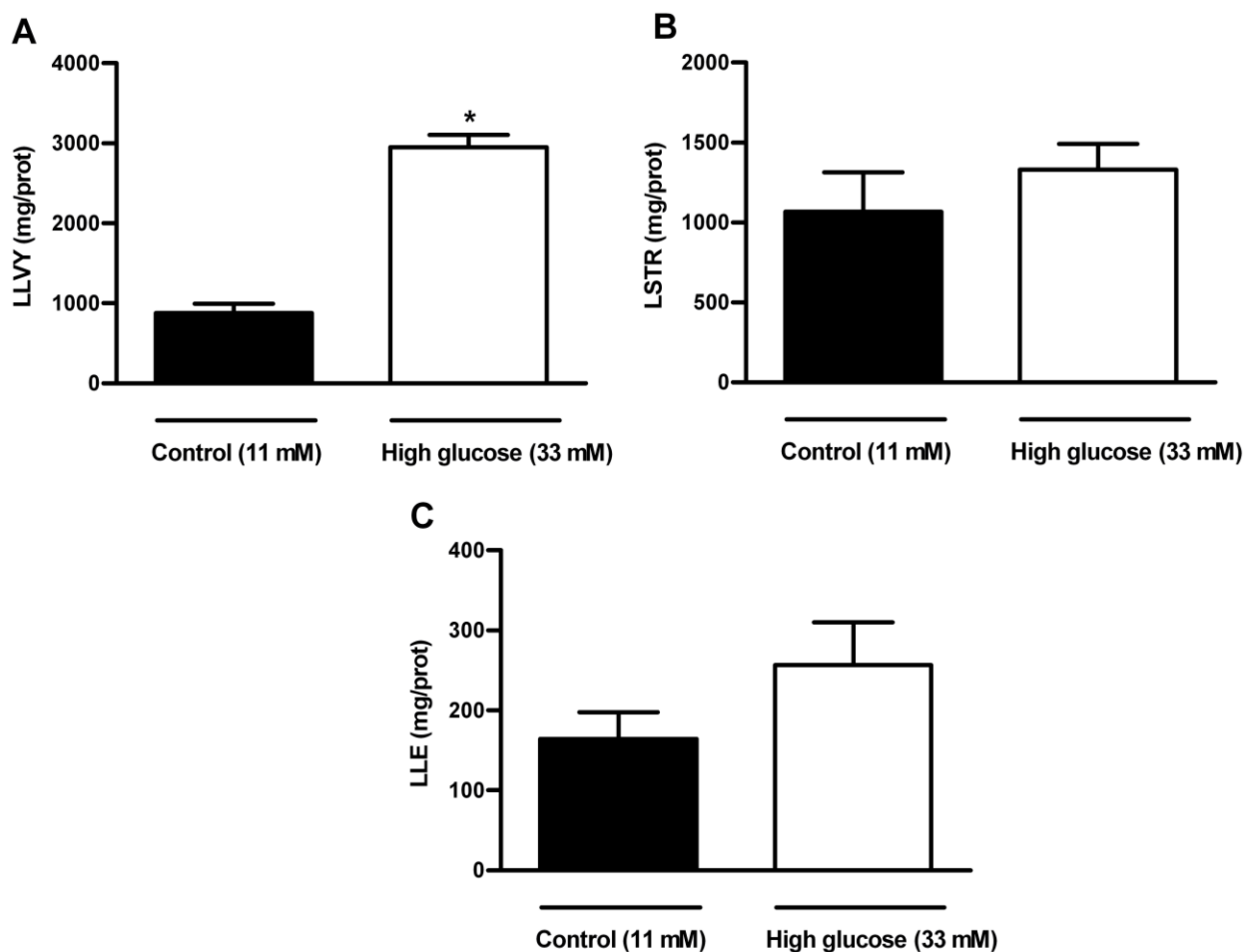


**Figure 3.19 Increased trypsin-like proteasomal activity in hearts under high glucose conditions without ischemia and reperfusion.** Isolated rat hearts were perfused under high glucose conditions vs. controls and subjected to ischemia and reperfusion. A) Trypsin-like proteasomal, (B) chymotrypsin-like, and (C) caspase-like activities after 60 min of reperfusion under high glucose conditions (33 mM) vs. control (11 mM). Values are expressed as mean  $\pm$  SEM (n=9). \*p<0.05 vs. respective control.

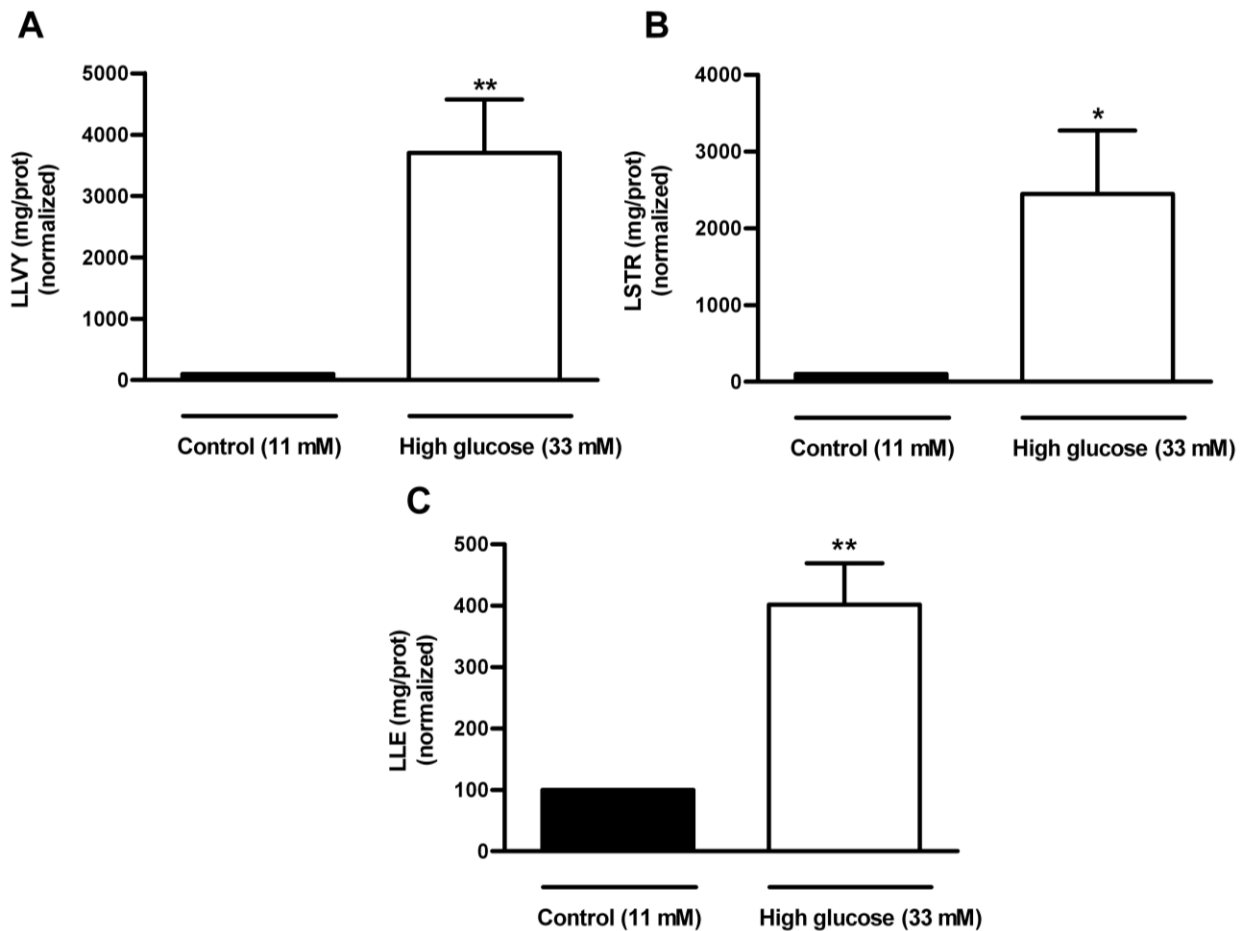


**Figure 3.20 Increased total proteasomal activity in hearts subjected to ischemia and reperfusion under high glucose conditions.** Isolated rat hearts were perfused under high glucose conditions vs. controls and subjected to ischemia and reperfusion. A) Trypsin-like proteasomal, (B) chymotrypsin-like, and (C) caspase-like activities after 60 min of reperfusion under high glucose conditions (33 mM) vs. control (11 mM). Values are expressed as mean  $\pm$  SEM (n=9). \* $p < 0.05$ , \*\* $p < 0.01$  vs. respective controls.

For 11 mM glucose perfusions, OA treatment decreased chymotrypsin-like proteasomal activity compared to the untreated control ( $p < 0.05$ ), but did not result in any significant effects on trypsin-like and caspase-like proteasomal activities (Figure 3.21A-C). Furthermore, OA treatment significantly diminished trypsin-like and chymotrypsin-like proteasomal activities in high glucose exposed rat hearts (Figure 3.21D and 3.21E). However, it had no effect on caspase-like activity in these hearts (Figure 3.21F).



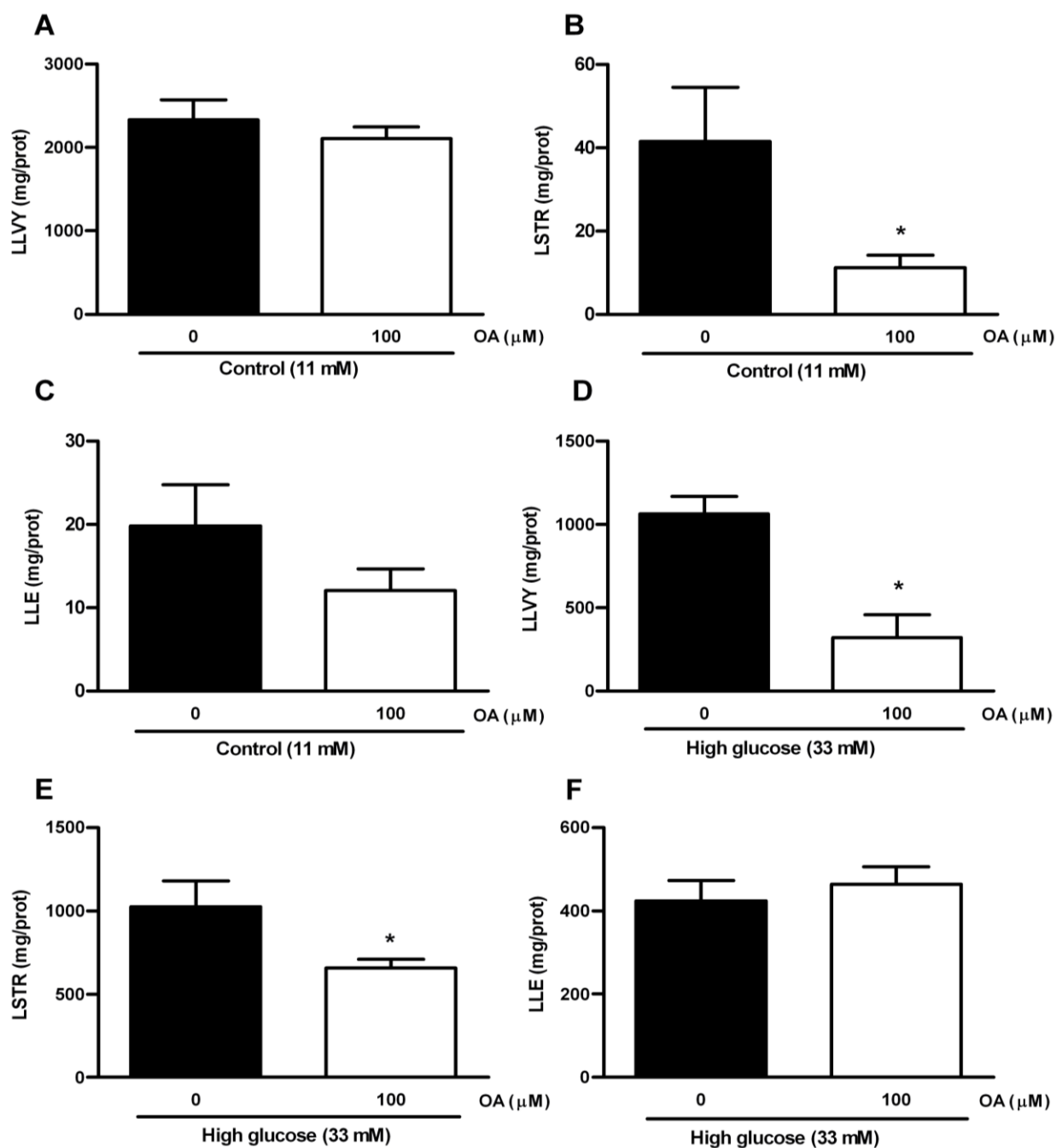


**Figure 3.21 OA attenuates high glucose-induced trypsin-like and chymotrypsin-like proteasomal activity following ischemia and reperfusion.** Isolated rat hearts were perfused under high glucose conditions vs. controls and subjected to ischemia and reperfusion. For OA treatment groups, 100  $\mu\text{M}$  OA was added during the first 20 min of reperfusion. (A) Trypsin-like proteasomal, (B) chymotrypsin-like, and (C) caspase-like activities after 60 min of reperfusion at baseline (11 mM glucose). (D) Trypsin-like proteasomal, (E) chymotrypsin-like, and (F) caspase-like activities after 60 min of reperfusion under high glucose conditions (33 mM glucose). Values are expressed as mean  $\pm$  SEM (n=9). \* $p < 0.05$  vs. respective controls.

### 3.4 Discussion

The damaging alliance between hyperglycemia and myocardial infarctions necessitates the development of novel therapeutic interventions that offer cardio-protection within this context. Moreover, stress-induced hyperglycemia in non-diabetic patients suffering an acute myocardial infarction also results in damaging outcomes, e.g. increased in-hospital mortality (56, 62). For the current study we explored whether OA acts as a novel cardio-protective factor in response to ischemia and reperfusion under hyperglycemic conditions. We tested our hypothesis by employing cell culture studies, *ex vivo* and *in vivo* rat heart perfusion models, and long-term OA treatment of diabetic rats as experimental systems. The main findings of this study are that OA treatment results in cardio-protection for rat hearts by attenuating hyperglycemia-induced oxidative stress, apoptosis, and proteasomal activity following ischemia and reperfusion.

We initially investigated our hypothesis by exposing isolated rat hearts to ischemia and reperfusion and found a marked decline in contractile function under high glucose perfusion conditions (simulated acute hyperglycemia). However, OA treatment resulted in a striking increase in functional recovery and demonstrates, for the first time as far as we are aware, that it triggers cardio-protection in high glucose perfused rat hearts. Post-ischemic increased coronary flow, decreased end diastolic pressure and our infarct size data further corroborated these findings. The increased coronary flow may be as a result of the vasodilatory effects of OA due to its nitric oxide production properties (68, 72). It may be that it prevents post-ischemic damage by increasing supply of oxygen to the myocardium, thus promoting oxidative phosphorylation and improving post-ischemic function (45). Moreover, OA administration following *in vivo* coronary artery ligations in hyperglycemic rats also decreased infarct sizes in the STZ-diabetic rats. Although OA-mediated cardio-protection was previously reported following ischemia and reperfusion, such studies were performed on hearts isolated from rats that were pre-treated with OA for several days (17, 24). Furthermore, these experiments were completed

under normoglycemic perfusion conditions. We also performed experiments for long-term OA treatment and found that it restored heart function in isolated rat heart perfusions. Collectively, our data therefore demonstrate that OA treatment initiated *after* an ischemic insult elicited cardio-protection, thus meaning that our findings may offer therapeutic value to actual clinical settings (versus pre-treatments).

To gain further insight into underlying mechanisms responsible for OA-mediated cardio-protection, we next evaluated whether it displays anti-oxidant and anti-apoptotic properties in our experimental systems. Here we found that OA diminished high glucose-induced myocardial oxidative stress and apoptosis in both our *in vitro* and *ex vivo* experimental models. Here the speculation is that the anti-apoptotic effects of OA *in vitro* are concentration-dependent with a lower ED50 vs. the anti-oxidant effects that were significant with a higher dose and not the lower dose. Moreover, our *ex vivo* data show significantly elevated superoxide levels together with decreased SOD activity in simulated acute hyperglycemic hearts following an ischemic insult. The superoxide ions may be coming from several sources in the heart some of which include the mitochondria via the ETC, glucose auto-oxidation and uncoupled nitric oxide synthase (ucNOS). The bulk of these free radicals were derived from the mitochondria (8, 9, 16), glucose auto-oxidation and ucNOS (8, 14, 21, 61, 86) under both hyperglycemic conditions with ischemia and reperfusion. How does OA exert its anti-oxidant effects in hyperglycemic hearts exposed to ischemia and reperfusion? Although the precise mechanisms of OA-mediated anti-oxidant effects are unclear, earlier data support a direct scavenging role, i.e. by decreasing superoxide and hydrogen peroxide levels together with reduced lipid peroxidation (1, 71). Here OA (a lipophilic compound) is proposed to intercalate into the lipid matrix and stabilize myocardial cell membranes under stressful conditions (34). In addition, OA contains a single phenolic hydroxyl group that is likely to be the bioactive group for scavenging free radicals (23). Our time course studies suggest that this likely occurs quite rapidly after an ischemic insult, peaking at about 20 minutes and thereafter sustained up to 60 minutes post-ischemia.

Previous studies established that OA treatment also results in transcriptional effects that increase expression of several anti-oxidant defense genes, including  $\alpha$ -tocopherol, glutathione peroxidase, catalase, thioredoxin peroxidase and superoxide dismutase (17, 23, 69, 76, 82, 83). Higher gene expression in this case is probably mediated by MAP kinases (JNK and ERK) that may regulate target transcriptional modulators (83). The basic leucine zipper transcription factor, nuclear factor erythroid 2 p45-related factor 2 (Nrf2), is strongly implicated in this process (83). Nrf2 plays a key role in protecting cells from oxidative stress by binding anti-oxidant-response elements (ARE) of gene promoters to induce expression of numerous target genes, e.g. glutathione peroxidase, heme oxygenase, and thioredoxin (35, 41, 48). Earlier work determined that OA upregulated Nrf2 expression in hepatocytes, with MAPK activation implicated in this process (83). Furthermore, Ichikawa *et al.* (40) found that dh404 (novel OA derivative) increased Nrf2 translocation to the nucleus to enhance Nrf2-driven transcription and suppress oxidative stress in H9c2 cardiomyoblasts. In support of its anti-oxidant properties OA attenuated protein carbonylation in hearts exposed following ischemia and reperfusion. Protein carbonylation is one of the more prominent ways through which proteins can be oxidized (53). The process of protein carbonylation is irreversible and often leads to loss of function and the need for degradation of damaged proteins mainly by the UPS. The exact mechanisms on how it occurs are unknown, however it involves non-enzymatic introduction of carbonyl groups to proteins by (i) direct oxidation of protein side chains or oxidative cleavage of the protein backbone, (ii) introduction of 4-hydroxy-2-noneal (HNE), 2-propenal or malondialdehyde from lipid peroxidation to a Cys, His or Lys residue and (iii) formation of advanced glycation end-products. Whether the probability and mechanism of carbonylation are constant or differ with increasing oxidative stress are still open questions. Collectively these data show that OA acts as an anti-oxidant and that its effects are mediated both by a direct scavenging role and also by induction of various anti-oxidant defense genes.

We propose that the improved functional effects detected with OA treatment stems from its anti-apoptotic effects observed in both our experimental models, that likely occur downstream of elevated

oxidative stress. There are several ways how this may happen. Firstly, rat hearts exposed to high glucose displayed increased superoxide and nitric oxide generation that favors the production of peroxynitrite and nitrotyrosine with damaging consequences (14). For example, others found that peroxynitrite inhibits the mitochondrial respiratory chain (7, 85) and triggers myocardial apoptosis (2). Our time course studies support the concept that myocardial apoptosis occurs downstream of the initial post-ischemic oxidative stress burst. Here we found that myocardial apoptosis in high glucose perfused hearts only increased from the 40 minute after the ischemic insult.

Secondly, our data show that OA exerts cardio-protective effects by attenuating HBP flux in hyperglycemic rat hearts. These data are in agreement with previous work from our laboratory that established that hyperglycemia results in greater oxidative stress, increased BAD O-GlcNAcylation and BAD-Bcl-2 dimer formation, thereby mediating HBP-induced myocardial apoptosis in H9c2 cardiomyoblasts (65). Thirdly, it is also possible that the OA-mediated decrease in oxidative stress may also limit hyperglycemia-induced inactivation of the sarco(endo)plasmic reticulum  $Ca^{2+}$ -ATPase (SERCA) (78) and electrophysiological alterations (arrhythmias, QT prolongation) (14, 25, 27). Thus our study shows that OA exerts anti-oxidant effects that attenuate myocardial apoptosis and thereby improve contractile functional recovery following ischemia and reperfusion of hyperglycemic rat hearts. Our *ex vivo* pre-ischemic data suggest that the cardio-protective effects of OA are not dependent on any inherent inotropic effects, but rather involve anti-oxidant and anti-apoptotic mechanisms. The potent hypotensive properties of OA confirm previous observations in Dahl salt sensitive (75) and STZ-diabetic rats (55). These data therefore offer significant clinical promise considering that hypertension is a robust risk factor for diabetes-induced CVD and non-diabetic heart diseases. The mechanisms underlying this interesting phenomenon were, however, not elucidated in this study. It is possible that OA treatment may also act to modulate the nervous system, but further studies are required to prove this.

We next investigated the role of the UPS in hyperglycemic hearts exposed to ischemia and reperfusion since it is the major non-lysosomal pathway for degradation of ubiquitinated proteins (87). We reasoned that since UPS dysregulation occurs during ischemia and reperfusion, it may be an important contributing factor to reduced contractile function found under these conditions (87). However, conflicting data have been published with both inhibition and activation of the UPS linked to improved heart function in response to ischemia–reperfusion [reviewed in (3, 81)]. It is likely that the discordant data may be due to differences in experimental models and protocols employed. We detected diminished proteasomal activities in 11 mM perfused rat hearts following ischemia (versus pre-ischemic hearts) (Figure 3.19). By contrast, high glucose perfused hearts exhibited a robust upregulation of trypsin-like, chymotrypsin-like and caspase-like proteasomal activities following ischemia (Figure 3.20). We propose that ischemia and reperfusion together with hyperglycemia trigger greater oxidative stress that may result in increased misfolded proteins that are targeted for removal by UPS degradation. In support of this notion, the increased protein carbonylation observed under hyperglycemic conditions also result in increased UPS to remove the misfolded proteins (46). However, excessively high UPS activation may result in the activation of damaging signaling pathways, e.g. nuclear factor-kappa B (NF- $\kappa$ B) (57). Here greater UPS activity will degrade I $\kappa$ B (NF- $\kappa$ B inhibitor) and release unbound NF- $\kappa$ B to the nucleus to induce expression of various genes that may exacerbate inflammation and reperfusion injury (4, 30). In support of this concept, Pye *et al.* (2003) (64) ascertained that proteasomal inhibition blunted NF- $\kappa$ B activation during reperfusion, thereby resulting in decreased reperfusion injury. Moreover, hyperglycemic rats treated with bortezomib (protease inhibitor) exhibited diminished UPS, inflammation and myocardial damage in response to ischemia and reperfusion (57). In agreement, we found that OA treatment attenuated proteasomal activities in high glucose hearts following ischemia and reperfusion. Together our data show that hearts exposed to high glucose levels and subjected to ischemia and reperfusion display UPS over-activity that may impair the heart's functional recovery. Moreover, we established that OA treatment inhibits the UPS and that this is linked with improved cardiac contractile function following ischemia and reperfusion under simulated hyperglycemic conditions.

How does our data differ from previous studies that implicate glucose-insulin-potassium (GIK) in cardio-protection? We propose that the protective effects of GIK may largely depend on the actions of insulin i.e. via a) its direct cardio-protective (anti-apoptotic) effects (4, 19, 43, 70) and b) its glucose lowering abilities. It is well established that insulin administration should increase plasma glucose clearance thus limiting damaging effects of acute and chronic hyperglycemia ('glucotoxicity'). Moreover, insulin promotes glucose uptake and the generation of glycolytic ATP that is linked with cardio-protection (19). GIK treatment has resulted in mixed success, e.g. GIK treatment for patients with acute myocardial infarction (CREATE-ECLA trial) did not result in any significant cardio-protective effects (59). Here it is proposed that the potential protective effects of GIK may have been abolished by higher blood glucose levels in GIK-treated patients (4). Finally, a recent study investigating glucose-insulin treatment in patients undergoing coronary artery bypass grafting (while maintaining normoglycemia) found that it is cardio-protective and improves myocardial function (13). Together these data strongly indicate that insulin acts as the major protective component of GIK, and that higher blood glucose levels are damaging to the cardiovascular system.

In summary, this study demonstrates that OA acts as a novel cardio-protective agent in hearts exposed to high glucose levels by decreasing oxidative stress, reducing apoptosis and the UPS, leading to cardio-protection following ischemia and reperfusion. These data are promising since it may eventually result in novel therapeutic interventions to treat stress-induced acute hyperglycemia (in non-diabetic patients) and also diabetic patients with associated CVD complications. Furthermore, in addition to its anti-inflammatory properties OA (32) use may be applicable in other cardiac diseases where inflammation is present e.g. in heart failure. We are of the opinion that this is particularly relevant within the developing world context, where it may provide a cost-effective therapeutic intervention for the treatment of acute myocardial ischemia in these individuals. The next chapter describes the second therapeutic agent benfotiamine addressing its effect on some aspects already highlighted in this chapter moreso on flux via the non-oxidative glucose pathways.

### 3.5 References

1. **Ali M, Jahangir M, Hussan S, Choudhary M.** Inhibition of  $\alpha$ -glucosidase by oleanolic acid and its synthetic derivatives. *Phytochem* 60: 295–299, 2002.
2. **Arstall M, Sawyer D, Fukazawa R, Kelly R.** Cytokine-mediated apoptosis in cardiac myocytes: the role of inducible nitric oxide synthase induction and peroxynitrite generation. *Circ Res* 85: 829–840, 1999.
3. **Baldwin AJ.** The NF-kappa B and I kappa B proteins: new discoveries and insights. *Annu Rev Immunol* 14: 649–683, 1996.
4. **Van den Berghe G.** Coronary bypass surgery: protective effects of insulin or of prevention of hyperglycemia, or both? *J Clin Endocrinol Metab* 96: 1272–1275, 2011.
5. **Boudina S, Abel ED.** Diabetic cardiomyopathy revisited. *Circulation* 115: 3213–3223, 2007.
6. **Bradshaw D, Norman R, Pieterse D, Levitt NS, Comparative A, Assessment R.** Estimating the burden of disease attributable to diabetes in South Africa in 2000. *S Afric Med J* 97: 701–706, 2007.
7. **Brown G.** Regulation of mitochondrial respiration by nitric oxide inhibition of cytochrome c oxidase. *Biochim Biophys Acta* 1504: 46–57, 2001.
8. **Brownlee M.** Biochemistry and molecular cell biology of diabetic complications. *Nature* 414: 813–820, 2001.
9. **Brownlee M.** The pathobiology of diabetic complications a unifying mechanism. *Diabetes* 54: 1615–1625, 2005.
10. **Bulteau AL, Lundberg KC, Humphries KM, Sadek HA, Szweda PA, Friguet B, Szweda LI.** Oxidative modification and inactivation of the proteasome during coronary occlusion/reperfusion. *J Biol Chem* 276: 30057–30063, 2001.
11. **Cai L, Li W, Wang G, Guo L, Jiang Y, Kang YJ.** Hyperglycemia-induced apoptosis in mouse myocardium: mitochondrial cytochrome c-mediated caspase-3 activation pathway. *Diabetes* 51: 1938–1948, 2002.
12. **Capes SE, Hunt D, Malmberg K, Gerstein HC.** Stress hyperglycaemia and increased risk of death after myocardial infarction in patients with and without diabetes: a systematic overview. *Lancet*: 355: 773–778, 2000.
13. **Carvalho G, Pelletier P, Albacker T, Lachapelle K, Joannis D, Al E.** Cardioprotective effects of glucose and insulin administration while maintaining normoglycemia (GIN therapy) in patients undergoing coronary artery bypass grafting. *J Clin Endocrinol Metab* 96: 1469–1477, 2011.
14. **Ceriello A, Quagliaro L, Amico MD, Filippo C Di, Marfella R, Nappo F, Berrino L, Rossi F, Giugliano D.** Acute hyperglycemia induces nitrotyrosine formation and apoptosis in perfused heart from rat. *Diabetes* 51: 1076–1082, 2002.



15. **Ceriello A.** Oxidative stress and glycemic regulation. *Metab Clin Exp* 49: 27–29, 2000.
16. **Chen Q, Vazquez EJ, Moghaddas S, Hoppel CL, Lesnefsky EJ.** Production of reactive oxygen species by mitochondria: central role of complex III. *J Biol Chem* 278: 36027–36031, 2003.
17. **Choi C, You H, Jeong H.** Nitric oxide and tumor necrosis factor- $\alpha$  production by oleanolic acid via nuclear factor- $\kappa$ B activation in macrophages. *Biochem Biophys Res Commun* 288: 49–55, 2001.
18. **Claude B, Morin P, Lafosse M, Andre P.** Evaluation of apparent formation constants of pentacyclic triterpene acids complexes with derivatized  $\beta$ - and  $\chi$ -cyclodextrins by reversed phase liquid chromatography. *J Chromatogr A* 1043: 37–42, 2004.
19. **Cross H, Clarke K, Opie L, Radda G.** Is lactate-induced myocardial ischemic injury mediated by decreased pH or increased intracellular lactate? *J Mol Cell Cardiol* 27: 1369–1381, 1995.
20. **Cunningham MJ, Apstein CS, Weinberg EO, Vogel WM, Lorell BH.** Influence of glucose and insulin on the exaggerated diastolic and systolic dysfunction of hypertrophied rat hearts during hypoxia. *Circ Res* 66: 406–415, 1990.
21. **Desco M, Asensi M, Márquez R, Martínez-Valls J, Vento M, Pallardó F, Sastre J, Viña J.** Xanthine oxidase is involved in free radical production in type 1 diabetes: protection by allopurinol. *Diabetes* 51: 1118–1124, 2002.
22. **Deuchar GA, Opie LH, Lecour S.** TNF $\alpha$  is required to confer protection in an in vivo model of classical ischaemic preconditioning. *Life Sci* 80: 1686–1691, 2007.
23. **Du Y, Ko K.** Oleanolic acid protects against myocardial ischemia-reperfusion injury by enhancing mitochondrial antioxidant mechanism mediated by glutathione and alpha-tocopherol in rats. *Planta Med* 72: 222–227, 2006.
24. **Du Y, Ko KM.** Effects of pharmacological preconditioning by emodin / oleanolic acid treatment and / or ischemic preconditioning on mitochondrial antioxidant components as well as the susceptibility to ischemia-reperfusion injury in rat hearts. *Mol Cell Biochem* 288: 135–142, 2006.
25. **D'Amico M, Marfella R, Nappo F, Di Filippo C, De Angelis L, Ai E.** High glucose induces ventricular instability and increases vasomotor tone in rats. *Diabetologia* 44: 464–470, 2001.
26. **Eyer K.** Complications of transfemoral coronary arteriography and their prevention using heparin. *Am Heart J* 86: 428, 1973.
27. **Di Filippo C, Cuzzocrea S, Marfella R, Fabbroni V, Scollo G, Ai E.** M40403 prevents myocardial injury by acute hyperglycaemia in perfused rat heart. *Eur J Pharmacol* 497: 65–74, 2004.
28. **Friguet B, Bulteau A, Conconi M, Petropoulos I.** Redox control of 20S proteasome. *Methods Enzymol* 353: 253–262, 2002.

29. **Ge F, Zeng F, Liu S, Guo N, Ye H, Song Y, Fan J, Wu X, Wang X, Deng X, Jin Q, Yu L.** In vitro synergistic interactions of oleanolic acid in combination with isoniazid , rifampicin or ethambutol against Mycobacterium tuberculosis. *J Med Microbiol* 59: 567–572, 2010.
30. **Ghosh S, May M, Kopp E.** NF-kappa and Rel proteins: evolutionarily conserved mediators of immune responses. *Annu Rev Immunol* 16: 225–260, 1998.
31. **Gokhroo R, Mittal SR.** Electrocardiographic correlates of hyperglycemia in acute myocardial infarction. *Intern J Cardiol* 22: 267–269, 1989.
32. **Gupta M, Bhalla T, Gupta G, Mitra C, Bhargava K.** Anti-inflammatory activity of natural products (I) triterpenoids. *Eur J Pharmacol* 6: 67–70, 1969.
33. **Gurib-Fakim A.** Medicinal plants: traditions of yesterday and drugs of tomorrow. *Mol Aspects Med* 27: 1–93, 2006.
34. **Han S, Ko Y, Park S, Jin I, Kim Y.** Oleanolic acid and ursolic acid stabilize liposomal membranes. *Lipids* 32: 769–773, 1997.
35. **Harvey C, Thimmulappa R, Singh A, Blake D, Ling G, Al E.** Nrf2-regulated glutathione recycling independent of biosynthesis is critical for cell survival during oxidative stress. *Free Radic Biol Med* 46: 443–453, 2009.
36. **Hearse D, Sutherland F.** The isolated blood and perfusion fluid perfused heart. *Pharmacol Res* 41: 613–627, 2000.
37. **Hostettmann K, Marston A.** *Chemistry and pharmacology of natural products: saponins.* UK: Cambridge University Press, 1995.
38. **Howarth F, Qureshi M.** Characterisation of ventricular myocyte shortening after administration of streptozotocin (STZ) to neonatal rats. *Arch Physiol Biochem* 109: 200–205, 2001.
39. **Hsu H, Yang J, Lin C.** Effects of oleanolic acid and ursolic acid on inhibiting tumor growth and enhancing the recovery of hematopoietic system postirradiation in mice. *Cancer Lett* 111: 7–13, 1997.
40. **Ichikawa T, Li J, Meyer C, Janicki J, Hannink M, Al E.** Dihydro-CDDO-trifluoroethyl amide (dh404), a novel Nrf2 activator, suppresses oxidative stress in cardiomyocytes. *PLoS One* 4: e8391, 2009.
41. **Jaiswal A.** Nrf2 signaling in coordinated activation of antioxidant gene expression. *Free Radic Biol Med* 36: 1199–1207, 2004.
42. **Jeong D, Kim Y, Kim H, Ji H, Yoo S, Choi W, Lee S, Han C, Lee H.** Dose-linear pharmacokinetics of oleanolic acid after intravenous and oral administration in rats. *Biopharm. Drug Dispos* 28: 51–57, 2007.
43. **Jonassen A, Sack M, Mjøs O, Yellon D.** Myocardial protection by insulin at reperfusion requires early administration and is mediated via Akt and p70s6 kinase cell-survival signalling. *Circ Res* 89: 1191–1198, 2001.

44. **Kaiserova K, Srivastava S, Hoetker JD, Awe SO, Tang X, Cai J, Bhatnagar A.** Redox activation of aldose reductase in the ischemic heart. *J Biol Chem* 281: 15110–15120, 2006.
45. **Kassiotis C, Rajabi M, Taegtmeyer H.** Metabolic reserve of the heart: the forgotten link between contraction and coronary flow. *Prog Cardiovasc Dis* 51: 74–88, 2008.
46. **Kastle M, Grune T.** Protein oxidative modification in the aging organism and the role of the ubiquitin proteasomal system. *Curr Pharm Des* 17: 4007–4022, 2011.
47. **Kelly RF, Lamont KT, Somers S, Hacking D, Lacerda L.** Ethanolamine is a novel STAT-3 dependent cardioprotective agent. *Basic Res Cardiol* 105: 763–770, 2010.
48. **Kensler T, Wakabayashi N, Biswal S.** Cell survival responses to environmental stresses via the Keap1-Nrf2-ARE pathway. *Ann Rev Pharmacol Toxicol* 47: 89–116, 2007.
49. **Kim N, Lee M, Park M, Kim S, Park H, Choi J, Kim S, Cho S, Lee J.** Momordin Ic and oleanolic acid from *Kochia* Fructus reduce carbon tetrachloride-induced hepatotoxicity in rats. *J Med Food* 8: 177–183, 2005.
50. **Li J, Guo W, Yang Q.** Effects of ursolic acid and oleanolic acid on human carcinoma cell line HCT15. *World J Gastroenterol* 8: 493–495, 2002.
51. **Liu J, Liu Y, Parkinson A, Klaassen C.** Effect of oleanolic acid on hepatic toxicant-activating and detoxifying systems in mice. *J Pharmacol Exp Ther* 257: 768–774, 1995.
52. **Liu J.** Pharmacology of oleanolic acid and ursolic acid. *J Ethnopharmacol* 49: 57–68, 1995.
53. **Madian A, Regnier F.** Proteomic identification of carbonylated proteins and their oxidation sites. *J. Proteome Res* 9: 3766–3780, 2010.
54. **Mahato S, Kundu A.** <sup>13</sup>C NMR Spectra of pentacyclic triterpenoids—a complication and some salient features. *Phytochem* 37: 1517–1573, 1994.
55. **Mapanga R, Tufts M, Shode F, Musabayane C.** Renal effects of plant-derived oleanolic acid in streptozotocin-induced diabetic rats. *Ren Fail* 31: 481–491, 2009.
56. **Marfella R, Di Filippo C, Portoghese M, Ferraraccio F, Rizzo MR, Siniscalchi M, Musacchio E, D'Amico M, Rossi F, Paolisso G.** Tight glycemic control reduces heart inflammation and remodeling during acute myocardial infarction in hyperglycemic patients. *J Am Coll Cardiol* 53: 1425–1436, 2009.
57. **Marfella R, Di Filippo C, Portoghese M, Siniscalchi M, Martis S, Ferraraccio F, Guastafierro S, Nicoletti G, Barbieri M, Coppola A, Rossi F, Paolisso G, D'Amico M.** The ubiquitin-proteasome system contributes to the inflammatory injury in ischemic diabetic myocardium: the role of glycemic control. *Cardiovasc Pathol* 18: 332–345, 2009.
58. **Mazonne T, Chait A, Plutzky J.** Cardiovascular disease risk in type 2 diabetes mellitus: insights from mechanistic studies. *Lancet* 371: 1800–1809, 2008.

59. **Mehta S, Yusuf S, Diaz R, Zhu J, Pais P, Al E.** CREATE-ECLA Trial Group investigators. Effect of glucose-insulin-potassium infusion on mortality in patients with acute ST segment elevation myocardial infarction: the CREATE-ECLA randomized controlled trial. *JAMA* 293: 437–446, 2005.
60. **Musabayane C, Tufts M, Mapanga R.** Synergistic antihyperglycemic effects between plant-derived oleanolic acid and insulin in streptozotocin-induced diabetic rats. *Ren Fail* 32: 832–839, 2010.
61. **Nishikawa T, Edelstein D, Du XL, Yamagishi S, Matsumura T, Kaneda Y, Yorek MA, Beebek D, Oates PJ, Hammes H, Giardino I, Brownlee M, Ave MP, York N.** Normalizing mitochondrial superoxide production blocks three pathways of hyperglycaemic damage. *Nature* 404: 787–790, 2000.
62. **Oswald GA, Smith CC, Betteridge DJ, Yudkin JS.** Determinants and importance of stress hyperglycaemia in non-diabetic patients with myocardial infarction. *Br Med J (Clin Res)* 293: 917–922, 1986.
63. **Powell SR.** The ubiquitin-proteasome system in cardiac physiology and pathology. *Am J Physiol Heart Circ Physiol* 291: H1–H19, 2006.
64. **Pye J, Ardeshirpour F, McCain A, Bellinger D a, Merricks E, Adams J, Elliott PJ, Pien C, Fischer TH, Baldwin AS, Nichols TC.** Proteasome inhibition ablates activation of NF-kappa B in myocardial reperfusion and reduces reperfusion injury. *Am J Physiol Heart Circ Physiol* 284: H919–H926, 2003.
65. **Rajamani U, Essop MF.** Hyperglycemia-mediated activation of the hexosamine biosynthetic pathway results in myocardial apoptosis. *Am J Physiol Cell Physiol* 299: C139–C147, 2010.
66. **Rajamani U, Joseph D, Roux S, Essop MF.** The hexosamine biosynthetic pathway can mediate myocardial apoptosis in a rat model of diet-induced insulin resistance. *Acta Physiol (Oxf, Eng)* 202: 151–157, 2011.
67. **Requena J, Levine R, Stadtman E.** Recent advances in the analysis of oxidized proteins. *Amino Acids* 25: 221–226, 2003.
68. **Rodriguez-Rodriguez R, Stankevicius E, Herrera MD, Østergaard L, Andersen MR, Ruiz-Gutierrez V, Simonsen U.** Oleanolic acid induces relaxation and calcium-independent release of endothelium-derived nitric oxide. *Br J Pharmacol* 155: 535–546, 2008.
69. **Rong Z, Gong X, Sun H, Li Y, Ji H.** Protective effects of oleanolic acid on cerebral ischemic damage in vivo and H<sub>2</sub>O<sub>2</sub>-induced injury in vitro. *Pharm Biol* 49: 78–85, 2011.
70. **Sack M, Yellon D.** Insulin therapy as an adjunct to reperfusion after acute coronary ischemia: a proposed direct myocardial cell survival effect independent of metabolic modulation. *J Am Coll Cardiol* 41: 1404–1407, 2001.
71. **Senthil S, Sridevi M, Pugalendi K V.** Cardioprotective effect of oleanolic acid on isoproterenol-induced myocardial ischemia in rats. *Toxicol Pathol* 35: 418–423, 2007.

72. **Simonsen U, Rodriguez-Rodriguez R, Dalsgaard T, Buus NH, Stankevicius E.** Novel approaches to improving endothelium-dependent nitric oxide-mediated vasodilatation. *Pharmacol Rep* 61: 105–115, 2009.
73. **Skrypiec-Spring M, Grotthus B, Szeląg A, Schulz R.** Isolated heart perfusion according to Langendorff- Still viable in the new millennium. *J Pharmacol Toxicol Methods* 55: 113–126, 2007.
74. **Somova L, Nadar A, Rammanan P, Shode F.** Cardiovascular, antihyperlipidemic and antioxidant effects of oleanolic and ursolic acids in experimental hypertension. *Phytomed* 10: 115–121, 2003.
75. **Somova LI, Shode FO, Ramnanan P, Nadar A.** Antihypertensive, antiatherosclerotic and antioxidant activity of triterpenoids isolated from *Olea europaea*, subspecies *africana* leaves. *J Ethnopharmacol* 84: 299–305, 2003.
76. **Soobrattee M, Neergheen V, Luximon-Ramma A, Aruoma O, Bahorun T.** Phenolics as potential antioxidant therapeutic agents: mechanism and actions. *Mutant Res* 579: 200–213, 2005.
77. **Stamler J, Vaccaro O, Neaton J, Wentworth D.** Diabetes, other risk factors, and 12-yr cardiovascular mortality for men screened in the Multiple Risk Factor Intervention Trial. *Diab Care* 16: 434–444, 1993.
78. **Tang W, Cheng W, Kravtsov G, Tong X, Hou X, Ai E.** Cardiac contractile dysfunction during acute hyperglycemia due to impairment of SERCA by polyol pathway-mediated oxidative stress. *Am J Physiol Cell Physiol* 299: C643–C653, 2010.
79. **Tang X, Gao J, Fang F, Chen J, Xu L, Zhao X, Xu Q.** Hepatoprotection of oleanolic acid is related to its inhibition on mitochondrial permeability transition. *Am J Chin Med* 33: 627–637, 2005.
80. **Walker W, Mundall S, Broderick H, Prasad B, Kim J.** Systemic heparinization for femoral percutaneous coronary arteriography. *New Eng J Med* 288: 826–828, 1973.
81. **Wang X, Li J, Zheng H, Su H, Powell S.** Proteasome functional insufficiency in cardiac pathogenesis. *Am J Physiol Heart Circ Physiol* 301: H2207– H2219, 2011.
82. **Wang X, Li Y, Wu H, Liu J, Hu J, Ai E.** Antidiabetic effect of oleanolic acid: a promising use of a traditional pharmacological agent. *Phytotherapy Res* 25: 1031–1040, 2011.
83. **Wang X, Ye X, Liu R, Chen H, Bai H, Ai E.** Antioxidant activities of oleanolic acid in vitro: possible role of Nrf2 and MAP kinases. *Chem Biol Interact* 184: 328–337, 2010.
84. **Wild S, Roglic G, Green A, Sicree R, King H.** Global prevalence of diabetes: estimates for the year 2000 and projections for 2030. *Diab Care* 27: 1047–1053, 2004.
85. **Xie Y, Wolin M.** Role of nitric oxide and its interaction with superoxide in the suppression of cardiac muscle mitochondrial respiration. Involvement in response to hypoxia/reoxygenation. *Circ* 94: 2580–2586, 1996.

86. **Yamagishi S, Edelstein D, Du X, Brownlee M.** Hyperglycemia potentiates collagen-induced platelet activation through mitochondrial superoxide overproduction. *Diabetes* 50: 1491–1494, 2001.
87. **Yu X, Kem DC.** Proteasome inhibition during myocardial infarction. *Cardiovasc Res* 85: 312–320, 2010.

## CHAPTER 4

### **Acute Benfotiamine Treatment Counteracts Hyperglycemia-mediated Contractile Dysfunction following Ischemia and reperfusion**

Hyperglycemia (chronic and acute) is an important risk factor for acute myocardial infarction. With hyperglycemia, activation of non-oxidative glucose metabolic circuits i.e. the polyol pathway, hexosamine biosynthetic pathway (HBP), advanced glycation end products (AGE), and protein kinase C (PKC) activation can elicit the onset of cardiovascular complications. Previous studies found that benfotiamine (BFT) – vitamin B1 derivative - stimulates transketolase (pentose phosphate pathway [PPP] enzyme) thereby shunting flux away from these four pathways. We therefore hypothesized that acute BFT treatment activates PPP leading to cardio-protection following ischemia and reperfusion under hyperglycemic conditions. We employed several experimental systems: 1) Isolated rat hearts were perfused *ex vivo* with Krebs-Henseleit buffer containing 33 mM glucose vs. controls (11 mM glucose) for 90 min, followed by 30 min global ischemia and 60 min reperfusion  $\pm$  BFT treatment added during the first 20 min of reperfusion; 2) Infarct size determination as in #1) but with 20 min regional ischemia and 2 hr reperfusion  $\pm$  acute BFT treatment; and 3) *In vivo* coronary ligations performed on streptozotocin-treated rats  $\pm$  acute BFT treatment during early reperfusion. Our data show that acute BFT treatment significantly decreased myocardial oxidative stress and apoptosis, and provided cardio-protection in response to ischemia and reperfusion under hyperglycemic conditions. In parallel, BFT blunted hyperglycemia-induced activation of four non-oxidative glucose pathways in the rat heart. This study therefore demonstrates that acute BFT treatment initiated after an ischemic insult offers significant potential as a novel therapeutic agent for acute myocardial infarctions under conditions of acute and chronic hyperglycemia.

## 4.1 Introduction

Diabetes poses a huge health burden that may result in devastating human and economic costs if no effective measures are implemented (104). Cardiovascular diseases frequently manifest in diabetic patients, and here chronic hyperglycemia presents as an important risk factor for acute myocardial infarction (AMI) (15, 125). Furthermore, stress-induced, acute hyperglycemia in non-diabetic individuals with AMI is associated with increased in-hospital deaths (86, 105). Thus, both acute and chronic hyperglycemia are able to trigger biochemical and electrophysiological perturbations that contribute to contractile dysfunction (19).

Under hyperglycemic conditions, enhanced flux through non-oxidative glucose metabolic circuits - polyol pathway, hexosamine biosynthetic pathway (HBP), formation of advanced glycation end products (AGE), protein kinase C (PKC) activation - may trigger reactive oxygen species (ROS) production and the development of micro- and macrovascular complications. Moreover, a positive feedback loop also exists where hyperglycemia-mediated oxidative stress activates non-oxidative glucose metabolic pathways. We previously found that hyperglycemia-induced ROS activated the HBP leading to greater O-GlcNAcylation (HBP end-product) of target proteins and myocardial apoptosis (109, 110). Moreover, we recently demonstrated that increased oxidative stress, HBP activation and apoptosis contribute to impaired contractile function in response to ischemia and reperfusion under acute and chronic hyperglycemic conditions (84). The underlying mechanisms responsible for hyperglycemia-mediated cardiac damage are, however, not precisely clear. An emerging paradigm suggests that hyperglycemia-induced ROS result in DNA damage and the subsequent activation of poly-ADP-ribose polymerase (PARP) as a restorative mechanism (12). However, PARP activation may also attenuate glyceraldehyde-3-phosphate dehydrogenase (GAPDH), a key glycolytic enzyme, thereby diverting upstream glycolytic metabolites into certain non-oxidative glucose pathways, with maladaptive consequences (Figure 4.1) (35, 47).



Ongoing research work is therefore focusing on ways to blunt this damaging sequence of events and to limit activation of certain non-oxidative glucose pathways under these conditions. In addition to oleanolic acid, this chapter investigates the potential use of another alternative therapeutic agent, benfotiamine (S-benzoylthiamine O-monophosphate, BFT). BFT is a synthetic S-acyl derivative of thiamine is emerging as a putative therapeutic agent since it stimulates transketolase, a key enzyme of the non-oxidative branch of the pentose phosphate pathway (PPP), thereby shunting flux away from the four non-oxidative glucose pathways earlier discussed and resulting in beneficial outcomes (Figure 4.1) (1, 82). Thiamine-derived compounds were discovered from plants on Allium genus such as onions, shallots and leeks and named as allithiamines (43). BFT was identified as the most effective compound with anti-AGEs properties. It is a lipid soluble molecule with an open thiazole ring that enables its entry directly through the cell membrane, hence it possesses increased bioavailability approximately five times that of thiamine (8, 81, 147). The thiazole ring closes once it is absorbed producing biologically active thiamine. After oral administration, BFT is first dephosphorylated to S-benzoylthiamine by the ecto-alkaline phosphatase in the brush borders of intestinal mucosal cells and enters the circulation. Studies reported that benfotiamine is delivered into cells via the reduced folate carrier-1 (RFC-1), and then de-benzoylated to thiamine monophosphate by cellular and plasma esterases (8, 130). Evidence suggest that BFT is an effective and safe compound to use. The classification of benfotiamine as a lipophilic agent is disputed by findings that showed its increased solubility in aqueous solutions e.g. water at pH < 7; and not in organic solvents e.g. benzene (135, 136). Thus, it is likely that benfotiamine is an amphipathic agent. Thiamine and its analogs are initially metabolized to thiamine monophosphate, then TPP/ thiamine diphosphate (TDP) that is required by TK.

Chronic BFT treatment of diabetic rodents prevented experimental retinopathy (47), and also enhanced post-myocardial infarction survival and functional recovery (70). Moreover, others emphasized the protective role of angiogenesis and pro-survival pathways (e.g. Akt) as potential mechanisms whereby BFT may offer cardio-protection within the setting of ischemia and reperfusion

(70). However, as far as we are aware, no-one has previously tested the effects of acute BFT administration in response to ischemia and reperfusion (under acute and chronic hyperglycemic conditions), and its impact on the four non-oxidative glucose pathways earlier discussed. In light of this, we hypothesized that acute BFT treatment will enhance myocardial PPP flux, thereby attenuating hyperglycemia-mediated activation of four non-oxidative glucose pathways (AGE, HBP, polyol pathway, PKC activation) and resulting in cardio-protection following ischemia and reperfusion. We believe this research question is highly relevant within the clinical setting since, if our hypothesis is indeed correct, BFT could be rapidly administered to both diabetic and non-diabetic patients after suffering an AMI.

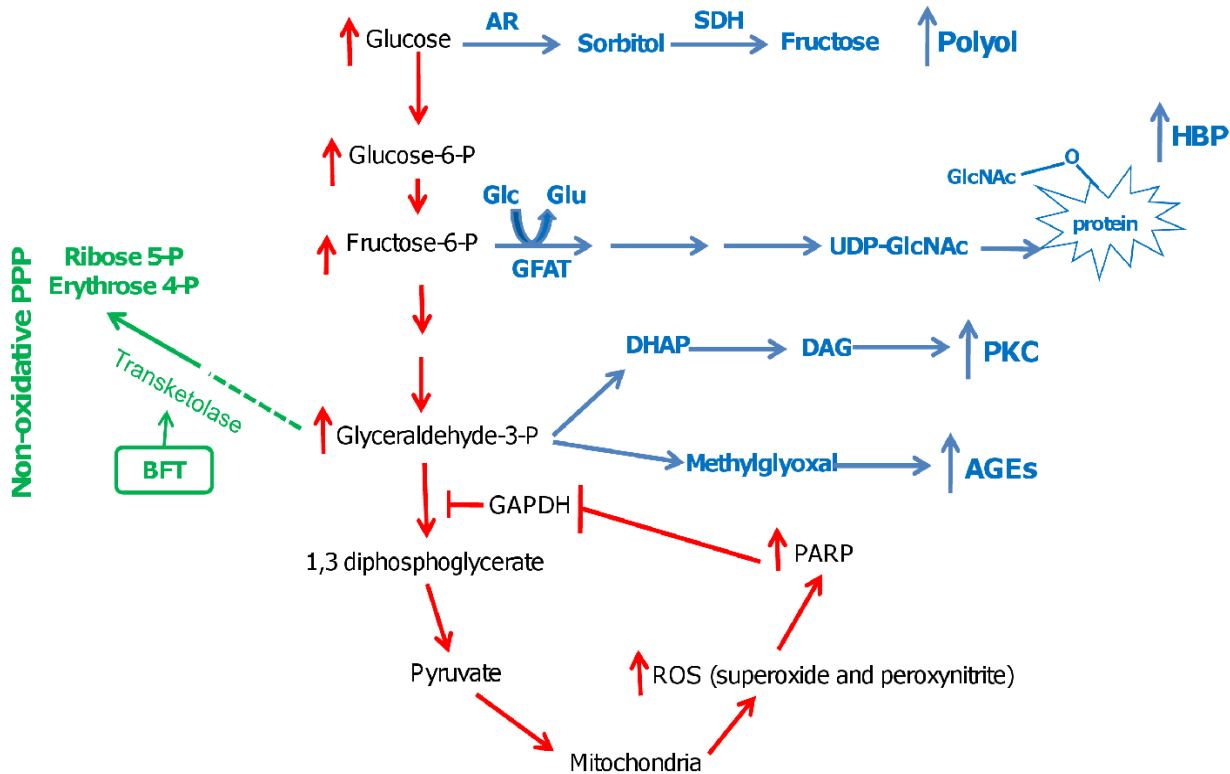


**Figure 4.1 Hyperglycemia activates non-oxidative pathways of glucose metabolism.** Under hyperglycemic conditions there is elevated glycolytic flux and increased mitochondrial ROS production. PARP is subsequently activated to restore DNA damage but also attenuate GAPDH activity leading to pooling of upstream glycolytic metabolites (refer red arrows). The latter subsequently fuels activation of non-oxidative pathways of glucose metabolism: polyol pathway, HBP, PKC and AGE (refer blue arrows and text). By contrast, BFT activates transketolase and the non-oxidative branch of the pentose phosphate pathway (PPP), thereby shunting flux away from the polyol, HBP, AGE and PKC pathways (refer green arrows and text). AR: aldose reductase; SDH: sorbitol dehydrogenase; Glc: glucosamine; Glu: glutamate; GFAT: glutamine: fructose-6-phosphate amidotransferase; UDP-GlcNAc: uridine diphosphate-*N*-acetylglucosamine; DHAP: dihydroacetone phosphate; DAG: diacylglycerol; ROS: reactive oxygen species.

Flux through the polyol, AGE, PKC and HBP can be inhibited by various inhibitors at different targets. In this study we used zopolrestat (ZOPO), aminoguanidine (AMG), chelerythrine chloride (CHE) and 6-diazo-5-norleucine (DON). It is imperative therefore to describe the pharmacology of these drugs. Firstly ZOPO/ Alond/ CP-73,8503/ 4-dihydro-4-oxo-3-[[5-(trifluoromethyl)-2-benzothiazolyl] methyl]-1-phthalazineacetic acid is a carboxylic acid that inhibits AR. ZOPO has been shown to normalize sorbitol, fructose and myo-inositol levels in sciatic nerve, retina and kidney in diabetic rats (6) and to normalize kidney function in galactosemic rats (100). The half maximal inhibitory concentration (IC<sub>50</sub>) of ZOPO against AR and its median effective dose (ED<sub>50</sub>) in the acute *in vitro* and *in vivo* test of diabetic complications were  $3.1 \times 10^{-9}$  M and 3.6 mg/kg, respectively. Under chronic test conditions the ED<sub>50</sub>s of ZOPO in reversing already elevated sorbitol accumulation in rat sciatic nerve, retina, and lens was reported to be 1.9, 17.6, and 18.4 mg/kg, respectively.

ZOPO is well absorbed in diabetic patients, resulting in high blood levels, and a highly favorable plasma half-life (27.5 h), and is undergoing further clinical evaluation (95). Furthermore, the mean steady-state maximum plasma concentration (C<sub>max</sub>) was reported to be 127 and 144 µg/ml, respectively, for normal and diabetic rats. The time of maximal plasma concentrations for nearly all tissues was 4 hr after oral dosing with 50 mg/kg, and the half-life of radioactivity in most tissues (8-10 hr) was similar to the half-life in plasma (63, 116). In rats less than 2% of ZOPO is excreted unchanged in urine after 48 hr following dosing (orally 50 mg/kg) with no accumulation in the liver and plasma; however it accumulates in nerve, kidney and lens (63). By contrast in humans after dosing with ZOPO (50- 1200 mg/kg orally) 34 to 45 % is excreted in urine after 48 hr with renal clearance ranging from 2.6 to 5.6 mL/min, and appeared to decrease as the dose was increased. In a 2-week multiple dose study, the mean steady-state minimum and maximum plasma concentrations, C<sub>min</sub> and C<sub>max</sub>, were 91.5 and 196 micrograms/mL for subjects administered 800 mg/day, and 131 and 281 micrograms/mL for subjects administered 1200 mg/day. Steady-state AUC(0-24) was also dose proportional. The mean steady state half-life of about 30.3 hours was consistent with the observed

2.2-fold accumulation in plasma. Apparent oral clearance ( $Cl_{po}$ ) was 5.2 mL/min, and apparent volume of distribution ( $V_{dss}/F$ ) was 12 L (62, 63).

Aminoguanidine/pimagedine is a diamine oxidase inhibitor that prevents formation of irreversible AGEs by trapping dicarbonyl compounds such as 3-deoxyglucosone (11, 131, 132). AMG was introduced in 1986, however, results from the phase III clinical trials showed that it had a high toxicity, low efficacy and increased urinary clearance (9, 41); therefore its development and use has been stopped. In addition to inhibition of AGEs formation, AMG is an inhibitor of NOS, more potent on iNOS, ( $IC_{50} = 31 \mu M$ ) than on nNOS ( $IC_{50} = 170 \mu M$ ) and eNOS ( $IC_{50} = 330 \mu M$ ) (23). Because the  $IC_{50}$  of AMG for inhibition of protein glycation in humans is  $203 \mu M$  (80), it is likely that it also inhibits iNOS and nNOS (132). AMG has shown antioxidant effects in various experimental models, for example by quenching hydroxyl radicals and lipid peroxidation (45, 60, 107). In several models of diabetes, AMG has shown an improvement of renal (39, 124), cardiac (99) and nerve function (48).

CHE is a benzophenanthridine alkaloid that interacts with the catalytic domain of PKC (52). It is considered a highly specific PKC inhibitor ( $IC_{50}$  of  $0.66 \mu M$ ) with a number of other effects such as activation of caspase 3 leading to induction of apoptosis, induction (127) with cyclic nucleotide phosphodiesterases (38) and inositol metabolism (24). It also inhibits other kinases such as protein kinase A, calcium/calmodulin dependent protein kinase with  $IC_{50}$  ranging 100 to  $170 \mu M$  (52). Several other effects of CHE have been reported and these include: inhibition of thymidine incorporation into DNA (3), inhibition of alanine aminotransferase ( $IC_{50}$  of  $4 \mu M$ ) (137) and  $Na^+/K^+$ -ATPase ( $IC_{50}$  of 30- $50 \mu M$ ) (22). Additionally it has anti-platelet activity (71) and is cytotoxicity in L-1210 tumor cells ( $IC_{50}$  of  $0.53 \mu M$ ) (52).

Lastly, 6-diazo-5-oxo-L-norleucine (DON) is a non-standard amino acid antibiotic that antagonizes glutamine and was first isolated from *Streptomyces* in a sample of Peruvian soil (31). It has been shown to possess antitumor properties in different animal models (149) and clinical trials but was

never approved (92). DON is a water soluble yellowish powder which can also be dissolved in aqueous solutions of methanol, acetone or ethanol. It is used as an inhibitor of various glutamine utilizing enzymes due to its similarity to glutamine by covalently binding to their catalytic centres (103, 106). DON is reported to be a cytotoxic inhibitor of many nucleotide synthesis enzymes *in vitro* leading to apoptosis (53, 142). More recently we have shown beneficial effects of DON under hyperglycemic conditions through inhibition of GFAT an amidotransferase. This effect was associated with decreased oxidative stress and apoptosis (53, 109, 110, 142).

## 4.2 Materials and Methods

### 4.2.2 Animals and ethics statement

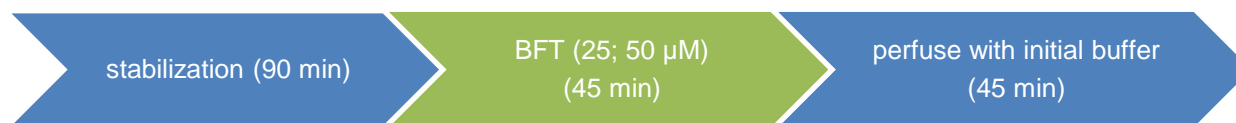
All animals were treated in accordance with the Guide for the Care and Use of Laboratory Animals of the National Academy of Sciences (NIH publication No. 85-23, revised 1996). The study was carried out with the approval of the Animal Ethics Committees of Stellenbosch University and the University of Cape Town (South Africa) (see Appendices 1 and 2, respectively).

### 4.2.3 *Ex vivo* global ischemia during simulated acute hyperglycemia

Male Wistar rats weighing 180-220 gr were used throughout the study. Rats were anesthetized (pentobarbitone, 100 mg/kg i.p) and hearts rapidly excised and perfused in a modified Langendorff model as described before (84). Briefly, Krebs-Henseleit buffer containing (in mM) 11 Glucose, 118 NaCl, 4.7 KCl, 1.2 MgSO<sub>4</sub>·7H<sub>2</sub>O, 2.5 CaCl<sub>2</sub>·2H<sub>2</sub>O, 1.2 KH<sub>2</sub>PO<sub>4</sub>, 25 NaHCO<sub>3</sub> (refer to Appendix 3 for preparation of the buffer) was equilibrated with 95% O<sub>2</sub>-5% CO<sub>2</sub> (37°C, pH 7.4) at a constant pressure (100 cm). Buffer was not recirculated and the hearts were allowed to beat at their natural rate. During perfusion, a latex balloon attached to a pressure transducer (Stratham MLT 0380/D, ADInstruments Inc, Bella Vista NSW, Australia) compatible with the PowerLab System ML410/W (ADInstruments Inc, Bella Vista NSW, Australia) was inserted into the left ventricle via the mitral valve and inflated to produce a systolic pressure of 80-120 mmHg and a diastolic pressure of 4-12 mm Hg. The temperature of the heart was maintained at 37°C by suspending it in a heated water jacket. Contractile parameters assessed throughout the experiment included heart rate (HR), left ventricular developed pressure (LVDP), end diastolic pressure, end systolic pressure, coronary flow and rate-pressure product (RPP = HR x LVDP).

Hearts were randomly distributed into three initial experimental groups for perfusions: 1) baseline control (11 mM glucose)  $\pm$  BFT; and 2) high glucose (22 mM glucose)  $\pm$  BFT (n=6 for each group) and high glucose (33 mM glucose)  $\pm$  BFT (n=6 for each group). High glucose perfusions were used to simulate acute hyperglycemia within the clinical setting. The buffer mimics the key ionic content of rat plasma or blood (51, 123) and it does not result in any hemodynamic dysfunction in the *ex vivo* heart perfusion system (25). Moreover, since *ex vivo* Langendorff perfusions are typically performed with 11 mM glucose at baseline, we are of the opinion that the 22 mM and 33 mM concentrations are representative of a 2-fold and 3-fold elevation of glucose levels (above normal), respectively, within the clinical setting. After these initial experiments further work was done using only 11 mM and 33 mM  $\pm$  and the highest concentration of BFT as these concentrations showed a more clear significant difference.

**A**



**B**



**C**



**Figure 4.2** Schematic diagrams showing the perfusion protocols for assessment of effects BFT on heart contractile function without ischemia (A), with ischemia (B) and on infarct size (C).

Our initial experiments were carried out to determine the BFT concentration to use, and here we employed a non-ischemic protocol, where hearts exposed to baseline glucose (11 mM) were allowed

to stabilize for 90 min whereafter 25 or 50  $\mu\text{M}$  BFT was added to the perfusate for 45 min (refer Figure 4.2A). Subsequently, hearts were perfused for a further 45 min with the same buffer used in the stabilization period (total perfusion time: 180 min). The ischemia and reperfusion protocol comprised a 90 min stabilization period, 30 min of global ischemia and 60 min of reperfusion. The cardio-protective effects of various concentrations of BFT (25, 50 and 100  $\mu\text{M}$ ), added during the first 20 min of reperfusion, were evaluated (see Figure 4.2B). Additional experiments were carried out in order to rule out the effects of osmotic pressure on heart function. Here hearts were perfused with 22 mM mannitol plus 11 mM glucose (total molarity = 33 mM) and subjected to ischemia and reperfusion as before.

To assess the contribution and activation of each of the hyperglycemia-induced pathways (AGE, PKC, HBP and polyol), specific pathway inhibitors were added to the perfusate (similar to BFT treatments). These experiments were carried out for both control and hyperglycemic groups using the ischemia reperfusion protocol, as outlined above. The following inhibitors (purchased from Sigma Aldrich, St Louis MO) were employed: AGE pathway - AMG (100  $\mu\text{M}$ ); PKC - CHE (5  $\mu\text{M}$ ); HBP – DON (40  $\mu\text{M}$ ); and polyol pathway - ZOPO (1  $\mu\text{M}$ ) (see Figure 4.3). All doses used were selected based on previously published studies (29, 30, 134, 146). At the end of each experiment hearts were removed and ventricular tissue was freeze-clamped with pre-cooled Wollenberger tongs whereafter it was stored at  $-80^{\circ}\text{C}$  for further molecular and biochemical analysis.



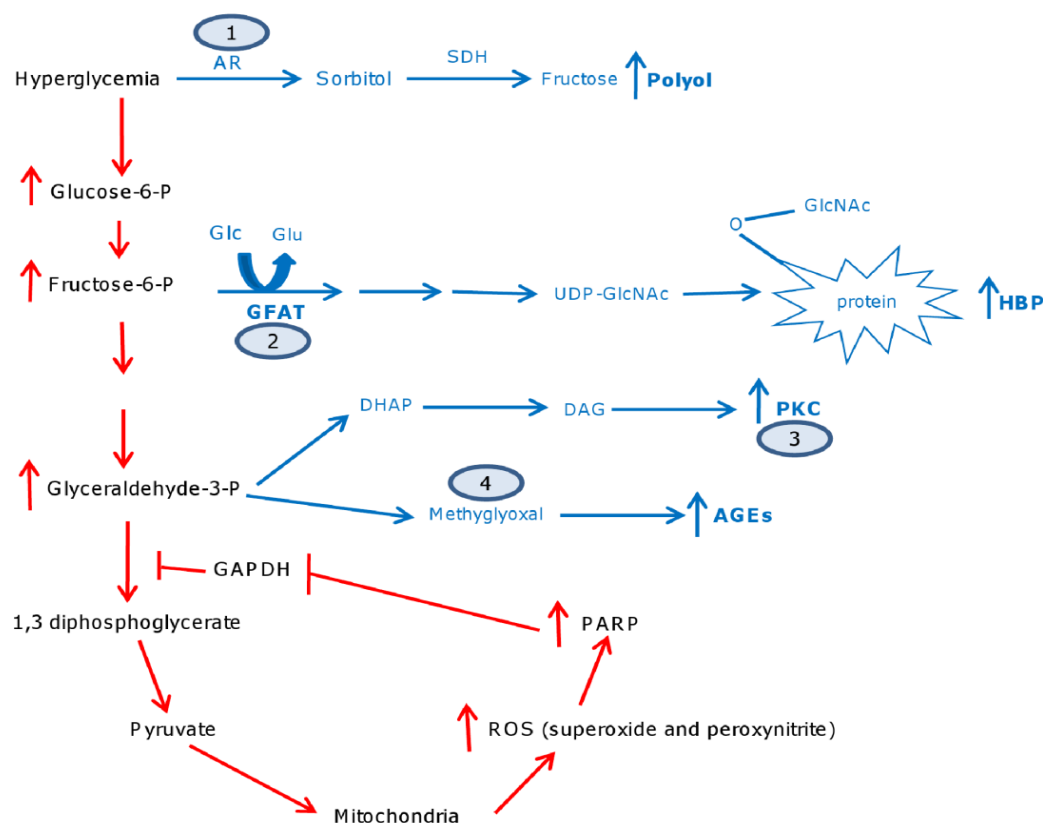


**Figure 4.3 Target sites for inhibition of non-oxidative glucose pathways.** Under hyperglycemic conditions there is elevated glycolytic flux and increased mitochondrial ROS production. PARP is subsequently activated to restore DNA damage but also attenuate GAPDH activity leading to pooling of upstream glycolytic metabolites (refer red arrows). The latter subsequently fuels activation of non-oxidative pathways of glucose metabolism: polyol pathway, HBP, PKC and AGE (refer blue arrows and text) which can be inhibited by (1) zopolrestat; (2) 6-diazo-5-oxo-L-norleucine; (3) chelerythrine chloride and (4) aminoguanidine, respectively. AR: aldose reductase; SDH: sorbitol dehydrogenase; Glc: glucosamine; Glu: glutamate; GFAT: glutamine: fructose-6-phosphate amidotransferase; UDP-GlcNAc: uridine diphosphate-N-acetylglucosamine; DHAP: dihydroacetone phosphate; DAG: diacylglycerol; ROS: reactive oxygen species.

#### 4.2.4 *Ex vivo* regional ischemia and reperfusion during simulated acute hyperglycemia

Perfusion experiments were carried out by employing male Wistar rats (180-220 gr) to determine the effect of BFT treatment on infarct size in our experimental system. This was performed using regional ischemia with a reperfusion time of 2 hr, as described previously (84). A 3/0 silk suture was placed around the proximal portion of the left anterior descending coronary artery. The ends of the suture were passed through a plastic tube to form a snare. For induction of regional ischemia, the snare was

occluded. After 20 min, the snare was released to initiate reperfusion. The efficacy of ischemia was confirmed by regional cyanosis and a substantial decrease in coronary flow.

#### **4.2.5 Determination of infarct size**

After completion of each regional ischemia and reperfusion experiment the snare was re-tightened and 2.5% Evans blue dye (in Krebs buffer) was perfused through the hearts for identification of the area at risk of ischemia. Hearts were subsequently removed from the Langendorff apparatus, blotted dry, suspended (using suture) within 50 ml plastic tubes and frozen at -20°C for 3 days. Thereafter, frozen hearts were sliced into 2 mm transverse sections and incubated with 1% 2,3,5-triphenyl tetrazolium chloride (TTC) in phosphate-buffered saline for 20 min at 37°C to distinguish non-infarcted (stained) from infarcted (non-stained) tissues. The area that was not stained with Evans Blue was defined as the area at risk (AAR). The area which demonstrated neither blue nor red was defined as the infarct site. Slices were then fixed in 10% formalin for 24 hr at room temperature before being placed between glass plates for scanning for preparation of the phosphate buffered saline). The infarct size (IS) and the area at risk (AAR) were determined using Image J software (v1.46p, National Institutes of Health, USA) as described in Appendices 11 and 12. Infarct size was expressed as a percentage of the AAR.

#### **4.2.6 *In vivo* regional ischemia and reperfusion in streptozotocin-treated rats (chronic hyperglycemia)**

The effects of BFT on infarct size in diabetic rats (chronic hyperglycemia) were assessed using an *in vivo* model of ischemia and reperfusion injury. These experiments were completed at the University of Cape Town (South Africa). Hyperglycemia was induced in Wistar rats as previously described (84, 85, 94). In brief, age-matched male Wistar rats weighing 250-300 gr were injected with a single dose of streptozotocin (STZ) (60 mg/kg, i.p). Control rats were injected with the vehicle (0.1 M citrate buffer,

pH 6.2; see Appendix 13). Blood glucose concentrations were measured using an Accu-Chek glucose monitor (Boehringer Mannheim Diagnostics, Indianapolis IN), and glucose levels of  $\geq 20$  mmol/l after one week were considered as a stable diabetic state. Body weights and non-fasting blood glucose levels before STZ induction and after a week of diabetes induction were also recorded.

For the *in vivo* coronary artery ligation experiments, rats were divided into control (citrate-treated) and diabetic (STZ-treated) groups. Each group was subjected to coronary artery ligations  $\pm$  BFT treatment (0.5 mg/kg i.v) (as described in detail below). The BFT was dissolved in 0.9% saline immediately prior to administration. Ligation experiments were performed one week after STZ injection and confirmation of a stable diabetic state. Rats were anesthetized with sodium pentobarbital (60 mg/kg i.p.), intubated, and thereafter ventilated with room air (2.5 ml/stroke) at a rate of 75 strokes per min via a rodent ventilator (Model 681, Harvard Apparatus, Holliston MA). Body temperature was monitored by a rectal temperature probe and a constant temperature was maintained throughout the surgical procedure by placing rats on a custom-made heating block. The depth of anesthesia was checked by assessing the pedal withdrawal reflex and by monitoring heart rate. Maintenance doses of anesthetic (6 mg/kg i.p) were administered as required. Lead II electrocardiogram (ECG) was recorded via an Animal Bio Amplifier (ML136, ADInstruments, Bella Vista NSW, Australia). Carotid arterial blood pressure was recorded via a custom-made cannula attached to a pressure transducer (MLT0670, ADInstruments, Bella Vista NSW, Australia). Since formation of clots around intra-arterial cannulae poses a potential risk for arterial thrombosis, heparin (1000 IU/kg i.p) was injected concurrently with anesthetic (84).

A left thoracotomy was performed through the 4<sup>th</sup> intercostal space and the left lung collapsed using a damp swab. The left anterior descending coronary artery was thereafter ligated as previously described (84). A 5/0 silk suture was placed around the left anterior descending coronary artery and its ends passed through a plastic tube to form a snare. For induction of regional ischemia the snare was occluded for 30 min. The efficacy of ischemia was confirmed by regional cyanosis and ECG changes. S-T elevation (ECG) was used to confirm coronary artery ligation. After 30 min, the snare was

released to initiate reperfusion. Rat hearts were subjected to 30 min ischemia followed by 2 hr of reperfusion. The penile vein was cannulated for drug administration. BFT rats were given a bolus concentration of BFT (0.5 mg/kg i.v) (135) at the onset of reperfusion (within 1 min of releasing the snare) and thereafter reperfused for 2 hr as before. Vehicle solution was administered to control rats. After the reperfusion period, the heart was removed, flushed with saline and the coronary artery was re-occluded with the suture that had been left in place. The heart was then stained with 2.5% Evans blue to reveal the AAR. TTC staining and infarct sizes were determined as described for the *ex vivo* model.

#### **4.2.7 Myocardial superoxide levels**

The heart tissue was pulverized and homogenized in 100 volumes of perchloric acid (10% v/v) and centrifuged for 20 min at 13, 000 *g* (65). Protein-free supernatant (0.1 ml) was subsequently incubated with 0.25 mM lucigenin (Sigma-Aldrich, St. Louis MO) at room temperature for 5 min in the dark and chemiluminescence measured in a white-walled luminometer 96-well microtiter plate (Corning Inc, Corning NY). Superoxide levels were expressed as chemiluminescence (RLU) per mg tissue.

#### **4.2.8 Measurement of superoxide dismutase (SOD) activity**

We assessed the total SOD activity (cytosolic and mitochondrial components) as detailed in the instructions of a commercially obtained kit (Biovision K335-100, Mountain View CA). The assay depends on utilizing a highly water-soluble tetrazolium salt, WST-1 (2-(4-iodophenyl)-3-(4-nitrophenyl)-5-(2,4-disulfo-phenyl)-2H-tetrazolium, monosodium salt), that produces a water-soluble formazan dye upon reduction with a superoxide anion. The rate of WST-1 reduction by superoxide anion is linearly related to the xanthine oxidase activity and is inhibited by SOD. Formazan levels can be measured by absorption with a spectrophotometer at 450 nm.

Briefly, collected heart tissues were homogenized with modified ice-cold RIPA buffer (see Appendix 5), the supernatant centrifuged twice at 4, 300 g for 10 min at 4°C. The samples were incubated with the enzyme and WST working solutions for 20 min at 37°C in a 96-well microtiter plate (Corning Inc, Corning NY) in an orbital shaker incubator. Absorbance was read at 450 nm with a microplate reader (EL 800 KC Junior Universal Microplate reader, Bio-Tek Instruments, Winooski VT). Optimization of the kit was done using a negative and a positive control provided with the kit. SOD activity was calculated according to the following formula: % inhibition =  $(A_{\text{control}} - A_{\text{sample}})/A_{\text{control}} \times 100$ . Lower absorbance of the reaction mixture indicated greater activity.

#### **4.2.9 Isolation of proteins for carbonylation and proteasome activity experiments**

Heart tissues were cut into small slices and homogenized in 1 ml of Tris-HCl buffer (pH 7.4) using an IKA Ultra Turrax T25 homogenizer (IKA Labortechnik, Staufen, Germany) and incubated on ice for 10 min before centrifugation at 9, 000 g for 15 min to remove cell debris. The supernatant was used for protein quantification using the BCA assay.

#### **4.2.10 ELISA carbonyl protocol**

Protein carbonyls are formed by a variety of oxidative mechanisms and are sensitive indices of oxidative injury. Protein carbonylation was determined by the carbonyl ELISA assay developed in the GEICO laboratory (Université de La Réunion, Saint Denis de La Réunion, France) based on recognition of protein-bound DNPH in carbonylated proteins with an anti-DNP antibody (115). Here 5 µl of protein from tissue lysates (0.2-0.6 µg) was denatured by adding 10 µl 12% SDS solution. Subsequently, proteins were derivatized to DNP hydrazone with 10 µl of DNPH solution (10 mM in 6 M guanidine hydrochloride, 0.5 M potassium phosphate buffer, pH 2.5). DNPH is a chemical compound that specifically reacts and binds to carbonylated proteins. Samples were incubated at room

temperature for 30 min and the reaction was neutralized and diluted in coating buffer (10 mM sodium carbonate buffer, pH 9.6) to yield a final protein concentration of 0.2 - 0.6 ng/ $\mu$ l.

Diluted samples were added to wells of a Nunc Immuno Plate Maxisorp (Dutscher, Brumath, France) and incubated at 37°C for 3 hr, and thereafter washed 5x with PBS/Tween (0.1%) between each of the following steps: blocking the wells with 1% BSA in PBS/Tween (0.1%) overnight at 4°C; incubation with anti-DNP antibody (Sigma-Aldrich, St Louis, MO) (1:2000 dilution in PBS/Tween [0.1%]/BSA [1%]) at 37°C for 3 hr; incubation with horse radish peroxidase-conjugated polyclonal anti-rabbit immunoglobulin (GE Healthcare, Mannheim, Germany) (1:4000 dilution in PBS/Tween [0.1%]/BSA [1%]) for 1 hr at 37°C; addition of 100  $\mu$ l of TMB substrate solution and incubation for 10 min before stopping the coloration with 100  $\mu$ l of 2 M sulphuric acid. Absorbances were read at 490 nm against the blank (DNP reagent in coating buffer without protein) with a Fluostar microplate reader (BMG Labtech, Ortenberg, Germany). Results are expressed as percentage of absorbance compared to control cells (treatment of samples with 11 mM glucose) after normalization with protein concentrations.

#### 4.2.11 Proteasome activity measurements

Chymotrypsin-like, trypsin-like, and caspase-like activities of the proteasome were assayed using fluorogenic peptides (Sigma-Aldrich, St Louis, MO): Suc-Leu-Leu-Val-Tyr-7-amido-4-methylcoumarin (LLVY-MCA at 25  $\mu$ M), N-t-Boc-Leu-Ser-Thr-Arg-7-amido-4-methylcoumarin (LSTR-MCA at 40  $\mu$ M) and N-Cbz-Leu-Leu-Glu-b-naphthylamide (LLE-NA at 150  $\mu$ M), respectively (42). Assays were performed with ~50  $\mu$ g of protein lysate (in 25 mM Tris-HCl, pH 7.5) and the appropriate substrate that were incubated together for 0-30 min at 37°C. Aminomethylcoumarin and  $\beta$ -naphthylamine fluorescence were measured at excitation/emission wavelengths of 350/440 and 333/410 nm, respectively, using a Fluostar fluorometric microplate reader (BMG Labtech, Ortenberg, Germany). Peptidase activities were measured in the absence/presence of 20  $\mu$ M of the proteasome inhibitor,

MG132 (N-Cbz-Leu-Leu-leucinal), and the difference between the two values was attributed to proteasome activity. Data were normalized to protein concentrations.

#### **4.2.12 Evaluation of myocardial apoptosis**

We evaluated apoptosis by employing a caspase activity assay (Biovision, Mountain View CA). Briefly, tissues were homogenized with modified ice-cold RIPA buffer (see Appendix 5), the supernatant centrifuged twice at 13, 000 *g* for 10 min at 4°C and protein levels determined by the Bradford assay. The caspase activity assay is based on spectrophotometric detection of the chromophore, *p*-nitroaniline (pNA), after cleavage of the labeled substrate amino acid sequence Asp-Glu-Val-Asp (DEVD)-pNA. The samples were added onto a 96-well microtiter plate (Corning Inc, Corning NY) and incubated with the reaction mixture and DEVD-pNA for 2 hr at 37°C for 60 min in an orbital shaker incubator. The color intensity was quantified with a microplate reader (EL 800 KC Junior Universal Microplate reader, Bio-Tek Instruments, Winooski VT) at 505 nm. The caspase activity was expressed as arbitrary units per mg protein.

We further ascertained myocardial apoptosis by performing Western blotting analysis for the pro-apoptotic factors, BAD and caspase-3, as described (109). The detailed protocol for SDS-PAGE, sample preparation and Western blotting is described in detail in Appendices 6-10. Briefly, collected heart tissues were homogenized with modified ice-cold RIPA buffer (see Appendix 5), the supernatant was centrifuged twice at 13, 000 *g* for 10 min at 4°C then stored at -80°C until further use. Protein expression was determined by SDS-PAGE as described before by us (109, 110) for total BAD and caspase-3 (Cell Signaling, Danvers MA). Protein expression was quantified by densitometric analysis and  $\beta$ -actin (Cell Signaling, Danvers MA) employed as a loading control.

#### 4.2.13 PARP assay

Poly ADP-ribosylation of nuclear proteins is a post-translational event that occurs in response to DNA damage. PARP catalyzes the NAD-dependent addition of poly(ADP-ribose) to itself and adjacent nuclear proteins such as histones. The assay was carried out as stipulated by the manufacturers (Trevigen, Gaithersburg MD). Briefly, collected heart tissues were homogenized with modified ice-cold RIPA buffer (see Appendix 5), the supernatant was centrifuged twice at 4, 300 g for 10 min at 4°C. The wells of the 96 well-plate were initially rehydrated with 50 µl of the 1x PARP buffer and incubated at room temperature for 30 min. For the standard curve the PARP enzyme was diluted such that the total activity ranged between 0.00 to 1 unit per 25 µl, with the 0/blank wells acting as negative controls. This was added to the first wells of the 96-well plate and 25 µl of each sample to be tested added to the remaining wells. Thereafter 25 µl of the 1x PARP cocktail (contains the PARP cocktail, activated DNA and PARP buffer) was added to the wells and the plate was incubated at room temperature for 60 min. The wells were then washed with 1x PBS (see Appendix 14) and 0.1% Triton X-100 (200 µl/well) followed by two washes with 1x PBS, and tapping wells onto paper towels. Strep-HRP was then added to the wells and the plate incubated for 60 min at room temperature (on a shaker). The washing and drying steps were repeated before addition of the pre-warmed TACS-Sapphire™ colorimetric substrate, followed by 15 min incubation in the dark at room temperature. The reaction was stopped by 5% phosphoric acid and readings done at 450 nm using a micro plate reader (EL 800 KC Junior Universal Microplate reader, Bio-Tek Instruments, Winooski VT).

#### 4.2.14 GAPDH assay

We utilized a GAPDH activity assay according to the kit's instruction manual (Biomedical Research Service Centre, University at Buffalo NY). The assay is based on the reduction of a water-soluble tetrazolium salt, 2-(4-Iodophenyl)-3-(4-nitrophenyl)-5-phenyl-2H-tetrazolium chloride, to formazan



(NADH-coupled reaction) exhibiting an absorption maximum at 492 nm. The intensity of the red color produced corresponds to the degree of GAPDH activity.

Briefly, tissue samples were lysed with cell lysis buffer and protein concentrations diluted to fall within 0.2-2 mg/ml range as stipulated in the kit's manual. Ten  $\mu$ l of each sample was thereafter pipetted onto the 96-well plate (Corning Inc, Corning NY) and the reaction initiated by adding 50  $\mu$ l of the GAPDH assay solution to each well. The plate was incubated at 37°C for 60 min in an orbital shaker incubator. The reaction was stopped by addition of 50  $\mu$ l of 3% acetic acid and the absorbance measured at 492 nm using a microplate reader (EL 800 KC Junior Universal Microplate reader, Bio-Tek Instruments, Winooski VT). GAPDH activity is expressed as the absorbance units per mg protein.

#### **4.2.15 Determination of non-oxidative pathway activation**

##### **4.2.15.1 AGE**

Methylglyoxal (MG) derivatives are formed from the non-enzymatic reaction of reducing carbohydrates such as glucose and carbonyl compounds (glyceraldehyde) in the Maillard reaction - products of this reaction are referred to as AGEs. Therefore, MG concentrations, measured using the OxiSelect™ Methylglyoxal (MG) ELISA Kit (Cell Biolabs, San Diego CA), were used as a marker for AGE pathway activation. The kit measures the quantity of MG adduct in protein samples by comparing its absorbance with that of a known MG-BSA standard curve.

Briefly, tissues were homogenized in modified ice-cold RIPA buffer (see Appendix 5) and the supernatant was centrifuged twice at 13,000 *g* for 10 min at 4°C. Protein quantification was performed using the Bradford assay. Standards (including a negative and a positive control) and protein samples were pipetted onto the 96-well plate (Corning Inc, Corning NY). Thereafter the plate was incubated overnight at 4°C for the MG in the standard and protein samples to adsorb onto plate wells. This was

followed by probing with an anti-MG specific monoclonal antibody for 60 min at room temperature on an orbital shaker. After a series of washing steps, an HRP-conjugated secondary antibody was added to all wells and incubated for an hour at room temperature. A substrate solution was next added and incubated for 5 - 20 min at room temperature on an orbital shaker to allow for color development. The latter reaction was terminated by adding a 'stop solution' before reading absorbances at 450 nm with a microplate reader (EL 800 KC Junior Universal Microplate reader, Bio-Tek Instruments, Winooski VT). MG levels were calculated from the standard curve and are expressed as nmol per  $\mu\text{g}$  protein.

#### **4.2.15.2 PKC assay**

The PKC assay was carried out as detailed in the kit's instruction manual (Enzo Life Sciences, Farmingdale NY). This is an ELISA-based method where a synthetic substrate is used for PKC activation that is measured by employing a polyclonal antibody that recognizes its phosphorylated form. Samples were homogenized in modified ice-cold RIPA buffer (see Appendix 5) and the supernatant was centrifuged twice at 13, 000  $g$  for 10 min at 4°C. The active PKC control provided was serially diluted and added onto a 96-well microtiter plate (Corning Inc, Corning NY) as positive controls whereas the blanks were the negative controls. The tissue samples were subsequently added to appropriate wells, followed by ATP addition to initiate the reaction. The plate was thereafter incubated for 90 min at 30°C and the kinase reaction then terminated by emptying contents of each well. We next added the phosphospecific substrate to wells followed by an incubation step for 60 min at room temperature. A peroxidase-conjugated secondary antibody was thereafter added and the assay was developed with tetramethylbenzidine substrate, where the color intensity is proportional to PKC phospho-transferase activity. Color development was stopped with an acid solution and color intensity recorded in a microplate reader (EL 800 KC Junior Universal Microplate reader, Bio-Tek Instruments, Winooski VT) at 450 nm. PKC activity was determined from the standard curve and expressed per volume of lysate per minute.

#### 4.2.15.3. Hexosamine biosynthetic pathway (HBP)

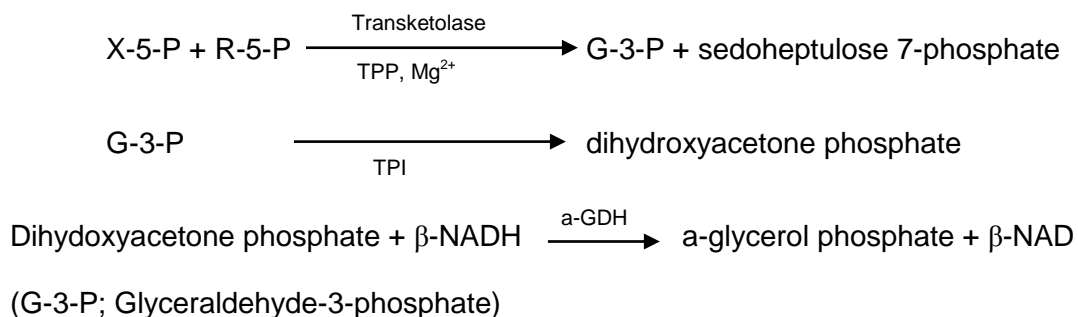
We employed Western blotting analysis to determine myocardial HBP activation in response to ischemia and reperfusion under high glucose conditions. Briefly, collected heart tissues were homogenized with modified ice-cold RIPA buffer (see Appendix 5), the supernatant was centrifuged twice at 13, 000 g for 10 min at 4°C then stored at -80°C until further use. Total O-GlcNAc expression was determined by SDS-PAGE as described before by us (84) (see Appendices 6-10) using an O-GlcNAc antibody (CTD110.6, Santa Cruz Biotechnology, Santa Cruz CA). Total O-GlcNAcylation (per lane) was quantified by densitometric analysis, and  $\beta$ -actin (Cell Signaling, Danvers MA) was utilized as a loading control for all blots.

#### 4.2.15.4 Polyol pathway

D-sorbitol, an intermediate of the polyol pathway, was measured as an index of the activity of this pathway. Total D-sorbitol levels (cytosolic and mitochondrial components) were measured as detailed in the instructions of a commercially obtained kit (Biovision K 631-100, Mountain View CA). Briefly, collected heart tissues were homogenized with modified ice-cold RIPA buffer (see Appendix 5) and the supernatant was centrifuged twice at 13, 000 g for 10 min at 4°C. Samples and optimizing standards with controls (negative and positive) were subsequently incubated with 50  $\mu$ l of the reaction mixture (assay buffer, enzyme mix, developer and probe) for 30 min at 37°C in a 96-well microtiter plate (Corning Inc, Corning NY) in an orbital shaker incubator. Sorbitol levels were determined by evaluating the oxidation of sorbitol to fructose and the reaction's absorbance was recorded at 560 nm with a microplate reader (EL 800 KC Junior Universal Microplate reader, Bio-Tek Instruments, Winooski VT). We calculated the sorbitol concentration (C) of samples by using the sample amount (nmol) from the standard curve ( $S_a$ ), sample volume ( $\mu$ l) used ( $S_v$ ) and the dilution factor (D);  $C = S_a / S_v * D$ .

#### 4.2.15.5 Non-oxidative pentose phosphate pathway (PPP)

We used a modified protocol (EC 2.2.1.1) from Sigma Aldrich (St. Louis MO) to determine transketolase activity as a marker for non-oxidative PPP activation. The reagents used were of analytical grade and purchased from Sigma Aldrich (St. Louis MO) and included: 216 mM glycylglycine buffer, 3.3 mmol/l xylulose 5-phosphate (X-5-P), 1.7 mmol/l ribose 5-phosphate (R-5-P), 0.002% (w/v) cocarboxylase (thiamine pyrophosphate solution) (TPP), 0.14 mmol/l reduced  $\beta$ -nicotinamide adenine dinucleotide ( $\beta$ -NADH), 15 mmol/l magnesium chloride ( $\text{MgCl}_2$ ), 20 units  $\alpha$ -glycerophosphate dehydrogenase/triophosphate isomerase enzyme solution ( $\alpha$ -GDH/TPI) and transketolase enzyme solution. The detailed protocol for the assay is in Appendix 16. The principle of the assay is based on the reactions below:



Briefly, heart tissues were homogenized in ice-cold RIPA buffer (see Appendix 5) and protein concentrations determined by the Bradford assay. The chemical reagents were freshly prepared and pipetted into a 96-well plate (Corning Inc, Corning NY) and mixed on an orbital shaker at room temperature. Absorbance was monitored using a microplate reader (EL 800 KC Junior Universal Microplate reader, Bio-Tek Instruments, Winooski VT) until constant, whereafter the samples and enzyme solution were added and the relative decrease in absorbance monitored for 10 min. In the assay the blank was used as the negative control and the enzyme solution for standards as positive controls.

Transketolase activity was calculated as follows:

$$\text{Units/ml of enzyme} = \frac{(\Delta A_{340\text{nm}} / \text{min test} - \Delta A_{340\text{nm}} / \text{min blank}) (0.3)(\text{df})}{(6.22)(0.01)}$$

$$\text{The values were presented as units/mg protein} = \frac{\text{units / ml enzyme}}{\text{mg protein / ml enzyme}}$$

( $\Delta$ - change increment; A-absorbance; df-dilution factor; ml-milliliter; mg-milligram;  
 6.22 = millimolar extinction coefficient of  $\beta$ -NADH at 340 nm;  
 0.01 = volume (in milliliters) of enzyme used; 0.3 = total volume (in milliliters) of assay)

#### 4.2.16 Statistical analysis

Data are presented as mean  $\pm$  standard error of mean (SEM). Differences between treatment groups and time points were analyzed using one way analysis of variance (ANOVA). Mann-Whitney unpaired t-test was used when comparisons were made between only two groups. Significant changes between groups were further assessed by means of the Tukey –Kramer *post hoc*. All statistical analyses were performed using GraphPad Prism version 5.01 (Graphpad Software, Inc, San Diego, USA). Values were considered significant when  $p < 0.05$ .

## 4.3 Results

### 4.3.1 Acute high glucose exposure impairs contractile heart function following ischemia and reperfusion

Our results indicate that acute hyperglycemia during the onset of ischemia and reperfusion elicits detrimental effects on the heart as shown by the reduced LVDP (Figure 4.4A) and RPP recovery (Figure 4.4B,  $p < 0.05$  vs. control). In control hearts, LVDP improved to  $42.2 \pm 3.9\%$  whereas high glucose perfused hearts recovered to only  $20.8 \pm 4.6\%$  after 60 min of reperfusion. Likewise RPP recovered much better in control hearts compared to hyperglycemic hearts after 60 min of reperfusion ( $39.5 \pm 3.7\%$  vs.  $11.0 \pm 2.6\%$ ,  $p < 0.05$ ). To rule out the possibility of attributing the effects of hyperglycemia on heart function to changes in osmolarity, we performed separate experiments where we perfused with 11 mM glucose plus 22 mM mannitol (mannitol control- total molarity 33 mM). Our data demonstrate higher LVDP and RPP recovery for the osmotic control group compared to hearts perfused under high glucose conditions ( $p < 0.05$ ) (Figure 4.4C and 4.4D). LVDP of the osmotic control improved to  $35.7 \pm 6.7\%$  of baseline and RPP to  $37.5 \pm 3.7\%$  of baseline compared to the respective high glucose perfused hearts.

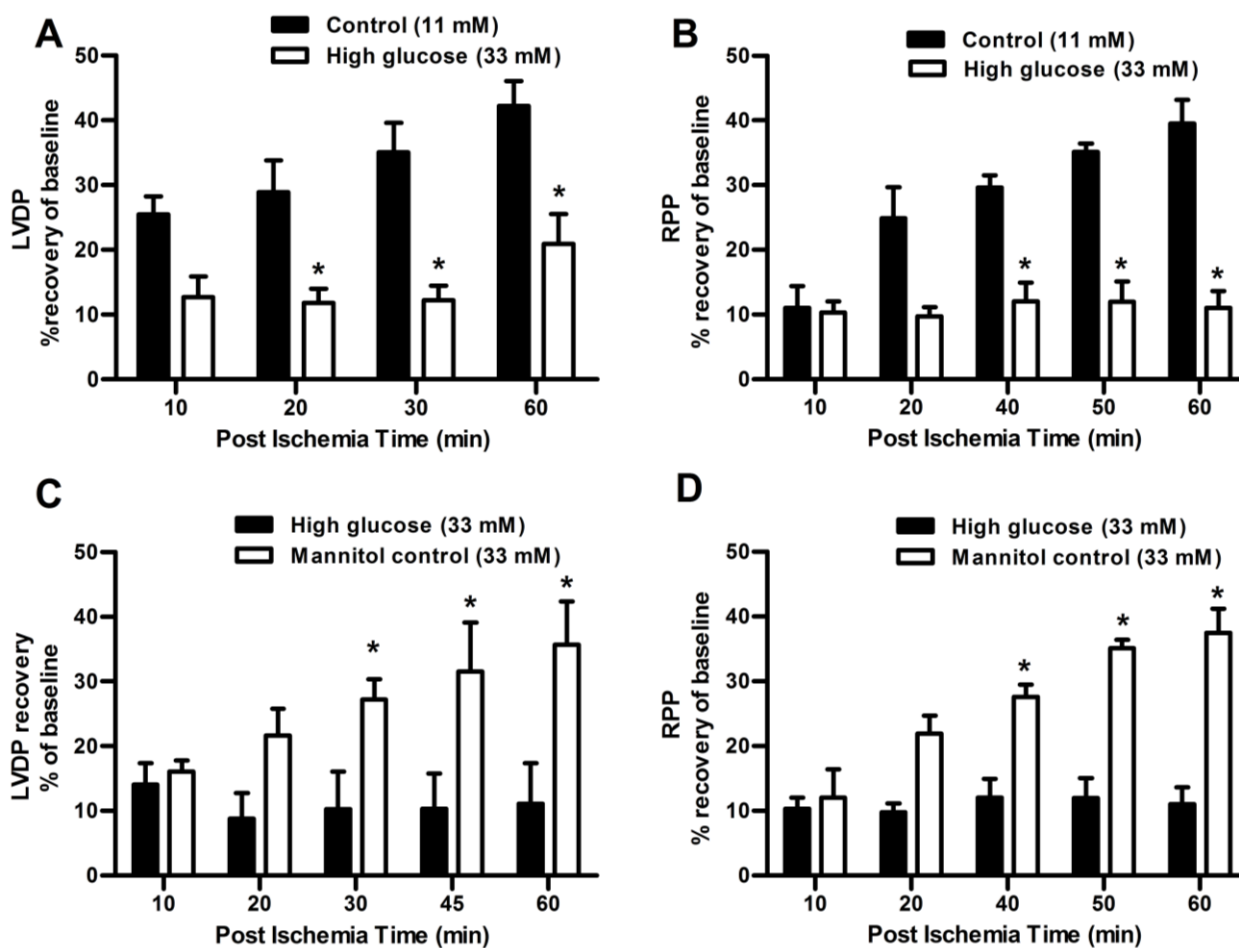


**Figure 4.4 High glucose-induced cardiac contractile dysfunction indicated by the decrease in % recovery of both LVDP and RPP in rat hearts exposed to high glucose conditions vs. hearts at baseline glucose concentrations. Effect is independent of osmotic increase as hearts perfused with mannitol + glucose (33 mM) performed to the same extent as hearts perfused with 11 mM glucose.** Isolated rat hearts were perfused under high glucose conditions (33 mM glucose) vs. controls (11 mM glucose) and subjected to 30 min of global ischemia, followed by 60 min of reperfusion. (A) Left ventricular developed pressure (% recovery) and (B) rate pressure product (RPP) (% recovery) between control and high glucose perfused groups. In parallel experiments, groups were perfused similarly under hyperosmotic conditions (mannitol control - 33 mM i.e. 22 mM mannitol + 11 mM glucose). (C) Left ventricular developed pressure (% recovery) and (D) rate pressure product (RPP) (% recovery) between high glucose and hyperosmotic perfused groups. Values are expressed as mean  $\pm$  SEM (n=6). \*p<0.05 vs. respective controls.

Changes in contraction ( $dP/dt_{max}$ ) reflected a similar trend (Figure 4.5A and 4.5C) as for LVDP recovery and RPP though there were no significant differences. There were no differences on the heart rate under high glucose conditions and with the osmotic control group (Figure 4.5B and 4.5D).

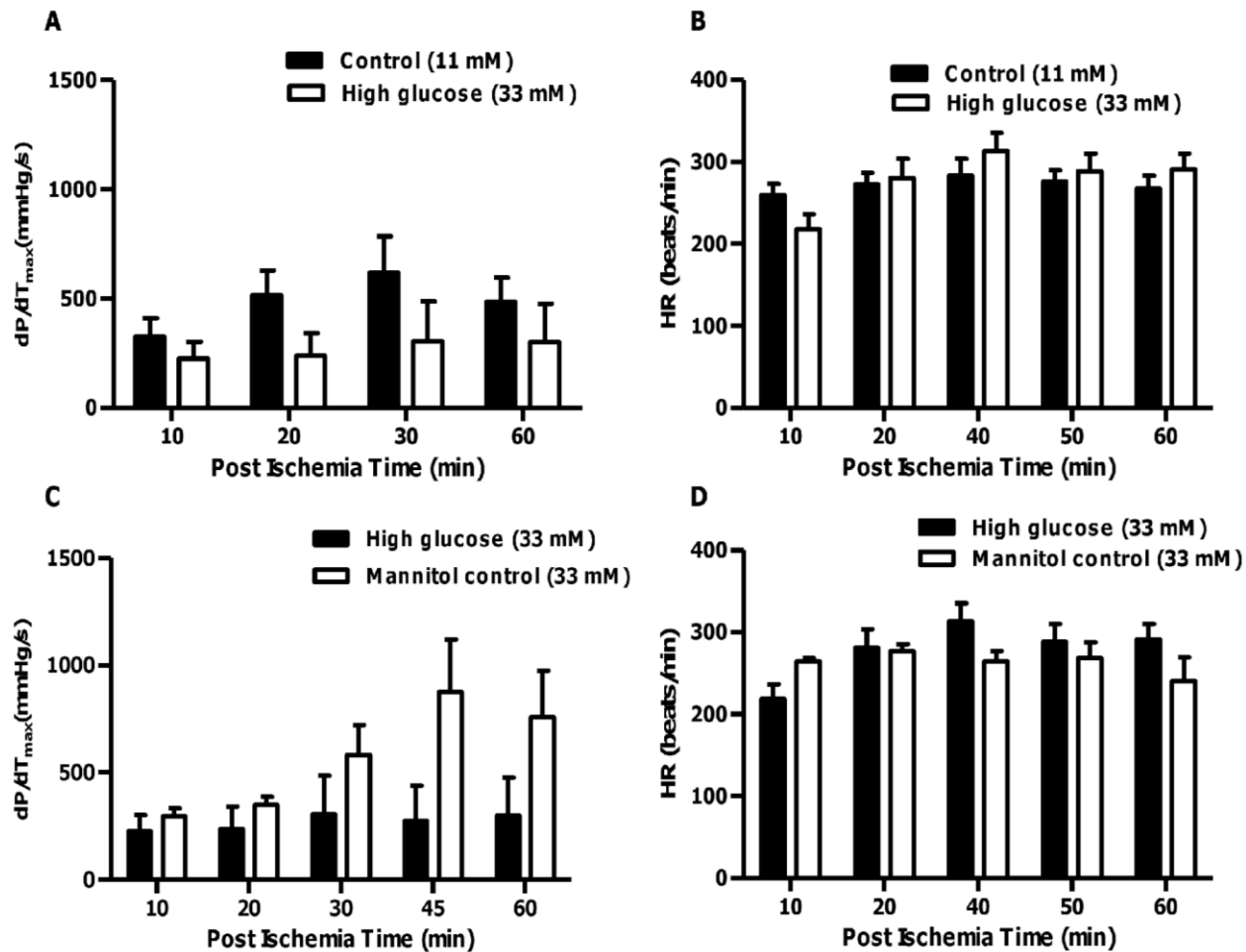


**Figure 4.5 Velocity of contraction and heart rate showed the same trend at baseline, hyperglycemic and osmotic control conditions.** Isolated rat hearts were perfused under high glucose conditions (33 mM glucose) vs. controls (11 mM glucose) and subjected to 30 min of global ischemia, followed by 60 min of reperfusion. (A) maximal velocity of contraction,  $dP/dt_{max}$ (mmHg/s) and (B) heart rate (beats/min) between control and high glucose perfused groups. In parallel experiments, groups were perfused similarly under hyperosmotic conditions (mannitol control 33 mM i.e. 22 mM mannitol + 11 mM glucose). (C) maximal velocity of contraction,  $dP/dt_{max}$ (mmHg/s) and (D) heart rate (beats/min) between high glucose and hyperosmotic perfused groups. Values are expressed as mean  $\pm$  SEM (n=6). \*p<0.05 vs. respective controls.



### 4.3.2 Acute BFT treatment enhances non- and post-ischemic contractile function

Our findings show that acute BFT treatment (40 min) significantly improved LVDP at baseline (11 mM glucose) (Figure 4.6A) and concomitantly decreased heart rate (Figure 4.6B). Overall, this did not translate into significant outcomes on the RPP (Figure 4.6C). There were no differences in  $dP/dt_{max}$  (Figure 4.6D).

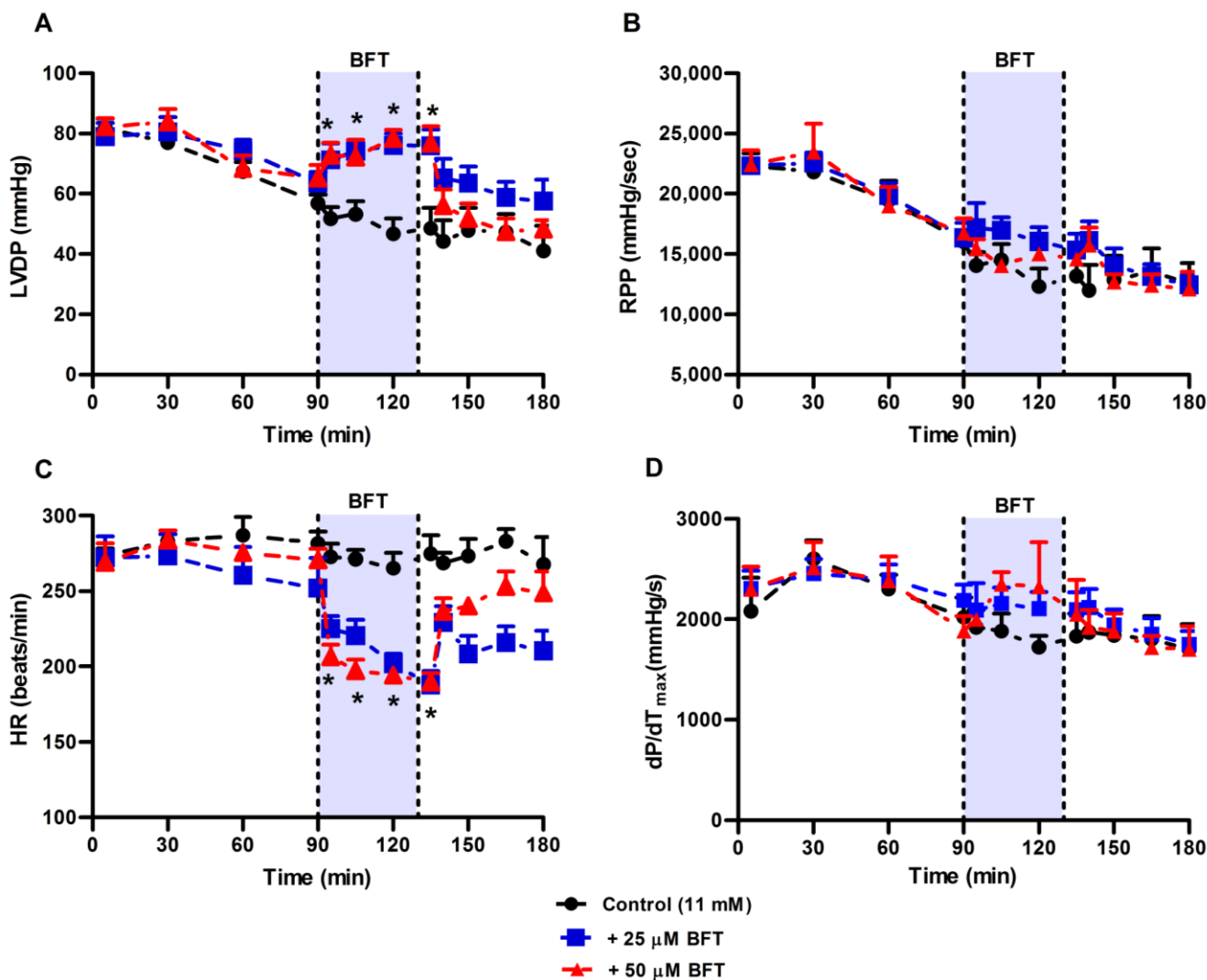


**Figure 4.6 Acute BFT treatment increases cardiac contractile function under baseline glucose and non-ischemic conditions reflected by increased LVDP, however HR is significantly decreased vs. untreated hearts.** Isolated rat hearts were perfused under baseline conditions (11 mM glucose)  $\pm$  25 or 50  $\mu$ M BFT treatment. We initially perfused for 90 min, whereafter BFT was added for a 40 min period. Subsequently, the buffer initially used was returned and hearts reperfused for an additional 40 min. (A) Left ventricular developed pressure, (B) rate pressure product (RPP) and (C) heart rate (HR) and maximal velocity of contraction ( $dP/dt_{max}$ ) at baseline  $\pm$  BFT. Values are expressed as mean  $\pm$  SEM (n=8). \* $p < 0.05$  vs. respective controls.

We next determined the effects of acute BFT administration within the setting of ischemia and reperfusion. Our data reveal that all BFT concentrations enhanced post-ischemic LVDP (Figure 4.7A) at baseline (11 mM glucose), with no differences in the three concentrations used. There was no effect on RPP (Figure 4.7B), however the low concentration of BFT improved  $dP/dt_{max}$  vs. control (Figure 4.7C). All the three concentrations of BFT decreased heart rate in the initial period of reperfusion (Figure 4.7D).

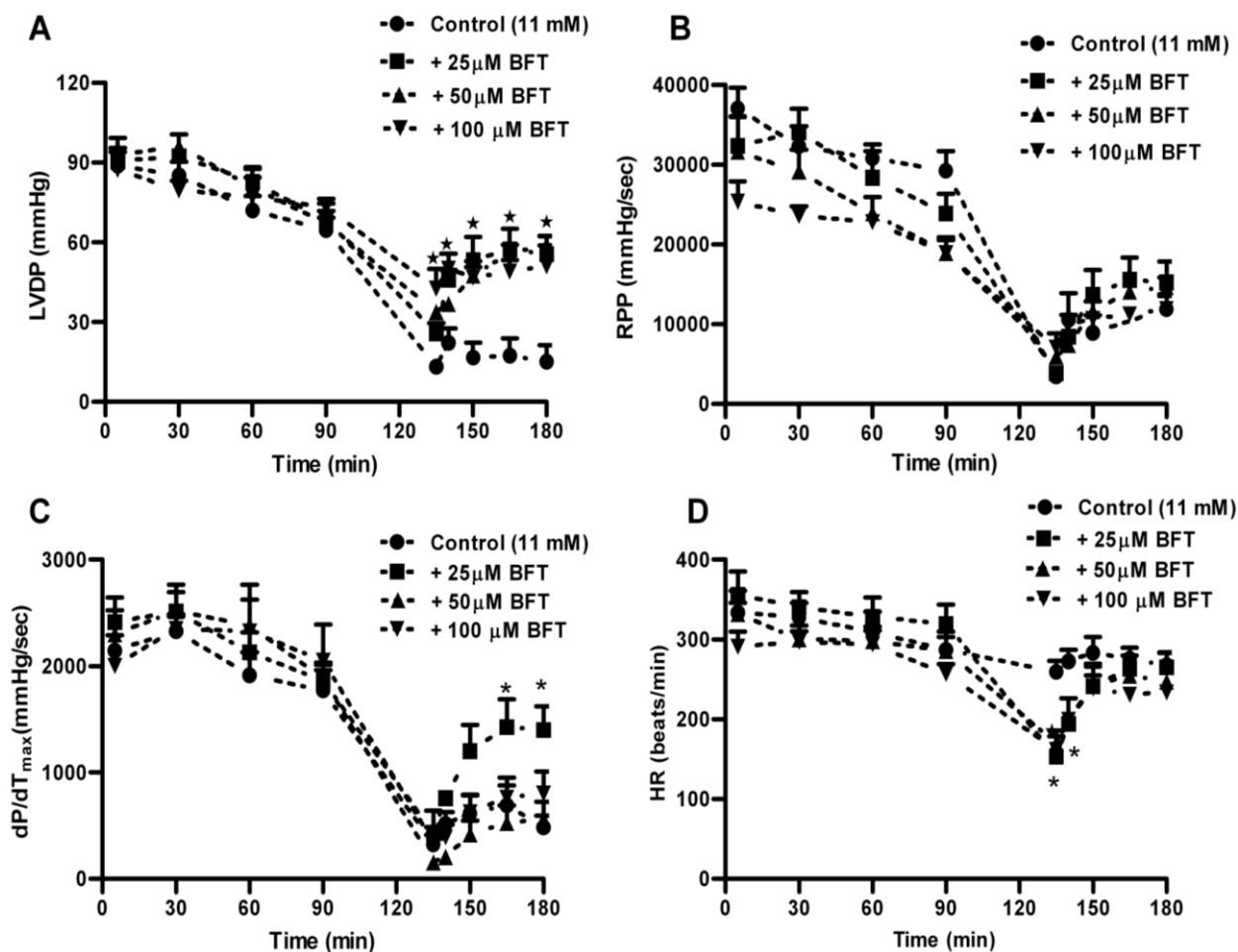


**Figure 4.7 Acute BFT treatment blunts cardiac dysfunction following ischemia and reperfusion at baseline glucose conditions since both LVDP and velocity of contraction are higher than in untreated hearts. In contrast BFT treatment reduced HR.** Isolated rat hearts were perfused under baseline glucose (11 mM glucose) and subjected to 30 min of global ischemia, followed by 60 min of reperfusion. For BFT treatment groups; 25, 50 or 100 μM was added during the first 20 min of reperfusion. (A) Left ventricular developed pressure (LVDP) and (B) rate pressure product (RPP), (C) maximal velocity of contraction ( $dP/dt_{max}$ ) and (D) heart rate (HR). Values are expressed as mean  $\pm$  SEM (n=6). \* $p < 0.05$  vs. respective controls.

Similarly all BFT concentrations improved LVDP in high glucose perfused hearts (22 mM) vs. untreated hearts (Figure 4.8A), however, there was no effect on RPP and  $dP/dt_{max}$  (Figures 4.8B and 4.8C). As seen in the baseline hearts, heart rate was also decreased ( $p < 0.05$ ) in the early phase of reperfusion in BFT treated groups vs. control (Figure 4.8D).

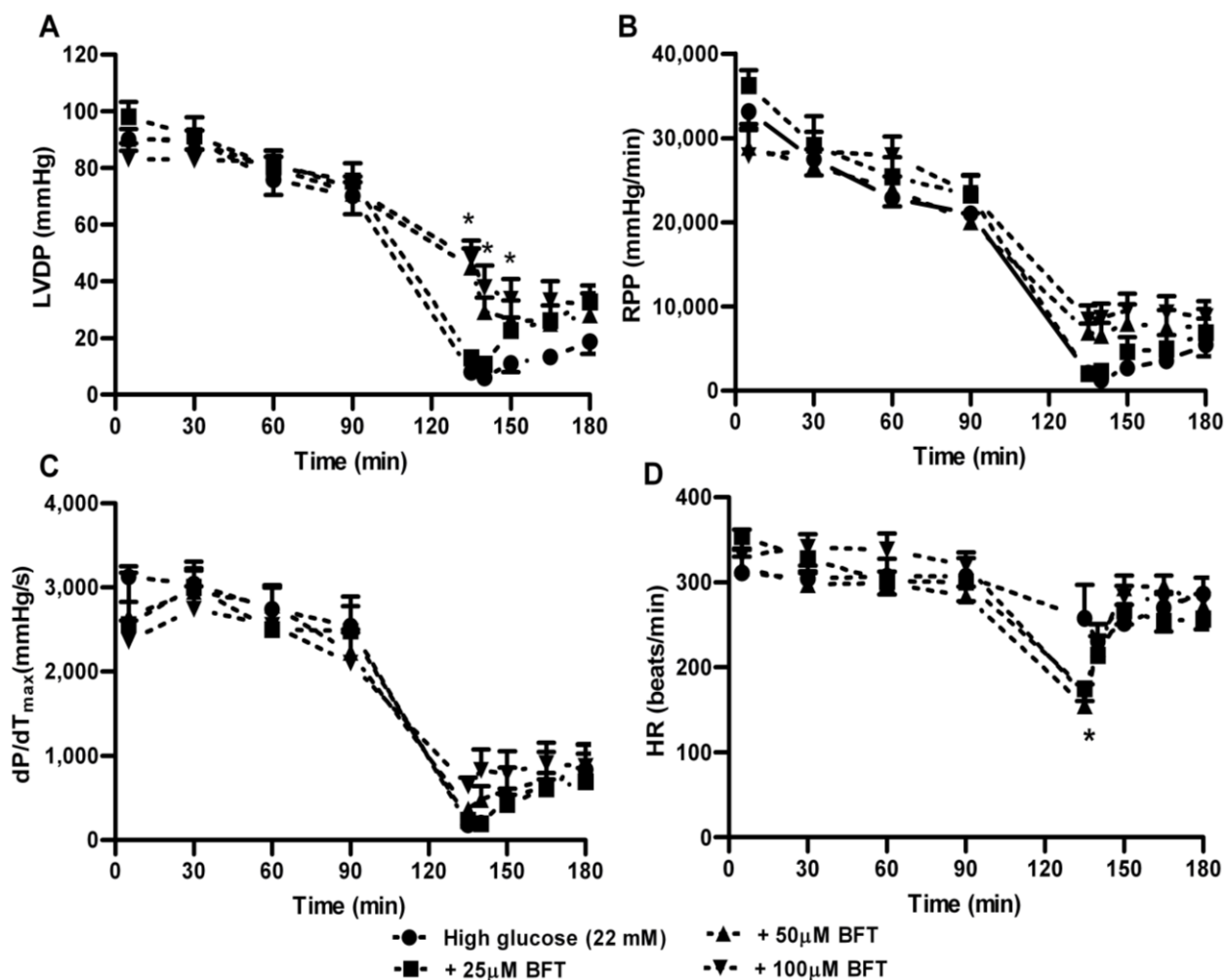


**Figure 4.8 Acute BFT treatment blunts high glucose-induced cardiac dysfunction following ischemia and reperfusion since LVDP recovery was higher in comparison to untreated hearts.** Isolated rat hearts were perfused under simulated hyperglycemic conditions (22 mM glucose) and subjected to 30 min of global ischemia, followed by 60 min of reperfusion. For BFT treatment groups; 25, 50 or 100 μM was added during the first 20 min of reperfusion. (A) Left ventricular developed pressure (LVDP) and (B) rate pressure product (RPP), (C) maximal velocity of contraction ( $dP/dt_{max}$ ) and (D) heart rate (HR) with high glucose exposure (22 mM). Values are expressed as mean  $\pm$  SEM ( $n=6$ ). \* $p < 0.05$  vs. respective controls.

With our highest glucose concentrations in simulated acute hyperglycemia (33 mM) the data show that all BFT concentrations significantly improved post-ischemic LVDP with the highest concentration of 100  $\mu$ M eliciting a robust effect during the early reperfusion period (Figure 4.9A), reaching  $\sim 71.1 \pm 5.9\%$  ( $p < 0.01$  vs. respective control). A similar pattern was found for post-ischemic RPP (Figure 4.9B), reaching a peak of  $\sim 12,904.3 \pm 2,500.6$  mmHg/sec vs.  $3,033.0 \pm 1,729.3$  mmHg/sec. Additionally all the concentrations enhanced post-ischemic  $dP/dt_{max}$  (Figure 4.9C) ( $p < 0.05$ ) by the end of the reperfusion period. As observed in hearts perfused with 11 mM and 22 mM glucose concentrations; heart rate was also reduced during the 20 min of reperfusion (Figure 4.9D).

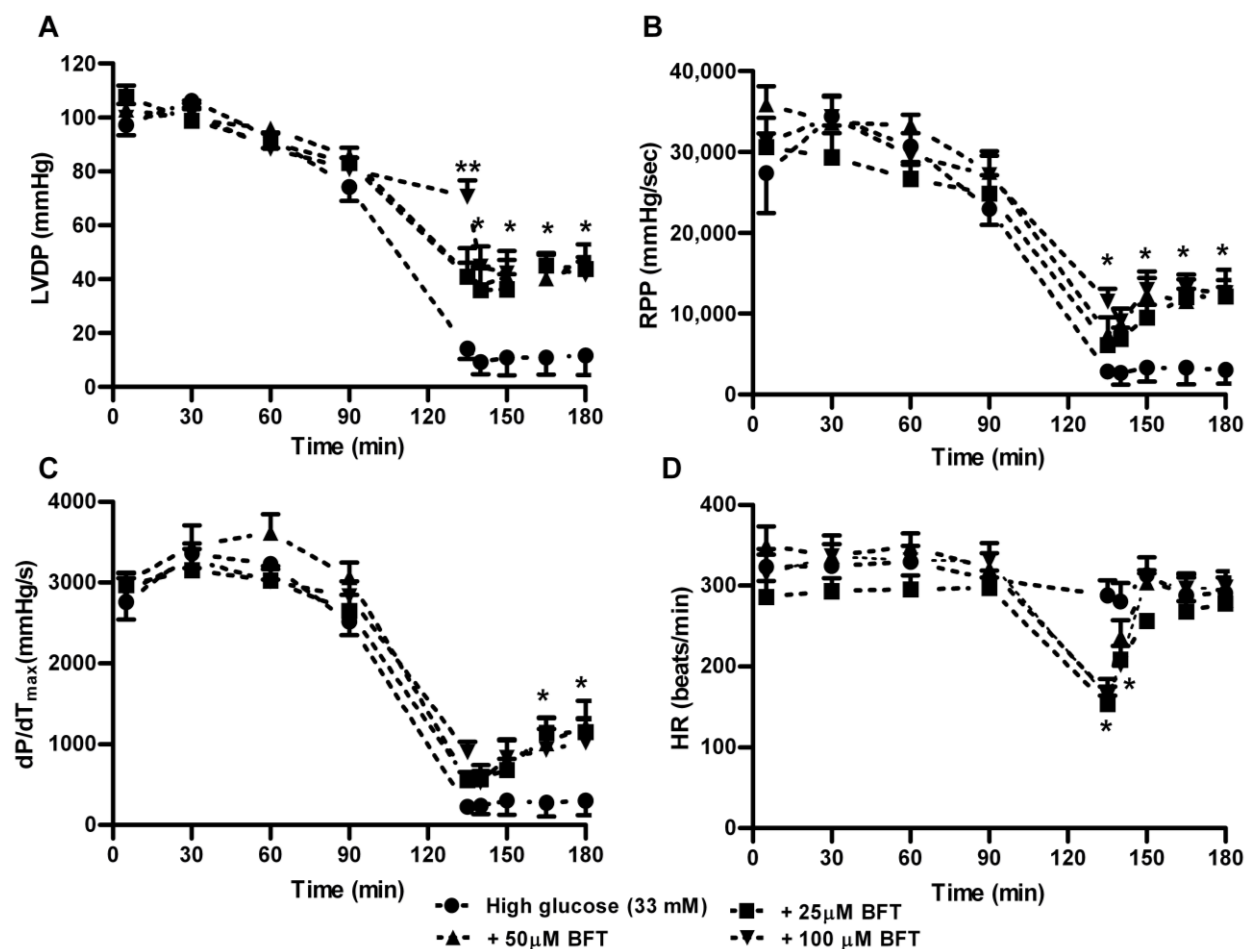


**Figure 4.9 Acute BFT treatment blunts high glucose-induced cardiac dysfunction following ischemia and reperfusion indicated by increased LVDP, RPP and velocity of contraction vs. untreated hearts.** Isolated rat hearts were perfused under simulated hyperglycemic conditions (33 mM glucose) and subjected to 30 min of global ischemia, followed by 60 min of reperfusion. For BFT treatment groups; 25, 50 or 100  $\mu$ M was added during the first 20 min of reperfusion. (A) Left ventricular developed pressure (LVDP) and (B) rate pressure product (RPP), (C) maximal velocity of contraction ( $dP/dt_{max}$ ) and (D) heart rate (HR) with high glucose exposure (33 mM). Values are expressed as mean  $\pm$  SEM ( $n=6$ ). \* $p < 0.05$ , \*\* $p < 0.01$  vs. respective controls.

Changes in coronary flow and end-diastolic pressure under baseline (11 mM) and with simulated hyperglycemia  $\pm$  BFT concentrations are shown in Table 4.1. There were no differences in coronary flow between hearts exposed to high glucose (22 and 33 mM) conditions vs. hearts at baseline glucose levels. However, BFT increased coronary flow in high glucose (22 and 33 mM) exposed hearts vs. their respective untreated controls. End-diastolic pressure was significantly elevated in high glucose exposed rat hearts vs. hearts in the control group. Moreover, there was a significant increase in end diastolic pressure for all the groups during post-ischemia, i.e. ranging from ~ 30 mmHg to 90 mmHg, with values higher in the high glucose untreated groups (22 and 33 mM) vs. baseline glucose exposed hearts. With BFT treatment end-diastolic pressure was significantly reduced in the high glucose exposed rat hearts, though there were no differences in the control group.

**Table 4.1.** Coronary flow and end-diastolic pressure (EDP) under high (22 and 33 mM) vs. baseline (11 mM) glucose conditions during the first ten min of stabilization and at the end of reperfusion.

	Coronary Flow (ml/min)		EDP (mmHg)	
	Pre Ischemia	Post Ischemia	Pre Ischemia	Post Ischemia
<b>Control (11 mM)</b>	12 $\pm$ 1	8 $\pm$ 2	12 $\pm$ 0	30 $\pm$ 6
+ 25 $\mu$ M BFT	14 $\pm$ 2	12 $\pm$ 1	10 $\pm$ 2	28 $\pm$ 4
+ 50 $\mu$ M BFT	15 $\pm$ 3	10 $\pm$ 2	11 $\pm$ 1	25 $\pm$ 5
+ 100 $\mu$ M BFT	10 $\pm$ 1	9 $\pm$ 2	8 $\pm$ 3	29 $\pm$ 7
<b>High Glucose (22 mM)</b>	13 $\pm$ 3	6 $\pm$ 1	7 $\pm$ 2	79 $\pm$ 7#
+ 25 $\mu$ M BFT	11 $\pm$ 3	8 $\pm$ 3	8 $\pm$ 1	43 $\pm$ 6*
+ 50 $\mu$ M BFT	14 $\pm$ 2	11 $\pm$ 1*	13 $\pm$ 4	46 $\pm$ 6*
+ 100 $\mu$ M BFT	13 $\pm$ 1	10 $\pm$ 2*	9 $\pm$ 3	36 $\pm$ 4*
<b>High Glucose (33 mM)</b>	14 $\pm$ 2	6 $\pm$ 3	10 $\pm$ 2	87 $\pm$ 6#
+ 25 $\mu$ M BFT	15 $\pm$ 4	13 $\pm$ 3*	11 $\pm$ 3	45 $\pm$ 5*
+ 50 $\mu$ M BFT	16 $\pm$ 2	12 $\pm$ 2*	11 $\pm$ 1	39 $\pm$ 4**
+ 100 $\mu$ M BFT	13 $\pm$ 1	11 $\pm$ 1*	14 $\pm$ 4	32 $\pm$ 8**

Values are expressed as mean  $\pm$  SEM. \*p<0.05; \*\*p<0.01 vs. respective control; #p<0.05 vs 11 mM control. (n=6 in each group)

### 4.3.3 Acute BFT administration decreases infarct size and attenuates high glucose-induced oxidative stress and apoptosis

Our data demonstrate that BFT reduced infarct sizes at baseline (11 mM glucose) and under high glucose conditions following regional ischemia (Figure 4.10A). Treatment with 100  $\mu$ M BFT diminished infarct size to  $39.0 \pm 2.5\%$  and  $49.7 \pm 7.4\%$  versus  $52.3 \pm 2.8\%$  and  $74.5 \pm 4.9\%$  at baseline and high glucose perfusions, respectively. There were no differences in the area at risk amongst all the groups (Figure 4.10B).

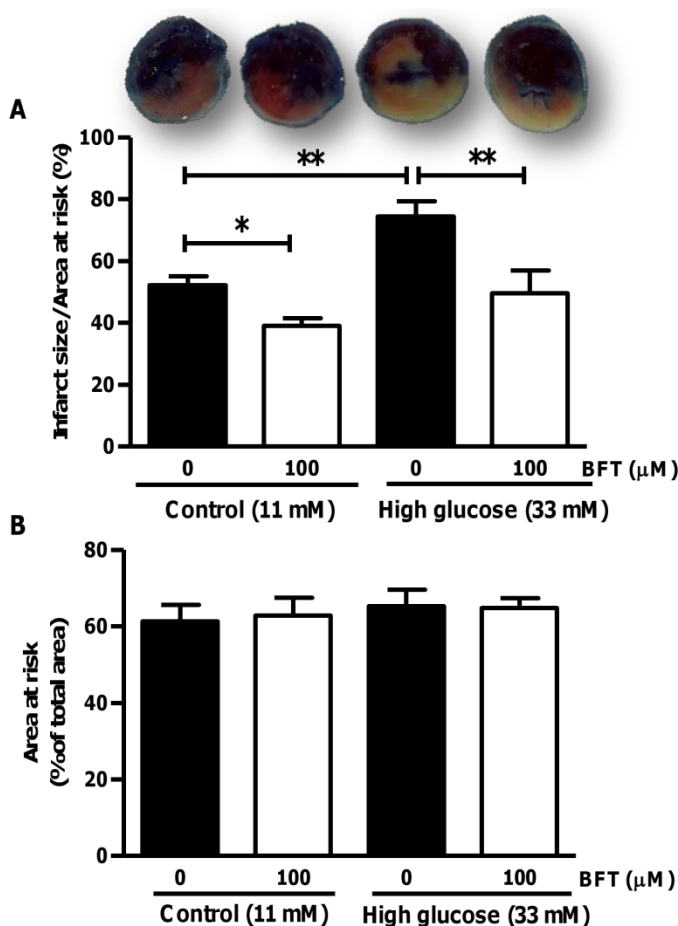


**Figure 4.10 Acute BFT treatment decreases infarct size following ischemia and reperfusion *ex vivo*.** Isolated rat hearts were perfused under normal or high glucose conditions and subjected to regional ischemia. For BFT treated groups, 100  $\mu$ M BFT was added during the first 20 min of the 2 hr reperfusion period. (A) infarct size/area at risk (%) and (B) area at risk under baseline (simulated normoglycemia) vs. high glucose perfusions. Evans blue dye and TTC staining enabled visualization of viable tissue, infarcted area and the area at risk. Values are expressed as mean  $\pm$  SEM. \* $p$ <0.05; \*\* $p$ <0.01 vs. respective control. (n=6 in each group).

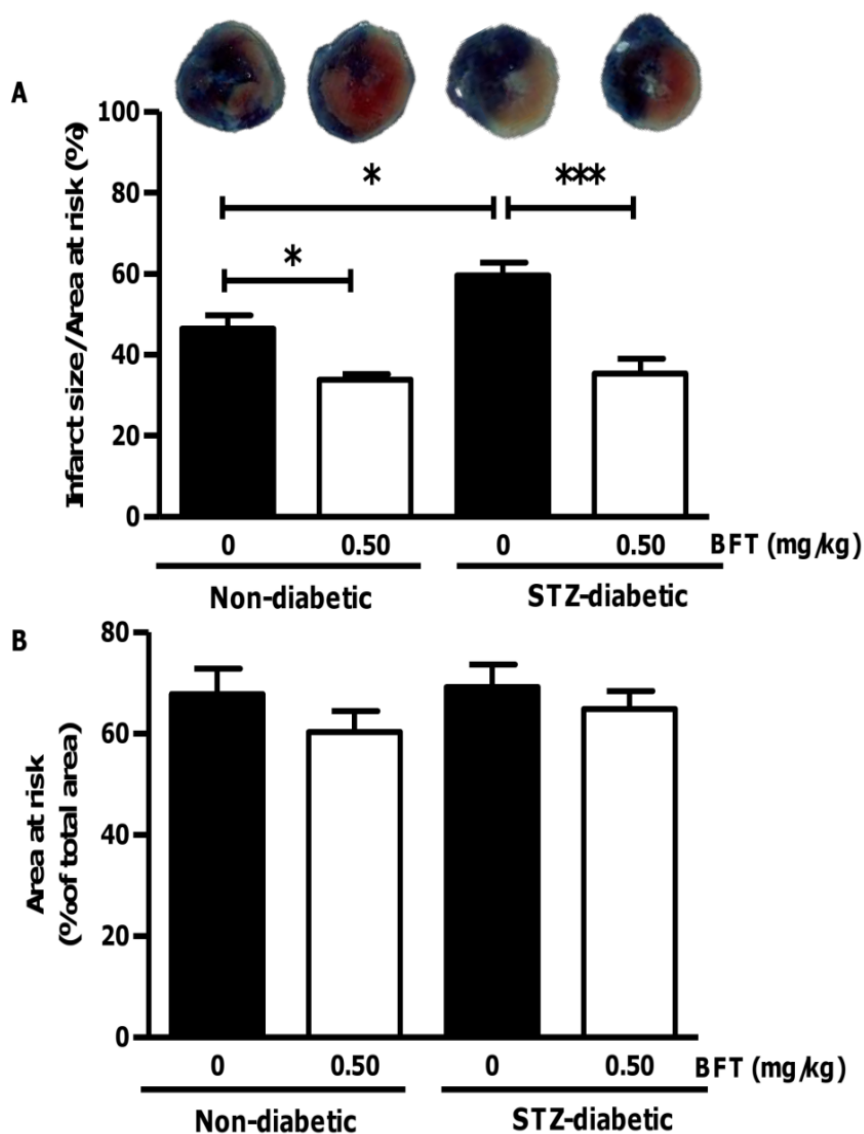
We next evaluated the cardio-protective effects of BFT treatment within the *in vivo* context, i.e. by employing coronary artery ligations in STZ-treated hyperglycemic rats. Our findings revealed markedly elevated blood glucose levels in STZ-diabetic rats compared to matched controls ( $p < 0.01$ ) (Table 4.2). This was associated with decreased weight gain in the STZ-diabetic rats ( $p < 0.01$  vs. matched controls).

**Table 4.2** Body weight and blood glucose levels after 1 week of STZ injection.

	<b>% Body weight change</b>	<b>Non-fasting blood glucose (mmol/l)</b>
<b>Non diabetic</b>	9.7 ± 1.7	6.9 ± 0.4
<b>STZ-diabetic</b>	-7.0 ± 2.6**	23.8 ± 1.8**

Data are expressed as mean ± SEM,  $n \geq 4$  in each group. \*\* $p < 0.01$  vs. non-diabetic control group.

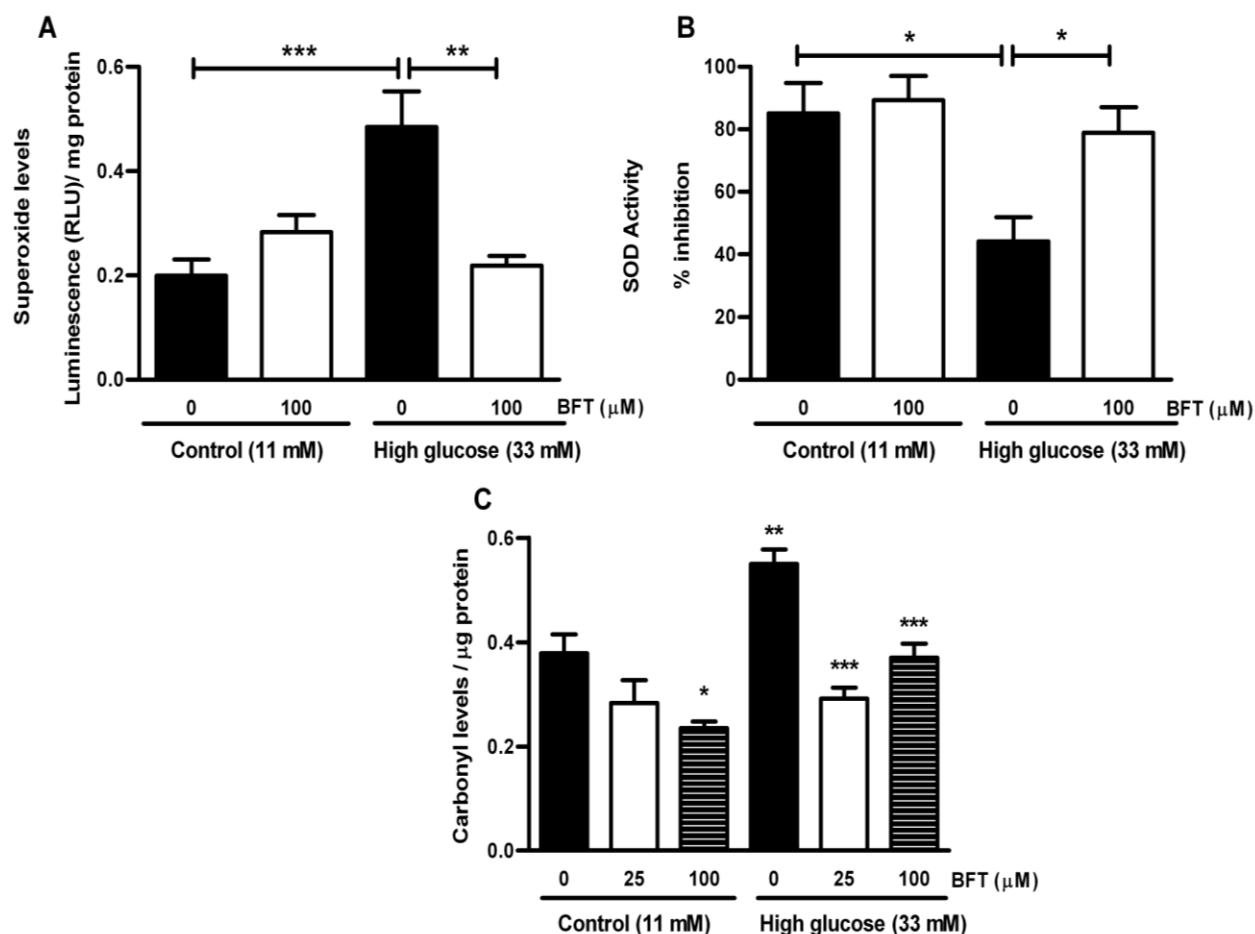
In agreement with our *ex vivo* perfusion data, we found that infarct size was significantly increased for the STZ-treated rats versus controls ( $59.6 \pm 3.1\%$  vs.  $46.4 \pm 3.3\%$ ) following 30 min coronary artery ligation and 2 hr reperfusion (Figure 4.11A). Moreover, this effect was blunted by BFT treatment in control and STZ-treated rat hearts. There were no differences in the area at risk amongst all the groups (Figure 4.11B).



**Figure 4.11 Acute BFT treatment decreases infarct size following ischemia and reperfusion *in vivo*.** Wistar rats were injected with STZ and followed for a 1-week period. Subsequently, 0.50 mg/kg BFT was injected via the penile vein within the first two min of reperfusion. (A) infarct size/area at risk (%) and (B) area at risk under baseline vs. high glucose conditions. Evans blue dye and TTC staining enabled visualization of viable tissue, infarcted area and the area at risk. Values are expressed as mean  $\pm$  SEM. \* $p < 0.05$ ; \*\*\* $p < 0.01$  vs. respective control. (n=6 in each group).

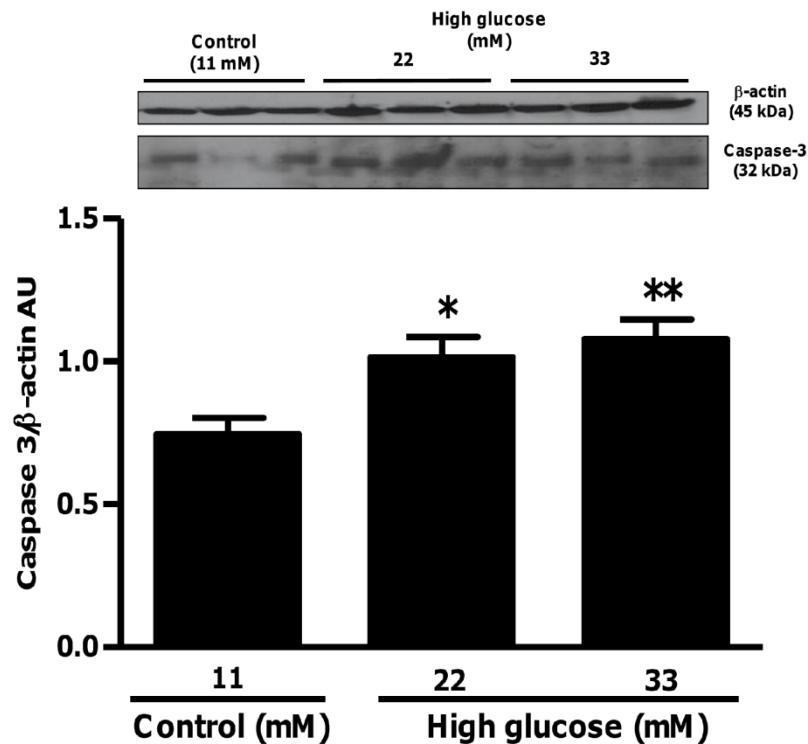


BFT attenuated high glucose-induced oxidative stress, i.e. reduced superoxide levels in high glucose perfused hearts following ischemia and reperfusion (Figure 4.12A), and concomitantly enhanced SOD activity ( $p < 0.05$  vs. untreated high glucose) (Figure 4.12B). To corroborate these antioxidant effects, 25  $\mu\text{M}$  and 50  $\mu\text{M}$  BFT concentration decreased protein carbonylation from  $0.55 \pm 0.03$  carbonyl levels/ $\mu\text{g}$  protein in high glucose untreated hearts to  $0.29 \pm 0.02$  carbonyl levels/ $\mu\text{g}$  protein and  $0.37 \pm 0.03$  carbonyl levels/ $\mu\text{g}$  protein respectively, under high glucose conditions. This effect was also observed under high glucose conditions with the highest concentration of BFT (Figure 4.12C).



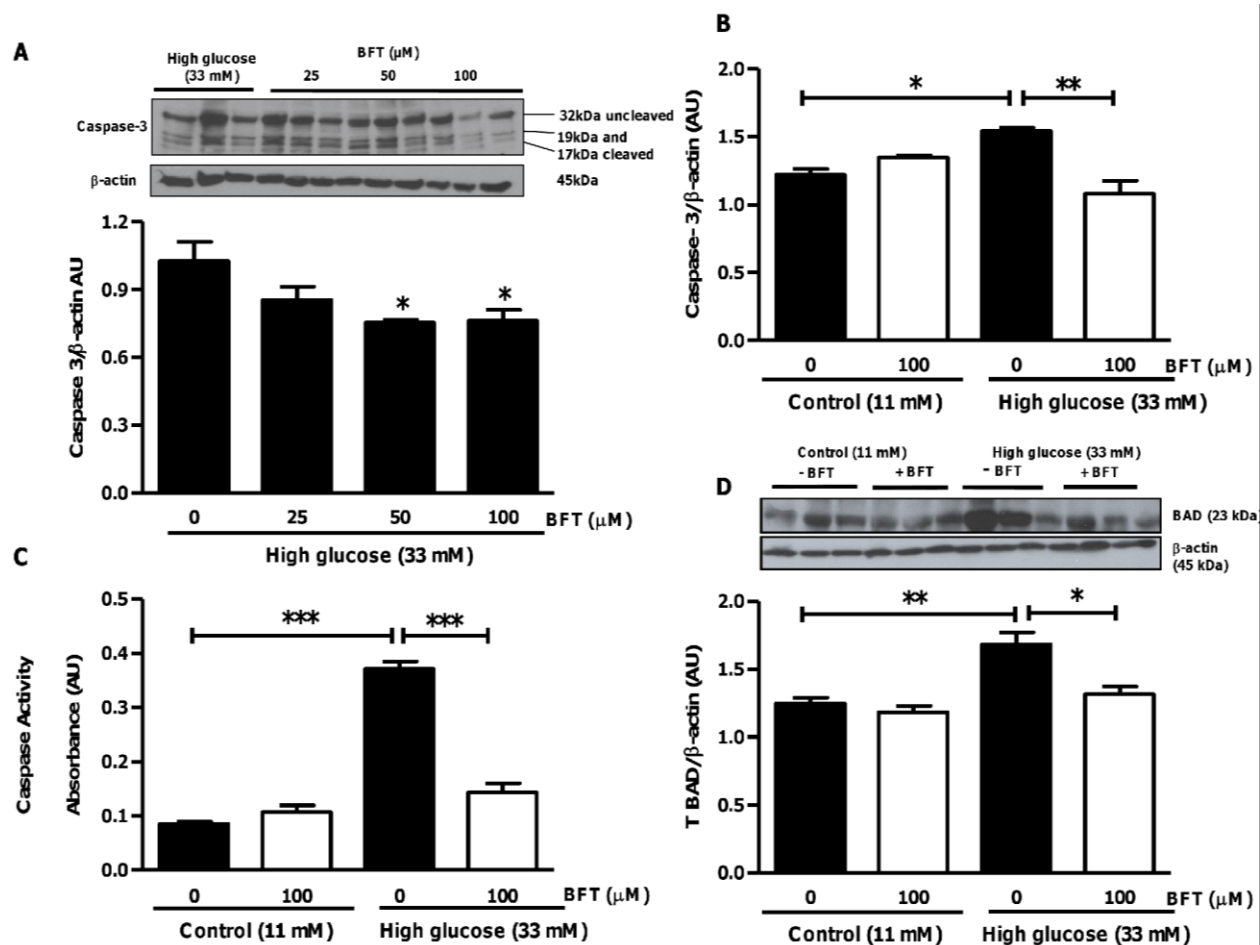
**Figure 4.12 Acute BFT treatment blunts high glucose-induced oxidative stress by decreasing superoxide levels, increasing SOD activity and attenuating protein carbonylation.** Isolated rat hearts were perfused under normal or high glucose conditions following ischemia and reperfusion. For BFT treated groups, 100  $\mu\text{M}$  BFT was added during the first 20 min of the 2 hr reperfusion period. (A) Superoxide levels under high glucose conditions vs. control  $\pm$  BFT treatment; (B) Superoxide dismutase (SOD) activity (% inhibition) in response to high glucose vs. control  $\pm$  BFT treatment and (C) carbonylation levels/ $\mu\text{g}$  protein in response to high glucose vs. control  $\pm$  25  $\mu\text{M}$  and 100  $\mu\text{M}$  BFT treatment. Values are expressed as mean  $\pm$  SEM ( $n=6$ ). \* $p < 0.05$ , \*\* $p < 0.01$ , \*\*\* $p < 0.001$  vs. respective controls.

Myocardial apoptosis was increased under high glucose conditions (both 22 and 33 mM) vs. baseline glucose conditions (Figure 4.13).



**Figure 4.13. Increased myocardial apoptosis in response to high glucose conditions indicated by increased expression of caspase-3.** Caspase-3 expression (uncleaved) in isolated rat hearts perfused under high glucose (22 and 33 mM) vs. baseline glucose (11 mM). Western blot analysis is shown with  $\beta$ -actin as loading control. Densitometric analysis for caspase-3 is displayed below gel image (normalized to corresponding  $\beta$ -actin values). Values are expressed as mean  $\pm$  SEM (n=6). \*p<0.05, \*\*p<0.01 vs control.

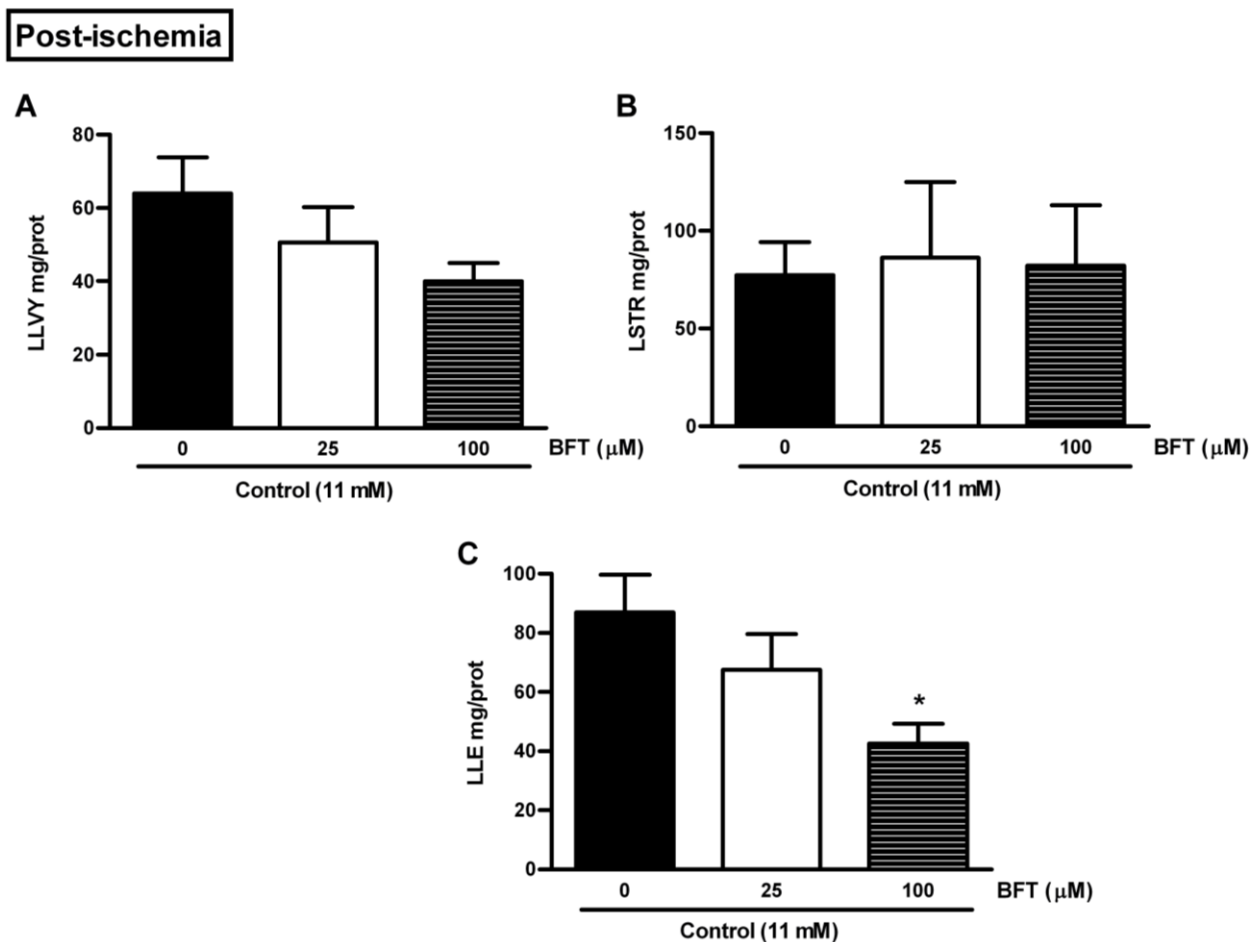
BFT treatment significantly blunted apoptosis as shown by the decreased cleaved caspase-3 peptide levels (Figure 4.14A and 4.14B), caspase activity (Figure 4.14C) and total BAD expression (Figure 4.14D) in high glucose (33 mM) perfused hearts compared to respective controls.



**Figure 4.14 Anti-apoptotic effects of BFT in hearts subjected to ischemia and reperfusion under high glucose conditions shown by decreased caspase-3 expression (un/cleaved), decreased caspase 3/7 activity and decreased total BAD expression.** Isolated rat hearts were perfused under high glucose conditions vs. controls and subjected to ischemia and reperfusion. For BFT treatment groups, various concentrations were added during the first 20 min of reperfusion. (A) Caspase-3 (cleaved) peptide levels under high glucose conditions with 25, 50 or 100  $\mu$ M BFT, respectively, and (B) with 100  $\mu$ M BFT vs. controls. (C) Caspase activity and (D) total BAD (BAD) peptide levels. Values are expressed as mean  $\pm$  SEM (n=9). \* $p$ <0.05, \*\* $p$ <0.01, \*\*\* $p$ <0.001 vs. respective controls.

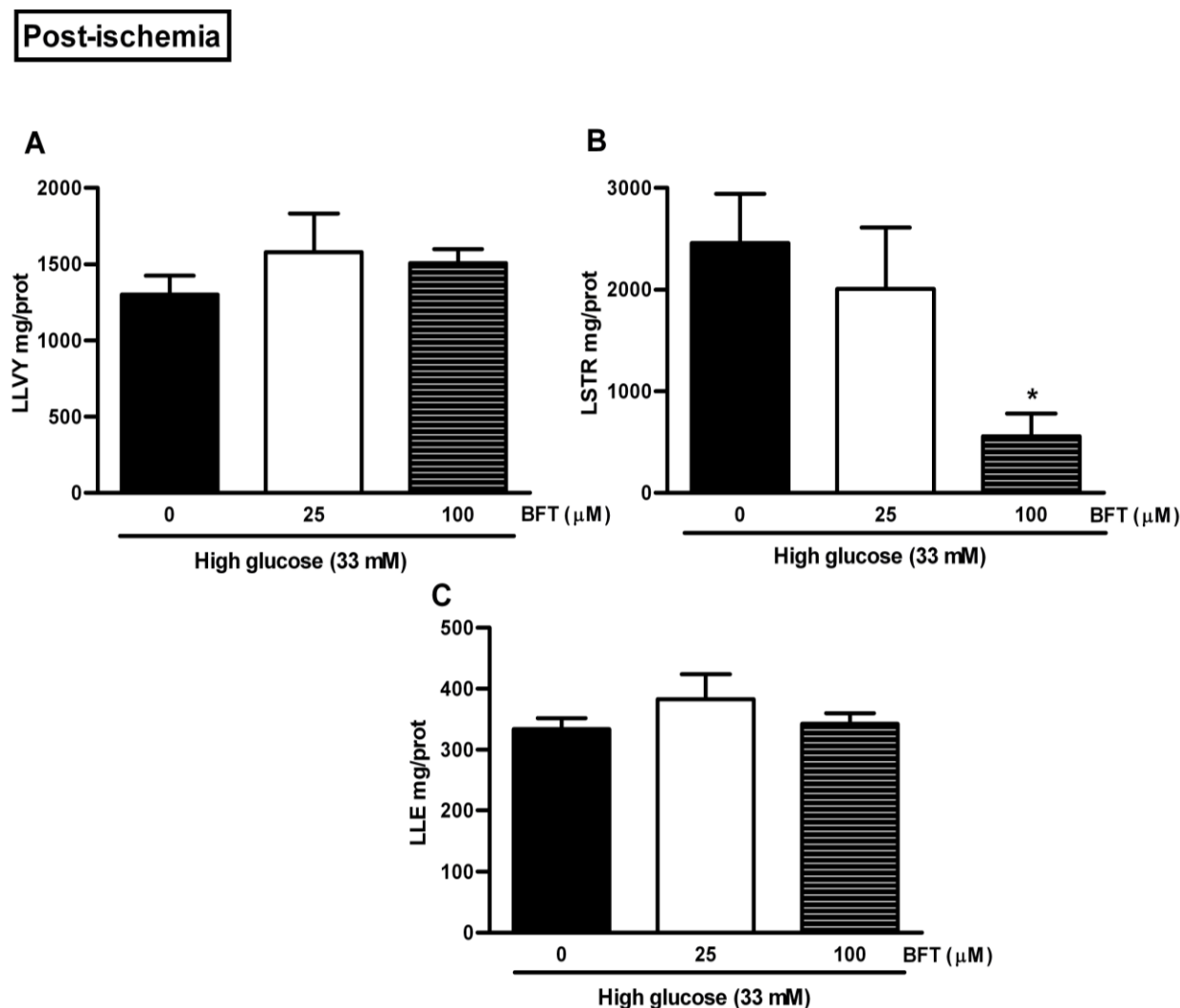
#### 4.3.4 BFT treatment decreased chymotrypsin proteasomal activity

The effect of high glucose perfusion conditions vs. control on post-ischemia proteasomal activity is shown in Chapter 3 (see Figure 3.19). There was no effect on post-ischemic chymotrypsin-like and trypsin-like activities with both the low and high concentrations of BFT (Figures 4.15A and 4.15B). However, the highest concentration of BFT blunted post-ischemic caspase-like proteasomal activity under baseline conditions (Figure 4.15C).



**Figure 4.15 The highest dose of BFT attenuates caspase-like proteasomal activity under baseline glucose conditions following ischemia and reperfusion.** Isolated rat hearts were perfused under baseline glucose conditions vs. controls and subjected to ischemia and reperfusion. For the treatment groups, 25  $\mu\text{M}$  and 100  $\mu\text{M}$  BFT were added during the first 20 min of reperfusion. (A) Trypsin-like proteasomal, (B) chymotrypsin-like, and (C) caspase-like activities after 60 min of reperfusion at baseline (11 mM glucose). Values are expressed as mean  $\pm$  SEM (n=9). \*p<0.05 vs. respective controls.

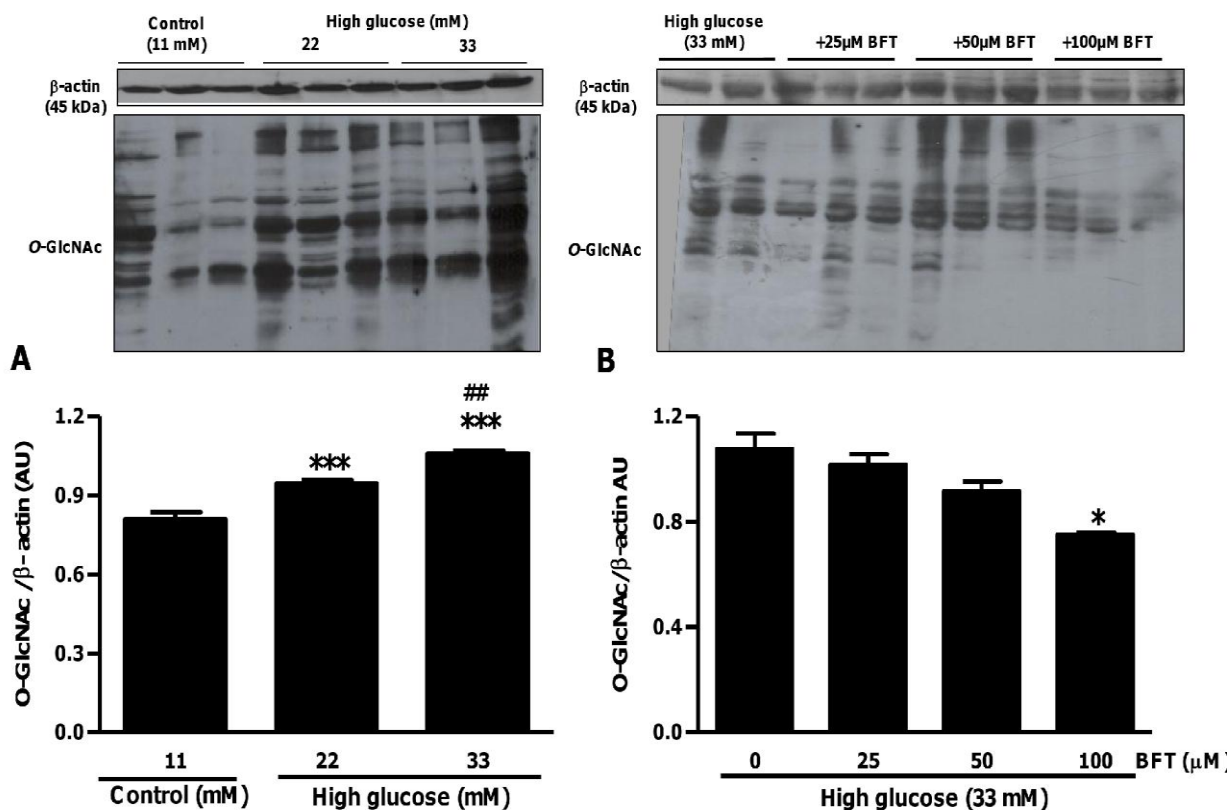
A similar observation was observed with hearts exposed to high glucose conditions with no effect on post-ischemic trypsin-like and caspase-like activities (Figures 4.16A and 4.16C). However, the highest BFT concentration blunted post-ischemic chymotrypsin-like proteasomal activity (Figure 4.16B) ( $p < 0.05$  vs. untreated hearts).



**Figure 4.16 The highest dose of BFT attenuates high glucose-induced chymotrypsin-like proteasomal activity following ischemia and reperfusion under high glucose conditions.** Isolated rat hearts were perfused under high glucose conditions vs. controls and subjected to ischemia and reperfusion. For the treatment groups, 25  $\mu\text{M}$  and 100  $\mu\text{M}$  BFT were added during the first 20 min of reperfusion. (A) Trypsin-like proteasomal, (B) chymotrypsin-like, and (C) caspase-like activities after 60 min of reperfusion under high glucose conditions (33 mM glucose). Values are expressed as mean  $\pm$  SEM ( $n=9$ ). \* $p < 0.05$  vs. respective controls.

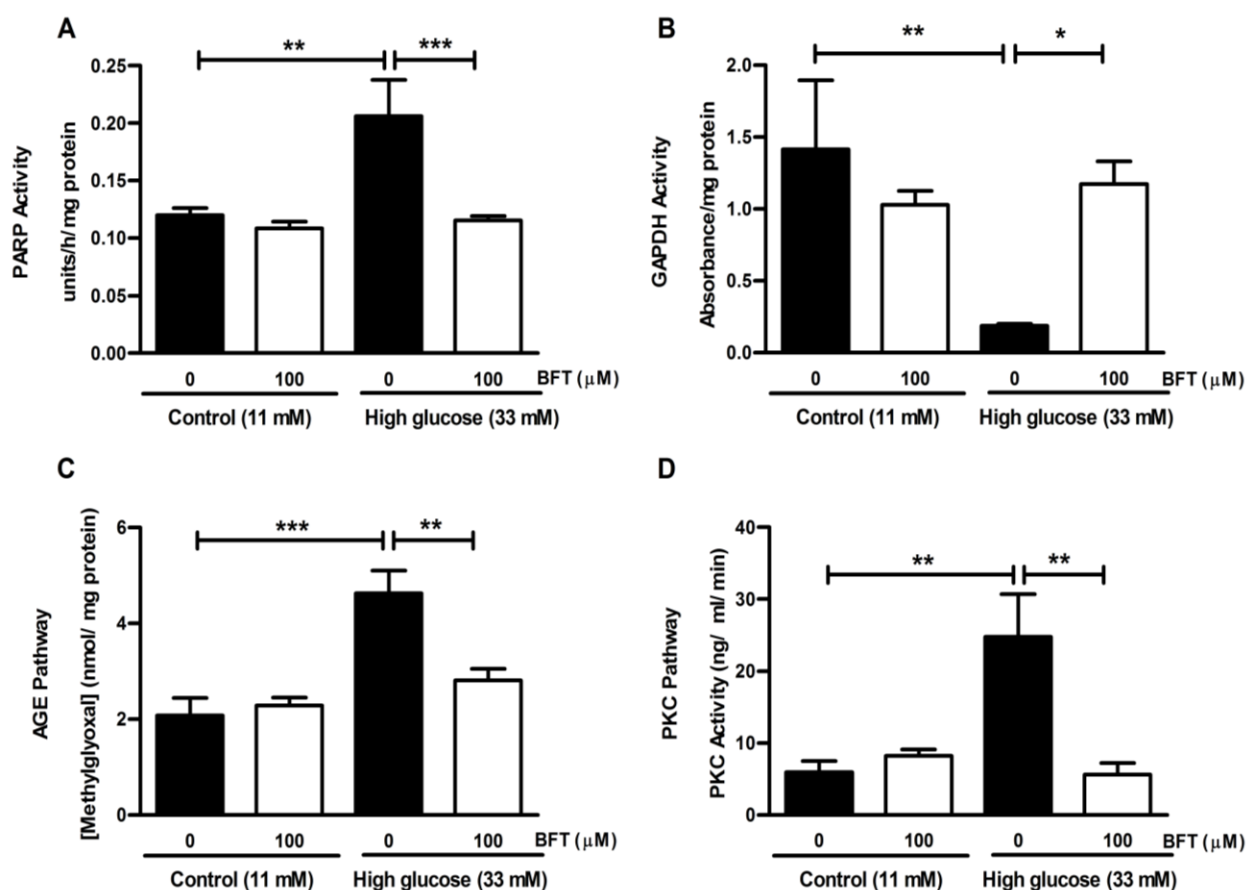
### 4.3.5 BFT blunts high glucose-induced metabolic dysfunction and activation of non-oxidative glucose utilizing pathways.

Hearts perfused under high glucose conditions (22 and 33 mM) showed increased O-GlcNAcylation vs. control group (Figure 4.17A). Treatment with BFT attenuated HBP flux, however, only the highest concentration showed a significant effect ( $p < 0.05$ ) vs. untreated hearts under high glucose perfusion conditions (Figure 4.17B).



**Figure 4.17 BFT treatment attenuates O-GlcNAcylation in hearts subjected to ischemia and reperfusion under high glucose conditions.** Isolated rat hearts were perfused under high glucose conditions vs. controls and subjected to ischemia and reperfusion  $\pm$  BFT treatment during reperfusion. Western blot analysis for overall O-GlcNAcylation is shown with  $\beta$ -actin as loading control. Densitometric analysis for O-GlcNAcylation is displayed below gel image (normalized to corresponding  $\beta$ -actin values). (A) O-GlcNAc levels under high glucose (22 and 33 mM) vs. control group (B) O-GlcNAc levels under high glucose (33 mM) conditions with varying concentrations of BFT. Values are expressed as mean  $\pm$  SEM (n=6). \* $p < 0.05$ , \*\* $p < 0.01$  vs. respective controls.

In line with our hypothesis, we next determined the impact of acute BFT treatment on non-oxidative pathways of glucose metabolism. BFT diminished hyperglycemia-mediated PARP activation ( $p < 0.001$  vs. respective control) (Figure 4.18A) and in parallel restored GAPDH activity ( $p < 0.01$  vs. respective control) (Figure 4.18B). As predicted, increased GAPDH activity within this context resulted in less activation of the four non oxidative pathways here investigated. We found attenuated AGE ( $p < 0.01$  vs. respective control), PKC activity ( $p < 0.01$  vs. respective control), HBP ( $p < 0.01$  vs. respective control), and polyol pathway activation following acute BFT treatment (Figure 4.18C- 4.18G). By contrast, acute BFT treatment restored transketolase activity in high glucose hearts following ischemia and reperfusion (Figure 4.18H).



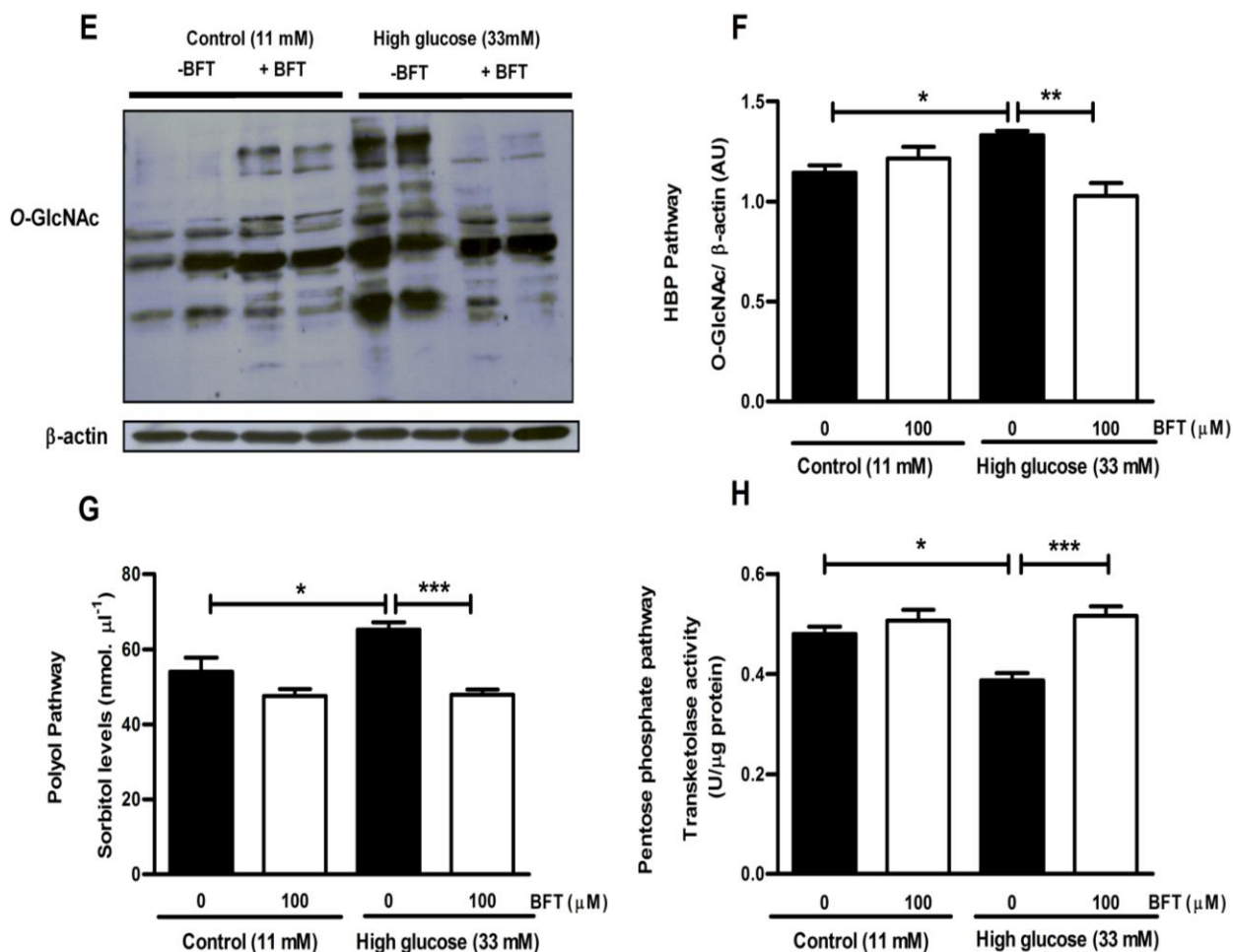


**Figure 4.18 Acute BFT administration attenuates high glucose-induced metabolic dysfunction and activation of non-oxidative glucose pathways.** Isolated rat hearts were perfused under high glucose conditions vs. controls and subjected to ischemia and reperfusion. (A) PARP activity, (B) GAPDH activity, (C) AGE activation (methylglyoxal concentration), (D) PKC activity, (E) O-GlcNAc peptide levels, (F) quantification of total O-GlcNAc peptide levels, (G) polyol pathway activation (sorbitol levels), and pentose phosphate pathway activation (transketolase activity). Values are expressed as mean  $\pm$  SEM (n=6). \*p<0.05, \*\*p<0.01, \*\*\*p<0.001 vs. respective controls



Interestingly, these data reveal that the PKC and AGE pathways showed greatest activation under high glucose conditions and were most sensitive to acute BFT treatment (Figure 4.19).

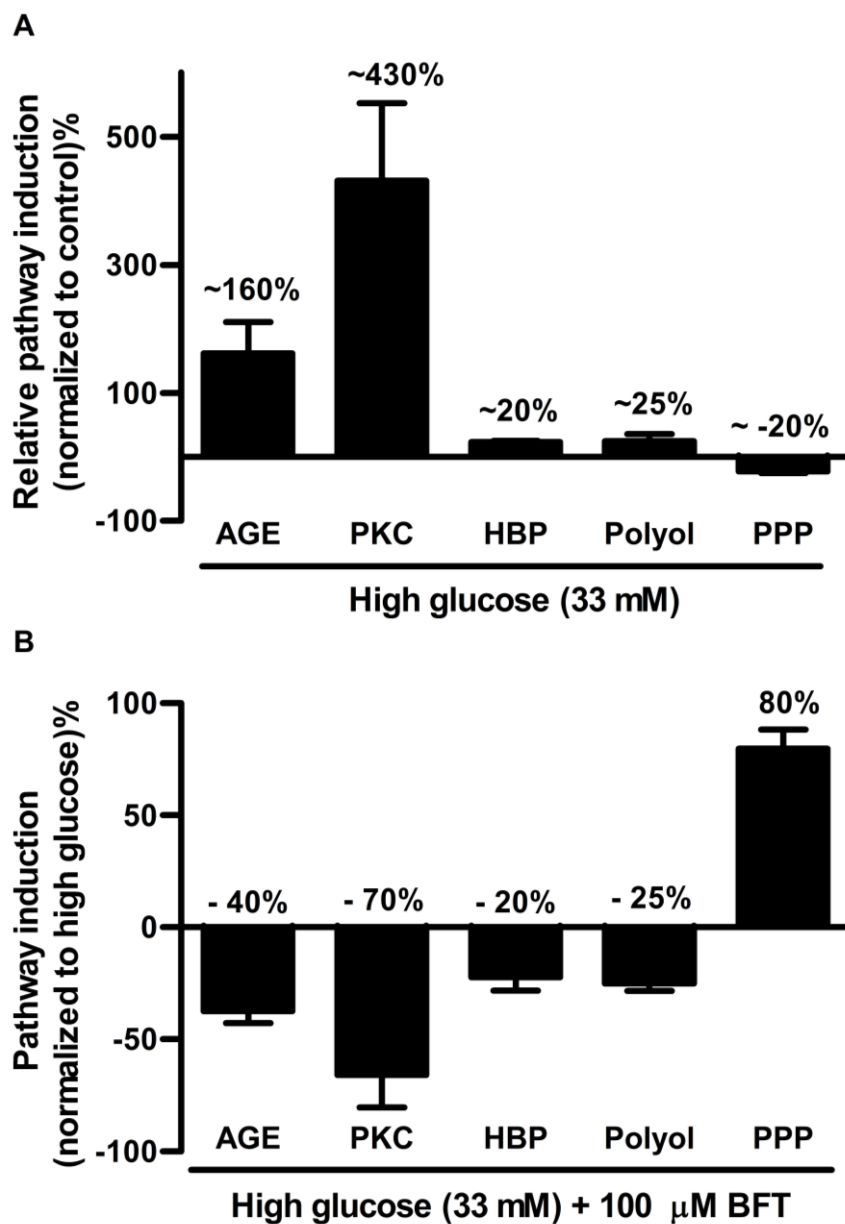


**Figure 4.19 Activation of non-oxidative pathways in high glucose perfusions relative to baseline conditions  $\pm$  BFT treatment.** (A) Relative pathway activation (without BFT treatment) in high glucose perfused hearts following ischemia and reperfusion (normalized to baseline glucose perfused hearts). (B) Changes in pathway activation in high glucose perfused hearts (with BFT treatment) following ischemia and reperfusion (normalized to high glucose perfused hearts). Values are expressed as mean  $\pm$  SEM (n=6).

#### **4.3.6 Acute inhibition of flux through the non-oxidative glucose pathways blunts high glucose-induced contractile dysfunction following ischemia and reperfusion**

Our data shows that inhibition of flux through the non-oxidative glucose pathways had no effect on both LVDP (% recovery) and RPP (Figure 4.20A and 4.20B) following ischemia and reperfusion after 60 min of reperfusion at baseline with the exception of polyol pathway inhibition that showed a strong ( $p < 0.05$ ) increase in LVDP (% recovery). By contrast, inhibition of the PKC, polyol, AGE and HBP pathways in high glucose perfused hearts showed improved contractile function vs. the untreated high glucose perfused hearts ( $p < 0.05$ ) (Figure 4.20C). LVDP recovery for inhibitor-treated hearts reached  $43.6 \pm 4.5\%$  vs. untreated high glucose perfused hearts that only recovered to  $20.8 \pm 4.6\%$  after 60 min of reperfusion. There was no significant effect of pathway inhibition on RPP in high glucose perfused hearts (Figure 4.20D).

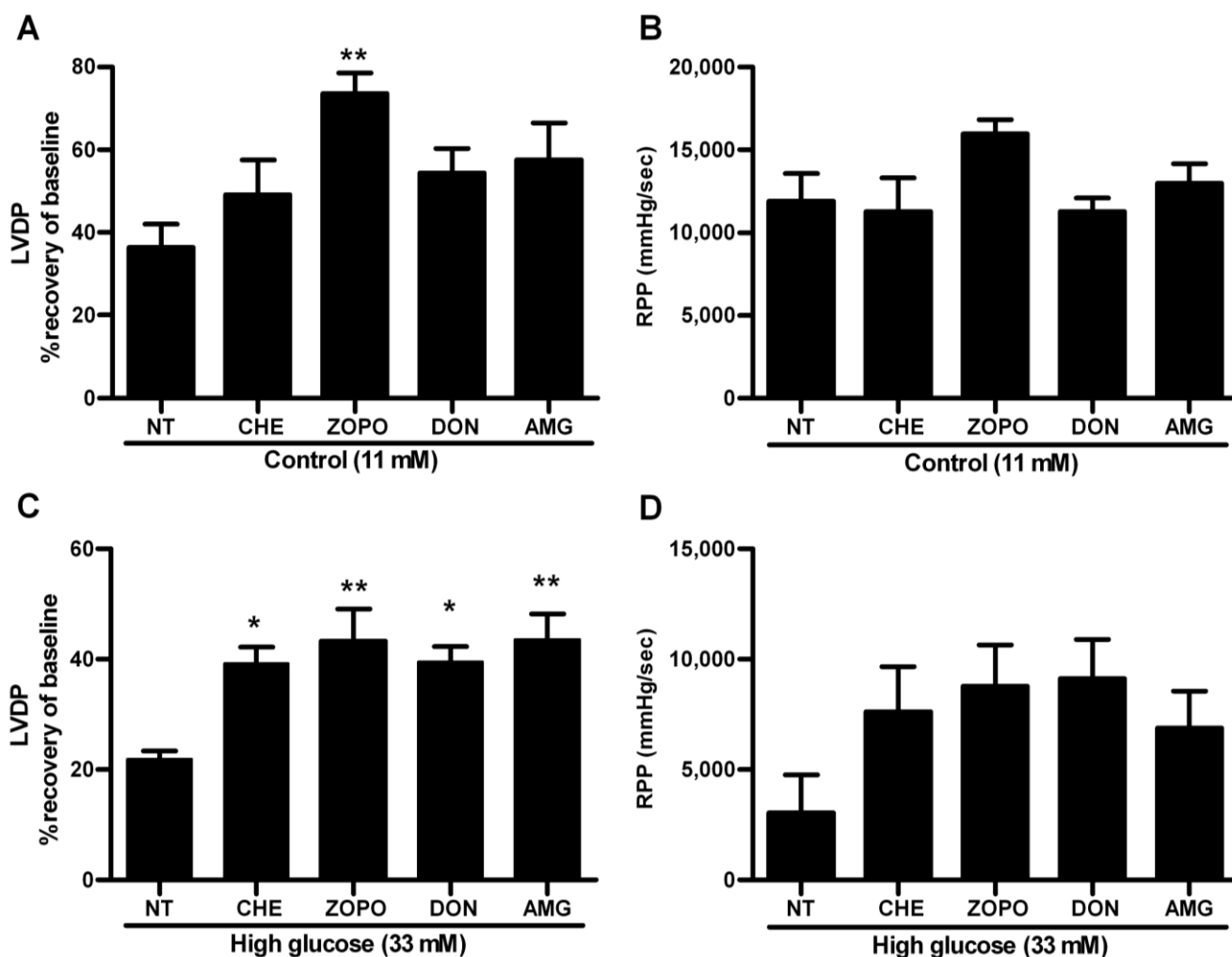


**Figure 4.20 High-glucose induced cardiac dysfunction blunted by acute non-oxidative pathway inhibition following ischemia and reperfusion.** Acute treatment with specific pathway inhibitors (100  $\mu$ M aminoguanidine (AMG) (for AGE pathway), 5  $\mu$ M chelerythrine chloride (CHE) (for PKC pathway), 40  $\mu$ M 6-diazo-5-oxonorleucine (DON) (for HBP), and 1  $\mu$ M zopolrestat (ZOPO) (for polyol pathway) during the first 20 min of reperfusion in isolated rat hearts. (A) LVDP recovery and (B) post-ischemic RPP ( $\text{mmHgsec}^{-1}$ ) under baseline conditions (11 mM glucose) and (C) LVDP recovery and (D) post-ischemic RPP ( $\text{mmHgsec}^{-1}$ ) under high glucose conditions (33 mM glucose) at 60 min of reperfusion. Values are expressed as mean  $\pm$  SEM ( $n=8$ ). \* $p<0.05$ , \*\* $p<0.01$  vs. respective controls.

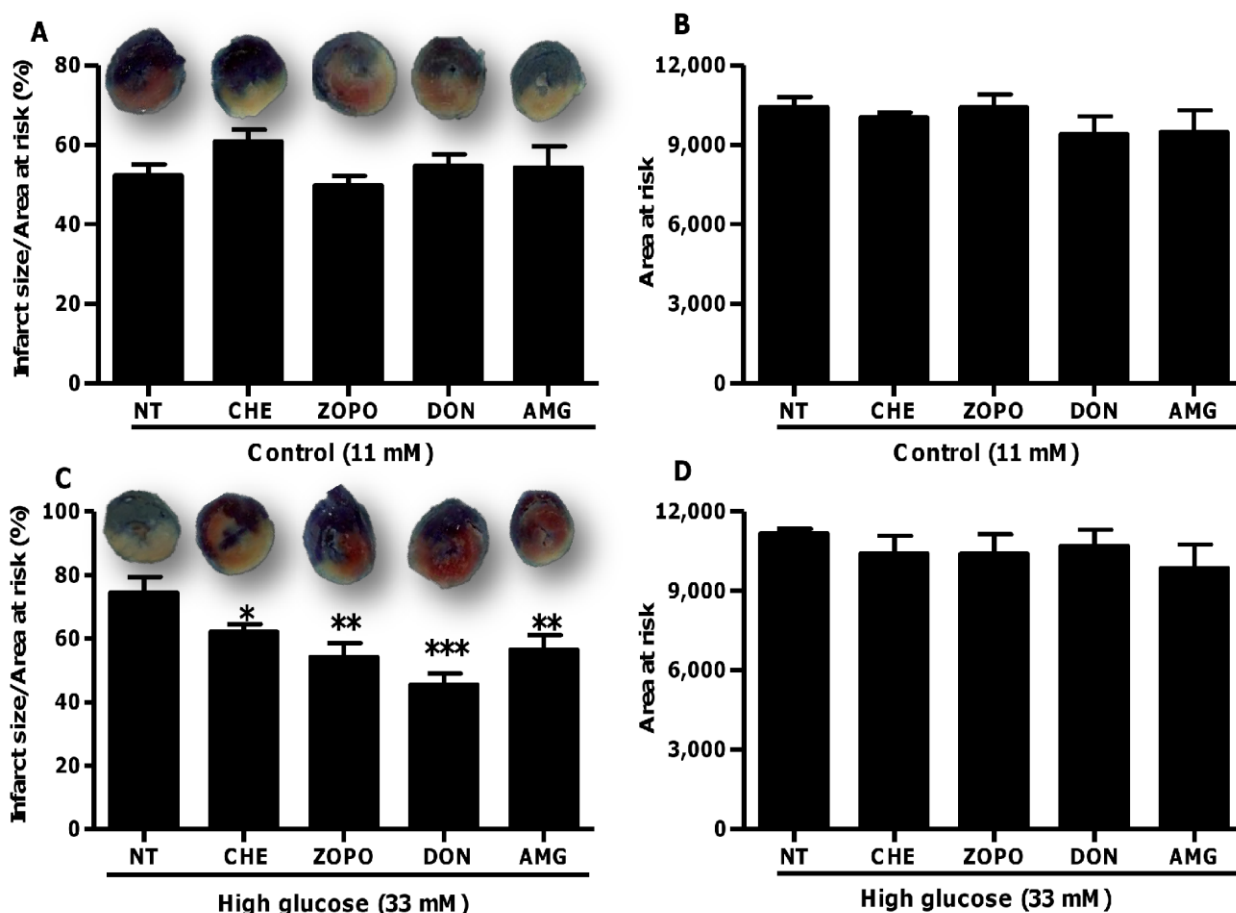
There were additional various effects on other parameters for contractile function following inhibition of flux through the individual non-oxidative glucose utilizing pathways. As shown in Table 4.3, no significant changes were found for coronary flow and heart rate in baseline and high glucose perfused rat hearts  $\pm$  inhibitor treatment. End-diastolic pressure was decreased following inhibition of the AGE and PKC pathways under high glucose conditions vs. untreated group. Furthermore,  $dP/dt_{max}$  was lower in the high glucose untreated rat hearts (33 mM) vs. control group (11 mM). This was, however, blunted ( $p < 0.05$ ) by specific inhibitors for the non-oxidative glucose pathways that resulted in elevated values to  $\sim 1,500$  mmHg/s vs.  $\sim 750$  mmHg for untreated high glucose perfused hearts (Table 4.3).

**Table 4.3** Coronary flow, end-diastolic pressure, heart rate and velocity of contraction for hearts under high glucose (33 mM) vs. control (11 mM)  $\pm$  NOGP inhibitors at the end of reperfusion.

	Coronary Flow (ml/min)	EDP (mmHg)	Heart rate (beats/min)	$dP/dt_{max}$ (mmHg/s)
<b>Control (11 mM)</b>	8 $\pm$ 2	38 $\pm$ 6	278 $\pm$ 19	1385 $\pm$ 56
<b>+ 5 <math>\mu</math>M CHE</b>	11 $\pm$ 1	42 $\pm$ 11	248 $\pm$ 9	1345 $\pm$ 63
<b>+ 1 <math>\mu</math>M ZOPO</b>	7 $\pm$ 2	36 $\pm$ 5	274 $\pm$ 17	1452 $\pm$ 23
<b>+ 40 <math>\mu</math>M DON</b>	9 $\pm$ 2	32 $\pm$ 12	276 $\pm$ 16	1265 $\pm$ 35
<b>+ 100 <math>\mu</math>M AMG</b>	6 $\pm$ 3	43 $\pm$ 12	282 $\pm$ 12	1300 $\pm$ 47
<b>High Glucose (33 mM)</b>	6 $\pm$ 1	87 $\pm$ 7*	310 $\pm$ 17	745 $\pm$ 91**
<b>+ 5 <math>\mu</math>M CHE</b>	9 $\pm$ 3	60 $\pm$ 6**	285 $\pm$ 14	1262 $\pm$ 126*
<b>+ 1 <math>\mu</math>M ZOPO</b>	10 $\pm$ 3	67 $\pm$ 4	283 $\pm$ 18	1310 $\pm$ 144*
<b>+ 40 <math>\mu</math>M DON</b>	11 $\pm$ 2	69 $\pm$ 4	309 $\pm$ 19	1350 $\pm$ 264*
<b>+ 100 <math>\mu</math>M AMG</b>	7 $\pm$ 3	61 $\pm$ 5*	281 $\pm$ 16	1500 $\pm$ 232*

NOGP- non-oxidative glucose pathways; EDP- end diastolic pressure;  $dP/dt_{max}$ - maximal velocity of contraction. (100  $\mu$ M aminoguanidine (AMG) (for AGE pathway), 5  $\mu$ M chelerythrine chloride (CHE) (for PKC pathway), 40  $\mu$ M 6-diazo-5-oxo-norleucine (DON) (for HBP), and 1  $\mu$ M zopolrestat (ZOPO) (for polyol pathway). Values are expressed as mean  $\pm$  SEM. \* $p < 0.05$ ; \*\* $p < 0.01$  vs. respective control. (n=6 in each group)

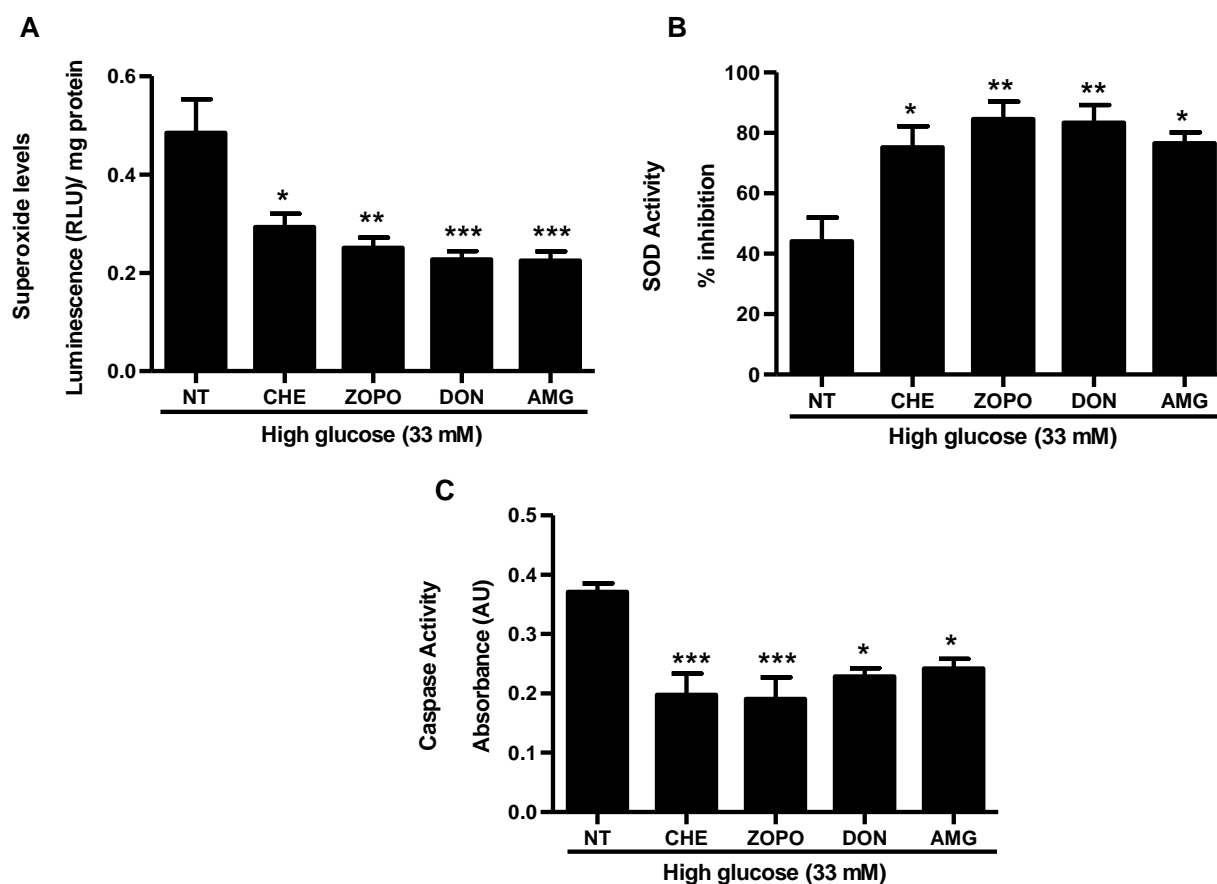
No changes were observed in infarct size/area at risk (%) under baseline glucose conditions (Figure 4.21A). However, infarct sizes decreased following inhibitor treatment – thus in line with our improved functional data (Figure 4.21C). There were no differences in the area at risk under baseline and high glucose perfusion conditions.



**Figure 4.21 Acute inhibition of non-oxidative glucose pathways decreases infarct size under high glucose conditions.** Isolated rat hearts were perfused under normal or high glucose conditions and subjected to regional ischemia. Acute treatment with specific pathway inhibitors (100  $\mu$ M aminoguanidine (AMG) (for AGE pathway), 5  $\mu$ M chelerythrine chloride (CHE) (for PKC pathway), 40  $\mu$ M 6-diazo-5-oxo-norleucine (DON) (for HBP), and 1  $\mu$ M zopolrestat (ZOPO) (for polyol pathway) during the first 20 min of reperfusion in isolated rat hearts of the 2 hr reperfusion period. (A) infarct size/area at risk (%) and (B) area at risk under baseline (simulated normoglycemia) vs. (C) infarct size/area at risk (%) and (D) area at risk under high glucose perfusions (simulated hyperglycemia). Evans blue dye and TTC staining enabled visualization of viable tissue, infarcted area and the area at risk. Values are expressed as mean  $\pm$  standard error of means (SEM). \* $p$ <0.05; \*\* $p$ <0.01; \*\*\* $p$ <0.001 vs untreated high glucose group.

#### 4.3.7 Hyperglycemia-induced oxidative stress and apoptosis is blunted by acute inhibition of flux through the damaging non-oxidative glucose pathways

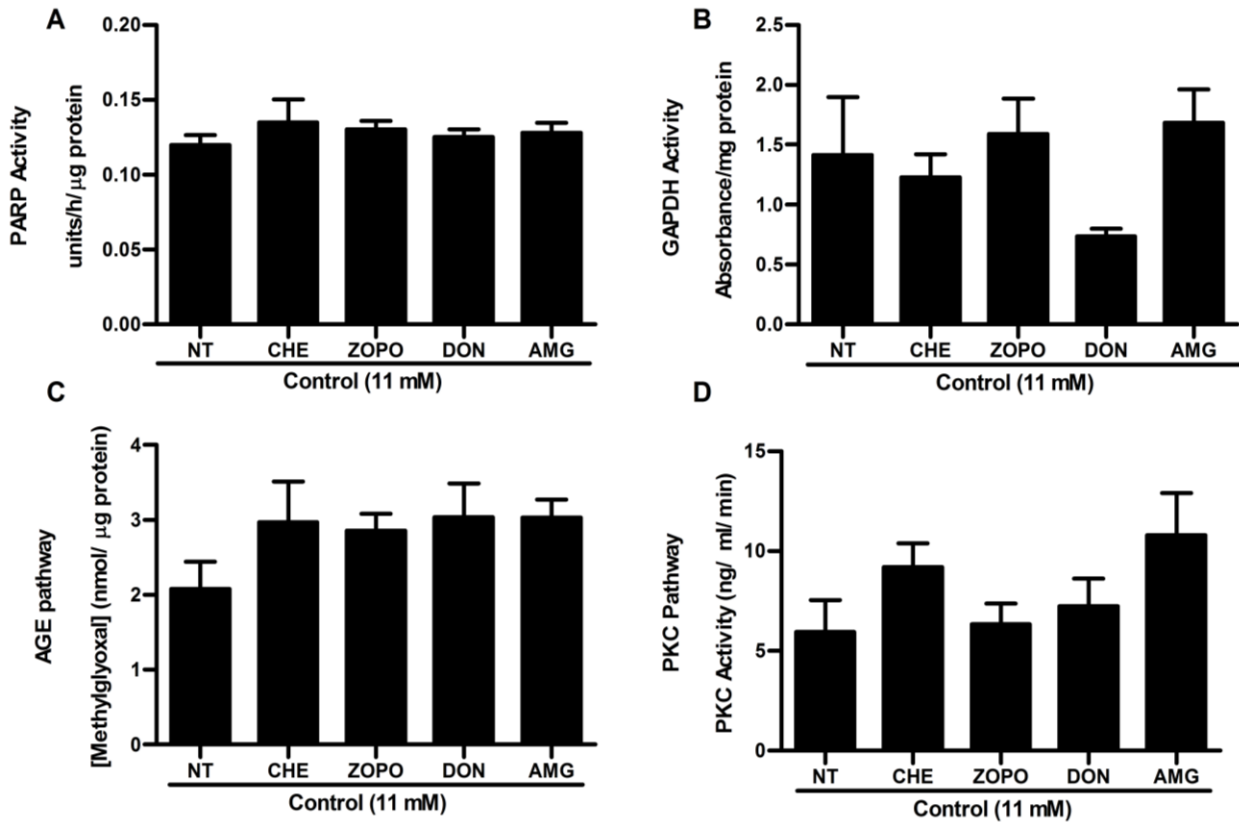
Our data shows that oxidative stress is blunted by inhibition of flux through PKC, AGE, HBP and polyol as shown by decreased superoxide levels (Figure 4.22A); increased SOD activity (Figure 4.22B); decreased caspase activity (Figure 4.22C).

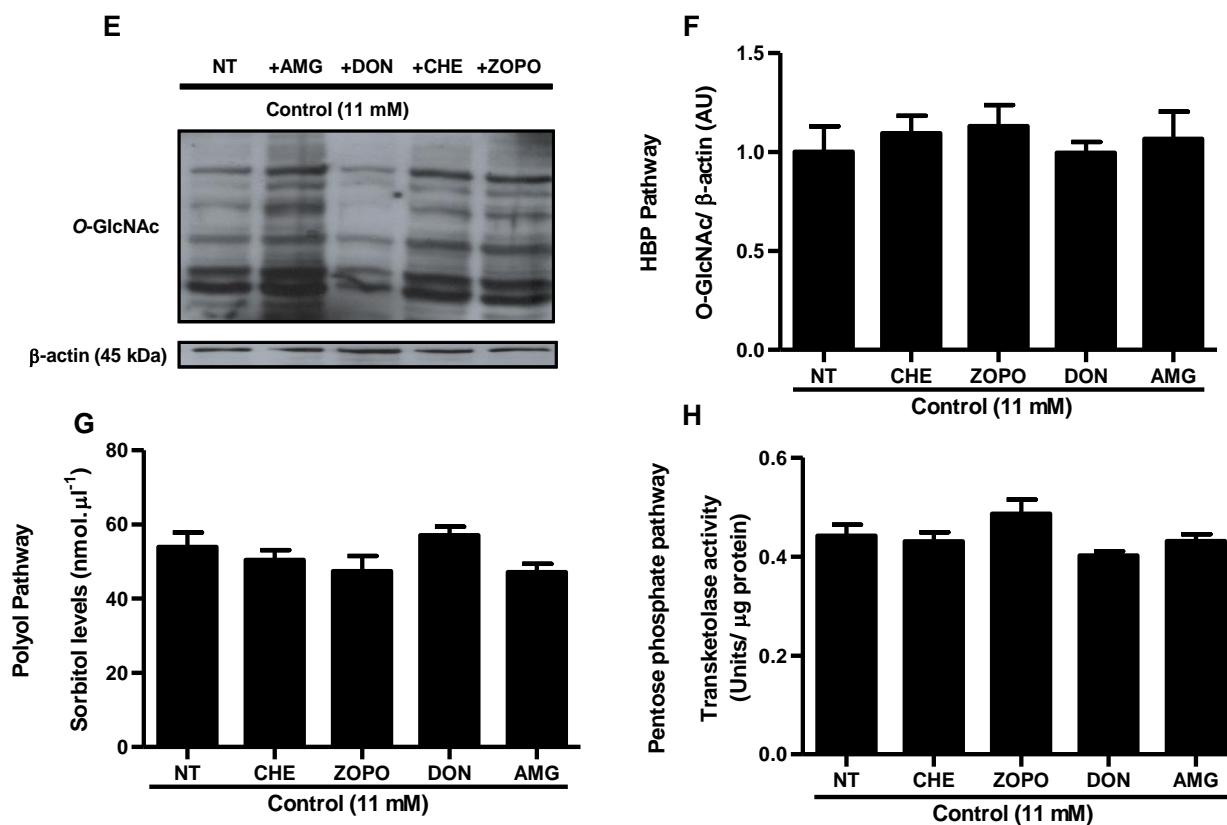


**Figure 4.22 Inhibition of the non-oxidative glucose pathways attenuate high glucose-induced oxidative stress (decreased superoxide levels and increased SOD activity) and apoptosis as shown by decreased caspase 3/7 activity.** Isolated rat hearts were perfused under high glucose conditions vs. controls and subjected to global ischemia  $\pm$  inhibitor treatments during the first 20 min of the 1hr reperfusion period (100  $\mu$ M aminoguanidine (AMG) (for AGE pathway), 5  $\mu$ M chelerythrine chloride (CHE) (for PKC pathway), 40  $\mu$ M 6-diazo-5-oxo-norleucine (DON) (for HBP), and 1  $\mu$ M zopolrestat (ZOPO) (for polyol pathway). NT: non-treated controls). (A) superoxide levels, (B) superoxide dismutase activity and (C) caspase activity. Values are expressed as mean  $\pm$  SEM (n=6). \*p<0.05, \*\*p<0.01, \*\*\*p<0.001 vs. respective controls.

### 4.3.8 The interlink of non-oxidative glucose pathways in attenuating hyperglycemia-induced metabolic dysfunction

Specific inhibition of individual non-oxidative glucose pathways showed no effect on flux through the other respective pathways in hearts under baseline glucose conditions (Figure 4.23).

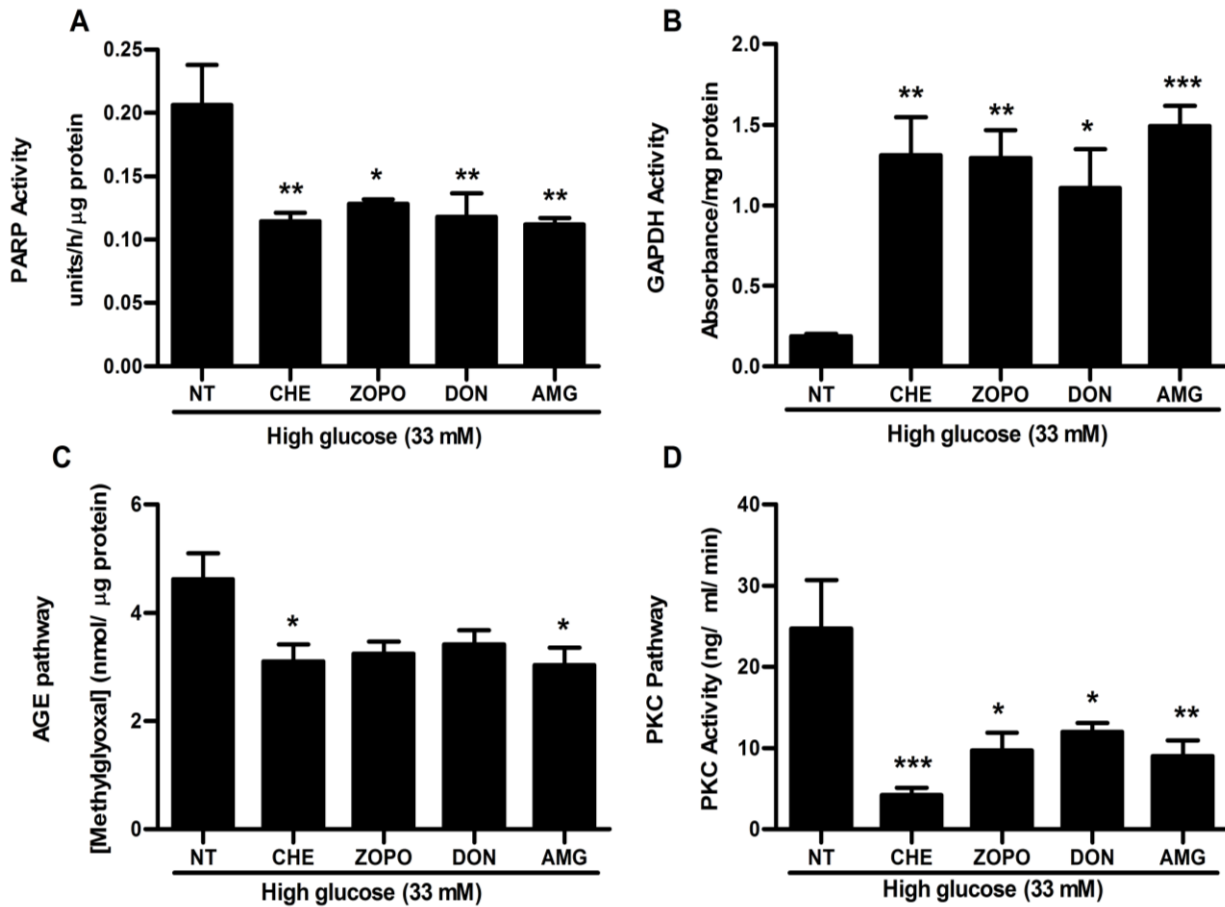




**Figure 4.23 Cardiac metabolic function at baseline glucose conditions with acute non-oxidative pathway inhibition following ischemia and reperfusion.** Acute treatment with specific pathway inhibitors (100  $\mu$ M aminoguanidine (AMG) (for AGE pathway), 5  $\mu$ M chelerythrine chloride (CHE) (for PKC pathway), 40  $\mu$ M 6-diazo-5-oxo-norleucine (DON) (for HBP), and 1  $\mu$ M zopolrestat (ZOPO) (for polyol pathway) during the first 20 min of reperfusion in isolated rat hearts. (A) PARP activity, (B) GAPDH activity, (C) AGE activation (methylglyoxal concentration), (D) PKC activity, (E) O-GlcNAc peptide levels, (F) quantification of total O-GlcNAc peptide levels, (G) polyol pathway activation (sorbitol levels), and (H) pentose phosphate pathway activation (transketolase activity). Values are expressed as mean  $\pm$  SEM (n=6).



However, inhibition of non-oxidative glucose pathway flux under high glucose conditions blunted metabolic dysfunction as shown by attenuation of PARP activity and normalizing of GAPDH activity (Figures 4.24A and 4.24B). Interestingly, inhibition of individual pathways attenuated activation through the other respective pathways (Figure 4.24C-4.24G). There was no effect, however, of the individual pathway inhibition on the pentose phosphate pathway.



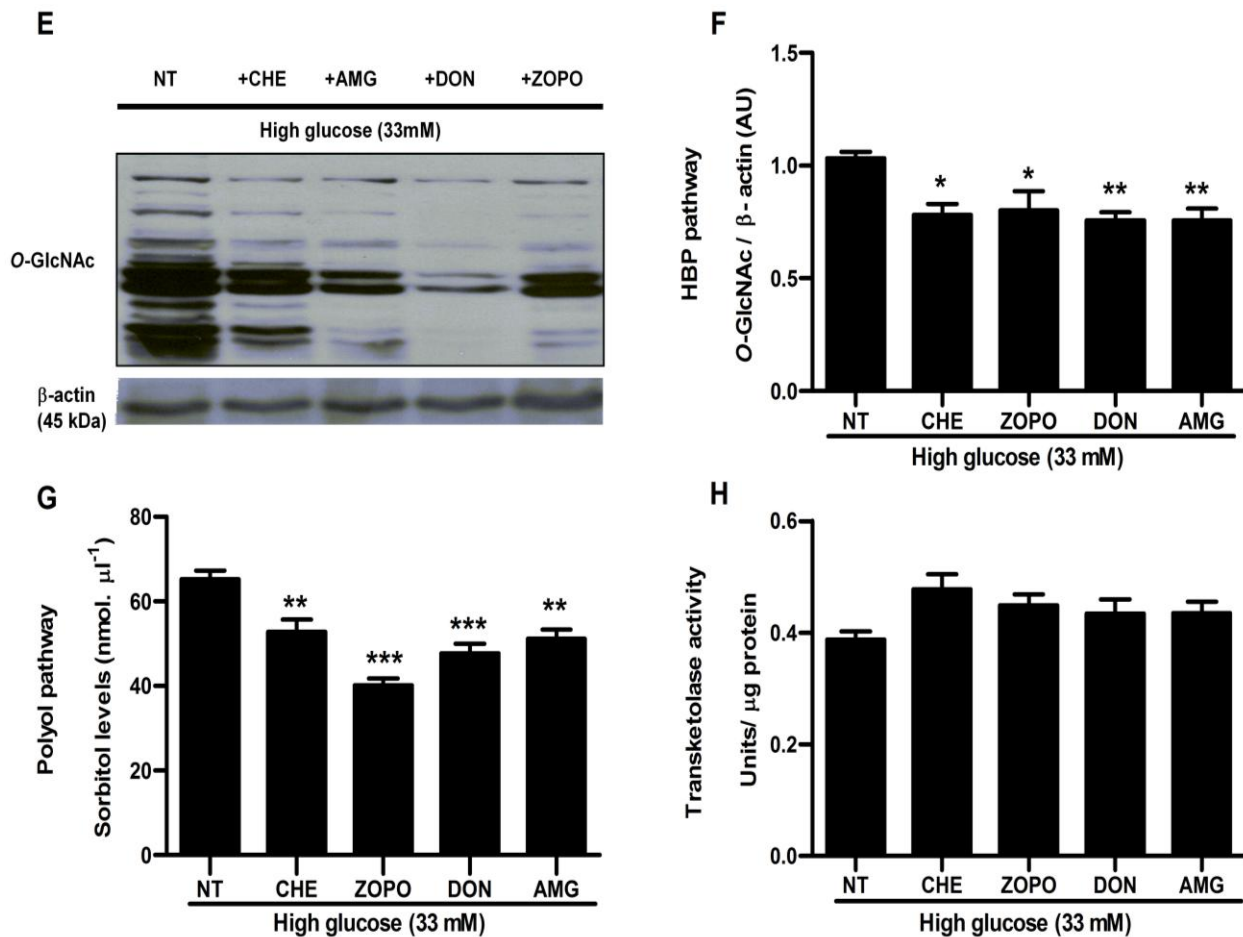


**Figure 4.24 High-glucose induced cardiac metabolic dysfunction blunted by acute non-oxidative pathway inhibition following ischemia and reperfusion.** Acute treatment with specific pathway inhibitors (100  $\mu$ M aminoguanidine (AMG) (for AGE pathway), 5  $\mu$ M chelerythrine chloride (CHE) (for PKC pathway), 40  $\mu$ M 6-diazo-5-oxo-norleucine (DON) (for HBP), and 1  $\mu$ M zopolrestat (ZOPO) (for polyol pathway) during the first 20 min of reperfusion in isolated rat hearts. (A) PARP activity, (B) GAPDH activity, (C) AGE activation (methylglyoxal concentration), (D) PKC activity, (E) O-GlcNAc peptide levels, (F) quantification of total O-GlcNAc peptide levels, (G) polyol pathway activation (sorbitol levels), and (H) pentose phosphate pathway activation (transketolase activity). Values are expressed as mean  $\pm$  SEM (n=6). \*p<0.05, \*\*p<0.01, \*\*\*p<0.001 vs. respective controls.

Thus our data shows that the individual non-oxidative glucose utilizing pathways are interrelated, i.e. inhibition of AGE, PKC, HBP and polyol down-regulated activation through all the other non-oxidative glucose utilizing pathways (Figures 4.25A to 4.25D).

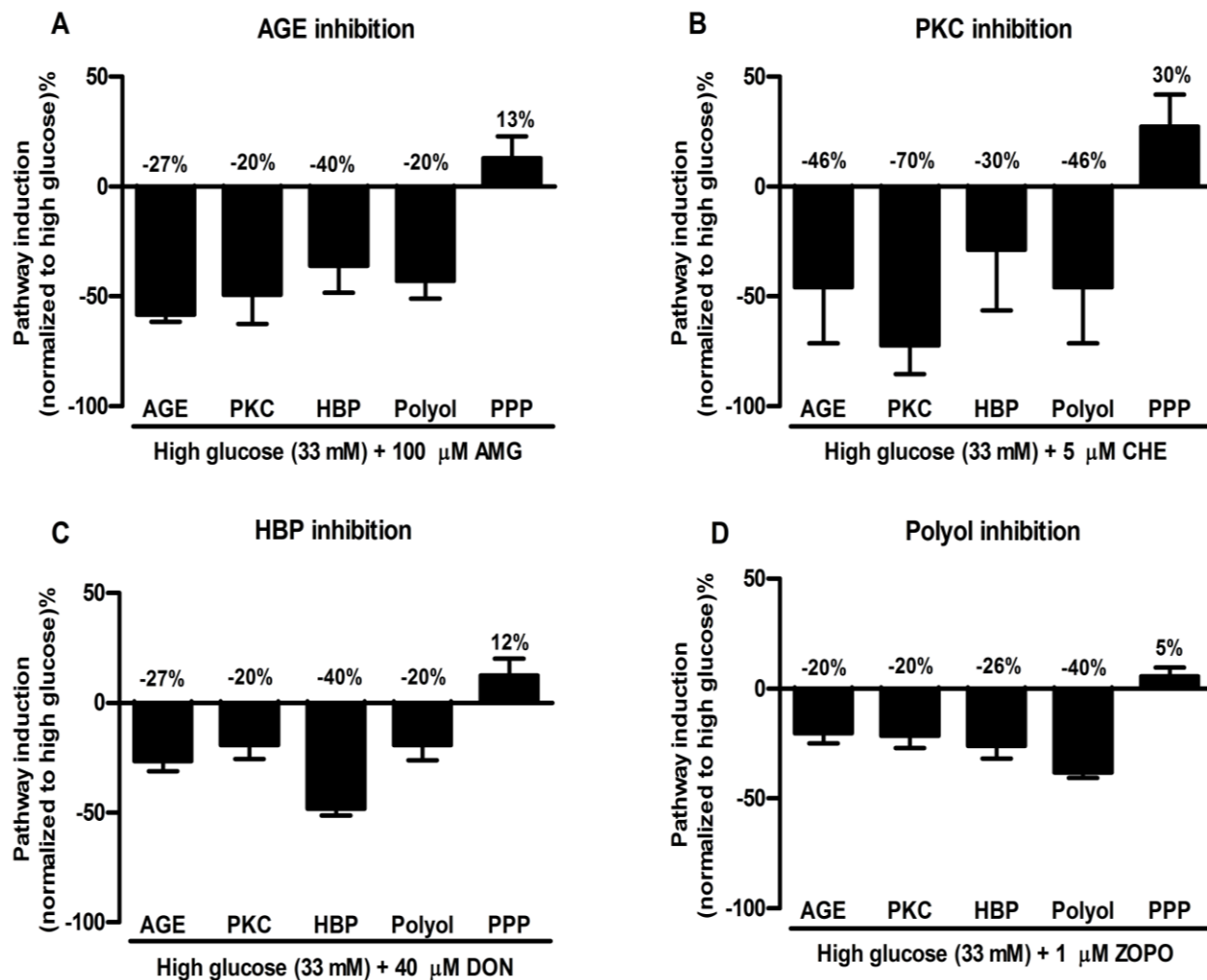


**Figure 4.25 Activation of non-oxidative pathways in high glucose perfusions with pathway inhibitors relative to high glucose conditions without treatment.** Relative pathway activation after inhibition of (A) AGE pathway, (B) PKC pathway, (C) HBP pathway and (D) polyol pathway. Values are expressed as mean  $\pm$  SEM (n=6).

## 4.4 Discussion

The damaging alliance between hyperglycemia and myocardial infarctions necessitates the development of novel therapeutic interventions for both chronic (diabetic individuals) and acute hyperglycemia (non-diabetic patients) (86, 105). In light of this, we employed *ex vivo* and *in vivo* models to investigate whether acute BFT administration - immediately following an ischemic insult – offers cardio-protection in response to ischemia and reperfusion under hyperglycemic conditions. The main findings of this study are that: 1) acute hyperglycemia triggers oxidative stress, the coordinated induction of non-oxidative glucose metabolic pathways and impaired contractile function following an ischemic insult under hyperglycemic conditions; and 2) post-ischemic BFT treatment resulted in cardio-protection by attenuating the detrimental effects of hyperglycemia with ischemia and reperfusion.

### 4.4.1 Acute hyperglycemia triggers oxidative stress, the coordinated induction of non-oxidative glucose metabolic pathways and impaired contractile function

Our *ex vivo* perfusion experiments revealed that acute hyperglycemia resulted in decreased contractile function following ischemia and reperfusion (independent of osmotic effects). Moreover, this was associated with higher myocardial superoxide levels and a concomitant decrease in SOD activity. This is in agreement with others where oxidative stress increased with hyperglycemia while activities of antioxidant enzymes decreased (16, 17, 26). Increased superoxide production was previously found in *ex vivo* models of hyperglycemia following ischemia and reperfusion (84), and it may also be converted to the damaging free radical, peroxynitrite (18). Our data are in agreement with the unifying hypothesis put forward by the Brownlee laboratory, that hyperglycemia-induced oxidative stress plays a crucial role in triggering damaging sequelae that contribute to the onset of type 2 diabetes (12, 13). Potential sources for hyperglycemia-induced ROS include greater superoxide levels

due to impaired mitochondrial function (13, 98) and/or higher NADPH oxidase activity (120), and glucose auto-oxidation (140). Moreover, ischemia and reperfusion *per se* also elevates cardiac ROS levels (20, 91, 118) thus further contributing to the overall oxidative stress here observed.

We also discovered increased PARP and attenuated GAPDH activities following ischemia and reperfusion in hearts exposed to high glucose. These findings are consistent with higher PARP activation operating as a restorative mechanism to alleviate hyperglycemia-induced DNA damage (66). However, its activation also leads to diminished GAPDH activity (28, 35, 153). Furthermore, GAPDH itself is susceptible to hyperglycemia-generated ROS (57), e.g. S-thiolation by hydrogen peroxide (10, 117, 121) and nitroalkylation by nitroalkene derivatives (5). Such modifications can cause GAPDH to form aggregates that translocate to the nucleus where it may participate in the induction of apoptosis (96). Lower GAPDH activity may also be due to the effects of ischemia (90).

Previous research established that PARP-mediated blunting of GAPDH activity leads to greater flux into the non-oxidative pathways of glucose metabolism – AGE, HBP, PKC and the polyol pathway - with damaging outcomes (35, 47). In parallel, PPP flux decreases under these conditions (35, 47). For our study we demonstrate that this scenario occurs within the setting of ischemia and reperfusion in response to acute hyperglycemia. Moreover, we determined - for the first time as far as we are aware – the relative degree of non-oxidative pathway activation, with AGE and PKC showing a marked increase under hyperglycemic conditions. However, does pathway activation in this instance *actually* result in harmful outcomes? Our data strongly support this since individual pathway inhibitor administration resulted in reduced myocardial ROS levels and apoptosis. In parallel, individual pathway inhibitors also decreased infarct sizes. Interestingly, the functional effects of individual pathway inhibitors did not significantly differ from each other and provides additional support for the idea of a unifying hypothesis and the inter-relatedness of the pathways (13). We propose that higher activation of AGE and PKC may further fuel flux through the HBP and polyol pathways with harmful effects. Furthermore, AGE and PKC activation may also trigger alternate functional outcomes not

investigated in the present study. Thus our data show that certain non-oxidative glucose pathways can be rapidly induced in response to acute hyperglycemic exposure and leads to serious implications for the heart's contractile abilities.

By what mechanisms do the non-oxidative pathways elicit its detrimental effects on the heart? Here the non-enzymatic attachment of proteins to glucose produces AGE that may eventually impair extracellular matrix and intracellular protein function (12, 49). Moreover, augmented MG levels (AGE precursor) may contribute to the pathogenesis of diabetic complications (114, 141). However, these findings were reported in response to chronic elevations in blood glucose and are therefore unlikely to play a role in our study. Since AGE accumulation may also trigger oxidative stress and myocardial apoptosis (77), we are of the opinion that this likely applies in our case.

Under hyperglycemic conditions excess glycolytic intermediates can lead to increased *de novo* synthesis of DAG, a well-known activator of the PKC pathway (reviewed in (44)). Moreover, PKC may also be activated as a result of lower ATP levels that occur due to the ischemic insult itself, thus resulting in a compounding effect together with hyperglycemia (126). Which PKC is implicated here since there are multiple isoforms that are expressed in the rat heart? We are of the opinion that the PKC- $\alpha$ , - $\beta$ 1 and - $\beta$ 2 isoforms likely play a role since earlier work established its up-regulation in the hyperglycemic heart (reviewed in (44)). However, further studies are required to delineate PKC isoforms activated in response to ischemia and reperfusion under acute hyperglycemic conditions. PKC activation may impair contractile function by decreasing activity of the Na<sup>+</sup>/K<sup>+</sup> ATPase pump (145). Here PKC activation increases cytosolic phospho-lipase A2 activity that enhances production of arachidonate and prostaglandin E2, known inhibitors of the Na<sup>+</sup>/K<sup>+</sup> ATPase pump (145). Moreover, PKC activation may also further elevate myocardial ROS production by activation of NADPH oxidases (4, 143).

Although we found relatively lower activation of the HBP and polyol pathways with high glucose exposure, its stimulation also contributes to higher myocardial oxidative stress, apoptosis and infarct sizes. This is supported by our data generated by respective HBP and polyol pathway inhibitors, demonstrating lower cardiac ROS levels and apoptosis together with cardio-protection. Moreover, previous research from our laboratory demonstrated that hyperglycemia results in greater oxidative stress that triggered HBP-induced myocardial apoptosis in cardiomyoblasts (109). Activation of the polyol pathway is also linked with detrimental effects e.g. increased oxidative stress, sorbitol-induced osmotic effects, and perturbations in  $\text{Na}^+/\text{K}^+$  ATPase activity (reviewed in (129)).

We also established that myocardial transketolase activity decreased in rat hearts following ischemia and reperfusion under hyperglycemic conditions, and this may occur due to its modification by oxidative stress (154). Our findings are in agreement with previous work that reported lower transketolase and glucose-6-phosphate dehydrogenase (G6PD) activities in the diabetic heart (70). Since the PPP generates NADPH (via G6PD reaction in oxidative branch) it allows for regeneration of reduced glutathione (GSH), thus playing a pivotal role in the myocardium's antioxidant defense system (70). Together our data therefore demonstrate that hyperglycemia-induced activation of non-oxidative glucose pathways together with reduced PPP activation trigger damaging effects (ROS and apoptosis) that contribute to contractile dysfunction in response to ischemia and reperfusion under hyperglycemic conditions.

#### **4.4.2 Acute BFT treatment attenuates the detrimental effects of hyperglycemia with ischemia and reperfusion**

We initially tested two BFT concentrations at baseline (11 mM glucose) under non-ischemic perfusion conditions. Our data show that BFT treatment enhanced contractile function, implying that it possesses intrinsic inotropic properties. Moreover, we found that BFT also decreased the heart rate under these conditions. We are unclear how precisely this occurs, but previous research work

suggests that this may constitute an energy conserving mechanism (by promoting glucose oxidation (40) and/or a direct effect of BFT on neuro-hormonal modulation (70). However, these interesting possibilities require further investigation.

We next tested whether acute BFT treatment could mediate cardio-protection in response to ischemia and reperfusion under hyperglycemic conditions. Our results demonstrate that all three BFT concentrations significantly improved contractile function and decreased infarct sizes. The increase in coronary flow may contribute to post-ischemic neovascularization previously reported (70), thus promoting oxygen supply and removing damaging metabolites to improve post-ischemic recovery (46, 54, 87). Adequate blood flow during reperfusion therefore allows efficient relaxation of the ventricles (decreased workload) (69) as observed by the decrease in end diastolic pressure with BFT treatment.

We also investigated whether BFT administration would lead to similar effects in response to chronic glucose exposure. Here acute intravenous BFT administration to STZ-induced diabetic rats following *in vivo* coronary artery ligations resulted in smaller infarct sizes compared to respective controls. Together these data show that post-ischemic BFT administration following acute and chronic hyperglycemia effectively blunts the harmful effects of excess glucose supply on contractile function. Of note, these findings are distinct from previous studies that employed *chronic* BFT treatment before the ischemic insult as a therapeutic strategy to offer cardio-protection to diabetic animals that were subjected to ischemia and reperfusion (70).

Our experiments also revealed an unexpected finding, i.e. that BFT acted as a novel cardio-protective agent when ischemia and reperfusion was performed under baseline conditions (simulated normoglycemia). We are unclear how exactly this occurs; however, our data indicate that the mechanism is likely independent of shunting of glycolytic metabolites to the pentose phosphate pathway. Several possibilities emerge that include activation of the reperfusion injury signaling kinase



(50, 83) and JAK-STAT pathways (70), and/or by alternate mechanisms. These possibilities are currently being investigated in our laboratory.

How does acute BFT treatment exert its cardio-protective effects (under hyperglycemic conditions) following an ischemic insult? The present study established that BFT administration markedly elevated transketolase activity thereby activating the non-oxidative branch of the PPP. In parallel, we found decreased activation of four non-oxidative glucose pathways thus confirming that BFT effectively shunted flux away from these detrimental pathways. Moreover, these data emphasize that there are distinct differences between non-oxidative glucose pathways with activation of AGE, HBP, polyol pathway and PKC linked to detrimental cardio-metabolic effects, while stimulation of the non-oxidative PPP branch was associated with protective effects. Our data also show that individual pathway inhibition resulted in attenuated myocardial superoxide levels for each respective pathway. In parallel, BFT supply reduced cardiac superoxide levels and concomitantly restored SOD function. Together these data demonstrate that BFT decreases overall myocardial oxidative stress by blunting ROS generation via certain non-oxidative pathways of glucose metabolism. Furthermore, BFT may also a) increase G6PD activity (70) (feed forward mechanism) and thereby further enhance myocardial anti-oxidant capacity, and b) attenuate ROS generated as a result of ischemia and reperfusion.

Benfotiamine administration concomitantly elicited cardio-protection in high glucose perfused hearts together with reduced cardiac cell death i.e. apoptosis and necrosis (decreased infarct size). Cardio-protection in this instance, likely results from BFT's upstream effects, i.e. by lowering myocardial oxidative stress and attenuating cell death. Moreover, by shunting flux away from the AGE, HBP, PKC and polyol pathway, BFT effectively blunts the other damaging effects that these pathways may have on the heart's function (earlier discussed). It is possible that BFT may have inhibited inflammation that occurs with ischemia and reperfusion, thus it may have additional beneficial effects in cardiac pathologies with inflammation such as arthritis. One of our interesting novel findings was inhibition of chymotrypsin-like proteasomal activity by BFT under high glucose conditions following ischemia and

reperfusion. As been discussed earlier in chapter 3 UPS activity varies with hyperglycemia and following ischemia and regulation. Literature also shows that posttranslational modification of UPS plays a role in regulating its activity. For example UPS activity is inhibited by protein kinase A phosphorylation (150), O-GlcNAcylation (151, 152) and glycation by AGEs (67, 108). We speculate that BFT inhibition of NOGP flux under high glucose conditions relieved the UPS of HBP-induced inhibition of the 26S. However, considering that BFT-inhibition on the AGE pathway is incomplete it implies that inhibition of the UPS chymotrypsin-like activity may be due to AGEs (67, 108) and possibly BFT itself.

#### **4.4.3 Individual acute inhibition of NOGP attenuates the detrimental effects of hyperglycemia with ischemia and reperfusion**

We tested effects of NOGP inhibition by employing various inhibitors specific for each pathway. Interestingly, inhibition of the polyol pathway at baseline significantly improved cardiac contractile function following ischemia and reperfusion with a corresponding decrease in infarct size (though did not reach statistical significance). This outcome supports previous observations regarding the role of the polyol pathway in ischemia and reperfusion damage, independent of hyperglycemia (2, 58, 59). It has been reported that ischemia increases AR activity approximately 3-fold possibly due to increased ROS produced during ischemia (65). Increased AR further increases ROS by peroxynitrite production and depletion of one a major antioxidant, i.e. glutathione (128). Furthermore, increased ROS secondary to AR activation can also occur due to opening of the mitochondrial permeability transition pore (mPTP) (2). The increased activation of the polyol subsequently causes cardiac contractile dysfunction by enhancing tyrosine nitration of the SERCA and oxidation of ryanodine proteins thus impairing its functional role in cardiac contractility (65, 128). Increased oxidative stress by the polyol pathway also involves its close relationship to the AGE pathway. For example, AR catalyzes the reversible reduction of MG to hydroxyacetone with consumption of NADPH (64). Additionally, MG is also a substrate for SDH (79).

Ischemia and reperfusion under hyperglycemic conditions further increases ROS production and its effects are further exacerbated by altered glucose metabolism (76, 102). The polyol pathway also provides potent substrates for AGE formation, hence further increasing ROS levels and leading to impaired cardiac contractile function (65, 74). Furthermore, GSH depletion implies a decrease in the detoxification of MG by the GSH-dependent glyoxal system (133). Our findings show that inhibition of the polyol pathway attenuates oxidative stress as indicated by decreased superoxide levels, increased SOD, restored GAPDH and PARP activities. Thus polyol pathway inhibition under normoglycemic and hyperglycemic conditions results in cardio-protection by improving energy homeostasis (112, 113), attenuation of ROS production and changes in intracellular sodium and calcium (101, 128, 134, 139). The decreased oxidative stress with zopolrestat implies restored glycolysis, GAPDH activity and consequently PARP activity (34, 35, 47) following polyol inhibition.

Attenuation of oxidative stress may also explain the decreased caspase activity since oxidative stress can directly induce apoptosis (14, 32, 37, 68). Indeed, AR inhibition attenuates TNF $\alpha$  and PKC activation, and p38 MAPK and c-Jun N-terminal kinase phosphorylation (93, 111).

We found that the inhibitor effects were much more pronounced under hyperglycemic perfusion conditions. Increased MG levels under hyperglycemic conditions in untreated hearts may impair contractile cardiac function by glycative inhibition of thioredoxin activity, thus further increasing oxidative stress (138). Moreover, various ROS are produced during AGE formation thus contributing to increased oxidative stress, apoptosis, decreased GAPDH and increased PARP activities as we and other investigators have previously reported (33–35, 138). MG can increase oxidative stress by causing glycation and subsequent inactivation of glutathione reductase and glutathione peroxidase (89). Furthermore, MG can directly deplete GSH and increase oxidative stress. This in turn will further impair degradation of MG and establish a vicious cycle that leads to even greater MG levels (133).

The damaging effects of AGE may occur directly or via its interaction with RAGE binding can initiate important signaling pathways involving activation of PKC (88, 119), tyrosine phosphorylation of JAK/STAT, (56), recruitment of PI 3-K to MAPK (78) or PKC (27, 72, 75, 122) and induction of oxidative stress cascades which culminate in NF- $\kappa$ B and AP-1 transcription (7, 12, 148). Thus by inhibiting AGE formation all these damaging effects are blunted and thereby resulting in improved cardiac function.

There has been a growing body of evidence in the central role of PKC in signal transduction pathways in hyperglycemia-induced complications (61, 144). We observed increased PKC activity in our untreated hearts exposed to high glucose, and this likely occurs due to elevated DAG levels (12, 61, 144). Of note, PKC activity and expression can increase during ischemia and reperfusion in acute ischemia/ reperfusion models (126). This may either be cardio-protective or damaging depending on which isoform is activated.

Lastly we also found greater HBP activation in association with decreased cardiac function, increased oxidative stress, apoptosis, attenuated GAPDH and enhanced PARP activity in untreated hearts under hyperglycemic conditions following ischemia and reperfusion. Increased O-GlcNAcylation under hyperglycemic conditions has been previously reported to elicit similar detrimental effects on cardiac contractile function (21, 55, 84). It is likely that detrimental effects are mainly due to altered protein function, for e.g. increased protein O-linked GlcNAcylation diminished expression of cardiac SERCA and lead to impaired myocardial contractility (21, 55). Increased HBP activation also causes PKC activation thus leading to more ROS and consequently apoptosis (36, 97). Moreover, HBP-mediated induction of FAO may also blunt cardiac function under these conditions (73).

In conclusion, our data demonstrate that acute BFT treatment initiated *after* an ischemic insult offers significant promise as a novel therapeutic agent for AMIs under conditions of acute and chronic hyperglycemia. This may be especially useful for the alarming number of diabetic individuals suffering cardiovascular complications, and also for non-diabetic patients that exhibit stress-induced

hyperglycemia within the clinical setting. Of note, acute BFT treatment also resulted in cardio-protection in control hearts, thereby highlighting that it actually has a broader therapeutic utility than what would be expected. Additionally, the current study demonstrates that acute NOGP inhibition initiated after an ischemic insult offers significant potential as therapeutic agent(s) for myocardial infarction under acute hyperglycemic conditions. Moreover, our findings establish for the first time that there is a convergence of downstream NOGP effects in our experimental systems, i.e. increased myocardial oxidative stress, further pathway activation, apoptosis, and impaired contractile function. Thus we propose a unique model to explain our intriguing findings. Here a vicious metabolic cycle is established whereby hyperglycemia-induced NOGP further fuels its own activation by generating even more oxidative stress, thereby exacerbating damaging effects on the heart under these conditions (Figure 4.26).

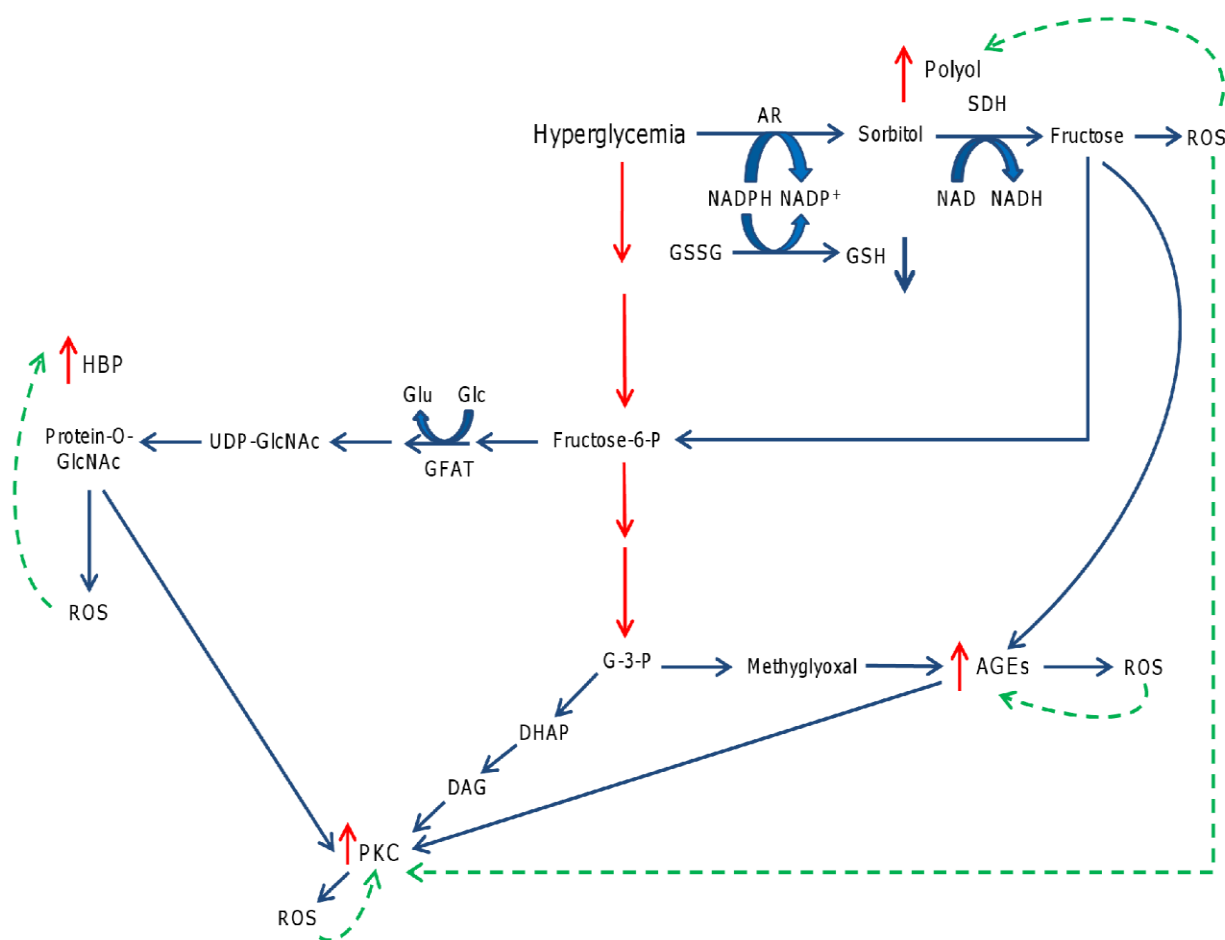


**Figure 4.26 Model to explain metabolic vicious cycle whereby hyperglycemia-mediated activation of non-oxidative pathways fuels oxidative stress and detrimental outcomes.** With acute hyperglycemia, ROS are produced by activation of non-oxidative pathways of glucose metabolism: polyol pathway, HBP, PKC and AGE (refer blue arrows). This results in a vicious metabolic cycle i.e. pathway activation further increasing ROS generation and again activating non-oxidative glucose pathways. AR: aldose reductase; SDH: sorbitol dehydrogenase; Glc: glucosamine; Glu: glutamate; GFAT: glutamine: fructose-6-phosphate amidotransferase; UDP-GlcNAc: uridine diphosphate-*N*-acetylglucosamine; DHAP: dihydroacetone phosphate; DAG: diacylglycerol; AR: aldose reductase; SDH: sorbitol dehydrogenase; ROS: reactive oxygen species; G 3-P: glyceraldehyde 3-phosphate; GSSG: oxidized glutathione; GSH: reduced glutathione.

## 4.5 References

1. **Alexander-Kaufman K, Harper C.** Transketolase: Observations in alcohol-related brain damage research. *Int J Biochem Cell Biol* 41: 717–720, 2009.
2. **Ananthakrishnan R, Kaneko M, Hwang YC, Quadri N, Gomez T, Li Q, Caspersen C, Ramasamy R.** Aldose reductase mediates myocardial ischemia-reperfusion injury in part by opening mitochondrial permeability transition pore. *Am J Physiol Heart Circ Physiol* 296: H333–H341, 2009.
3. **Barg J, Belcheva M, Coscia C.** Evidence for the implication of phosphoinositol signal transduction in mu-opioid inhibition of DNA synthesis. *J Neurochem* 59: 1145–1152, 1992.
4. **Basuroy S, Bhattacharya S, Leffler CW, Parfenova H.** Nox4 NADPH oxidase mediates oxidative stress and apoptosis caused by TNF-alpha in cerebral vascular endothelial cells. *Am J Physiol Cell Physiol* 296: C422–C432, 2009.
5. **Batthyany C, Schopfer FJ, Baker PRS, Durán R, Baker LMS, Huang Y, Cerveñansky C, Branchaud BP, Freeman BA.** Reversible post-translational modification of proteins by nitrated fatty acids in vivo. *J Biol Chem* 281: 20450–20463, 2006.
6. **Beyer T, Siegel T, Beebe D, Aldinger C, Ellery C, Ashton M, Pustilnik L, Morehouse L.** Low doses of aldose reductase inhibitors dissociate sorbitol accumulation from myo-inositol depletion in tissues of the diabetic rat. *Diabetes* 39: 187A, 1990.
7. **Bierhaus A, Schiekofler S, Schwaninger M, Andrassy M, Humpert PM, Chen J, Hong M, Luther T, Henle T, Klötting I, Morcos M, Hofmann M, Tritschler H, Weigle B, Kasper M, Smith M, Perry G, Schmidt A-M, Stern DM, Haring H-U, Schleicher E, Nawroth PP.** Diabetes-associated sustained activation of the transcription factor nuclear factor- B. *Diabetes* 50: 2792–2808, 2001.
8. **Bitsch R, Wolf M, Möller J, Heuzeroth L, Grünekle D.** Bioavailability assessment of the lipophilic benfotiamine as compared to a water-soluble thiamin derivative. *Ann Nutr Metab* 35: 292–296, 1991.
9. **Bolton W, Cattran D, Williams M, Adler S, Appel G, Cartwright K, Foiles P, Freedman B, Raskin P, Ratner R, Spinowitz B, Whittier F, Wuerth J.** Randomized trial of an inhibitor of formation of advanced glycation end products in diabetic nephropathy. ACTION I Investigator Group. *Am J Nephrol* 24: 32–40, 2004.
10. **Brodie AE, Reed DJ.** Reversible oxidation of glyceraldehyde 3-phosphate dehydrogenase thiols in human lung carcinoma cells by hydrogen peroxide. *Biochem Biophys Res Comm* 148: 120–125, 1987.
11. **Brownlee M, Vlassara H, Kooney A, Ulrich P, Cerami A.** Aminoguanidine prevents diabetes-induced arterial wall protein cross-linking. *Science* 232: 1629–1632, 1986.
12. **Brownlee M.** Biochemistry and molecular cell biology of diabetic complications. *Nature* 414: 813–820, 2001.

13. **Brownlee M.** The pathobiology of diabetic complications a unifying mechanism. *Diabetes* 54: 1615–1625, 2005.
14. **Cai L, Li W, Wang G, Guo L, Jiang Y, Kang YJ.** Hyperglycemia-Induced apoptosis in mouse myocardium: mitochondrial cytochrome c-mediated caspase-3 activation pathway. *Diabetes* 51: 1938–1948, 2002.
15. **Capes SE, Hunt D, Malmberg K, Gerstein HC.** Stress hyperglycaemia and increased risk of death after myocardial infarction in patients with and without diabetes: a systematic overview. *Lancet* 355: 773–778, 2000.
16. **Catherwood MA, Powell LA, Anderson P, McMaster D, Sharpe PC, Trimble ER.** Glucose-induced oxidative stress in mesangial cells. *Kidney Int* 61: 599–608, 2002.
17. **Ceriello A, Morocutti A, Mercuri F, Quagliaro L, Moro M, Damante G, Viberti G.** Defective intracellular antioxidant enzyme production in type 1 diabetic patients with nephropathy. *Diabetes* 49: 2170–2177, 2000.
18. **Ceriello A, Quagliaro L, Amico MD, Filippo C Di, Marfella R, Nappo F, Berrino L, Rossi F, Giugliano D.** Acute hyperglycemia induces nitrotyrosine formation and apoptosis in perfused heart from rat. *Diabetes* 51: 1076–1082, 2002.
19. **Ceriello A.** Oxidative stress and glycemic regulation. *Metab Clin Exp* 49: 27–29, 2000.
20. **Chowdhury AK, Watkins T, Parinandi NL, Saatian B, Kleinberg ME, Usatyuk P V, Natarajan V.** Src-mediated tyrosine phosphorylation of p47phox in hyperoxia-induced activation of NADPH oxidase and generation of reactive oxygen species in lung endothelial cells. *The Journal of biological chemistry* 280: 20700–11, 2005.
21. **Clark RJ, McDonough PM, Swanson E, Trost SU, Suzuki M, Fukuda M, Dillman WH.** Diabetes and the accompanying hyperglycemia impairs cardiomyocyte calcium cycling through increased nuclear O-GlcNAcylation. *J Biol Chem* 278: 44230–44237, 2003.
22. **Cohen H, Seifen E, Straub K, Tiefenback C, Stermitz F.** Structural specificity of the NaK-ATPase inhibition by sanguinarine, an isoquinoline benzophenanthridien alkaloid. *Biochem Pharmacol* 27: 2555–2558, 1978.
23. **Corbett J, Tilton R, Chang K, Hasan K, Ido Y, Wang J, Sweetland M, Lancaster, JR Jr, Williamson J, McDaniel M.** Aminoguanidine, a novel inhibitor of nitric oxide formation, prevents diabetic vascular dysfunction. *Diabetes* 41: 552–556, 1992.
24. **Le Corvoisier P, Lacotte J, Laplace M, Crozatier B.** Interaction of chelerythrine with inositol phosphate metabolism. *Fundamental Clin Pharmacol* 16: 31–37, 2002.
25. **Cunningham MJ, Apstein CS, Weinberg EO, Vogel WM, Lorell BH.** Influence of glucose and insulin on the exaggerated diastolic and systolic dysfunction of hypertrophied rat hearts during hypoxia. *Circulation Research* 66: 406–415, 1990.
26. **Davì G, Falco A, Patrono C.** Lipid peroxidation in diabetes mellitus. *Antioxid Redox Signal* 7: 256–268, 2005.



27. **Deora AA, Win T, Vanhaesebroeck B, Lander HM.** A redox-triggered ras-effector interaction. Recruitment of phosphatidylinositol 3'-kinase to Ras by redox stress. *J Biol Chem* 273: 29923–29928, 1998.
28. **Dimmelers S, Lottspeich F, Brune B.** Nitric oxide causes adp- ribosylation and inhibition of glyceraldehyde-3-phosphate dehydrogenase. *J Biol Chem* 267: 16771–16774, 1992.
29. **Ding H, Zhu H, Dong J, Zhu W, Zhou Z.** Intermittent hypoxia protects the rat heart against ischemia / reperfusion injury by activating protein kinase C. *Life Sci* 75: 2587 – 2603, 2004.
30. **Ding H-L, Zhu H, Dong J, Zhu W, Yang W, Yang H, Zhou Z.** Inducible nitric oxide synthase contributes to intermittent hypoxia against ischemia/reperfusion injury. *Acta Pharmacol Sin* 26: 315–322, 2005.
31. **Dion HW, Al E.** 6-diazo-5-oxo-L-norleucine, A new tumor inhibitory substance. II: Isolation and Characterization". *Antibiotics Chemother* 78: 3075–3077, 1954.
32. **Droge W.** Free radicals in the physiological control of cell function. *Physiol Rev* 82: 47–95, 2002.
33. **Du X, Edelstein D, Brownlee M.** Oral benfotiamine plus  $\alpha$ -lipoic acid normalises complication-causing pathways in type 1 diabetes. *Diabetes* (2008).
34. **Du X, Edelstein D, Rossetti L, Fantus IG, Goldberg H, Ziyadeh F, Wu J, Brownlee M.** Hyperglycemia-induced mitochondrial superoxide overproduction activates the hexosamine pathway and induces plasminogen activator inhibitor-1 expression by increasing Sp1 glycosylation. *Proc Natl Am Sci* 97: 12222–12226, 2000.
35. **Du X, Matsumura T, Edelstein D, Rossetti L, Zsengellér Z, Szabó C, Brownlee M.** Inhibition of GAPDH activity by poly (ADP-ribose) polymerase activates three major pathways of hyperglycemic damage in endothelial cells. *J Clin Invest* 112: 1049–1057, 2003.
36. **D'Alessandris C, Andreozzi F, Federici M, Cardellini M, Brunetti A, Ranalli M, Del Guerra S, Lauro D, Del Prato S, Marchetti P, Lauro R, Sesti G.** Increased O-glycosylation of insulin signaling proteins results in their impaired activation and enhanced susceptibility to apoptosis in pancreatic beta-cells. *Fed Am Soc Exp Biol J* 18: 959–961, 2004.
37. **Earnshaw WC, Martins LM, Kaufmann SH.** Mammalian caspases: structure, activation, substrates, and function during apoptosis. *Annu Rev Biochem* 68: 383–424, 1999.
38. **Eckly-Michel AE, Le Bec A, Lugnier C.** Chelerythrine, a protein kinase C inhibitor, interacts with cyclic nucleotide phosphodiesterases. *Eur J Pharmacol* 324: 85–88, 1997.
39. **Forbes J, Soulis T, Thallas V, Panagiotopoulos S, Long D, Vasan S, Wagle D, Jerums G, Cooper M.** Renoprotective effects of a novel inhibitor of advanced glycation. *Diabetologia*. 44: 108–114, 2001.
40. **Fraser DA, Hessvik NP, Nikolić N, Aas V, Hanssen KF, Bøhn SK, Thoresen GH, Rustan AC.** Benfotiamine increases glucose oxidation and downregulates NADPH oxidase 4

expression in cultured human myotubes exposed to both normal and high glucose concentrations. *Genes Nutri* 7: 459–469, 2012.

41. **Freedman B, Wuerth J, Cartwright K, Bain R, Dippe S, Hershon K, Mooradian A, Spinowitz B.** Design and baseline characteristics for the aminoguanidine Clinical Trial in Overt Type 2 Diabetic Nephropathy (ACTION II). *Control Clin Trials* 20: 493–510, 1999.
42. **Friguet B, Bulteau A, Conconi M, Petropoulos I.** Redox control of 20S proteasome. *Methods Enzymol* 353: 253–262, 2002.
43. **Fujiwara M, Watanabe H, Matsui K.** Allithiamine, a newly found derivative of vitamin B1. *J Biochem* 41: 29–39, 1954.
44. **Geraldes P, King GL.** Activation of protein kinase C isoforms and its impact on diabetic complications. *Circ Res* 106: 1319–1331, 2010.
45. **Giardino I, Fard A, Hatchell D, Brownlee M.** Aminoguanidine inhibits reactive oxygen species formation, lipid peroxidation, and oxidant-induced apoptosis. *Diabetes* 47: 1114–1120, 1998.
46. **Guth BD, Wisneski JA, Neese RA, White FC, Heusch G, Mazer CD.** Myocardial lactate release during ischemia in swine. Relation to regional blood flow. *Circ* 81: 1948–1958, 1990.
47. **Hammes H, Du X, Edelstein D, Taguchi T, Matsumura T, Ju Q, Lin J, Bierhaus A, Nawroth P, Hannak D, Neumaier M, Bergfeld R, Giardino I, Brownlee M.** Benfotiamine blocks three major pathways of hyperglycemic damage and prevents experimental diabetic retinopathy. *Nat Med* 9: 294–299, 2003.
48. **Hammes H, Martin S, Federlin K, Geisen K, Brownlee M.** Aminoguanidine treatment inhibits the development of experimental diabetic retinopathy. *Proc Natl Acad Sci USA* 88: 11555–11558, 1991.
49. **Hartog JW, Voors AA, Bakker SJL, Smit AJ, Van Veldhuisen DJ.** Advanced glycation end-products (AGEs) and heart failure: pathophysiology and clinical implications. *Eur J Heart Fail* 9: 1146–1155, 2007.
50. **Hausenloy DJ, Yellon DM.** Reperfusion injury salvage kinase signalling: taking a RISK for cardioprotection. *Heart Fail Rev* 12: 217–234, 2007.
51. **Hearse D, Sutherland F.** The isolated blood and perfusion fluid perfused heart. *Pharmacol Res* 41: 613–627, 2000.
52. **Herbert JM, Augereau JM, Gleye J, Maffrand JP.** Chelerythrine is a potent and specific inhibitor of protein kinase C. *Biochem Biophys Res Commun* 172: 993–999, 1990.
53. **Hiramoto K, Fujino T, Kikugawa K.** DNA strand cleavage by tumor-inhibiting antibiotic 6-diazo-5-oxo-L-norleucine. *Mutat Res* 360 (2): 95–100 360: 95–100, 1996.
54. **Hoffman JI.** Transmural myocardial perfusion. *Prog Cardiovasc Dis* 29: 429–464, 1987.

55. **Hu Y, Belke D, Suarez J, Swanson E, Clark R, Hoshijima M, Dillman WH.** Adenovirus-mediated overexpression of O-GlcNAcase improves contractile function in the diabetic heart. *Circ Res* 96: 1006–1013, 2005.
56. **Huang JS, Guh JY, Hung WC, Yang ML, Lai YH, Chen HC, Chuang LY.** Role of the Janus kinase (JAK)/signal transducers and activators of transcription (STAT) cascade in advanced glycation end-product-induced cellular mitogenesis in NRK-49F cells. *Biochem J* 342: 231–238, 1999.
57. **Hwang NR, Yim S, Kim YM, Jeong J, Song EJ, Lee Y, Lee JH, Choi S, Lee K.** Oxidative modifications of glyceraldehyde-3-phosphate dehydrogenase play a key role in its multiple cellular functions. *Biochem J* 423: 253–264, 2009.
58. **Hwang YC, Kaneko M, Bakr S, Liao H, Lu Y, Lewis ER, Yan S, Li S, Itakura M, Rui L, Skopicki H, Homma S, Schmidt AM, Oates PJ, Szabolcs M, Ramasamy R.** Central role for aldose reductase pathway in myocardial ischemic injury. *Fed Am Soc Exp Biol* 18: 1192–1199, 2004.
59. **Hwang YC, Sato S, Tsai JY, Bakr S, Yan SD, Oates PJ, Ramasamy R.** Aldose reductase activation is a key component of myocardial response to ischemia. *Fed Am Soc Exp Biol J* 16: 243–245, 2002.
60. **Ihm S, Yoo H, Park S, Ihm J.** Effect of aminoguanidine on lipid peroxidation in streptozotocin-induced diabetic rats. *Metab* 48: 1144–1145, 1999.
61. **Inoguchi T, Battan R, Handler E, Sportsman JR, Heath W, King GL.** Preferential elevation of protein kinase C isoform beta II and diacylglycerol levels in the aorta and heart of diabetic rats: differential reversibility to glycemic control by islet cell transplantation. *Proc Natl Acad Sci USA* 89: 11059–11063, 1992.
62. **Inskeep P, Ronfeld R, Peterson M, Gerber N.** Pharmacokinetics of the aldose reductase inhibitor, zopolrestat, in humans. *J Clin Pharmacol* 34: 760–766, 1994.
63. **Inskeep PB, Reed AE, Ronfeld RA.** Pharmacokinetics of zopolrestat, a carboxylic acid aldose reductase inhibitor, in normal and diabetic rats. *Pharmaceut Res* 8: 1511–1515, 1991.
64. **Vander Jagt D, Robinson B, Taylor K, Hunsaker L.** Reduction of trioses by NADPH-dependent aldo-keto reductases. Aldose reductase, methylglyoxal, and diabetic complications. *J Biol Chem* 267: 4363–4369, 1992.
65. **Kaiserova K, Srivastava S, Hoetker JD, Awe SO, Tang X, Cai J, Bhatnagar A.** Redox activation of aldose reductase in the ischemic heart. *J Biol Chem* 281: 15110–15120, 2006.
66. **Kajstura J, Fiordaliso F, Andreoli A M, Li B, Chimenti S, Medow MS, Limana F, Nadal-Ginard B, Leri A, Anversa P.** IGF-1 overexpression inhibits the development of diabetic cardiomyopathy and angiotensin II-mediated oxidative stress. *Diabetes* 50: 1414–1424, 2001.
67. **Kapphahn RJ, Bigelow EJ, Ferrington DA.** Age-dependent inhibition of proteasome chymotrypsin-like activity in the retina. *Exp Eye Res* 84: 646–654, 2007.
68. **Karin M.** The beginning of the end: I $\kappa$ B kinase (IKK) and NF- $\kappa$ B activation. *J Biol Chem* 274: 27339–27342, 1999.

69. **Kassiotis C, Rajabi M, Taegtmeyer H.** Metabolic reserve of the heart: the forgotten link between contraction and coronary flow. *Prog Cardiovasc Dis* 51: 74–88, 2008.
70. **Katare R, Caporali A, Emanuelli C, Madeddu P.** Benfotiamine improves functional recovery of the infarcted heart via activation of pro-survival G6PD/Akt signaling pathway and modulation of neurohormonal response. *J Mol Cell Cardiol* 49: 625–638, 2010.
71. **Ko FN, Chen IS, Wu SJ, Lee LG, Haung TF TC.** Antiplatelet effects of chelerythrine chloride isolated from *Zanthoxylum simulans*. *Biochim Biophys Acta* 1052: 360–365, 1990.
72. **Koya D, Jirousek MR, Lin YW, Ishii H, Kuboki K, King GL.** Characterization of protein kinase C beta isoform activation on the gene expression of transforming growth factor-beta, extracellular matrix components, and prostanoids in the glomeruli of diabetic rats. *J Clin Invest* 100: 115–126, 1997.
73. **Laczy B, Fülöp N, Onay-Besikci A, Des Rosiers C, Chatham JC.** Acute regulation of cardiac metabolism by the hexosamine biosynthesis pathway and protein O-GlcNAcylation. *PLoS One* 6: e18417, 2011.
74. **Lal S, Randall WC, Taylor AH, Kappler F, Walker M, Brown TR, Szwegold BS.** Fructose-3-phosphate production and polyol pathway metabolism in diabetic rat hearts. *Metab* 46: 1333–1338, 1997.
75. **Lander HM, Tauras JM, Ogiste JS, Hori O, Moss RA, Schmidt AM.** Activation of the receptor for advanced glycation end products triggers a p21ras-dependent mitogen-activated protein kinase pathway regulated by oxidant stress. *J Biol Chem* 272: 17810–17814, 1997.
76. **Li Q, Hwang YC, Ananthakrishnan R, Oates PJ, Guberski D, Ramasamy R.** Polyol pathway and modulation of ischemia-reperfusion injury in Type 2 diabetic BBZ rat hearts. *Cardiovasc Diabetol* 7: 33, 2008.
77. **Li S, Sigmon V, Babcock S, Ren J.** Advanced glycation endproduct induces ROS accumulation, apoptosis, MAP kinase activation and nuclear O-GlcNAcylation in human cardiac myocytes. *Life Sci* 80: 1051–1056, 2007.
78. **Lin L.** RAGE on the toll road? *Cell Mol Immunol* 3: 351–358, 2006.
79. **Lindstad R, McKinley-McKee J.** Methylglyoxal and the polyol pathway. Three-carbon compounds are substrates for sheep liver sorbitol dehydrogenase. *FEBS Lett* 330: 31–35, 1993.
80. **Lo T, Selwood T, Thornalley P.** The reaction of methylglyoxal with aminoguanidine under physiological conditions and prevention of methylglyoxal binding to plasma proteins. *Biochem Pharmacol* 48: 1865–1870, 1994.
81. **Loew D.** Pharmacokinetics of thiamine derivatives especially of benfotiamine. *Int J Clin Pharmacol Ther* 34: 47–50, 1996.
82. **Lonsdale D.** A review of the biochemistry, metabolism and clinical benefits of thiamin(e) and its derivatives. *Evid Based Complement Alternat Med* 3: 49–59, 2006.

83. **López-Neblina F, Toledo-Pereyra LH.** Phosphoregulation of signal transduction pathways in ischemia and reperfusion. *J Surg Res* 134: 292–299, 2006.
84. **Mapanga R, Rajamani U, Dlamini N, Zungu-Edmondson M, Kelly-Laubscher R, Shafiullah M, Wahab A, Hasan M, Fahim M, Rondeau P, Bourdon E, Essop M.** Oleanolic acid: a novel cardioprotective agent that blunts hyperglycemia-induced contractile dysfunction. *PloS one* 7: e47322, 2012.
85. **Mapanga R, Tufts M, Shode F, Musabayane C.** Renal effects of plant-derived oleanolic acid in streptozotocin-induced diabetic rats. *Ren Fail* 31: 481–491, 2009.
86. **Marfella R, Di Filippo C, Portoghese M, Ferraraccio F, Rizzo MR, Siniscalchi M, Musacchio E, D'Amico M, Rossi F, Paolisso G.** Tight glycemc control reduces heart inflammation and remodeling during acute myocardial infarction in hyperglycemic patients. *J Am Coll Cardiol* 53: 1425–1436, 2009.
87. **Marshall RC, Nash WW, Shine KI, Phelps ME, Ricchiuti N.** Glucose metabolism during ischemia due to excessive oxygen demand or altered coronary blood flow in the isolated arterially perfused rabbit septum. *Circ Res* 49: 640–648, 1981.
88. **Menè P, Pascale C, Teti A, Bernardini R, Cinotti GA, Pugliese F.** Effects of advanced glycation end products on cytosolic Ca<sup>2+</sup> signaling of cultured human mesangial cells. *J Am Soc Nephrol* 10: 1478–1486, 1999.
89. **Miyata T, Van Ypersele De Strihou C, Imasawa T, Yoshino A, Ueda Y, Ogura H, Kominami K, Onogi H, Inagi R, Nangaku M, Kurokawa K.** Glyoxalase I deficiency is associated with an unusual level of advanced glycation end products in a hemodialysis patient. *Kidney Int* 60: 2351–2359, 2001.
90. **Mochizuki S, Neely R.** Control of glyceraldehyde-3-phosphate dehydrogenase in cardiac muscle. *J Mol Cell Cardiol* 11: 221–236, 1979.
91. **Mollen KP, McCloskey C a, Tanaka H, Prince JM, Levy RM, Zuckerbraun BS, Billiar TR.** Hypoxia activates c-Jun N-terminal kinase via Rac1-dependent reactive oxygen species production in hepatocytes. *Shock (Augusta, Ga.)* 28: 270–7, 2007.
92. **Mueller C, Al-Batran S, Jaeger E, Schmidt B, Bausch M, Unger C, Sethuraman N.** A phase IIa study of PEGylated glutaminase (PEG-PGA) plus 6-diazo-5-oxo-L-norleucine (DON) in patients with advanced refractory solid tumors. *J Clin Oncol* 26, 2008.
93. **Murata M, Ohta N, Sakurai S, Alam S, Tsai J, Kador PF, Sato S.** The role of aldose reductase in sugar cataract formation: aldose reductase plays a key role in lens epithelial cell death (apoptosis). *Chem Biol Interact.* 130-132: 617-625, 2001.
94. **Musabayane C, Tufts M, Mapanga R.** Synergistic antihyperglycemic effects between plant-derived oleanolic acid and insulin in streptozotocin-induced diabetic rats. *Renal Fail* 32: 832–839, 2010.
95. **Mylari B, Larson E, Beyer T, Zembrowski W, Aldinger C, Dee M, Siegel T, Singleton D.** Novel, potent aldose reductase inhibitors: 3,4-dihydro-4-oxo-3-[[5-(trifluoromethyl)-2-benzothiazolyl] methyl]-1-phthalazineacetic acid (zopolrestat) and congeners. *J Med Chem* 34: 108–122, 1991.

96. **Nakajima H, Amano W, Kubo T, Fukuhara A, Ihara H, Azuma Y, Tajima H, Inui T, Sawa A, Takeuchi T.** Glyceraldehyde-3-phosphate dehydrogenase aggregate formation participates in oxidative stress-induced cell death. *J Biol Chem* 284: 34331–34341, 2009.
97. **Nakamura M, Barber AJ, Antonetti DA, LaNoue KF, Robinson KA, Buse MG, Gardner TW.** Excessive hexosamines block the neuroprotective effect of insulin and induce apoptosis in retinal neurons. *J Biol Chem* 276: 43748–43755, 2001.
98. **Nishikawa T, Edelstein D, Du XL, Yamagishi S, Matsumura T, Kaneda Y, Yorek MA, Beebek D, Oates PJ, Hammes H, Giardino I, Brownlee M, Ave MP, York N.** Normalizing mitochondrial superoxide production blocks three pathways of hyperglycaemic damage. *Nature* 404: 787–790, 2000.
99. **Norton GR, Candy G, Woodiwiss AJ.** Aminoguanidine prevents the decreased myocardial compliance produced by streptozotocin-induced diabetes mellitus in rats. *Circ* 93: 1905–1912, 1996.
100. **Oates P, Ellery C.** Aldose reductase inhibitors sorbinil and CP-73,850 prevent galactose-induced hyperperfusion of the renal cortex. *Diabetes* 39: 184A, 1990.
101. **Obrosova IG, Minchenko AG, Vasupuram R, White L, Abatan OI, Kumagai AK, Frank RN, Stevens MJ.** Aldose reductase inhibitor fidarestat prevents retinal oxidative stress and vascular endothelial growth factor overexpression in streptozotocin-diabetic rats. *Diabetes* 52: 864–871, 2003.
102. **Obsorova IG.** Increased sorbitol pathway activity generates oxidative stress in tissue sites for diabetic complications. *Antioxid Redox Signal* 7: 1543–1552, 2005.
103. **Ortlund E, Lacount M, Lewinski K, Lebioda L.** Reactions of Pseudomonas 7A glutaminase-asparaginase with diazo analogues of glutamine and asparagine result in unexpected covalent inhibitions and suggests an unusual catalytic triad Thr-Tyr-Gl. *Biochem* 39 (6): 39: 1199–1204, 2000.
104. **Osei K, Schuster DP, Amoah AGB, Owusu SK.** Diabetes in Africa. Pathogenesis of type 1 and type 2 diabetes mellitus in sub-Saharan Africa: implications for transitional populations. *J Cardiovasc Risk* 10: 85–96, 2003.
105. **Oswald GA, Smith CC, Betteridge DJ, Yudkin JS.** Determinants and importance of stress hyperglycaemia in non-diabetic patients with myocardial infarction. *Br Med J (Clin Resd.)* 293: 917–922, 1986.
106. **Pinkus LM.** Glutamine binding sites. *Methods Enzymol* 46: 414–427, 1977.
107. **Price D, Rhett P, Thorpe S, Baynes J.** Chelating activity of advanced glycation end-product inhibitors. *J Biol Chem* 276: 48967–48972, 2001.
108. **Queisser MA, Yao D, Geisler S, Hammes H, Schleicher ED, Brownlee M, Preissner KT.** Hyperglycemia impairs proteasome function by methylglyoxal. *Diabetes* 59: 670–678, 2010.
109. **Rajamani U, Essop MF.** Hyperglycemia-mediated activation of the hexosamine biosynthetic pathway results in myocardial apoptosis. *Am J Physiol Cell Physiol* 299: C139–C147, 2010.

110. **Rajamani U, Joseph D, Roux S, Essop MF.** The hexosamine biosynthetic pathway can mediate myocardial apoptosis in a rat model of diet-induced insulin resistance. *Acta Physiol (Oxford, England)* 202: 151–7, 2011.
111. **Ramana K V, Friedrich B, Bhatnagar A, Srivastava SK.** Aldose reductase mediates cytotoxic signals of hyperglycemia and TNF- $\alpha$  in human lens epithelial cells. *Fed Am Soc Exp Biol J* 17: 315–317, 2003.
112. **Ramasamy R, Oates PJ, Schaefer S.** Aldose reductase inhibition improves the altered glucose metabolism of isolated diabetic rat hearts. *Diabetes* 46: 292–300, 1997.
113. **Ramasamy R, Trueblood NA, Schaefer S.** Metabolic effects of aldose reductase inhibition during low-flow ischemia and reperfusion. *Am J Physiol Heart Circ Physiol* 275: H195–H203, 1998.
114. **Randell EW, Vasdev S, Gill V.** Measurement of methylglyoxal in rat tissues by electrospray ionization mass spectrometry and liquid chromatography. *J Pharmacol Toxicol Methods* 51: 153–157, 2005.
115. **Requena J, Levine R, Stadtman E.** Recent advances in the analysis of oxidized proteins. *Amino Acids* 25: 221–226, 2003.
116. **Schneider R, Fouda H, Inskeep P.** Tissue distribution and biotransformation of zopolrestat, an aldose reductase inhibitor, in rats. *Drug Metab Dispos* 26: 1149–1159, 1998.
117. **Schuppe-Koistinen I, Moldéus P, Bergman T, Cotgreave I A.** S-thiolation of human endothelial cell glyceraldehyde-3-phosphate dehydrogenase after hydrogen peroxide treatment. *Eur J Biochem* 221: 1033–1037, 1994.
118. **Schäfer M, Schäfer C, Ewald N, Piper HM, Noll T.** Role of redox signaling in the autonomous proliferative response of endothelial cells to hypoxia. *Circ Res* 92: 1010–1015, 2003.
119. **Scivittaro V, Ganz MB, Weiss MF.** AGEs induce oxidative stress and activate protein kinase C-beta(II) in neonatal mesangial cells. *Am J Physiol Renal Physiol* 278: F676–F683, 2000.
120. **Serpillon S, Floyd BC, Gupte RS, George S, Kozicky M, Neito V, Recchia F, Stanley W, Wolin MS, Gupte S a.** Superoxide production by NAD(P)H oxidase and mitochondria is increased in genetically obese and hyperglycemic rat heart and aorta before the development of cardiac dysfunction. The role of glucose-6-phosphate dehydrogenase-derived NADPH. *Am J Physiol Heart Circ Physiol* 297: H153–H162, 2009.
121. **Shenton D, Grant CM.** Protein S-thiolation targets glycolysis and protein synthesis in response to oxidative stress in the yeast *Saccharomyces cerevisiae*. *Biochem J* 374: 513–519, 2003.
122. **Simm A, Munch G, Seif F, Schenk O, Heidland A, Richter H, Vamvakas S, Schinzel R.** Advanced glycation endproducts stimulate the MAP-kinase pathway in tubulus cell line LLC-PK1. *FEBS Lett.* .
123. **Skrypiec-Spring M, Grotthus B, Szeląg A, Schulz R.** Isolated heart perfusion according to Langendorff- Still viable in the new millennium. *J Pharmacol Toxicol Methods* 55: 113–126, 2007.

124. **Soulis T, Cooper M, Vranes D, Bucala R, Jerums G.** Effects of aminoguanidine in preventing experimental diabetic nephropathy are related to the duration of treatment. *Kidney Int* 50: 627–634, 1996.
125. **Stamler J, Vaccaro O, Neaton J, Wentworth D.** Diabetes, other risk factors, and 12-yr cardiovascular mortality for men screened in the Multiple Risk Factor Intervention Trial. *Diabetes Care* 16: 434–444, 1993.
126. **Strasser RH, Braun-Dullaes R, Walendzik H, Marquetant R.** Alpha 1-receptor-independent activation of protein kinase C in acute myocardial ischemia. Mechanisms for sensitization of the adenylyl cyclase system. *Circ Res* 70: 1304–1312, 1992.
127. **Sweeney JF, Nguyen PK, Atkins KB, Hinshaw DB.** Chelerythrine chloride induces rapid polymorphonuclear leukocyte apoptosis through activation of caspase-3. *Shock* 13: 464–471, 2000.
128. **Tang WH, Cheng WT, Kravtsov GM, Tong XY, Hou XY, Chung SK, Chung SSM.** Cardiac contractile dysfunction during acute hyperglycemia due to impairment of SERCA by polyol pathway-mediated oxidative stress. *Am J Physiol Cell Physiol* 299: C643–C653, 2010.
129. **Tang WH, Martin KA, Hwa J.** Aldose reductase, oxidative stress, and diabetic mellitus. *Frontiers in pharmacology* 3: 1–8, 2012.
130. **Thornalley P, Babaei-Jadidi R.** Prevention of microvascular complications of diabetes by high dose S-benzoylthiamine monophosphate (Benfotiamine): mechanism of thiamine delivery into cells. *Diabetologia* 48: Suppl 1, 2005.
131. **Thornalley P, Yurek-George A, Argirov O.** Kinetics and mechanism of the reaction of aminoguanidine with the alpha-oxoaldehydes glyoxal, methylglyoxal, and 3-deoxyglucosone under physiological conditions. *Biochem Pharmacol* 60: 55–65, 2000.
132. **Thornalley P.** Use of aminoguanidine (Pimagedine) to prevent the formation of advanced glycation endproducts. *Arch Biochem Biophys* 419: 31–40, 2003.
133. **Thornalley PJ.** Glutathione-dependent detoxification of alpha-oxoaldehydes by the glyoxalase system: involvement in disease mechanisms and antiproliferative activity of glyoxalase I inhibitors. *Chem Biol Interact* 111: 137–151, 1998.
134. **Tracey WR, Magee WP, Ellery CA, MacAndrew JT, Smith AH, Knight DR, Oates PJ.** Aldose reductase inhibition alone or combined with an adenosine A3 agonist reduces ischemic myocardial injury. *Am J Physiol Heart Circ Physiol* 279: 1447–1452, 2000.
135. **Volvert M, Seyen S, Piette M, Evrard B, Gangolf M, Plumier J, Bettendorff L.** Benfotiamine, a synthetic S-acyl thiamine derivative, has different mechanisms of action and a different pharmacological profile than lipid-soluble thiamine disulfide derivatives. *BMC Pharmacol* 8: 10, 2008.
136. **Wada T, Takagi H, Minakami H, Hamanaka W, Okamoto K, Ito A, Sahashi Y.** A new thiamine derivative, S-benzoylthiamine O-monophosphate. *Science* 134: 195–196, 1961.



137. **Walterová D, Ulrichová, Preininger V, Simánek V, Lenfeld J, Lasovský J.** Inhibition of liver alanine aminotransferase activity by some benzophenanthridine alkaloids. *J Med Chem* 24: 1100–1103, 1981.
138. **Wang X-L, Lau WB, Yuan Y, Wang Y, Yi W, Christopher TA, Lopez BL, Liu H, Ma X.** Methylglyoxal increases cardiomyocyte ischemia-reperfusion injury via glycative inhibition of thioredoxin activity. *Am J Physiol Endocrinol Metab* 299: E207–E214, 2010.
139. **Williamson JR, Chang K, Frangos M, Hasan KS, Ido Y, Kawamura T, Nyengaard JR, Van den Enden M, Kilo C, Tilton RG.** Hyperglycemic pseudohypoxia and diabetic complications. *Diabetes* 42: 801–813, 1993.
140. **Wolff SP, Dean RT.** Glucose autoxidation and protein modification. The potential role of “autoxidative glycosylation” in diabetes. *Biochem. J* 245: 243–250, 1987.
141. **Wu L, Juurlink B.** Increased Methylglyoxal and Oxidative Stress in Hypertensive Rat Vascular Smooth Muscle Cells. *Hypertension* 39: 809–814, 2002.
142. **Wu, F, Lukinius A, Bergström M, Eriksson B, Watanabe Y, Långström B.** A mechanism behind the antitumour effect of 6-diazo-5-oxo-L-norleucine (DON): disruption of mitochondria. *Eur J Cancer* 35: 1155–1161, 1996.
143. **Xia L, Wang H, Goldberg HJ, Munk S, Fantus IG, Whiteside CI.** Mesangial cell NADPH oxidase upregulation in high glucose is protein kinase C dependent and required for collagen IV expression. *Am J Physiol Renal Physiol* 290: F345–F356, 2006.
144. **Xia P, Inoguchi T, Kern TS, Engerman RL, Oates PJ, King GL.** Characterization of the mechanism for the chronic activation of diacylglycerol-protein kinase C pathway in diabetes and hypergalactosemia. *Diabetes* 43: 1122–1129, 1994.
145. **Xia P, Kramer RM, King GL.** Identification of the mechanism for the inhibition of Na<sup>+</sup>,K<sup>(+)</sup>-adenosine triphosphatase by hyperglycemia involving activation of protein kinase C and cytosolic phospholipase A2. *J Clin Invest* 96: 733–740, 1995.
146. **Xu P, Wang J, Kodavatiganti R, Zeng Y, Kass IS.** Activation of protein kinase C contributes to the isoflurane-induced improvement of functional and metabolic recovery in isolated ischemic rat hearts. *Anesth Analg* 99: 993–1000, 2004.
147. **Yadav U, Subramanyam S, Ramana K.** Prevention of endotoxin-induced uveitis in rats by benfotiamine, a lipophilic analogue of vitamin B1. *Invest Ophthalmol Vis Sci* 50: 2276–2282, 2009.
148. **Yonekura H, Yamamoto Y, Sakurai S, Watanabe T, Yamamoto H.** Current perspective roles of the receptor for advanced glycation endproducts in diabetes-induced vascular injury. *J Pharmacol Sci* 311: 305–311, 2005.
149. **Yoshioka K, Takehara H, Okada A, Komi N.** Glutamine antagonist with diet deficient in glutamine and aspartate reduce tumor growth. *Tokushima J Exp Med* 39: 69–76, 1992.
150. **Zhang F, Hu Y, Huang P, Toleman C, Paterson A, Kudlow J.** Proteasome function is regulated by cyclic AMP-dependent protein kinase through phosphorylation of RPT6. *J Biol Chem* 282: 22460–22471, 2007.

151. **Zhang F, Paterson AJ, Huang P, Wang K, Kudlow JE.** Metabolic control of proteasome function. *Physiol (Bethesda, Md.)* 22: 373–9, 2007.
152. **Zhang F, Su K, Yang X, Bowe D, Paterson A, Kudlow J.** O-GlcNAc modification is an endogenous inhibitor of the proteasome. *Cell* 115: 715–725, 2003.
153. **Zhang J, Snyder SH.** Nitric oxide stimulates auto-ADP-ribosylation of glyceraldehyde-3-phosphate dehydrogenase. *Proc Natl Acad Sci U S A* 89: 9382–9385, 1992.
154. **Zhao J, Zhong C.** A review on research progress of transketolase. *Neurosc Bull* 25: 94–99, 2009.

## Chapter 5

### Final conclusions, limitations and recommendations

#### 5.1 Conclusions

This study examined the damaging effects of hyperglycemia in the setting of ischemia and reperfusion. Several conclusions can be drawn from our work. We initially demonstrated that significant metabolic dysregulation occurs with ischemia and reperfusion under hyperglycemic conditions (acute and chronic). Specifically, we found that oxidative stress plays a key role in this process by triggering activation of non-oxidative glucose pathways (NOGP) metabolism that results in damaging outcomes for the heart. This sequence of events were deduced by evaluating our hypothesis in multiple experimental systems, i.e. *in vitro*, *ex vivo* and *in vivo* models of hyperglycemia using H9c2 cells, Langendorff heart perfusions and STZ-induced diabetic rats, respectively.

Another key objective was to identify novel therapeutic agents that are able to blunt the detrimental effects of hyperglycemia in the context of ischemia and reperfusion. Our findings show that both oleanolic acid (OA) and benfotiamine (BFT) offer exciting prospects to treat acute and chronic hyperglycemia-induced cardiac contractile dysfunction. Of note, acute BFT treatment also resulted in cardio-protection in control hearts, thereby highlighting that it actually has a broader therapeutic utility than what would be expected. This therefore opens up significant opportunities to effectively translate our basic findings into the clinical setting. However, more pre-clinical and small-scale clinical studies are required to further test the cardio-protective effects of OA and BFT. Our data also indicate that the UPS may be a unique therapeutic target to treat ischemic heart disease in individuals that present with stress-induced, acute hyperglycemia. However, this interesting possibility requires further investigation. The current study also establishes for the first time – as far as we are aware - that there is a convergence of downstream NOGP effects in our model, i.e. increased myocardial oxidative stress, further NOGP pathway activation, apoptosis, and impaired contractile function.

There are various mechanisms we speculate the inhibitors of the NOGPs may have exerted their cardio-protective effects under hyperglycemic conditions following ischemia and reperfusion. Inhibition of the polyol pathway may have attenuated oxidative stress by prevention of activation of other NOGPs or opening of the mitochondrial permeability transition pore (mPTP) independent of hyperglycemia, restored calcium homeostasis by preventing tyrosine nitration of the sarcoplasmic endoplasmic reticulum calcium ATPase (SERCA) and oxidation of ryanodine proteins. These same mechanisms may also have been involved in the improved function with polyol inhibition at baseline glucose levels. Furthermore, inhibition of the polyol pathway has shown improved cardiac energy metabolism under both normoglycemic and hyperglycemic conditions. AGE inhibition also attenuates oxidative stress and improves contractile function since glycation of thioredoxin and phosphorylation of glycogen synthase 3-beta do not occur. Inhibition of PKC implies that there is no downward activation of PKC-dependent damaging signaling pathways such as activation of nuclear factor kappa beta. With the use of an inhibitor for the HBP pathway there is less O-GlcNAcylation hence protein function maintained and restored expression of SERCA (calcium homeostasis).

In summary, our data demonstrate that both OA and BFT may be useful therapies in the setting of acute myocardial infarction, especially for the alarming number of non-diabetic and diabetic individuals saddled with acute and chronic hyperglycemia, respectively. We are of the opinion that this is particularly relevant within the developing world context, where it may provide cost-effective therapeutic interventions for the treatment of acute myocardial ischemia in such individuals.

## **5.2 Limitations and future recommendations**

For the *in vitro* studies there were no parallel experiments carried out to rule out the osmotic effect as previously described in our laboratory (2). Furthermore superoxide levels were the major oxidant measured, however, we acknowledge that other ROS and RNS may also be implicated in the

damaging effects of hyperglycemia. Although lucigenin chemiluminescence was used to measure superoxide levels, this method has shortfalls since superoxide are short-lived and lucigenin auto-oxidizes to produce superoxide and may therefore decrease sensitivity of superoxide detection (1). For future studies it is recommended that a variety of alternative markers of oxidative stress be measured e.g. aconitase, reduced and oxidized glutathione levels, dihydroethidium and lipid peroxidation. The source of superoxide ions was not determined in all the studies and hence these may have to be determined in future studies for example: *in vitro* with various markers (e.g. mitoSox for mitochondrial superoxide), using L-NG-Nitroarginine Methyl Ester (L-NAME) for inhibition of NOS; cyclosporine to determine mPTP opening contribution). Furthermore expression of the enzymes involved in superoxide production may be determined by Western blotting or immunohistochemistry. Another point to consider is that for NOGP activation we measured metabolite concentrations as markers of pathway stimulation. However, an assessment of *actual* metabolic flux will further strengthen our existing data (3). The effects of OA, BFT and the specific inhibitor drugs used may be due to their non-specific effects hence in order to rule out these effects dose-dependent experiments should be performed using *in vitro*, *ex vivo* and *in vivo* models to analyze NOGP activation, oxidative stress, apoptosis, and cardiac functional effects. For future studies it is recommended to investigate effects of standard anti-diabetic drugs (e.g. insulin, metformin) on flux via NOGP. Finally, we propose that additional studies are required to elucidate the protective mechanisms of BFT at baseline glucose levels (e.g. JAK/STAT pathways).

### 5.3 References

1. **Fridovich I.** Superoxide anion radical (O<sub>2</sub><sup>-</sup>), superoxide dismutases, and related matters. *J Biol Chem* 272: 18515–18517, 1997.
2. **Rajamani U, Essop MF.** Hyperglycemia-mediated activation of the hexosamine biosynthetic pathway results in myocardial apoptosis. *Am J Physiol Cell Physiol* 299: C139–C147, 2010.
3. **Stephanopoulos G.** Metabolic fluxes and metabolic engineering. *Metab Eng* 1: 1–11, 1999.

## APPENDICES

### Appendix 1



UNIVERSITEIT-STELLENBOSCH-UNIVERSITY  
jou kennisvermoë • your knowledge partner

4 June 2010

Prof. M. F. Essop  
Physiological Sciences  
Stellenbosch University  
Stellenbosch

Dear Prof Essop

**Application for Ethical Clearance:**  
**BENFOTIAMINE ATTENUATES HYPERGLYCEMIA-MEDIATED DECREASE IN**  
**MYOCARDIAL FUNCTION IN RESPONSE TO ISCHEMIA-REPERFUSION**  
**Ref: 10NF\_ESS01**

Your application for ethical clearance has been approved by the SU ACU committee. Please note that this clearance is only valid for a period of twelve months. Ethical clearance of protocols spanning more than one year must be renewed annually through submission of a progress report, up to a maximum of three years.

**Applicants are reminded that they are expected to comply with accepted standards for the use of animals in research and teaching as reflected in the South African National Standards 10386: 2008. The SANS 10386: 2008 document will be available on the Division for Research Development's website [www.sun.ac.za/research](http://www.sun.ac.za/research) , shortly.**

Please feel free to contact Mr. Winston Beukes if any additional information is needed.

Kind regards

  
PP: Ms M Fouche (Manager: Research Support)



Mr. Winston Beukes  
Address: Naverzingsdreef 146 • Division: Research Development  
Private: Sakhisibo Bldg-Matieland 7602-Stellenbosch, South Africa  
Tel: +27 21 808 9015 • E-mail: [w-beukes@sun.ac.za](mailto:w-beukes@sun.ac.za) • Faxed/Fax: +27 021 808 4537

## Appendix 2



UNIVERSITY OF CAPE TOWN

Health Sciences Faculty  
Research Ethics Committee  
Room E53-24 Grootte Schuur Hospital Old Main Building  
Observatory 7925  
Telephone [021] 406 6338 • Facsimile [021] 406 6411  
e-mail: nosi.tsarna@uct.ac.za

29 June 2012

AEC REF NO: 012/039

Dr R Kelly-Laubscher  
Human Biology  
Anatomy Building

Dear Dr Kelly-Laubscher

**PROJECT TITLE: NOVEL AGENTS THAT BLUNT HYPERGLYCEMIA-INDUCED CARDIAC DYSFUNCTION IN THE RAT.**


Thank you for submitting your study to the Faculty of Health Sciences Animal Research Ethics Committee for review.

It is a pleasure to inform you that the FHS AEC has authorised the above mentioned study specifically for the use of 170 Wistar rats for the period of 18 months.

*Please note that the first annual progress report is due in June 2013.*

Please quote the REC. REF in all your correspondence.

Yours sincerely

  
**PROF GRAHAM LOUW**  
**CHAIR, HSF AEC**

tsarni

## Appendix 3

### Krebs-Henseleit stock solutions

1. NaCl (279g/ 2L)
2. NaHCO<sub>3</sub> (83.6g/ 2L)
3. KCl (17.6g) +  
K H<sub>2</sub>PO<sub>4</sub> (8.1 g) in 2 L
4. MgSO<sub>4</sub>· 7H<sub>2</sub>O (7.4g) +  
NaSO<sub>4</sub> (4.2g) in 1L
5. CaCl<sub>2</sub>·2H<sub>2</sub>O (18 g) in 1L

To make up the 5 L working Krebs-Henseleit buffer mix 250ml of 1 and 2; add 100ml of 3 and 4 then add glucose and finally # 5. Filter and p.H to 6.7 with HCl or NaOH. To make up 11 mM glucose add 9.9 g and increase twice or thrice for 22 mM and 33 mM buffer solutions, respectively.

## Appendix 4

### Caspase-Glo® 3/7 assay

H9c2 cells in a 96-well format

Preparation of working reagent solution and storage:

Mix the Caspase-Glo® 3/7 buffer reagent gently and allow to equilibrate at room temperature. Transfer the lyophilized substrate to the buffer and mix by swirling. Store at -20°C. (Note that reconstituted reagent that is freeze thawed will display diminished signal over time – approximately 60% compared to freshly prepared reagent after 4 weeks according to the manufacturer. However, little reduction in signal intensity was noticed over longer time periods of freeze thawing in our experiments.)

#### Assay protocol:

Allow the working buffer reagent to equilibrate at room temperature for at least 30 minutes. Remove plates containing cells from 37°C growing conditions to allow them to equilibrate at room temperature. (At least 10 minutes). Transfer 50 µl (1:1) of working reagent to each well containing cells. Mix plates on a shaker for 30 seconds. Incubate plates in the dark for 1 hour at *constant* room temperature. (Can incubate for up to 3 hours). Measure the luminescence in a luminometer.



## Appendix 5

### Modified RIPA Buffer:

A 100 ml modified RIPA buffer contains:

- 50 mM Tris-HCl (790 mg of Tris in 75 ml distilled water and 900 mg of NaCl and pH made 7.4 using HCl)
- 10 ml of 10% NP-40 [final concentration 1%]
- 2.5 ml of 10% sodium deoxycholate [final concentration 0.25%]
- 1 ml of 100 mM EDTA pH 7.4 [final concentration 1 mM]
- Protease inhibitors
  - 500  $\mu$ L of 200 mM phenylmethylsulfonyl fluoride (PMSF) [final concentration 1 mM]
  - 100  $\mu$ L of Leupeptin (1 mg/ml water) [final concentration 1  $\mu$ g/ml]
  - 80  $\mu$ L of SBT1 (5 mg/ml water) [final concentration 4  $\mu$ g/ml]
  - 100  $\mu$ L of Benzamidine (1 M) [final concentration 1 mM]
- Protein phosphatase inhibitors
  - 500  $\mu$ L of 200 mM activated sodium orthovanadate ( $\text{Na}_2\text{VO}_3$ ) [final concentration 1 mM]
  - 500  $\mu$ L of 200 mM NaF [final concentration 1 mM]
- 1 ml Triton X-100

This buffer is then made up to a final volume of 100 ml with distilled water and stored at  $-20^\circ\text{C}$ .

## Appendix 6

### Bradford protein quantification method:

Bradford reagent

- 500 mg of Coomassie Brilliant Blue G in 250 ml of 95% ethanol
- 500 ml of phosphoric acid

This is made up to 1 litre using distilled water, filtered and stored at 4°C.

Working solution:

The Bradford stock is diluted in 1:5 ratio using distilled water, filtered and used for protein quantification.

Bradford method:

BSA (1 mg/ml) is diluted in a 1:4 ratio using distilled water. A protein standard with varying protein concentrations is prepared as follows:

BSA ( $\mu\text{L}$ )	BSA concentration ( $\mu\text{g}$ )	Volume of distilled water ( $\mu\text{L}$ )
0	Blank	100
10	2	90
20	4	80
40	8	60
60	12	40
80	16	20
100	20	0
5	Unknown protein sample	95

To all these protein and BSA standards, 900  $\mu\text{L}$  of Bradford working solution is added and vortexed gently. Samples were allowed to stand for  $\sim 5$  minutes. The absorbancies of each sample was read using a spectrophotometer at 595 nm. (If the protein absorbancies fall outside the protein standard, the proteins must be diluted with RIPA buffer and reading taken again). The absorbancies were then plotted to construct a linear plot for the standards. Thereafter the amounts of protein in unknown samples were quantified in relation to the linear standard plot.

## Appendix 7

### 3x Sample buffer (*pre-made, bench*)

For a 0.5 M Tris solution, add 3.03 g to 50 ml distilled water and adjust the pH to 6.6. Take 33.3 ml and add 8.8 g SDS, 20 g Glycerol and a tiny bit Bromophenol blue. Fill up to 75 ml with  $\text{dH}_2\text{O}$ .

### Sample preparation (tissue lysates) Western blotting- SDS-PAGE:

Set heating block temperature to 99  $^{\circ}\text{C}$  and keep samples on ice, and allow to thaw. A stock solution of sample buffer containing 850  $\mu\text{L}$  sample buffer and 150  $\mu\text{L}$  mercaptoethanol is prepared. A volume of sample buffer equivalent to 1/3 final volume of the sample is added (under the fume hood). The appropriate amounts of proteins are added to each tube calculated previously. Tiny holes are punched on the lids of microfuge tubes (containing the prepared sample) and placed in boiling water for about 5 minutes. The tubes are then briefly spun in a table top centrifuge. Samples can now be used for Western blot analysis or alternatively be stored at  $-80^{\circ}\text{C}$  for later use.

SDS = denature proteins, constant anionic charge-to-mass ration

Glycerol = give sample a higher density than buffer to "sink" to the bottom of the well

Mercaptoethanol = reduce disulfide bonds present in protein sample

## Appendix 8

### SDS-PAGE -Western blotting

Clean pairs of large and small glass plates with methanol and a paper towel. Place the small glass plate onto the large plate and slide these into the green assembly. Tighten the assembly by pushing the green clips outward. Place the assembly onto the rubber base, pushing down gently. Prepare two small beakers, two Pasteur pipettes and a small stirring bar. Fill one beaker with H<sub>2</sub>O and prepare isobutanol.

Gel recipe for 10% 0.75mm gels:

	2gels:	4 gels
	µl	µl
dH <sub>2</sub> O	3850	7700
1.5M Tris-HCl pH 8.8 (68.1 g Tris base dissolved in 1 liter dH <sub>2</sub> O)	2500	5000
10 % SDS (stock)	100	200
10 % APS (0.1 g/ml)	20	40
Acrylamide (40 %) ( <i>carcinogenic</i> )	2500	5000
Temed ( <i>add at very end in fume hood</i> )	5	10

Mix solution and pour between the glass plates using a Pasteur pipette leaving enough space for the stacking gel. Add a layer of isobutanol using a fresh Pasteur pipette.

Allow to set for 45 minutes - 1 hour.

In the meantime prepare running buffer in a 1:10 dilution.

After 30- 45 minutes has passed begin to prepare the stacking gel (4% recipe):

	2gels:	4 gels
	$\mu\text{l}$	$\mu\text{l}$
dH <sub>2</sub> O	3050	6100
0.5M Tris-HCl pH 8.8 (6.06 g Tris base dissolved in 1 liter dH <sub>2</sub> O)	1250	2500
10 % SDS (stock)	50	100
10 % APS (0.1 g/ml)	50	100
Acrylamide (40%)	500	1000
Temed	10	10

Once the gels are set (after ~1 h), wash off the isobutanol and ensure the plates are dry. Add Temed to the stacking solution, quickly and add stack between the plates. Gently push the combs (of the correct width) into the stacking gel. Allow to set for 30 minutes. Retrieve prepared samples from the -80 C freezer and allow to thaw on ice. Once thawed, vortex each sample briefly before denaturing on the heating block for 5 minutes.

In the meantime, remove the combs carefully from the gels and wash gently with deionized water being careful not to damage the wells. Take the gel plates out of the assembly stand and place them in the U-shaped adaptor cassette with the small plates facing inward. Place the U-shaped adaptor into the loading system and push the latches closed, away from your body. Carefully pour running buffer into the middle compartment between the gel plates, allowing the buffer to flow over the wells. Add 10  $\mu\text{l}$  of pre-stained weight marker (peqGOLD, PEQLAB Biotechnologie GMBH, Germany) into the first well on the left of each gel for orientation and electrophoretic determination of molecular weights of specific bands.

Hereafter add 50 µg of protein samples into each well in the desired order using a micropipette and clean loading tips for every sample. Place the system into the outer running chamber, add the running buffer until ~1cm below the wells. Place the green lid with electrical leads onto the cell system, making sure to attach the electrodes correctly i.e. red to red and black to black. Run gels were run for 60 minutes at 100 V (constant) and 400 mA (Mini Protean System, Bio-Rad, USA) for 10 minutes then the voltage was increased to 200 V with the same current for 60 minutes.

## **Appendix 9**

### **Electrotransfer of proteins:**

Cut two chromatography filter papers and one 0.2 micron polyvinylidene fluoride (PVDF) membranes (Immunibilon, Millipore, USA). Soak filter papers in transfer buffer and for the membrane first soak in methanol for 15 seconds, thereafter wash with distilled water before soaking in transfer buffer. Place on filter paper onto the semi-dry apparatus (Bio-Rad, USA) and carefully place the PVDF membranes on top. Roll with a wet tube to remove any bubbles. Hereafter place gels onto membranes making sure to get rid of any bubbles with a wet tube. To complete the sandwich place filter paper on top of the gel, close the system and run at limit 0.5 A and 15 V for ~ 1 h.

## Appendix 10

### Detection of proteins (Western blots): Probing the membrane

In order to prevent non-specific binding membranes were blocked in 5 % (weight/volume) fat-free milk in 0.1 % Tris Buffered Saline-Tween 20 (TBS-T see Appendix 14) for 2 hours at room temperature. Membranes were then incubated with the respective primary antibody diluted in 5 % (w/v) fat-free milk in 0.1 % TBS-T (1: 1000), overnight at 4 °C. Hereafter on the following day, membranes were washed a further three times in TBS-T (3x5 minutes) before being incubated in the secondary anti-mouse/rabbit/sheep/goat HRP monoclonal antibody (1:4000) for 1 hour at room temperature with gentle agitation.

For detection of the antibodies, membranes were treated with 2 ml ECL LumiGLO Reserve™ chemiluminescent substrate kit (KPL, Inc., USA) as per manufacturer's instructions. It was then dried on tissue paper, placed between transparencies and was then developed in a dark room where bands were exposed to autoradiography film (Hyperfilm, Amersham Biosciences, UK). The film was then developed by placing it in developing solution until bands appeared followed by 15 seconds in a fixative. This film was then visualised and quantified by densitometry using the UNSCAN-IT© densitometry software (Silk Scientific Corporation, Utah, USA). All bands were expressed as optical density readings relative to a control present on the same blot.

## **Appendix 11**

### **Preparation of the triphenyl-tetrazolium chloride (TTC) solution**

Make up a high pH phosphate buffer by dissolving 14.2 mg of  $\text{Na}_2\text{HPO}_4$  in a liter of distilled water and a low pH phosphate buffer by dissolving 12 mg of  $\text{NaH}_2\text{PO}_4$  in a liter of distilled water. Mix in a ratio of 8 parts of the high pH buffer to 2 for the low pH buffer. pH to 7.4. For every heart use 5 ml of the mixed phosphate buffers and weigh 10 mg of the TTC salt for every 1 ml of the solution. Incubate the cut heart slices at 37 °C for 20 min shaking at least once.

## **Appendix 12**

### **Determination of infarct size and area at risk using Image J software**

Select the heart slices using the third tool for polygon selections in the tools bar and pressing down on the Shift key of the keyboard. Determine the total area by clicking the Edit tab then select clear outside, thereafter click the Analyze tab and select Measure. A table with the first set of results shows and for infarct size use the area values. Thereafter click on the Image tab, select Split channels. Here 3 windows will open i.e. green, red, and blue channels. Close the blue channel, use values from the green channel will be used for calculating infarct size and from the red channel area at risk. Here, it is advisable to do the analysis with a picture of the heart alongside. In either of the green or red channel, click on the Image tab, select Adjust threshold and using the eighth tool select the respective highlighted area in the heart slices corresponding to the infarct size and area at risk, respectively. Thereafter click on the Analyze tab and select measure. At the end three readings should appear for total area, infarct size and area at risk. For the calculations subtract the second and third readings from the total area to obtain infarct size and area at risk values, respectively. These are calculated for both sides of the heart slices and expressed as infarct size/area at risk.



## Appendix 13

### Preparation of citrate buffer for dissolving streptozotocin

To make the buffer prepare 0.1 M sodium citrate and 0.1 M citric acid as follows:

Weigh 0.192 g citric acid and dissolve in 10 ml dH<sub>2</sub>O. Weigh 0.294 g sodium citrate and dissolve in 10 ml dH<sub>2</sub>O.

Pipette 1.8 ml citric acid and add to 8.2 ml of sodium citrate. Bring final volume to 100 ml with dH<sub>2</sub>O and adjust pH to 6.2 with sodium hydroxide or hydrochloric acid.

## Appendix 14

### Phosphate buffered saline (PBS) preparation

Dissolve the following in 800 ml of dH<sub>2</sub>O:

- 8 g NaCl
- 0.2 g KCl
- 1.44 g Na<sub>2</sub>HPO<sub>4</sub>
- 0.24 g KH<sub>2</sub>PO<sub>4</sub>

Adjust pH as desired, add more dH<sub>2</sub>O to make it 1L, sterilize and autoclave. Store at room temperature.

## Appendix 15

### Buffers used during Western blotting

#### **10 x TBS** (STOCK – store in fridge)

- 48.4 g Tris
- 160 g NaCl

Dissolve in 500 ml distilled water, set pH to 7.6 with concentrated HCl and then make up to 2 L.

#### **10X running buffer** (STOCK – store in fridge)

- Tris base 60.6 g
- Glycine 288 g
- 10 % SDS 20 g

Dissolve in 2 liter distilled water.

#### **Transfer buffer (ready to use)**

In a 1L bottle add :

- 100 ml Biorad 10X transfer buffer
- 200 ml methanol
- 700 ml dH<sub>2</sub>O

## Appendix 16

### Transketolase assay protocol

Prepare:

- 250 mM of Glycylglycine buffer, pH 7.7 at 25°C in dH<sub>2</sub>O using Glycylglycine, Free Base.
- 1 ml 100 mM Xylulose 5-Phosphate solution (X 5-P) in dH<sub>2</sub>O using D-X 5-P, Sodium Salt.
- 1 ml 50 mM Ribose 5-Phosphate Solution (R 5-P) in dH<sub>2</sub>O using D-Ribose 5-Phosphate, Disodium Salt.
- 1 ml 0.10% (w/v) Cocarboxylase (Thiamine Pyrophosphate) Solution in cold dH<sub>2</sub>O using Cocarboxylase (**PREPARE FRESH.**)
- Dissolve the contents of one 5 mg vial of β-NADH, Disodium Salt (**PREPARE FRESH.**)
- 1 ml 300 mM Magnesium Chloride Solution (MgCl<sub>2</sub>) in deionized water using Magnesium Chloride
- a solution containing 2000 TPI units/ml of α-Glycerophosphate Dehydrogenase/ Triosephosphate Isomerase (α-GDH/TPI) (Immediately before use) in cold dH<sub>2</sub>O
- a solution containing 5.0 units/ml of Transketolase Enzyme Solution in cold Glycylglycine buffer
- (Immediately before use)

Pipette in a 96 well microtiter plate as follows:

	μl	μl
Glycylglycine buffer	248	248
X 5-P	10	10
R 5-P	10	10
Cocarboxylase solution	5	5
NADH solution	10	10
MgCl <sub>2</sub>	15	15
α-GDH/TPI solution	1	1
Sample/dH <sub>2</sub> O for blank	10	10

Immediately mix and record decrease in Absorbance at 340nm for approximately 10 minutes.